Summer 8-13-2010

Enhancing Mesenchymal Stem Cell Chondrogenesis for Cartilage Tissue Engineering

Alice H. Huang
University of Pennsylvania, halice@seas.upenn.edu

Enhancing Mesenchymal Stem Cell Chondrogenesis for Cartilage Tissue Engineering

Abstract
Articular cartilage provides a bearing surface for transmitting forces across joints. The poor ability of cartilage to self-repair has motivated efforts to engineer replacement tissues, and mesenchymal stem cells (MSCs), which can undergo chondrogenesis, have emerged as a promising cell source. To date however, the functional properties of MSC-based constructs remain lower than those of the native tissue and of chondrocyte-based constructs cultured identically. Therefore, the overall objective of this thesis is to better understand the transcriptional and functional limitations underlying chondrogenic differentiation and enhance MSC chondrogenesis.

Toward this end, established tissue engineering strategies from the chondrocyte literature were applied. Specifically, the effects of cell seeding density, media formulation and mechanical stimulation were examined with respect to functional growth. Transient application of TGF-β3 improved the compressive properties of MSC-laden constructs, but only when constructs were formed at a higher seeding density. Long-term dynamic compression initiated 3 days after MSC encapsulation impaired functional properties; in contrast, dynamic compression initiated after 3 weeks of chondrogenic pre-culture improved mechanical function. While these strategies enhanced functional chondrogenesis, the compressive properties achieved were ~50% of native tissue levels and did not reach chondrocyte levels. To understand the basis of this difference, microarray analysis was carried out to compare these two cells types and a set of molecular factors were identified as mis-expressed during MSC chondrogenesis.

Although work up to this point focused on optimizing compressive properties, the tensile properties of articular cartilage are also critical to its functional role. In this work, we characterized the tensile properties of MSC-based constructs and demonstrated functional parity with chondrocyte-based constructs. To further enhance these properties, a novel sliding contact bioreactor was developed to better replicate physiologic joint loading conditions. Long-term application of loading to MSC-laden constructs improved not only tensile properties, but instilled biochemical inhomogeneity, reminiscent of native articular cartilage.

Overall, the work outlined in this thesis represents a significant advancement in engineering cartilage replacements as well as in understanding MSC chondrogenesis. Using a multi-faceted approach, we explored potential routes toward overcoming limitations in chondrogenesis and demonstrated that MSCs are responsive to their chemical and mechanical environment.

Degree Type
Dissertation

Degree Name
Doctor of Philosophy (PhD)

Graduate Group
Bioengineering

First Advisor
Robert L. Mauck

Keywords
mesenchymal stem cells, tissue engineering, bioreactors, chondrogenesis, mechanical stimulation

Subject Categories
Molecular, Cellular, and Tissue Engineering

ENHANCING MESENCHYMAL STEM CELL CHONDROGENESIS FOR CARTILAGE TISSUE ENGINEERING

Alice H. Huang

A Dissertation in Bioengineering

Presented to the Faculties of the University of Pennsylvania in Partial Fulfillment of the Requirements for the Degree of Doctor of Philosophy, 2010

Supervisor of Dissertation

_____

Robert L. Mauck
Assistant Professor of Orthopaedic Surgery and Bioengineering
University of Pennsylvania

Graduate Group Chair

_____

Susan S. Margulies
Professor of Bioengineering and Neurosurgery
University of Pennsylvania

Dissertation Committee

Jason A. Burdick, Associate Professor of Bioengineering, University of Pennsylvania

Maurizio Pacifici, Professor of Orthopaedic Surgery, Thomas Jefferson University

Dawn M. Elliott, Associate Professor of Orthopaedic Surgery, University of Pennsylvania

Kurt Hankenson, Assistant Professor of Cell Biology, University of Pennsylvania

ENHANCING MESENCHYMAL STEM CELL CHONDROGENESIS FOR CARTILAGE TISSUE ENGINEERING

ACKNOWLEDGEMENTS

I would first like to thank my advisor, Dr. Robert Mauck. Given Rob's penchant for farm animal idioms, it seems appropriate to co-opt one of his favorites – you can't make a silk purse from a sow's ear. If there is anyone who has proven this idiom wrong, it is Rob, as whatever progress I have made from sow's ear toward silk purse is largely due to his tireless support and guidance. During my time here, his dedication to his students and his enthusiasm for science was a constant source of energy and created an environment that was both fun and intellectually rewarding; I will always be grateful for this experience.

I would also like to thank the other members of my thesis committee, Drs. Dawn Elliott, Jason Burdick, Maurizio Pacifici and Kurt Hankenson for their thoughtful suggestions and advice. Not only have they improved my work significantly, but they have also provided valuable career guidance as I transition to the next stage of my studies.

This work would also not have been possible without the assistance of several talented undergraduate and graduate students. In particular, I would like to acknowledge Ashley Stein, an undergraduate student who was involved in nearly every aspect of my work, as well as the other members (past and present) of the cartilage tissue engineering group, Isaac Erickson, Megan Farrell, Minwook Kim, Jenny Yuan and Meira Yeger-McKeever, for helpful discussions and moral support. In addition, I'd like to thank several current and former members of the McKay Orthopaedic Research Laboratory for facilitating my studies; in no particular order, these include Nelly Andarawis, Ashwin Nathan, Albert Gee, Lachlan Smith, Barbara Gibson, Eileen Shore, and Lou Soslowsky. And finally, I

am fortunate to have conducted my entire graduate career alongside my two close friends and officemates, Brendon Baker and Nandan Nerurkar. Always available for discussion of data or to lend a hand in experiments, they have made me a better scientist, writer and student. They have also helped me maintain my sense of humor and mental equilibrium, mainly through TTA.

Last but not least, I would like to thank my mom, Betty, and my sister, Jessica for their constant love and support. Even from a distance of 3000 miles, their presence has been an important part of my life. I also thank my aunt in Taiwan, Pi-Chin, for giving me many opportunities that would not have been otherwise possible and my brother in law, Ryan. Finally I acknowledge Tony the cat for being an ideal roommate and source of jolliness.

ABSTRACT

ENHANCING MESENCHYMAL STEM CELL CHONDROGENESIS FOR CARTILAGE TISSUE ENGINEERING

Alice H. Huang

Robert L. Mauck

Articular cartilage provides a bearing surface for transmitting forces across joints. The poor ability of cartilage to self-repair has motivated efforts to engineer replacement tissues, and mesenchymal stem cells (MSCs), which can undergo chondrogenesis, have emerged as a promising cell source. To date however, the functional properties of MSC-based constructs remain lower than those of the native tissue and of chondrocyte-based constructs cultured identically. Therefore, the overall objective of this thesis is to better understand the transcriptional and functional limitations underlying chondrogenic differentiation and enhance MSC chondrogenesis.

Toward this end, established tissue engineering strategies from the chondrocyte literature were applied. Specifically, the effects of cell seeding density, media formulation and mechanical stimulation were examined with respect to functional growth. Transient application of TGF-β3 improved the compressive properties of MSC-laden constructs, but only when constructs were formed at a higher seeding density. Long-term dynamic compression initiated 3 days after MSC encapsulation impaired functional properties; in contrast, dynamic compression initiated after 3 weeks of chondrogenic pre-culture improved mechanical function. While these strategies enhanced functional chondrogenesis, the compressive properties achieved were ~50% of native tissue levels

and did not reach chondrocyte levels. To understand the basis of this difference, microarray analysis was carried out to compare these two cells types and a set of molecular factors were identified as mis-expressed during MSC chondrogenesis.

Although work up to this point focused on optimizing compressive properties, the tensile properties of articular cartilage are also critical to its functional role. In this work, we characterized the tensile properties of MSC-based constructs and demonstrated functional parity with chondrocyte-based constructs. To further enhance these properties, a novel sliding contact bioreactor was developed to better replicate physiologic joint loading conditions. Long-term application of loading to MSC-laden constructs improved not only tensile properties, but instilled biochemical inhomogeneity, reminiscent of native articular cartilage.

Overall, the work outlined in this thesis represents a significant advancement in engineering cartilage replacements as well as in understanding MSC chondrogenesis. Using a multi-faceted approach, we explored potential routes toward overcoming limitations in chondrogenesis and demonstrated that MSCs are responsive to their chemical and mechanical environment.

TABLE OF CONTENTS

LIST OF TABLES

LIST OF FIGURES

CHAPTER 1: INTRODUCTION

Mesenchymal stem cells are a multipotent cell type capable of differentiating toward a number of lineages of the musculoskeletal system, including bone, cartilage and fat. This multipotential capacity was first described over three decades ago, and since then, the potential use of MSCs for regenerative therapies has generated tremendous excitement and focus. MSCs are attractive for these applications for several reasons: in addition to their ability to take on multiple phenotypes, MSCs are readily expandable in culture and retain their multipotential characteristics with expansion. Further, MSCs and other similar progenitor cells can be isolated from a wide variety of tissue sources, thereby avoiding additional damage to diseased/injured tissues. These considerations drive the use of MSCs in cartilage tissue engineering efforts and significant advances have been made toward generating functional cartilage replacements. Not all progress with mesenchymal stem cell based cartilage has been successful, however, and considerable challenges remain in the realization of MSC-based cartilage for load-bearing applications. Despite their early promise, MSCs have yet to produce constructs with the mechanical and biochemical properties approaching that of the native tissue. The collagen matrix formed by these cells remains structurally disorganized, and further limit the mechanical function of engineered constructs. Therefore the overall objective of this work is to better understand the molecular and functional limitations underlying chondrogenic differentiation and enhance MSC chondrogenesis to generate functional replacement cartilage.

Thus the intent of Chapter 2 is to define the functional metrics required for the tissue engineering of articular cartilage, and to situate the current state of MSC-based constructs within this framework. In doing so, the components and function of articular cartilage are defined, and the progress made to date using differentiated cartilage cells (chondrocytes) for cartilage tissue engineering is reviewed. Discussion of this work includes methods of formation, biochemical formulations for enhancing *in vitro* development, as well as the use of mechanical forces to further direct the maturation of these engineered constructs. Finally, an overview of adult MSCs for cartilage applications is presented, as well as a discussion on MSC mechanobiology and the potential of mechanical stimulation to further the chondrogenic phenotype of these cells.

In Chapter 3, standard tissue engineering strategies successful in the chondrocyte literature (presented in Chapter 2) were applied to optimize MSC chondrogenesis in 3D culture. Specifically, the effects of increasing initial cell seeding density and the application of a novel media formulation (transient exposure to TGF-β3) were evaluated on MSC-laden agarose constructs. This study tested two hypotheses: 1) that increasing the initial MSC seeding density would result in proportional increases in matrix accumulation, with resultant increases in mechanical properties and 2) that transient application of TGF-β3 would generate constructs with superior GAG content and mechanical properties relative to constructs continuously exposed to TGF-β3.

Chapter 4 describes the effects of mechanical stimulation on functional MSC chondrogenesis. The motivation for this study is self evident as mechanical forces play

an important role in cartilage development and have been shown to modulate the growth of chondrocyte-based constructs. In Chapter 4, mechanical stimulation in the form of dynamic compression (a well characterized loading modality) was applied to MSC-laden constructs after 3 days or 3 weeks of chondrogenic pre-culture. The effects of long-term loading on functional growth of these constructs was examined with respect to pre-culture duration (3 days or 3 weeks), loading duration (1 or 4 hours per day), frequency of the applied load (0.1 or 1 Hz) and TGF-β3 supplementation (with or without) during loading.

In Chapter 5, the molecular profiles of chondrogenic MSCs were compared to that of undifferentiated MSCs and fully differentiated chondrocytes. As MSCs do not form functional matrix on par with that of chondrocytes, this study was carried out to identify molecular differences between the two cell types and establish new criteria for successful chondrogenesis. Donor-matched MSC- and chondrocyte-laden constructs from three donors were cultured under chondrogenic conditions. Functional growth was characterized throughout the culture duration and molecular profiles were assessed via microarray analysis for undifferentiated MSCs (day 0), chondrogenic MSCs (day 28) and chondrocytes (day 28). From this evaluation, a set of molecular factors was identified as potentially dis-regulated during chondrogenesis. Expression of these genes was confirmed in a separate study and differential deposition of identified ECM proteins examined.

While the focus of the studies presented in Chapters 3-5 (as well as current work in the field) has been on optimizing the compressive properties of MSC-based constructs, the tensile properties of articular cartilage are also crucial to its load-bearing role in the joint. The evolution of these properties in native cartilage is described in Chapter 2, however few studies have characterized the tensile properties of engineered constructs. Therefore, in Chapter 6, the tensile properties of MSC-laden constructs are described, relative to that of chondrocyte-laden constructs cultured identically.

To optimize tensile properties, a novel bioreactor was developed to apply sliding contact to cell-seeded agarose strips. As physiologic loading within the joint consists of two articulating cartilage layers sliding against one another, a better recapitulation of this mechanical environment may improve both the tensile and compressive properties of MSC-laden constructs, as well as instill structural anisotropy and inhomogeneity. To test this hypothesis, the study described in Chapter 7 examined the effects of short-term sliding contact on chondrogenesis under a range of axial strains in the presence or absence of TGF-β3. Long-term sliding contact was applied using optimized parameters established from short-term studies and functional growth was assessed.

In Chapter 8, a high-throughput screening method was developed to rapidly screen chemical libraries for modulators of MSC chondrogenesis. To date, the majority of studies rely on one chemically defined media formulation to induce chondrogenic differentiation of MSCs. Though this formulation is successful to a certain extent, additional inducers may be necessary for a more complete conversion of phenotype.

Identification of chemical modulators (both inducers and inhibitors) of known action may also be useful in elucidating the signaling pathway underlying MSC chondrogenesis.

And finally, Chapter 9 contains a summary of the major findings stemming from this work, as well as a discussion of its implications for the field of cartilage tissue engineering and potential future research directions.

CHAPTER 2: BACKGROUND

2.1 Clinical Significance

Articular cartilage is a unique tissue whose function is predicated on a precise balance of extracellular matrix (ECM) components and chondrocytes. Together, these components produce and maintain structure and mechanical function over a lifetime of use. Disruption of the articulating cartilages, either through trauma or progressive degenerative diseases such as osteoarthrititis (OA), engenders pain and loss of function to millions in the US, and hundreds of millions worldwide. The antecedents of OA have yet to be fully elucidated, but certain mechanical, genetic, and lifestyle risk factors have been identified (Felson et al. 2000). Pathologies associated with OA arise both within the articulating cartilage layers (fissuring, loss of matrix properties, progressive vascularization and eburnation), as well as within the subchondral bone supporting the cartilage layer. Many of the same features that enable cartilage function (a dense ECM, a lack of vascularity) also appear to impede normal healing responses in the tissue, and predispose a loss in functional capacity once the careful regulatory mechanisms that maintain the tissue become imbalanced.

This lack of endogenous healing necessitates methods for repair to restore joint function, the most common of which is total joint replacement. This replacement of bone and soft tissue with metal and plastic components represents the most significant advance in orthopaedic medicine over the last several decades; joint replacement has restored function to millions of patients who otherwise would be incapable of carrying out the functions of daily life. Indeed, with the aging of the US population, as well as increases

in lifespan, total joint replacement procedures are only becoming more common. A recent study suggested that the number of total knee replacements would increase by >600% by 2030, reaching as many as 3.5 million procedures performed per year in the US alone (Kurtz et al. 2007). Despite the successes of joint replacement in restoring function, the lifetime of implanted prosthetic components range between 10-15 years, and surgical methods are limited to only one revision procedure (in which a failing implant is replaced with a new component). Given the prevalence of this disease, the number of replacements performed annually, and the limited alternatives available, solutions to OA are increasingly in demand.

To address this pressing clinical need, the field of tissue engineering has focused on biologic reconstruction of articulating joints. Tissue engineering is loosely defined as the combination of cells and biocompatible materials to generate new, living, biologic tissues for implantation. A tenet of this approach is that biologic substitution is superior to material implantation as a biologic substitute by definition can remodel and sustain itself through normal cellular processes, much like the normal functioning tissue. Early successes in the production of cartilage and bone from cells cultured *ex vivo* as replacement tissue have suggested that tissue engineering may be a viable approach that can eliminate or forestall the need for joint replacement. Even in the absence of full functionality with engineered biologics, provision of an additional decade of joint health via a biologic substitute (prior to joint replacement) would immeasurably improve patient health, particularly as life expectancies continue to improve in the aged population.

2.2 Articular Cartilage

To fully comprehend the challenge of articular cartilage tissue engineering, an in-depth appreciation of the structure, composition, and function of the native tissue is required. The following sections briefly describe the main structural and mechanical features of cartilage that are critical to its functional role, as well as the events that underlie its formation, maturation, and maintenance through a lifetime of use.

2.2.1 Articular Cartilage: Composition and Mechanical Properties

As the load bearing material of diarthrodial joints, articular cartilage lines the bony surfaces and functions to transmit the high stresses that originate with motion through an elegant transition from soft to hard tissue, (**Figure 2-1**). Articular cartilage consists of both a solid matrix (Muir 1970; Clarke 1971; Eyre 1980; Eyre 2004) and a fluid phase (Lipshitz et al. 1976; Mankin et al. 1994). The solid matrix is composed of a dense network of type II collagen fibrils enmeshed in a solution of charged, aggregated proteoglycans (PGs: aggrecan core protein plus glycosaminoglycan (GAG) side chains). Collagen content ranges from 5-30% by wet weight and PG content from 2-10% (Muir 1980; Williamson et al. 2001), with the remainder of the tissue made up of water. Collagen forms a cross-linked co-polymeric network composed of collagen types II, IX and XI (Eyre 2004), and acts to immobilize proteoglycans within the ECM (Mankin et al. 1994). In developing articular cartilage, the proportions of collagens are roughly ≥10% IX, ≥10% XI, ≥80% II, falling to ~1% IX, ~3% XI, ≥90% II in adult cartilage (Eyre 2004). Mutations in collagen types II, IX and XI genes have been associated with the onset of cartilage degeneration and OA-like features (Reginato et al. 2002; Hu et al.

2006). Trifunctional hydroxypyridinium cross-links stabilize these collagen components and contribute to the tensile properties of the tissue. Chondrocytes make up less than 10% of the tissue (Mankin et al. 1994) and produce ECM to balance continual degradation and remodeling by MMPs (collagenases and aggrecanases) (Malemud et al. 1999; Nagase et al. 2003; Stanton et al. 2005). The composition, architecture, and remodeling of cartilage are uniquely adapted to function over a lifetime of repetitive use.

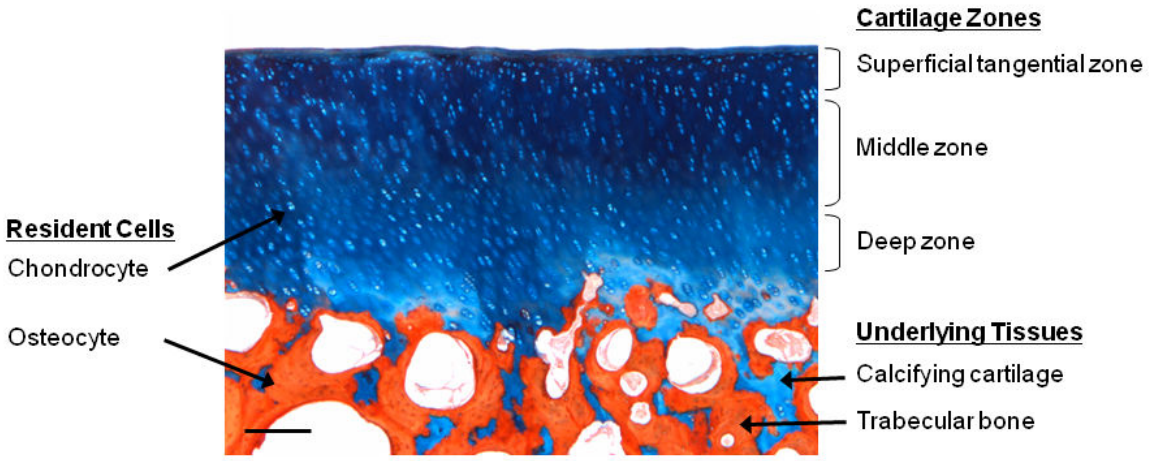

Figure 2-1: Articular cartilage histology showing zonal dependence and integration with underlying bone. Ovine tissue sample stained for proteoglycan (alcian blue) and collagen (picrosirius red). Scale bar: 200 µm.

A normally active adult takes 1-2 million steps per year (Weightman 1976) and the resulting forces acting on cartilage range from 2.5 to 4.9 times the body weight (Paul et al. 1975; Armstrong et al. 1979). Loading is cyclical/intermittent (Dillman 1975; Paul et al. 1975) and stresses at the cartilage surface can range from 2-10 MPa (Fukubayashi et al. 1980; Ahmed et al. 1983; Brown et al. 1983). The dense PG-rich collagenous matrix of cartilage resists this loading environment with its high equilibrium compression modulus of 0.2-1.4 MPa (Mow et al. 1980; Frank et al. 1987; Athanasiou et al. 1991; Ateshian et al. 1997; Chen et al. 2001; Wang et al. 2002) and even higher tensile modulus

of 1-30 MPa (Woo et al. 1976; Roth et al. 1980; Grodzinsky et al. 1981; Akizuki et al. 1986; Schmidt et al. 1990) in the plane of the tissue. The organization and prevailing direction of collagen fibers (the split line direction, **Figure 2-2**) is of particular importance for the tensile properties, which are highest at the surface and in the split line direction (Woo et al. 1976; Mow et al. 2002; Chahine et al. 2004; Huang et al. 2005). Split lines have a different organization in loaded and unloaded regions of joints (Gomez et al. 2000) that is similar between patients (**Figure 2-3**), consistent with the idea that use defines structural organization (Below et al. 2002).

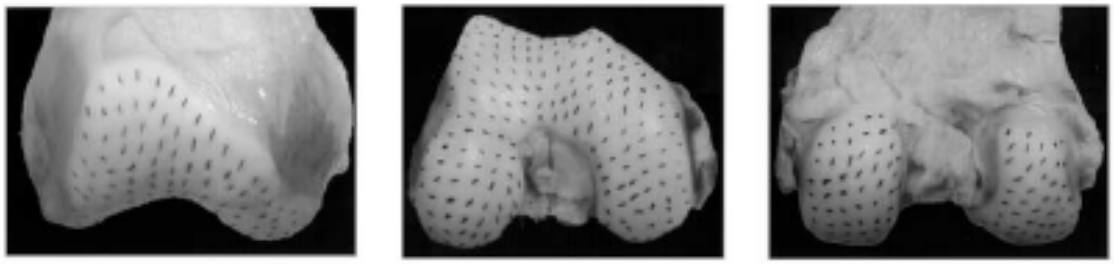

Figure 2-2: Representative split-line patterns of cadaveric femoral articular cartilage. (Below et al. 2002).

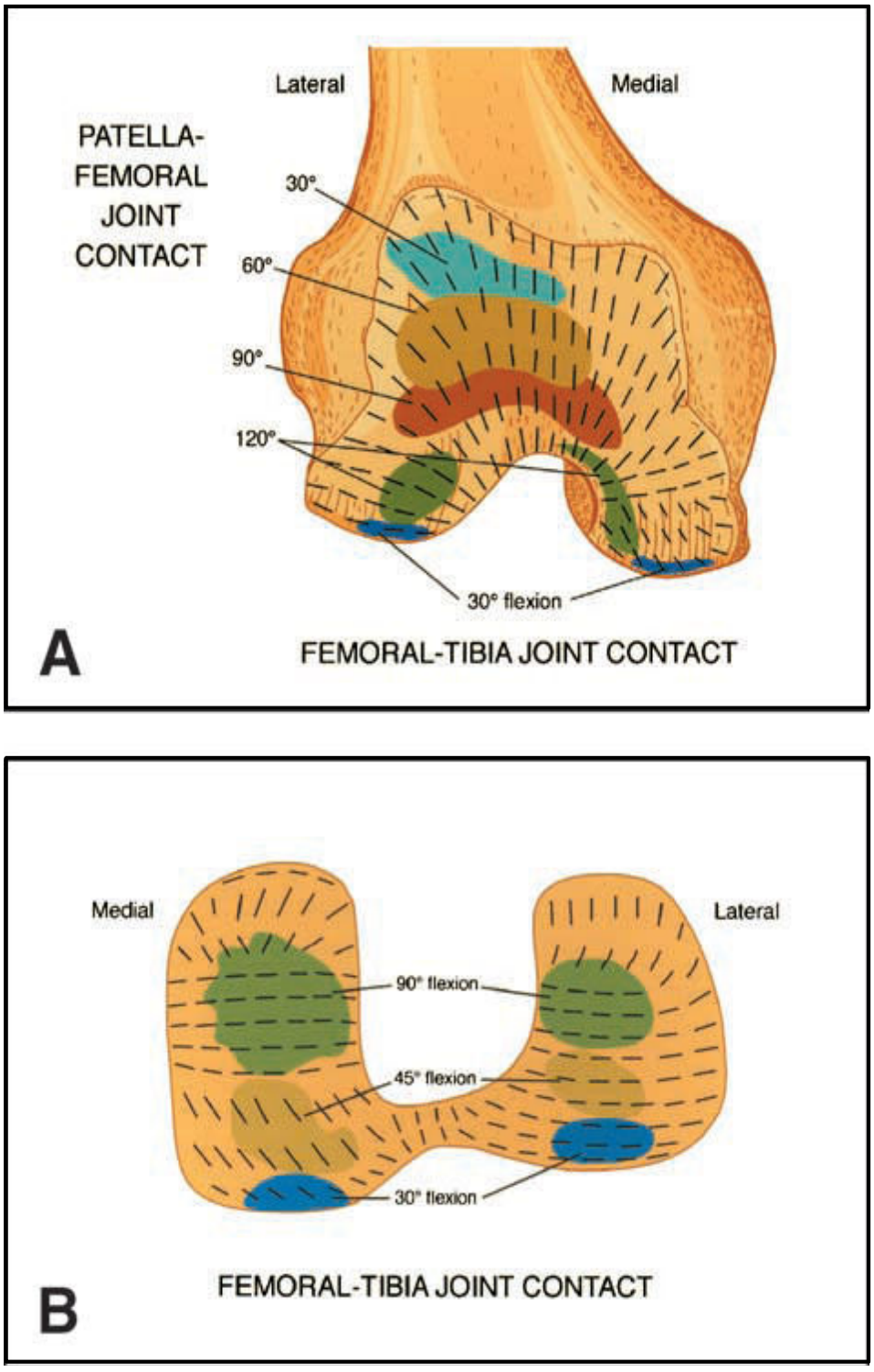

Figure 2-3: Schematic drawings representing the generic split-line pattern of the distal femur and the areas of joint contact. (A) Anterior-inferior view and (B) posterior view. (Below et al. 2002).

With this dense specialized matrix, cyclical compressive loading at physiologic frequencies (0.1-2 Hz) causes the interstitial fluid pressure to increase (Lee et al. 1981), resulting in a higher dynamic modulus than equilibrium modulus (Park et al. 2004). This is enhanced by the disparity between the tensile and compressive moduli (Cohen et al. 1998; Soulhat et al. 1999; Bursac et al. 2000; Soltz et al. 2000; Huang et al. 2001; Li et al. 2003). In addition to these factors, the dynamic compressive modulus is also dependent on the collagen content and tensile properties of the tissue (Huang et al. 2001; Park et al. 2004; Park et al. 2006). Treatment with collagenase results in marked reduction of the dynamic compressive modulus of cartilage explants (Toyras et al. 1999; Laasanen et al. 2003; Park et al. 2008). With contact loading, the enhanced fluid pressurization at the point of contact supports >90% of applied stress, shielding the solid matrix from excess deformation (Soltz et al. 1998; Soltz et al. 2000). Remarkably, with its high contact stresses, cartilage thickness *in vivo* changes by <6-20% with use (Armstrong et al. 1979; Macirowski et al. 1994; Eckstein et al. 1998; Wayne et al. 1998). This mechanical interplay between the solid and fluid components of cartilage has been defined by sophisticated biphasic and poroelastic models (Soltz et al. 2000; Li et al. 2003). It is precisely this combination of tensile and compressive properties, promoting fluid pressurization, which enables cartilage mechanical function and must be recapitulated in any successful repair.

2.2.2 Articular Cartilage: Formation and Maturation

While the current understanding of articular cartilage structure and function is fairly extensive, the mechanism by which cartilage develops these properties is less clear. It is

also unclear how articular chondrocytes acquire and maintain their characteristic phenotype during embryogenesis. A better understanding of these developmental processes is important from a tissue engineering standpoint as it would allow researchers to more effectively engineer replacement tissues with a stable phenotype. The first appearance of a cartilage-like tissue (dense organization of PG and type II collagen) is in the limb bud (Gilbert 2000). Limb bud cells aggregate and undergo chondrogenesis under a complex array of morphogenetic and transcription factors, and other signaling cues (Gilbert 2000). While this material is 'cartilage', it is transient in nature, and much of it is eventually replaced through endochondral ossification (Zhou et al. 2000; Jimenez et al. 2001; Malemud 2006). Articular chondrocytes however, escape hypertrophy and ossification, and acquire permanent phenotypic traits that allow them to maintain and remodel cartilage throughout a lifetime of use. The origin of these cells and the factors directing the development of their unique phenotype are only beginning to be elucidated. The formation of articular joints (a process known as cavitation) begins with the interruption of the cartilage template (the anlagen) within the limb bud by a specialized layer called the interzone. This specialization is directed by a host of molecular factors, including GDF-5, Wnt-4, ERG and PTHrP. Wnt-4 is a soluble factor expressed early in the developing joint, and may be an important molecule in determination of the interzone site. GDF-5 is a member of the BMP family and appears to play many roles during joint development, including cavitation and joint patterning. PTHrP is expressed in cartilage cells from the embryonic stage through adulthood, and may maintain the articular cartilage phenotype (O'Keefe et al. 1997; Iwamoto et al. 2007). While the precise sequence of events has yet to be definitively mapped, at least a portion of the interzone

appears to be populated by invading cells from the anlagen periphery (Hyde et al. 2008; Koyama et al. 2008). Cells within the interzone differentiate into all of the fibrous joint structures, and occupy at least the superficial and middle zones of the eventual permanent articular cartilage. In addition to biological factors, mechanical forces are essential for articular joint formation (Mitrovic 1982; Persson 1983). For example, inhibitors of muscle contraction *in ovo* lead to incomplete joint formation and decreased properties (Mikic et al. 2000; Pitsillides 2003; Mikic et al. 2004; Kahn et al. 2009). Many signaling factors, including PTHrP (Chen et al. 2008), are themselves modulated by mechanical factors, suggesting that the promotion and maintenance of the chondrocyte phenotype is a highly regulated process in development.

After birth, articular cartilage undergoes dramatic maturational changes that results in an adult tissue with unique load-bearing capacity. Collagen fiber organization within the tissue is transformed from an isotropic arrangement to a mature configuration with superficial fibers arranged into split lines parallel to the surface (**Figure 2-4**) (Archer et al. 2003).

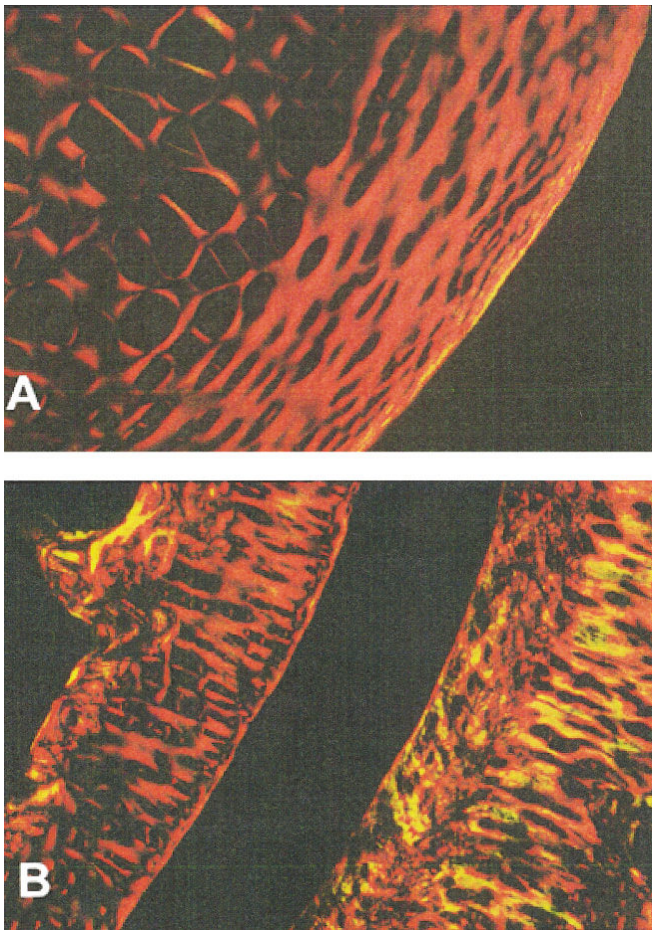

Figure 2-4. Articular cartilage from (A) 2- and (B) 8-month-old animals stained with picrosirius red and viewed under polarizing light. While the arrangement of collagen fibers in the younger animal lie predominantly parallel to the articular surface, the fibers are perpendicular to the cartilage surface in the older animal, indicative of extensive matrix remodeling with cartilage growth (Archer et al. 2003).

Compared to the initial anlagen formation, less is known about the cells in the articulating cartilage, and the signaling events that define their maturation. Unlike cells within other skeletal structures, articulating cartilage cells never undergo hypertrophy. Pacifici and co-workers recently reviewed the extant literature on these articular chondrocytes, and concluded that articular cells that retain a permanent cartilage phenotype are distinguishable from the transient chondrocytes that form the initial anlagen and growth plate (Pacifici et al. 2005). While these different cell types likely

share some signaling mechanisms, it is not yet clear whether these factors act in the same fashion. Nevertheless, what is clear is that the maturation of cartilage results in dramatic increases in tissue mechanics (particularly tensile properties) (Kempson 1982; Kempson 1991; Athanasiou et al. 2000). In mice, MMPs-2,-3, and -9 are absent at birth and peak 2 weeks later, suggesting intense early ECM remodeling (Gepstein et al. 2002; Gepstein et al. 2003). In the cow, mechanical and biochemical properties increase rapidly in juvenile compared to fetal cartilages (Williamson et al. 2001; Williamson et al. 2003), with increases in tensile properties correlated to increases in collagen content and cross-linking. At the same time, tissue cellularity decreases markedly, from 120 million cells/mL in fetal calf tissue to 50 million cells/mL in adult tissues (Jadin et al. 2005). When embryonic and juvenile bovine cartilage explants are removed from the joint environment, tensile properties decrease (Williamson et al. 2003). While one cannot overstate the importance of biologic factors in the *in situ* milieu, these findings also suggest that the demands placed on cartilage, coincident with use, help define organization and properties (e.g., collagen split lines, **Figure 2-2**), allowing the tissue to achieve its mature load bearing capacity.

Thus, a developmental cascade of events, from formation in the embryo through maturation in the adult, results in the unique properties of the native tissue – incorporation of this understanding, and application of these principles may aid in the generation of functional engineered cartilage constructs.

2.3 Cartilage Tissue Engineering

As cartilage healing is limited, there exists a growing demand for cell-based strategies for cartilage repair. A now standard tissue engineering approach consists of a chondrocytic cell type encapsulated in or seeded on a three-dimensional (3D) biomaterial support. Chondrocytes are a well-characterized and useful cell type for these applications, as they readily produce a cartilage-like matrix composed of PGs and collagens *in vitro* in a number of supportive media and material conditions.

2.3.1 Biomaterials for Cartilage Tissue Engineering

A number of materials have been employed in cartilage tissue engineering, including porous scaffolds (foams and fibrous meshes) fabricated from poly(α-hydroxy esters) including poly(glycolic acid), poly(lactic acid), and their copolymers (Puelacher et al. 1994; Vunjak-Novakovic et al. 1999; Davisson et al. 2002; Rotter et al. 2002; Schaefer et al. 2002). Foams and meshes based on natural materials (types I and II collagen, PG/collagen composites) support cartilage growth as well (Nehrer et al. 1997; Yates et al. 2005). Chondrocytes cultured on these porous scaffolds form ECM and increased mechanics with culture. However, uniform seeding throughout the scaffold expanse is a challenge; cells flatten and line the pore spaces, collagen contents remain lower than native tissue, and directionality of formed matrix has not been achieved. Alternatively, hydrogels are attractive biomaterials for cartilage regeneration and many natural (e.g., collagen and alginate) and synthetic polymers (e.g., Pluronics) have been investigated. Specific examples in the literature include alginate (Hauselmann et al. 1994; Paige et al. 1995; Rowley et al. 1999), agarose (Mauck et al. 2002; Mauck et al. 2003), fibrin

(Brittberg et al. 1997; Nixon et al. 1999), types I and II collagen (Kawamura et al. 1998; Hunter et al. 2002), peptide gels (Kisiday et al. 2002), and poly(ethylene glycol) (PEG) (Bryant et al. 2001; Burdick et al. 2001; Elisseeff et al. 2002), to list but a few. This focus on hydrogels is motivated by the observation that in hydrogel culture, chondrocytes can be well dispersed and cells may assume their natural round shape and phenotype. This shape is particularly important, as it has long been demonstrated that de-differentiated chondrocytes can regain their cartilage ECM producing capacity when seeded in even simple hydrogels (Benya et al. 1982). Furthermore, these gels efficiently entrap the cartilage-like ECM produced by the cells (Benya et al. 1982; Buschmann et al. 1992), and can rapidly assemble a neo-cartilage matrix with functional properties. Combinations of gels and fibrous structures might be particularly valuable, as demonstrated in work by Moutos and co-workers developing a cell-laden gel-infused fiber scaffold using advanced weaving technologies (**Figure 2-5**) (Moutos et al. 2007).

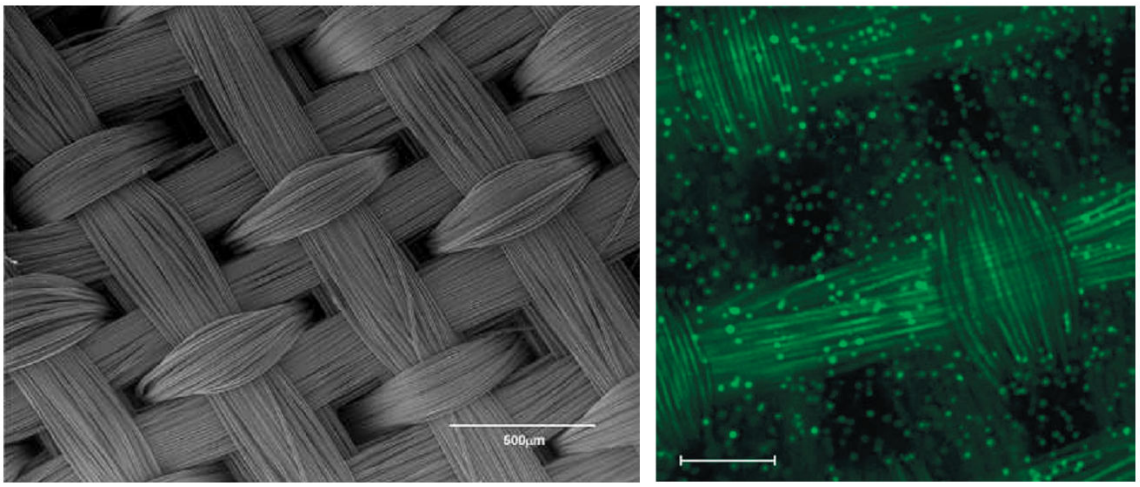

Figure 2-5: (Left) Fiber architecture of a 3D orthogonally woven structure. (Right) Fluorescent image of a freshly seeded construct. Porcine articular chondrocytes in a fiber-reinforced 2% agarose (small pore scaffold) show a spatially uniform initial distribution of cells with rounded morphology (fluorescent labeling with calcein-AM) (Moutos et al. 2007).

Recent focus has also turned to highly functionalized hydrogels, including photopolymerizable networks that can be optimally modified to elicit specific cell responses *in vivo* and *in vitro*. Elisseeff *et al.* first used a transdermally polymerized hydrogel formed from dimethacrylated poly(ethylene oxide) and semi-interpenetrating linear poly(ethylene oxide) chains (Elisseeff et al. 2001). This work illustrated both the ability to photoencapsulate viable chondrocytes in a hydrogel network with light transmitted through dermal tissue and the production of neocartilage with both PG and collagen present. Bryant and Anseth later showed that photocrosslinked scaffolds could be fabricated that span the thickness of native cartilage found *in vivo* while maintaining PG production (Bryant et al. 2001). More recently, chemically and photocrosslinked natural materials such as elastin like protein (ELP) and hyaluronic acid (HA) have been employed in the formation of chondrocyte-seeded hydrogels (Betre et al. 2002; Nettles et al. 2004; Burdick et al. 2005; Chung et al. 2008). A number of investigators have examined how changes in hydrogel properties (e.g., crosslinking density) influence the synthesis and distribution of collagen and PGs by encapsulated chondrocytes (Bryant et al. 1999; Bryant et al. 2004; Bryant et al. 2004). This work generally showed that higher crosslinking densities limit matrix distribution. To hasten matrix distribution, dynamic hydrogels have been developed that either incorporate degradable linkages or have enzymatic treatment methods applied to cell-seeded constructs during maturation. For example, agarase (which degrades agarose) has been applied to remove the remnants of this gel from the neo-tissue (Ng et al. 2009). Others have engineered the hydrogel itself via the inclusion of hydrolytically degradable linkages in synthetic PEG gels; findings from this work show a markedly greater level of collagen deposition and distribution by

chondrocytes seeded within (Bryant et al. 2003). Other gels have been designed with MMP-cleavable linkages and backbones, such that remodeling of a synthetic matrix can occur by natural, cell-mediated mechanisms (Lutolf et al. 2005). For example, an MMP-sensitive PEG based gel developed by Lutolf (Lutolf et al. 2003) was used to encapsulate bovine chondrocytes (Park et al. 2004). This study showed a greater distribution of formed matrix in gels with MMP-sensitive linkages, as well as greater expression of aggrecan and type II collagen. From this body of work it is clear that a cell encapsulating material can be appropriately designed to promote maximum levels of matrix formation, as well as eventually be removed to further ECM distribution throughout the construct.

2.3.2 Functional Cartilage Tissue Engineering

Simply supporting matrix formation is sufficient for enabling cartilage-like tissue formation, but absent other cues, this tissue does not typically develop into a tissue construct with native tissue properties. Articular cartilage exists in a mechanically challenging environment, and this environment is critical in the development of mechanical properties, as the dynamic environment guides new tissue formation. Drawing on this concept, the primary goal of functional tissue engineering is to recapitulate critical structural and mechanical benchmarks necessary to restore function in the joint (Butler et al. 2000). This approach incorporates our understanding of the mechanical signals that arise in the tissue microenvironment (Guilak et al. 1997), and then uses these signals to inform *in vitro* culture conditions to better direct tissue growth and modulate cell behavior. To that end, bioreactors that provide an appropriate mechanical environment for constructs are an important element in tissue engineering.

Constructs can be cultured in the presence of mechanical signals, including hydrostatic pressurization (e.g., (Smith et al. 1996)), fluid flow (e.g., (Gemmiti et al. 2006)), or direct mechanical stimulation through mechanical compression (e.g., (Mauck et al. 2000; Mauck et al. 2002; Mauck et al. 2003; Hung et al. 2004)). Since mechanical stimulation plays a crucial role in the native environment of cartilage, mechanical preconditioning may be an especially suitable strategy for engineering cartilage (Hung et al. 2004). Studies in hydrogels have shown that biosynthesis of collagen and proteoglycans are up-regulated with compressive loading (Buschmann et al. 1995) and are modulated by amplitude, frequency and loading duration (Shieh et al. 2003; Waldman et al. 2003). In chondrocyte-based constructs, long-term application of dynamic compression enhances both the mechanical properties and biochemical content of loaded gels (Mauck et al. 2000). To date, however, the collagen content of engineered constructs remain well below native values; failure of constructs to achieve the dynamic compressive properties and tensile properties found in cartilage can be attributed to this lack in collagen content and organization (Riesle et al. 1998).

2.3.3 New Media Formulations for Cartilage Tissue Engineering

In addition to mechanical loading, a number of other optimization strategies have been employed to improve engineered cartilage formation. Several studies have shown that increasing the initial cell number within the construct can lead to more rapid and/or greater cartilage-ECM formation and mechanics (Puelacher et al. 1994; Vunjak-Novakovic et al. 1998; Chang et al. 2001; Mauck et al. 2002; Mauck et al. 2003). Increased levels of nutrient supplementation can likewise increase growth rates (Mauck

et al. 2003). Specific inclusion of anabolic growth factors normally found in the maturing and mature synovial fluid (such as IGF-1, TGF-β family members, and FGF) can further improve cartilage-like tissue development in engineered constructs (Gooch et al. 2001; Blunk et al. 2002; Gooch et al. 2002; Pei et al. 2002; Mauck et al. 2003). In a series of recent studies we have shown that such approaches can lead to rapid and robust growth. Specifically, transient (rather than continuous) application of TGF-β3 in a serum-free, chemically defined medium dramatically enhances the compressive properties and GAG content of chondrocyte-laden hydrogels to near-native levels (Lima et al. 2007; Byers et al. 2008). In these studies, after removal of the growth factor, constructs undergo an explosive growth phase, and reach equilibrium compressive moduli of ~0.8 MPa and proteoglycan levels of 6-7% wet weight in less than 2 months of culture (**Figure 2-6**). These findings have particular implications for clinical use, as the media used for culture does not contain poorly characterized and potentially immunogenic serum elements, and induction is superior when growth factor is discontinued, as would be the case when such constructs are implanted *in vivo*. While promising, however, it should be noted that both collagen content and dynamic modulus of such constructs remains well below that of native tissue, suggesting that further optimization will be required to achieve full functionality. Towards that end, we applied dynamic loading to these constructs and showed that in the presence of TGF-β3, loading reduced the mechanical properties of chondrocyte-seeded constructs relative to free-swelling controls. In contrast, sequential application of TGF-β3 followed by dynamic compression (after removal of TGF-β3) significantly enhanced mechanical properties, with constructs reaching a compressive moduli in excess of 1 MPa. These findings

indicate that the biologic and mechanical environments are highly interactive, and that optimization of growth can be tuned to the current state of the microenvironment.

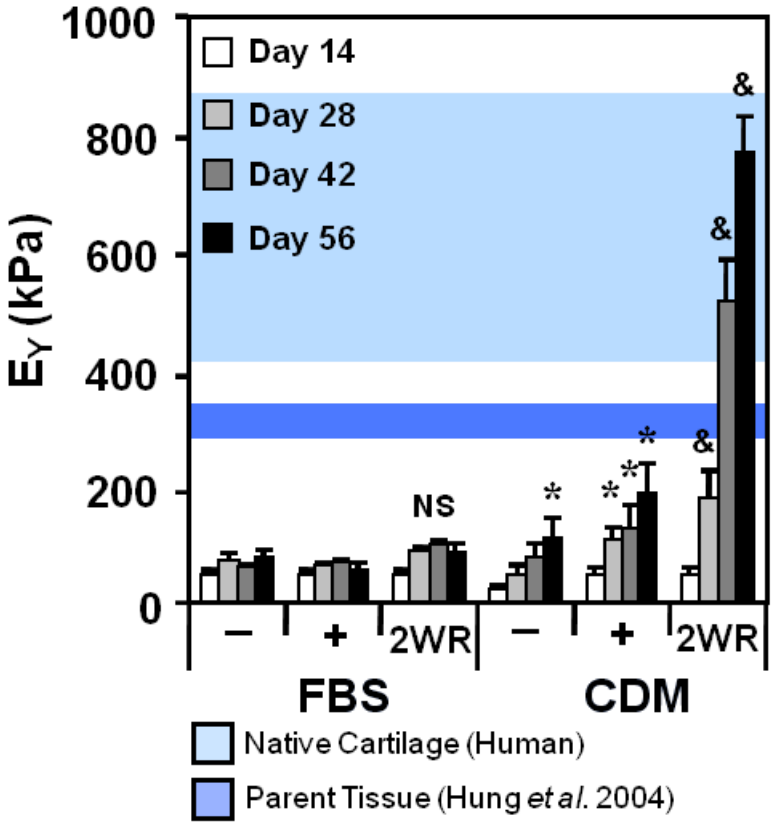

Figure 2-6: Equilibrium unconfined compressive modulus of chondrocyte-seeded constructs maintained in serum-containing (FBS) or chemically defined (CDM) media supplemented continuously with (+), transiently with (2WR), or in the absence of (-) 10 ng/mL TGF-β3. Data represent mean and standard deviation of 8-22 samples from two to five replicate studies. * indicates significant difference versus day 14, & indicates significant difference from all other time-matched samples, p<0.05 (Byers et al. 2008).

2.4 Cartilage Tissue Engineering with Mesenchymal Stem Cells

Despite these successes in cartilage tissue engineering with primary cells, limitations in chondrocyte availability and donor site morbidity may preclude their use in clinical applications. Therefore, over the last decade, there has been increasing interest in mesenchymal stem cells (MSCs) as an alternative cell type for cartilage engineering.

2.4.1 Mesenchymal Stem Cell Isolation and Chondrogenesis

MSCs are a self-renewing and multi-potent cell type with great potential for cell-based regenerative therapies. In the original descriptions of MSC multi-potentiality, MSCs were induced toward bone, fat, and cartilage phenotypes (Prockop 1997; Pittenger et al. 1999), and these assays remain the accepted metric for characterization of these cells. Although there is no definitive marker for MSC selection, hematopoietic surface antigens (i.e., CD45, CD34 and CD14) are not present on MSCs (Pittenger et al. 1999). Because there is no single defining surface marker for MSC identification, cell selection through plastic adhesion and colony formation is widely utilized. As a result, the starting population of cells may include a heterogeneous mixture of MSCs and other cells. MSCs can be readily isolated from a wide variety of tissue sources; while bone marrow is a common source of MSCs, these cells (and cells with similar multi-lineage capacity) have been derived from adipose tissue (Erickson et al. 2002), periosteum (Choi et al. 2008), synovium (Sakaguchi et al. 2005), and trabecular bone chips (Noth et al. 2002). In standard assays of MSC chondrogenesis, cells are collected into high-density pellets to induce a rounded morphology (mimicking mesenchymal condensation in the limb bud). Indeed, in some ways, these cells possess a similar capacity as limb bud mesenchyme cells, as they can form both bone and cartilage. It should be noted that these two cell types are distinct; while limb bud cells transit through cartilage and on to an osteogenic lineage *in vitro* in micromass culture without specific additives, adult MSCs must be treated with specific biofactors to take on a cartilage phenotype. Common chondrogenic media formulations for MSCs include TGF-β superfamily members and dexamethasone presented in a chemically defined serum-free medium (Caplan 1991; Prockop 1997;

Johnstone et al. 1998; Pittenger et al. 1999). Under these conditions, MSCs synthesize a cartilage-specific ECM rich in sulfated GAGs and type II collagen and express cartilage markers, including the transcription factor sox 9. In addition to their chondrogenic potential, there is also evidence suggesting that MSCs are nonimmunogenic or hypoimmunogenic, which may be useful for therapeutic applications (Barry et al. 2005).

2.4.2 Mechanical Properties of MSC-Based Engineered Constructs

As noted above, MSCs are a particularly ideal cell source for cartilage tissue engineering. Since the early descriptions of chondrogenesis in 3D cell pellet culture (Prockop 1997; Johnstone et al. 1998; Pittenger et al. 1999), the ability of these cells to generate cartilage-like tissues has been widely investigated. Indeed, a number of studies have demonstrated that, when presented with a chemically defined media including TGF/BMP family members, MSC chondrogenesis occurs in scaffolding materials previously employed for chondrocyte-based cartilage tissue engineering (**Table 2-1**). However, viability of MSCs in these materials is sometimes less robust than with chondrocytes (Salinas et al. 2007). Further material modifications, including covalent linking of matrix adhesion moieties (e.g., RGD and collagen mimetic peptides) can modulate both the viability of MSCs in these materials, as well as their phenotypic conversion (Connelly et al. 2007; Lee et al. 2008). In most studies, the shift of MSCs towards the chondrogenic phenotype is demonstrated via the induction of a relatively small set of phenotypic markers. Most commonly, these include expression of major ECM components specific to hyaline cartilage, including aggrecan and type II collagen. These molecules play a central role in the establishment of the mechanical function of the native tissue.

However, a host of other less prevalent matrix elements (including COMP, link protein, collagen type IX to name but a few) also play critical roles in matrix organization and retention, and are occasionally monitored during chondrogenesis as well. These 'minor' ECM components engender significant deficits in cartilage function and/or durability when absent from the tissue in disease or knockout animal models (Hu et al. 2006).

While these markers are appropriate evidence that a chondrogenic event has occurred, they do not necessarily correlate with mechanical function. For clinical translation, and demonstration of efficacy, the mechanical properties of engineered constructs will ultimately dictate in vivo success. However, few studies of MSC chondrogenesis have considered this critical metric. Those few studies that have measured mechanical properties suggest a puzzling scenario. That is, while most markers of the 'chondrocyte' phenotype are expressed (in some cases, to a greater extent than chondrocytes) the mechanical properties of constructs populated by these cells are typically inferior to both native tissue and to comparable tissue engineered constructs formed by fully differentiated chondrocytes. Where available, the mechanical properties of engineered MSC-based cartilage are provided in **Table 2-1**.

Table 2-1: Examples of engineered cartilage derived from MSCs and other progenitor cell sources

BIOMATERIAL	CELL SOURCES	OUTCOME ASSAYS	MECHANICAL PROPERTIES	REFERENCE
Alginate	Human, bone marrow derived	Gene expression, histology, SEM, GAG content	NA	(Wang et al. 2009)
	Human	Gene expression	NA	(Xu et al. 2008)
Alginate (RGD-modified)	Bovine, bone marrow derived	Gene expression, biochemical analysis	NA	(Connelly et al. 2007)
Agarose	Bovine, bone marrow derived	Biochemical analysis, histology, compressive properties	Eq. modulus: 48 kPa Dyn. Modulus: 800 kPa	(Mauck et al. 2006)
	Bovine, bone marrow derived	Biochemical analysis, histology, tensile properties	Tensile modulus: 363 kPa Toughness: 420 kPa Ultimate Strain: 63%	(Huang et al. 2008)
Chitosan scaffold	Human, bone marrow and adipose derived	Gene expression, histology, SEM	NA	(Seda Tigli et al. 2009)
Collagen type I	Human, bone marrow derived	Gene expression, biochemical analysis, histology	NA	(Dickhut et al. 2008)
Collagen type II	Human, bone marrow derived	Histology	NA	(Chang et al. 2007)
Fibrin	Human, bone marrow derived	Gene expression, biochemical analysis, histology	NA	(Dickhut et al. 2008)
	Human, bone marrow derived	Gene expression, proliferation	NA	(Pelaez et al. 2008)
Gelatin	Human, bone marrow derived	Histology, biochemical analysis	NA	(Ponticiello et al. 2000)
	Human, adipose derived	Biochemical analysis, histology, compressive and shear properties	Eq. compressive modulus: ~15 kPa Eq. shear modulus: ~4 kPa Complex shear modulus: ~6 kPa	(Awad et al. 2004)
Hyaluronic Acid	Bovine, bone marrow derived	Biochemical content, compressive properties	Eq. Modulus: 60 kPa Dyn. Modulus: 40 kPa	(Erickson et al. 2009)
	Human, bone marrow derived	Gene expression, biochemical analysis, histology, compressive properties	Eq. modulus: 50-60 kPa	(Chung et al. 2009)
	Human, bone marrow derived	Gene expression, biochemical analysis, histology, immunohistochemistry	NA	(Nesti et al. 2008)
Matrigel	Human, bone marrow derived	Gene expression, biochemical analysis, histology	NA	(Dickhut et al. 2008)

BIOMATERIAL	CELL SOURCES	OUTCOME ASSAYS	MECHANICAL PROPERTIES	REFERENCE
oligo(poly(ethylene glycol)fumarate) (OPF) scaffolds	Rabbit, bone marrow derived	Gene expression, confocal microscopy	NA	(Park et al. 2009)
poly(ε-caprolactone) (PCL) nanofiber scaffolds	Human, bone marrow derived	Gene expression, biochemical analysis, histology, SEM	NA	(Li et al. 2005)
poly(ethylene glycol) (PEG)	Human, bone marrow derived	Gene expression, immunohistochemistry	NA	(Chung et al. 2009)
	Human, bone marrow derived	Biochemical analysis, histology, immunohistochemistry	NA	(Buxton et al. 2007)
Poly(ethylene oxide) diacrylate (PEODA) with collagen mimetic peptides	Goat, bone marrow derived	Gene expression, biochemical analysis, histology	NA	(Lee et al. 2008)
Polyglycolic acid (PGA)	Rabbit, bone marrow derived	Histology, immunohistochemistry	NA	(Zhou et al. 2008)
poly lactic-co-glycolic acid (PLGA) scaffold	Rabbit, bone marrow derived	Histology, biochemical analysis	NA	(Zhang et al. 2009)
poly(l-lactic acid) (PLLA) nanofiber scaffolds	Human, bone marrow derived	Gene expression, histology, compressive properties	Eq. Modulus: 12 kPa	(Janjanin et al. 2008)
Puramatrix	Bovine, bone marrow derived	Biochemical analysis, compressive properties	Eq. Modulus: 80 kPa Dyn. Modulus: 120 kPa	(Erickson et al. 2009)
Silk fibroin scaffold	Human, bone marrow derived	Gene expression, biochemical analysis, histology, compressive properties	Aggregate modulus: 40 kPa	(Hofmann et al. 2006)
	Human, bone marrow and adipose derived	Biochemical analysis, histology	NA	(Seda Tigli et al. 2009)

While somewhat limited in number, these studies do show that the compressive properties of MSC-based constructs increase with culture duration, and do so in a number of materials, including hydrogels, non-woven meshes, and porous foams (Awad et al. 2004). For example, **Figure 2-7** shows the time course of accumulation of mechanical and biochemical properties of constructs formed from bovine MSCs embedded within agarose, self-assembling peptide, and photocrosslinked hyaluronic acid hydrogels. These

properties increase substantially over the 8 weeks of *in vitro* culture, with robust deposition of proteoglycan evident in histological sections (Erickson et al. 2009).

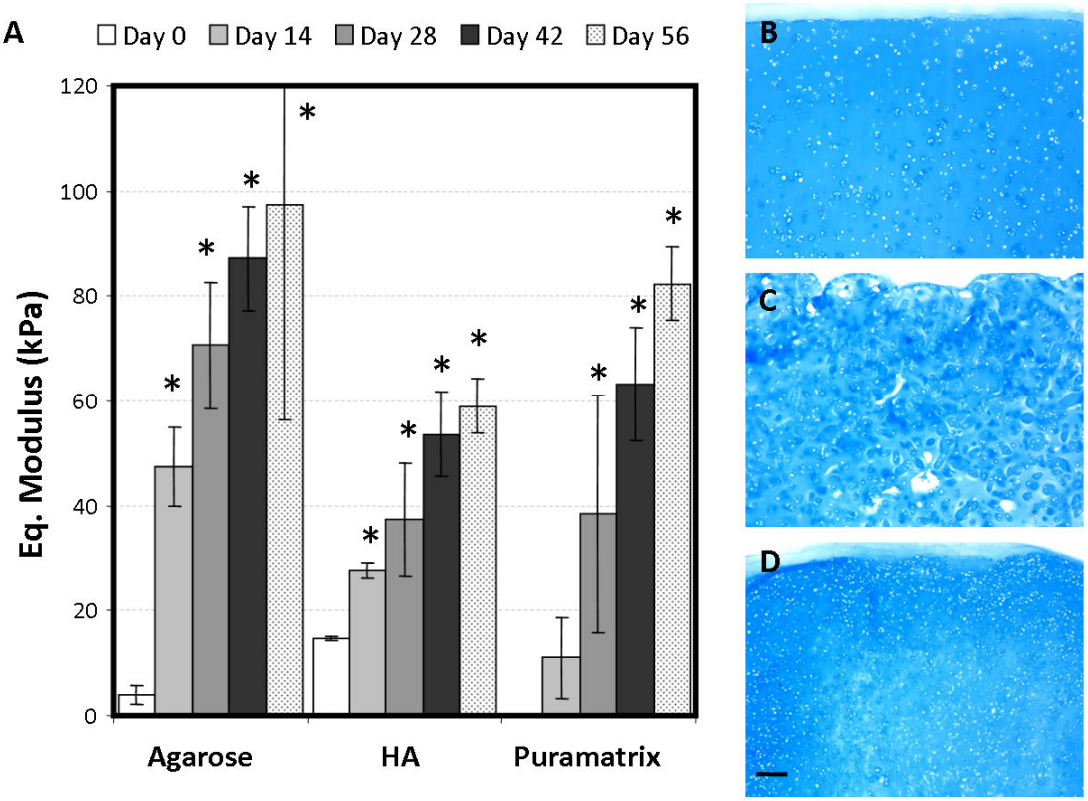

Figure 2-7: (A) Equilibrium compressive modulus of MSC-seeded agarose, photo-crosslinked hyaluronic acid (HA), and self-assembling Puramatrix hydrogels (20 million cells/mL) after long-term culture in a chemically defined media containing 10 ng/mL TGF-β3. Data represent the mean and standard deviation of 3-4 samples per time point; * indicates $p<0.05$ versus Day 0. (B-D) Alcian blue staining demonstrates robust proteoglycan deposition in agarose (B), HA (C) and Puramatrix (D) hydrogels on day 56. Scale Bar: 100 μm (Erickson et al. 2009).

More recent studies have shown that human MSCs in a natural ECM-derived material can reach a compressive modulus of ~0.15 MPa, and that bovine MSCs in agarose can reach a modulus of ~0.2 MPa with proteoglycan contents approaching 2-3% of the wet weight (Cheng et al. 2008; Huang et al. 2009). These values are significant when viewed in the context of chondrocyte-based tissue engineering efforts using serum containing media, but are deficient when compared to the properties of chondrocyte-based constructs

cultured identically in pro-chondrogenic chemically defined, growth factor supplemented media. For example, chondrocytes in agarose with transient exposure to TGF-β3 regularly achieve native tissue levels of compressive moduli (on the order of 0.7-1.0 MPa) and proteoglycan content (5-6%) (Lima et al. 2007; Byers et al. 2008). These data support the growing appreciation that the functional capacity of MSCs has yet to be fully realized.

2.4.3 Mechanical Preconditioning of MSC-Based Cartilage Constructs

To improve the functional outcome of MSC-based constructs and better instill the phenotypic traits associated with articular cartilage, one potential strategy for optimization is direct mechanical stimulation. Mechanical stimulation methods have been widely employed in chondrocyte-based cartilage tissue engineering, with many studies showing improvements in mechanical properties and biochemical composition when the loading conditions are appropriately tuned (Mauck et al. 2000; Connelly et al. 2004; Kisiday et al. 2004; Grad et al. 2005; De Croos et al. 2006; Hu et al. 2006; Appelman et al. 2009). The rationale for taking a similar approach for MSC-based constructs is easily identified from the crucial role mechanical forces play during normal joint development. For example, inhibition of muscle forces results in incomplete formation of the joint and mechanical signals modulate the expression of important molecular factors, such as PTHrP, which may regulate the phenotypic state of mesenchymal cells during development (Vortkamp et al. 1996; Mikic et al. 2000; Mikic et al. 2004; Chen et al. 2008). In addition, mechanical regulation remains important after birth, as cartilage undergoes additional remodeling and mechanical maturation with load-

bearing use (Williamson et al. 2003; Williamson et al. 2003) and the maintenance of healthy cartilage and the retention of the chondrogenic phenotype in normal articular chondrocytes is dependent on mechanical loading (Chen et al. 2008). Further, compressive loading of chick limb-bud mesenchyme cells (a distinct but related cell type to MSCs) in agarose enhances chondrogenesis; this response is modulated by both the frequency and duration of the applied load (Elder et al. 2000; Elder et al. 2001).

Taken together, these findings form the basis for mechanical preconditioning of MSC-based constructs for cartilage tissue engineering applications, and indeed, results from several studies indicate that MSCs are responsive to mechanical loading. For example, hydrostatic pressurization, an indirect loading modality, enhances the expression of chondrogenic genes in MSC pellets and MSC-seeded constructs (Angele et al. 2003; Miyanishi et al. 2006; Finger et al. 2007; Wagner et al. 2008). More direct modes of mechanical perturbation, both in compression and tension, have also been examined, however, the effects of these loading modalities on MSC chondrogenesis and the development of functional properties remains unclear. Early studies of MSC mechanotransduction have focused on short-term application of load and limited outcome measures to gene expression and matrix synthesis. In one of the first studies examining the relationship between mechanical stimulation and MSC differentiation, Huang and co-workers applied dynamic compression to MSC-seeded agarose and induced several transcription factors known to mediate TGF-β signaling, including sox 9, AP-1 and c-Jun (Huang et al. 2005). When MSC-seeded porous hyaluronan-gelatin constructs were subjected to compressive loading, the expression levels of chondrogenic genes were

upregulated relative to non-loaded controls (Angele et al. 2004). In another study, short-term loading of MSC-laden agarose cultures in the absence of TGF-β increased aggrecan promoter activity, but decreased collagen type II promoter activity (Mauck et al. 2007).

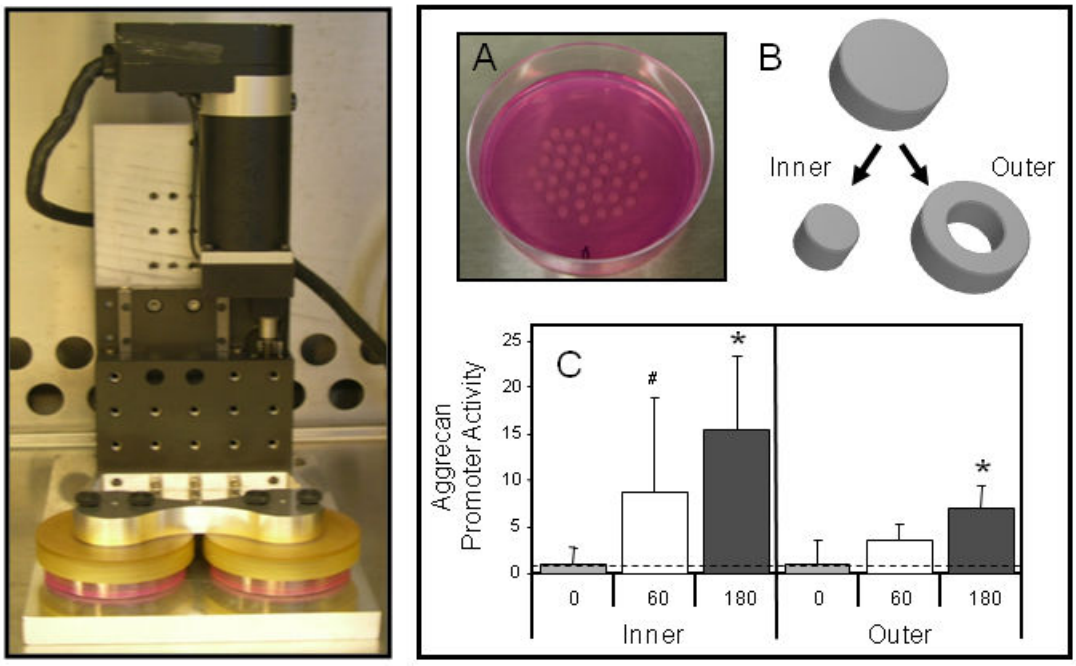

Figure 2-8: (A) Compression loading bioreactor for mechanical stimulation of cell-seeded hydrogel constructs. (B) MSC-seeded agarose disks in prepared mold for dynamic loading. (C) Schematic of agarose disk cored into inner and outer regions to determine region-specific gene expression responses with dynamic loading. (D) Aggrecan promoter activity in the inner and outer regions of MSC-seeded constructs after 0, 60 and 180 minutes of dynamic compressive loading. # indicates p<0.1 versus free-swelling, * indicates p<0.05 versus free swelling, n=7-8 per group (Mauck et al. 2007).

Consistent with this, Kisiday and colleagues recently demonstrated that 12 hours of continuous loading in the absence of TGF-β improved proteoglycan synthesis levels, though these values did not reach those attained with inclusion of TGF-β under free swelling conditions. In cultures loaded in the presence of TGF-β, matrix synthesis levels diminished (Kisiday et al. 2009). In these studies, application of load was initiated before elaboration of ECM, yet pre-culturing constructs before loading may also modulate cell properties. A single application of cyclic compression improved both collagen type II

and aggrecan expression when MSC-seeded agarose gels were pre-cultured in TGF-β1 containing media for 16 days; these effects were not observed with a pre-culture time of 8 days (Mouw et al. 2007). Under cyclic tension (10% strain, 1Hz), the rate of GAG synthesis was enhanced in MSCs seeded on collagen-GAG scaffolds (McMahon et al. 2008; McMahon et al. 2008), suggesting a positive role for cyclic tensile loading in chondrogenesis. However, tensile loading can also induce apoptosis of MSC-seeded silicon membranes at strains of 7.5% or greater (Kearney et al. 2008).

Collectively, these studies affirm that MSCs are mechanically sensitive and that MSC chondrogenesis can be modulated by mechanical stimulation. While these findings suggest that dynamic loading may be beneficial in inducing/enhancing chondrogenesis, and that the presence or absence of TGF-β may define this response, few studies have examined the effects of long-term loading or have assessed functional outcomes. One recent study showed that long-term mechanical compression impairs functional growth of MSC-based engineered constructs. When loaded daily for 42 days in TGF-β containing media, the compressive modulus and GAG content of MSC-seeded agarose constructs were considerably reduced compared to free-swelling controls (Thorpe et al. 2008). From this study, it appears that MSC and chondrocyte response to mechanical stimulation are not identical.

Although these studies indicate that long-term compressive loading may be detrimental to the development of functional properties in MSC-based constructs, a recent study by Teracciano and co-workers provides evidence that pre-differentiation of stem cells may

modulate the effects of compressive loading. In this study, embryonic stem cells embedded in a hydrogel environment responded adversely to applied load in the absence of TGF-β; however, after a period of chondrogenic induction, applied mechanical load elicited positive effects on cartilaginous gene expression (Terraciano et al. 2007). These findings suggest that the establishment of a chondrogenic phenotype prior to the initiation of loading may be a crucial determinant of MSC response. A more complete understanding of the mechanotransduction pathways occurring during loading will enable better tuning of the loading regimes applied to optimize functional outcomes.

CHAPTER 3: TRANSIENT EXPOSURE TO TGF-B3 IMPROVES THE MECHANICAL PROPERTIES OF MSC-LADEN CARTILAGE CONSTRUCTS IN A DENSITY DEPENDENT MANNER

3.1 Introduction

Articular cartilage lines the surfaces of joints and functions to absorb shock and distribute the forces arising from joint movement. This load-bearing role is enabled by a dense extracellular matrix (ECM) composed of proteoglycans and type II collagen (Muir 1980; Williamson et al. 2001; Ateshian et al. 2003), which are responsible for the unique mechanical properties of cartilage as described in Section 1. To date, few strategies exist for restoring damaged articular surfaces; therefore, cartilage tissue engineering (TE) has emerged as a means to generate replacement tissues (Hunziker 1999). To optimize growth and maturation of TE constructs, various methodologies have been employed, including three-dimensional (3D) culture in a wide range of biomaterials (Kisiday et al. 2002; Mouw et al. 2005; Ng et al. 2005; Li et al. 2006; Chung et al. 2008), coupled with mechanical stimulation (Grodzinsky et al. 2000; Mauck et al. 2003; Kisiday et al. 2004; Seidel et al. 2004) and growth factor supplementation (Blunk et al. 2002; Gooch et al. 2002). In addition to these strategies, variations in cell-seeding density and medium formulations have also been shown to have pronounced effects on the final properties accrued by engineered cartilage (Mauck et al. 2003; Kisiday et al. 2005; Williams et al. 2005).

While significant progress has been made with these chondrocyte-based approaches, the use of chondrocytes for cartilage TE may prove impractical, due to limitations in cell

availability and donor site morbidity. Therefore, recent efforts have utilized mesenchymal stem cells (MSCs), which readily undergo chondrogenesis when cultured in chemically defined media with TGF-β family members (Johnstone et al. 1998; Pittenger et al. 1999). While MSCs can generate cartilage-like ECM, it has also been shown that MSCs do not reach functional parity with donor-matched chondrocytes cultured under the same conditions. Our previous work suggests that MSCs, starting at the same seeding density, reach at best 50% of the compressive equilibrium properties of chondrocyte-seeded agarose constructs (Mauck et al. 2006). A number of studies have examined the effects of varying cell seeding density on MSC chondrogenesis; however in most studies, the seeding densities employed were low (less than 10 million cells/mL) relative to those used in cartilage TE with chondrocytes, and functional properties were not assayed (Ponticiello et al. 2000; Kavalkovich et al. 2002; Huang et al. 2004; Park et al. 2007; Huang et al. 2008; Hui et al. 2008). Cell-cell contact and/or communication is a recognized factor in the initiation of chondrogenesis in pellet cultures (Tuli et al. 2003), although the effect of variation in this parameter has yet to be investigated in the context of emerging mechanical properties of MSC-seeded 3D constructs.

In addition to cell density effects, recent studies have also shown that transient application of TGF-β3 in a serum-free, chemically defined medium enhances the compressive properties and GAG content of chondrocyte-laden hydrogels to near-native tissue levels (Lima et al. 2007; Byers et al. 2008). In those studies, after removal of the growth factor, constructs achieved equilibrium compressive moduli of ~0.8 MPa and proteoglycan levels of 6-7% wet weight in less than 2 months of culture. It is not yet

clear whether similar transient application of growth factor can accelerate the maturation of MSC-based constructs. Two recent studies using MSC-laden hydrogels indicate that this phenomenon may be operative for MSCs in 3D culture (Caterson et al. 2001; Mehlhorn et al. 2006). In one study by Mehlhorn et al, human MSCs in alginate beads synthesized lower amounts of aggrecan after transient application of TGF-β3 compared to constructs cultured continuously with TGF-β3 over a two week time course. However, the level of aggrecan accrued was still greater than that of control constructs and chondrogenic genes remained expressed, suggesting maintenance of the chondrocytic phenotype (Mehlhorn et al. 2006). Indeed, differentiated MSCs were resistant to subversion of the chondrogenic phenotype when challenged with osteogenic media. However, this study did not examine mechanical properties of the formed constructs. Caterson et al also observed a continued chondrogenic response by MSCs in alginate treated with a single pulse of TGF-β1 (50 ng/mL) for three days (Caterson et al. 2001). At 21 days of culture, treated constructs stained for proteoglycans and type II collagen, and continued to express aggrecan, type II and type IX collagens. Interestingly, constructs also briefly expressed osteocalcin at 14 days of culture.

Taken together, these studies indicate that a brief exposure to TGF-β may be sufficient to initiate and maintain chondrogenesis; however, the impact of this treatment on mechanical function was not investigated. It is also unknown whether transient application of TGF-β enhances MSC chondrogenesis and improves the development of functional properties of MSC-based constructs. While standard practice relies on continuous treatment with TGF-β, previous studies using chondrocyte-based constructs

suggest temporal exposure to this morphogen is more effective in generating tissue replacements with near-native properties. To date, the effects of transient TGF-β treatment has not been investigated in terms of mechanical properties of MSC-laden constructs. In addition, as TGF-β is known to suppress chondrocyte hypertrophy (Ballock et al. 1993), and can retard or abrogate osteogenic progression of MSCs in monolayer culture (Moioli et al. 2006; Moioli et al. 2007), it is also not clear whether removal of the growth factor will initiate mineralization or other hypertrophic changes in our stem cell populations.

To specifically address these questions, this study evaluated mechanical and biochemical properties in chondrocyte- and MSC-laden hydrogels with transient exposure of TGF-β3 in a chemically defined medium. In addition, we explored the effects of varying seeding density in MSC-laden constructs on resultant functional properties. We hypothesized that increasing seeding density would improve mechanical properties and biochemical content. We also hypothesized that transient application of TGF-β3 would improve functional properties of MSC-laden constructs, and that these changes would be marked by differences in cartilaginous gene expression.

3.2 Materials and Methods

3.2.1 Mesenchymal Stem Cell and Chondrocyte Isolation and Culture

Bone marrow derived MSCs were harvested from the carpal bones of 3-6 month old calves (Fresh Farms Beef, Rutland, VT and Research 87, Boylston, MA). Typically, six separate marrow isolations (minimum of three animals) were carried out. Trabecular

regions were removed with a saw and agitated in a solution of high glucose Dulbecco's Modified Eagle's Medium (DMEM) supplemented with 2% penicillin/streptomycin/Fungizone (PSF) and 300 U/mL of heparin. The resulting solution was centrifuged (5 min, 300×g) and plated into 10 cm tissue culture plates. Cultures were maintained in DMEM supplemented with 1% penicillin/streptomycin/fungizone (PSF) and 10% fetal bovine serum (FBS) changed twice weekly until confluence. Sub-culturing was carried out at a 1:3 ratio up to passage two. To isolate chondrocytes, cartilage pieces were harvested from the carpometacarpal joints of the same group of animals, rinsed in DMEM containing 2% PSF and 10% FBS, and incubated at 37°C in a humidified 5% CO_2 incubator for five days (one medium change) to ensure sterility. Pieces were then combined and digested sequentially with pronase and collagenase (Mauck et al. 2003). Chondrocyte suspensions were filtered (70μm cell strainer, BD Falcon, Bedford, MA), pelleted (5 min, 300×g), resuspended in DMEM, and viable cells counted. Chondrocytes were encapsulated immediately upon isolation.

3.2.2 Construct Fabrication and Long-Term 3D Culture

Primary chondrocytes or MSCs were suspended in a chemically defined medium (CM) and combined 1:1 with sterile type VII agarose (49°C, 4% w/v, Sigma, St Louis, MO) in phosphate buffered saline (PBS) at room temperature. CM consisted of DMEM supplemented with 1X PSF, 0.1 μM dexamethasone, 50 μg/mL ascorbate 2-phosphate, 40 μg/mL L-proline, 100 μg/mL sodium pyruvate, 1X ITS+ (6.25 μg/ml insulin, 6.25 μg/ml transferrin, 6.25 ng/ml selenous acid, 1.25 mg/ml bovine serum albumin, and 5.35 μg/ml

linoleic acid). Chondrocytes were seeded at a density of 20 million cells/mL and MSCs were seeded at either 20 or 60 million cells/mL. The resultant cell-agarose mixture was cast between parallel plates to create a 2.25 mm sheet and allowed to gel for 20 minutes at room temperature. After gelation, disks (Ø4 mm) were cored and cultured with continuous or transient TGF-β3 treatment in 1 mL of CM per construct. In the continuous treatment group, disks were cultured in CM supplemented with 10 ng/mL TGF-β3 (CM+, R&D Systems, Minneapolis, MN) for 7 weeks. In the transient TGF-β3 treatment group, disks were maintained in CM+ for the first 3 weeks and then cultured in CM without TGF-β3 for an additional 4 weeks. At 3, 5, and 7 weeks, constructs were evaluated for mechanical properties, biochemical content and gene expression. Constructs were measured with digital calipers at each time point to monitor dimensional stability. Each experiment was repeated at least once to confirm results with data from all samples pooled.

3.2.3 Mesenchymal Stem Cell Pellet Formation And Long-Term Culture

Pellets containing 250,000 MSCs per pellet were formed by centrifugation (5 min, 300×g) in 96-well polypropylene conical plates (Nalge Nunc International, Rochester, NY). Pellets were cultured with continuous or transient application of TGF-β3 as described above. At 3, 5, and 7 weeks, pellets were evaluated for sulfated glycosaminoglycans (GAG) and DNA content. Histological analysis was performed at 7 weeks.

3.2.4 Mechanical Testing of Engineered Constructs

A custom mechanical testing device was used to evaluate compressive properties of engineered constructs (Mauck et al. 2006). Disks were tested in unconfined compression

between two impermeable platens in a PBS bath. First, samples were equilibrated in creep under a static load of 2 grams for 5 minutes. After creep testing, samples were subjected to 10% strain (calculated from post-creep thickness values) applied at 0.05%/s followed by relaxation for 1000 seconds until equilibrium. Dynamic testing was performed by applying 1% sinusoidal deformation at 1.0 Hz. The equilibrium modulus was determined from the equilibrium stress (minus tare stress) normalized to the applied strain. The dynamic modulus was determined from the slope of dynamic stress-strain response. After mechanical testing, constructs were frozen at -20°C for biochemical evaluation.

3.2.5 Biochemical Analysis

To assess biochemical content, samples were digested for 16 hours in papain (0.56 units/ml in 0.1M sodium acetate, 10M cysteine HCL, 0.05M EDTA, pH 6.0) at 60°C. Agarose disks were digested in 1 mL/construct of papain and cell pellets were digested in 300 μL/sample of papain with three pellets combined per sample. Following digestion, the 1,9-dimethylmethylene blue dye-binding assay was used to determine GAG content in digests against a standard curve of chondroitin-6-sulphate. Digested samples were also evaluated for collagen content after acid hydrolysis using the orthohydroxyproline (OHP) assay (Stegemann et al. 1967), with a 1:7.14 OHP:collagen ratio used as described previously (Neuman et al. 1950). DNA content was determined from papain digests using the PicoGreen dsDNA assay (Molecular Probes, Eugene, OR). GAG and collagen values are reported as percentage of construct wet weight while DNA content is reported as quantity per disk.

3.2.6 Real-Time Polymerase Chain Reaction

Total RNA was extracted by two sequential isolations in TRIZOL-chloroform and quantified using a Nanodrop ND-1000 spectrophotometer (Nanodrop Technologies, DE). Reverse transcription was performed using the First Strand cDNA Synthesis kit (Invitrogen Life Technologies) and cDNA amplification was carried out using an Applied Biosystems 7300 real-time PCR system with intron-spanning primers and SYBR Green Reaction Mix (Applied Biosystems). Expression levels of seven cartilage-specific markers [chondroitin-4-sulfotransferase-1 (C4ST-1), chondroitin-4-sulfotransferase-2 (C4ST-2), xylosyltransferase (XT-1), GalNAc4,6S-disulfotransferase (Galnac), aggrecan, collagen II and link protein] and two bone-related markers [collagen type I and osteocalcin] were determined and normalized to the housekeeping gene, GAPDH.

3.2.7 Histology

Samples for histology were fixed in 4% paraformaldehyde, dehydrated in a graded series of ethanol, and embedded in paraffin (Paraplast, Lab Storage). Samples were sectioned at 8 μm thickness and stained with hematoxylin and eosin (H&E, Sigma, St. Louis, MO), Alcian Blue (pH 1.0), or Picrosirius Red (0.1% w/v in saturated picric acid) for cell distribution, sulfated proteoglycans and collagens, respectively. Mineralization in engineered constructs was assessed by Von Kossa staining according to manufacturer's instructions (American Mastertech, Lodi, CA) with a positive calcium control slide stained simultaneously for comparison. Color images were captured at 10X or 20X magnification using a microscope equipped with a color CCD digital camera and the QCapturePro acquisition software.

3.2.8 Immunohistochemistry

For immunohistochemical analysis, 8 μm sections were deparaffinized and rehydrated in a graded series of ethanol to water. Antigen retrieval was performed by incubating sections in citrate buffer (10 mM citric acid with 0.05% Tween 20 at pH 6.0) heated to 99°C for 25 minutes. Citrate buffer and samples were then transferred to room temperature and allowed to cool for an additional 20 minutes. Following antigen retrieval, samples were incubated for 1 hour at room temperature in 300 μg/mL hyaluronidase (Type IV, Sigma) in PBS. Primary antibodies to collagen type I (MAB3391, Millipore), collagen type II (11-116B3, Developmental Studies Hybridoma Bank, Iowa City, IA) and collagen type X (X-AC9, Developmental Studies Hybridoma Bank, Iowa City, IA) were used for immunolabeling according to manufacturer's directions . Briefly, samples were treated with 3% H_20_2 followed by treatment with a blocking reagent (DAB150 IHC Select, Millipore), and incubated with primary antibodies in 3% BSA with non-immune controls. Following incubation with primary antibodies, samples were treated with biotinylated goat anti-rabbit IgG secondary antibodies and Streptavidin HRP, then reacted with DAB chromogen reagent (DAB150 IHC Select, Millipore). Color images were captured at 10X magnification as above.

3.2.9 Statistical Analysis

Statistical analysis was performed using SYSTAT software (v10.2, SYSTAT Software Inc., San Jose, CA). Mechanical and biochemical data for cell-seeded constructs was analyzed via two way ANOVA with significance set at $p<0.05$. Biochemical content of

cell pellets was assessed via one way ANOVA with significance set at $p<0.05$. Where significance was indicated by ANOVA analysis, Tukey's posthoc testing was carried out to enable comparisons between groups. All values are reported as mean ± standard deviation.

3.3 Results

3.3.1 Compressive Properties of Cell-Seeded Agarose

To optimize functional properties of MSC-laden constructs, MSCs were seeded at 20 (M20) or 60 (M60) million cells/mL agarose and cultured under continuous (+) or transient (T) exposure to TGF-β3 for 7 weeks in chemically defined, serum-free medium. Chondrocytes were seeded at 20 million cells/mL (C20) and maintained under these same conditions. Over time in culture, CH- and MSC-seeded constructs became increasingly opaque and, consistent with previous findings, increased in volume relative to starting values. Construct thickness did not change with transient exposure to TGF-β3, however, at every time point assayed, MSC-seeded gels were thicker than CH-seeded gels, regardless of seeding density. There were no observable differences in MSC-seeded construct diameters until day 49. As with thickness measurements, diameter size was comparable between M20 and M60 at every time point, and both were larger than C20 by day 49 (**Table 3-1**).

Table 3-1: Changes in construct dimensions with time. * indicates significant difference from day 21 within cell type and seeding density (p<0.05), # indicates significant difference from C20 within each time point and media group (p<0.05).

	THICKNESS (mm)			DIAMETER (mm)		
	Day 21	Day 35	Day 49	Day 21	Day 35	Day 49
CH20+	2.24±0.02	2.42±0.06*	2.48±0.07*	4.01±0.01	4.06±0.07	4.18±0.17
CH20-T	NA	2.41±0.04*	2.45±0.06*	NA	4.02±0.03	4.04±0.05
M20+	2.55±0.10#	2.63±0.09#	2.71±0.16#	4.08±0.11	4.13±0.09	4.40±0.15*
M20-T	NA	2.58±0.13#	2.67±0.12#	NA	4.13±0.08	4.33±0.23*#
M60+	2.58±0.08#	2.67±0.08#	2.81±0.10#	4.22±0.25	4.28±0.14	4.53±0.12*#
M60-T	NA	2.69±0.11#	2.76±0.09#	NA	4.35±0.08#	4.41±0.20#

For all groups, the equilibrium and dynamic compressive modulus improved with time in culture ($p<0.05$). Consistent with our previous findings (Mauck et al. 2006), the equilibrium modulus of C20+ disks increased through week 7, reaching 203±27 kPa ($p=0.008$), while M20+ constructs plateaued by 3 weeks at a lower level of 107±23 kPa ($p=1.0$, **Figure 3-1A**). There was no difference in equilibrium modulus between M20+ and M60+ at any time point ($p>0.9$), although the modulus of both groups were much greater than starting agarose values (typically 5-10 kPa). Also consistent with our previous findings (Byers et al. 2008), the equilibrium modulus of the C20-T group increased dramatically, with an 8-fold increase 4 weeks after removal of TGF-β3 ($p<0.001$), compared to only a 4-fold increase over the same time period with continuous exposure ($p<0.001$). While the equilibrium properties of M20 constructs did not change in transient compared to continuous medium conditions ($p=0.9$), a 4-fold increase to 193±40 kPa was observed in M60 constructs by week 7 when cultured in transient compared to continuous media exposure ($p<0.001$). These M60-T samples reached modulus values similar to that of week 7 C20+ constructs ($p=1.0$, **Figure 3-1A**). Despite the difference in the equilibrium

modulus between C20+ and M20+, the dynamic moduli of these constructs were not significantly different by week 7 ($p=0.9$). At 7 weeks, the dynamic modulus of M20+ was also similar to that of M60+ ($p=0.1$). Under transient medium conditions, the dynamic moduli of C20 and M20 constructs did not improve relative to control constructs in + conditions ($p>0.2$). However, the dynamic modulus of M60-T constructs was greater than that of M60+ ($p=0.003$, **Figure 3-1B**).

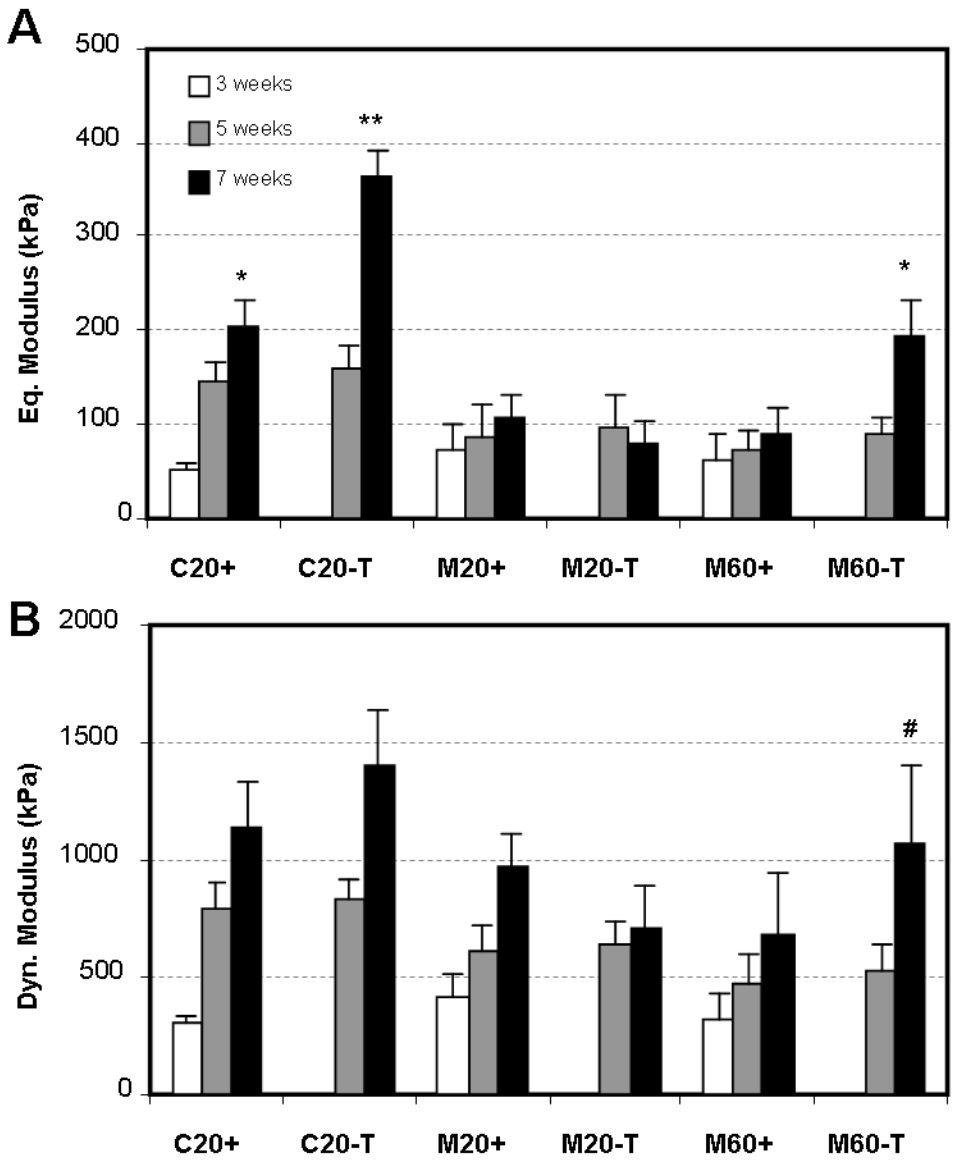

Figure 3-1: Time-dependent compressive properties of engineered constructs with variation in cell type, seeding density and media formulation. (A) Equilibrium and (B) dynamic modulus of cell-seeded constructs. * indicates greater than C20+ at 5 weeks ($p<0.05$); ** indicates greater than C20+ at week 7 ($p<0.05$), # indicates greater than M60+ at 7 weeks. Data represent the mean and standard deviation of 7-8 samples per group per time point.

3.3.2 Biochemical Content of Cell-Seeded Agarose

Biochemical content for C20+ and M20+ disks increased with time, with more GAG deposited in C20+ compared to M20+ by week 7 ($p<0.001$, **Figure 3-2A**). As with the

equilibrium modulus, the GAG content of C20+ continued to improve through the final timepoint ($p<0.001$) while M20+ disks plateaued by week 3 ($p>0.4$, **Figure 3-2A**). Under transient conditions, a marked increase in GAG content was observed in C20-T and M60-T groups ($p<0.001$, **Figure 3-2A**) compared to their continuous exposure controls. While the total GAG content of week 7 M60-T constructs was markedly higher compared to all other MSC groups, it remained below that of week 7 chondrocyte-laden constructs. Collagen content was not significantly different between groups by week 7, except in the M60+ group which was lower compared to C20+ and M60-T ($p<0.05$, **Figure 3-2B**). Assessment of DNA content showed that higher cell density was maintained in the 60M-seeded MSC groups and that transient application of TGF-β3 had no effect on cell proliferation, regardless of cell type ($p=1.0$, **Figure 3-2C**). When normalized to DNA content, GAG content in M60 constructs cultured in either medium condition was dramatically reduced compared to M20 constructs similarly maintained, suggesting that GAG synthesis per cell was impaired with increasing cell number (not shown).

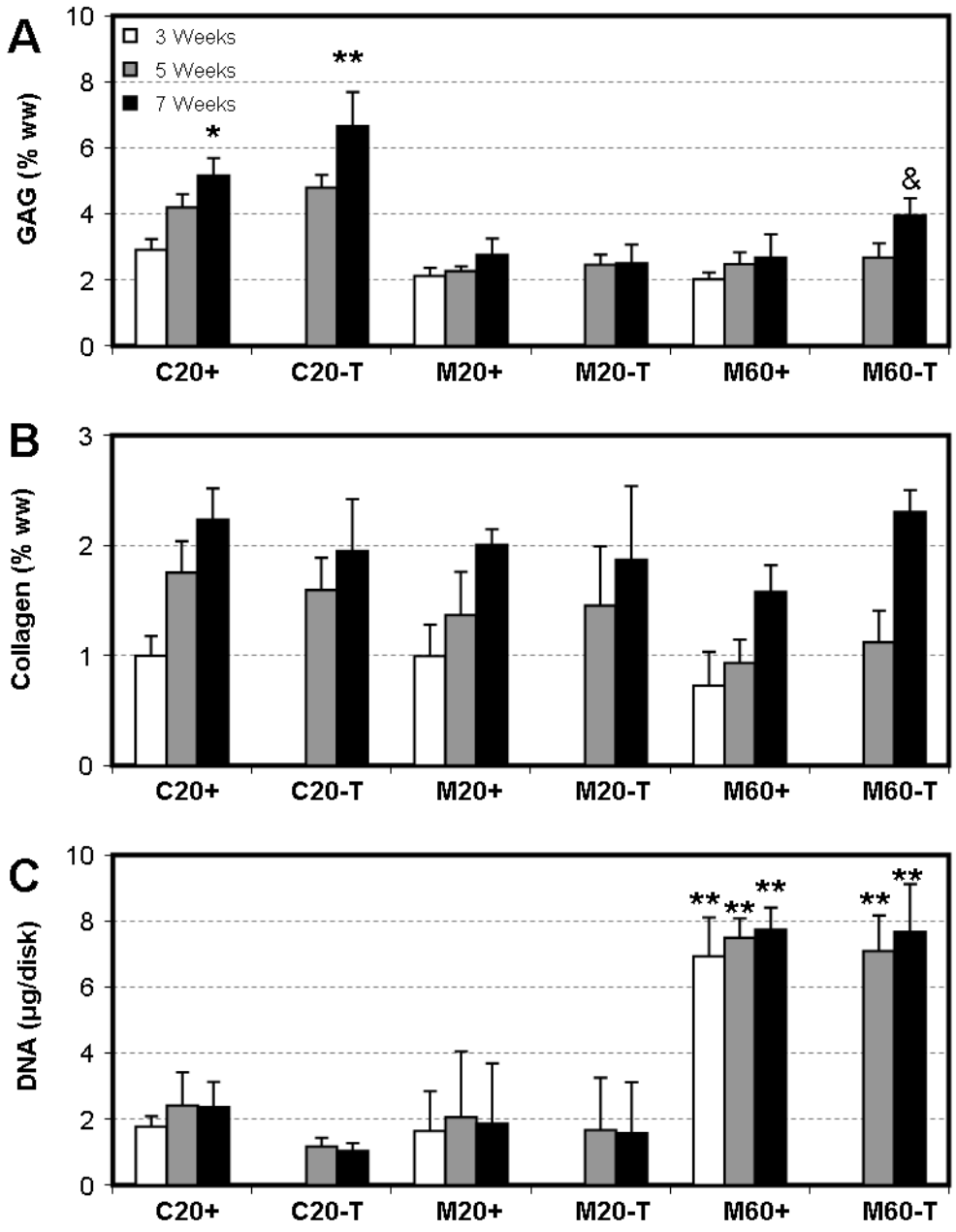

Figure 3-2: Biochemical composition of engineered constructs with variation in time in culture, cell type, seeding density and media formulation. (A) GAG, (B) collagen and (C) DNA content of chondrocyte- and MSC-laden gels. * indicates greater than C20+ at 5 weeks ($p<0.05$), ** indicates greater than C20+ at 7 weeks, & indicates no difference from C20+ at 5 weeks ($p>0.05$). Data represent the mean and standard deviation of 7-8 samples per group per time point.

3.3.3 Histological Analysis of Cell-Seeded Agarose

Histological staining for cellularity, GAG, and collagen deposition largely confirmed biochemical measures. Consistent with biochemical analyses of DNA content, H&E staining for cell distribution at week 7 showed greater cell density for gels seeded at 60M cells/mL compared to those seeded at 20M cells/mL (**Figure 3-3**). From H&E staining, it appeared that transient application of TGF-β3 resulted in larger cell lacunae in both the C20 and M60 groups. These C20-T and M60-T groups also showed increased staining for proteoglycan deposition relative to controls with continuous medium conditions (**Figure 3-3**).

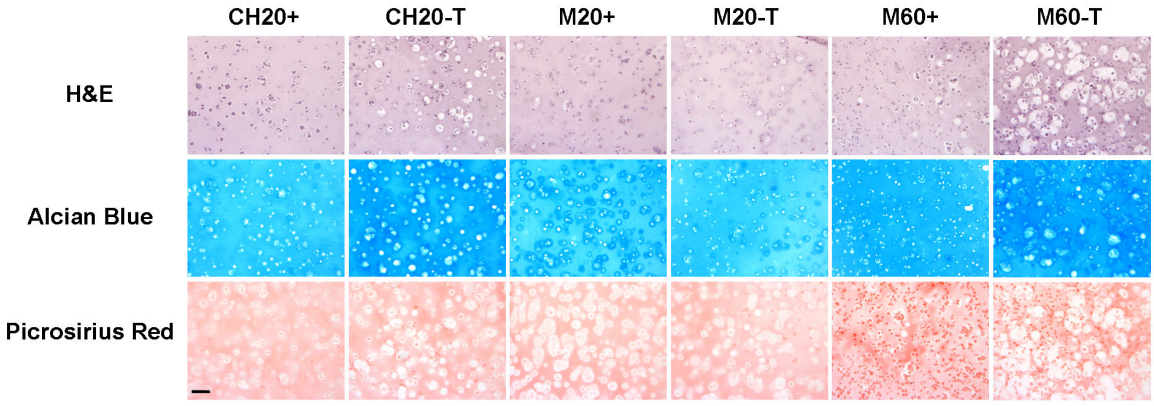

Figure 3-3: Histological appearance of engineered constructs after 7 weeks of culture. Hematoxylin and Eosin, Alcian Blue, and Picrosirius Red staining of C20, M20 and M60 constructs cultured in + and T media. C20-T and M60-T showed increased proteoglycan deposition as well as changes in cell morphology consistent with hypertrophic events. Images were acquired at 10x magnification. Scale bar: 100 μm.

Constructs showed little discernible difference in collagen staining with variation in cell type or seeding density. Collagen deposition was further assessed by immunohistochemistry to distinguish between type I, type II and type X collagens. At week 7, all groups showed weak pericellular staining for type I collagen and intense interterritorial staining for type II collagen (**Figure 3-4**).

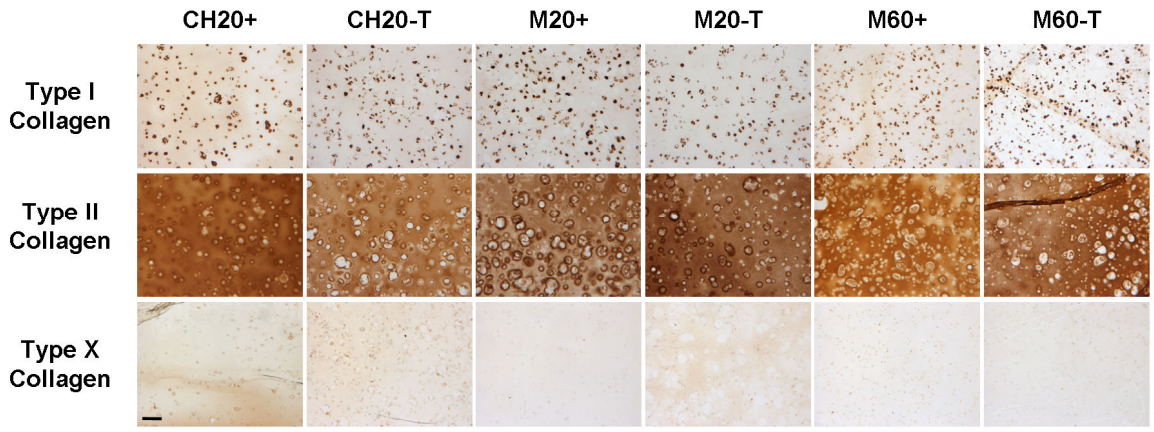

Figure 3-4: Distribution of collagen types I, II and X in engineered constructs cultured in + or T medium for 7 weeks. Chondrocyte- and MSC-laden constructs showed weak pericellular staining for type I collagen and intense staining for type II collagen regardless of initial seeding density or media formulation. Type X collagen was not apparent in any group. Scale bar: 100 μm.

There was no increase in type I collagen accumulation with removal of TGF-β3 in any group, nor was type X collagen staining evident under any condition. Von Kossa staining for calcium was also performed to assess mineralization in cell-seeded gels; no evidence of calcium deposition was observed in any group (**Figure 3-5**).

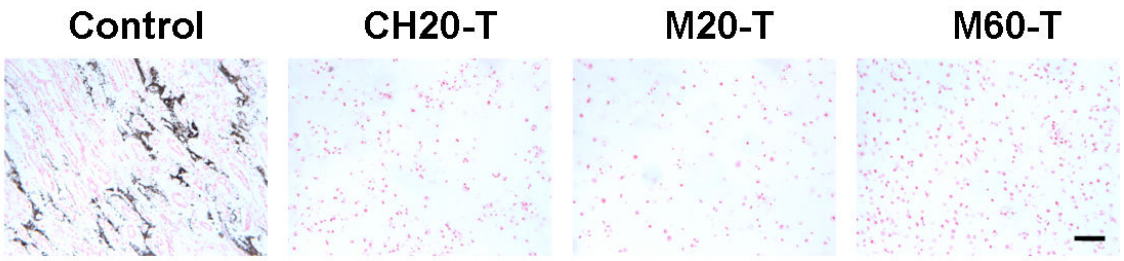

Figure 3-5: Von Kossa staining of engineered constructs cultured in T medium for 7 weeks. Mineralization (black staining) was not observed in chondrocyte- or MSC-laden gels. Images were acquired at 10x magnification. Scale bar: 100 μm.

3.3.4 Biochemical and Histological Analysis of MSC Pellets

Because MSC response to transiently applied TGF-β3 appeared to be dependent on the initial seeding density, a cell pellet model of chondrogenesis was used to determine whether results similar to that achieved with gels seeded at 60M cells/mL could be generated when cultured under transient conditions. Cells are tightly packed in pellet culture (i.e., no ECM at the initiation of culture), they may be considered 'infinite' with respect to the other seeding densities used in this study (20 or 60 million cells/mL). MSC pellets accrued increasing amounts of GAG with time through week 7 when cultured continuously with TGF-β3. With transient exposure to TGF-β3, the GAG content of pellets was significantly greater by week 7 compared to the GAG content of pellets cultured continuously with TGF-β3 ($p<0.001$, **Figure 3-6A**). Contrary to our findings in 3D hydrogel culture, DNA content of pellets decreased for both groups at week 7, with greater loss in pellets cultured under transient medium conditions compared to continuous exposure (**Figure 3-6B**). When normalized to cell number, the difference in GAG content at week 7 between pellets cultured under transient and continuous conditions was even more pronounced, with a 2.6-fold difference in GAG deposition (**Figure 3-6C**).

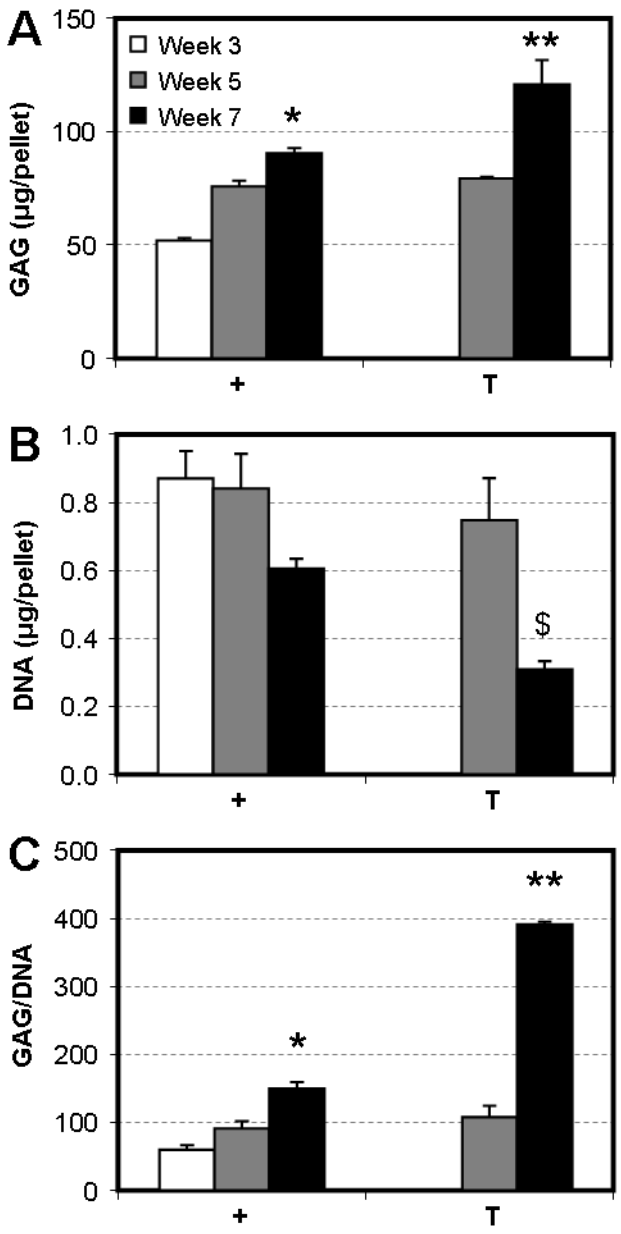

Figure 3-6: Biochemical composition of MSC pellets with variation in time in culture and media formulation. (A) GAG (µg/pellet), (B) DNA (µg/pellet) and (C) GAG/DNA content of MSC pellets. Transient application of TGF-β3 increased GAG deposition relative to pellets cultured continuously with TGF-β3. * indicates greater than + pellets at 5 weeks ($p<0.05$), ** indicates greater than + pellets at 7 weeks ($p<0.001$), $ indicates lower than + pellets at 7 weeks and T pellets at 5 weeks ($p<0.01$). Data represent the mean and standard deviation of 3 samples per group per time point.

No differences in collagen content were observed with transient application of TGF-β3 (not shown). By week 7, there was a noticeable difference in cell number between pellets

maintained continuously or transiently in TGF-β3, as shown in the H&E stains. As with cell-seeded constructs, Alcian Blue staining for proteoglycans demonstrated conspicuously darker regions of staining in pellets cultured under transient conditions compared to continuous, consistent with biochemical measures of GAG content. Picrosirius red staining for collagen was of equal intensity between the two groups (**Figure 3-7**).

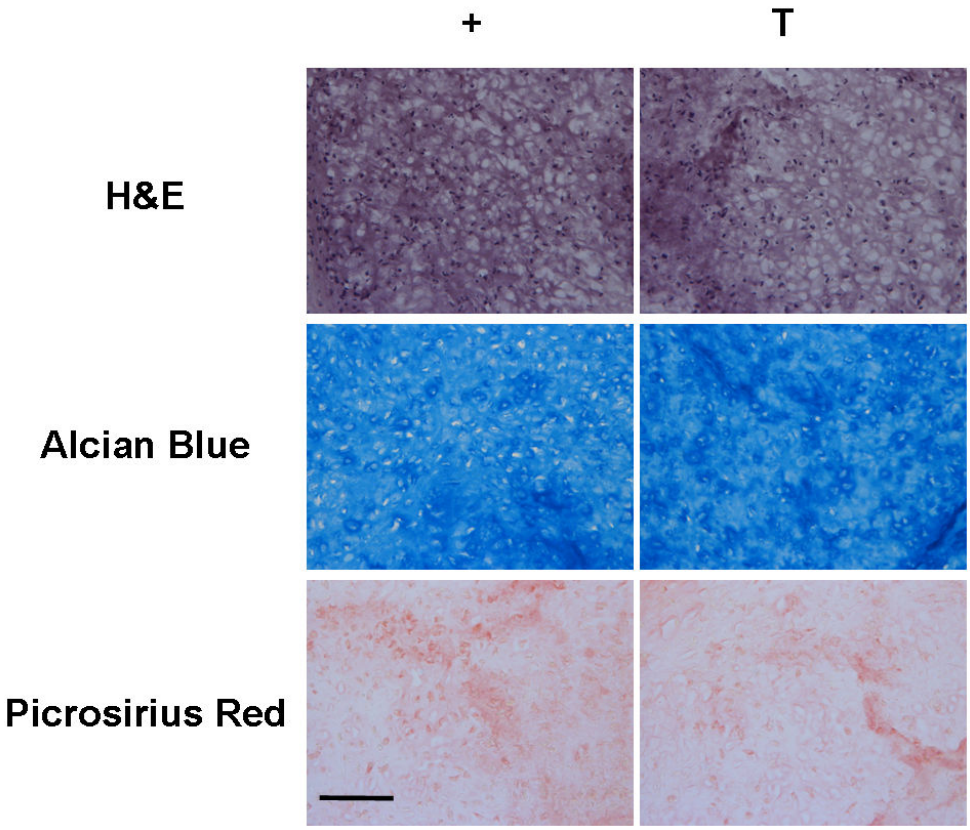

Figure 3-7: Histologic appearance of MSC pellets after 7 weeks of culture. H&E, Alcian Blue, and Picrosirius Red staining of MSC pellets cultured in + and T media. Images were taken at 20x magnification. Scale bar: 100 μm.

3.3.5 Gene Expression

Chondrogenic markers were expressed by all groups cultured continuously with TGF-β3. Removal of TGF-β3 did not adversely affect the chondrocytic phenotype of MSCs seeded at either 20 or 60 million cells/mL. Expression levels of C4ST-1 and Galnac continued to

increase for both M20-T and M60-T after 3 weeks, while aggrecan, and collagen type II expression remained relatively stable (**Figure 3-8**). C20-T groups followed a similar pattern of expression, with large increases in Galnac by 7 weeks relative to 3 weeks. For all MSC and chondrocyte groups exposed transiently to TGF-β3, Galnac expression at 7 weeks was markedly higher compared to control gels maintained continuously with TGF-β3. These data are from two biologic replicates (separate studies) with similar findings in each. Although collagen type I was expressed by all groups, osteocalcin expression was undetectable (not shown).

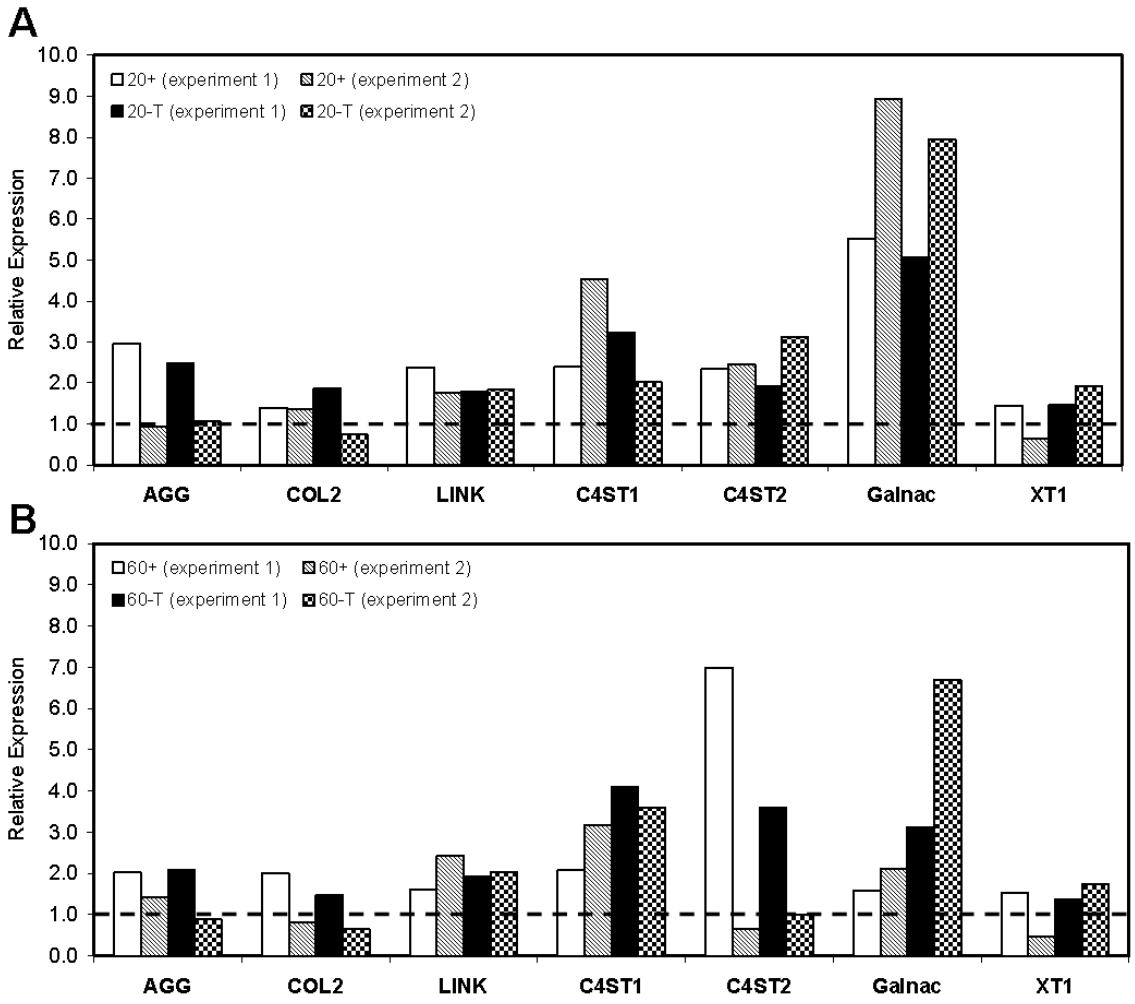

Figure 3-8: Expression of cartilage markers in MSC-laden constructs with variation of initial seeding density. Relative gene expression normalized to 3 week control constructs (dashed line) of (A) M20 and (B) M60 constructs at 7 weeks in + and T media. The chondrocyte-like phenotype is maintained in constructs cultured in T media 4 weeks after TGF-β3 withdrawal. Data from two experiments are presented.

3.4 Discussion

Bone marrow derived mesenchymal stem cells (MSCs) are an attractive cell source for regenerative medicine, given their ready isolation and expansion capacity, and their ability to differentiate towards a number of musculoskeletal lineages. For cartilage tissue engineering, MSCs readily undergo chondrogenesis in 3D culture in the presence of specific biofactors, and deposit a cartilage-like matrix. This matrix formation improves

mechanical properties critical to the function of the native tissue, including both the compressive and tensile properties (Mauck et al. 2006; Huang et al. 2008). Despite their maturation potential, engineered cartilage formed from MSCs is limited by the reduced equilibrium compressive properties generated compared to fully differentiated chondrocytes. Consistent with previous findings (Mauck et al. 2006), this study showed that the mechanical properties of MSC-laden constructs were lower than chondrocyte-laden constructs similarly maintained. To further optimize chondrogenesis, we examined the effects of two parameters, initial seeding density and transient application of TGF-β3, on the mechanical properties and biochemical content of MSC-laden gels. In chondrocyte-seeded hydrogels, both factors have been previously shown to improve equilibrium compressive properties (Mauck et al. 2003; Byers et al. 2008).

Contrary to our original hypothesis, MSCs seeded in agarose at 20 and 60 million cells/mL and maintained continuously with TGF-β3 showed no differences in functional properties or biochemical content after 7 weeks in free swelling culture. While several studies have reported enhanced chondrogenesis with increasing seeding density (Ponticiello et al. 2000; Kavalkovich et al. 2002; Huang et al. 2004; Hui et al. 2008), the range of cell densities assayed were generally below 10 million cells/mL (Huang et al. 2004; Hui et al. 2008) and outcome parameters were limited to biochemical measures or gene expression. In one study comparing seeding densities above 10 million cells/mL, total GAG deposition was indistinguishable between constructs seeded at 12-48 million cells/mL, consistent with the current findings (Ponticiello et al. 2000). In another study comparing human MSCs seeded at different densities in alginate, an initial density of 25

million cells/mL resulted in significantly increased GAG synthesis per cell after 14 days of culture compared to constructs seeded at 50 million cells/mL (Kavalkovich et al. 2002). In keeping with this observation, we found a marked reduction in GAG deposition per cell (~75% reduction) in constructs seeded at 60 million MSCs/mL relative to constructs seeded at 20 million MSCs/mL.

During chondrogenesis in the limb bud and in *in vitro* micromass models using these cells, increased cellularity promotes cell-cell contact and enhances differentiation (Tacchetti et al. 1992; Oberlender et al. 1994). Our results and those of others suggest that there exists an optimal MSC density that maximizes GAG production per cell, even when cells are not in direct contact in 3D hydrogel systems. At seeding densities higher than this optimal value, chondrogenesis may be adversely affected. Studies using chondrocyte-based constructs have also shown that while matrix biosynthesis is initially high during early culture periods, when the pericellular environment is being established *de novo*, a decline in synthesis rate is observed with gradual accumulation of ECM (Buschmann et al. 1992). At earlier time points than those assayed in our studies, a higher seeding density may promote matrix biosynthesis until a certain threshold value of bulk GAG content is attained. To assess whether such negative feedback mechanisms regulate matrix accumulation rates in MSC-based constructs, future work will assess GAG synthesis at earlier time points. Alternatively, a deficit in nutrient supply may reduce the extent of differentiation or matrix production observed at the higher seeding density. For example, we have shown more robust production of ECM in chondrocyte-

seeded gels in medium containing 20% FBS compared to 10% FBS medium (Mauck et al. 2003). Additional studies will be required to address this important question.

To further enhance MSC chondrogenesis, we also examined the effect of transient application of TGF-β3 in the context of changing seeding densities. While chondrocytes responded favorably to transient exposure of TGF-β3 by dramatically increasing the equilibrium modulus, MSCs seeded at the same density (20 million/mL) showed no change with removal of the growth factor. Although the 'release' phenomenon was not observed in MSCs seeded at this density, removal of TGF-β3 did not abrogate accrued properties, indicating that MSCs were able to maintain their differentiated phenotype and functional properties. Conversely, when MSCs were seeded at a higher density (60 million cells/mL), transient application of TGF-β3 had a pronounced effect on the equilibrium modulus and GAG accumulation. This finding suggests the potential for quorum sensing in triggering the 'release' phenomenon in MSCs, where by paracrine signaling between cells may potentiate the 'release' response after TGF-β3 withdrawal. Alternatively, at a higher seeding density (i.e. 60 million cells/mL), a smaller fraction of MSCs may undergo chondrogenesis or the extent of chondrogenesis might be limited in induced cells, potentially through negative feedback mechanisms or nutrient limitations and growth factor supply. The improvement in total GAG content and equilibrium compressive properties in these constructs with removal of TGF-β3 may be due to enhanced recruitment of undifferentiated cells or enhanced GAG production by committed MSCs. Whether the triggering response is initiated by chondrogenically committed or uncommitted cells is as yet unknown.

Despite improved GAG production in these MSC-laden constructs with the removal of TGF-β3, the GAG content on a per cell basis remained markedly reduced compared to MSC constructs seeded at 20 million cells/mL (~ 65% lower). This suggests that simply adding additional MSCs does not overcome their inherent matrix forming limitations compared to fully differentiated chondrocytes. Furthermore, while MSCs seeded at 20 million cells/mL did not respond to 'release' in general, in two instances (out of six), increases in equilibrium modulus was observed on par with that of cells seeded at 60M cells/mL. This observation implies that if this response is dependent on the initial seeding density, 20 million cells/mL may be close to the threshold density. To test whether seeding density was a factor in this 'release' response, we also cultured MSC pellets under transient conditions and assessed GAG content and histological features. Consistent with findings for MSC constructs seeded at 60 million cells/mL, transient exposure to TGF-β3 induced significant increases GAG accumulation in MSC pellets.

The ability of MSCs to generate functional matrix is merely one aspect of engineering viable replacement tissue. For clinical application, the phenotype of these cells must be maintained once removed from the controlled, pro-chondrogenic and chemically defined culture environment to the much less defined, and often inflammatory, *in vivo* setting. As other *in vitro* studies have demonstrated, we have shown here that a chondrocyte-like phenotype is maintained in constructs after initiation of chondrogenesis with transient exposure to TGF-β3. Furthermore, we have shown continuous expression of genes encoding cartilage matrix elements as well as four genes encoding enzymes involved in

proteoglycan synthesis. While most of these genes were insensitive to TGF-β3 withdrawal, the expression levels of Galnac increased rapidly after removal of the growth factor. This was consistent across all 'release' groups, including MSCs seeded at 20 million cells/mL (which did not improve in properties), and the levels achieved by 7 weeks exceeded that of the continuous exposure control groups. While the expression of Galnac may be modulated to some extent by 'release,' the complete molecular mechanism underlying the dramatic increases in mechanical properties and GAG content associated with the 'release' response is still unclear. Larger scale screening methods (such as microarray analysis) may be required to fully understand this phenomenon. Alternatively, factors not examined in this study, such as post-translational modifications may play a crucial role and warrant further study.

Although transient application and removal of TGF-β3 from the culture medium did not adversely affect chondrogenic gene expression, histological analysis of our constructs revealed enlarged cell lacunae. This morphological feature is prominent in cells with high metabolic activities (producing large amounts of highly charged proteoglycan) (Quinn et al. 2002), but is also consistent with the hypertrophic changes associated with endochondral ossification. This morphology was not detected in MSCs seeded at 20 million cells/mL or in constructs cultured continuously in TGF-β3 (i.e., groups not undergoing a 'release' response). Despite the presence of these enlarged cells, there was no additional evidence indicative of hypertrophic transitions taking place. There was no evidence of matrix mineralization or a shift to type I collagen production 4 weeks after removal of TGF-β3, and type X collagen deposition was also not observed. This finding

is supported by one study, which showed that TGF-β withdrawal alone was not sufficient to induce hypertrophy or mineralization in MSC pellets (Mueller et al. 2008).

While we did not observe phenotypic changes in our MSC constructs in this study, the long term stability of the cartilage phenotype of differentiated MSCs in the absence of pro-chondrogenic factors remains to be determined. Recent work assessing the chondrogenic commitment of MSCs demonstrated pronounced instability of phenotype when cultured under *in vivo* conditions (Pelttari et al. 2006; Jukes et al. 2008). Implantation of chondrogenically differentiated MSCs resulted in extensive mineralization, coupled with the persistence of cartilage-like regions. Remarkably, articular chondrocytes showed no signs of ossification or hypertrophy when implanted *in vivo*, suggesting intrinsic differences remain between these two cell types. In this study, enlarged lacunae were observed in both chondrocyte and MSC seeded constructs undergoing release. While TGF-β removal may not be sufficient to induce phenotypic changes, its absence may create a permissive environment for other factors present *in vivo* to drive osteogenesis in cells that are less complete in their commitment to the chondrocyte phenotype. In one *in vitro* study, Mueller et al induced mineralization of chondrogenically differentiated MSC pellets by the addition of triiodothyronine and β-glycerophosphate after withdrawing TGF-β (Mueller et al. 2008). Additional work, using both chondrocyte- and MSC-seeded constructs, will be required to demonstrate the stability of the cartilage phenotype in our 'released' constructs if they are to be viable candidates for regenerative therapies.

The work described herein demonstrates that functional MSC chondrogenesis is regulated by initial seeding density and transient application of TGF-β3. The equilibrium modulus reported here (~200 kPa) for constructs seeded at 60 million cells/mL and cultured with transient TGF-β3 exposure is the highest value we have yet achieved for MSCs seeded in agarose hydrogels. This modulus is ~50% that of native bovine tissue (Athanasiou et al. 1991; Ateshian et al. 1997), and suggests the potential of these cells for the production of functional engineered cartilage constructs. While the parameters used in this study generated MSC constructs with the highest equilibrium modulus we have ever achieved using these cells, the properties attained still fall below chondrocyte construct values when cultured under similar conditions. This finding further underscores the inherent differences that remain between these two cells types, even after MSCs commit to the chondrocyte phenotype. While GAG content and compressive equilibrium properties approached native levels, collagen content and dynamic properties remained low for all cell-seeded constructs. Continuing optimization strategies should focus on these critical aspects of engineered cartilage constructs. We and other have deployed novel materials (Connelly et al. 2007; Kisiday et al. 2008) and constructed mechanical loading systems (Mauck et al. 2007; Mouw et al. 2007) that may better foster the chondrogenic differentiation process. These advances have the potential to generate functional cartilage replacements based on MSCs, especially if combined with the defined media regimes and seeding density requirements indicated from our results. Recent work using chondrocyte-based constructs demonstrate that mechanical loading applied in concert with transient exposure to TGF-β3 can generate neo-tissues with mechanical properties exceeding that of either treatment alone (Lima et al. 2007). Despite this potential,

expectations must be tempered regarding the capacity of a newly differentiated cell type relative to fully differentiated cells, and must take heed of the continuing necessity of promoting and maintaining the differentiated phenotype and functional properties after in vivo implantation.

CHAPTER 4: LONG-TERM DYNAMIC LOADING IMPROVES THE MECHANICAL PROPERTIES OF CHONDROGENIC MESENCHYMAL STEM CELL-LADEN HYDROGELS

4.1 Introduction

The practical use of MSCs for cartilage regeneration has thus far been limited by the inferior mechanical properties generated by constructs based on these cells. As Chapter 3 demonstrated, these limitations in functional chondrogenesis are not simply due to insufficient cell number within the constructs (Kavalkovich et al. 2002; Huang et al. 2009). While transient exposure to TGF-β3 enhanced GAG content and mechanical properties when applied to MSC-laden constructs seeded at 60 million cells/mL, on a per cell basis, these properties remained lower than that of constructs seeded at 20 million cells/mL. In addition, the final properties achieved do not meet the mechanical benchmarks of the native tissue described in Chapter 2. Limitations in functional MSC chondrogenesis then, may be due to an intrinsic limitation in TGF-β mediated chondrogenesis, in the absence of additional stimuli. Given the mechanically demanding environment of articular cartilage, the ability of MSC-based constructs to function within this environment is an important consideration and will directly affect clinical success.

Therefore, mechanical stimulation may be one strategy for optimizing chondrogenesis and overcoming these functional limitations as mechanical loading plays a vital role in the development, remodeling and maintenance of normal articular cartilage. During development, inhibition of muscle contraction and forces acting on skeletal elements

results in abnormal joint formation (Mikic et al. 2000; Mikic et al. 2004). After birth, loading-induced remodeling of articular cartilage leads to dramatic changes in tissue structure (particularly of the collagen network) and increases in mechanical properties; in the absence of loading, this remodeling is not observed (Williamson et al. 2001; Williamson et al. 2003; Williamson et al. 2003). In addition, normal joint loading has also been implicated in the maintenance of the chondrogenic phenotype of articular chondrocytes within cartilage (Chen et al. 2008).

For cartilage tissue engineering, dynamic compression has proven especially effective in improving the functional properties of chondrocyte-seeded constructs (Mauck et al. 2000; Mauck et al. 2003; Lima et al. 2006). While less is known regarding the mechanoresponsivity of MSC-based constructs, recent work with MSCs and related cell types show that dynamic compression modulates the chondrogenic phenotype of these cells (Elder et al. 2000; Elder et al. 2001; Elder 2002). In general, loading of human or rabbit MSCs increases expression of aggrecan and collagen type II (Angele et al. 2004; Huang et al. 2004), and is mediated by induction of the TGF-β signaling pathway (Huang et al. 2005). The presence/absence of TGF-β also dictates the response of MSCs to compressive loading. Loading in the absence of TGF-β improves proteoglycan synthesis levels of equine MSCs relative to free swelling controls while in cultures loaded in the presence of TGF-β, matrix synthesis levels diminish (Kisiday et al. 2009). Taken together, these findings suggest that dynamic compression modulates MSC chondrogenic differentiation and that the presence/absence of TGF-β influences this process.

While promising, the majority of the studies noted above were limited to short-term loading durations and focused on changes in gene expression and instantaneous measures of ECM synthesis. These studies have not established a link between these transient events and functional outcomes related to matrix accumulation and mechanical properties of the forming tissue. Indeed, repeated exposure to physical stimuli is often required for transient perturbations in ECM synthesis to culminate in changes in functional properties (Angele et al. 2003). In one recent study, dynamic compression (initiated immediately after porcine MSC encapsulation in agarose) was carried out over 42 days in the presence of TGF-β. Findings from this study showed a marked reduction in the mechanical properties of loaded constructs compared to free-swelling controls (Thorpe et al. 2008). In this previous work, loading was initiated before chondrogenesis had developed or deposition of local ECM had occurred, however, others have suggested that these initial phenotypic transitions may regulate MSC response to physical signals. For example, Mouw et al. showed that a single application of dynamic compression improved both collagen type II and aggrecan expression when bovine MSC-seeded constructs were pre-cultured in TGF-β1 containing media for longer culture durations (Mouw et al. 2007). Similarly, Terraciano et al. demonstrated that human embryonic stem cells in 3D culture responded adversely to compressive loading in the absence of TGF-β; but responded positively when loading was initiated after a period of chondrogenic pre-differentiation (Terraciano et al. 2007).

Collectively, these foundational studies on MSC mechanobiology suggest that dynamic compressive loading can modulate MSC chondrogenesis, though it is important to

consider species differences when interpreting these findings as a number of these studies utilized MSCs derived from various species. These same studies also indicate that loading-mediated improvements in functional maturation of MSC-seeded constructs with dynamic loading may require the establishment of a chondrogenic phenotype before exposure to mechanical perturbation. To test this hypothesis, we applied long-term dynamic compressive loading to MSC-seeded constructs and evaluated the resulting changes in construct mechanical properties over 6 weeks of culture. We assessed whether varying pre-culture duration, loading regimens and inclusion of TGF-β3 during loading would affect functional outcomes and phenotypic transitions. While long-term loading initiated soon after MSC encapsulation reduced the mechanical properties of constructs, loading initiated after a short period of chondrogenesis and matrix elaboration dramatically improved construct mechanical properties. These findings show, for the first time, that the mechanical properties of MSC-seeded constructs can be enhanced by dynamic compressive loading, and point towards improved clinical translation of MSC-based cartilage constructs.

4.2 Materials and Methods

4.2.1 Dynamic Compression of MSC-Seeded Constructs

MSCs were isolated and expanded as described in Section 3.2.1. MSCs from at least two donors were combined for each study with a total of 8 donors used (donor sets A, B, C and D). To carry out these studies, MSC-laden constructs (Ø4 mm x 2.25 mm) were formed with a final cell seeding density of 20 million cells/mL as in Section 3.2.2 and cultured in chemically defined media. For all studies, dynamic unconfined compression

was applied using a custom bioreactor with impermeable platens (**Figure 4-1**) (Mauck et al. 2007). The loading protocol consisted of a 10% dynamic strain superimposed on a static 2% tare strain, with constructs in unconfined conditions (i.e., allowed to expand radially with axial compression). For all studies, loading was carried out at 37°C in a humidified incubator for 5 days per week for 3 weeks with free-swelling controls cultured in parallel.

A total of five independent studies were carried out as outlined in **Figure 4-1D,** with cells combined from two donors for each study (each distinct donor set is indicated accordingly). In Study 1, dynamic compression was initiated 3 days after MSC encapsulation. Loading was applied at 1 Hz for 4 hours per day in CM supplemented with (CM+) or without (CM-) 10 ng/mL TGF-β3 (R&D Systems, Minneapolis, MN). Gene expression was assessed weekly by real-time PCR. For Studies 2-5, dynamic compression was initiated after a 3 week pre-culture period in CM+. In Study 2, pre-cultured constructs were loaded in CM- or CM+ at 1 Hz for 4 hours per day. In Study 3, loading was applied for 1 hour or 4 hours per day at 1 Hz in CM+. In Study 4, dynamic compression was applied for 4 hours per day at 1 Hz or 0.01 Hz in CM+ medium. In Study 5, free-swelling constructs were cultured in CM- or CM+ for 6 weeks and loading was applied in CM+ at 1 Hz for 4 hours daily beginning at week 3. For all studies, mechanical and biochemical analyses were carried out at 3 and 6 weeks according to protocols established in Sections 3.2. For Study 5, global gene expression was assessed by microarray.

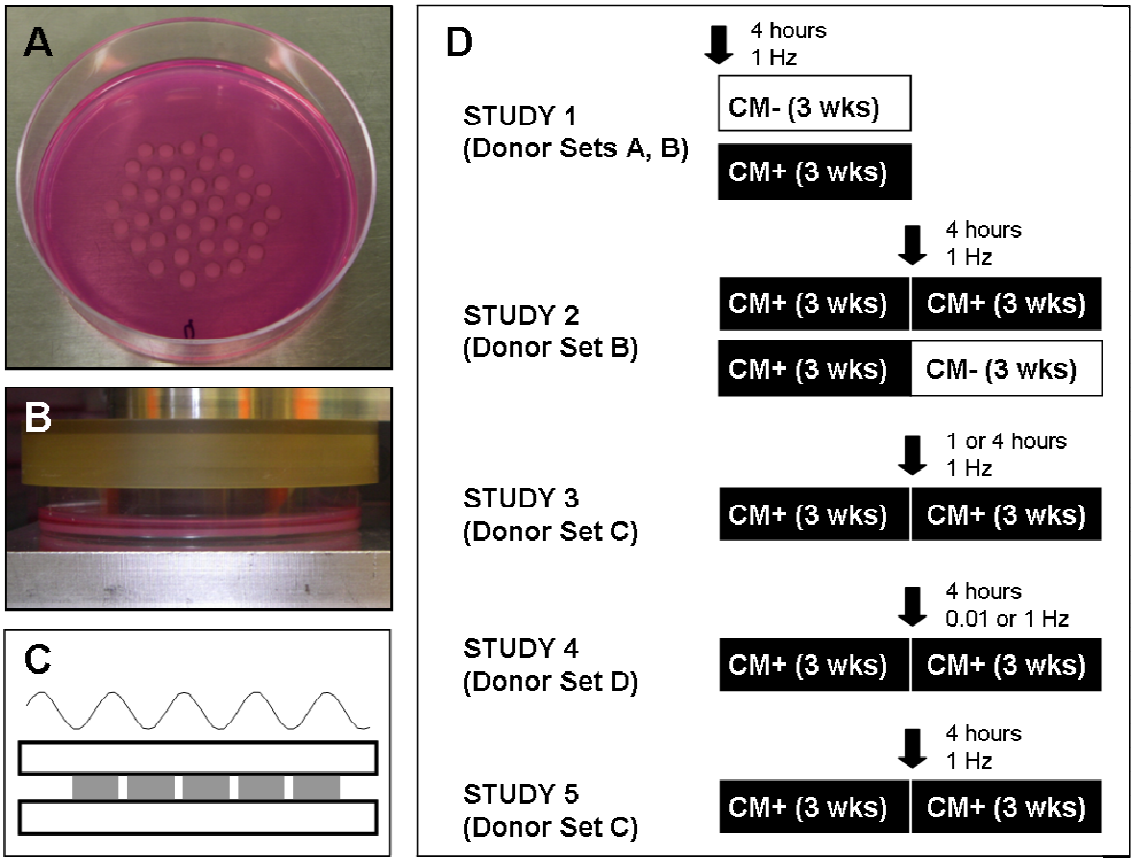

Figure 4-1: Unconfined dynamic compressive loading of MSC-laden constructs in a custom bioreactor system. (A) To hold constructs in place, molds were fabricated by casting a thin layer (~ 1.5 mm thickness) of sterile 4% agarose; Ø5 mm wells were made after gelation and MSC-seeded constructs (Ø4 mm) were maintained in these wells throughout the culture duration. (B) Impermeable platens were used to apply a (C) sinusoidal displacement to MSC-seeded constructs. (D) Separate studies were carried out to examine the effects of pre-culture, loading duration, loading frequency, and dependence on TGF-β3.

4.2.2 Microarray Hybridization and Analysis

Total RNA was extracted and quantified as described in Section 3.2.6. Microarray services were provided by the Penn Microarray Facility, including quality control tests of total RNA by Agilent Bioanalyzer and Nanodrop spectrophotometry. All protocols were conducted as described in the NuGEN Ovation manual and the Affymetrix GeneChip Expression Analysis Technical Manual. Briefly, 100 ng of total RNA was converted to first-strand cDNA using reverse transcriptase primed by a poly(T) oligomer that

incorporated a synthetic RNA sequence. Second-strand cDNA synthesis was followed by ribo-SPIA (Single Primer Isothermal Amplification, NuGEN Technologies Inc. San Carlo, CA) for linear amplification of each transcript, and the resulting cDNA was fragmented, assessed by Bioanalyzer, and biotinylated. cDNA yields ranged from 5-10 μg, and 5 μg were added to Affymetrix hybridization cocktails, heated at 99ºC for 2 min and hybridized for 16 h at 45ºC to 9 Bovine GeneChips (Affymetrix Inc., Santa Clara, CA). Microarrays were washed at low (6X SSPE) and high (100mM MES, 0.1M NaCl) stringency and stained with streptavidin-phycoerythrin. Fluorescence was amplified by adding biotinylated anti-streptavidin and an additional aliquot of streptavidin-phycoerythrin stain. Fluorescence signals were collected after excitation at 570 nm by the Affymetrix Gene Chip Scanner 3000 (Affymetrix Inc.).

Output (.cel) files from scanning were processed using Microarray Suite (v.5, Affymetrix Inc., Santa Clara, CA) and gene expression was assessed after normalization. Expression levels were evaluated for free-swelling week 6 MSCs in CM-, free-swelling week 6 MSCs in CM+ and dynamically loaded MSCs in CM+ at week 6. Microarray data were analyzed using Spotfire Software (Tibco, Somerville, MA). All microarray data discussed in this manuscript have been deposited in NCBI's Gene Expression Omnibus and are accessible through GEO Series accession number GSE18879 (http://www.ncbi.nlm.nih.gov/geo/query/acc.cgi?acc=GSE18879).

4.2.3 Histology and Immunohistochemistry

Paraffin sections (8 μm) were stained with hematoxylin and eosin (H&E, Sigma, St. Louis, MO), Alcian Blue (pH 1.0), or Picrosirius Red for cell distribution, sulfated proteoglycans

and collagens, respectively (Section 3.2.7). For immunohistochemistry, antigen retrieval was performed by incubating sections in proteinase K (20 μg/mL in TE buffer, pH 8.0) at 37°C for 15 minutes, then at 25°C for 10 minutes. Collagens type I (MAB3391, Millipore, Billerica, MA) and type II (11-116B3, Developmental Studies Hybridoma Bank, Iowa City, IA) primary antibodies were used. Subsequent reaction and visualization with DAB chromogen reagent (DAB150 IHC Select, Millipore, Billerica, MA) was carried out according to manufacturer's instructions as in Section 3.2.8. Color images were captured at 2.5X or 10X magnification using a microscope equipped with a color CCD digital camera and the QCapturePro acquisition software.

4.2.4 Fourier Transform Infrared Imaging Spectroscopy (FT-IRIS)

FT-IRIS was carried out using a Spectrum Spotlight 300 spectrometer (Perkin-Elmer, Waltham, MA) equipped with an optical microscope and an array detector. Sections (8 μm) were mounted onto barium fluoride windows and scanned with a spatial resolution of 25 μm and a spectral resolution of 4 cm^{-1}. The acquired spectra were analyzed using ISys software 5.0 (Malvern Instruments Ltd., Worcestershire, UK). Collagen and proteoglycan distributions were determined by molecular vibrations at specific frequencies (wavenumber, cm^{-1}); the amide I absorbance band (1720-1592 cm^{-1}; C=O stretch) was used to map collagen while proteoglycans were visualized using the 1176-960 cm^{-1} band (C-O-C and C-OH ring vibrations)(Kim et al. 2005; Boskey et al. 2007). FT-IRIS analysis was performed on three samples per group.

4.2.5 Statistical Analysis

Statistics were performed on mechanical and biochemical data using ANOVA. For Studies 1 and 2, a two way ANOVA was used with media and loading condition as independent variables. For Studies 3-5, a one way ANOVA was carried out. Where significance was indicated by ANOVA, Tukey's posthoc tests were performed. Significance was determined at $p \leq 0.05$ and a trend toward significance determined at $p < 0.1$. All values are reported as mean ± standard deviation.

4.3 Results

4.3.1 Dynamic Compression Initiated Before Chondrogenesis Impairs Functional Maturation of MSC-Seeded Constructs

To examine the effects of direct mechanical stimulation on functional chondrogenesis, MSC-seeded constructs were subjected to repeated dynamic compression over 3 weeks. In Study 1, dynamic loading (DL) was initiated 3 days after MSC encapsulation and carried out in the presence (CM+) or absence (CM-) of TGF-β3. Free swelling (FS) controls were cultured and analyzed identically. The equilibrium and dynamic compressive moduli improved with time in culture for all groups cultured in CM+, regardless of loading ($p < 0.05$). Consistent with our previous studies (Huang et al. 2009), the equilibrium and dynamic modulus of FS CM+ constructs reached ~80 kPa and ~350 kPa, respectively, by 3 weeks. Conversely, the modulus of FS CM- constructs remained similar to that of acellular 2% agarose (~2 kPa, **Figure 4-2A**). Long-term DL initiated 3 days after construct fabrication significantly reduced the mechanical properties of CM+ constructs at 3 weeks relative to FS CM+ controls ($p < 0.05$). At 3 weeks, the equilibrium

and dynamic moduli of DL CM+ constructs were ~35 kPa and ~230 kPa, respectively (**Figure 4-2A, B**). Although significantly greater than day 0 properties (equilibrium modulus: ~ 2 kPa, dynamic modulus: ~ 45 kPa), these values were less than two thirds that of FS CM+ constructs.

While DL did not change the mechanical properties of CM- constructs (**Figure 4-2A, B**), GAG content was reduced with DL (trend, $p=0.07$), although DNA and collagen contents were not affected (**Figure 4-2C-E**). DL applied in CM+ reduced all biochemical measures relative to FS CM+. Despite this reduction, DNA and GAG contents remained significantly higher in DL CM+ compared to either FS CM- or DL CM- groups, indicating that successful chondrogenesis had occurred, but to a lesser extent. DNA content for both FS and DL groups at 3 weeks was also significantly higher than day 3 starting values, while GAG content on a per cell basis (GAG/DNA) was comparable between 3 week FS and DL CM+ groups (not shown). These quantitative biochemical findings were mirrored qualitatively in histological sections, with less intense staining for proteoglycans and collagens in DL CM+ compared to FS CM+ sections (**Figures 4-2F-K**).

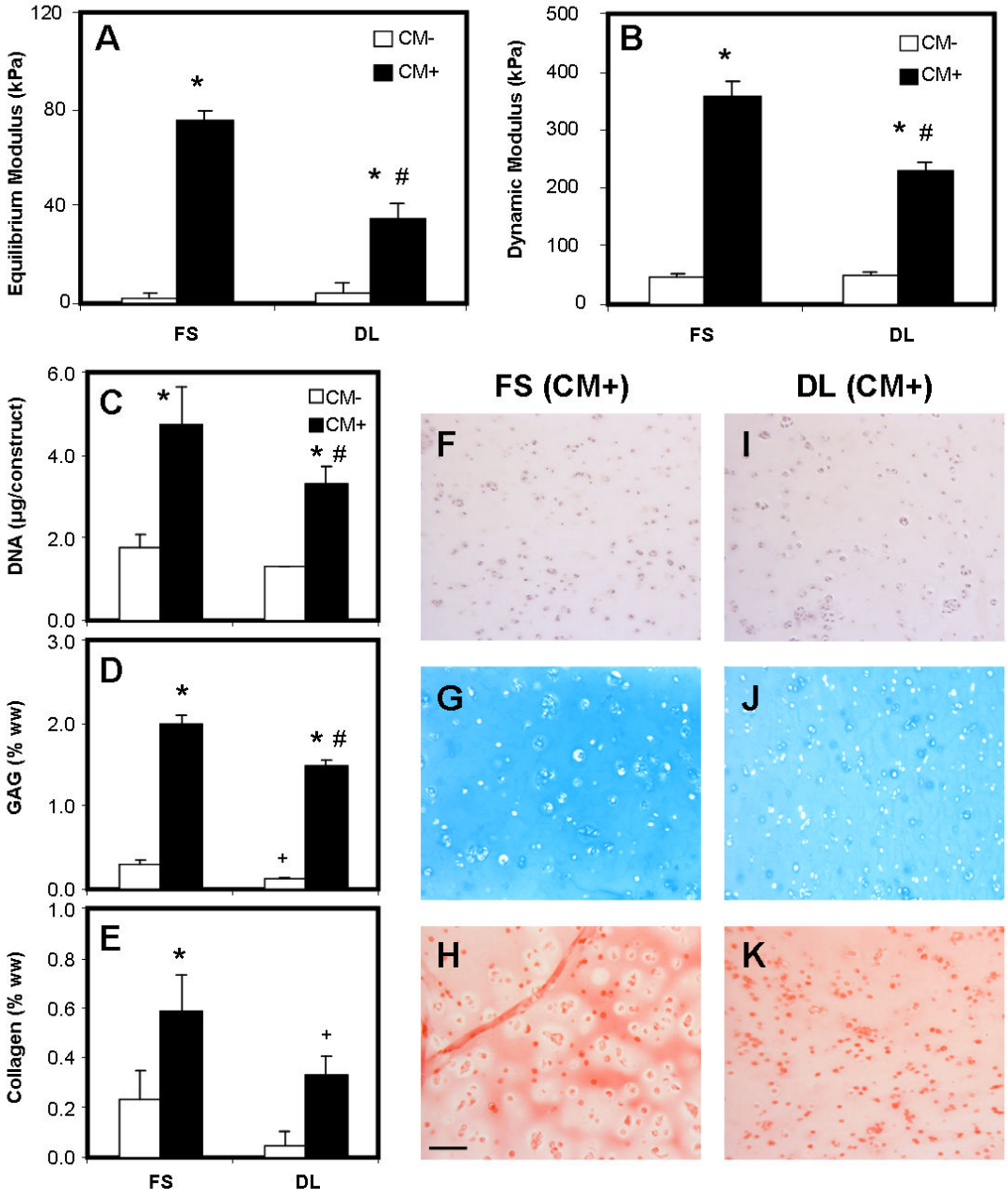

Figure 4-2: Long-term dynamic compression initiated directly after construct fabrication blocks functional maturation. (A) The equilibrium and (B) dynamic moduli of MSC-seeded constructs loaded in CM+ were impaired by 3 weeks of dynamic compression. (D) DNA, (E) GAG, and (F) collagen contents were similarly affected. Histological analysis confirmed these findings with (F, I) H&E, (G, J) Alcian Blue, and (H, K) Picrosirius Red staining for cell content, proteoglycans and collagens, respectively. Scale bar: 100 µm. * indicates greater than CM- ($p<0.05$), # indicates lower than FS CM+ ($p<0.05$), + indicates lower than FS control within media condition ($p<0.1$). Data represent the mean and standard deviation of three samples per group per time point.

Real-time PCR analysis of these MSC-seeded constructs showed that while DL reduced mechanical and biochemical measures, DL increased expression of both AGC1 and COL2A1 at almost every time point assayed in both CM- and CM+ media relative to FS controls (**Figure 4-3**).

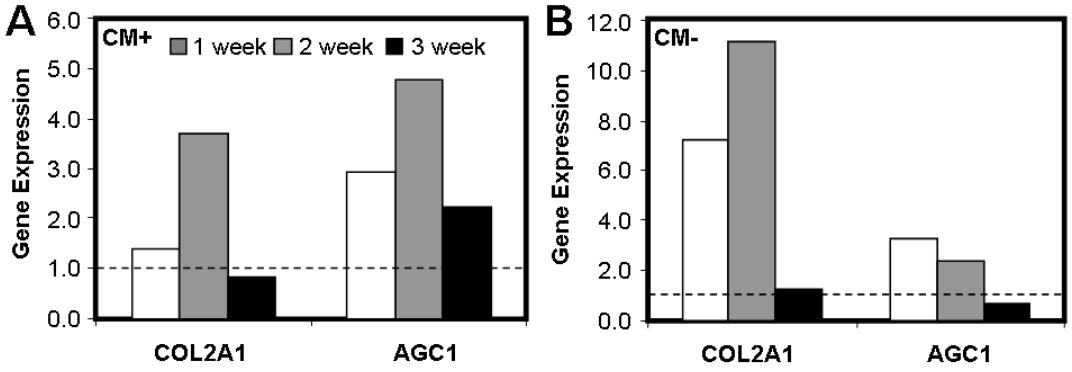

Figure 4-3: Long-term dynamic compression initiated directly after construct fabrication improves chondrogenic gene expression. At nearly every timepoint, COL2A1 and AGC1 expression improved with loading in (A) CM+ and (B) CM- media. Expression levels were normalized to free-swelling controls at each timepoint (indicated by the dashed line).

4.3.2 Long-Term Dynamic Compression Initiated After Chondrogenic Pre-Culture Improves Functional Properties of MSC-Seeded Constructs

To assess whether a period of chondrogenic pre-culture alters functional maturation in response to DL, MSC-seeded constructs were differentiated in TGF-β3 containing media prior to the initiation of loading (Study 2). Constructs were cultured in CM+ for 3 weeks (weeks 1-3) and then subjected to 3 weeks of dynamic loading (weeks 4-6) in CM+ or CM-. As we have previously observed (Huang et al. 2009), the mechanical properties of MSC-seeded constructs increased with time, but plateaued after 3 weeks, with no significant difference in mechanical properties between the 3 and 6 week FS groups in CM+ (not shown). In contrast to Study 1, the equilibrium and dynamic properties of pre-

cultured constructs with 3 additional weeks of DL in CM+ were significantly higher than FS controls in CM+ (**Figure 4-4A**). DL CM+ constructs reached equilibrium and dynamic moduli at week 6 of ~150 kPa (65% increase vs. FS CM+) and ~800 kPa (38% increase vs. FS CM+), respectively. This increase in properties with DL was only observed when loading was applied in CM+. In the absence of TGF-β3 (CM- from week 4 to week 6), DL did not change mechanical properties. To better understand the threshold for DL-induced improvements in functional properties, Studies 3 and 4, examined the influence of loading duration (1 or 4 hours) and loading frequency (0.01 or 1 Hz) on construct properties. While DL in CM+ for 4 hours per day at 1 Hz always increased mechanical properties compared to FS controls, DL for 1 hour per day at 1 Hz or 4 hours per day at 0.01 Hz had no effect on these measures (**Figures 4-4B, C**).

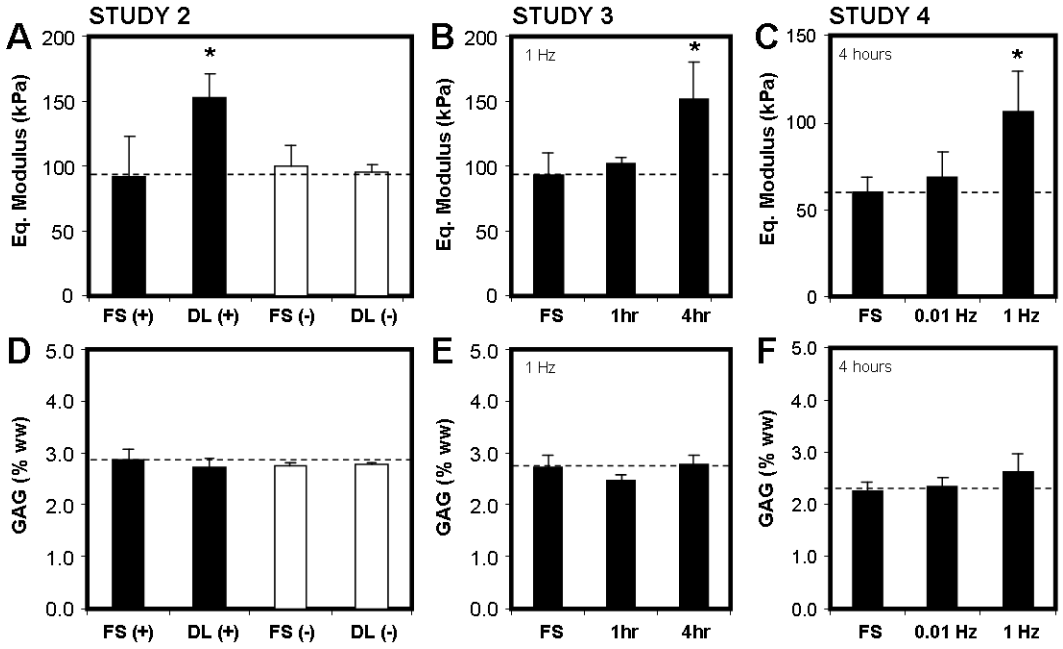

Figure 4-4: Long-term dynamic loading initiated after chondrogenic pre-culture improves mechanical properties. (A-C) The equilibrium modulus of MSC-seeded constructs improved only when loading was applied in CM+ for 4 hours per day at 1 Hz. No improvement in mechanical properties was observed when other loading regimens were employed. (D-F) GAG content was not affected by loading. Black bars indicate CM+ media and white bars indicate CM- media. * indicates greater than control ($p<0.05$). Data represent the mean and standard deviation of three to five samples per group per time point.

Despite increases in mechanical properties, GAG (**Figures 4-4D-F**) and collagen (**Figure 4-5**) contents were not different between any of the CM+ groups. Similarly, GAG released into the media was not different when comparing FS to DL (data not shown). DNA content was not affected by loading in Studies 2 and 4, but was slightly reduced in the 4 hour loaded samples compared to FS conditions in Study 3 (**Figure 4-5**).

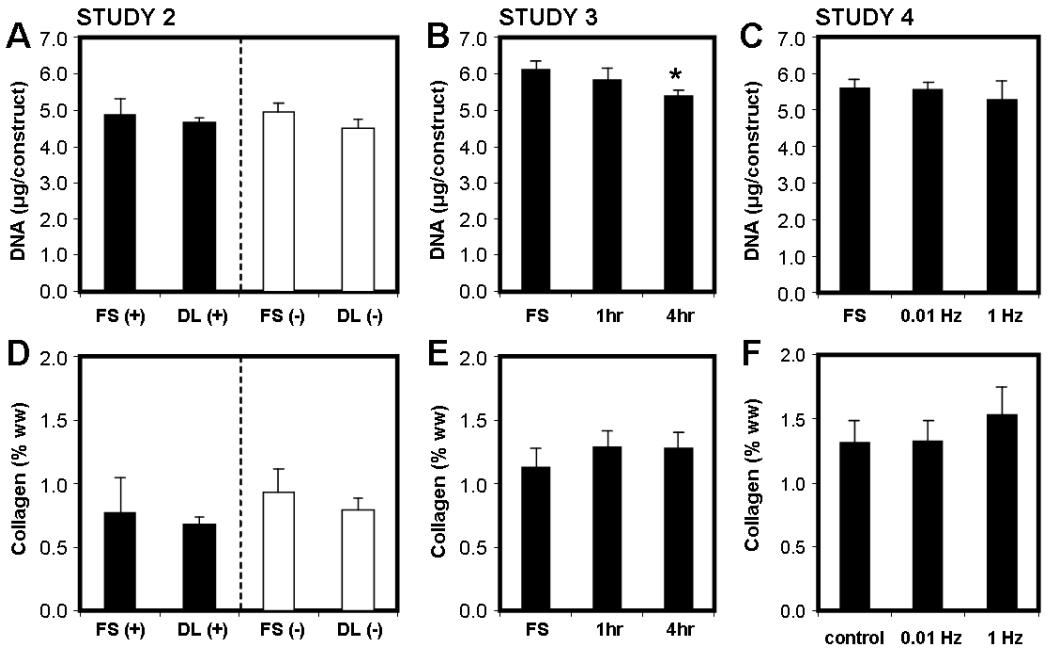

Figure 4-5: Long-term dynamic loading initiated after chondrogenic pre-culture does not improve biochemical content. (A-C) The DNA and (D-F) collagen contents of MSC-seeded constructs were largely unchanged with dynamic compressive loading. Black bars indicate CM+ media and white bars indicate CM- media. * indicates greater than control ($p<0.05$). Data represent the mean and standard deviation of three to five samples per group per time point.

4.3.3 Long-Term Dynamic Compression Enhances Matrix Distribution

Based on Studies 1-4, a dynamic compressive loading protocol of 4 hours per day at a frequency of 1 Hz, initiated after 3 weeks of pre-culture, was applied in a final study designed to further elucidate the mechanism of load-induced increases in mechanical properties of MSC-seeded constructs (Study 5). As before, loading was carried out for 5 days per week for 3 weeks. Consistent with these previous iterations, the equilibrium modulus improved with DL, but bulk GAG and collagen contents were not different compared to FS (**Figure 4-6A, B**). FS CM- constructs did not deposit appreciable ECM with long-term culture; these findings were confirmed histologically, with weak pericellular staining for proteoglycans and collagens observed. At the microscopic level, GAG distribution was similar between CM+ DL and FS constructs, while collagen

content was more uniformly distributed in the CM+ DL groups (**Figure 4-6**). At the final time point, all CM+ constructs stained strongly for type II collagen and weakly for type I collagen (**Figure 4-7**), regardless of loading condition (**Figure 4-6J, K**). Type II collagen was more uniformly distributed with DL, consistent with the Picrosirius Red stains. Despite the absence of TGF-β3, by week 6, a subset of MSCs in CM- had undergone chondrogenesis to a limited extent, depositing a small amount of type II collagen in the immediate pericellular space (**Figure 4-6I**).

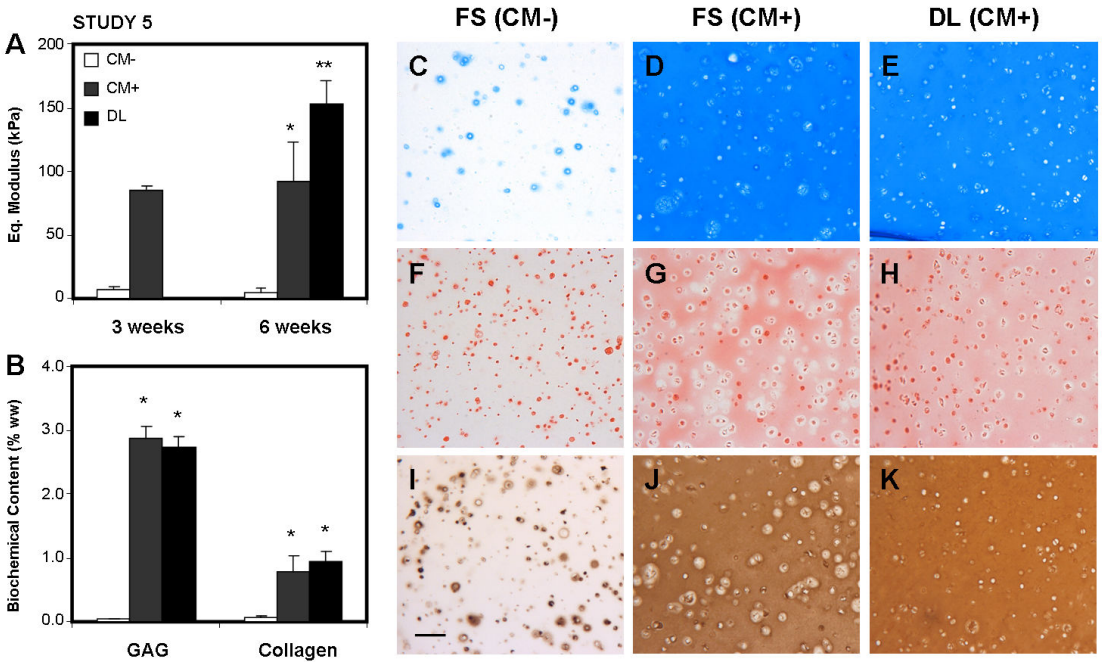

Figure 4-6: Long-term dynamic loading initiated after 3 weeks of chondrogenic pre-culture improves microscopic ECM distribution. (A) The equilibrium modulus of MSC-seeded constructs was higher in CM+ compared to CM- at 3 and 6 weeks; dynamic loading in CM+ for 3 weeks further improved mechanical properties. (B) Biochemical content of dynamically loaded constructs was not different compared to CM+ controls. (C-E) Alcian Blue staining showed equal distribution of proteoglycans between CM+ controls and loaded constructs with weak staining in CM- controls. (F-H) Picrosirius Red staining and (I-K) collagen type II immunostaining showed more homogeneous distribution of collagen in loaded constructs compared to controls, on the microscopic level. Scale bar: 100 μm. * indicates greater than CM- controls ($p<0.05$), ** indicates greater than CM+ controls ($p<0.05$). Data represent the mean and standard deviation of three samples per group per time point.

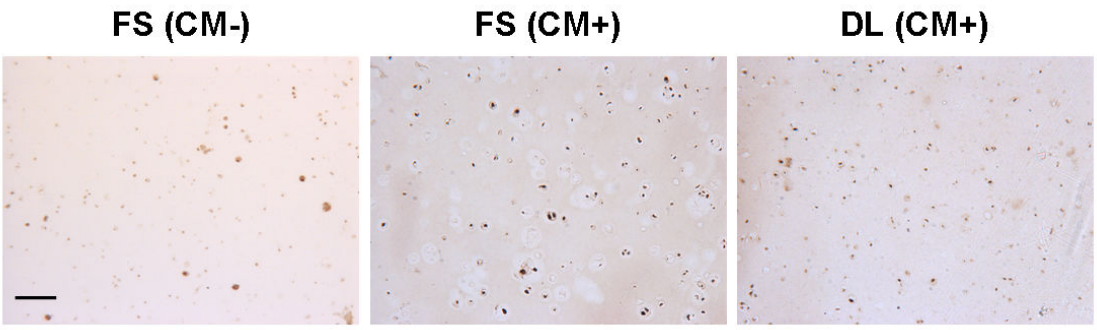

Figure 4-7: Type I collagen staining of free-swelling and dynamically loaded constructs. Weak, pericellular staining for type I collagen was observed for all constructs, regardless of loading. Scale bar: 100 μm.

Finally, FT-IRIS was performed as a more sensitive measure of proteoglycan and collagen distribution across the construct expanse. Characteristic spectra for proteoglycans and collagens showed consistently improved distribution with DL, particularly in the construct central regions (**Figure 4-8**).

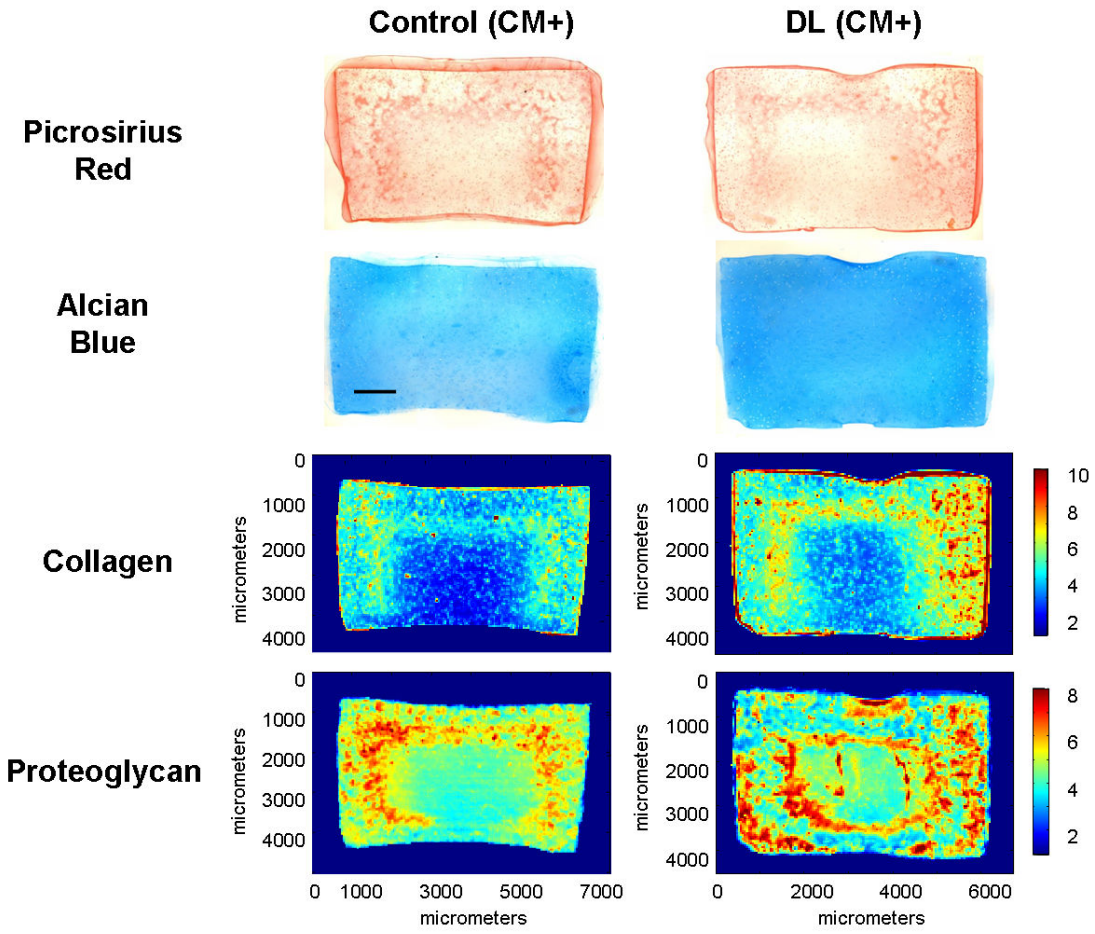

Figure 4-8: FT-IRIS assessment of matrix distribution. Whole construct views of Picrosirius Red and Alcian Blue stained cross-sections showing distributions of collagen and proteoglycan within FS and DL constructs. Spectral data obtained from FT-IRIS analysis, a more sensitive and semi-quantitative measurement technique, showed improved collagen and proteoglycan distribution within MSC-seeded constructs with dynamic compressive loading. Scale bar: 1mm.

4.3.4 Expression Profiles With Chondrogenic Induction and Long Term Dynamic Compression

In a final analysis, a preliminary microarray screen was performed to visualize shifts in molecular topography that might underlie the observed differences in mechanical properties with dynamic loading. This screen compared whole genome expression profiles for week 6 FS CM- samples (undifferentiated), FS CM+ samples (differentiated), and DL

CM+ samples. CM- and CM+ groups were chosen as undifferentiated and differentiated controls, respectively, in order to identify markers associated with functional chondrogenesis. Heat maps at week 6 showed changes in gene expression with chondrogenesis (CM+ vs. CM-), with higher and lower levels of expression for individual genes depicted in red and green, respectively (**Figure 4-9A**). While the molecular fingerprints between FS CM+ and DL CM+ were more alike compared to FS CM-, DL modulated the expression of a number of genes (**Figure 4-9A**). Venn diagrams showed 5449 genes that were chondrogenic, but not mechanically sensitive; of these genes, 4280 were up-regulated and 1169 were down-regulated during chondrogenesis (**Figure 4-9B, C**). In addition, numerous genes associated with chondrogenesis were further modulated by DL (413 up-regulated, 139 down-regulated). A complete list of the genes modulated by DL can be found in **Appendix 1**.

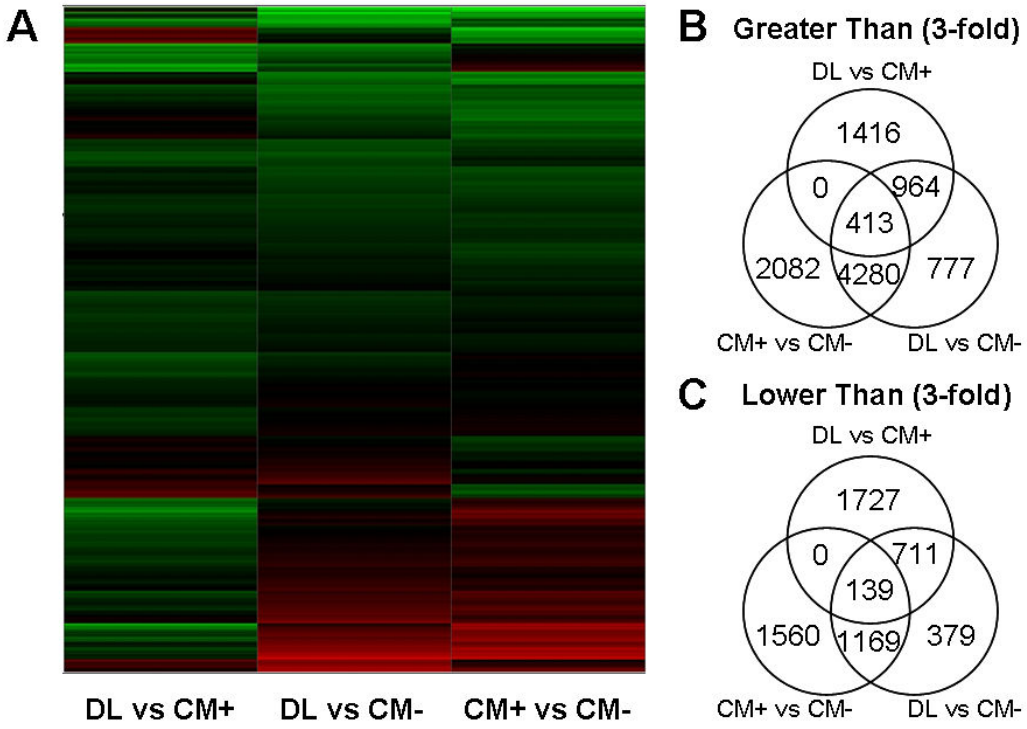

Figure 4-9: Molecular topography of chondro-induction and mechanosensitivity. (A) Heat map generated from microarray data showing differential gene expression (green = greater, red = lower) between CM- free-swelling (FS) controls (CM-), CM+ FS controls (CM+) and constructs dynamically loaded (DL) in CM+ at day 42. (B, C) Venn diagrams of CM-, CM+ and DL indicate a number of genes that were differentially regulated with chondrogenic induction (CM+) in 3D culture and with dynamic compressive loading (>3-fold).

4.4 Discussion

Mesenchymal stem cells (MSCs) are an ideal candidate for cartilage tissue engineering given their ability to undergo chondrogenesis in 3D culture. Under pro-chondrogenic conditions, MSCs deposit a cartilage-specific matrix and accrue increasingly robust mechanical properties with time. However, recent findings suggest that further optimization may be required to generate properties akin to that of the native tissue, or that of articular chondrocytes cultured similarly (Mauck et al. 2006; Huang et al. 2009). As mechanical stimulation plays a unique role in both cartilage development and the maturation of chondrocyte-based engineered constructs, we examined long-term dynamic

compressive loading as a means of modulating MSC-seeded construct properties and chondrogenesis

Consistent with previous findings, long-term dynamic loading initiated soon after MSC encapsulation in the presence of TGF-β3 reduced the mechanical properties of constructs compared to free-swelling controls (Thorpe et al. 2008). While biochemical content was lower in these dynamically loaded samples, GAG content per cell was not different from controls and chondrogenic gene expression was up-regulated with loading at each time point assayed. As loading did not affect cell viability, this data suggests that long-term loading in the presence of TGF-β3 reduced MSC proliferation with commensurate decreases in bulk biochemical and mechanical properties, but did not impair chondrogenic differentiation. Dynamic compression alone, in the absence of TGF-β3, failed to induce chondrogenesis; in fact, after three weeks of loading, GAG content decreased in loaded groups, though chondrogenic gene expression increased. Thus, while long-term dynamic compression, initiated prior to cell differentiation or matrix deposition, may improve the expression of AGC1 and COL2A1, mechanical properties and GAG content are inferior in these samples, regardless of TGF-β supplementation. Whether this lower GAG content in loaded constructs is due to poor retention of synthesized GAG (caused by differences in molecule size/assembly or possible upregulation of catabolic agents), or due to an actual reduction in GAG synthesis is currently unclear.

In contrast to these findings, loading initiated after chondrogenesis and matrix elaboration in the presence of TGF-β3 consistently improved the mechanical properties of MSC-seeded constructs. As all other factors remained constant, the timing of load initiation was crucial in determining functional outcomes. These divergent responses to loading can be attributed to changes in MSC phenotype and construct properties with maturation. Work in ligament tissue engineering support the notion that the timing of mechanical stimulation with MSC developmental stage may be a critical determinant of cell response to load (Chen et al. 2006). Similarly, dynamic compression applied after an extended pre-culture time improved chondrogenic gene expression of MSCs, as well as embryonic stem cells (Mouw et al. 2007; Terraciano et al. 2007). As the nuclei of undifferentiated stem cells deform more readily than that of differentiated cells (Pajerowski et al. 2007), the differentiation status of MSCs may play an important role in how these cells perceive external mechanical stimulation. Cell-matrix interactions may also affect load-induced response; since agarose is an inert material, these interactions emerge only as MSCs differentiate and generate local ECM. With matrix elaboration, the physical environment of the cells under dynamic compression is also altered. As construct composition shifts from 2% agarose to a denser, cartilage-like matrix of proteoglycans and collagen and construct permeability decreases, the stresses induced by dynamic compression are higher and largely borne through fluid pressurization (Soltz et al. 1998); this is apparent from our mechanical testing results showing marked increases in the dynamic modulus with culture duration. These differences in fluid pressurization and fluid flow may underlie the profoundly disparate outcomes we observe with dynamic compressive loading, depending on construct maturity. This is consistent with several studies showing

that application of hydrostatic pressure to human MSC aggregates improves cartilaginous matrix deposition and gene expression (Angele et al. 2003; Miyanishi et al. 2006).

Interestingly, in the absence of TGF-β3, compressive loading initiated after chondrogenic pre-culture did not elicit any changes in functional properties, indicating that the load-induced increase in mechanics is dependent on TGF-β3. This is consistent with previous findings showing improved matrix synthesis and pSmad2/3 protein levels in pre-cultured bovine MSC-seeded agarose with a single application of loading, when loading was applied in the presence of TGF-β1 and dexamethasone (Mouw et al. 2007). In contrast to MSCs, repeated dynamic compression of pre-cultured chondrocyte-seeded agarose improved the mechanical properties of these constructs when loading was applied in the absence of TGF-β3 (Lima et al. 2007). Long-term dynamic compression initiated prior to matrix elaboration also improved the functional properties of chondrocyte-based constructs, though these studies were conducted in the presence of serum (Mauck et al. 2000). Collectively, these studies suggest that the mechanotransduction pathways initiated by dynamic compression may be fundamentally different between chondrocytes and undifferentiated or chondrogenically differentiated MSCs and underscores the need for better characterization of these cell types relative to one another.

While it is unclear how dynamic compression may improve functional MSC chondrogenesis, one potential mechanism may be facilitated nutrient/growth factor transport with dynamic deformation. Theoretical models of dynamic compression of porous permeable materials indicate that solute transport into constructs may be

improved by dynamic loading and that higher frequencies enhance this phenomenon (Mauck et al. 2003). Recent experimental findings validate these theoretical predictions and show that, in particular, the transport of large solutes (with molecular weights similar to that of growth factors such as TGF-β) is facilitated by dynamic compression and is dependent on loading duration (Albro et al. 2008; Chahine et al. 2009). In one set of experiments with acellular agarose gels of varying concentrations, solute uptake increased for higher concentration gels (Albro et al. 2008). These results parallel findings from the current study, where mechanical properties only increased when dynamic loading was initiated after pre-elaboration of matrix (denser construct), and applied at longer durations (4 hours vs. 1 hour) at a higher frequency (1 Hz vs. 0.01 Hz). Notably, loading in the absence of exogenous TGF-β3 (after chondrogenic pre-culture) failed to elicit any changes in mechanical properties.

Although enhanced transport of nutrients or TGF-β is one possible mechanism, MSC responsivity to mechanical stimulus may also be an important factor. To assess MSC response on the molecular level, we carried out microarray analysis of loaded and free-swelling constructs and saw marked overlap in chondrogenic gene expression, indicating successful induction and stability of the chondrogenic phenotype. Consistent with these findings, all constructs stained strongly for collagen type II and weakly for collagen type I. As bulk GAG and collagen contents were not affected by loading (despite increases in mechanical properties), minor elements involved in matrix remodeling and refinement may be of consequence. Though preliminary, microarray analysis indicated modulation of several genes from the MMP/TIMP family, as well as specialized cross-linking molecules.

Additional analyses will be necessary to validate these findings and determine the potential role of these genes under dynamic compression. Although measurement of gene expression is not necessarily a reliable predictor of functional chondrogenesis (i.e. Study 1), evidence for matrix remodeling was found by histology and FT-IRIS. These analyses showed improved matrix distribution after 3 weeks of repeated loading. Histological stains showed better pericellular distribution of collagen and FT-IRIS showed enhanced macroscopic distribution of proteoglycans and collagens throughout the construct expanse. This is consistent with previous studies of chondrocyte-based constructs showing improved collagen organization (assessed by polarized light microscopy) with dynamic compressive loading (Kelly et al. 2006).

To our knowledge, this is the first study to demonstrate improved mechanical properties of MSC-based engineered cartilage through the long-term application of dynamic compressive loading. While the mechanism underlying these increased properties is not yet established, we show that improved matrix distribution, suggestive of matrix remodeling and refinement occur with dynamic compression. Although we achieved a ~65% improvement in mechanical properties over 3 weeks of loading, these values remain lower than native cartilage. Future studies will optimize these parameters over longer culture durations to further explicate load-induced increases in mechanical properties. We will also evaluate MMP activity and the expression and distribution of minor elements indicated from microarray analysis, as well as assess proteoglycan size and collagen crosslinking with dynamic loading. The use of other biomaterials, including materials that mimic the native ECM or materials that include hydrolytic or MMP-cleavable components

to allow better matrix distribution, may also aid matrix remodeling and further enhance functional outcomes (Lutolf et al. 2003; Park et al. 2004; Chung et al. 2009; Erickson et al. 2009). The combination of these tunable materials with our optimized loading regime will generate clinically-relevant, mechanically robust MSC-based constructs for articular cartilage repair.

CHAPTER 5: EVALUATION OF THE COMPLEX MOLECULAR TOPOGRAPHY OF MESENCHYMAL STEM CELL CHONDROGENESIS FOR CARTILAGE TISSUE ENGINEERING

5.1 Introduction

If MSC-based solutions for cartilage degeneration are to be successful, certain critical considerations must be evaluated. Because cartilage exists in a harsh load-bearing environment, engineered MSC-based neo-cartilage must replicate key functional (i.e., mechanical) features of the native tissue (Chapter 2). Toward that end, MSCs have been cultured in a number of 3-dimensional (3D) hydrogels (Huang et al. 2010). These materials support chondrogenesis and the deposition of an increasingly stiff matrix when cultured in the presence of TGF-β superfamily members (Kavalkovich et al. 2002; Buxton et al. 2007; Kisiday et al. 2008; Chung et al. 2009; Erickson et al. 2009; Erickson et al. 2009). While this chondrogenic potential in 3D culture is encouraging, comparisons to differentiated chondrocytes cultured identically consistently show that MSC-based constructs do not achieve the same functional properties (Mauck et al. 2006; Huang et al. 2009). Standard means of enhancing functional growth in chondrocyte-based constructs, such as increasing cell-seeding density or the application of long-term dynamic compressive loading protocols, as described in Chapters 3 and 4, have thus far not improved the compressive properties of MSC-based constructs to native levels (Thorpe et al. 2008; Huang et al. 2009).

These findings underscore the inherent differences between chondrocytes and chondrogenically induced MSCs, and suggest the need for a more complete evaluation of chondrogenesis in relation to differentiated cells, and how this phenotypic transition relates to mechanical function. To date, most work in the field has focused on whether or not chondrogenesis has occurred (defined by the expression of a few key cartilaginous genes and the deposition of proteoglycans and collagen type II), and on identifying genes associated with this differentiation process. For example, several studies have characterized the temporal profiles of known chondrogenic markers during MSC chondrogenesis, at both the molecular and tissue levels (Barry et al. 2001; Sekiya et al. 2002; Xu et al. 2008). Other recent microarray studies identified new candidate markers by comparing undifferentiated MSCs and cartilage (Boeuf et al. 2007), while still others have employed microarray analysis to evaluate differentiation and subsequent dedifferentiation of MSCs to identify 'differentiation' and 'stemness' genes through multiple lineage progression (Song et al. 2006).

Collectively, these studies provide important information on the molecular events underlying MSC chondrogenesis, and have identified key factors in this process. However, most have taken a "yes/no" approach in defining chondrogenesis and have not assessed the differences in functional capacity between chondrogenically differentiated MSCs and fully differentiated chondrocytes in a 3D, tissue engineering context. The current standard of reference for chondrogenic induction of MSCs is often an undifferentiated MSC or a healthy or osteoarthritic chondrocyte. To our knowledge, there exists no study comparing the molecular fingerprints of donor-matched healthy

MSCs and chondrocytes maintained under identical culture conditions *in vitro* in 3D culture. As it is under these conditions that we observe robust growth of chondrocyte-based constructs (Lima et al. 2007; Byers et al. 2008) and functional limitations in MSC chondrogenesis (Mauck et al. 2006), it is under these conditions that we must identify the underlying molecular differences that define these functional disparities.

To address this issue, the current study was undertaken to identify markers of functional MSC chondrogenesis. A genome-wide screen using bovine microarrays was carried out using healthy donor-matched cells (chondrocytes and MSCs) seeded in 3D culture. Three donors were evaluated after long-term culture under identical, pro-chondrogenic conditions, and the molecular profiles of undifferentiated MSCs, chondrogenically differentiated MSCs and chondrocytes were evaluated. Through this process, we defined a novel set of factors that were differentially regulated between these groups and showed that these differences in expression existed in both the absolute and temporal sense. This study provides critical new insight into the complexity of chondrogenesis on a molecular level, and provides new targets for enhancing their functional maturation and clinical potential.

5.2 Materials and Methods

5.2.1 Construct Fabrication and Long-Term 3D Culture

Donor-matched chondrocytes and MSCs were isolated as described in Section 3.2.1 from three juvenile calves. Cell-seeded constructs (20 million cells/mL, Ø4 x 2.25 mm) were formed as in Section 3.2.2, with each donor kept separate. Constructs were cultured for 56

days in 1 mL/disk of chemically defined media (CM, Section 3.2.2) supplemented with 10 ng/mL TGF-β3 (CM+, R&D Systems, Minneapolis, MN). At biweekly intervals, constructs were evaluated for mechanical properties and biochemical content as in Sections 3.2.4 and 3.2.5. Gene expression of day 0 and day 28 MSC-seeded constructs as well as day 28 chondrocyte-seeded constructs were evaluated using microarrays (described below) and real-time PCR (as in Section 3.2.6). In subsequent studies assessing gene expression over long-term culture, MSC- and chondrocyte-seeded constructs were fabricated as above with cells from three donors combined. Cell-seeded constructs were cultured in CM+ for 56 days. Gene expression was evaluated biweekly, and mechanical properties were assessed at day 56.

5.2.2 Microarray: Target Preparation and Hybridization

Total RNA was extracted and quantified as described in Section 3.2.6. Microarray services were provided by the Penn Microarray Facility, including quality control tests of total RNA by Agilent Bioanalyzer and Nanodrop spectrophotometry. All protocols were conducted as described in the NuGEN Ovation manual and the Affymetrix GeneChip Expression Analysis Technical Manual. Briefly, 100 ng of total RNA was converted to first-strand cDNA using reverse transcriptase primed by a poly(T) oligomer that incorporated a synthetic RNA sequence. Second-strand cDNA synthesis was followed by ribo-SPIA (Single Primer Isothermal Amplification, NuGEN Technologies Inc. San Carlo, CA) for linear amplification of each transcript, and the resulting cDNA was fragmented, assessed by Bioanalyzer, and biotinylated. cDNA yields ranged from 5-10 μg, and 5 μg were added to Affymetrix hybridization cocktails, heated at 99ºC for 2 min

and hybridized for 16 h at 45ºC to 9 Bovine GeneChips (Affymetrix Inc., Santa Clara, CA). Microarrays were washed at low (6X SSPE) and high (100mM MES, 0.1M NaCl) stringency and stained with streptavidin-phycoerythrin. Fluorescence was amplified by adding biotinylated anti-streptavidin and an additional aliquot of streptavidin-phycoerythrin stain. Fluorescence signals were collected after excitation at 570 nm by the Affymetrix Gene Chip Scanner 3000 (Affymetrix Inc.).

5.2.3 Microarray Data Analysis

Output (.cel) files from scanning were processed (Partek, St. Louis, MO) and gene expression was assessed after normalization with the RMA algorithm. Principal component analysis was carried out to determine global variation. To determine statistical significance, a two-way mixed model ANOVA was applied with donor and cell type as the independent variables. Three pairwise contrasts were evaluated to assess fold-changes in gene expression levels. Changes in expression were assessed between donor-matched undifferentiated MSCs (day 0) and differentiated MSCs (day 28), undifferentiated MSCs (day 0) and chondrocytes (day 28), as well as differentiated MSCs (day 28) and chondrocytes (day 28). P-values were generated for donor, cell type and each pairwise contrast. To determine false discovery rates, the Benjamini Hochberg method was applied to the generated p-values and step-up p-values were calculated. Genes that were considered under-expressed during chondrogenesis were defined as those that were at least 2-fold greater in chondrocytes compared to both day 0 and day 28 MSCs and no more than 2 fold less or 3 fold greater in day 28 MSCs compared to day 0 MSCs. Genes that were considered over-expressed were defined as genes that were at

least 2-fold greater in both day 0 and day 28 MSCs compared to chondrocytes, and no more than 2-fold greater in day 28 MSCs compared to day 0 MSCs. Genes of interest were identified using a false discovery rate (FDR) of 10% (Spotfire software; Tibco, Somerville, MA). Expression was verified by real-time PCR for the genes listed in **Figure 5-6C**. The primer sequences used are listed in **Table 5-1** below. All microarray data discussed in this manuscript have been deposited in NCBI's Gene Expression Omnibus and are accessible through GEO Series accession number GSE18394 (http://www.ncbi.nlm.nih.gov/geo/query/acc.cgi?acc=GSE18394).

Table 5-1: Primer sequences of genes identified from microarray screening.

Gene	Forward Primer	Reverse Primer
Dikkopf-1	GCTCCAGGAATTCCGTTTGA	GATACGGCTGGTGGTTGTCA
Periostin	CCTGATTCTGCCAAACAAGTTATTG	GGGCCACAAGGTCTGTGAA
CXCL14	CAGAGCACCAAGCGGTTCA	TAGACCCTGCGCTTCTCGTT
HOX4A	TGGAGGATCGCATCTTAGTGTTGGG	GCAGGTCTTGGAGCTGGAGAAAGAG
Calpain 6	GCTCAGGGAGCTGACTATGGA	GTAGCCACGAGCCAGATTCC
Caspase 4	CGACTCATCACATGCTTCCAA	TTTTCAAATGATTGTTGTACCTTCCT
ID1	TCCAGCACGTCATCGACTACA	ACGTGGGATTCCGAGTTGAG
Chondromodulin	GGGAGCGACAATCACATTTACA	CATTGACCCATCTTGCAACTTC
SOSTDC1	GTTCAAGTAGGCTGCCGAGAA	GCACTGGCCGTCTGAGATG
Leiomodin 1	TGCTCAGCTTCTGTGAAAAGGA	CCTTTTTCGCATCTGTCTTGGT
THBS4	CGTGATCTCCACCTTCAAGCT	GAAGAGTAAAGGCCGAAGATGGT
MAGEL2	GCAGCTGCCCCACAAGTG	GCTCAGCCGAGGTCTTTGAG
Fas	CCTCCTGGCAAACGGAAA	GCAGAGCACACATTCTGGTGTATC
Meis homeobox 2	TCTATGGGCACCCGTTGTTT	TCGCCAGCTCGCACTTCT
EVA1	GACGTTGATGGGCTGATTGG	ATGGCCAGAGCCAGGAAGT
RGDCAP	TGGCCCCCATGAATTCTGT	TTTGTCCGGGCATTAATCG
PRG4	GCAACGGTAGGCCAGTAGATG	AATGACCTCGAAATGCAACTAATG
Protocadherin 10	GCCAGTCAGCTGGTATGGATCT	ACCGATCTGAGTGGCCAAGT

5.2.4 Histology and Immunohistochemistry

Paraffin sections (8 μm) were deparaffinized, rehydrated and stained with hematoxylin and eosin (H&E, Sigma, St. Louis, MO), Alcian Blue (pH 1.0), or Picrosirius Red for cell distribution, sulfated proteoglycans and collagens, respectively. For immunohistochemical

analysis, antigen retrieval was performed by incubating sections in citrate buffer (10 mM citric acid with 0.05% Tween 20 at pH 6.0) heated to 99°C for 25 minutes, cooling for 20 minutes (25°C), and incubating in hyaluronidase (Huang et al. 2008). Collagen type I (MAB3391, Millipore, Billerica, MA), collagen type II (11-116B3, Developmental Studies Hybridoma Bank, Iowa City, IA), proteoglycan 4 (PRG4, ab28484, Abcam, Cambridge, MA) and transforming-growth-factor-beta induced 68 kDa protein (TGFBI, ab66957, Abcam) primary antibodies were used to identify matrix components. Primary and secondary antibody hybridization and subsequent visualization with DAB chromogen was carried out as in Section 3.2.8. Color images were captured at 10X magnification as previously described (Section 3.2.7).

5.2.5 Statistical Analysis

Statistical analysis was performed on mechanical and biochemical data using three way ANOVA with time, cell type and donor as independent variables. Where significance was indicated, Tukey's posthoc tests were carried out. For all measures, significance was determined at $p<0.05$. All values are reported as mean ± standard deviation.

5.3 Results

5.3.1 Mechanical Properties

Three donor-matched sets of chondrocytes and MSCs were encapsulated in agarose and cultured in defined media containing TGF-β3 for 56 days. Consistent with previous studies, the compressive properties of cell-seeded constructs improved with time in culture. For all donors, the equilibrium modulus of chondrocyte-seeded constructs increased

through day 42 while MSC-seeded constructs did not improve after day 28 (p=1.0, **Figure 5-1A**). Chondrocyte-seeded constructs attained equilibrium moduli of 180-240 kPa while MSC-seeded constructs reached moduli of 75-114 kPa. In all constructs, the dynamic modulus continued to develop beyond day 28, regardless of cell type (**Figure 5-1B**). Both equilibrium and dynamic properties were significantly lower for all MSC groups compared to chondrocytes at the final time point, with the exception of donor 3 dynamic properties.

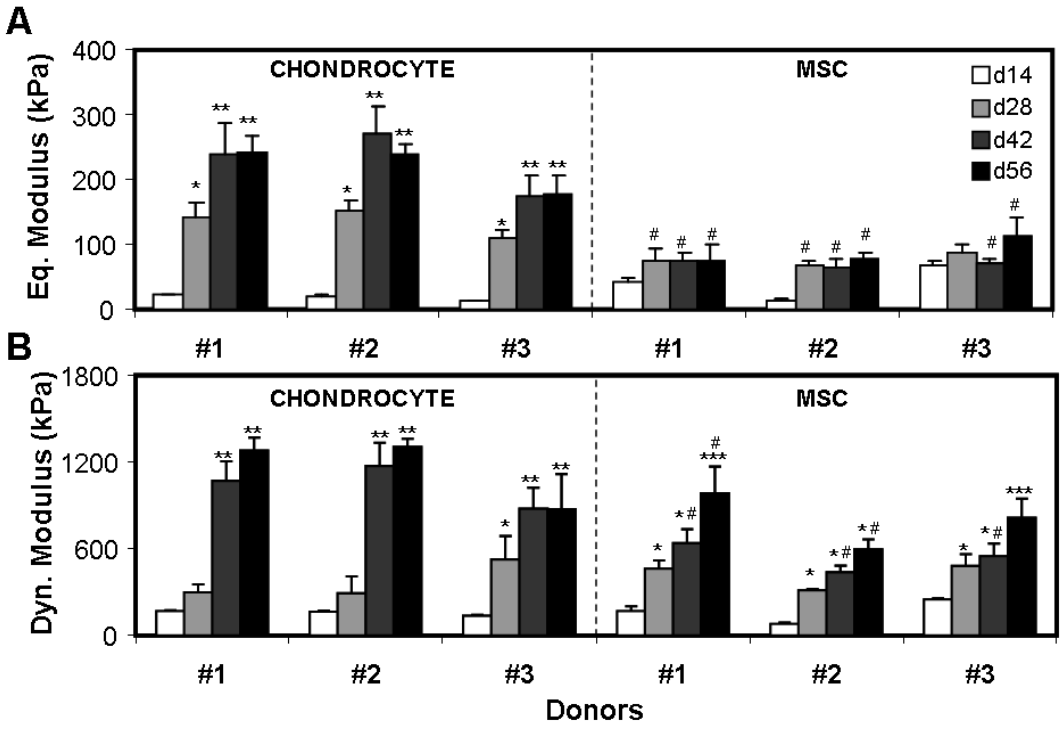

Figure 5-1: Time-dependent compressive (A) equilibrium and (B) dynamic modulus (kPa) of chondrocyte- and MSC-seeded constructs with culture in a chemically defined medium supplemented with 10 ng/mL TGF-β3. * indicates greater than d14 within donors and cell type (p<0.001); ** indicates greater than d28 within donors and cell type (p<0.02); * indicates greater than d28 within donors and cell type (p<0.05); # lower compared to donor-matched chondrocytes at the same timepoint (p<0.01). Data represent the mean and standard deviation of four samples per group per time point.**

5.3.2 Biochemical Content and Chondrogenic Gene Expression

Consistent with mechanical data, the biochemical content for chondrocyte- and MSC-seeded constructs increased with time, with chondrocyte-seeded constructs increasing more rapidly and achieving significantly higher levels by day 42. DNA content was comparable between groups (**Figure 5-2A**). While GAG and collagen content improved for both chondrocyte- and MSC-seeded constructs, MSC-seeded groups failed to attain the levels achieved by their donor-matched chondrocyte constructs (**Figure 5-2B, C**). Histological analysis showed uniform GAG and collagen distribution throughout each construct (**Figure 5-3**). At the final time point, all constructs stained strongly for collagen type II and weakly for collagen type I, regardless of cell type or donor (**Figure 5-2D**).

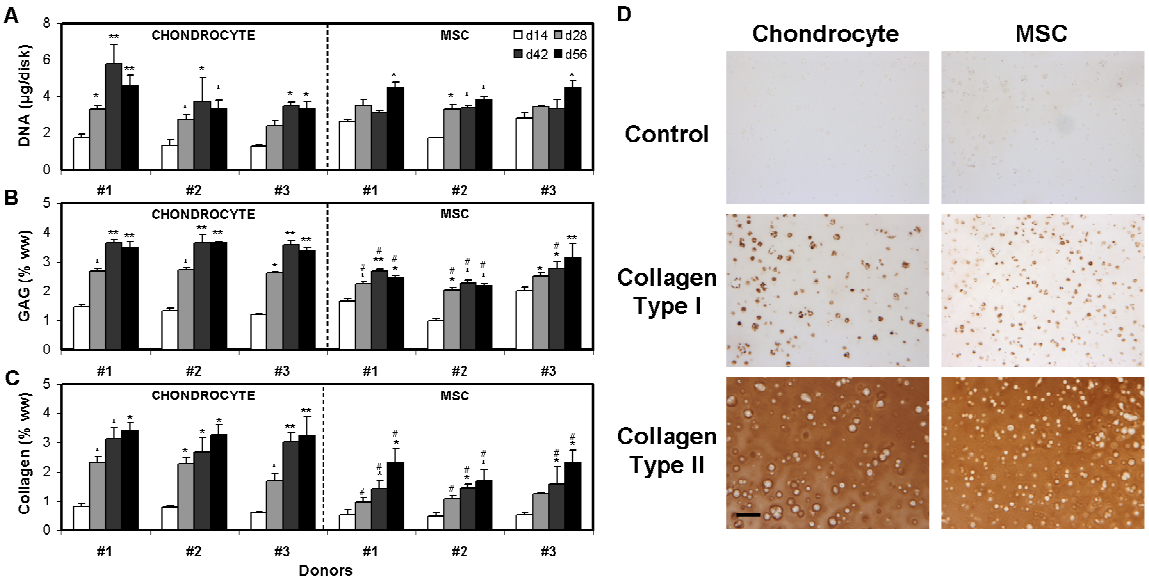

Figure 5-2: Biochemical composition of constructs with variation in time in culture, donor and cell type. (A) DNA content (□g/disk), (B) GAG (% ww) and (C) collagen content (% ww) of chondrocyte- and MSC-seeded constructs. (D) Immunohistochemical analysis of collagen types I and II distribution in cell-seeded constructs for a single donor. * indicates greater than d14 within donors and cell type ($p<0.015$); ** indicates greater than d28 within donors and cell type ($p<0.025$); # lower compared to donor-matched chondrocytes at the same timepoint ($p<0.04$). Data represent the mean and standard deviation of four samples per group per time point. Scale Bar: 100 μm.

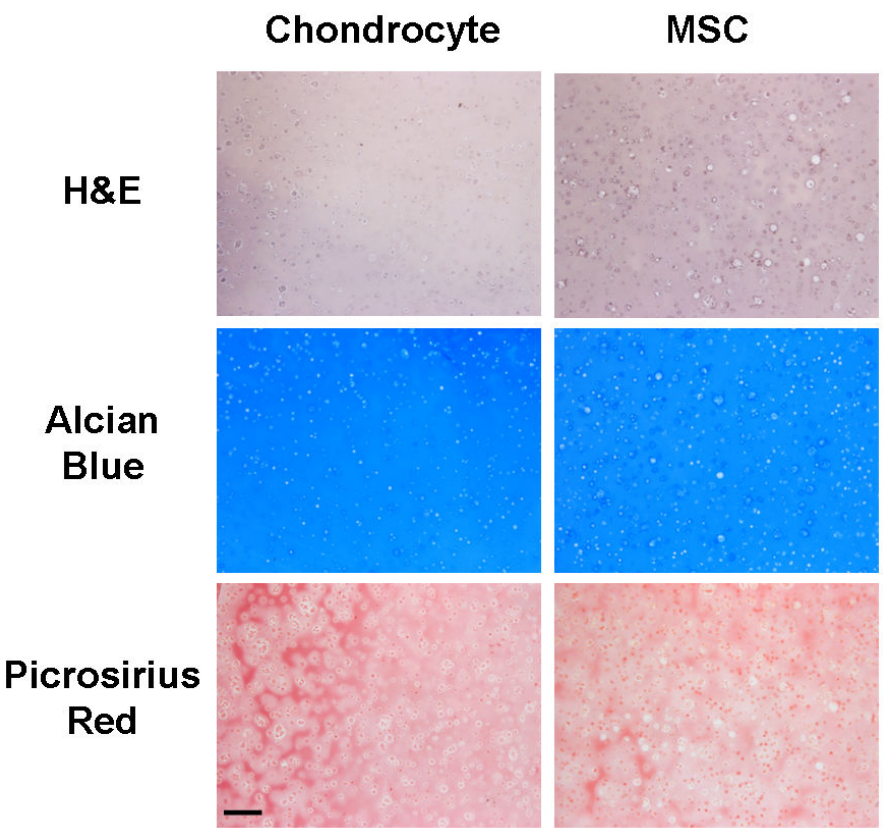

Figure 5-3: Histological staining for chondrocyte- and MSC-seeded constructs after 56 days of culture in the presence of TGF-β3. Constructs were stained with H&E, Alcian Blue and Picrosirius Red for cellularity, proteoglycans and collagens, respectively. Scale Bar: 100 μm.

Expression of cartilage-specific ECM structural components (aggrecan, Type II, IX and XI collagen) at day 28 showed higher expression in differentiated MSC-seeded constructs compared to chondrocyte-seeded constructs for each donor (**Figure 5-4**). These genes were expressed at negligible levels in undifferentiated MSCs (data not shown).

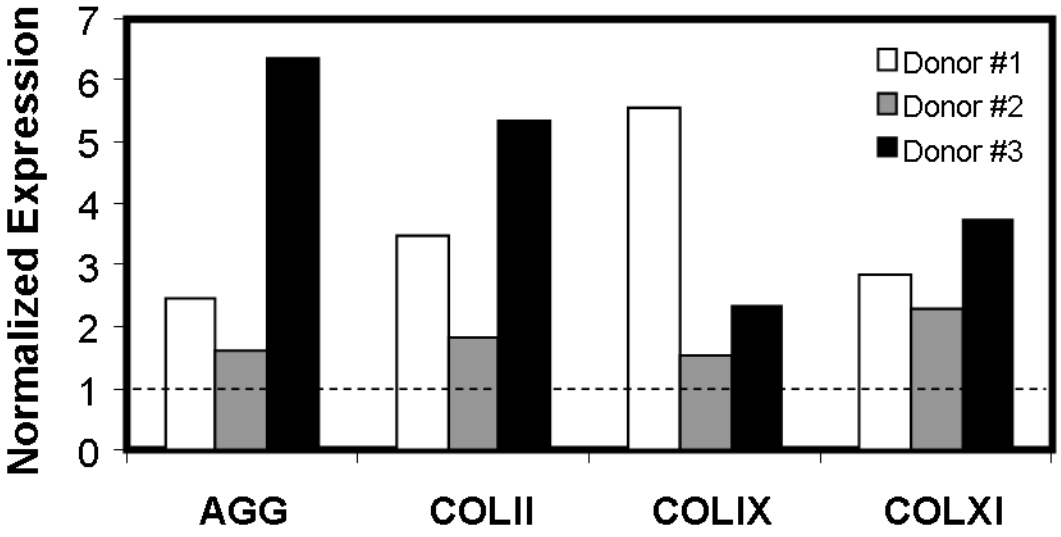

Figure 5-4: Expression of cartilage ECM genes in MSC-seeded constructs normalized to chondrocytes-seeded constructs after 28 days of culture in TGF-β3 containing medium. For all three donors, aggrecan, types II, IX and XI collagen expression levels were higher in MSC-seeded constructs.

5.3.3 Microarray Screening

Microarray screening was then carried out to identify additional genes that are mis-expressed during MSC chondrogenesis. In this screen, day 0 MSCs (M0, undifferentiated MSCs), day 28 MSCs (M28, chondrogenically differentiated MSCs) and day 28 chondrocytes (C28) in 3D culture were processed for three donors. Samples were chosen for analysis at day 28 as this marks the point where the mechanical properties of chondrocyte- and MSC-based constructs began to diverge significantly (**Figure 5-1**), with MSC-based construct properties plateauing after this point. Principal component analysis (PCA) of the microarray data indicated that while chondrogenically differentiated MSCs and chondrocytes were more similar to one another compared to undifferentiated MSCs (PC1), significant differences persisted between these two groups (PC2, **Figure 5-5A**).

Heat map visualization further confirmed this observation, with higher and lower levels of expression for individual genes depicted in red and green, respectively (**Figure 5-5B**).

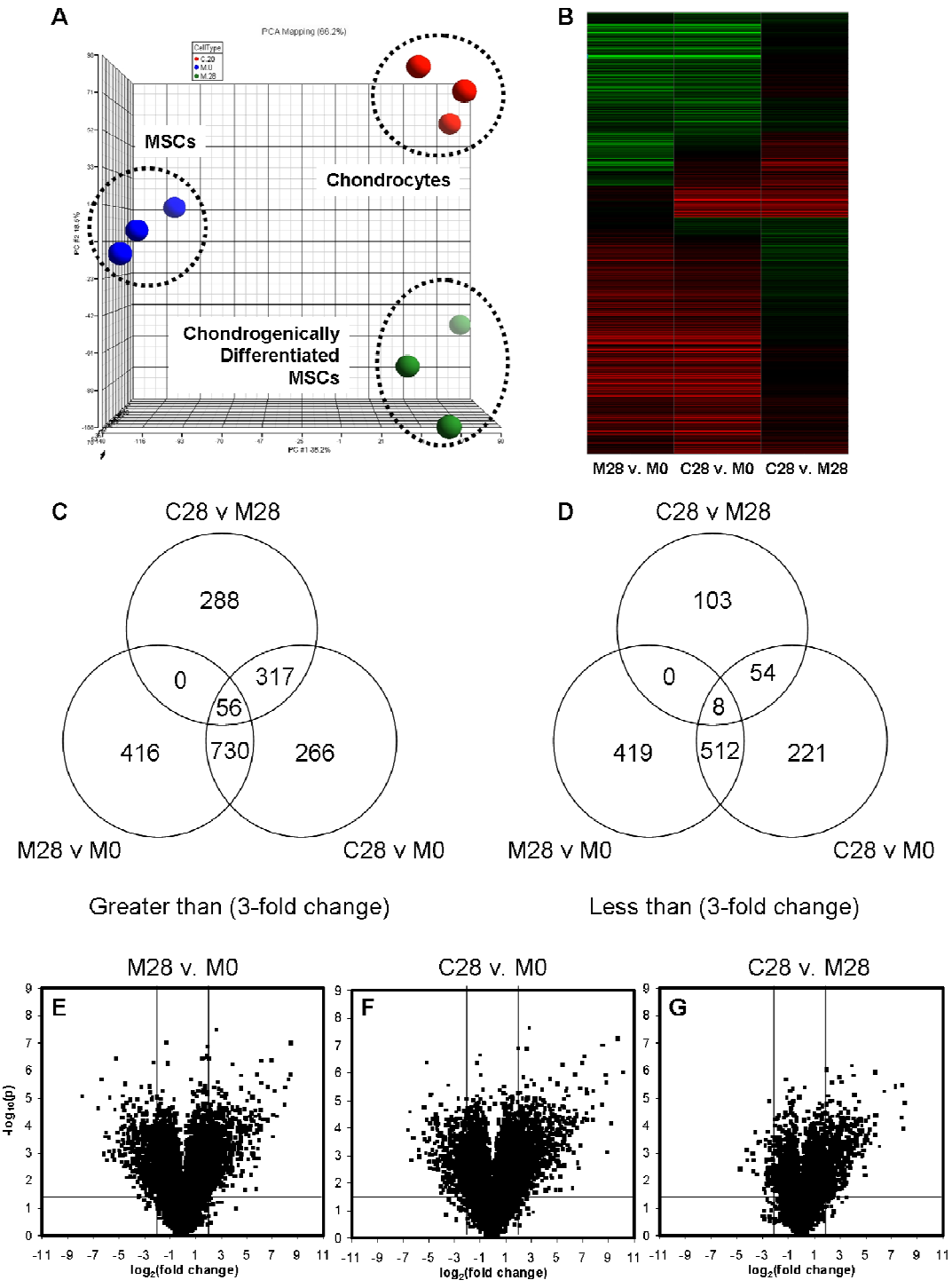

Figure 5-5: (A) Principal component analysis and (B) heat map generated from microarray data showing differential gene expression (green = greater, red = lower) between undifferentiated MSCs at day 0 (M0), chondrogenically differentiated MSC-seeded constructs at day 28 (M28) and chondrocyte-seeded constructs at day 28 (C28). (C-D) Venn diagrams and (E-G) volcano plots for M0, M28 and C28 indicates number of genes and dispersion of genes that were differentially regulated with chondrogenic induction in 3D culture.

With chondrogenic induction, 1202 genes were upregulated in M28 compared to M0 (**Figure 5-5C**). Of these genes, 730 genes were comparably expressed by M28 relative to C28 while 56 genes failed to attain C28 expression levels. Of the 730 genes induced, several were known cartilage markers, including COMP and SERPINA1 (>300 fold relative to M0), chondroadherin (>200 fold relative to M0), collagen type XI (>100 fold relative to M0), collagen types II and IX and aggrecan 1 (>40 fold relative to M0). Microarray analysis also revealed 317 genes that were not changed during MSC chondrogenesis at day 28. Although these 317 genes were expressed by chondrocytes, they remained not expressed or poorly expressed (less than 3-fold change) by MSCs compared to chondrocytes, regardless of MSC differentiation status. A similar analysis of genes suppressed during chondrogenesis identified 939 genes that were lower in M28 compared to M0 (**Figure 5-5D**). Within this group, 512 genes were similar between M28 and C28 while only 8 genes were highly expressed in M0, moderately expressed in M28 and poorly expressed in C28. There were 54 genes that were over-expressed in both M0 and M28 and the expression of these genes at day 28 was not affected by chondrogenesis.

These observations were visually confirmed by volcano plots summarizing fold-changes in gene expression and statistical criteria (**Figure 5-5E-G**). Most notably, the C28 to M28 comparison indicated that the most significant differences were those of higher expression in the C28 group. Using specific criteria (greater than 2 fold change) and a false discovery rate (FDR) of 10%, 252 genes and 72 genes were identified as potentially under-expressed or over-expressed during MSC chondrogenesis, respectively (**Appendix 2**). A subset of these genes was selected for further analysis and real-time PCR was used to validate the

results for 18 of these genes. Of these genes, 14 were poorly expressed in day 0 and day 28 MSC-seeded constructs relative to chondrocyte-seeded constructs while 4 genes remained highly expressed in the MSC populations even after chondrogenesis but were absent or very low in chondrocytes (**Figure 5-6C**). Representative results for PRG4 and Fas demonstrate the patterns of this transcriptional mis-regulation during MSC chondrogenesis (**Figure 5-6A, B**).

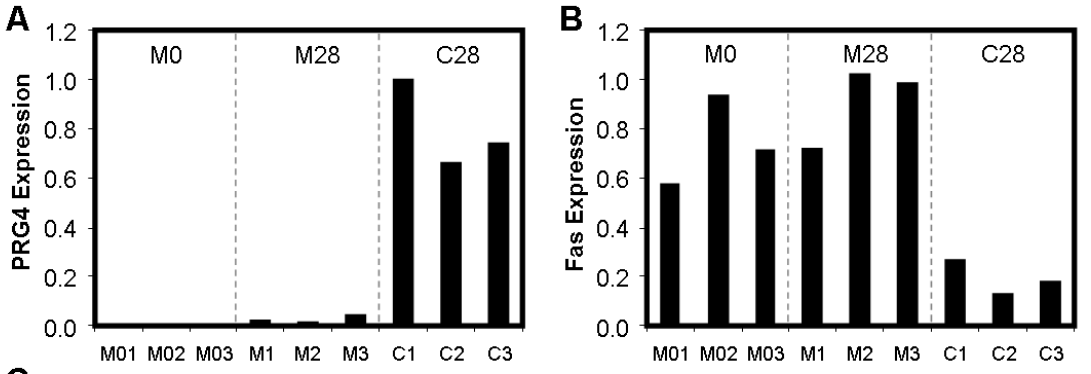

C

Gene (Under-expression)	Fold Diff.	Gene (Over-expression)	Fold Diff.
Similar to MAGEL2 protein	> 2	Similar to leiomodin 1	< -2
CXCL14	> 2	Caspase 4	< -2
Dickkopf-1	> 2	Meis homeobox 2	< -5
Periostin	> 2	Fas	< -5
ID1	> 5		
Chondromodulin	> 5		
Similar to TGFBI	> 5		
Hox4A	> 10		
SOSTDC1	> 10		
Thrombospondin 4	> 15		
Epithelial V-like Antigen 1	> 15		
Proteoglycan 4 (PRG4)	> 25		
Similar to Protocadherin 10	> 25		
Calpain 6	> 30		

Figure 5-6: Gene expression of (A) PRG4 and (B) Fas, illustrating genes that were under- or over-expressed in MSC-seeded constructs relative to chondrocyte-seeded constructs. (C) Genes confirmed by real-time PCR to be differentially expressed with fold difference indicated for C28 compared to M0 and M28.

5.3.4 Gene Expression Profiles

One limitation in this previous analysis was that only a single time point was analyzed (day 28). To assess the temporal profiles of identified genes, chondrocyte- and MSC-seeded constructs were maintained in chondrogenic media for 56 days and the expression levels of the previously identified genes (**Figure 5-6**) were evaluated biweekly. Distinct patterns of

expression emerged from this analysis, as demonstrated by representative graphs of PRG4, TGFBI, chondromodulin and dickkopf-1. While chondromodulin and dickkopf-1 expression remained markedly under-expressed in MSC-seeded constructs compared to chondrocyte-seeded constructs at every time point assayed (**Figure 5-7C, D**), delayed expression of PRG4 and TGFBI was observed in MSC-seeded constructs, with increasing levels of expression at later time points (**Figure 5-7A, B**). PRG4 expression in MSC-seeded constructs was highest at day 42 (compared to day 28 for chondrocyte-seeded constructs), although the peak expression level in MSC-seeded constructs remained lower than the peak level in chondrocyte-seeded constructs for the time points evaluated. Conversely, TGFBI expression increased continually in MSC-seeded constructs at day 56. It is unknown whether the expression level of this gene would continue to increase past day 56 and reach eventual parity with peak chondrocyte-seeded construct levels (day 28). Temporal expression profiles of Fas and caspase 4 showed that expression of these genes in MSC-seeded constructs remained consistently higher than chondrocyte-seeded constructs throughout the culture duration (**Figure 5-7E, F**).

To evaluate whether these differences in gene expression were translated to matrix formation, two molecules, PRG4 and TGFBI, were selected for further analysis. For all donors, chondrocyte-seeded constructs on day 56 stained intensely for both PRG4 and TGFBI, although deposition was localized to the center of the constructs. In contrast, extracellular deposition of PRG4 and TGFBI was not observed for any of the MSC-seeded constructs (**Figure 5-7G**). Consistent with previous reports (Schumacher et al. 1999), PRG4 immunostaining was discernible in superficial regions of articular cartilage section

taken from juvenile bovine carpal joints, with little to no staining in the middle or deep zones (not shown).

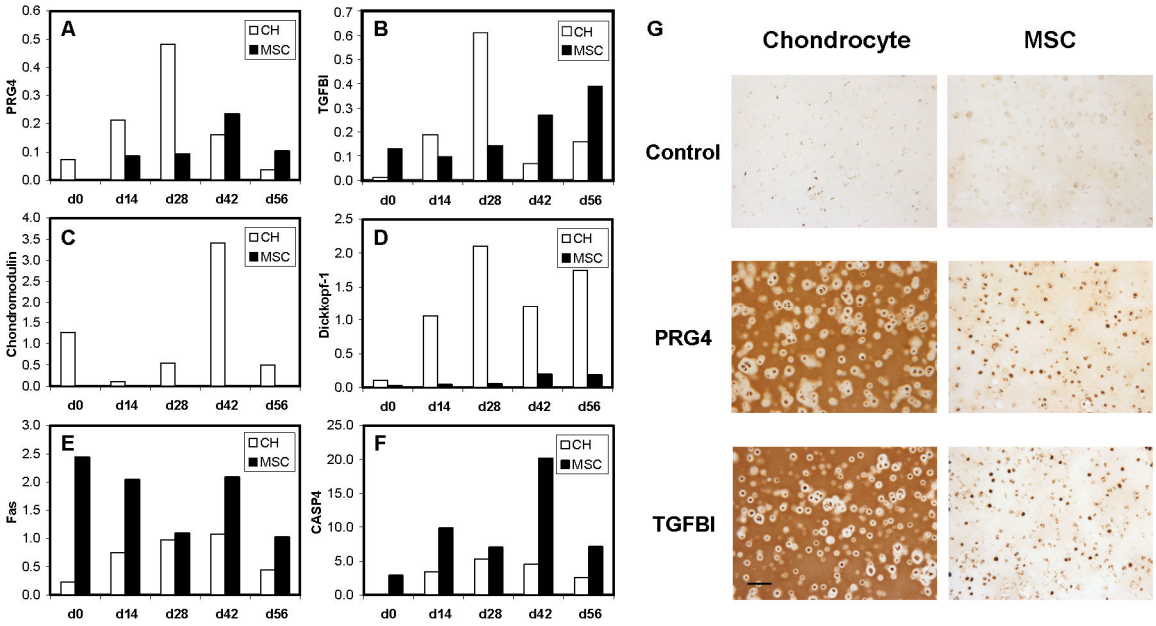

Figure 5-7: Expression profiles of (A) PRG4, (B) TGFBI, (C) chondromodulin, (D) DKK1, (E) Fas and (F) CASP4 show different temporal patterns for chondrogenically induced MSC-seeded constructs compared to chondrocyte-seeded constructs cultured identically for 56 days. (G) Immunohistochemical detection of PRG4 and TGFBI for day 56 cell-seeded constructs show robust staining in chondrocyte-seeded constructs and weak staining in MSC-seeded constructs. Scale Bar: 100 µm.

5.4 Discussion

The ability of bone marrow derived MSCs to undergo chondrogenesis and accumulate functional matrix has provided impetus for their use in cartilage tissue engineering. While promising, the extent of MSC conversion toward the chondrogenic phenotype remains in question; these concerns are sparked in part, by the limited functional capacity of MSCs in 3D hydrogel culture (Mauck et al. 2006; Huang et al. 2009). To better understand the basis of this limitation and develop new benchmarks for chondrogenesis, we characterized the molecular profiles of chondrogenically induced MSCs. In particular, we focused on the molecular differences distinguishing differentiated MSCs

from donor-matched articular chondrocytes, as identification of these deficits may lead to potential targets for therapeutic intervention.

Consistent with previous findings, after long-term culture in pro-chondrogenic conditions, the compressive properties and biochemical content of MSC-laden constructs fell short of those attained by chondrocytes for all three donors. Standard cartilage markers, such as aggrecan and collagen types II, IX and XI, were consistently upregulated during MSC chondrogenesis and expression was maintained at high levels at day 28. Surprisingly, MSCs expressed higher levels of these genes compared to donor-matched chondrocytes at this timepoint, suggesting that the observed discrepancy in functional properties was not due to expression deficits of these standard matrix molecules. Collagen type II immunostaining further confirmed this observation, as chondrocyte- and MSC-laden constructs stained with equal intensity for this important ECM protein. These findings suggest that while standard markers are expressed, they are insufficient predictors of mechanical functionality of chondrogenically induced MSC populations in 3D culture.

To elucidate the topography of chondro-induction, we carried out a genome-wide screen via microarray analysis and identified 324 genes that were transcriptionally misregulated over the course of chondrogenesis. These genes were either 2-fold higher or lower in undifferentiated and chondrogenically differentiated MSC-seeded constructs relative to chondrocyte-seeded constructs at day 28. Of these genes, a subset of 18 genes was confirmed by real time PCR and their temporal expression profiles assessed over 56 days.

This time course was chosen because construct properties typically equilibrate by this time. While some genes such as chondromodulin and Dikkopf-1 were never expressed by MSCs undergoing chondrogenesis, others including PRG4 and TGFBI showed delayed patterns of expression. Immunostaining at the terminal timepoint showed robust deposition of PRG4 and TGFBI in chondrocyte-seeded constructs and no staining in MSC-seeded constructs for all three donors. This is consistent with the findings of Gleghorn et al, who demonstrated that PRG4 was retained in chondrocyte-seeded, but not MSC-seeded alginate (Gleghorn et al. 2007). Interestingly, that study also found greater PRG4 secretion into the media by MSCs compared to chondrocytes. The lack of synthesis or retention of these minor molecules may play a critical role in functional outcomes, particularly if their role is to nucleate ECM formation or regulate ECM organization.

In addition, these molecules may also be indicative of the state of phenotypic conversion. For example, TGFBI, a type II collagen binding protein (Hashimoto et al. 1997), inhibits mineralization and maintains the chondrocytic phenotype in hypertrophic chondrocytes (Ohno et al. 2002). Furthermore, expression of this gene is highest in the pre-hypertrophic stage of developing cartilage (Ohno et al. 2002). Poor expression of TGFBI in MSCs may thus reflect incomplete or incorrect induction toward the chondrogenic phenotype. Indeed, recent data suggest that the phenotype achieved by differentiated MSCs may be more akin to that of 'transient' rather than 'permanent' chondrocytes. During development, 'transient' chondrocytes undergo hypertrophy and eventual ossification while 'permanent' chondrocytes maintain a fixed chondrogenic

phenotype (Pacifici et al. 2000). Microarray analysis of mouse articular cartilage and growth plate cartilage showed considerable differences in gene expression between these chondrocyte populations, though standard cartilage markers, including aggrecan, were expressed by both (Yamane et al. 2007). Notably, collagens types II, IX and XI were expressed at higher levels in the 'transient' chondrocytes compared to the 'permanent' articular chondrocytes, paralleling the findings of the current study with differentiated MSCs and articular chondrocytes. Other data also suggest that the chondrogenic commitment of induced MSCs may be flexible in vivo (Pelttari et al. 2006; Jukes et al. 2008). Implantation of chondrogenically differentiated MSCs resulted in extensive mineralization of the cartilage matrix, mirroring 'transient' chondrocyte phenotypic transitions. In contrast, articular chondrocytes showed no signs of phenotypic instability in vivo, further delineating the differences between fully committed articular chondrocytes and chondrogenically differentiated MSCs.

In this study, we identified a subset of genes that is mis-expressed during MSC chondrogenesis. While important, these missing elements of MSC chondrogenesis may not represent the molecular limitations of chondrogenesis in its entirety, as all of the genes described here were identified from analysis of a single timepoint, day 28. From temporal expression profiles, it is apparent that even within this subset of genes, patterns of expression vary dramatically. Microarray analyses of early and later stage chondrogenesis will be necessary to capture the complete topography of molecular dysfunction and may well identify additional targets for consideration. In addition, it is as yet unclear what role these genes play with respect to the mechanical maturation of MSC-based constructs; future knockdown studies will be required to establish functional

correlations between gene expression and construct mechanical properties. Once correlation is established, the manipulation of the expression of these genes may enhance the functional capacity of MSCs for cartilage repair.

Taken together, our studies establish a better understanding of the complex molecular topography of MSC chondrogenesis and in particular, our limitation in the creation of mechanically functional constructs based on this cell source. Having now established new molecular benchmarks of chondrogenesis, these features can be applied to gauge the efficacy of a given culture environment or media supplement. For example, we have recently probed small molecule libraries for novel biochemical mediators of chondrogenesis using high-throughput screening (Huang et al. 2008); these new markers may prove useful in such optimizations. Alternatively, these same markers may be helpful in the tuning of interactions between MSCs and their biomaterial microenvironment (Connelly et al. 2008; Erickson et al. 2009) as well as the timing and magnitude of mechanical perturbation (Mouw et al. 2007; Thorpe et al. 2008; Huang et al. 2010). For example, as a subset of the identified genes are sensitive to mechanical stimulation (**Figure 5-8**), the modulation of their expression in response to loading can be used to optimize loading parameters for chondrogenesis. Benchmarking all such efforts against molecular profiles that generate functional neo-cartilage constructs will improve MSC-based cartilage tissue engineering and lead to a mechanically competent, phenotypically stable, cartilage replacement.

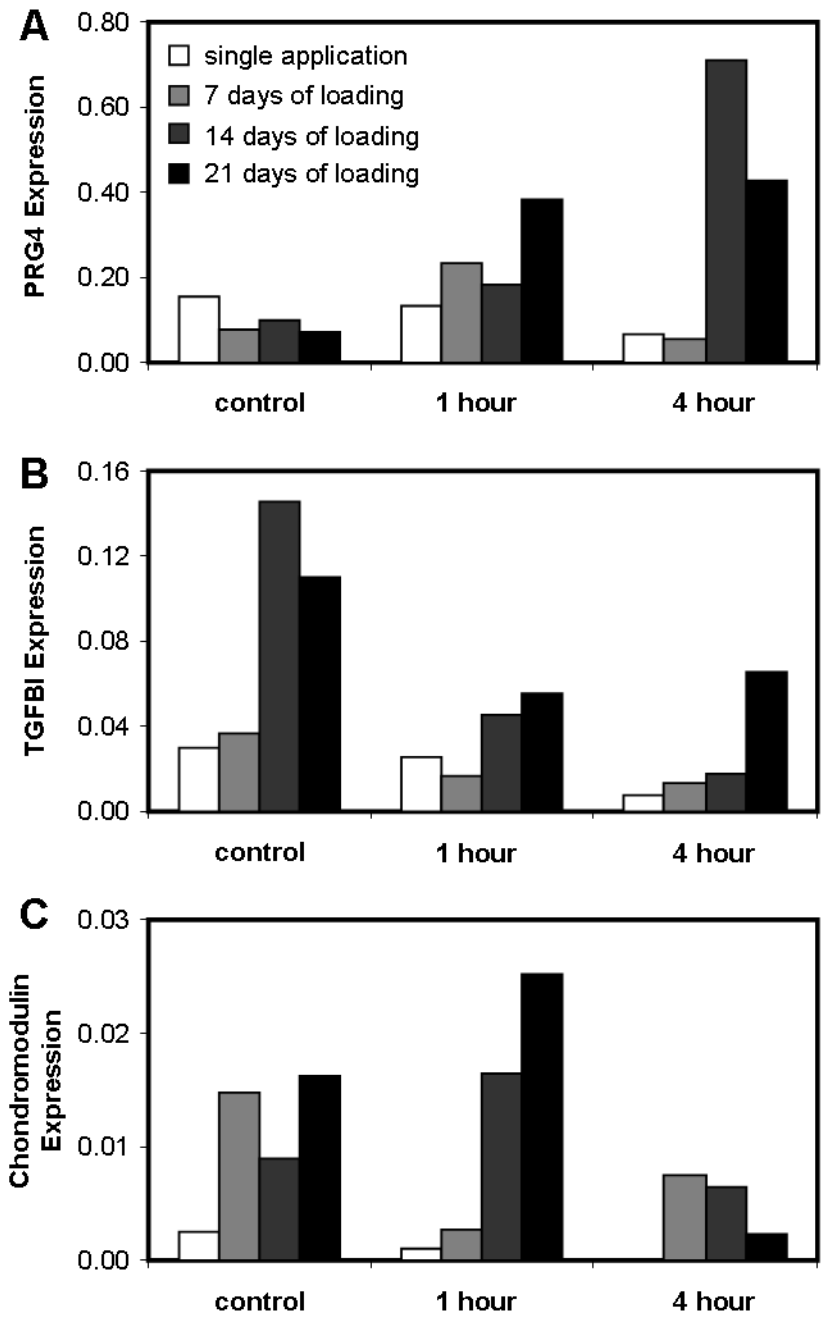

Figure 5-8: Repeated dynamic compressive loading of MSC-seeded constructs over 21 days modulated the expression of (A) PRG4, (B) TGFBI and (C) chondromodulin. Loading was applied at 10% strain and 1 Hz, 1 or 4 hours per day over a period of 3 weeks in CM+ media. At day 21, PRG4 expression was upregulated with loading while TGFBI was downregulated, regardless of loading duration. In contrast, chondromodulin expression was upregulated when loaded for 1 hour but downregulated after 4 hours.

CHAPTER 6: TENSILE PROPERTIES OF ENGINEERED CARTILAGE FORMED FROM CHONDROCYTE- AND MSC-LADEN HYDROGELS

6.1 Introduction

Work up to this point have focused on improving the functional properties of MSC-based constructs and in particular, the compressive properties. Regardless of cell source, cartilage constructs are routinely evaluated after *in vitro* or *in vivo* culture for ECM content, gene expression, and histological appearance. When used as an outcome parameter, mechanical properties of constructs have primarily been assessed in compression (confined and unconfined). Several studies have shown that the compressive properties of the chondrocyte-seeded constructs improve with increasing culture duration and cell seeding density (Puelacher et al. 1994; Chang et al. 2001; Mauck et al. 2002) as well as with the inclusion of anabolic growth factors and/or increased serum supplementation (Gooch et al. 2001; Pei et al. 2002; Mauck et al. 2003). With long-term culture using specialized media and/or bioreactor culture, equilibrium properties have matched that of the native tissue (Freed et al. 1997; Byers et al. 2008). For example, we have recently shown that a defined serum free media supplemented with TGF-β3 markedly improved the compressive properties of chondrocyte-seeded agarose compared to those maintained in the absence of TGF-β3 or in serum containing medium (Mauck et al. 2006). However, in that same study, MSCs produced inferior properties compared to age and donor-matched chondrocytes. Strategies effective in improving chondrocyte-seeded construct properties (such as increasing seeding density) have not proven effective in improving MSC-seeded construct properties to chondrocyte levels (Chapter 3).

In addition to these oft measured compressive properties, the tensile properties of cartilage play a significant role in its mechanical function. It has long been noted that cartilage tensile properties are higher than compressive properties (Chahine et al. 2004). Kempson reported that the ramp tensile modulus of human superficial zone femoral head cartilage ranges from 75-150 MPa (Kempson 1991). For superficial bovine samples, equilibrium tensile moduli increase with age and range from 6-15 MPa (with failure strains of ~60%), while compressive properties at equilibrium are much lower (<1MPa) (Williamson et al. 2003; Charlebois et al. 2004). The large disparity in tensile and compressive properties is termed tension compression non-linearity (TCNL) (Huang et al. 2001; Huang et al. 2005). Under certain compressive loading configurations (e.g., unconfined compression), failure to include TCNL results in poor theoretical predictions of transient response (Soltz et al. 2000). Therefore, many of the poroelastic and biphasic cartilage models have been altered to incorporate TCNL (Soulhat et al. 1999; Soltz et al. 2000). Further highlighting the importance of these properties, cartilage tensile properties decrease rapidly after insult and are a precursor to further degeneration (Elliott et al. 1999).

While critical for cartilage function, few studies have directly examined the tensile properties of engineered cartilage. Rather, most studies indirectly assess this parameter by measuring the dynamic modulus in unconfined compression (a measure dependent on both the compressive and tensile modulus). It has been noted that even when the equilibrium compressive modulus (and GAG content) matches that of the native tissue,

the dynamic modulus (and collagen content) remains lower (~25% of native) (Lima et al. 2007). While less common, several studies have directly measured the tensile properties of engineered constructs (Table 1). Collectively, these studies indicate that the tensile properties of chondrocyte monolayers, masses, and cell-seeded hydrogels remain well below native tissue levels, even after extensive periods of *in vitro* or *in vivo* culture. While illustrative, these studies did not employ a defined media with growth factor supplementation, nor did they assess the potential of MSCs to recapitulate this important property in 3D culture.

Therefore, the purpose of this study was to assess the tensile properties of hydrogel-based constructs seeded with chondrocytes and MSCs and maintained in a defined media. Based on our previous findings of robust increases in compressive properties in this media with TGF-β3, we hypothesized that this treatment would similarly increase construct tensile properties. Further, based on previous studies focusing on compressive properties, we hypothesized that increasing chondrocyte seeding density would produce constructs with greater tensile properties. Finally, we hypothesized that MSC-laden constructs would increase in tensile properties only when exposed to TGF-β3, but would do so to a lesser extent than chondrocyte-laden constructs.

To test these hypotheses, chondrocyte-seeded constructs were formed at two seeding densities (10 and 30 million cells/mL) and cultured for 8 weeks in a defined medium, with or without TGF-β3. Additionally, donor-matched MSCs were seeded (10 million cells/mL) and cultured similarly. At biweekly intervals, the ramp modulus, ultimate

strain and toughness were determined using tensile tests to failure. Biochemical content (DNA, GAG, and collagen) was analyzed and ECM distribution and collagen type determined via histology and immunohistochemistry. Findings show that the tensile properties of cell-seeded constructs increased with increasing culture duration and the application of TGF-β3. Interestingly, increasing chondrocyte density increased the initial rate of accumulation of ECM and tensile modulus, but did not alter the modulus values achieved after 8 weeks. Further, when cultured at the same seeding density, chondrocytes and MSCs generated similar increases in tensile properties. Neither cell type nor higher seeding density resulted in constructs whose tensile properties matched that of native cartilage, highlighting the need for further refinement of these engineered constructs to enable their load bearing role once implanted *in vivo*.

6.2 Materials and Methods

6.2.1 Construct Fabrication and 3D Culture

MSCs and chondrocytes were isolated as described in Section 3.2.1. For all studies, type VII agarose (Sigma, St Louis, MO) in PBS was cast in 2.25 mm thick sheets, gelled for 20 minutes at 25^{o}C, and cut into strips (7mm x 40mm). For validation studies, acellular strips of 2, 3, 4 and 5% w/v were prepared. For seeding studies, sterile agarose (49°C, 4% w/v) was combined 1:1 with chondrocytes (20 or 60 million cells/mL) or MSCs (20 million cells/mL) at 25^{o}C in chemically defined medium (CM, Section 3.2.2). Constructs were cultured for 56 days in 6 mL/strip with (CM+) or without (CM-) 10 ng/mL TGF-β3 (R&D Systems, Minneapolis, MN). Strips from two replicate experiments with different cell isolations were used and media was changed twice weekly. At biweekly intervals,

constructs were evaluated for tensile properties, biochemical content, and ECM distribution.

6.2.2 Construct Mechanical Testing

To evaluate tensile properties, an Instron 5848 Microtester (Instron, Canton, MA) was used to apply uniaxial tension to strips seated into 120 grit sandpaper-coated grips at 25^{o}C. Sample dimensions were measured via digital caliper, and gauge length noted after placement in grips. Samples were moistened with PBS during the test. Elongation was prescribed at a quasi-static 0.5%/sec strain rate until failure. To validate our tensile testing protocol and to ensure that slippage at the grips was not occurring in these samples, texture correlation was used to compare local strains in a central region of interest (ROI) of the gel to the nominal grip-to-grip strain. To enable this analysis, graphite markers were encapsulated in acellular 2% and 5% agarose gels prepared as above. Strips were tested at 0.5%/sec strain rate until failure. Images were acquired of the central region of the construct every second during elongation with a digital camera controlled via a custom LABVIEW program (Guerin et al. 2007). Average local strain in the longitudinal direction within the ROI was determined from this image series via a particle tracking algorithm using the Vic2D software (Correlated Solutions Inc, West Columbia, SC) and was compared to grip-to-grip strain derived from the Instron output file. In another subset of acellular samples, the equilibrium tensile modulus was determined using a tensile stress relaxation test. In this test, strips were subjected to three steps of 2% elongation at a rate of 0.05%/sec with a relaxation period of 80 seconds following each ramp. Equilibrium tensile stress was plotted against applied strain and the tensile modulus calculated from a linear fit

to this data. The ramp tensile modulus was calculated from the measured geometry on the day of testing and the linear region of the stress-strain curve. Ultimate strain (strain at maximum stress) and toughness (integrated area under the stress-strain curve) was calculated for each sample.

6.2.3 Immunohistochemistry

For immunohistochemistry, sections were deparaffinized, rehydrated, and incubated for 1 hour at 37°C in 300µg/mL hyaluronidase (Type IV, Sigma) in PBS. Samples were washed, treated with 3% H_20_2, and incubated with a blocking reagent (DAB150 IHC Select, Millipore, Billerica, MA). Collagens were identified with 5µg/ml dilutions of primary antibodies specific for either collagen I (MAB3391, Millipore) or collagen II (11-116B3, Developmental Studies Hybridoma Bank, Iowa City, IA) in 3% BSA in PBS. Non-immune controls were prepared with 3% BSA in PBS without primary antibody. Biotinylated goat anti-rabbit IgG secondary antibodies with Streptavidin HRP bound the primary antibody and were reacted with DAB chromogen reagent for 10 minutes (DAB150 IHC Select, Millipore). Color images were captured at 5X magnification using a microscope equipped with a color CCD digital camera and the QCapturePro acquisition software. For each antibody, all samples were stained at the same time and imaged under the same conditions to enable comparison between groups.

6.2.4 Statistical Analysis

All statistical analysis was performed with SYSTAT software (v10.2, SYSTAT Software Inc., San Jose, CA). Significance was set at $p<0.05$ and data analyzed using two separate

ANOVA analyses. Time, culture medium (CM- or CM+) and either seeding density (10 or 30 million cell/mL) or cell type (Chondrocyte or MSC) were the independent variables. When the ANOVA analysis indicated significance, Fisher's LSD posthoc tests were applied to enable comparisons between groups. All data are reported as mean ± SD of 7-10 samples.

6.3 Results

6.3.1 Tensile Properties of Acellular Agarose

Preliminary testing of acellular agarose gels showed that little stress relaxation occurred when a series of step tensile deformations was applied in a stress relaxation test (**Figure 6-1A, B**, percent relaxation ~8%, solid line). This is in marked contrast to the behavior of agarose in compression, during which conspicuous stress relaxation is observed (**Figure 6-1B**, percent relaxation ~34%, dotted line,). Indeed, while long durations are required to determine equilibrium properties of agarose in compression, the tensile properties of 2% and 5% agarose strips were comparable to one another when determined from ramp and equilibrium testing (**Figure 6-1C**). Testing a range of concentrations of acellular gels in both tension (ramp) and compression (equilibrium) demonstrated that increasing agarose concentration increased both compressive and tensile moduli. Significant increases were observed for each percentage increase over 2% in both tension and compression, with tensile moduli being 5-25 times higher than the compressive moduli at each concentration (**Figure 6-1D**). This indicates that even for acellular agarose gels, a significant tension/compression non-linearity exists, similar to native cartilage tissue (Huang et al. 2001; Huang et al. 2005).

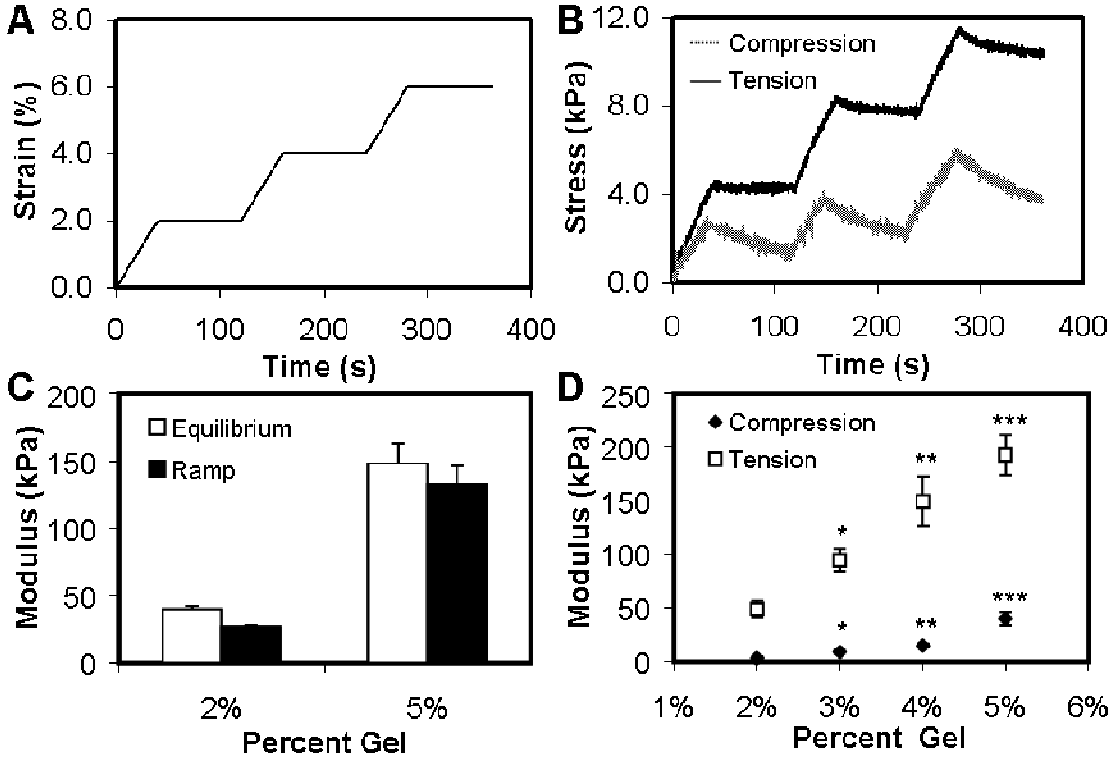

Figure 6-1: Tensile and compressive properties of acellular agarose gels. (A) Plot of 3 sequential ramps of 2% tensile or compressive strain applied to a 5% agarose gel followed by 80 seconds of relaxation. (B) Stress relaxation response of 5% agarose gel with extension (solid line) or compression (dotted line). Note the marked relaxation with compressive stress relaxation. (C) Equilibrium and ramp tensile moduli of 2% and 5% agarose gels. (D) Tensile (derived from ramp testing) and compressive (derived from equilibrium testing) properties of acellular gels as a function of agarose content (% w/v). Data represents the mean and standard deviation of ten samples per group. * Indicates greater than all values lower $p<0.05$; ** indicates greater than all values lower $p<0.05$; * indicates greater than all values lower $p<0.05$.**

To verify that the clamping protocol we employed did not allow slipping at the grips, texture correlation of surface deformation was used to analyze local strains during ramp testing. Good agreement was found between measured local strains in the central region of the construct compared with the applied grip-to-grip strains over the linear region from which the ramp modulus was calculated (0-5%, **Figure 6-2**). Based on these results and

those from the stress relaxation testing, the ramp modulus was used to evaluate tensile properties for subsequent studies of cell-laden gels.

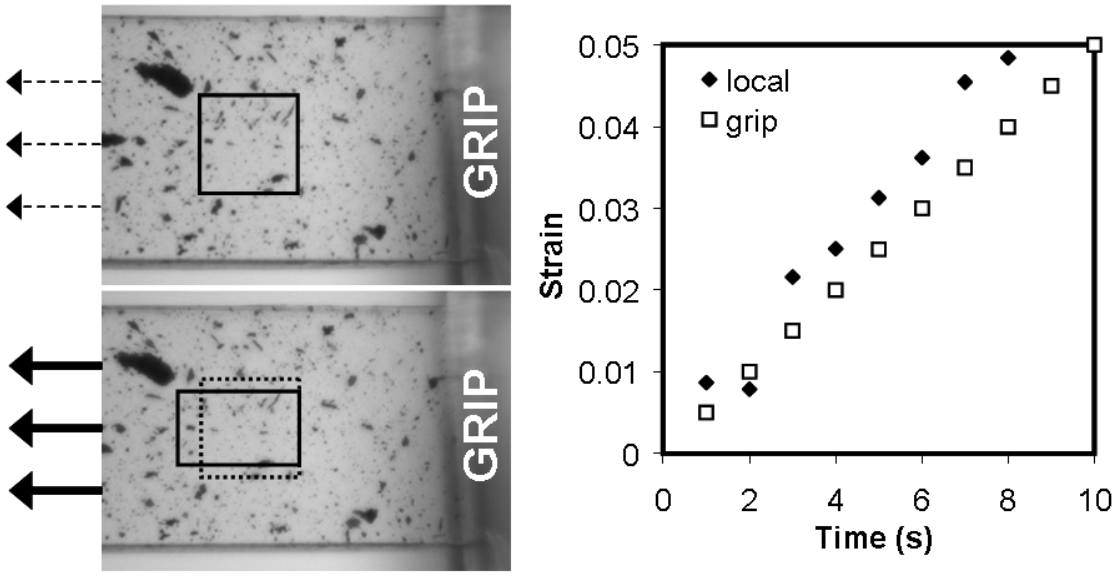

Figure 6-2: Analysis of bulk and local strain during tensile testing of agarose strips. (A) Representative image of speckled acellular gels at the outset (top image) and after 3% grip-to-grip strain (bottom image) during the tensile test. Boxes represent undeformed and deformed region of interest for analysis of local strains. (B) Representative correlation of local strain (closed diamonds) with grip-to-grip strain (open squares) for a central region of an acellular construct. Good agreement is observed between local and grip-to-grip strains in the linear region of the force-elongation curves used to calculate tensile properties.

While the ramp tensile modulus increased for each percentage increase in agarose concentration (**Figure 6-3**, $p<0.05$), the ultimate strain in these acellular gels was relatively insensitive to increasing concentration, with failure occurring at <15%. A small decrease in ultimate strain was observed at agarose concentrations greater than 2% (**Figure 6-3**, $p<0.05$).

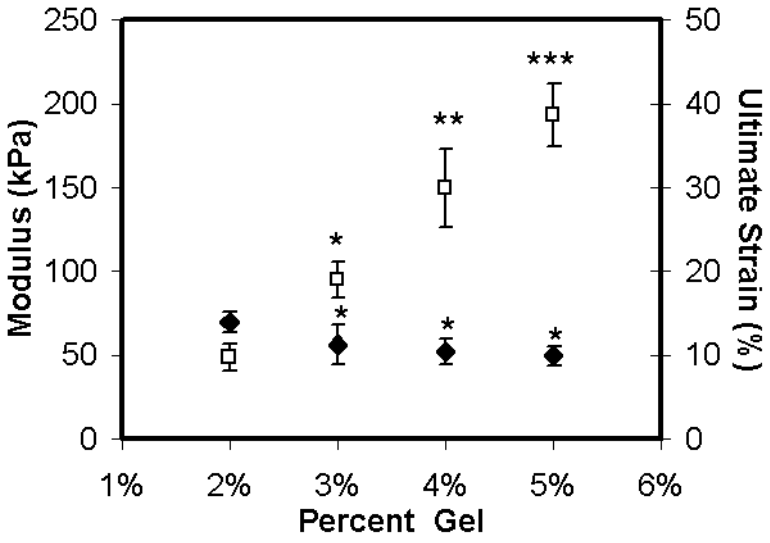

Figure 6-3: Tensile properties of acellular agarose hydrogels. Tensile ramp modulus (white squares) and ultimate strain (black diamonds) of acellular gels as a function of agarose content (% w/v). Data represents the mean and standard deviation of ten samples per group. * Indicates difference from 2% group, p<0.05; ** indicates greater than 3% group, p<0.05; * indicates greater than 4% group, p<0.05.**

6.3.2 Biochemical Content of Cell-Seeded Agarose

6.3.2a Effect of Cell Density

After test validation, chondrocyte-laden constructs, seeded at 10 and 30 million cells/mL (CH10M and CH30M, respectively), were fabricated and maintained in long-term culture in either CM- or CM+. DNA content increased with time in CH10M groups in CM+ ($p<0.01$ vs. day 14, Figure 2), but showed no increase until day 56 compared to day 14 in CM- ($p=0.015$ vs. day 14). In contrast, DNA content remained stable for CH30M groups in CM+ ($p>0.06$ vs. day 14). DNA content was higher at all time points except day 56 for CH30M compared to CH10M in CM+ ($p<0.05$). Both GAG and collagen content were dependent on culture duration and media composition ($p<0.001$, **Figure 6-4**). After day 14 for the CH10M group, and after day 28 for the CH30M group, increased GAG and collagen were found in constructs in CM+ compared to CM-. With seeding at the

higher density and culture in CM+, CH30M constructs contained greater GAG and collagen compared to CH10M constructs at all time points after day 14 ($p<0.04$). Interestingly, CH30M strips maintained in CM- synthesized comparable GAG and collagen by day 56 compared to CH10M groups in CM+ ($p=0.129$ for GAG, $p=0.905$ for collagen).

6.3.2b Effect of Cell Type

To evaluate the ability of MSCs to produce functional matrix, donor-matched MSCs were seeded at 10 million cells/mL (MSC10M) and compared to the CH10M group. DNA content of MSC10M groups did not change with time, regardless of media condition ($p>0.08$, **Figure 6-4**). MSC10M in CM+ produced similar GAG compared to CH10M CM+ at all time points ($p>0.25$). Although collagen content was similar between MSC10M and CH10M at the terminal time point ($p>0.1$), collagen increased more rapidly in MSC10M groups. MSC10M constructs maintained in CM- failed to deposit appreciable amounts of GAG or collagen regardless of time in culture.

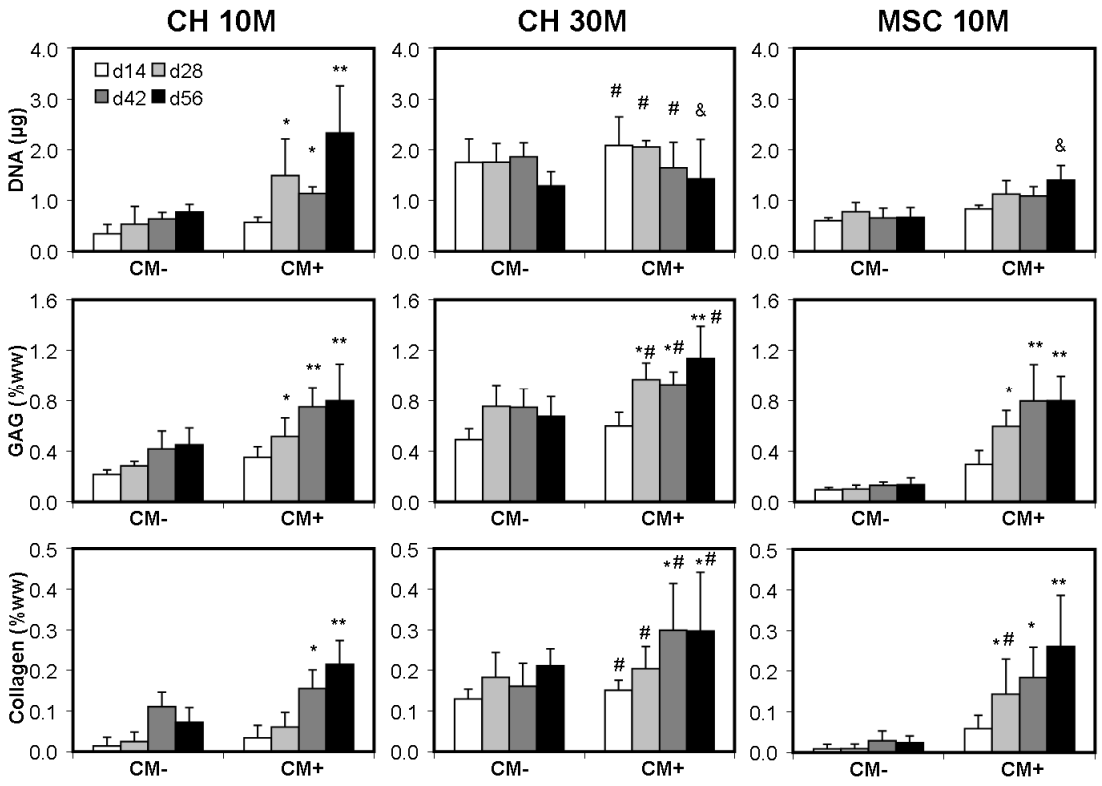

Figure 6-4: Biochemical composition of tensile strips with variation in time in culture, media condition, cell type, and cell density. Top row: DNA content (□g/disk); middle row: sGAG content (%ww); bottom row: collagen content (%ww). * Indicates greater than all values lower in both CM- and CM+ conditions within cell and seeding density group ($p<0.05$); ** indicates greater than all values lower in both CM- and CM+ conditions within cell and seeding density group ($p<0.05$); # indicates greater than corresponding CH10M value at same time point and media condition ($p<0.05$); & indicates lower than corresponding CH10M value at same time point and media condition ($p<0.05$). Data represent the mean and standard deviation of seven to ten samples per group per time point.

6.3.3 Tensile Properties of Cell-Seeded Agarose

6.3.3a Effect of Cell Density

The tensile modulus of CH10M constructs increased with time in culture in CM+, reaching 405±127 kPa by day 56 ($p<0.001$ vs. day 14, **Figure 6-5**). In contrast, constructs in CM- were significantly weaker in tension, only reaching 104±76 kPa at the terminal time point ($p<0.001$). When maintained in CM+, CH30M constructs increased in tensile properties with time ($p<0.001$), and did so more rapidly than CH10M constructs

(e.g., note higher modulus in CH30M on day 42). However, the tensile modulus achieved in the CH30M group plateaued by day 42 at a value of 354±125 kPa. When maintained in CM-, CH30M constructs improved in tensile modulus with time ($p<0.001$ at day 56 vs. day 14) and at day 56, attained similar tensile properties as day 28 CH10M constructs in CM+ ($p>0.9$). Interestingly, although biochemical content was higher in CH30M constructs in CM+ compared to CH10M, the tensile modulus was not different on day 56. The ultimate strain and toughness of chondrocyte-laden constructs were dependent on time in culture ($p<0.01$) and media condition ($p<0.001$), but not on seeding density ($p>0.8$). Unlike the tensile modulus, which rose steadily through the culture duration, the ultimate strain and toughness of the CH10M and CH30M groups in CM+ reached their highest values by day 28 and were not different from one another thereafter ($p>0.1$). The ultimate strain achieved was higher for constructs in CM+ compared to CM- at all time points, regardless of seeding density ($p<0.05$). In contrast, the toughness of constructs in CM+ was not different than CM- constructs until day 28 ($p>0.07$ day 14 CM+ vs. CM-).

6.3.3b Effect of Cell Type

As expected based on the weak deposition of matrix, MSC10M constructs in CM- did not show any improvement in tensile properties with time ($p>0.8$ at day 56 vs. day 14). In CM+, however, MSC10M constructs increased in tensile modulus with time ($p<0.001$), and did so more rapidly than CH10M constructs. Tensile moduli in these constructs plateaued at day 42 to values of 363±99 kPa. The ultimate strain and toughness of

MSC10M constructs were dependent on time in culture ($p<0.01$) and media condition ($p<0.001$), but were not different than the CH10M group similarly maintained ($p>0.25$).

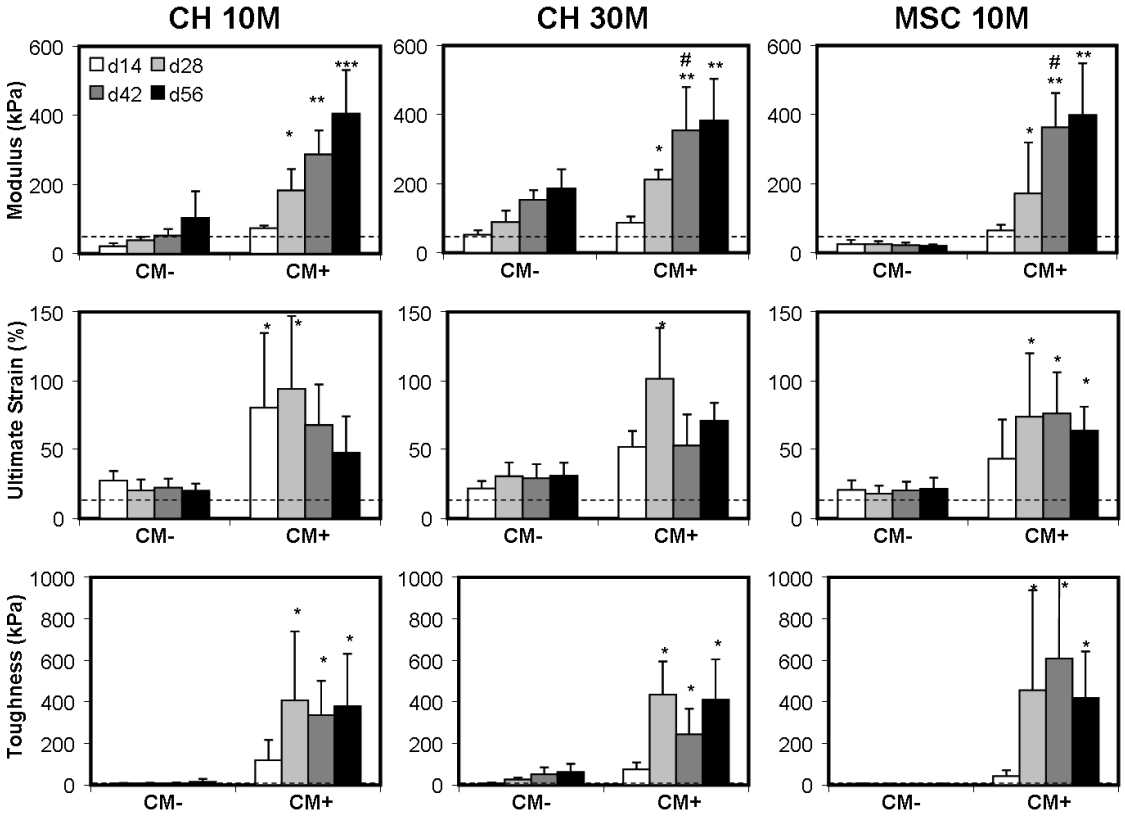

Figure 6-5: Time-dependent tensile modulus (kPa), ultimate strain (%), and toughness (kPa) of constructs with culture in CM- or CM+ medium. * Indicates greater than all values lower in both CM- and CM+ conditions within cell and seeding density group ($p<0.05$); ** indicates greater than all values lower in both CM- and CM+ conditions within cell and seeding density group ($p<0.05$); * indicates greater than all lower values within same cell type and seeding density group ($p<0.05$); # indicates greater than corresponding CH10M value at same time point and media condition ($p<0.05$). Data represent the mean and standard deviation of seven to ten samples per group per time point. Dotted line indicates corresponding property of 2% agarose from acellular studies.**

6.3.4 Histological Analysis

Histological analysis showed an increasing amount of matrix deposition with culture duration, with more intense staining with culture in CM+ (not shown). Very little matrix was deposited in the MSC10M group maintained in CM-. As expected from analysis of biochemical content, day 56 constructs cultured in CM+ showed little difference in

staining intensity with variations in seeding density and cell type with respect to cellularity, and GAG and collagen deposition (**Figure 6-6**).

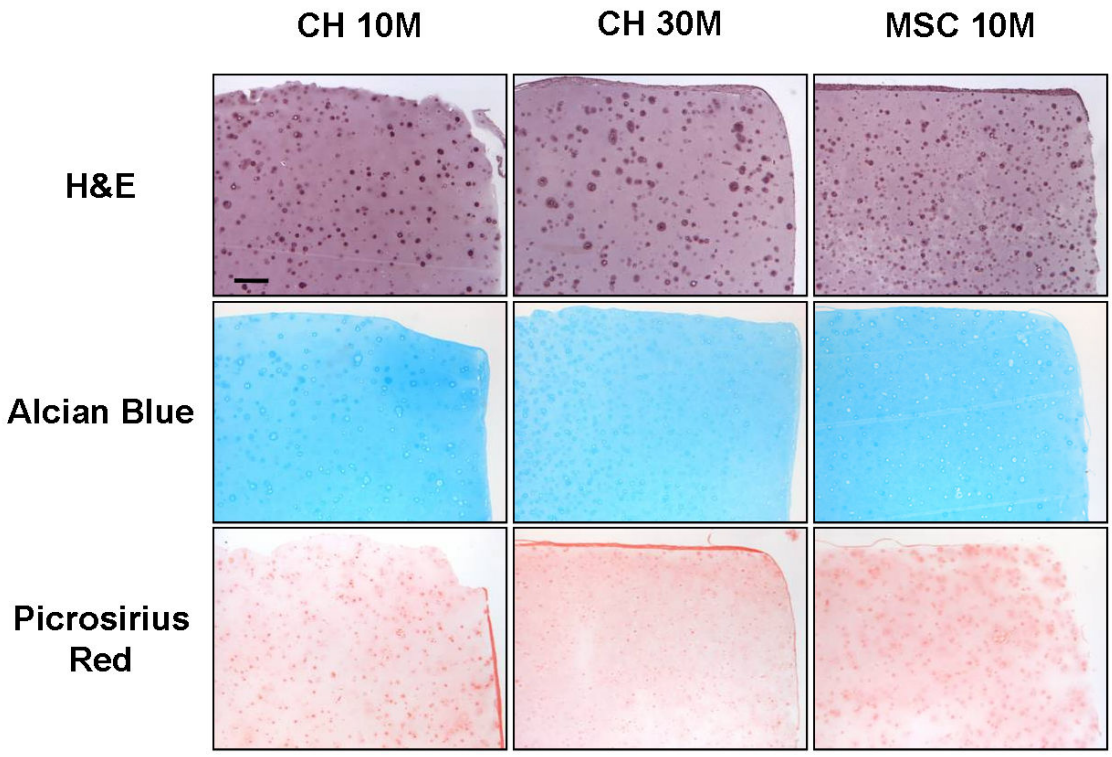

Figure 6-6: Histologic appearance of constructs on day 56. H&E, Alcian Blue and Picrosirius Red staining of CH10M, CH30M and MSC10M constructs cultured in CM+ reveals no differences between groups at day 56. Constructs cultured in CM- conditions (not shown) showed lower staining intensities for chondrocyte groups, and absence of stain for MSCs. Scale bar: 200μm.

The type of collagen deposition in the different culture conditions was analyzed using immunohistochemistry (**Figure 6-7**). Interestingly, chondrocytes at either density deposited a mixture of type I and type II collagen in CM-. Addition of TGF-β3 resulted in a dramatic shift in matrix deposition in these constructs, with nearly all collagen deposited being type II. Conversely, MSC-laden constructs showed weak pericellular staining of type I collagen and no type II collagen in CM-, indicative of their lack of chondrogenic phenotype in this media. However, when cultured in CM+, a robust

deposition of type II collagen was observed, and pericellular type I collagen staining was lost.

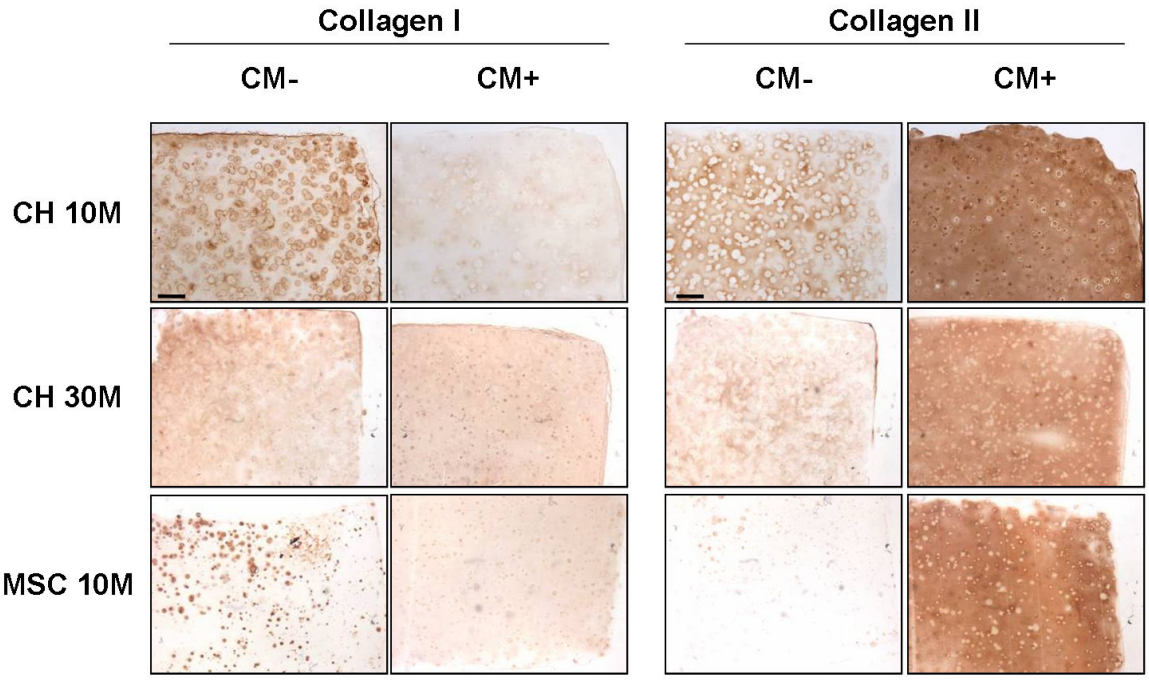

Figure 6-7: Immunohistochemical detection of amount and distribution of collagen type I and type II in day 56 constructs cultured in CM- or CM+ medium. Chondrocyte-laden constructs stained for both type I and type II collagen in CM- conditions, with an intense shift to predominantly type II collagen and loss of type I staining in CM+ conditions, regardless of seeding density. MSCs showed some pericellular staining of type I collagen and no type II collagen in CM- conditions, but a robust deposition of type II collagen throughout the construct with culture in CM+ conditions. Scale bar: 200μm.

To determine organization of the newly formed collagen, Picrosirius Red staining was carried out on a subset of the day 56 CM+ CH10M constructs that had been sectioned *en face* (parallel to the construct surface). These stained sections showed a much lower collagen staining intensity than native articular cartilage prepared and stained similarly (**Figure 6-8**). Furthermore, polarized light imaging of constructs revealed a distinct lack of collagen organization in these engineered constructs compared to the native tissue. In the engineered section, little birefringent material was present, and that which was present showed no directional consensus. Conversely, native tissue showed intense

birefringence, that when analyzed for preferred orientation, showed a prevailing fiber direction of 107 degrees with a coefficient of variation of 21 degrees.

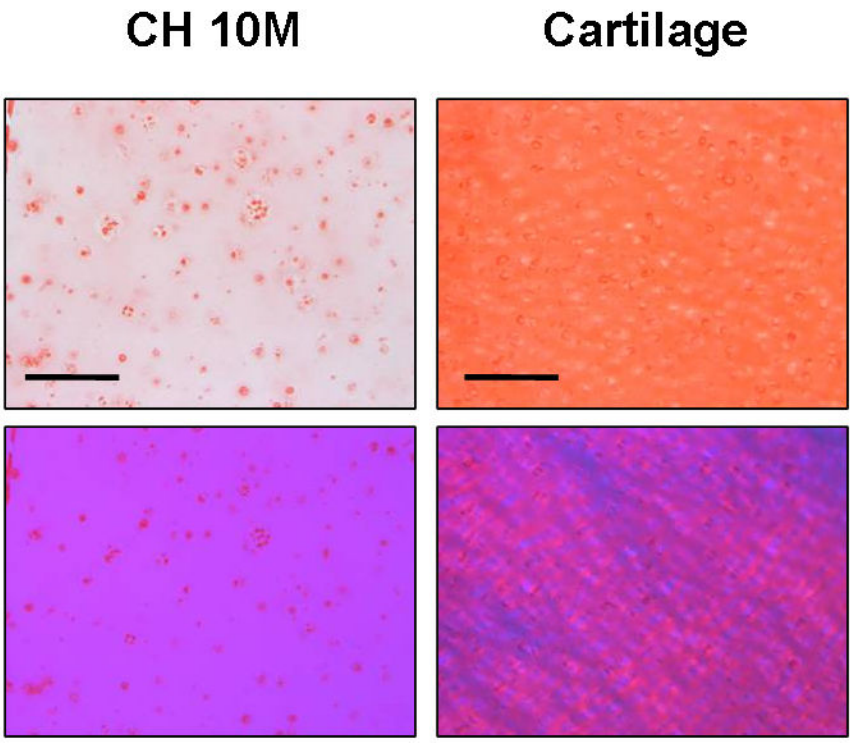

Figure 6-8: Collagen deposition and alignment in engineered cartilage constructs and the superficial zone of native tissue. Picrosirius red staining (top) and polarized light imaging (bottom) of en face sections from the superficial zone of a CH10M construct cultured in CM+ at day 56 and bovine carpal articular cartilage. Engineered constructs stained less intensely for collagen compared to native cartilage and showed no specific collagen organization. Scale bar: 200μm.

6.4 Discussion

The load bearing capacity of articular cartilage is enabled by a high compressive modulus and an even higher tensile modulus. While compressive properties have been widely studied as a benchmark of mechanical functionality in engineered cartilage, few studies using hydrogels have examined tensile properties or have sought to optimize this critical determinant of cartilage mechanical function. In this study, we directly measured the tensile properties of cell-laden agarose, a commonly used hydrogel in cartilage TE. In

agreement with previous studies (Normand et al. 2000), agarose tensile properties were dependent on the percent composition, and acellular gels failed at strains of >15%, independent of percent composition. When seeded with chondrocytes or MSCs, these properties increase with culture duration, with the largest improvement in tensile properties observed in a chemically defined medium containing TGF-β3. Such seeded constructs increased in ultimate strain to >50% (matching native values); however, the tensile moduli achieved after 8 weeks were a fraction (10% or lower) of native values, which range from 5-50MPa (Huang et al. 2005).

In addition to assessing baseline tensile properties, this study explored several parameters for improving construct maturation. First, we used a chemically defined medium with (CM+) or without (CM-) TGF-β3 supplementation. We have previously shown that chondrocytes cultured in agarose cylinders in this medium increase in compressive properties with time in culture, with markedly larger improvements with the inclusion of TGF-β3 (Mauck et al. 2006). In this study, CM+ medium similarly resulted in larger increases in the biochemical composition (GAG and collagen content) as well as the tensile properties of chondrocyte-laden constructs compared to those maintained in CM-. Additionally, while both type I and type II collagen were deposited by chondrocytes in CM-, a pronounced shift to the accumulation of type II collagen was observed in CM+.

Additional experiments demonstrated that increasing the initial chondrocyte seeding density modulated the rate and amount of construct ECM deposition. In general, an increased starting cellularity led to more rapid and/or higher final biochemical content.

For example, constructs seeded with chondrocytes at 30 million cells/mL in CM- reached higher tensile moduli and greater biochemical content on day 56 than 10 million cells/mL constructs similarly maintained. These findings are consistent with previous short-term (14 day) studies that directly measured tensile properties of chondrocyte-laden alginate gels at varying seeding densities (Williams et al. 2005). This increase in biochemical content with increased seeding density was apparent in CM+ as well. However, despite higher GAG and collagen content at the terminal time point (day 56) in the higher seeding density constructs, the tensile properties achieved were comparable between the two groups. This suggest that factors other than GAG and bulk collagen content, such as collagen cross-linking or expression and deposition of other cross-linking elements, may play a role in increasing tensile properties. Furthermore, given the relatively low collagen levels (0.8-1.1%) observed in these constructs, our findings suggest that there exists a threshold below which composition does not correlate with tensile properties as it does for the native tissue.

Finally, a separate set of experiments explored the capacity of MSCs to develop tensile properties comparable to chondrocytes. In a previous study, we showed that MSCs were unable to achieve comparable compressive properties compared to chondrocytes. One interesting observation in that study was that collagen contents were similar between MSC and chondrocyte-laden cylinders. In this study, MSC-laden constructs attained similar collagen content and tensile properties on day 56 compared to donor-matched chondrocytes at the same density. Staining for collagen type showed that MSCs and chondrocytes responded differently to the varying media conditions. While chondrocytes

deposited matrix containing both type I and II collagens in the absence of TGF-β3, MSCs showed only slight accumulation of type I collagen. This finding indicated that MSCs were viable in CM-, but deposited very little ECM. Addition of TGF-β3 shifted the phenotype of both cell types towards one that was strongly chondrogenic, with the majority of collagen deposited being type II. These quantitative and qualitative measures demonstrate, for the first time, that MSCs can form cartilaginous constructs with tensile properties similar to those formed by chondrocytes in a 3D hydrogel environment. This potential is critical for the optimization of this cell source as a viable alternative to chondrocytes for cartilage TE.

From these studies, it is clear that the culture of either chondrocytes or MSCs in agarose results in lower tensile properties and collagen content (~1% of wet weight) than that of the native tissue. This finding is consistent with previous studies that have matched the GAG content and compressive properties of the native tissue in engineered constructs, but have failed to achieve physiologic collagen content, resulting in significantly lower dynamic moduli in unconfined compression (Lima et al. 2007; Byers et al. 2008),. Additionally, collagen organization (assessed via polarized light microscopy) was isotropic and disorganized in these constructs compared to the ordered collagen alignment in the cartilage superficial layer. Given that tensile properties are based on a dense, ordered collagen component and are critical to cartilage function, these limitations must be resolved to enable successful engineering of this unique tissue.

Several enabling technologies may be considered for the improvement of these tensile properties. First, it may be that the non-biodegradable agarose used in this study interferes with the distribution and remodeling of the forming collagen network. Previous studies using pulse-chase radiolabeling have shown that spatial and temporal gradients in newly formed matrix constituents control the distance from the cell that products migrate (Quinn et al. 2002). Hydrogels that are engineered to degrade on a specific time scale (Burdick et al. 2001) or via hydrolysis of enzymatically cleavable elements (Park et al. 2004) might improve ECM distribution, and may likewise promote increases in tensile properties. Alternatively, fabrication of hydrogels from biologics, such as hyaluronic acid (HA) or chondroitin sulfate (CS), may permit natural ECM remodeling with construct maturation (Burdick et al. 2005; Chung et al. 2006), (Li et al. 2004).

Collectively, the results of this study suggest that ECM deposition by chondrocytes and MSCs can improve the tensile properties of engineered constructs. However, the low tensile properties achieved under these free swelling conditions are a significant impediment to load-bearing use. These limitations correlate with the poor construct collagen content and the overall lack of ECM organization. Engineering methods, such as mechanical stimulation, that borrow from developmental concepts of remodeling and physiologic use may be necessary to improve construct tensile properties and enable their load bearing capacity upon implantation.

CHAPTER 7: SLIDING CONTACT ENHANCES MESENCHYMAL STEM CELL CHONDROGENESIS IN 3D CULTURE

7.1 Introduction

The load-bearing role of articular cartilage is enabled by a set of unique properties that are both inhomogeneous (depth-dependent) and anisotropic (direction-dependent). As described in Chapter 2, the collagen content of mature cartilage is highest in the superficial zone, and is organized parallel to the surface (Mankin et al. 1994). In the middle zone, collagen orientation is disorganized and in the deep zone, collagen is oriented perpendicular to the subchondral bony surface. In the superficial zone, collagen is also organized along split-line directions, which change directions across the surface (Below et al. 2002). The tensile properties of cartilage vary accordingly, and are highest in the split-line direction (parallel to collagen fibers) (Huang et al. 2005). Cartilage maturation and the development of these depth- and direction-dependent properties is directed by mechanical forces; loading induces remodeling of the immature matrix (Archer et al. 2003), leading to increases in compressive and tensile properties (Kempson 1982; Kempson 1991; Athanasiou et al. 2000). In bovine cartilage, these increases in tensile properties correlate with increases in collagen content and cross-linking (Williamson et al. 2001; Williamson et al. 2003; Charlebois et al. 2004). When embryonic and juvenile bovine cartilage explants are removed from the loading environment, the tensile properties decrease in conjunction with decreases in collagen and cross-link density (Williamson et al. 2003). These findings suggest that the demands placed on cartilage, coincident with load-bearing use, lead to rapid changes in collagen content and organization, allowing the tissue to achieve its mature load bearing capacity.

Despite the importance of tensile properties to articular cartilage function, few studies have considered these properties in engineered tissue replacements. In the previous chapter, we charted the tensile properties of chondrocyte- and MSC-seeded constructs in free-swelling culture and found no differences between these cell types. As with the compressive properties, tensile properties initially increased with time in culture as matrix was deposited; however, within a few weeks tensile properties plateaued to levels far below those of the native tissue. Biochemical evaluation showed poor collagen deposition and little collagen organization.

From the work presented thus far (Chapters 3-6), generating MSC-based constructs with the mechanical complexity and integrity of cartilage remains a challenge; not only are the properties of MSC-seeded hydrogels consistently lower than those of the native tissue, but the structural organization of articular cartilage is completely absent. As mechanical stimulation is critical to cartilage development and maturation, bioreactor systems that simulate the native mechanical environment of cartilage may bridge these functional disparities. Indeed, as discussed extensively in Chapter 4, dynamic axial compression enhanced the compressive properties of MSC-based engineered cartilage, though collagen content remained low. Improvements in compressive properties were not related to improvements in bulk matrix content, but were perhaps due to load-induced matrix remodeling. In these constructs, type II collagen distribution was noticeably improved compared to free-swelling controls; this was apparent throughout the construct expanse (macro-scale) and at the pericellular level (micro-scale). While promising, these studies

were not designed to generate either depth-dependence or constructs with improved tensile properties. Therefore, to better enhance construct properties and instill depth- and direction-dependent properties, a loading modality more representative of the native joint environment may be required.

Physiologic loading within the joint is represented by two cartilage layers sliding relative to one another. In the knee joint, this sliding contact is carried out by the cartilages lining the femoral condyles and tibial plateau. Loading is characterized by a moving contact area across curved surfaces and the applied load is largely borne by fluid pressurization (Ateshian et al. 1995; Caligaris et al. 2008). To date, few studies have examined the effects of sliding contact on the functional growth of engineered constructs; in one study, a migrating contact applied to adult canine chondrocyte-seeded agarose disks improved the equilibrium compressive properties, though no differences were observed in biochemical content or spatial distribution of matrix (Bian et al.). Related studies applying rolling contact (Stoddart et al. 2006) or compression and shear (Grad et al. 2005; Grad et al. 2006; Grad et al. 2006) to chondrocyte-seeded constructs showed that these loading modalities can modulate chondrogenic gene expression and proteoglycan synthesis, however mechanical properties were not assessed. Compression and shear in these studies were applied using an oscillating spherical hip ball and the contact area remained constant with loading, with shear loading superimposed on dynamic compressive loading. Using this bioreactor system, recent studies have examined the effect of dynamic compression and shear on MSC-seeded fibrin-polyurethane sponges. While MSC gene expression was modulated by loading, the GAG content of constructs was not affected (Li et al. 2009; Li et

al. 2009). Changes in gene expression was also dependent on the presence and concentration of TGF-β1 during loading (Li et al. 2009). Though interesting, the physical signals arising from this loading system and the mechanical microenvironment of MSCs within these constructs was not characterized and is not well understood. In addition, none of the studies mentioned above was designed to examine the effect of loading on developing tensile properties or collagen content.

To overcome the above limitations, we developed and characterized a new sliding contact bioreactor system that can better recapitulate the mechanical stimuli arising from joint motion (two contacting cartilage layers). Using this bioreactor system, we demonstrated improved expression of chondrogenic genes with short-term sliding contact of MSC-seeded agarose; these changes in gene expression were dependent on both axial strain and TGF-β supplementation. We then applied long-term sliding contact to MSC-seeded agarose constructs using the optimized parameters previously determined from short-term studies, and showed improved tensile properties and depth-dependent matrix remodeling with sliding contact. Finally, FEM analysis of sliding contact showed that tensile strains (parallel to the sliding direction) and fluid efflux/influx were depth-dependent and highest in the region closest to the construct surface, consistent with histologic observations.

7.2 Materials and Methods

7.2.1 Sliding Contact Bioreactor

A custom, displacement controlled bioreactor (**Figure 7-1**) was constructed to apply sliding contact (SLC) to cell-seeded hydrogel strips. The bioreactor consisted of an array of

spherical polytetrafluoroethylene indenters (Ø25 mm) cut to 10 mm width and length, a lid to maintain sterility, removable polysulfone trays, and a motorized motion control system (Soloist, Aerotech, Pittsburgh, PA) to regulate sliding displacement (x-direction). Axial displacement (y-direction) was controlled manually with ball-bearing linear stages and actuators (Newport, Irvine, CA). Strips were maintained and loaded in rectangular wells within trays and held in place by clamps on either end, with up to 5 strips per tray. For all experiments, a sinusoidal sliding displacement was applied.

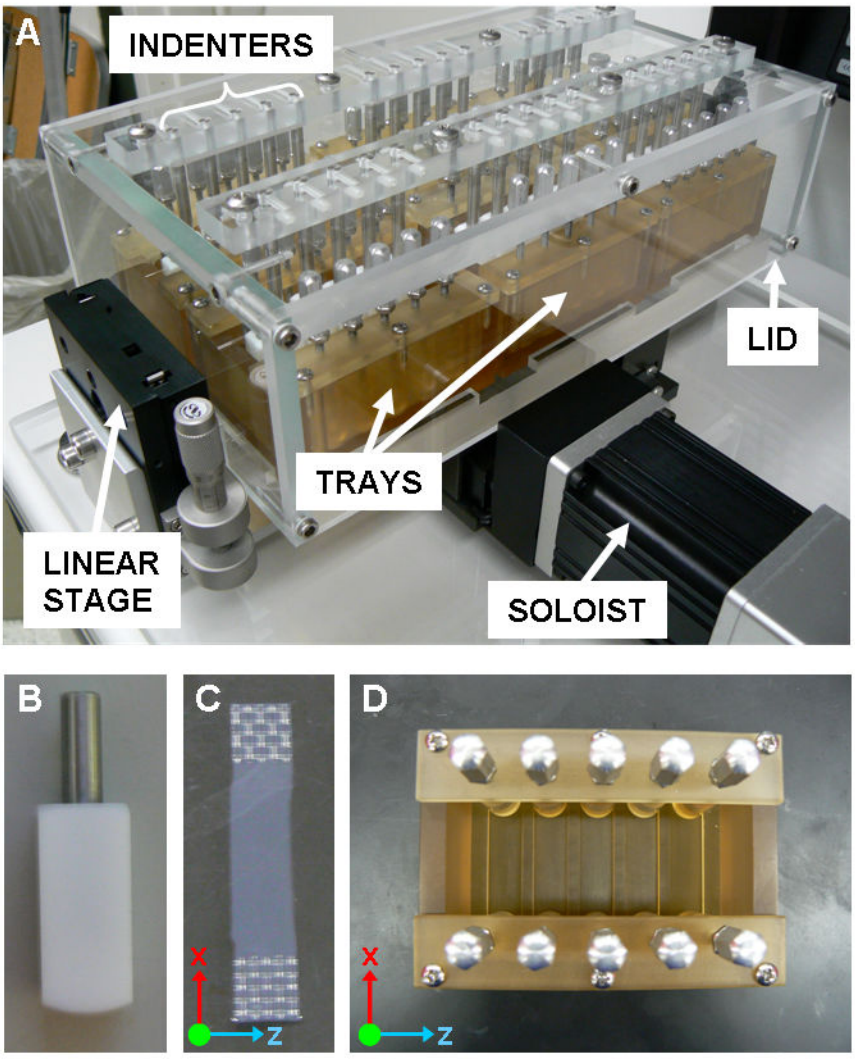

Figure 7-1: A custom, displacement-controlled bioreactor to apply sliding contact (SLC) to engineered cartilage constructs. (A) The bioreactor consisted of spherical indenters, a lid and removable trays. Axial and sliding displacements were controlled by linear stages and the Soloist motion controller, respectively. (B) SLC was applied using spherical indenters (original diameter: Ø25 mm). (C) Cell-seeded hydrogel strips were cast with nylon meshes on either end. (D) Strips were housed in removable trays and held in place by posts, with up to five strips per tray.

7.2.2 Sliding Contact Loading of Acellular and MSC-Seeded Constructs

For acellular studies, 2% and 6% type VII agarose (Sigma, St Louis, MO) in PBS were separately cast between parallel plates to form 1.5 mm thick sheets that were subsequently sectioned into rectangular strips (41.5 x 7.5 mm). Strips were subjected to one hour of SLC

at 5, 10 or 20% axial strain applied at a velocity of 2.5 mm/s. Additional intact strips were evaluated for tensile properties.

For all MSC-seeded studies, MSCs were isolated and cultured as previously described (Section 3.2.1). MSCs were then combined 1:1 with sterile type VII agarose to form constructs with a final seeding density of 20 million cells/mL. The cell-agarose solution was cast into small porous nylon webs at each end (**Figure 7-1C**) in 1.5 mm thick sheets and allowed to gel for 20 minutes at room temperature. Following gelation, strips (41.5 x 7.5 mm) were cut and maintained in CM supplemented with 10 ng/mL TGF-β3 (CM+, R&D Systems, Minneapolis, MN) with media (6 mL/strip) changed twice weekly.

After 21 days, mechanical and biochemical properties were evaluated as in Sections 3.2.4, 3.2.5, 6.2.2. To determine optimal loading parameters, additional pre-matured (21 days) strips were subjected to 3 hours of sliding at 5, 10 or 20% axial strain at 2.5 mm/s (0.1 Hz). Sliding was applied in the presence (CM+) or absence (CM-) of TGF-β3 with free-swelling controls cultured in parallel. Gene expression was assessed by real-time PCR directly after sliding as in Section 3.2.6. Samples for compression testing and gene expression were harvested from the loaded region of strips, while separate, intact strips were used for tensile testing. Two replicate experiments (with two different MSC isolations) were carried out with data from both experiments pooled. Cell viability after loading was assessed using the Live/Dead assay (Molecular Probes, Eugene, OR) for the 20% axial strain group.

From these preliminary studies, a loading regimen of 20% axial strain at 2.5 mm/s in CM+ media was used for subsequent long-term sliding experiments. After 21 days of pre-culture in CM+, strips were subjected to 21 days of sliding contact. Loading was applied for 3 hours daily, 5 days per week with free-swelling controls cultured in parallel. On days 21 and 42, strips were evaluated for tensile and compressive properties, as well as biochemical content and gene expression.

7.2.3 Histology and Immunohistochemistry

Paraffin sections (8 μm) were stained with hematoxylin and eosin (H&E, Sigma, St. Louis, MO), Alcian Blue (pH 1.0), or Picrosirius Red for cell distribution, sulfated proteoglycans and collagens, respectively. For immunohistochemistry, antigen retrieval was performed by incubating sections in proteinase K (20 μg/mL in TE buffer, pH 8.0) at 37°C for 15 minutes, then at 25°C for 10 minutes. Collagens type I (MAB3391, Millipore, Billerica, MA) and type II (11-116B3, Developmental Studies Hybridoma Bank, Iowa City, IA) primary antibodies were used. Subsequent reaction and visualization with DAB chromogen reagent (DAB150 IHC Select, Millipore, Billerica, MA) was carried out as in Section 3.2.8 (Huang et al. 2009). Color images were captured at 2.5X or 10X magnification using a microscope equipped with a color CCD digital camera and the QCapturePro acquisition software.

Depth-dependent inhomogeneity in matrix deposition was semi-quantitatively assessed on Alcian Blue and Picrosirius Red stains of construct cross-sections (Image J, National Institute of Health, Bethesda, MD). To carry out these analyses, color images were converted to 32-bit grayscale images. Each cross-section was divided into three layers of

equal thickness (surface, middle, deep). Mean intensity values were measured in the surface and deep layers (255: black, 0: white) of each construct.

7.2.4 Finite Element Analysis

A finite element model (FEM) was generated using experimentally-determined properties and geometries of day 21 MSC-seeded constructs (**Figure 7-4**). A biphasic, poroelastic material was used with incompressible fluid and solid phases. As fluid was allowed to exit and enter the construct, the volume of the overall mixture was not fixed. Sliding contact was modeled using an impermeable spherical indenter with a diameter of Ø25 mm. A velocity of 2.5 mm/s and an axial deformation of 20% was applied. The contact interface (between indenter and construct) was assumed to be frictionless and the bottom of the construct was fixed. Fluid was allowed to escape from the free boundaries not in direct contact with the indenter. FEM results were visualized using the FEBio Postview software.

7.2.5 Statistical Analysis

Statistical analysis was performed on mechanical and biochemical data using one way ANOVA. A two-way ANOVA was used to assess differences in gene expression, with independent variables of axial strain and media condition. Where significance was indicated by ANOVA, Tukey's posthoc tests were performed. Significance was determined at $p \leq 0.05$ and a trend toward significance determined at $p < 0.1$. All values are reported as mean ± standard deviation.

7.3 Results

7.3.1 Sliding Contact Bioreactor Characterization

A displacement-controlled bioreactor was constructed to apply sliding contact (SLC) to hydrogel constructs via spherical indenters (**Figure 7-1A-D**). Indenter sizes ranging from Ø2-Ø25 mm were initially considered. Calculations derived from the indenter geometry (spherical) and an assumed axial deformation of 10% showed that increasing indenter diameter increased the contact area, while decreasing the strain rate for a given sliding velocity (**Figure 7-2A**). As indenter curvature was less steep with increasing diameter, strain rates were minimized with larger indenter sizes. Assuming an indenter size of Ø25 mm and 10% axial strain, sliding velocities of 2.5-20 mm/s were then considered. Strain rates generated at 20 mm/s reached nearly 200%/s while lower sliding velocities generated much lower strain rates (~25-50%/s, **Figure 7-2B**). From these initial calculations, an indenter diameter size of Ø25 mm and sliding velocity of 2.5 mm/s were incorporated into the bioreactor design and used for all experiments. As the sliding contact path was ~13 mm in length, the frequency of sliding was ~0.1 Hz.

In addition to the above considerations, a range of axial strains was also applied to assess the effects of SLC on chondrogenesis. Calculations based on Ø25 mm indenter size and 2.5 mm/s sliding velocity showed that increasing the applied axial strain (5-20%) also increased indenter contact area. Strain rate was also higher with increasing axial strain, with non-uniform strain rates generated throughout the displaced region. While strain rates were lowest at the center of the indented region (regardless of the applied strain),

strain rates increased with increasing distance from the center due to the curvature of the indenter (**Figure 7-2C, D**).

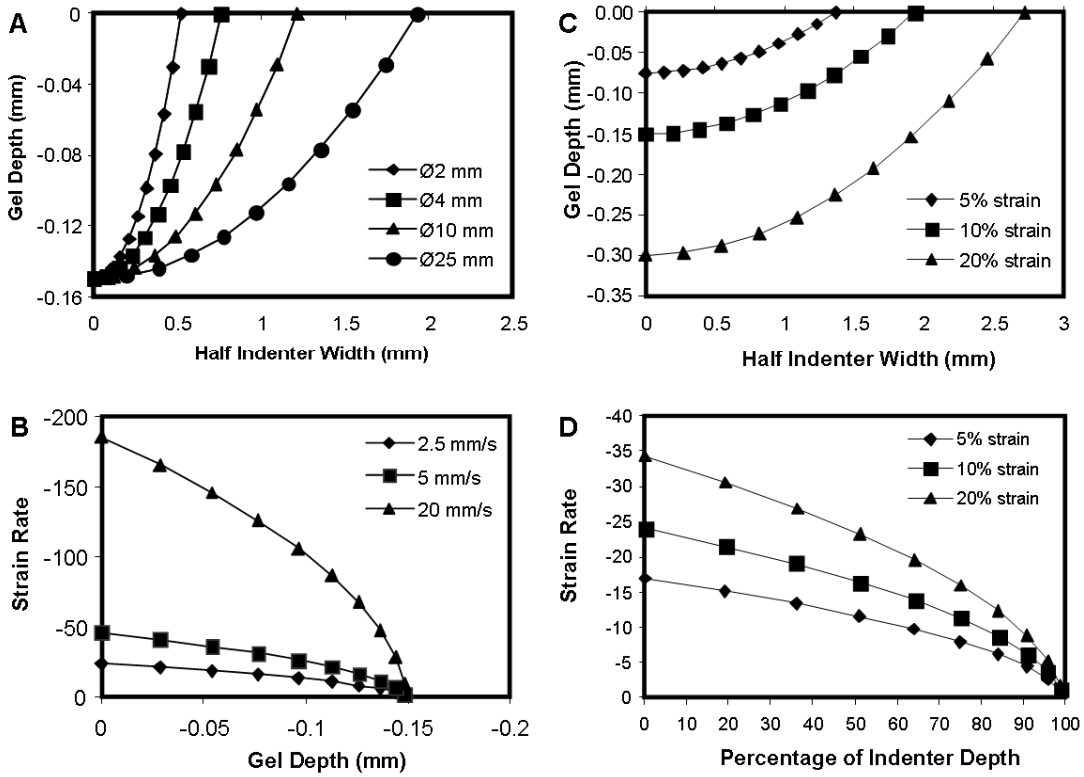

Figure 7-2: (A) Indenter displacement was calculated for a range of indenter diameters. (B) Strain rate was calculated for a range of sliding velocities. (C) Indenter displacement and (D) strain rate were calculated for axial displacements of 5, 10 and 20%.

After construction of the bioreactor system, initial studies were performed on acellular agarose constructs. Consistent with our previous studies (Huang et al. 2008), increasing agarose concentration resulted in a higher tensile modulus, without changing the ultimate strain (**Figure 7-3**). For both 2% and 6% acellular agarose constructs, ultimate tensile strain was ~10%. Under chondrogenic culture, the tensile modulus of MSC-seeded constructs was higher at day 21 (compared to 2% agarose starting values) and was akin to that of the 6% acellular agarose constructs (~270 kPa). The ultimate strain also improved

by day 21 to ~40% as matrix was deposited (compared to ~10% starting values, **Figure 7-3**). Similarly, the compressive properties and biochemical content increased with time in culture (**Figure 7-4A**). Under SLC, both 2% and 6% acellular gels consistently fractured through the midline (along the sliding contact path) for all axial strains applied (not shown). Fracture was observed in all cases within a few minutes after initiation of loading. In contrast, pre-cultured MSC-seeded constructs remained intact after 3 hours of SLC at 20% axial strain. No adverse effects on cell viability was observed with SLC compared to free-swelling (FS) controls (**Figure 7-4B**). Based on these findings, MSC-seeded constructs were chondrogenically pre-cultured for 21 days prior to the initiation of sliding for subsequent studies.

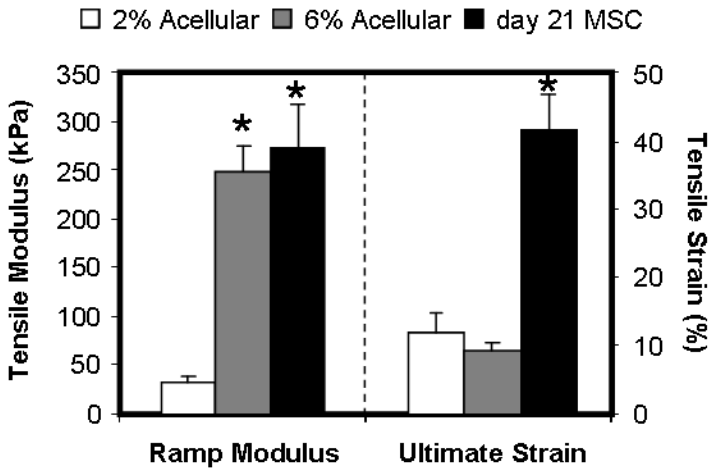

Figure 7-3: Tensile properties of acellular and MSC-seeded agarose constructs. While the tensile modulus increased with higher agarose concentration, the ultimate strain was comparable between 2% and 6% acellular agarose. After 21 days of culture in CM+, the tensile modulus of MSC-seeded constructs was the same as 6% agarose, but the ultimate strain was 4-fold higher compared to acellular constructs. * indicates greater than 2% agarose ($p<0.05$). Data represent the mean and standard deviation of three samples per group per time point.

A

Construct Properties	Value
Compressive modulus (kPa)	13.6 ± 5.5
Tensile modulus (kPa)	337 ± 104
DNA content (µg/construct)	1.45 ± 0.2
GAG content (% ww)	1.09 ± 0.2
Collagen content (% ww)	0.11 ± 0.04

B

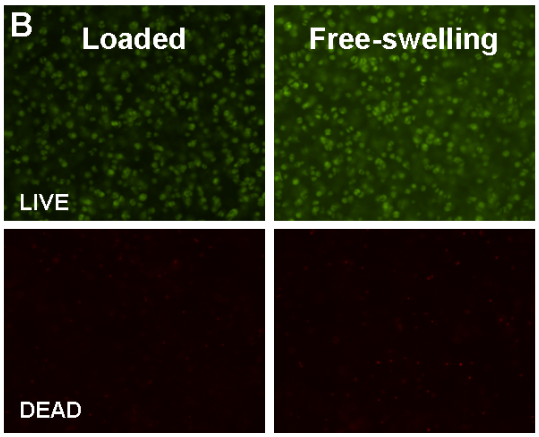

Figure 7-4: Mechanical and biochemical properties of MSC-seeded constructs cultured for 21 days in CM+ media. (A) Mechanical and biochemical properties improved with time in pro-chondrogenic culture. (B) Preliminary studies showed no adverse effect on cell viability when SLC was applied at 20% axial strain at 2.5 mm/s for 3 hours. Data represent the mean and standard deviation of six samples.

7.3.2 Chondrogenic Gene Expression in MSC-Seeded Constructs With Short-Term Application of Sliding Contact

To assess the effects of SLC on chondrogenic gene expression, loading was applied for 3 hours at 2.5 mm/s on MSC-seeded constructs following 21 days of pre-culture. Axial strains of 5%, 10% and 20% were evaluated and SLC was carried out in defined media in the presence (CM+) and absence (CM-) of TGF-β3. When SLC was applied in CM-, collagen type II and aggrecan expression were higher in groups subjected to 20% axial strain, compared to FS. An axial strain-dependent effect was observed in SLC constructs in CM+. While 5% strain did not alter collagen type II or aggrecan expression, SLC at 10% axial compression improved the expression of both of these genes (trend, $p<0.1$). Expression levels for these genes were further increased when SLC was applied at 20% strain, and were significantly higher compared to all other groups (**Figure 7-5**). An increase in proteoglycan 4 and collagen type I expression was only observed in SLC

constructs at 20% strain in CM+. As results from these studies demonstrated that SLC applied at 20% axial strain in CM+ was optimal for promoting chondrogenic gene expression, these parameters were employed for subsequent long-term studies.

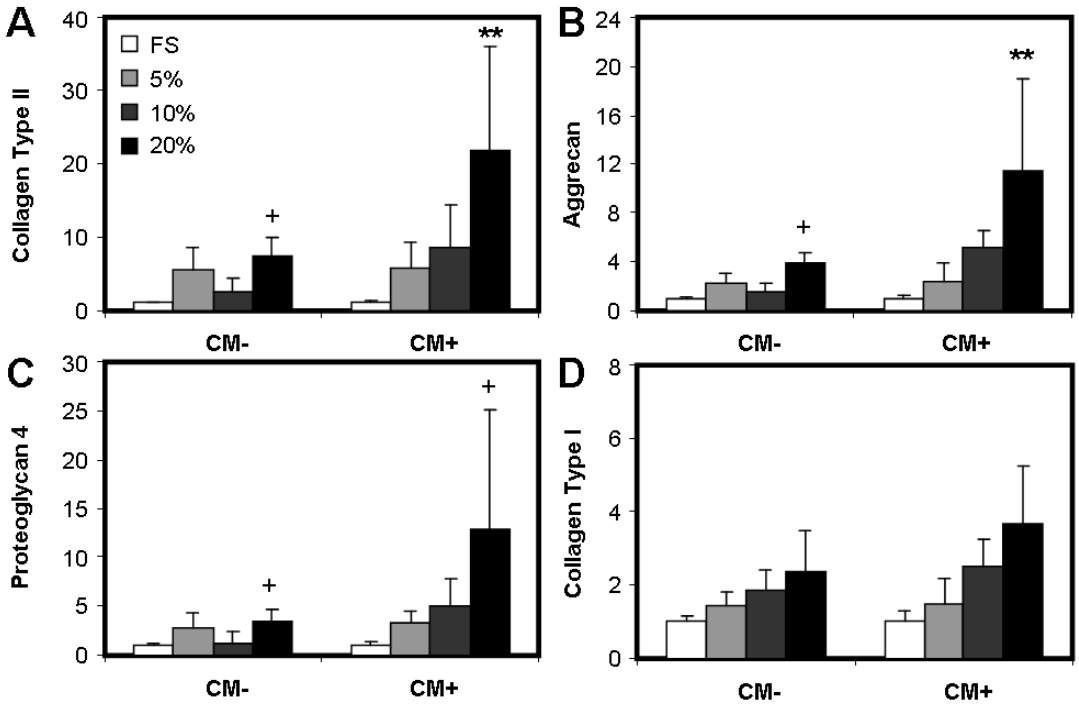

Figure 7-5: Cartilaginous gene expression with short-term application of SLC. (A) Collagen type II, (B) aggrecan, (C) proteoglycan 4 and (D) collagen type I gene expression was dependent on both media condition and axial strain. For all chondrogenic genes, expression was highest in CM+ with 20% axial strain. No significant difference was observed in collagen type I expression with SLC. Gene expression (normalized to GAPDH) was normalized to free-swelling controls within media type. At 20% axial strain, SLC applied in CM- was significantly lower compared to SLC applied in CM+. While SLC had some affect on PRG4 expression, the expression levels were much lower than collagen type II or aggrecan levels. Similarly, collagen type I expression was negligible compared to cartilaginous genes. Gene expression was normalized to GAPDH only. ** indicates greater than all within media condition ($p<0.05$), + indicates greater than free-swelling control within media condition ($p<0.05$). Data represent the mean and standard deviation of 4-6 samples per group per time point.

7.3.3 Functional Properties of MSC-Seeded Constructs After Long-Term Application of Sliding Contact

To evaluate whether long-term application of SLC could direct functional maturation, MSC-seeded constructs were subjected to 21 days of daily sliding contact (3 hours/day) following 21 days of pre-culture in CM+. By day 42, tensile properties were significantly greater compared to day 21, for both FS and SLC groups ($p<0.05$). The tensile stiffness and tensile modulus both increased with SLC, reaching values of ~0.8 N/mm and ~750 kPa, respectively (compared with ~0.6 N/mm and ~600 kPa for FS, **Figure 7-6A, B**). Day 21 and day 42 values for ultimate tensile strain were similar; this measure was unchanged with SLC and remained at ~40% (not shown).

Although DNA content was lower in SLC compared to FS at day 42, it was comparable to day 21 starting values. Both GAG and collagen contents were higher in SLC compared to FS (trend $p<0.1$); while GAG content was comparable in FS between days 42 and 21, collagen content was higher by day 42 ($p<0.01$, **Figure 7-6C-E**).

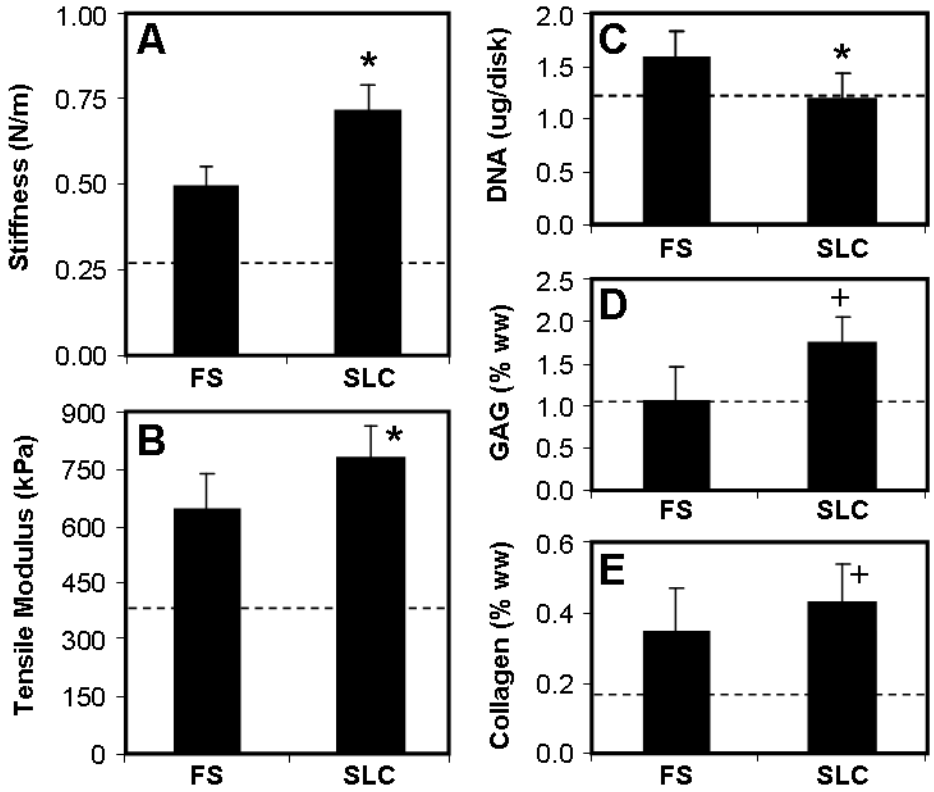

Figure 7-6: Mechanical and biochemical properties of MSC-seeded constructs after long-term application of SLC. (A) Tensile stiffness and (B) tensile modulus increased after 21 days of SLC. (C) DNA content (μg/construct) was lower for SLC compared to day 42 FS. Bulk measures of (D) GAG and (E) collagen content (% wet weight) were higher with SLC compared to FS at day 42. * indicates greater than day 42 controls ($p<0.05$), + indicates greater than day 42 controls ($p<0.1$). Data represent mean and standard deviation of six samples per group. Dashed line represents day 21 starting values.

7.3.4 Depth-Dependent Matrix Distribution in MSC-Seeded Constructs After Long-Term Sliding Contact

To assess whether matrix distribution was affected by SLC, cross-sections were stained with Alcian Blue to visualize proteoglycans (**Figure 7-7**), and staining intensity was quantified through the depth. Although bulk biochemical measures were not different with SLC (**Figure 7-6**), histological assessments showed distinct differences in depth-dependent matrix distribution at day 42. Alcian Blue intensity was comparable in the deep zones of FS and SLC constructs. While there was a slight increase in intensity at

the surface zones of FS constructs, the staining intensity at the surface of SLC constructs was much greater. Interestingly, while proteoglycan distribution was homogeneous through the depth in FS, type II collagen was non-uniform. The surface half of FS constructs exhibited even staining while the deep regions were marked by punctate type II collagen staining. In contrast, type II collagen was continuously distributed through the depth in SLC constructs; as with Alcian Blue stains, intense collagen staining was observed in the surface region (**Figure 7-8**).

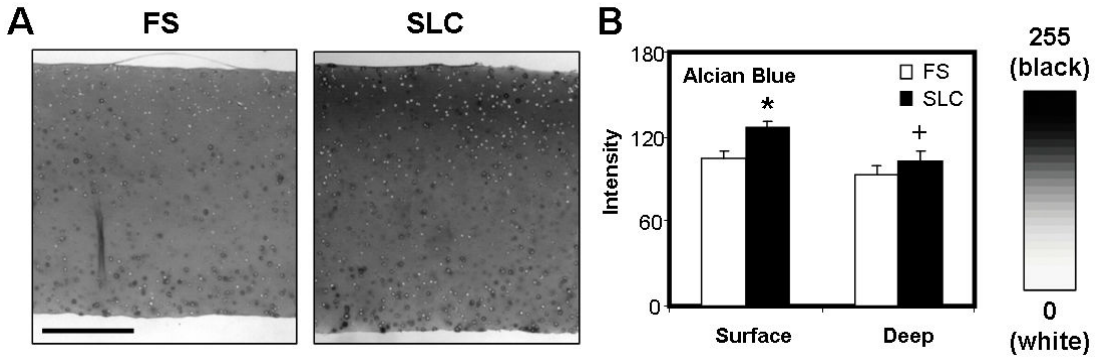

Figure 7-7: Depth-dependent distribution of ECM in MSC-seeded constructs after long-term application of SLC. Gray-scale images of (A) Alcian Blue stained cross-sections were assessed for zonal heterogeneity. (B) Intensity measurements at the surface zones were different between FS and SLC, with SLC constructs exhibiting more intense staining in the surface zone. Deep zone intensity measurements were not different between groups. * indicates higher than all values ($p<0.05$). Data represent mean and standard deviation of six samples per group. Scale bar: 0.5 mm.

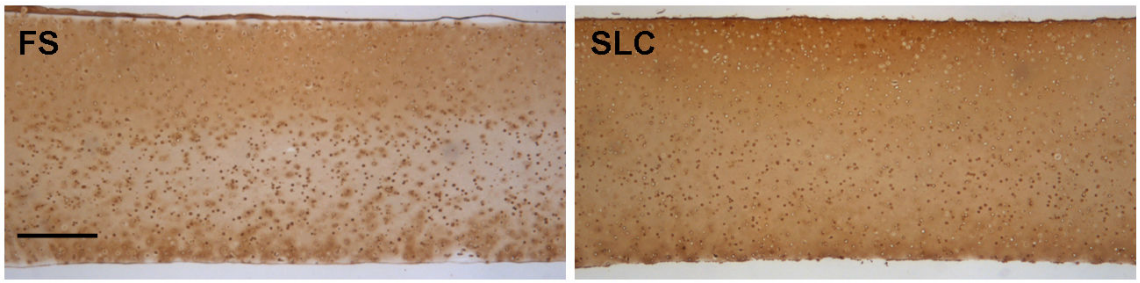

Figure 7-8: Type II collagen immunostaining of MSC-seeded constructs at day 42 showed more continuous distribution of collagen type II for SLC compared to FS. In addition, more intense staining was observed in the surface region of FS constructs. Scale bar: 0.5 mm.

7.3.5 Finite Element Modeling of Sliding Contact

A finite element model (FEM) was developed to better describe the mechanical signals imparted by SLC on MSC-seeded, pre-matured constructs. SLC was modeled using a 20% axial strain (y-direction), a sliding velocity of 2.5 mm/s and experimentally-derived construct properties at day 21 (**Figure 7-9A**). Physical signals were assessed at each of the nodes depicted in Figure 7A. FEM analysis of SLC demonstrated that fluid pressure was highest directly underneath the indenter (node 1). After indenter passage, fluid pressure at nodes 1 and 2 remained above baseline starting values (**Figure 7B**). In contrast, fluid pressure at node 4 remained at baseline levels throughout SLC. Interestingly, the regions of highest fluid flow did not extend to the outer edges of the construct; fluid flow in the z-direction was highest in nodes 2 and 3, and lowest in nodes 1 and 4 (**Figure 7-9C**). Increased tensile strain (x-strain) was observed at all nodes with SLC and was highest at node 1. Tensile strain was heterogeneous through the depth and primarily localized to the surface half of the construct (**Figure 7-9D**). As expected, the compressive strain (y-direction) was greatest directly under the indenter at 20% (**Figure 7-9E**), consistent with previous calculations (**Figure 7-2E**).

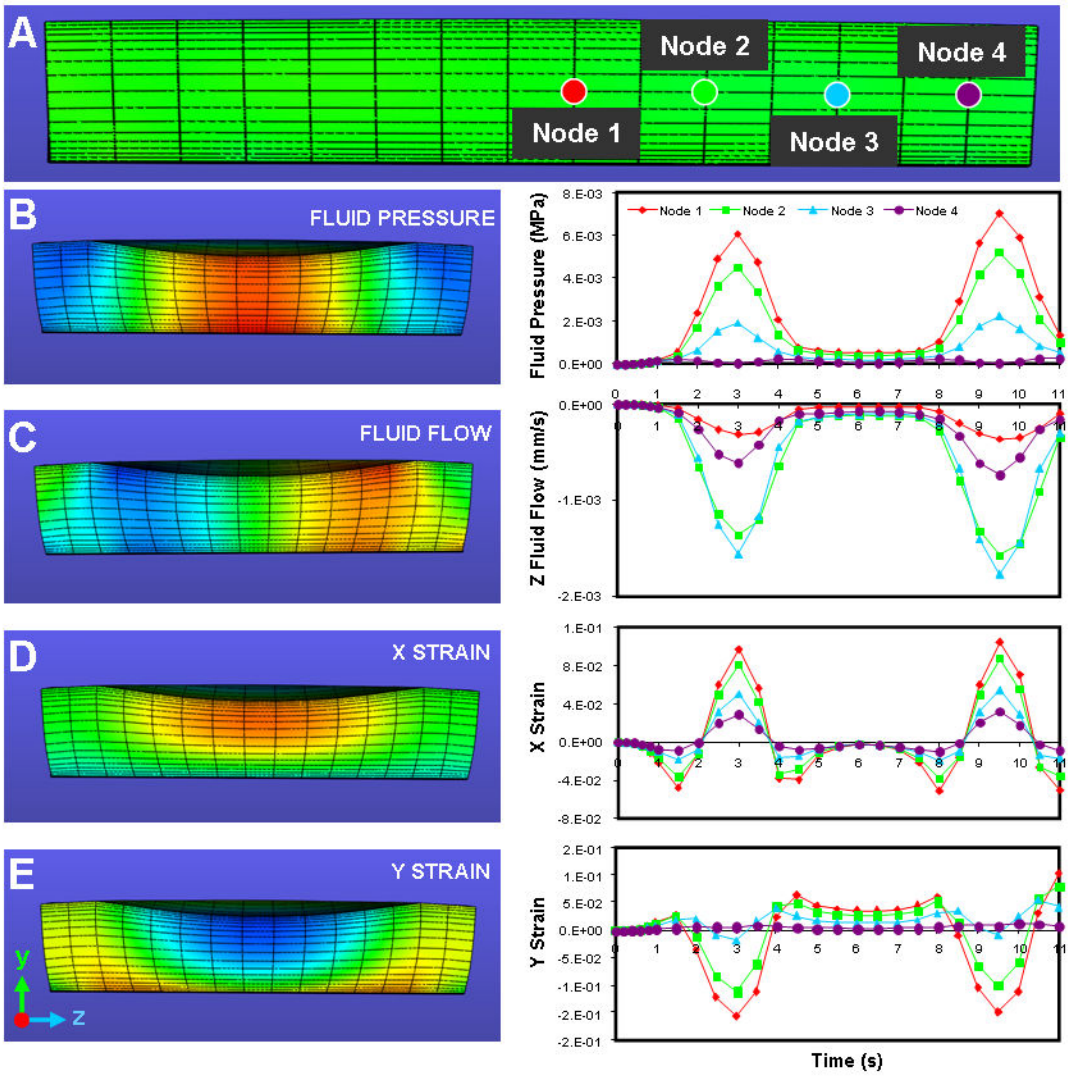

Figure 7-9: Modeling of spatial and temporal mechanobiologic signals arising from SLC on day 21 MSC-seeded constructs. (A) Location of nodes within construct. Cross-sectional views and graphical representations of (B) fluid pressure, (C) fluid flow, (D) x-strain (tensile) and (E) y-strain (compressive) as the indenter traveled along the construct length (time = 0-6) and back (time = 6-11). Length, depth and width of constructs are represented by x, y and z, respectively.

Fluid efflux/influx (y-direction) was also localized to the surface, but the pattern of flow was relatively complex compared to fluid flow in the x- and z-directions. In these directions, fluid moved symmetrically outward from the indenter during SLC and flow was not observed in the construct periphery (**Figure 7-10**). However, in the y-direction,

the pattern of flow was complicated by bulging at the construct periphery. With indenter passage (time = 3s), outward bulging was noted, coincident with influx of fluid at the surface (top view). Within the construct (cross-sectional view), fluid moved upward near these points. At time = 4s, the construct periphery recovered its initial dimensions and fluid efflux in the y-direction was noted at these regions. Within the construct at this time, fluid in the positive y-direction was localized to the central surface areas as the construct recovered from the applied axial deformation (**Figure 7-10**).

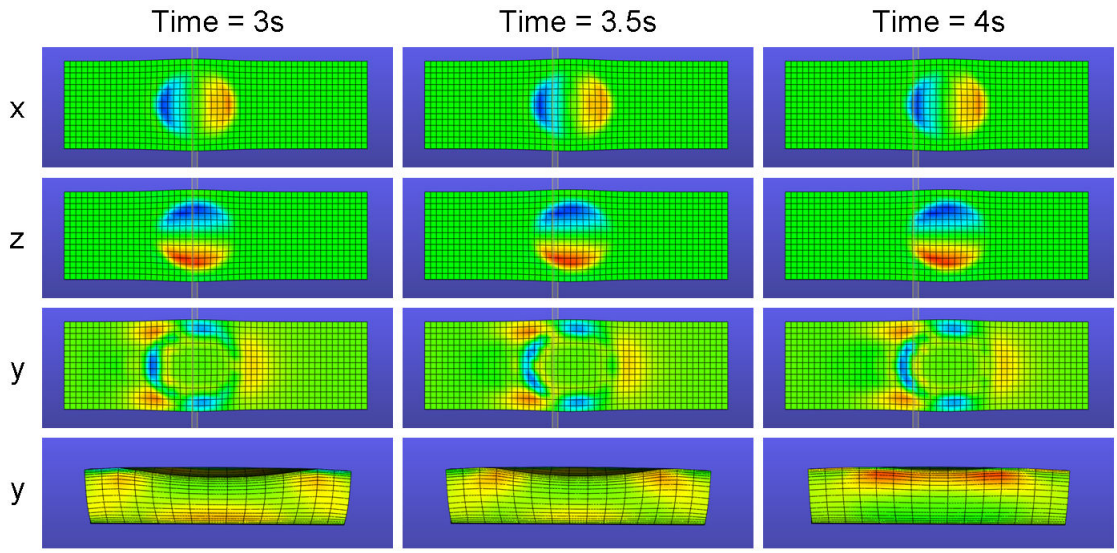

Figure 7-10: Modeling of spatial and temporal mechanobiologic signals arising from SLC on day 21 MSC-seeded constructs. Top view of fluid flow in the (First row) x-direction (Second row) z-direction and (Third row) y-direction. (Fourth row) Cross-sectional view of y-direction fluid flow.

7.4 Discussion

In Chapter 4, we showed that long-term mechanical stimulation of MSC-seeded constructs via dynamic compressive loading (initiated after a period of chondrogenic pre-culture) improved the compressive properties of these constructs and enhanced matrix distribution. Though these results were encouraging and showed that chondrogenically differentiated MSCs are able to translate mechanical signals to generate constructs with higher functional properties, several limitations remained. For example, the collagen content and those properties associated with collagen content (such as the dynamic compressive properties) were quite low relative to the native tissue. These studies were also not designed to instill key hallmark properties of articular cartilage (inhomogeneity and anisotropy) or to examine developing tensile properties. As these characteristic properties arise during cartilage maturation with the advent of physiologic loading, we hypothesized that a more representative loading environment may be required. To test this hypothesis, we constructed and characterized a novel sliding contact bioreactor to better replicate the mechanical loading environment within the knee joint.

During physiologic loading, the majority of the applied load is supported by pressurization of the interstitial fluid, which shields the solid matrix from excessive deformation. Theoretical predictions suggest that this fluid load support is enhanced by a large migrating contact area, which enables sustained fluid pressurization over a larger contact region (Ateshian et al. 1995; Caligaris et al. 2008). The same phenomenon is observed for higher indenter deformation (given a relatively large indenter radius), as this also leads to greater contact areas. Notably, this is only true for curved indenters, as

increasing the load applied with a flat indenter would not affect the contact area. With these considerations in mind, we designed our bioreactor system with spherical indenters and a moving contact area. Calculations were performed varying the indenter diameter, the travel velocity and the applied axial deformation to assess contact areas and strain rates, in order to best replicate *in vivo* conditions.

Using this sliding contact bioreactor system, initial short term loading studies showed that chondrogenic gene expression was dependent on the applied axial deformation and TGF-β3 supplementation. Aggrecan and collagen type II gene expression was enhanced under 20% axial deformation within both media conditions, but was greatest in the presence of TGF-β3. This was consistent with our previous studies in Chapter 4 showing that long-term improvements in functional chondrogenesis was only observed when TGF-β3 was present. Interestingly, human MSC-seeded fibrin-polyurethane sponges subjected to simultaneous compression and shear responded positively to loading only in the absence of TGF-β1 (Li et al. 2009). While chondrogenic gene expression was higher in groups treated with TGF-β1, no additional effect was observed with loading when exogenous TGF-β1 was present. This important difference may be due to the type of biomaterial used as MSCs within a fibrin-polyurethane composite construct may experience and translate mechanical signals differently than MSCs encapsulated within agarose, an inert biomaterial that maintains cells in an isolated, rounded morphology. In addition, the bioreactor system used in those studies is distinct from the current system, in that shear loading is superimposed on dynamic compressive loading. Though not

described, the physical signals arising from such a system is likely to be very different compared to the system used in the current work.

Based on our short-term studies, we then applied long-term sliding contact using optimized parameters (20% axial deformation with 10 ng/mL TGF-β3) and showed that after 3 weeks of loading, the tensile properties and biochemical content of MSC-based constructs were improved compared to non-loaded controls. We also observed biochemical inhomogeneity within the constructs subjected to sliding, with collagen type II localized to the surface region. Unexpectedly, inhomogeneity in proteoglycan distribution mirrored that of collagen, which is inconsistent with the structure of native articular cartilage, where proteoglycans are primarily localized to the middle and deep zones. These results suggest that sliding contact may therefore have a general stimulatory effect in this surface region. FEM analysis showed that the physical signals arising from sliding contact were indeed depth-dependent. Tensile strains and fluid influx/efflux in particular were localized to the surface regions, though compressive strains were non-uniform through the depth. In contrast, fluid pressure and fluid flow in the lateral directions spanned the construct depth. The tensile strains generated with sliding also exhibited direction-dependence with tensile strains of >10% observed parallel to the sliding direction. Interestingly, preliminary experiments with acellular agarose constructs showed that fracturing along the midline (parallel to the sliding direction) occurred soon after the initiation of sliding contact. While the tensile moduli of acellular constructs differed, the ultimate tensile strains were consistently 10%. As proof of principle, day 21 MSC-based constructs (ultimate tensile strain: ~40%) were able to

withstand hours of repeated loading, suggesting that the physical cues predicted by FEM analysis were reflected in our sliding contact system.

As indicated by FEM, the mechanical environment experienced by the cells in the surface half of constructs is complex. Tensile and compressive strains are both present, along with symmetric fluid pressure and non-symmetric fluid flow. While chondrocyte (Buschmann et al. 1995; Mauck et al. 2000; Mauck et al. 2002; Lima et al. 2007) and MSC (Huang et al. 2004; Mauck et al. 2007; Mouw et al. 2007; Thorpe et al. 2008; Huang et al. 2010) response under applied compressive strains is relatively well documented, fewer studies have assessed the effect of tensile strains in a cartilage tissue engineering context. In general, dynamic compressive loading enhances chondrogenic gene expression and in the case of chondrocytes, improves GAG content. Previous work applying dynamic tensile loading to chondrocyte-seeded fibrin showed reduced proteoglycan synthesis with loading (Connelly et al. 2004). Interestingly, tensile loading to superficial zone chondrocytes seeded in fibrin promoted proteoglycan synthesis, while the same loading applied to deep zone chondrocytes did not (Vanderploeg et al. 2008). When cyclic tension was applied to MSCs seeded in collagen-GAG scaffolds, the rate of GAG synthesis was enhanced (McMahon et al. 2008). In another study using MSC-seeded fibrin, proteoglycan synthesis was only enhanced during early stages of tensile loading while protein synthesis remained elevated at later stages (Connelly et al. 2010); collagen type I expression was also stimulated while no change was observed in collagen type II or aggrecan expression, consistent with a fibrocartilaginous phenotype. Although we observed a small increase in collagen type I expression with sliding contact, we saw a

far greater response in collagen type II and aggrecan expression levels. Collectively, these studies show that both compressive and tensile deformations applied to MSC-seeded constructs can enhance GAG and collagen content, consistent with the results of the current study.

While the tensile properties and collagen content improved with sliding contact by 25% and 15%, respectively, the values reached are still far lower than that of articular cartilage. Because the collagen content was relatively poor, collagen orientation was not readily assessed by polarized light microscopy and preliminary analysis of collagen alignment showed no differences between groups. It is possible that 3 weeks of sliding was insufficient and longer-term loading will be required to enhance collagen anisotropy. Alternative methods of analysis, such as FT-IRIS (Bi et al. 2005) or second harmonic imaging microscopy (Stoller et al. 2002), may also be used to capture early changes in collagen alignment that were not evident from polarized light microscopy analysis. In this study, tensile properties were only assessed parallel to the sliding direction; however these properties may also be assessed perpendicular to the sliding direction to evaluate the development of mechanical anisotropy.

While we chose a 3 week pre-culture duration based on our previous studies using dynamic compression, a longer pre-culture duration may enhance baseline construct properties prior to the initiation of sliding and lead to better outcomes. While compressive properties plateau after 3 weeks, tensile properties continue to increase past this timepoint, due to reduced rates of matrix accumulation. This is likely due to

differences in construct geometries, as the diffusion limitations in rectangular agarose strips is more severe compared to agarose cylinders. To overcome these limitations, dynamic culture conditions (agitation of media) may be investigated for future work. In addition, the presence of agarose itself may limit the extent of matrix remodeling as agarose is an inert biomaterial and does not degrade. The morphology of chondrocytes in the superficial zone of native cartilage is flattened in shape and oriented parallel to the surface; agarose may prevent cells from adopting this morphology. As a rounded phenotype is necessary for proper chondrogenic induction, a hydrogel that evolves with time in culture is ideal. Recent work suggests that hydrogels containing hydrolytically or MMP-degradable components enhance collagen deposition by increasing pore-size over time (Bryant et al. 2003; Chung et al. 2009). It may be that the use of these novel biomaterials will better enable MSC-mediated matrix remodeling in response to sliding contact.

CHAPTER 8: HIGH THROUGHPUT SCREENING FOR MODULATORS OF MESENCHYMAL STEM CELL CHONDROGENESIS

8.1 Introduction

Adult bone marrow derived MSCs are a multi-potential and self-renewing cell type that can be induced to differentiate along a variety of tissue-specific pathways, including cartilage (chondrogenesis) and bone (osteogenesis). Given their chondrogenic potential, MSCs are a promising cell source for investigating skeletal developmental paradigms and cartilage tissue engineering applications. Indeed, recent studies have shown that MSCs undergo chondrogenesis in 3D environments, such as fibrous networks, porous foams, and hydrogels (Angele et al. 1999; Huang et al. 2004; Li et al. 2005; Mauck et al. 2006), and deposit a cartilage-like ECM. However, the quantity and functional capacity of ECM formed by chondrogenic MSCs is reduced relative to the ECM formed by fully differentiated chondrocytes cultured under identical conditions (Mauck et al. 2006; Huang et al. 2008). Thus, further work is necessary to optimize MSC chondrogenesis for engineering replacement tissues.

A better understanding of the signaling pathways underlying MSC differentiation is critical to understanding functional chondrogenesis. To date, growth factors have been widely used to induce chondrogenesis, however, the molecular mechanisms involved in this phenotypic conversion are only partially defined. Several studies have used synthetic molecules to investigate signaling pathways known to be involved in cartilage development or chondrocyte biosynthesis to determine their functional roles in MSC differentiation. For example, MAPK and Wnt signaling pathways have been implicated

in TGF-β1-mediated chondrogenesis (Tuli et al. 2002; Tuli et al. 2003), and synthetic MAPK inhibitors block pellet formation. It has also been shown that Insulin-Like Growth Factor-1 (IGF-1) activates the PI3K pathway during chondrogenesis, while induction by TGF-β1 does not (McMahon et al. 2008). In micromass cultures of limb-bud cells (a related, but distinct, cell type), synthetic compounds that inhibit Rac and ROCK activity alter chondrogenic progression (Woods et al. 2005; Woods et al. 2007). Disruption of cytoskeletal dynamics in these same cells with cytochalasin D and colchicine can also influence chondrogenesis (Woods et al. 2006). Analogous to results from chondrocyte de- and re-differentiation studies (Brown et al. 1988), actin cytoskeleton disruption improves the chondrogenic differentiation of embryonic stem cells (Zhang et al. 2006). More recently, investigators have taken an informed approach by identifying factors involved in MSC chondrogenesis. For example, expression analysis suggests a decrease in retinoic acid receptor β is associated with chondrogenesis; subsequent treatment with a synthetic inhibitor (LE135) of this pathway induced chondrogenesis via a Sox 9-independent pathway (Kafienah et al. 2007). These studies demonstrate that a clearer understanding of the molecular mechanisms governing MSC chondrogenesis may provide insight into methods for optimizing functional differentiation, and that small molecule modulators will be critical in these efforts.

While induction of MSC chondrogenesis is well-defined using existing protocols and media formulations, the capacity and potency of alternative factors to regulate chondrogenesis remains largely unexplored. Although several studies have examined the chondrogenic effects of various combinations of growth factors and media supplements,

they have been limited in scope since execution, maintenance, and analysis remains a laborious and time-consuming process (Awad et al. 2003; Indrawattana et al. 2004; Toh et al. 2005; Estes et al. 2006; Im et al. 2006; Longobardi et al. 2006). Most chondrogenesis assays require a 'macro' pellet (>225,000 cells in 200μL of media) cultured in individual tubes to ensure sufficient ECM for subsequent quantification steps. Given this pellet size, the screening of large chemical libraries or numerous conditions is impractical; for example, a single screen of the >200,000 compounds in the NIH Small Molecule Repository (SMR) would require ~46 billion cells from a single donor. Recent efforts in minimizing handling have used 96-well conical plates (Penick et al. 2005; Welter et al. 2007); however, cell number in each pellet and time required to analyze differentiation end-points remains a limiting factor.

These limitations may be overcome by high-throughput screening (HTS), wherein the simultaneous layout and query of a large number of conditions may be realized within a single plate. HTS depends on the use of robotic liquid handling systems and on the development of sensitive and readily quantifiable assays (Walters et al. 2003). In a typical screen, a drug target or model system is reacted against a large range of chemicals contained in a compound library. Identified agents that modulate pathways of biologic interest are then verified via secondary confirmatory assays and characterization of dosage response. Numerous chemical libraries, such as the National Institute of Neurological Disorders and Stroke (NINDS) library and the Library of Pharmacologically Active Compounds (LOPAC), contain small molecules of known pharmacologic activity. Additionally, the recently developed SMR is populated by a vast

number of compounds with unknown activity. Few studies have assayed these libraries to study MSC differentiation towards skeletal phenotypes with HTS methods. One recent study used zebrafish as a model to screen >5000 compounds from commercial libraries and identified dorsomorphin, an inhibitor of bone morphogenic protein (BMP) type I receptor signaling (Yu et al. 2008). HTS was also used to identify osteogenic suppressors in MSC monolayers using an siRNA library (Zhao et al. 2007) and the osteogenic inducer purmorphamine from a custom chemical library (Wu et al. 2002). These studies illustrate the power of HTS for identifying new compounds. However, chondrogenic differentiation protocols are more complicated than the assays used to date and require specific adaptation of the standard protocol to be useful in HTS. This is the first report of a high-throughput assay for screening MSC chondrogenesis.

An HTS assay for chondrogenesis would enable the rapid optimization of effective media formulations for tissue engineering and would provide a platform for pharmaceutical screening to identify new chemical agents for the treatment of musculoskeletal pathologies. To optimize cell culture and assay procedures to enable high throughput screening of MSC chondrogenesis, we have focused on minimizing the cell number required, manual handling, and culture durations. A novel in-well digestion protocol was developed to enable rapid post-processing and to further minimize handling. In addition, a precise and robotic approach for layout, culture, and analysis of ECM deposition using 'micro' MSC pellets (10,000 cells in 50μL of media) in a 384-well format was validated. Following validation in this 384-well format, a combinatorial study analyzing the chondrogenic effects of TGF-β3, BMP-2, IGF-1, Fibroblast Growth Factor-2 (FGF-2)

and their combinations (81 combinations) using three different doses per growth factor (none, low, high) was executed. Finally, we carried out an initial screen of the NINDS small molecule library containing 1040 known compounds and demonstrated the feasibility of this technology for use in HTS for potential effectors of chondrogenesis. These methods and results provide a new approach to the rapid identification of compounds that influence chondrogenic fate decisions by MSCs.

8.2 Materials and Methods

8.2.1 HTS Assay Development

8.2.1a Minimization of Pellet Size, Media Exchange, and In-Well Analysis

MSC pellets were formed via centrifugation (300×g) for five minutes in conical 96-well polypropylene plates (Nalge Nunc International, Rochester, NY). Pellets contained 225,000, 150,000, 75,000, 30,000 and 15,000 MSCs with all assays performed in triplicate. Each pellet was maintained in 150 μL of CM. Pellets were cultured with (CM+) or without (CM-) 10ng/mL TGF-β3 (R&D Systems, Minneapolis, MN) for 7 days, with media changed twice, once or not at all. Three replicate experiments were carried out with consistent results (one replicate shown). On day 7, pellets were digested with direct addition of 30 μL concentrated papain solution (8.96 units/mL in 0.1M sodium acetate, 10M cysteine HCL, 0.05M EDTA, pH 6.0) into each well. Plates were sealed with optical adhesive covers (Applied Biosystems, Foster City, CA) and incubated in a 60°C waterbath overnight. To assess GAG content, 40 μL of digestate was manually combined with 250 μL of dimethylmethylene blue (DMMB) reagent and absorbance read at 540/595nm (Farndale et al. 1986). In a separate study, cartilage gene expression was

evaluated in pellets of different sizes (30,000 and 225,000 cells/pellet) with culture as above with no media changes. After 7 days, pellets were combined and gene expression analyzed via real-time PCR as in (Mauck et al. 2006). For gene expression analysis, 18 pellets (30K pellet size) or 3 pellets (225K pellet size) were pooled for each sample with n=3 samples per group assessed. PCR amplification was carried out with primers specific for aggrecan and type II collagen and expression was normalized to the housekeeping gene glyceraldehyde-3-phosphate dehydrogenase (GAPDH).

8.2.1b Inhibition of Chondrogenesis with IL-1β

To confirm that chemical screens may be performed, Interleukin-1β (IL-1β, R&D Systems, Minneapolis, MN), a known inhibitor of chondrogenesis, was used to block the chondrogenic effect of TGF-β3 (Majumdar et al. 2001). Large (225,000) and small (30,000) pellets were formed as described above in 96-well plates in 150μL of CM- or CM+ media supplemented with IL-1β at 0, 0.1, 1.0, 10.0 ng/mL. Pellets were cultured with no media changes and GAG content assessed on day 7.

8.2.1c Assessing DMSO Sensitivity

To assess the sensitivity of MSCs to dimethyl sulfoxide (DMSO), a common solvent in chemical libraries, small pellets (30,000) were formed in 96-well plates and exposed to CM- or CM+ media in the presence of graded concentrations of DMSO (0%, 0.10%, 0.25%, 0.50%, 0.75%, 1 %) for 7 days. GAG and DNA content was assessed via the DMMB and PicoGreen assays, respectively. The PicoGreen dsDNA assay (Molecular Probes, Eugene, OR) was carried out by reacting 10 μL of digested sample with 100 μL

of PicoGreen working reagent (50 μL PicoGreen reagent, 500μL 20X TE buffer, 9.45mL deionized water) (Huang et al. 2008). Following a five minute incubation in the dark, plates were read at 480nm excitation/520 nm emission (Bio-Tek Synergy HT Multi-Mode Microplate Reader).

8.2.1d Automation of Layout and Analysis in 384-well Format

For optimization of culture and analysis techniques in a 384-well format for HTS, a stream-lined protocol for chondrogenesis was applied (**Figure 8-1**). Total media volume and cell number was further reduced from 96-well procedures by a factor of three. Cells were dispensed automatically using a Matrix Technologies WellMate system with 10,000 cells pelleted in 50 μL of CM in 384-well conical plates (Greiner Bio-One, San Diego, CA). After centrifugation (5 minutes at 300×g), pellets were cultured for 7 days in CM- or CM+, with a Breathe-Easy membrane (Research Products International Corp, Mt. Prospect, IL) sealing all wells to minimize evaporation and allow for gas exchange. After culture for 7 days, the Breathe-Easy membrane was removed and in-well digestion was performed by automated addition of 10 μL of concentrated papain solution (3.36 units/mL) using the WellMate system. Plates were then sealed with ArctiSeal sealing mats (ArcticWhite LLC, Bethlehem, PA) and incubated in a 60°C waterbath as described above. Subsequently, a robotic liquid handling system (PerkinElmer Evolution P3 Pipetting Platform) mixed and transferred 10 μL of the digestate to a new flat-bottomed 384-well assay plate (Corning Inc., Corning, NY), and the GAG assay was performed by reaction with 60 μL DMMB dye solution as described above (PerkinElmer Envision 2102

Multilabel Reader). DNA content was similarly assessed by reaction of 1 µL of digestate with 10 µL of PicoGreen working reagent.

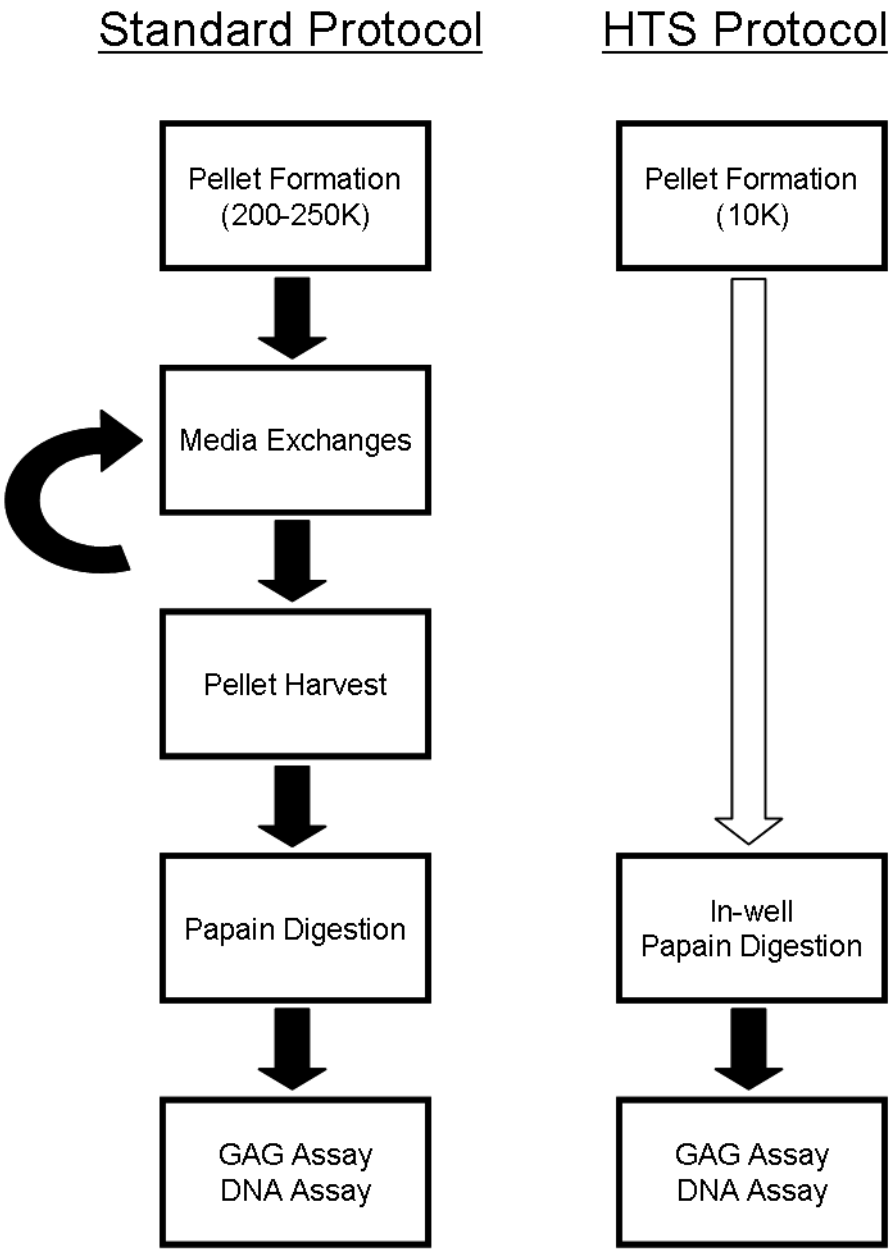

Figure 8-1: Schematic of chondrogenesis protocols. Flow diagram of the standard chondrogenesis protocol and the HTS-optimized chondrogenesis protocol with each handling step represented by a black arrow. White arrow indicates where handling steps have been eliminated.

8.2.2 Growth Factor Combinatorial Screen

To demonstrate the feasibility of assaying combinations of multiple growth factors at varying dosages, a screen was carried out using TGF-β3, BMP-2 (R&D Systems, Minneapolis, MN), IGF-1 (Peprotech, Rocky Hill, NJ) and FGF-2 (Peprotech, Rocky Hill, NJ). The effects of three different concentrations (none, low, high) were assessed for each growth factor. For TGF-β3 and FGF-2, the low and high concentrations were chosen as 1 ng/mL and 10 ng/mL, respectively. Low and high concentrations of BMP-2 and IGF-1 were chosen as 10 ng/mL and 100 ng/mL. Growth factor concentrations were selected based on previous studies of MSC chondrogenesis (Barry et al. 2001; Solchaga et al. 2005; Toh et al. 2005; Estes et al. 2006). The chondrogenic and proliferative effects of each growth factor was assessed alone and in combinations of two, three and four growth factors at all dosages for a total number of 81 groups (n=16 pellets per group). To carry out this study, MSCs were pelleted in 384-well plates as described above with 10,000 cells in 30 μL CM-. Growth factors were dispensed via automation at 5 μL volumes to achieve desired concentrations in 50 μL. CM- medium (5-20μL) was dispensed into wells containing three or fewer growth factors to bring the final volume per well to 50 μL. Papain digestion was executed as described above. An initial analysis of GAG deposition indicated that for certain combinations of growth factors, the amount of GAG accumulated exceeded the measurable range when assayed using our standard volume ratios. Therefore, the DMMB assay was performed by combining 5 μL of digestate with 80μL of DMMB dye. The DNA assay was performed via automation as described above.

8.2.3 NINDS Library Screen

After confirming assay sensitivity in the 384-well culture format and showing robustness of chondrogenesis in the presence of DMSO, HTS was performed using the NINDS library (1040 compounds, listed at http://www.msdiscovery.com/ninds.html) of small molecules. To execute this study, micro-pellets were formed as above in conical 384-well plates with 10,000 cells in 45 μL of CM- or CM+ media. Compounds from the NINDS library were prepared by diluting 10 mM stock solutions in CM-. Diluted compound solutions (5 μL) were added to achieve a final concentration of 10 μM in 50 μL (0.1% final DMSO concentration). Media only (CM-) and cell only (in CM- or CM+) controls were maintained in each plate. Papain digestion and GAG assays were performed via automation as described above. Possible inducers of chondrogenesis (CM- "hits") were identified by selecting values above a threshold (150% of average CM- control values) in CM-. Possible inhibitors (CM+ "hits") were identified by selecting values below a threshold (50% of average CM+ control values) in CM+. DNA content of the identified inhibitors was assessed to identify compounds that were cytotoxic rather than anti-chondrogenic. Compounds that reduced DNA content by more than 40% compared to CM+ control values were considered cytotoxic.

8.2.4 Statistical Analysis

For the following studies, data was analyzed via two way ANOVA with significance set at $p<0.05$. For cell pellet minimization studies, pellet size and media condition were the independent variables. For IL-1β inhibition studies, IL-1β concentration and media

condition were the independent variables. For DMSO sensitivity studies, DMSO concentration and media condition were set as the independent variables. Where significance was indicated by ANOVA analysis, Tukey's posthoc testing was carried out to enable comparisons between groups. For the growth factor combinations study, one way ANOVA was performed. Due to the large number of conditions, where significance was indicated by ANOVA analysis, posthoc testing was performed with Bonferroni corrections and significance set at $p<0.05$. Assay sensitivities in 96-well and 384-well formats were assessed via Z-factor analysis (Zhang et al. 1999).

8.3 Results

8.3.1 Minimization of Cell Number and Media Exchange

In order for HTS to be conducted practically and efficiently, screening assays must use a minimum number of cells and limited handling steps. We therefore optimized a standard MSC chondrogenesis assay for HTS, using GAG content as the measure for chondrogenesis. In these optimization studies, GAG content was dependent on both cell pellet size ($p<0.001$) and the presence of TGF-β3 in the media ($p<0.001$). Increasing cell number/pellet increased GAG content of pellets maintained in either media with (CM+) or without (CM-) TGF-β3 (**Figure 8-2A**). Above 15,000 cells/pellet, differences in GAG became appreciable, with higher levels in CM+ pellets compared to CM- ($p<0.05$). Normalizing GAG content to cell number showed that deposition was most efficient in CM+ at 30,000 cells/pellet or lower, regardless of media changes (**Figure 8-2B**). At 30,000 cells/pellet, the assay Z-factor was 0.6 (excellent). Expression of aggrecan and collagen II mRNAs by quantitative rt-PCR showed at least 4-fold and 10-fold increases,

respectively, in CM+ compared to CM- at both sizes, confirming MSC chondrogenesis at the transcriptional level (**Fig 8-2C, D**).

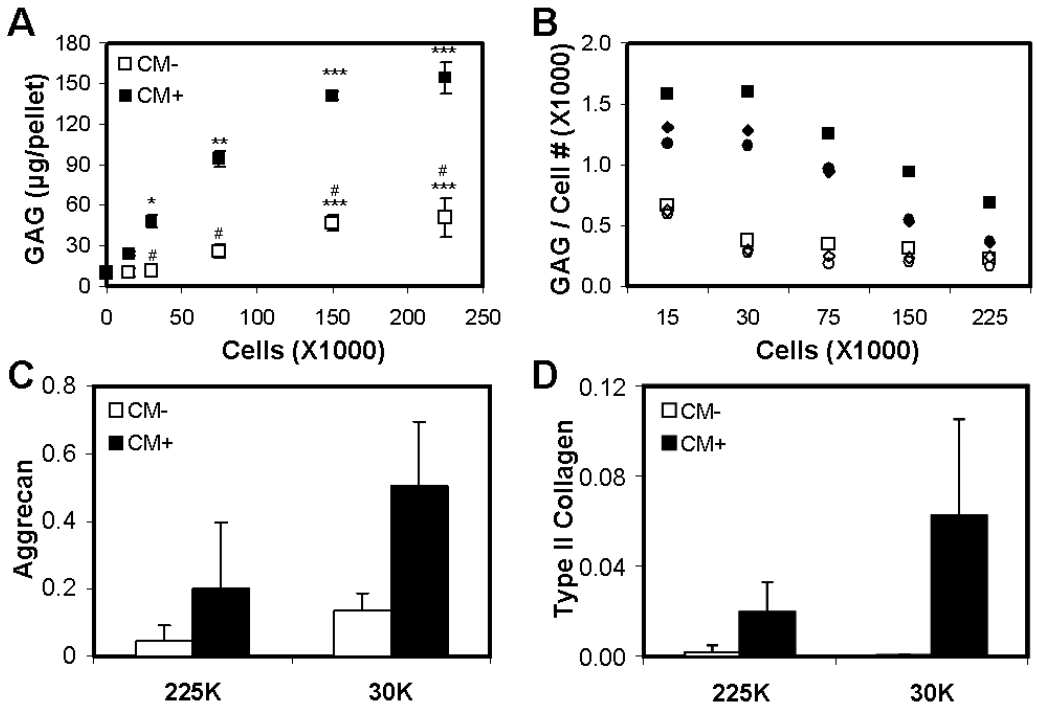

Figure 8-2: GAG deposition and cartilage gene expression with variation in pellet size, media exchange and media condition. (A) GAG content with increasing pellet size (no media change). (B) GAG content normalized to cell number. CM- or CM+ media (white or black markers) were changed twice, once or not at all (circles, diamonds or squares); increasing stars indicate greater than previous cell number within medium type ($p<0.05$), # lower than CM+ of corresponding pellet size ($p<0.001$), n=3. (C) Aggrecan and (D) type II collagen gene expression of large (225,000 cells/pellet) and small (30,000 cells/pellet) pellets, n=3.

8.3.2 Optimization of Culture and Analysis for 384-Well Format

To further reduce handling for HTS and enable robotic liquid dispensing, automated layout and analysis procedures were validated in micro-pellets (10,000 cells/pellet) in 384-well plates, with GAG content results similar to those found with large (225,000 cells/pellet) and small (30,000 cells/pellet) pellets in 96-well plates. In this 384-well format, GAG content was 62±6 µg/pellet in CM+ compared to 8±3 µg/pellet in CM-

(p=0.00025). Z-factor analysis showed that the assay sensitivity remained excellent (Z=0.6).

8.3.3 Effect of Combinations of TGF-β3, BMP-2, IGF-1 and FGF-2 on MSC Chondrogenesis

To assess the effects of different growth factors, their combinations and their doses, we carried out an aggressive combinatorial study comprised of four growth factors (TGF-β3, BMP-2, IGF-1 and FGF-2) at three doses (**Figure 8-3A**). When MSC pellets were cultured with a single growth factor, FGF-2, TGF-β3 and BMP-2 at both high and low doses enhanced GAG deposition compared to CM- controls ($p<0.025$, **Figure 8-3B**). IGF-1 had no discernible effect on GAG production at either dose ($p>0.13$, **Figure 8-3B**). When pellets were cultured with combinations of two growth factors, the effect on matrix accumulation became less clear, although all combinations yielded higher GAG values compared to CM- ($p<0.001$). While the high dose of BMP-2 showed a strong combinatorial effect with TGF-β3 and FGF-2 at both doses ($p<0.001$), the same effect was not found with the low dose of BMP-2 ($p>0.05$, **Figure 8-3C**). Combinations of IGF-1 or FGF-2 with TGF-β3 or BMP-2 yielded mixed results. A low dose of IGF-1 with a high dose of TGF-β3 enhanced GAG deposition ($p<0.001$), but IGF-1 had no effect on TGF-β3 activity when TGF-β3 was provided at the low dose ($p>0.4$, **Figure 8-3D**). Similarly, a low dose of IGF-1 enhanced the chondrogenic effect of low dose BMP-2 ($p<0.025$), but did not enhance high dose BMP-2 activity ($p>0.75$). Combinations of low dose TGF-β3 with both doses of FGF-2 improved GAG production compared to the low dose of TGF-β3 alone ($p<0.02$); however these values did not reach high dose TGF-

β3 levels ($p<0.001$, **Figure 8-3D**). Interestingly, combinations of FGF-2 and IGF-1 at any dose significantly increased GAG accumulation compared to FGF-2 alone, IGF-1 alone, or low dose TGF-β3 ($p<0.005$, **Figure 8-3E**).

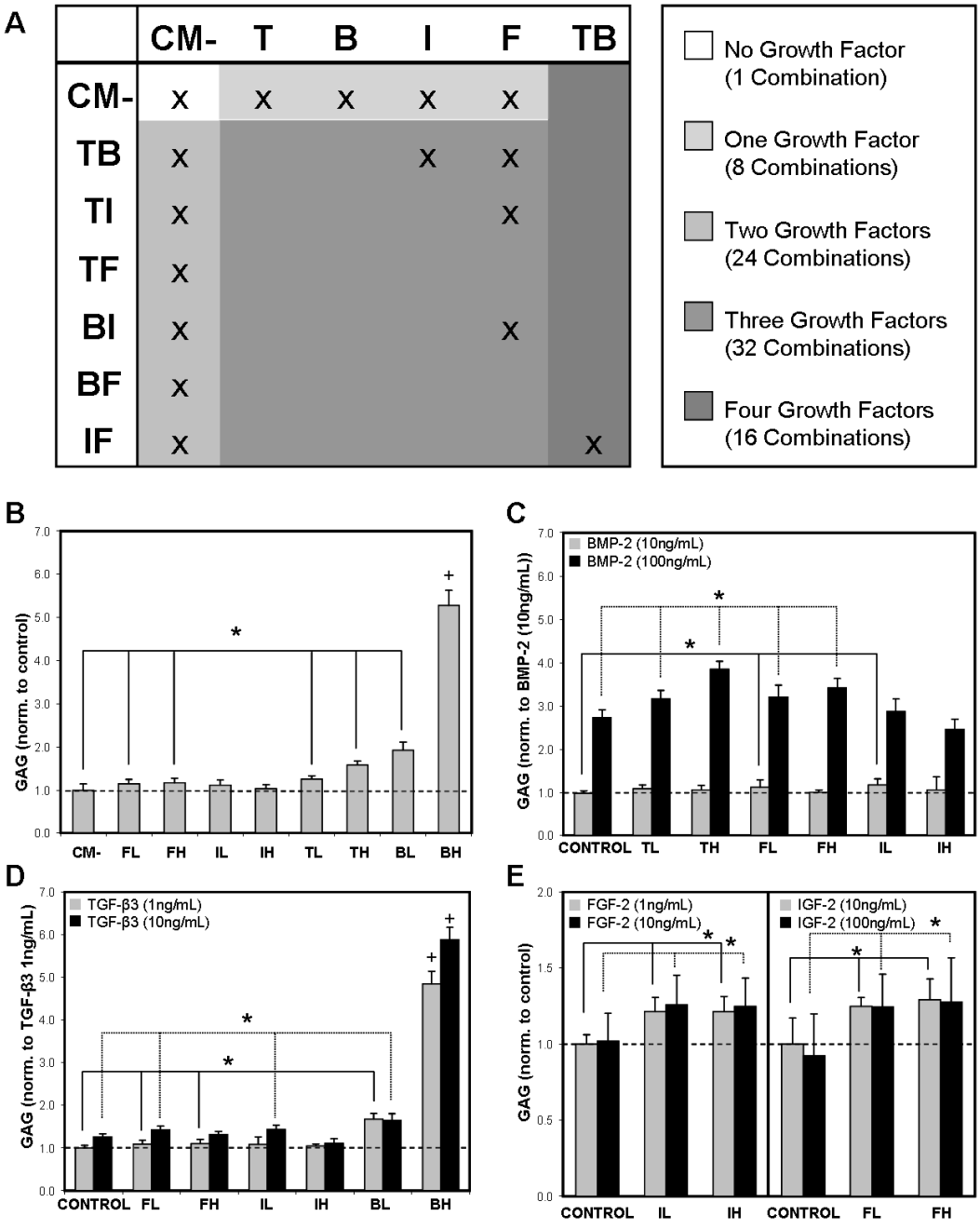

Figure 8-3: Growth factor combinatorial screen. (A) Growth factor combinations of TGF-β3 (T), BMP-2 (B), IGF-1 (I), and FGF-2 (F) were assayed in 81 combinations. CM- represents control condition. Each growth factor was given at one of three doses (none, low, high) where indicated by X. (B) GAG content of pellets cultured in the presence of a single growth factor: TGF-β3 (T), BMP-2 (B), IGF-1 (I), or FGF-2 (F) at a low (L) or high (H) dose. GAG content of pellets cultured with combinations of two growth factors: (C) BMP-2 with another growth factor, (D) TGF-β3 with another growth factor, and (E) combinations of FGF-2 and IGF-1. * greater than control ($p<0.05$). + greater than all other groups within the same dose ($p<0.05$).

With combinations of three or more growth factors, the effects of individual growth factors and their doses on chondrogenesis became more difficult to assess. While combinations involving high dose TGF-β3 with high dose BMP-2 consistently outperformed all other combinations (GAG values greater than 130 μg/pellet), improvements in GAG accrual were observed for other combinations as well (**Figure 8-4**). Analysis of DNA content suggests that while FGF-2 increased cell proliferation ($p<0.05$) and TGF-β3 enhanced matrix deposition (without increasing cell number, $p>0.25$), a high dose of BMP-2 improved both matrix deposition and cell number ($p<0.001$, **Figure 8-5**).

Effect of a Single Growth Factor on GAG Content

Growth Factor 1	CM-	FL	FH	IL	IH	BL	BH	TL	TH
Average GAG Content (µg/pellet)	**18.9**	**21.8**	**22.3**	**21.3**	**19.7**	**36.5**	**97.4**	**23.9**	**30.1**
Standard Deviation	*2.9*	*2.0*	*2.1*	*2.3*	*1.7*	*3.7*	*9.7*	*1.5*	*1.8*

Effect of Two Growth Factors on GAG Content

Growth Factor 1	TL	TL	TL	TL	TL	TL	TH	TH	TH	TH	TH	TH	BL	BL	BL	BL
Growth Factor 2	FL	FH	IL	IH	BL	BH	FL	FH	IL	IH	BL	BH	FL	FH	IL	IH
Average GAG Content (µg/pellet)	**26.0**	**26.4**	**26.0**	**24.9**	**41.3**	**116.9**	**34.2**	**31.5**	**34.3**	**26.6**	**39.4**	**142.7**	**41.1**	**37.3**	**47.6**	**46.0**
Standard Deviation	*2.2*	*2.4*	*4.1*	*1.4*	*6.1*	*8.2*	*2.0*	*1.8*	*2.3*	*2.6*	*3.7*	*11.4*	*3.9*	*4.7*	*14.2*	*14.5*

Growth Factor 1	BH	BH	BH	BH	IL	IL	IH	IH
Growth Factor 2	FL	FH	IL	IH	FL	FH	FL	FH
Average GAG Content (µg/pellet)	**117.3**	**125.1**	**105.1**	**105.0**	**26.6**	**27.5**	**26.5**	**22.7**
Standard Deviation	*10.1*	*7.8*	*10.6*	*26.5*	*2.1*	*2.4*	*2.4*	*8.9*

Effect of Three Growth Factors on GAG Content

Growth Factor 1	TL	TL	TL	TL	TH	TH	TH	TH	TL	TL	TL	TL	TH	TH	TH	TH
Growth Factor 2	IL	IL	IH	IH	IL	IL	IH	IH	BL	BL	BH	BH	BL	BL	BH	BH
Growth Factor 3	FL	FH	FL	FH	FL	FH	FL	FH	FL	FH	FL	FH	FL	FH	FL	FH
Average GAG Content (µg/pellet)	**26.1**	**28.9**	**30.1**	**28.3**	**36.4**	**32.7**	**35.2**	**32.7**	**40.3**	**28.5**	**122.2**	**127.8**	**42.0**	**35.5**	**157.2**	**146.6**
Standard Deviation	*8.4*	*2.5*	*2.1*	*1.8*	*2.2*	*2.3*	*2.1*	*2.9*	*3.2*	*3.0*	*11.1*	*9.6*	*2.7*	*2.8*	*10.7*	*9.1*

Growth Factor 1	TL	TL	TL	TL	TH	TH	TH	TH	BL	BL	BL	BL	BH	BH	BH	BH
Growth Factor 2	BL	BL	BH	BH	BL	BL	BH	BH	IL	IL	IH	IH	IL	IL	IH	IH
Growth Factor 3	IL	IH	IL	IH	IL	IH	IL	IH	FH	FL	FH	FL	FH	FL	FH	FL
Average GAG Content (µg/pellet)	**38.1**	**33.8**	**123.4**	**116.4**	**39.9**	**37.9**	**136.3**	**134.6**	**40.8**	**36.9**	**38.7**	**33.6**	**124.3**	**129.9**	**128.7**	**136.4**
Standard Deviation	*6.0*	*3.3*	*16.3*	*22.1*	*5.2*	*3.2*	*9.2*	*11.1*	*4.1*	*3.9*	*3.5*	*2.1*	*17.3*	*8.4*	*7.4*	*12.5*

Effect of Four Growth Factors on GAG Content

Growth Factor 1	TL	TL	TL	TL	TL	TL	TL	TL	TH	TH	TH	TH	TH	TH	TH	TH
Growth Factor 2	BL	BL	BL	BL	BH	BH	BH	BH	BL	BL	BL	BL	BH	BH	BH	BH
Growth Factor 3	IL	IL	IH	IH	IL	IL	IH	IH	IL	IL	IH	IH	IL	IL	IH	IH
Growth Factor 4	FL	FH	FL	FH	FL	FH	FL	FH	FL	FH	FL	FH	FL	FH	FL	FH
Average GAG Content (µg/pellet)	**45.1**	**34.8**	**38.7**	**32.3**	**121.8**	**124.3**	**118.1**	**121.1**	**40.7**	**35.5**	**38.2**	**35.8**	**132.7**	**122.7**	**141.7**	**138.6**
Standard Deviation	*8.1*	*3.0*	*4.2*	*2.0*	*18.7*	*7.1*	*18.8*	*10.2*	*9.8*	*10.1*	*9.4*	*3.7*	*13.3*	*24.3*	*9.5*	*6.5*

Figure 8-4: Growth Factor Combinations on GAG content.

Effect of a Single Growth Factor on DNA Content

Growth Factor 1	CM-	FL	FH	IL	IH	BL	BH	TL	TH
Average DNA Content (µg/pellet)	**2.76**	**2.95**	**3.21**	**2.74**	**3.12**	**2.90**	**4.29**	**2.39**	**2.38**
Standard Deviation	*0.80*	*1.50*	*1.18*	*1.31*	*1.23*	*2.01*	*1.59*	*0.58*	*0.77*

Effect of Two Growth Factors on DNA Content

Growth Factor 1	TL	TL	TL	TL	TL	TL	TH	TH	TH	TH	TH	TH	BL	BL	BL	BL
Growth Factor 2	FL	FH	IL	IH	BL	BH	FL	FH	IL	IH	BL	BH	FL	FH	IL	IH
Average DNA Content (µg/pellet)	**2.86**	**4.29**	**2.58**	**2.53**	**2.78**	**4.56**	**2.79**	**3.86**	**2.84**	**2.51**	**2.07**	**4.35**	**2.56**	**3.63**	**1.52**	**2.98**
Standard Deviation	*0.68*	*1.93*	*0.66*	*0.69*	*1.21*	*2.19*	*1.46*	*1.71*	*1.67*	*0.74*	*0.84*	*1.14*	*1.51*	*1.84*	*0.88*	*1.54*

Growth Factor 1	BH	BH	BH	BH	IL	IL	IH	IH
Growth Factor 2	FL	FH	IL	IH	FL	FH	FL	FH
Average DNA Content (µg/pellet)	**4.10**	**6.21**	**4.08**	**4.08**	**2.97**	**3.25**	**2.89**	**3.47**
Standard Deviation	*1.82*	*1.26*	*1.30*	*1.36*	*0.99*	*0.80*	*0.57*	*1.12*

Effect of Three Growth Factors on DNA Content

Growth Factor 1	TL	TL	TL	TL	TH	TH	TH	TH	TL	TL	TL	TL	TH	TH	TH	TH
Growth Factor 2	IL	IL	IH	IH	IL	IL	IH	IH	BL	BL	BH	BH	BL	BL	BH	BH
Growth Factor 3	FL	FH	FL	FH	FL	FH	FL	FH	FL	FH	FL	FH	FL	FH	FL	FH
Average DNA Content (µg/pellet)	**3.46**	**3.60**	**2.84**	**4.20**	**3.33**	**3.68**	**2.92**	**4.00**	**2.88**	**4.48**	**4.32**	**6.09**	**2.26**	**3.71**	**5.49**	**5.34**
Standard Deviation	*1.13*	*0.87*	*1.24*	*1.53*	*1.77*	*1.09*	*1.00*	*1.61*	*0.76*	*2.75*	*1.34*	*0.93*	*0.83*	*1.36*	*0.74*	*1.64*

Growth Factor 1	TL	TL	TL	TL	TH	TH	TH	TH	BL	BL	BL	BL	BH	BH	BH	BH
Growth Factor 2	BL	BL	BH	BH	BL	BL	BH	BH	IL	IL	IH	IH	IL	IL	IH	IH
Growth Factor 3	IL	IH	IL	IH	IL	IH	IL	IH	FL	FH	FL	FH	FL	FH	FL	FH
Average DNA Content (µg/pellet)	**2.27**	**2.98**	**5.14**	**4.12**	**2.02**	**2.35**	**4.88**	**4.92**	**3.13**	**3.98**	**2.72**	**3.27**	**4.77**	**5.95**	**4.80**	**5.54**
Standard Deviation	*1.71*	*1.89*	*1.84*	*1.53*	*1.57*	*0.72*	*1.01*	*0.97*	*1.47*	*2.09*	*0.94*	*0.92*	*1.49*	*0.67*	*0.87*	*0.87*

Effect of Four Growth Factors on DNA Content

Growth Factor 1	TL	TL	TL	TL	TL	TL	TL	TL	TH	TH	TH	TH	TH	TH	TH	TH
Growth Factor 2	BL	BL	BL	BL	BH	BH	BH	BH	BL	BL	BL	BL	BH	BH	BH	BH
Growth Factor 3	IL	IL	IH	IH	IL	IL	IH	IH	IL	IL	IH	IH	IL	IL	IH	IH
Growth Factor 4	FL	FH	FL	FH	FL	FH	FL	FH	FL	FH	FL	FH	FL	FH	FL	FH
Average DNA Content (µg/pellet)	**2.44**	**2.43**	**2.50**	**3.08**	**4.23**	**5.60**	**4.03**	**5.70**	**1.92**	**2.73**	**2.01**	**3.78**	**5.19**	**5.55**	**4.51**	**4.97**
Standard Deviation	*1.71*	*0.85*	*1.05*	*0.95*	*1.77*	*0.73*	*1.67*	*1.02*	*0.68*	*1.15*	*0.76*	*1.86*	*1.34*	*0.97*	*1.03*	*1.02*

Figure 8-5: Growth Factor Combinations on DNA content.

8.3.4 Sensitivity of MSC Pellets to Il-1β and DMSO

A pilot screen using IL-1β, a known inhibitor of chondrogenesis, showed that GAG deposition was dependent on both IL-1β concentration ($p<0.001$) and media condition ($p<0.001$). Increasing concentrations of IL-1β inhibited GAG production in CM+ (**Figure 8-6A, B**). For smaller pellets (30,000), inhibition was apparent at 0.1 ng/mL IL-1β ($p<0.01$), although complete inhibition was not seen until 1.0 ng/mL (compared to CM-, $p>0.29$, **Figure 8-6A**). At a concentration of 1.0 ng/mL, GAG deposition was

~50% of control CM+ values. Based on these results, 50% of control CM+ GAG was chosen as the inhibition threshold for future screens. Interestingly, large pellets (225,000) were less sensitive to inhibition by IL-1β; GAG deposition decreased from control values at 1.0 ng/mL ($p<0.01$) and complete inhibition was only noted at the highest dose (compared to CM-, $p>0.1$, **Figure 8-6B**). As expected, GAG content for CM- pellets did not change with addition of IL-1β ($p>0.5$, **Figure 8-6A, B**).

Since chemical compounds are often solubilized in DMSO, the effects of DMSO on chondrogenesis were examined. When exposed to graded concentrations of DMSO, pellets were insensitive to DMSO at levels up to 0.5%, regardless of media condition as assessed by DNA (CM-: $p>0.45$, CM+: $p>0.96$) and GAG (CM-: $p>0.85$, CM+: $p>0.7$) contents (**Figure 8-6C, D**). We therefore used 0.5% DMSO as the maximum allowable thresholds for library screens when compounds are dissolved in DMSO.

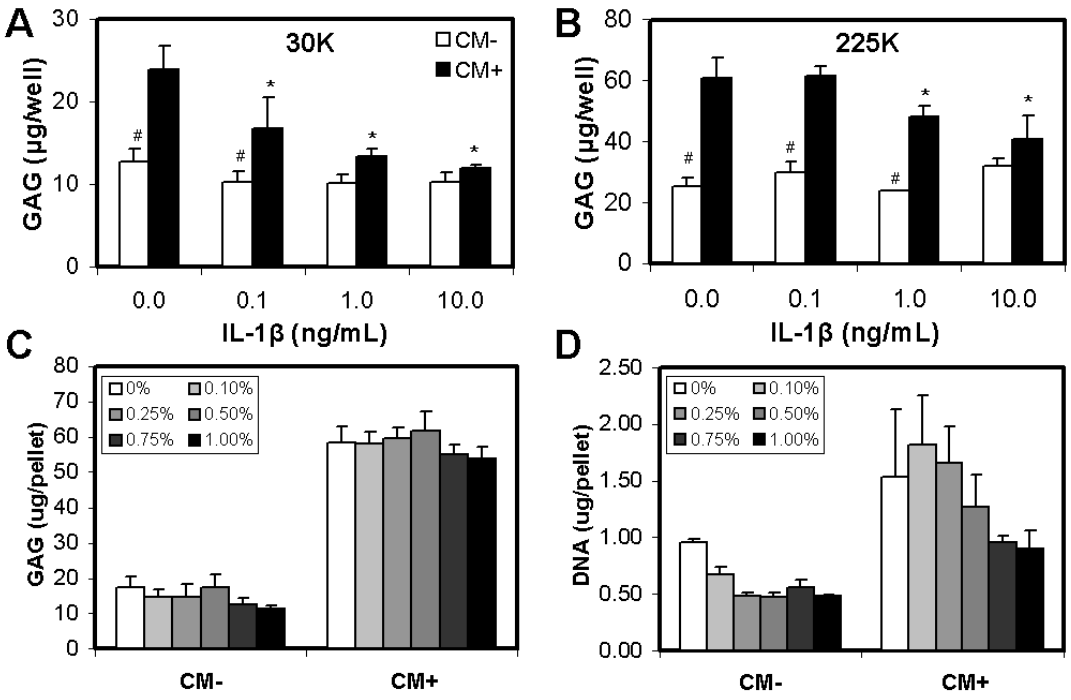

Figure 8-6: GAG accumulation with variation in IL-1β concentration, pellet size and media condition and the effect of DMSO on MSC chondrogenesis. (A) GAG content with increasing concentrations of IL-1β at the 30,000 pellet size. (B) GAG content with increasing concentrations of IL-1β at the 225,000 pellet size. * lower than 0ng/mL IL-1β within medium type ($p<0.01$), # lower than CM+ within IL-1β concentration ($p<0.001$), n=4. (C) DNA and (D) GAG content of micro-pellets with exposure to graded levels of DMSO. ** indicates lower than 0, 0.1, 0.25% DMSO within the same medium type ($p<0.05$). DNA: n=3; GAG: n=8.

8.3.5 Identification of Potential Inducers and Inhibitors of Chondrogenesis With NINDS Library Screen

After optimization and validation of our miniaturized culture and assay procedures, a screen of the NINDS library was undertaken to demonstrate the feasibility of HTS for MSC chondrogenesis. From this screen, 5 potential inducers and 39 potential inhibitors of chondrogenesis were identified based on GAG content assays (**Figure 8-7**).

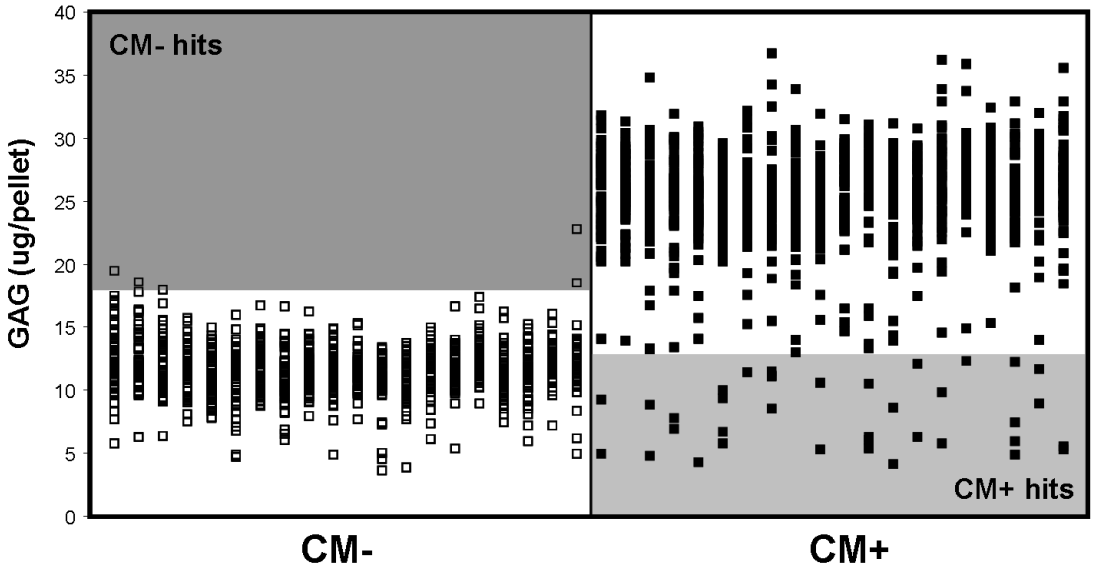

Figure 8-7: NINDS library screen. HTS of the NINDS library identified inducers (CM- hits) and inhibitors (CM+ hits) of MSC chondrogenesis.

Of these potential inhibitors, 15 were cytotoxic at the doses investigated, lowering DNA contents by 40-80% compared to control CM+ values (**Figure 8-8**). The remaining 24 compounds were selected as viable "hits" (**Table 8-1**). With a Z-factor of 0.5, assay sensitivity remained excellent for this screen.

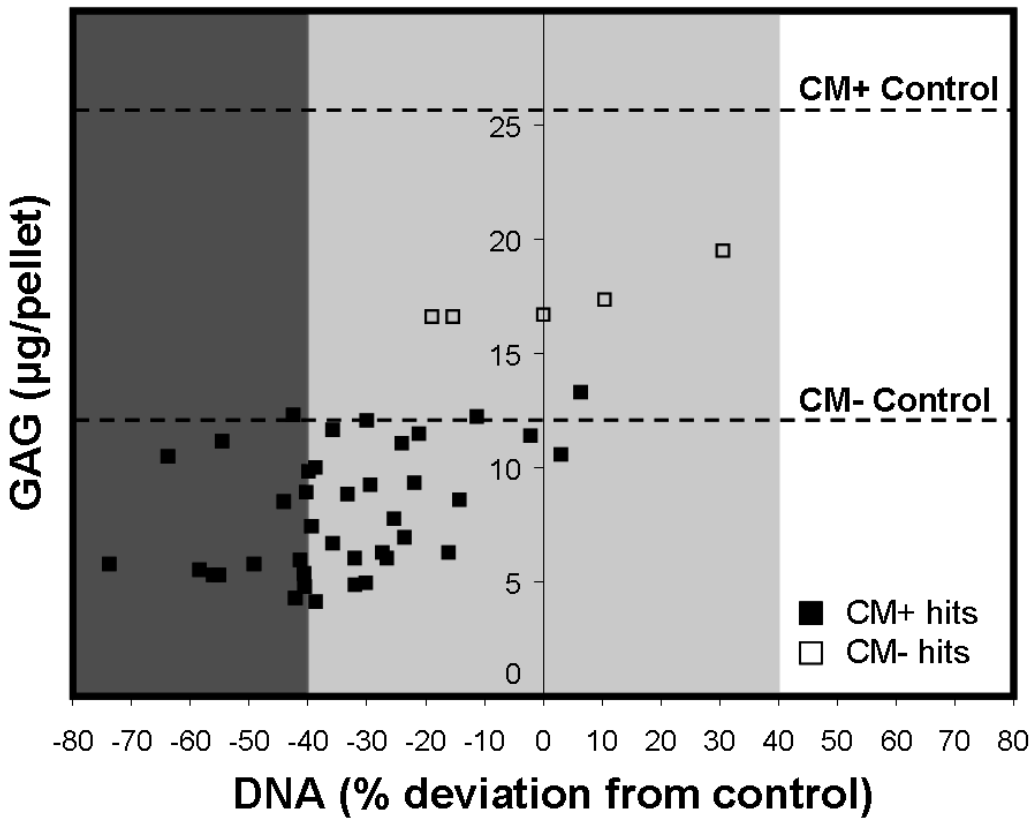

Figure 8-8: Identification of cytotoxic compounds from NINDS library screen. GAG (µg/pellet) and DNA (% deviation from control) content of identified inducers and inhibitors of chondrogenesis. Compounds with DNA content greater than 40% below CM+ control values were considered cytotoxic and excluded from further analysis.

Table 8-1: List of identified inhibitors and inducers.

NAME	CLASS	ACTIVITY
Doxylamine Succinate	Antihistamine, hypnotic	Inducer
Pergolide Mesylate	Dopamine receptor agonist	Inducer
Perphenazine	Antipsychotic	Inducer
Eszopiclone	Hypnotic	Inducer
Colforsin	Adenylate cyclase activator, vasodilator	Inducer
Hexachlorophene	Antiinfective	Inhibitor
Oxyphenbutazone	Antiinflammatory	Inhibitor
Colchicine	Antimitotic	Inhibitor
Glucosamine Hydrochloride	Antiarthritic	Inhibitor
Chlorohexidine	Antibacterial, disinfectant	Inhibitor
Digitoxin	Inotropic, cardiotonic	Inhibitor
Digoxin	Inotropic, cardiac stimulant	Inhibitor
Acriflavinium Hydrochloride	Antiinfective, intercalating agent	Inhibitor
Ouabain	Cardiotonic, Na/K ATPase inhibitor	Inhibitor
Vinblastine Sulfate	Antineoplastic, antimitotic	Inhibitor
Beta-ESCIN	Membrane permeabilizer	Inhibitor
Podofilox	Antineoplastic, antimitotic	Inhibitor
Teniposide	Antineoplastic	Inhibitor
Nocodazole	Antineoplastic, antimitotic	Inhibitor
Pyrithione Zinc	Antiseborrheic	Inhibitor
Azathioprine	Antineoplastic, immunosuppressant	Inhibitor
Puromycin Hydrochloride	Antineoplastic, protein synthesis inhibitor	Inhibitor
Avermectin B1	Antiparisitic	Inhibitor
Cyclohexamide	Protein synthesis inhibitor	Inhibitor
Valinomycin	Potassium transporter, antibiotic	Inhibitor
Irinotecan Hydrochloride	Antineoplastic, topoisomerase I inhibitor	Inhibitor
Pararosaniline Pamoate	Antischistosomal	Inhibitor
Salinomycin Sodium	Antibacterial	Inhibitor
Lasalocid Sodium	Antibacterial	Inhibitor

8.4 Discussion

Mesenchymal stem cells (MSCs) from bone marrow are an attractive cell source for regenerative medicine and the study of skeletal development. MSCs can differentiate into a number of relevant phenotypes, as well as transition from one phenotype to another (Song et al. 2004; Mueller et al. 2008). Despite considerable interest in MSC chondrogenesis, the signal transduction and molecular mechanisms that underlie this

process remain largely undefined. Furthermore, while defined media formulations have been developed to induce this phenotype, these media have yet to be optimized with respect to the functional capacity of the formed tissue. For example, using standard media formulations (containing TGF-β3 and dexamethasone), MSCs in 3D culture systems produce cartilaginous tissues with lower properties than donor matched chondrocytes maintained similarly (Mauck et al. 2006). To explore the signaling topology that underlies chondrogenesis, as well as to discover novel modulators of this process, we developed and optimized a high-throughput screening methodology compatible with MSC chondrogenesis In traditional pellet studies, chondrogenesis is evaluated after 21 days of culture using sizes of 200-250,000 cells/pellet. Here, we successfully reduced the number of cells required to 10,000 per pellet and assessed chondrogenesis after 7 days. Further, we developed an in-well digestion protocol to enable high-throughput analysis and minimize handling (**Figure 8-1**). We also demonstrated our ability to fully automate the layout, culture, and analysis of cartilage matrix production by MSCs in a 384-well format with Z-factor analysis confirming the excellent sensitivity of these miniaturized growth and assay procedures.

After validation of our assay system, we executed a comprehensive combinatorial screen of four growth factors: TGF-β3, BMP-2, IGF-1 and FGF-2. While previous studies have analyzed the effects of these factors on chondrogenesis, there has been no study assessing all combinations of these growth factors using multiple doses in a single experiment. Over a 7 day culture period, treatment with TGF-β3, BMP-2 and FGF-2 improved matrix production compared to control, while treatment with IGF-1 failed to induce

chondrogenesis. Our results also showed an enhanced effect when high doses of TGF-β3 and BMP-2 were given in concert. These findings are consistent with several previous studies of growth factor effects on MSC chondrogenesis (Majumdar et al. 2001; Schmitt et al. 2003; Indrawattana et al. 2004; Palmer et al. 2005; Toh et al. 2005). Although the chondrogenic effects of TGF-β3 and BMP-2 are well characterized, the effects of FGF-2 and IGF-1 are less established. In our study, short-term pellet culture with FGF-2 increased cell proliferation when given alone or with other growth factors. In monolayer studies, FGF-2 increased cell proliferation and enhanced the chondrogenic potential of MSCs (Im et al. 2006; Stewart et al. 2007). While IGF-1 has been shown to improve chondrogenesis when given with TGF-β3 (Indrawattana et al. 2004), our results were less decisive. Interestingly, combinations of IGF-1 and FGF-2 appeared to increase GAG deposition, independent of dosage.

In addition to our growth factor screen, we conducted an HTS campaign on the NINDS library (1040 compounds) and identified several potential inducers and inhibitors of chondrogenesis (**Table 8-1**). Inducers were from several different classes of molecules, including hypnotic agents and vasodilators. Inhibitors were largely anti-neoplastic or anti-protein synthesis agents. To eliminate cytotoxic inhibitors, the threshold for DNA content was set at 40% below control values. Dosage response studies will be necessary to determine whether inhibitory effects will be retained with minimal cytotoxicity at lower doses. Interestingly, of the identified inhibitors, several compounds, including those that altered sodium/potassium levels (ouabain and valinomycin), inhibited protein synthesis (puromycin and cyclohexamide), or inhibited microtubule formation

(colchicine and vinblastine), have previously been shown to block sulfate incorporation into GAGs in embryonic chick cartilage (Adamson et al. 1966; Audhya et al. 1976). These results reaffirm our ability to identify specific inhibitors and inducers of chondrogenesis. Unexpectedly, glucosamine hydrochloride, an amino monosaccharide with possible anti-arthritic properties (Reginster et al. 2001), was also identified as a potential inhibitor of MSC chondrogenesis. While the benefits of glucosamine as a therapeutic agent for osteoarthritis remains controversial (Verbruggen 2006), in one study of human MSC pellets, treatment with 100 μM of glucosamine enhanced chondrogenesis while treatment with 10 mM significantly inhibited chondrogenesis (Derfoul et al. 2007). However, the pellet size used in these experiments (1.5 million cells per pellet) was 150 times greater than the size used in our screen (10,000 cells per pellet). Our validation studies with IL-1β suggest that smaller pellet sizes may be more sensitive to inhibition, perhaps owing to decreased diffusional distances. Therefore, while 10 μM of glucosamine was inhibitory in our miniaturized pellets, a lower dose may prove to be beneficial.

The ability to effectively screen large numbers of compounds and uncover both inducers and inhibitors of chondrogenesis is a key strength of HTS. From this initial screen of a small chemical library, we were able to identify several known effectors of chondrogenesis and GAG production. Moreover, we identified several modulators whose actions on MSC chondrogenesis had been previously unknown. While inducers of chondrogenesis are of clear utility for tissue engineering applications, they may also possess chondroprotective properties useful for direct systemic treatment of osteoarthritis.

Similarly, inhibitors of chondrogenesis may be of clinical interest as therapeutic agents for skeletal pathologies, such as fibrodysplasia ossificans progressive (FOP). In FOP, progenitor cells in the soft tissues undergo chondrogenesis and ultimately osteogenesis, forming ectopic bone in an endochondral fashion. In addition to discovering novel modulators of chondrogenesis, we were also able to identify compounds widely used in orthopaedic practice that displayed no effect on chondrogenesis. These compounds include common antibiotics (vancomycin, ciprofloxacin and gentamicin), non-steroidal anti-inflammatory agents (rofecoxib and celecoxib) and corticosteroids (cortisone and methylprednisolone). Interestingly, while ciprofloxacin did not affect chondrogenesis, at high doses it has been shown to inhibit fracture healing in rats and inhibit proliferation and extracellular mineralization by osteoblastic cells (Huddleston et al. 2000). Vancomycin has also been shown to reduce cell proliferation in chondrocytes and osteoblasts; however, these effects were only evident at doses exceeding 2000 μg/mL (Antoci et al. 2007). Although we were able to identify several inducers and inhibitors of chondrogenesis, secondary screening tools must be developed to confirm our findings and eliminate false positives.

This work describes a new method for assaying MSC chondrogenesis using an HTS approach and presents findings from a preliminary chemical screen and combinatorial growth factor study. While the results are exciting, several limitations remain. In terms of methodology, we focused on the DMMB assay of GAG production as a primary screening tool. GAG is a sensitive and cost-effective (0.01¢ per well) measure of chondrogenesis. However, in this setup, we capture all GAG produced by MSCs over the

time course of the study, rather than that which is fixed within the ECM and most important for tissue formation. Future work may discriminate between soluble GAG and fixed GAG by assaying the media prior to papain digest. Additionally, more sensitive assays will be required to confirm early-stage chondrogenesis at the molecular level in identified compounds of interest. For example, we have previously used both aggrecan and type II collagen promoter-reporter assays to monitor cartilaginous gene expression in differentiating MSCs (Mauck et al. 2007), and these assays may be adapted for secondary screening in this HTS format. These assays are more expensive, but will serve as a specific indicator of the chondrogenic state. On a mechanistic level, it has recently been reported that centrifugation is not necessary for pellet formation (Welter et al. 2007); removal of this step might further decrease processing time for our anticipated larger library screens. In our studies, we observed a natural heterogeneity in response between the different donor MSC populations investigated. While differences with chondrogenic induction in all screens remain robust (Z-factors >0.5), as we transition from bovine to human sources, these differences will have to be carefully monitored. Additionally, we only assayed a single dose for the chemical factors in the library screen. As with all library screening, this allows for the existence of false-negatives – factors that are in fact inducers or inhibitors that fail to present based on improper dosing. Additional assays at higher doses may be performed to account for this limitation. Finally, these studies were executed over a relatively short duration of seven days. By focusing our screen for factors that induce chondrogenesis, we may fail to recognize late-stage modulators of this process that may prove valuable for tissue engineering efforts. To implement longer culture durations, the protocol may be tailored to include partial media exchanges, with

half the volume of media replaced once a week, to avoid aspiration of cell pellets during the exchange.

The results of this study demonstrate for the first time that HTS approaches can be used to screen large molecular libraries for modulators of MSC chondrogenesis. Furthermore, by fully automating the layout and analysis techniques, as well as reducing pellet size to 10,000 cells/pellet, we are now poised to screen even larger chemical libraries, such as the >200,000 compound NIH Small Molecule Repository, which contains many factors of chemical interest but unknown action. Newly identified modulators of chondrogenesis may find use in tissue engineering as well as in the treatment of musculoskeletal pathologies. For example, it has been reported that MSCs from osteoarthritic (OA) patients are themselves less robust than those from healthy patients of the same age (Murphy et al. 2002). Factors that improve MSC activity in these diseased cells may prove beneficial to this large and growing OA population. For skeletal pathologies like FOP, factors may be identified that block the promiscuous chondrogenesis that occurs in these cells, while not adversely impacting the natural chondrogenic events that are necessary for skeletal growth in this young population. In the same way that microarray technologies allow for unbiased discovery of new genes involved in a specific cellular process, HTS identifies novel modulators of biochemical action. Using this HTS approach coupled with large chemical libraries, new modulators of chondrogenesis can be identified and the signaling topology of this important event in cartilage and bone formation will be better understood. These advances will improve the clinical application

of MSCs for cartilage formation for regenerative medicine applications as well as for the treatment of skeletal pathologies.

CHAPTER 9: SUMMARY AND FUTURE DIRECTIONS

9.1 Summary

The function of articular cartilage within the joint is primarily load-bearing and this function is dependent on its unique structure. As outlined in Chapter 1, the structure and properties of articular cartilage vary through the depth, and the chondrocytes residing within these different zones present distinct phenotypes and morphologies. In addition, cartilage is anisotropic; type II collagen fibers within the superficial zone are oriented in distinct patterns across the joint surface, leading to direction-dependent tensile properties. To date, the foremost challenge confronting cartilage tissue engineering has been replicating this unique structure and generating mechanically functional tissue replacements using a clinically feasible cell source. Toward this end, the overall objective of this thesis was to better understand the molecular and functional underpinnings of mesenchymal stem cell chondrogenesis in 3D culture and to develop methods to enhance chondrogenesis for cartilage tissue engineering.

In Chapter 3, standard tissue engineering strategies effective in the chondrocyte literature were applied to optimize MSC chondrogenesis in 3D culture. Specifically, the effects of increasing initial cell seeding density and the application of a novel media formulation (transient exposure to TGF-β3) were evaluated on MSC-laden agarose constructs. In contrast to studies using chondrocytes, increasing the seeding density of MSCs (20 million vs. 60 million cells/mL) did not lead to commensurate increases in bulk mechanical or biochemical properties. Indeed, no differences were observed with seeding density under continuous exposure to TGF-β3. As previously observed, the

mechanical properties of MSC-based constructs remained dramatically reduced compared to chondrocytes cultured identically. Interestingly, transient application of TGF-β3 dramatically improved the GAG content and mechanical properties of MSC-seeded constructs, but only when constructs were seeded with 60 million cells/mL. While constructs seeded at 20 million cells/mL density did not respond favorably to transient TGF-β3 exposure, the mechanical properties and biochemical content did not decline with TGF-β3 removal. Chondrogenic gene expression remained at high levels in these constructs, suggesting maintenance of the cartilaginous phenotype despite the absence of TGF-β3. Notably, type I and X collagens were not observed under 'transient' conditions, consistent with previous observations that MSC hypertrophy and ossification is not induced *in vitro* with TGF-β abrogation, in the absence of other factors.

In Chapter 4, the effect of long-term dynamic compressive loading on functional MSC chondrogenesis was examined. Functional growth of constructs was markedly dependent on chondrogenic pre-culture; loading initiated after 3 days of pre-culture inhibited cell proliferation and the development of robust mechanical and biochemical properties while loading initiated after 3 weeks of pre-culture enhanced mechanical properties, though biochemical content was comparable to free-swelling cultures. Collagen was better distributed in the loaded samples, suggesting that this enhanced distribution may contribute to the improved mechanical properties. Variation of loading duration, frequency and TGF-β supplementation showed that loading-induced gains in mechanical properties were only observed for constructs loaded for 4 hours per day at 1 Hz in the presence of TGF-β3, suggesting that minimal thresholds of loading may exist. Methods

to elucidate the potential factors (MSC phenotype, cell-matrix interactions, solute transport) underlying these disparate responses to mechanical stimulation are described later in this chapter.

Results from Chapters 3 and 4 clearly demonstrate that while MSCs undergo chondrogenesis, the functional phenotype established by these cells under our culture system is distinct from that of articular chondrocytes. Therefore in Chapter 5, the molecular profiles of chondrogenic MSCs were compared to that of undifferentiated MSCs and fully differentiated chondrocytes to better understand the underpinnings of chondrogenesis. Transcriptional differences were established between these cell types and two of the genes identified (PRG4 and TGFBI) were further confirmed to be differentially translated. This work describes for the first time the transcriptional limitations of MSC chondrogenesis and begins to set new benchmarks for 'successful' differentiation.

While the focus of the studies presented in Chapters 3-5 (as well as current work in the literature) was toward optimizing the compressive properties of MSC-based constructs, the tensile properties of articular cartilage are also crucial to its load-bearing role in the joint. The evolution of these properties in native cartilage was described in Chapter 2, however very few studies have characterized the tensile properties of engineered constructs. Therefore, in Chapter 6, tensile testing methods were validated for hydrogel strips, and the development of tensile properties of MSC-laden constructs was investigated, relative to that of chondrocyte-laden constructs cultured identically. Tensile

properties were comparable between cell types by the final timepoint (day 56), however these properties were extremely poor compared to that of native cartilage. As expected, in the absence of external stimuli, the engineered tissue was isotropic and homogeneous, with respect to collagen orientation and localization.

To optimize tensile properties and collagen content, a novel bioreactor was developed to apply sliding contact to cell-seeded agarose strips to better replicate the physiologic loading environment within the joint. In Chapter 7, sliding contact loading was characterized by finite element analysis and preliminary studies on acellular constructs were performed. Based on the results generated by these acellular studies (and the data presented in Chapter 5), sliding contact was initiated after 3 weeks of chondrogenic pre-culture. We examined the effects of short-term sliding contact on chondrogenesis under a range of axial deformations in the presence or absence of TGF-β3. Long-term sliding contact was applied using optimized parameters established from these short-term studies (20% axial deformation with TGF-β3 supplementation) and functional growth was assessed. Results demonstrate for the first time that sliding contact not only improved the tensile properties of MSC-based constructs, but also instilled biochemical inhomogeneity.

While the latter part of the thesis focused on mechanical stimulation as a modulator of MSC chondrogenesis, it is not the sole mediator. In defined conditions, TGF-β is a powerful chondrogenic inducer, and the chemical makeup of the media utilized in all of the studies presented in this thesis is also the one that is most widely used in the field. Although this media formulation is currently the gold standard, our studies show

incomplete conversion of the MSC phenotype using this formulation. Therefore in Chapter 8, a high-throughput screening method was developed to rapidly screen chemical libraries for novel mediators of MSC chondrogenesis. In addition to improving chondrogenic differentiation, identification of chemical modulators (both inducers and inhibitors) of known action may be useful in elucidating the signaling pathway underlying MSC chondrogenesis.

Overall, this work outlines limitations in MSC functional chondrogenesis for cartilage tissue engineering and highlights key differences between this cell type and fully differentiated articular chondrocytes. Using a multi-pronged approach, we explored potential routes toward overcoming these limitations and demonstrated that MSCs are responsive to their chemical environment as well as their mechanical environment. Although encouraging, our results indicate that further optimization of these parameters will be necessary for clinical realization.

9.2 Limitations and Future Directions

9.2.1 Functional links between transcription and mechanical properties

In Chapter 5, we identified a set of genes that were misregulated during MSC chondrogenesis, however functional links have not yet been established. It is currently unknown which of these genes (if any) may underlie the functional (compressive properties, GAG content) or phenotypic (permanently vs. transiently chondrogenic) disparities we and others have observed between chondrogenic MSCs and chondrocytes. One challenge moving forward is identifying reasonable targets for further study. While

we have a list of candidate genes, this list may not be comprehensive. Our microarray analyses was limited to one timepoint (day 28), since the properties of MSC-based constructs do not improve past this time. Although other timepoints before and after day 28 would be useful in order to capture early and later stages of chondrogenesis (and these studies are ongoing), our time course analyses showed that several of the genes identified from the day 28 timepoint were also mis-expressed at timepoints before and after day 28. For example, chondromodulin and DKK1 were never expressed in MSCs at any timepoint.

While our description of MSC chondrogenesis is not yet comprehensive, we were able to generate a list of 324 genes as potential targets of intervention. Only a subset of these genes were further validated, as it was not feasible to validate all 324 of the identified genes. Based on a review of the existing literature, the genes selected were those that were related to functional properties (matrix elements) or phenotype (transcription factors or molecule indicative of cell differentiation). For example, PRG4, TGFBI and chondromodulin are matrix molecules important in cartilage function, SOSTDC1 and ID1 are involved in BMP signaling and MEIS2 and HOX4A are highly conserved transcription regulators that play important roles during development.

Using this list as a logical starting point, the connection between transcription and functional outcomes may first be established by assessing successful translation from expression to protein identification via MALDI-TOF mass spectroscopy (Hillenkamp et al. 1991), followed by siRNA knockdown studies in chondrocyte cultures. Attractive

candidate genes may then be over-expressed in MSC cultures to evaluate rescue of function or phenotype. Once links have been confirmed, these genes will serve as new benchmarks of "successful" functional chondrogenesis, in addition to the established set of chondrogenic markers (i.e. type II collagen, aggrecan). For example, we recently analyzed the microarray data generated from dynamic compressive loading studies (Chapter 4) against this list of mis-regulated genes and found some overlap with genes that were mechanically sensitive. Specifically, we observed that a sub-set of genes that were under-expressed in MSCs compared to chondrocytes were up-regulated after 3 weeks of dynamic compression. Similarly, a few genes that were over-expressed in MSCs were down-regulated by loading. These analyses will aid us in uncovering the mechanism(s) by which dynamic compressive loading improves functional MSC chondrogenesis. The complete list of these genes can be found in **Appendix 3**.

9.2.2 MSC phenotype *in vivo*

While some of the transcriptional differences between chondrogenic MSCs and chondrocytes may be due to differences of phenotype, these differences are not easily resolved *in vitro*. As a potent inducer of MSC chondrogenesis, TGF-β3 promotes the cartilaginous phenotype *in vitro* (evidenced by ample deposition of proteoglycans and type II collagen), while inhibiting osteogenesis. The chondrogenic phenotype of MSCs is maintained after TGF-β3 removal and hypertrophy and mineralization is not observed (Chapter 3). However, there is increasing evidence that while stable *in vitro*, the phenotype of chondrogenic MSCs shifts toward an osteogenic phenotype (concurrent

with vascular invasion) when exposed to *in vivo* conditions, thereby mimicking the process of endochondral ossification (Pelttari et al. 2006; Jukes et al. 2008). In marked contrast, implantation of articular chondrocytes does not induce this response, and the surrounding cartilaginous matrix remains inviolate. To overcome these limitations and enable accurate evaluation of the MSC phenotype, potential therapies and assays must either be tested against an *in vitro* environment that better replicates the *in vivo* one (which may require the addition of osteo-permissive factors such as β-glycerophosphate and thyroid hormone) (Mueller et al. 2008), or rigorous assessments of MSC phenotype must be carried out under *in vivo* conditions, following standard *in vitro* culture.

9.2.3 MSC mechanotransduction

In Chapters 4 and 7, we showed that the mechanical environment can modulate MSC chondrogenesis and that the application of mechanical signals can improve the compressive and tensile properties of MSC-based constructs. In these studies, the effects of dynamic compression were dependent on pre-culture duration, loading duration, frequency and TGF-β3 supplementation. Improved compressive modulus was only observed in cases where MSC-based constructs were pre-cultured for 3 weeks prior to the initiation of loading. These pre-cultured constructs differ from day 3 constructs in several respects: the MSCs are chondrogenic and have secreted a GAG-rich matrix, leading to decreases in construct porosity and increases in bulk compressive properties. It is currently unknown which of these factors might govern MSC response to loading, whether it is the differentiation status of MSCs, the effect of cell-matrix interactions or the changing material properties of the surrounding material.

To examine whether MSC phenotype may play a role in load-induced maturation, future studies will focus on the response of chondrogenic MSCs encapsulated in 2% agarose (devoid of external cell-secreted matrix). MSCs may be cultured in alginate or pellet culture in pro-chondrogenic conditions then dissociated from the surrounding matrix/polymer to free the chondrogenically differentiated cells. To examine the effect of cell-matrix interactions on loading response, biomaterials derived from cartilage matrix constituents, such as collagen, RGD-modified, or chondroitin sulfate biomaterials may be investigated. Scaffolds derived from the native cartilage matrix may also be useful as these scaffolds improve chondrogenesis of adipose derived stem cells; a similar formulation may enable better study of cell-matrix interactions during dynamic compressive loading. Loading may also be applied in the presence of blocking antibodies to inhibit integrin binding and permit identification of important signaling pathways. Assessment of phosphorylated MAPKs during loading may be another method to assess MSC mechanotransduction pathways and may be a more reliable early predictor of efficacy compared to gene expression.

To determine the importance of bulk construct properties on MSC mechanoresponsivity, gradual removal of proteoglycans or collagens (by graded digestion in chondroitinase or collagenase) may be carried out prior to the initiation of loading. Similarly, MSCs may be encapsulated in materials of different mechanical properties; while this is difficult to achieve with agarose due to its viscous nature, other materials with more tunable properties, such as hyaluronic acid or PEG hydrogels are attractive possibilities.

In addition to pre-culture considerations, loading must also be applied for 4 hours per day at 1 Hz to obtain favorable outcomes in mechanical properties. Other variations of this loading regime (1 hour per day at 1 Hz and 4 hours per day at 0.1 Hz) failed to modulate mechanical properties. While these duration and frequency parameters may influence solute transport (described in more detail in Chapter 5), MSC responsiveness to loading may also be related to the number of loading cycles experienced by the cells; for example, 4 hours at 1 Hz correspond to 14,400 cycles while 4 hours at 0.1 Hz and 1 hour at 1 Hz correspond to significantly fewer cycles (1,440 and 3,600 cycles, respectively). Frequency itself may be important as fluid pressure generated by loading is dependent on the frequency of the applied load. To address this question, parametric studies of loading cycle (at fixed frequency) or frequency (at fixed number of cycles) may be carried out to elucidate the effects of these different variables.

9.2.4 Development of mechanically-induced anisotropy

In Chapter 7, we developed a novel bioreactor to apply sliding contact loading to MSC-seeded constructs. While 3 weeks of sliding improved the tensile properties and collagen content of constructs relative to free-swelling, the overall properties remained low compared to native. Using semi-quantitative measures of histology, we were able to discern matrix inhomogeneity in constructs subjected to sliding; the surface region of constructs showed more intense staining of proteoglycans and type II collagen. However, due to low collagen content (resulting in light Picrosirius Red staining), assessment of collagen orientation by polarized light was not easily achieved; initial analyses indicated

no differences in collagen alignment with sliding. It may be that 3 weeks of sliding was insufficient and longer-term loading will be required to achieve observable differences in collagen remodeling. Our polarized light method may also not be sensitive enough to capture early differences in alignment. In this case, alternative methods established in the literature, such as polarized FT-IRIS (Bi et al. 2005) or second harmonic imaging microscopy (Stoller et al. 2002), can be explored. Lastly, as agarose is an inert biomaterial and does not degrade, the presence of the polymer may inhibit collagen remodeling. The morphology of chondrocytes in the superficial zone of native cartilage is flattened in shape and oriented parallel to the surface; agarose may prevent cells from adopting this morphology. Cell morphology may be important as collagen alignment and orientation is often preceded by cellular orientation (Hayes et al. 1999; Baker et al. 2007). Hydrolytically-degradable and MMP-degradable formulations have shown some promise in enhancing collagen deposition (Bryant et al. 2003); the use of these novel biomaterials may enable better collagen remodeling.

9.2.5 Chondrogenesis of human MSCs

One limitation of all of the studies presented in this thesis is the use of cells derived from bovine sources. While cells derived from animal sources may not be ideal, the use of these cells allows us to test many more conditions than would be possible with human cells, and allows comparisons to be made to healthy fully differentiated chondrocytes. With respect to functional cartilage tissue engineering in particular, the use of bovine MSCs also enables comparisons to be made to mechanical benchmarks set by foundational work based on juvenile bovine cartilage. Ultimately however, studies using

human MSCs will be necessary to enhance the clinical applicability of our findings, and these studies are underway. Thus far, preliminary work suggests that additional optimization will be required for successful chondrogenesis (and viability) of these cells, though factors such as age and the disease status of the donor cells must also be considered. Under defined media conditions in the presence of TGF-β3, human MSCs isolated from an osteoarthritic, aged patient (70 yrs, female) do not accrue appreciable levels of GAG after 28 days of culture and the mechanical properties of MSC-based hydrogels remain similar to that of starting values (**Figure 9-1**).

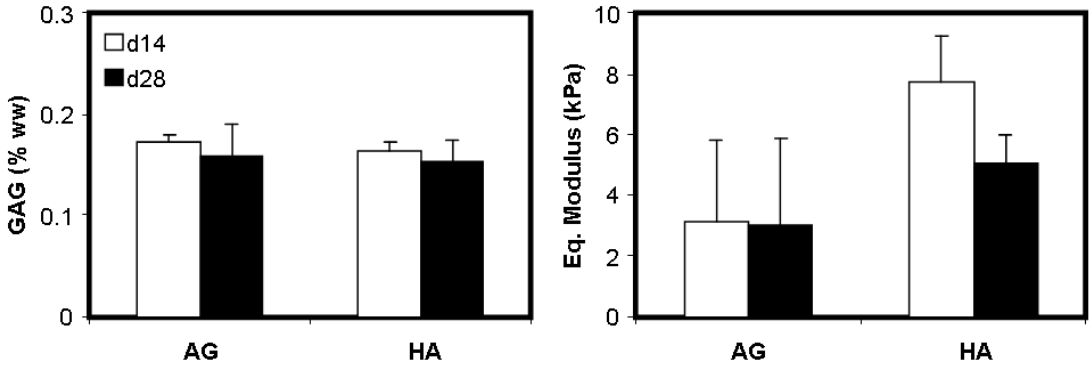

Figure 9-1: GAG content and equilibrium compressive modulus of human MSCs seeded in 2% agarose (AG) or 2% hyaluronic acid (HA) hydrogels for 28 days in chemically defined media containing TGF-β3. Data represent mean and standard deviations, n=3 per group.

MSC viability declines over the first 9 days of culture for both agarose and hyaluronic acid (HA) constructs (**Figure 9-2**); however, the surviving MSCs in agarose express increasing levels of aggrecan and type II collagen while MSCs in HA do not (**Figure 9-3**). From this preliminary work, it is evident that while human MSCs may undergo chondrogenesis on a transcriptional level in 3D, this does not translate to improvements in matrix deposition and functional properties. This may be due to the pronounced decrease in MSC viability early in culture; one way to overcome these limitations may be

the inclusion of mitogenic factors (such as FGFs) during MSC expansion or the use of biomaterials that promote cell adhesion or cell-cell communication (mimicking pellet culture conditions). Future work will examine these possibilities as well as investigate the effects of donor age and disease status on MSC chondrogenesis in a 3D culture environment.

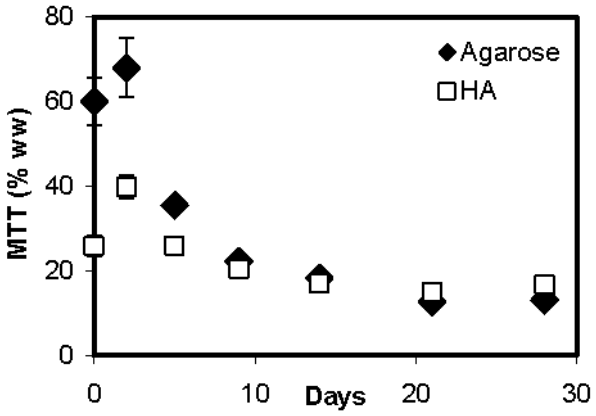

Figure 9-2: MTT assay for cell viability showed marked decrease in viability within 9 days of culture for human MSCs seeded in both agarose and HA constructs. Data represent mean and standard deviations, n=3 per group.

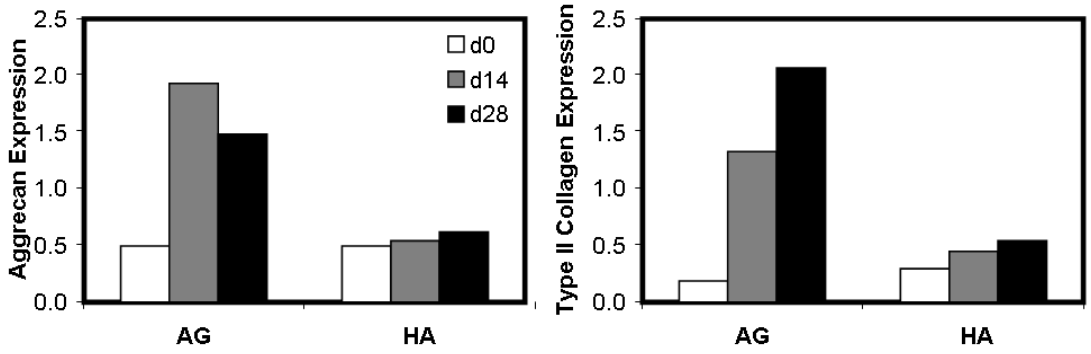

Figure 9-3: Human MSCs seeded in agarose improved cartilaginous gene expression with time in chondrogenic culture. When cells from the same donor were seeded in HA hydrogels and cultured in parallel identically, the expression levels of the same genes did not change with time.

9.2.6 Alternative growth factors to enhance functional chondrogenesis

Although TGF-β3 is a potent inducer of chondrogenesis and was used for all of the work presented here, it is not the only growth factor capable of stimulating chondrogenesis in

MSCs. While TGF-β1 and TGF-β2 isoforms also induce chondrogenesis of MSC pellets *in vitro*, TGF-β3 was specifically selected for these studies as exposure to this isoform resulted in markedly enhanced differentiation in human MSCs, compared to the other two isoforms (Barry et al. 2001). Other members of the TGF-β superfamily, including the bone morphogenic proteins (BMPs), can also stimulate chondrogenesis and several studies have demonstrated the chondrogenic potential of these growth factors, including BMP-2, 6, and 9 (Majumdar et al. 2001; Indrawattana et al. 2004). In Chapter 8, we showed that exposure of MSC micro-pellets to BMP-2 dramatically improved GAG deposition; GAG content was even higher when TGF-β3 was combined with BMP-2. Based on these findings, preliminary studies were performed investigating the effect of BMP-2 in normal MSC pellet culture (250,000 cells) and in 3D agarose culture. Consistent with our previous findings from the HTS screen, pellets cultured in defined media containing BMP-2 outperformed those cultured in TGF-β3. Pellet diameter was much greater in BMP-2 groups and GAG and collagen contents were also higher in these pellets (**Figure 9-4**). Additional studies comparing these growth factors showed that bovine MSCs seeded in agarose also responded more favorably to BMP-2, resulting in constructs with greater mechanical properties and GAG content (**Figure 9-5)**. While BMP-2 was applied at 100 ng/mL (compared to 10 ng/mL TGF-β3), dosage studies showed that at least 50 ng/mL of BMP-2 was required for chondrogenesis and no differences were observed at concentrations higher than 50 ng/mL. Similarly, 10 ng/mL of TGF-β3 was required for successful differentiation, with no additional benefits observed above that dosage (data not shown). Considerations of dosage (and the costs

associated) for each type of growth factor treatment will certainly affect clinical feasibility.

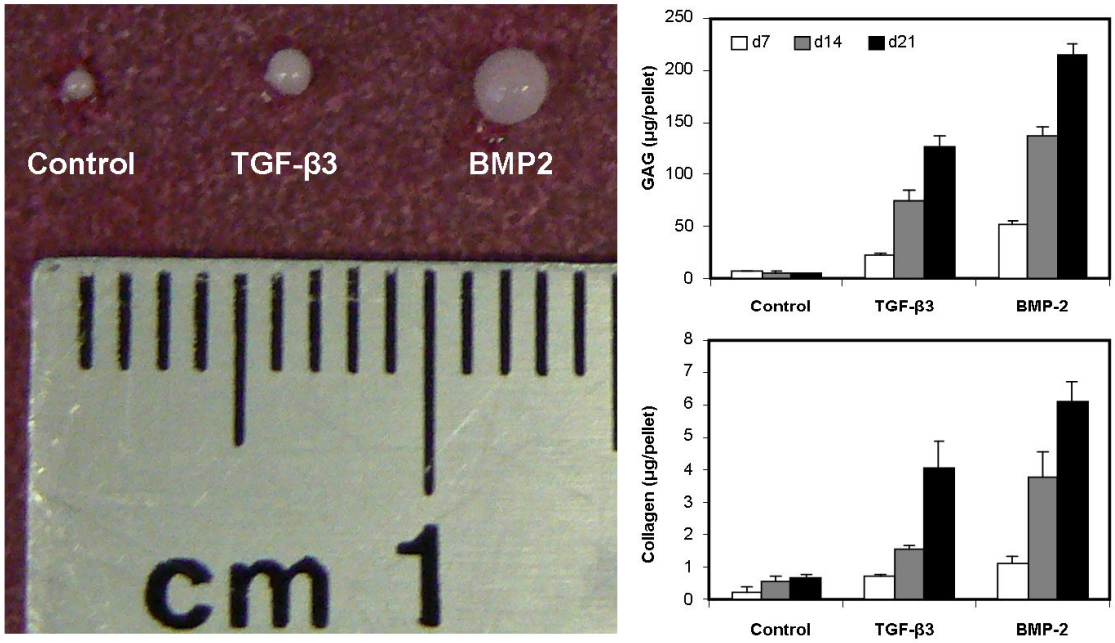

Figure 9-4: Bovine MSC pellets were cultured in control media (no growth factors), 10 ng/mL TGF-β3 or 100 ng/mL BMP-2 supplemented media for 21 days. (Left) Pellet diameter was highest for BMP-2 treated pellets. (Right) GAG and Collagen contents were also highest in BMP-2 treated pellets. Data represent mean and standard deviation, n=3 per group.

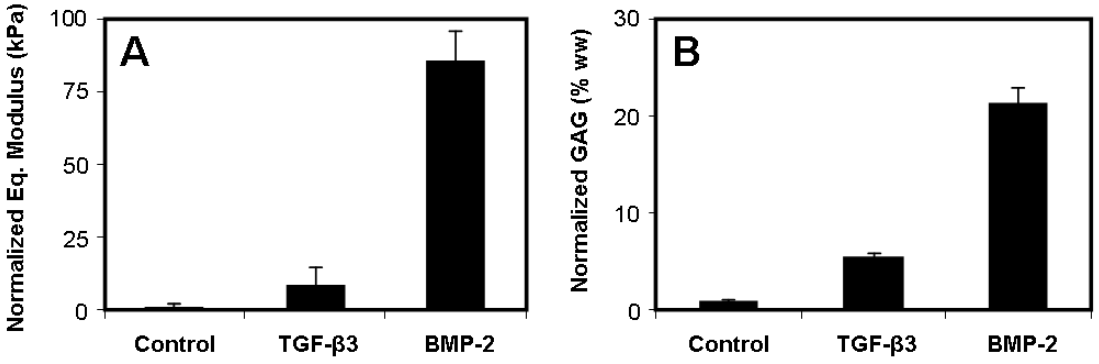

Figure 9-5: Bovine MSCs were seeded in agarose and cultured in control media (no growth factors), or 10 ng/mL TGF-β3 or 100 ng/mL BMP-2 supplemented media for 21 days. (A) Equilibrium modulus and (B) GAG content were highest for BMP-2 treated constructs. Data was normalized to control constructs and represent mean and standard deviation, n=3 per group.

From these preliminary studies, BMP-2 emerges as an attractive alternative to TGF-β3, though several caveats remain. First, while BMP-2 can successfully induce chondrogenesis, it is also an osteogenic inducer. BMPs and TGF-βs signal through alternative Smad pathways (Smads 1/5/7 vs. Smads 2/3, respectively) and the BMP signaling pathway is important in bone formation. For example, constitutive activation of a BMP receptor, ALK-2, causes ectopic bone formation via endochondral ossification (Shore et al. 2006; Kaplan et al. 2007). Our own studies show that pellets treated with BMP-2 deposit a large fibrous ring devoid of type II collagen or proteoglycans (**Figure 9-6**), indicating an inclination toward a fibro-cartilaginous phenotype. Therefore, while the phenotype of TGF-β-induced MSCs is already in question, the phenotype of BMP-induced MSCs may be even less stable. Future studies will focus on these potential differences, and determine the feasibility of BMP-2 as a chondrogenic factor.

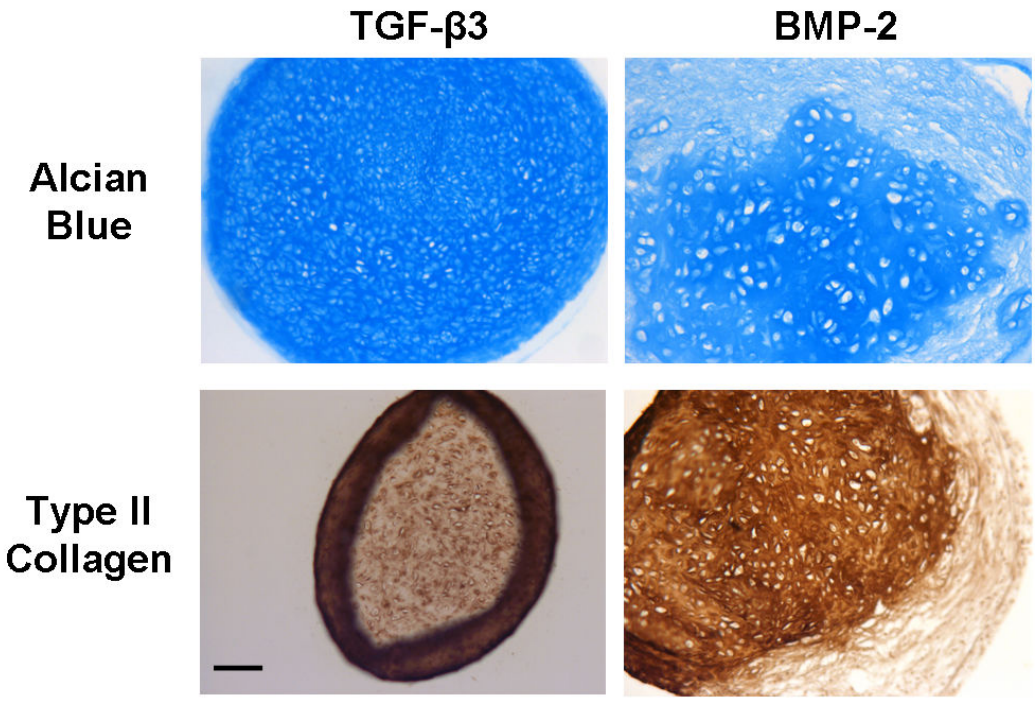

Figure 9-6: Alcian Blue and type II collagen immunostaining of bovine MSC pellets treated with 10 ng/mL TGF-β3 or 100 ng/mL BMP-2. Scale bar: 100 μm.

9.3 Conclusion

Despite the potential avenues open for future investigation, the work outlined in this thesis represents a significant advancement in the engineering of cartilage replacements as well as in our understanding of mesenchymal stem cell (MSC) chondrogenesis. We show that the established markers of chondrogenesis, while important, are insufficient indicators of functional MSC chondrogenesis and identify these transcriptional limitations, relative to fully differentiated articular chondrocytes. By better characterizing the transcriptional profiles of chondrogenesis, we achieve a better understanding of MSC differentiation and phenotype. We show that MSC chondrogenesis can be modulated by their chemical and mechanical environment; furthermore, we demonstrate for the first time that mechanical stimulation can improve

the compressive and tensile properties of MSC-based constructs for cartilage tissue engineering applications. The results presented here has important implications in the study of MSC mechanobiology, not only for the field of cartilage tissue engineering, but also for the engineering of other load-bearing tissues. Overall, the work described in this thesis provides a significant step forward toward clinical realization of a tissue engineered solution for cartilage regeneration.

APPENDIX 1: COMPLETE LIST OF GENES MODULATED BY DYNAMIC LOADING

Complete list of genes that were up-regulated (>3-fold) at week 6 with dynamic compressive loading compared to CM+ free-swelling control.

Probe Set ID	Gene Symbol	Gene Title
Bt.9979.1.S1_at	CHRNA5	cholinergic receptor, nicotinic, alpha 5
Bt.8132.1.S1_at	HRG	histidine-rich glycoprotein
Bt.26755.2.S1_a_at	LOC783009	similar to KIAA0674 protein
Bt.26636.1.S1_at	NKG7	natural killer cell group 7 sequence
Bt.26126.1.A1_at	LOC783038	Hypothetical protein LOC783038
Bt.25683.1.A1_at	MGC134028	similar to IIIG9 protein
Bt.22408.1.S1_at	LOC407176	calcium activated potassium channel beta subunit
Bt.21044.2.A1_at	---	Transcribed locus, moderately similar to NP_057236.1 retinoic acid receptor, bet
Bt.17231.1.A1_at	MGC179444	similar to putative protein product of HYST1046
Bt.1207.1.S1_at	MGC139592	similar to solute carrier family 16 (monocarboxylic acid transporters), member 1
Bt.11341.1.A1_at	NNAT	Neuronatin
Bt.8555.2.S1_at	LOC505941	similar to ribosome binding protein 1
Bt.8363.2.S1_at	KCNK1	potassium channel, subfamily K, member 1
Bt.729.1.S1_at	LOC788224	similar to Rse
Bt.7209.1.S1_at	CRHR1	corticotropin releasing hormone receptor 1
Bt.7196.1.S1_at	LOC404111	epidermal keratin VII
Bt.7168.1.S1_at	LOC513668	similar to collagen, type XXVII, alpha 1
Bt.6509.2.S1_at	LOC511043	Similar to laminin 5 gamma 2 subunit
Bt.6007.1.S1_at	LOC519777	Similar to Suppressor of variegation 4-20 homolog 2 (Drosophila)
Bt.5194.2.S1_a_at	WBP1	WW domain binding protein 1
Bt.4858.1.S1_at	LOC504250	similar to dihydropyrimidinase related protein-1
Bt.48.1.S1_a_at	CD28	CD28 molecule
Bt.4768.1.S1_at	JAM1	junctional adhesion molecule 1
Bt.4414.2.S1_at	LOC532273	hypothetical LOC532273
Bt.4298.3.S1_a_at	GPR172A	G protein-coupled receptor 172A
Bt.4133.1.S1_at	RGS16	regulator of G-protein signaling 16
Bt.4074.1.S1_at	FUT	alpha 1,3 fucosyltransferase
Bt.4057.2.S1_at	MYH10	myosin, heavy chain 10, non-muscle
Bt.37.2.S1_a_at	LHCGR	luteinizing hormone/choriogonadotropin receptor
Bt.29794.1.S1_at	---	Glucose induced gene (clone 2C) [cattle, thoracic aorta smooth muscle cells, mRN
Bt.29794.1.A1_at	---	Glucose induced gene (clone 2C) [cattle, thoracic aorta smooth muscle cells, mRN
Bt.29763.1.S1_at	TRB@	T cell receptor, beta cluster
Bt.29683.1.A1_at	HYAL2	Hyaluronoglucosaminidase 2
Bt.29462.1.S1_at	MGC137262	similar to cell division cycle associated 2
Bt.29179.1.S1_at	POLR2F	polymerase (RNA) II (DNA directed) polypeptide F
Bt.2867.1.S1_at	SCHIP1	schwannomin interacting protein 1
Bt.28401.2.A1_at	LOC514978	similar to lipopolysaccharide binding protein
Bt.2833.1.S1_at	LOC510764	similar to SAPS2 protein
Bt.28277.1.A1_at	LOC781988	hypothetical protein LOC781988
Bt.28014.1.S1_at	LOC407172	cAMP-gated channel
Bt.28004.2.S1_at	LOC505306	Hypothetical LOC505306
Bt.27681.1.A1_at	LOC539023	similar to tripartite motif-containing 36
Bt.27484.1.A1_at	PLXNA3	plexin A3
Bt.27329.1.A1_at	LOC541200	similar to 5-HT5A serotonin receptor
Bt.27319.1.A1_at	MGC151855	hypothetical LOC508022
Bt.26827.1.S1_at	KLHL12	kelch-like 12
Bt.26798.1.S1_at	GPR114	G-protein coupled receptor 114
Bt.26529.1.S1_at	DOK1	docking protein 1
Bt.26356.1.A1_at	MGC142602	similar to Glutamate decarboxylase 1 (Glutamate decarboxylase, 67 kDa isoform) (
Bt.26153.2.A1_at	LOC615350	Hypothetical LOC615350
Bt.25955.1.A1_at	LOC538986	similar to Fidgetin-like 1
Bt.25924.1.A1_at	MGC160119	similar to Family with sequence similarity 64, member A
Bt.25911.1.A1_at	LOC521943	similar to Zinc finger and BTB domain containing 8
Bt.25800.1.A1_at	FLJ32660	hypothetical protein LOC509524
Bt.25767.2.A1_at	LOC527517	similar to putative G protein-coupled receptor
Bt.25666.1.A1_at	FAM19A5	similar to TAFA5
Bt.2551.1.S1_at	CCNA2 ///	cyclin A2 /// similar to Cyclin A2

Probe Set ID	Gene Symbol	Gene Title
	LOC786906	
Bt.2519.1.S1_at	PLAU	plasminogen activator, urokinase
Bt.25040.1.S1_at	MGC142697	similar to Plakophilin-3
Bt.24882.2.S1_at	MAP1B	microtubule-associated protein 1B
Bt.24739.1.S1_at	ELA2	elastase 2, neutrophil
Bt.24643.1.S1_at	APOBEC2	apolipoprotein B mRNA editing enzyme, catalytic polypeptide-like 2
Bt.24381.2.S1_at	LOC784292	similar to dCMP deaminase
Bt.23582.1.A1_at	NOX4	NADPH oxidase 4
Bt.23480.1.S1_at	MGC143269	similar to distal-less homeobox protein
Bt.23250.3.A1_at	AHSG	Alpha-2-HS-glycoprotein
Bt.23126.2.A1_at	NOS2A	nitric oxide synthase 2A (inducible, hepatocytes)
Bt.23094.2.A1_at	LOC785762	similar to prostaglandin F synthase-like1 protein
Bt.22950.1.S1_at	CRISP-1	cysteine-rich secretory protein 1
Bt.22599.1.A1_at	MGC137443	similar to L-threonine dehydrogenase
Bt.21998.1.S1_at	LOC504797	similar to zinc finger transcription factor TReP-132
Bt.2121.2.S1_at	LOC522383	similar to nestin
Bt.21130.1.S1_at	LOC508029	similar to KNP3
Bt.21087.2.S1_at	MGC143310	similar to putative transcription factor
Bt.2092.3.S1_at	LOC506953	similar to Integrin alpha-7 precursor
Bt.20880.1.S1_at	MGC140206	similar to p53-regulated receptor for death and life
Bt.20778.2.S1_at	LOC510050	similar to TG-interacting factor
Bt.19690.1.A1_at	PON1	paraoxonase 1
Bt.19376.1.A1_at	G6PC	Glucose-6-phosphatase, catalytic subunit
Bt.19.2.A1_at	SLC24A1	solute carrier family 24 (sodium/potassium/calcium exchanger), member 1
Bt.18834.1.A1_at	LOC538993	similar to KIAA0748 protein
Bt.18616.2.A1_at	LOC537010	Similar to striatin, calmodulin binding protein
Bt.17928.2.A1_at	LOC532126	similar to transmembrane protein 16A
Bt.17928.1.A1_at	LOC532126	similar to transmembrane protein 16A
Bt.17885.1.A1_at	LOC531389	hypothetical LOC531389
Bt.17609.1.A1_at	LOC531398	similar to KIAA1290 protein
Bt.1745.1.S1_at	KRT18	keratin 18
Bt.17307.1.A1_at	LOC785202	similar to RIKEN cDNA 2510048L02 gene
Bt.17047.1.A1_at	MGC140771	similar to HUD3
Bt.16377.1.S1_at	MBP	myelin basic protein
Bt.16073.1.A1_at	LOC533166	similar to mosaic protein LR11
Bt.16047.1.S1_at	CDCA5	cell division cycle associated 5
Bt.15601.2.S1_at	XRCC3	X-ray repair complementing defective repair in Chinese hamster cells 3
Bt.14579.2.S1_at	WRNIP1	Werner helicase interacting protein 1
Bt.13922.1.A1_at	MGC140381	similar to hairy and enhancer of split 6
Bt.13721.1.S1_at	LOC512371	Similar to tumor protein p53 inducible protein 5
Bt.13470.2.S1_at	LOC787630	hypothetical protein LOC787630
Bt.13092.1.S1_at	MMP7	matrix metallopeptidase 7 (matrilysin, uterine)
Bt.13030.2.A1_at	COL2A1	collagen, type II, alpha 1
Bt.13003.9.S1_at	TRA@	T cell receptor, alpha
Bt.13003.9.A1_at	TRA@	T cell receptor, alpha
Bt.12989.1.S1_at	SEC14L2	SEC14-like 2 (S. cerevisiae)
Bt.12818.3.A1_x_at	TSPY	testis-specific protein, Y-encoded
Bt.12636.1.A1_at	LOC514609	similar to BCM-like membrane protein
Bt.12328.1.S1_at	LOC533089	similar to centromere protein F (350/400kD)
Bt.11506.1.A1_at	alpha globin	hemoglobin alpha chain
Bt.11410.1.A1_at	LOC512401	hypothetical LOC512401
Bt.11226.2.S1_at	LOC507102	similar to sterol regulatory element-binding transcription factor 2
Bt.11040.1.S1_at	LOC785319	similar to Neural cell adhesion molecule 1, 180 kDa isoform precursor (N-CAM 180
Bt.10719.1.S1_at	MGC140227	similar to Myosin light polypeptide 4 (Myosin light chain 1, embryonic muscle/at
Bt.106.1.S1_at	ALPI	alkaline phosphatase, intestinal
BtAffx.1.9.S1_at	NPPA	natriuretic peptide precursor A
BtAffx.1.6.S1_at	OSM	oncostatin M
BtAffx.1.16.S1_s_at	5-OPase	5-oxo-L-prolinase
Bt.9987.1.S1_at	LOC513008	similar to deleted in neuroblastoma 5
Bt.9986.2.S1_at	LOC513431	Hypothetical LOC513431
Bt.9957.1.S1_a_at	SFN	stratifin

Probe Set ID	Gene Symbol	Gene Title
Bt.9868.3.S1_a_at	LOC522614	similar to aarF domain containing kinase 5
Bt.9863.1.S1_at	LOC523367	hypothetical LOC523367
Bt.9832.2.S1_at	MUSTN1	musculoskeletal, embryonic nuclear protein 1
Bt.9789.1.S1_at	mash2	achaete-scute complex-like protein 2 /// achaete scute-like protein 2
Bt.9683.1.A1_at	MGC148604	similar to lymphocyte antigen 6 complex, locus G6E
Bt.9656.1.S1_at	MARK4	MAP/microtubule affinity-regulating kinase 4
Bt.9654.1.S1_at	LOC510193	similar to Apolipoprotein L, 3
Bt.964.1.S1_at	MGC148510	thymidine kinase 1, soluble
Bt.9632.1.S1_a_at	MUCIN	gall-bladder mucin
Bt.9595.1.S1_at	LOC509961	hypothetical LOC509961
Bt.9563.1.S1_at	ASZ1	ankyrin repeat, SAM and basic leucine zipper domain containing 1
Bt.9483.1.S1_at	ITGAD	integrin, alpha D
Bt.942.2.S1_at	LOC517717 /// MGC142499	hypothetical LOC517717 /// similar to SAM domain and HD domain-containing protei
Bt.9412.1.S1_at	LOC781493	similar to collagen, type XIV, alpha 1
Bt.9306.3.S1_at	MARS	methionyl-tRNA synthetase
Bt.9261.1.S1_at	LOC787353	hypothetical protein LOC787353
Bt.9196.1.A1_at	LOC513220	similar to antigen identified by monoclonal antibody Ki-67
Bt.9163.1.A1_at	P2RY10	purinergic receptor P2Y, G-protein coupled, 10
Bt.9159.1.S1_at	MOBKL2A	MOB1, Mps One Binder kinase activator-like 2A (yeast)
Bt.9139.1.A1_at	LOC616332	hypothetical LOC616332
Bt.9032.3.A1_at	TCRG	T-cell receptor gamma chain
Bt.9032.2.A1_at	TRGC3	T cell receptor gamma C3
Bt.9028.1.S1_at	TYR	tyrosinase
Bt.9025.1.S1_at	ITPR3	inositol 1,4,5-triphosphate receptor, type 3
Bt.891.1.S1_at	LOC508292	similar to Chromosome 16 open reading frame 77
Bt.8889.1.S1_at	LOC515924	Similar to ret proto-oncogene
Bt.8869.1.S1_at	LOC534002	similar to Serine/arginine repetitive matrix protein 2
Bt.8834.2.S1_a_at	NRM	nurim (nuclear envelope membrane protein)
Bt.8822.1.A1_at	MGC152173	similar to inward rectifier potassium channel Kir1.2
Bt.8804.1.S1_at	MGC166235	similar to nel-related protein 2
Bt.8694.2.S1_at	LOC789036	similar to cask-interacting protein 2
Bt.8624.2.S1_at	ARG2	arginase, type II
Bt.8601.1.S1_at	LOC617280	similar to Rho guanine nucleotide exchange factor (GEF) 19
Bt.86.1.S1_at	SERPINF2	serpin peptidase inhibitor, clade F (alpha-2 antiplasmin, pigment epithelium der
Bt.8597.2.S1_at	TOP3B	topoisomerase (DNA) III beta
Bt.8543.1.S1_at	TIMAP	CAAX box protein TIMAP
Bt.8479.1.A1_at	NOS2A	nitric oxide synthase 2A (inducible, hepatocytes)
Bt.8282.1.S2_at	DPP4 /// LOC784693	dipeptidyl-peptidase 4 (CD26, adenosine deaminase complexing protein 2) /// simi
Bt.8279.1.A1_at	MGC128000	Similar to nuclear protein E3-3
Bt.8232.1.S1_at	PPP1R16A	Protein phosphatase 1, regulatory (inhibitor) subunit 16A
Bt.8145.1.S1_at	SMCX	Smcx homolog, X chromosome (mouse)
Bt.8141.1.A1_at	UGT8	UDP glycosyltransferase 8 (UDP-galactose ceramide galactosyltransferase)
Bt.8127.1.S2_at	HPSE	heparanase
Bt.8030.2.S1_at	RGS3	regulator of G-protein signaling 3
Bt.8030.1.S1_at	RGS3	regulator of G-protein signaling 3
Bt.7990.2.S1_at	LOC517259	similar to molecule interacting with Rab13
Bt.797.1.S1_at	LOC616570	similar to Hydrogen voltage-gated channel 1
Bt.7960.1.S1_at	CD1A /// CD1B /// LOC618200	CD1b molecule /// CD1a molecule /// similar to CD1b3
Bt.7948.1.S1_at	LOC518833	similar to KIAA1168 protein
Bt.794.1.S1_at	MGC151650	similar to SCG10-related protein HiAT3
Bt.7872.1.S1_at	CBR1	carbonyl reductase 1
Bt.7860.2.S1_a_at	LOC534119	similar to beta-dystrobrevin
Bt.7741.1.S1_at	ApoC3	apolipoprotein C-III
Bt.7677.1.S1_at	TMEM59L	transmembrane protein 59-like
Bt.7641.1.S1_at	PDXK	pyridoxal (pyridoxine, vitamin B6) kinase
Bt.762.1.S1_at	TMUB1	transmembrane and ubiquitin-like domain containing 1
Bt.7338.1.S1_at	LOC539721	hypothetical LOC539721
Bt.73.1.S1_at	COL10A1	collagen, type X, alpha 1(Schmid metaphyseal chondrodysplasia)
Bt.7213.1.S1_at	IL12RB2	interleukin 12 receptor, beta 2
Bt.7211.1.S1_at	SIAT4A	sialyltransferase 4A (beta-galactosidase alpha-2,3-sialytransferase)
Bt.7179.1.S1_a_at	MMP23B	matrix metallopeptidase 23B
Bt.7174.1.S1_at	LOC533435	hypothetical LOC533435
Bt.7126.1.S1_at	LOC616326	similar to Chromosome 14 open reading frame 131
Bt.7034.1.S1_at	ITGB1BP3	integrin beta 1 binding protein 3
Bt.7003.2.S1_at	LPXN	leupaxin
Bt.6976.1.S1_at	SELPG	selectin P ligand
Bt.6849.1.S1_at	SEC23B	Sec23 homolog B (S. cerevisiae)
Bt.6724.2.S1_a_at	HGS	hepatocyte growth factor-regulated tyrosine kinase substrate
Bt.6710.2.S1_at	LOC516108	hypothetical LOC516108
Bt.6700.1.A1_at	LOC515917	similar to trophoblast Kunitz domain protein 2

Probe Set ID	Gene Symbol	Gene Title
Bt.6670.1.S1_at	CHF2	cardiovascular basic helix-loop-helix factor 2
Bt.6654.1.S1_at	LOC521224	similar to Ras GTPase-activating protein 4 (RasGAP-activating-like protein 2) (C
Bt.6620.1.S1_at	MYH7	myosin, heavy chain 7, cardiac muscle, beta
Bt.6509.3.S1_a_at	LOC511043	similar to laminin 5 gamma 2 subunit
Bt.6507.2.A1_s_at	LOC509889	Hypothetical LOC509889
Bt.6413.1.S1_at	MGC127064	hypothetical protein LOC616622
Bt.6116.3.S1_at	HTRA2	HtrA serine peptidase 2
Bt.6072.1.S1_a_at	STX1A	syntaxin 1A (brain)
Bt.6056.1.S1_at	LOC615408	similar to septin 5
Bt.6025.1.S1_at	SLC27A1	solute carrier family 27 (fatty acid transporter), member 1
Bt.597.1.S1_at	MMP20	matrix metallopeptidase 20 (enamelysin)
Bt.5945.1.A1_at	ITIH4	inter-alpha (globulin) inhibitor H4 (plasma Kallikrein-sensitive glycoprotein)
Bt.594.1.S1_at	LOC286871	uterine milk protein precursor
Bt.5878.2.S1_at	SDS	serine dehydratase
Bt.5848.1.S1_at	ATP2A1	ATPase, Ca++ transporting, cardiac muscle, fast twitch 1
Bt.5839.1.S1_at	TSEN2	tRNA splicing endonuclease 2 homolog (S. cerevisiae)
Bt.5819.1.S1_at	LOC513643	similar to Forkhead box protein M1 (Forkhead-related protein FKHL16) (Hepatocyte
Bt.5770.1.A1_at	SMPD2	sphingomyelin phosphodiesterase 2, neutral membrane (neutral sphingomyelinase)
Bt.576.1.S1_at	BSP30B	common salivary protein BSP30, form b
Bt.5718.1.S1_at	CACNA1G	calcium channel, voltage-dependent, T type, alpha 1G subunit
Bt.565.1.S1_at	CCRL1	chemokine (C-C motif) receptor-like 1
Bt.5585.1.S1_at	MGC137174	Similar to Protein KIAA0317
Bt.5579.1.S1_at	LOC540545	hypothetical LOC540545
Bt.5577.1.S1_at	LOC506293	similar to DEAD/H (Asp-Glu-Ala-Asp/His) box polypeptide 11
Bt.5550.1.S1_at	IMPG1	interphotoreceptor matrix proteoglycan 1
Bt.5525.1.S1_at	LOC524222	similar to extracellular matrix protein 1
Bt.549.1.A1_at	AMBP	alpha-1-microglobulin/bikunin precursor
Bt.5448.1.S1_at	CHGB	chromogranin B (secretogranin 1)
Bt.5430.1.S1_at	BCAN	brevican
Bt.5391.1.S1_at	KERA	keratocan
Bt.5360.2.S1_at	PAPOLB	poly(A) polymerase beta (testis specific)
Bt.5354.1.S1_at	CSN1S2	casein alpha-S2
Bt.5353.2.S1_a_at	SSBP4	single stranded DNA binding protein 4
Bt.5271.1.S1_at	LOC504986	similar to polycystin 1; polycystic kidney disease 1
Bt.5262.1.S1_at	MGC157179	similar to Cyclin F
Bt.5237.1.S1_at	IGFBP4	insulin-like growth factor binding protein 4
Bt.5194.3.S1_a_at	WBP1	WW domain binding protein 1
Bt.5177.1.S1_at	MGC137853	similar to BMP and activin membrane-bound inhibitor homolog precursor (Putative
Bt.5129.1.S1_a_at	NNAT	neuronatin
Bt.510.1.S1_at	TAP	tracheal antimicrobial peptide
Bt.5087.1.S1_at	PNPLA6	patatin-like phospholipase domain containing 6
Bt.507.1.S1_at	UCP1	uncoupling protein 1
Bt.5061.1.S1_at	PFKL	phosphofructokinase, liver
Bt.5046.2.A1_a_at	LOC506670	similar to Solute carrier family 7, (cationic amino acid transporter, y+ system)
Bt.5038.3.S1_at	FGF1	fibroblast growth factor 1 (acidic)
Bt.499.1.S1_a_at	PRLR	prolactin receptor
Bt.4899.1.S1_at	LOC510465	similar to Mucoepidermoid carcinoma translocated protein 1 (Transducer of regula
Bt.4865.1.S1_at	LOC540451	similar to emilin
Bt.4860.1.S1_at	LOC787239 /// SYT1	synaptotagmin I /// similar to Synaptotagmin-1 (Synaptotagmin I) (SytI) (p65)
Bt.4774.1.S1_at	GNAT1	guanine nucleotide binding protein (G protein), alpha transducing activity polyp
Bt.4760.1.S1_at	HSD3B1	hydroxy-delta-5-steroid dehydrogenase, 3 beta- and steroid delta-isomerase 1
Bt.473.1.S1_a_at	GNGT1	guanine nucleotide binding protein (G protein), gamma transducing activity polyp
Bt.4714.1.S1_at	MMP9	matrix metallopeptidase 9 (gelatinase B, 92kDa gelatinase, 92kDa type IV collage
Bt.4698.1.S1_at	TIE	tyrosine kinase with immunoglobulin and epidermal growth factor homology domains
Bt.4695.1.S1_at	PIGR	polymeric immunoglobulin receptor
Bt.4630.1.S1_at	RNASE1	ribonuclease
Bt.4614.1.S1_at	LOC511558	similar to glycerol 3-phosphate permease
Bt.4597.1.S1_at	GPR68	G protein-coupled receptor 68
Bt.4553.3.S1_a_at	LOC526472	similar to CLIM2
Bt.4547.2.S1_a_at	NTT73	homolog of rat orphan transporter v7-3
Bt.454.1.S1_at	LOC751563 /// PRP1	prolactin-related protein 1 /// prolactin-related protein 12
Bt.452.1.S1_at	GPLD1	glycosylphosphatidylinositol specific phospholipase D1
Bt.45.1.S1_at	CCIN	calicin
Bt.4480.1.S1_at	GUCY1A3	guanylate cyclase 1, soluble, alpha 3
Bt.448.1.S1_at	PLCB1	phospholipase C, beta 1 (phosphoinositide-specific)
Bt.4387.2.S1_at	NAGK	N-acetylglucosamine kinase
Bt.4375.1.S1_at	B4GALT3	UDP-Gal:betaGlcNAc beta 1,4- galactosyltransferase, polypeptide 3
Bt.4332.1.S1_at	CEBPA	CCAAT/enhancer binding protein (C/EBP), alpha
Bt.4321.1.S1_at	CISH	cytokine inducible SH2-containing protein
Bt.430.1.S1_a_at	CSH1	chorionic somatomammotropin hormone 1 (placental lactogen)
Bt.4297.1.S2_at	CYP11B1	cytochrome P450, subfamily XI B, polypeptide 1

Probe Set ID	Gene Symbol	Gene Title
Bt.423.1.S1_at	IL4	interleukin 4
Bt.4210.1.A1_a_at	KNG	kininogen
Bt.4194.1.S1_at	TTYH2	tweety homolog 2
Bt.4071.1.S1_at	MGC148652	Hypothetical LOC616916
Bt.3994.2.S1_a_at	SMN	survival motor neuron
Bt.3930.1.S1_at	ASMT	acetylserotonin O-methyltransferase
Bt.3885.4.S1_a_at	CLCA3 /// LOC784768	chloride channel, calcium activated, family member 3 /// similar to calcium-acti
Bt.3863.1.S1_at	ZFP36	zinc finger protein 36, C3H type, homolog (mouse)
Bt.3760.1.A1_at	MGC139033	similar to suppression of tumorigenicity 5
Bt.3757.1.S1_at	LOC523865	similar to Myeloid zinc finger 1
Bt.3731.1.S1_at	LOC787458	similar to fibrillin3
Bt.373.3.S1_a_at	AMELX /// AMELY	amelogenin (amelogenesis imperfecta 1, X-linked) /// amelogenin, Y-linked
Bt.372.1.S1_at	AKAP5	A kinase (PRKA) anchor protein 5
Bt.37.1.S1_at	LHCGR	luteinizing hormone/choriogonadotropin receptor
Bt.3686.1.S1_at	IL6	interleukin 6 (interferon, beta 2)
Bt.365.1.S2_at	SYNJ1	synaptojanin 1
Bt.3538.3.S1_at	MGC128098	similar to anterior pharynx defective 1a homolog
Bt.3457.1.S1_at	TBC1D10A	TBC1 domain family, member 10A
Bt.341.1.S1_at	IL2	interleukin 2
Bt.3406.1.S1_at	MGC139318	hypothetical LOC508503
Bt.3385.1.A1_at	POLR2A	Polymerase (RNA) II (DNA directed) polypeptide A, 220kDa
Bt.3371.1.S1_at	LOC510120	similar to MCM2 minichromosome maintenance deficient 2, mitotin (S. cerevisiae)
Bt.3360.2.S1_at	LOC521410	hypothetical LOC521410
Bt.3360.1.S1_at	MGC134547	similar to peptidylprolyl isomerase-like 2
Bt.3339.1.S1_at	SEMA4A	sema domain, immunoglobulin domain (Ig), transmembrane domain (TM) and short cyt
Bt.3323.1.S1_at	LOC508175	similar to KIAA0315
Bt.3315.1.A1_at	MGC139689	similar to D-lactate dehydrogenase isoform 2 precursor
Bt.3255.1.A1_at	ABP1	amiloride binding protein 1 (amine oxidase (copper-containing))
Bt.3225.3.A1_at	LOC506423	Similar to Glucose 6-phosphate translocase (Glucose 5-phosphate transporter) (So
Bt.3194.1.S1_at	LOC511594	similar to cell adhesion molecule JCAM
Bt.3046.1.S1_at	SNAI1	snail homolog 1 (Drosophila)
Bt.3027.1.S1_at	BAT3	HLA-B associated transcript 3
Bt.302.1.S1_at	RCV1	recoverin
Bt.29962.2.S1_at	MAP3K12	mitogen-activated protein kinase kinase kinase 12
Bt.29932.1.S1_at	LOC522068	similar to small optic lobes homolog
Bt.29930.1.S1_at	LOC508078	similar to mKIAA0870 protein
Bt.29927.1.S1_at	TRMT12	tRNA methyltransferase 12 homolog (S. cerevisiae)
Bt.29926.3.S1_at	MGC140559	similar to transmembrane protein 68
Bt.29899.1.S1_at	RBM15B	RNA binding motif protein 15B
Bt.29883.1.A1_at	IL-18Ra	IL-18 receptor alpha
Bt.29881.1.S1_at	LOC407218	calcitonin receptor-stimulating peptide-1
Bt.29876.1.S1_at	SP-A	surfactant protein A
Bt.29861.1.S1_at	hare	putative hyaluronan receptor for endocytosis
Bt.29847.1.S1_at	LOC407118	GABA transporter GAT-1 homolog
Bt.29835.1.S1_at	OMG	oligodendrocyte myelin glycoprotein
Bt.29833.1.S1_at	LOC540382	cannabinoid receptor 1
Bt.29819.1.A1_at	BOLA-NC1	Non-classical MHC class I antigen
Bt.29815.1.S1_x_at	BOLA	MHC class I heavy chain
Bt.29805.1.A1_at	---	Clone 2 immunoglobulin heavy chain variable region (VH)
Bt.29789.1.S1_at	SIAT1	Sialyltransferase 1 (beta-galactoside alpha-2,6-sialytransferase)
Bt.29787.1.S1_s_at	SIAT1	Sialyltransferase 1 (beta-galactoside alpha-2,6-sialytransferase)
Bt.29782.1.S1_at	---	Glutathione-S-transferase (GST) specific immunoglobulin heavy chain variable reg
Bt.29782.1.A1_at	---	Glutathione-S-transferase (GST) specific immunoglobulin heavy chain variable reg
Bt.29777.1.S1_at	---	Immunoglobulin lambda light chain variable region (Ig Vl1a)
Bt.29769.1.A1_at	LOC407184	steroidogenic factor 1
Bt.29767.1.S1_at	TRPC3	transient receptor potential cation channel, subfamily C, member 3
Bt.29761.1.A1_at	LOC509384	Similar to T-cell receptor beta chain
Bt.29739.1.S1_at	---	B4 cell-line anti-respiratory syncytial virus Ig lambda chain V region (IgL)
Bt.29739.1.A1_at	---	B4 cell-line anti-respiratory syncytial virus Ig lambda chain V region (IgL)
Bt.29732.1.S1_at	---	Immunoglobulin variable region
Bt.29710.1.A1_at	zo3	tight junction protein 3
Bt.29691.1.S1_at	BVd1.18 /// LOC786720	T cell receptor delta chain variable region /// hypothetical protein LOC786720
Bt.29688.1.A1_at	BVd1.22	T cell receptor delta chain variable region
Bt.29683.1.S1_x_at	HYAL2	Hyaluronoglucosaminidase 2
Bt.29682.1.S1_at	LOC407199	T cell receptor delta chain
Bt.2965.2.S1_at	MGC148363	similar to growth arrest specific 11
Bt.29631.1.A1_at	---	Transcribed locus, strongly similar to NP_033401.1 thyroglobulin [Mus musculus]
Bt.29612.1.A1_at	LOC538467	similar to putative T7-like mitochondrial DNA helicase
Bt.29515.1.A1_at	LOC509187	similar to high mobility group AT-hook 1-like 4

Probe Set ID	Gene Symbol	Gene Title
Bt.29469.1.A1_at	LOC526526	similar to small GTPase RAB6B
Bt.29298.1.A1_at	NKAPL	NFKB activating protein-like
Bt.29293.1.A1_at	MGC159470	similar to transcript expressed during hematopoiesis 2
Bt.2928.3.S1_a_at	PPP1R13L	protein phosphatase 1, regulatory (inhibitor) subunit 13 like
Bt.2928.1.S1_at	PPP1R13L	protein phosphatase 1, regulatory (inhibitor) subunit 13 like
Bt.29258.2.A1_at	LOC789849 /// MADCAM1	mucosal vascular addressin cell adhesion molecule 1 /// similar to mucosal addre
Bt.29147.1.S1_at	PSMD13	Proteasome (prosome, macropain) 26S subunit, non-ATPase, 13
Bt.29137.1.A1_at	FASTK	Fas-activated serine/threonine kinase
Bt.29133.1.A1_at	LOC782888 /// LOC784090	hypothetical protein LOC782888 /// hypothetical protein LOC784090
Bt.29080.1.A1_at	TINAG	tubulointerstitial nephritis antigen
Bt.29076.1.S1_at	LOC510079	similar to HSPC323
Bt.29059.1.A1_at	LOC513936	similar to N-benzoyl-L-tyrosyl-p-amino-benzoic acid hydrolase alpha subunit
Bt.29019.1.S1_at	FOV	foveolin precursor
Bt.28966.1.S1_at	LOC100125947 /// LOC507201	phospholipase A2 group IIA-like /// hypothetical protein LOC100125947
Bt.2892.1.S1_at	FABP7	fatty acid binding protein 7, brain
Bt.28908.1.A1_at	---	Transcribed locus, strongly similar to XP_869038.2 PREDICTED: similar to mFLJ003
Bt.28891.1.S1_at	LOC614174	similar to Double-headed protease inhibitor, submandibular gland
Bt.28865.1.A1_at	RPS8	ribosomal protein S8
Bt.28836.1.S1_at	LOC538749 /// MGC139910	similar to KIAA0666 protein /// hypothetical LOC538749
Bt.28828.1.S1_at	MGC148379	similar to LAMP
Bt.28826.1.A1_at	LOC511100	Similar to Opa interacting protein 5
Bt.288.1.S1_at	PAG15	pregnancy-associated glycoprotein 15
Bt.28797.2.S1_at	CENP-N	centromere protein N
Bt.28795.1.A1_at	CAPNS1	calpain, small subunit 1
Bt.28759.1.A1_at	LOC539452	similar to SLIT-ROBO Rho GTPase activating protein 1
Bt.28751.1.S1_at	LOC615257	similar to enterocytin
Bt.28745.1.S1_at	F2RL1	coagulation factor II (thrombin) receptor-like 1
Bt.28740.1.S1_at	REG4	regenerating islet-derived family, member 4
Bt.28707.1.S1_at	LOC618833	similar to IQ motif containing E
Bt.28675.1.S1_at	LOC407169	12-lipoxygenase
Bt.28664.1.A1_at	MGC140449	similar to catechol O-methyltransferase, membrane-bound form
Bt.28604.1.S1_at	MGC137499	hypothetical LOC511775
Bt.28552.2.S1_at	GPI7	GPI7 protein
Bt.28518.1.S1_at	LOC404103 /// PTI	spleen trypsin inhibitor /// pancreatic trypsin inhibitor
Bt.28510.1.S1_at	CHN2	chimerin (chimaerin) 2
Bt.28494.7.S1_at	LOC524810	IgM
Bt.28494.2.A1_at	LOC524810	IgM
Bt.28487.1.S1_at	ART4	ADP-ribosyltransferase 4 (Dombrock blood group)
Bt.28476.1.S1_at	MOGAT1	monoacylglycerol O-acyltransferase 1
Bt.28461.1.S1_a_at	INSR	insulin receptor
Bt.28461.1.A1_at	INSR	insulin receptor
Bt.28460.1.S1_at	SNRPD3	small nuclear ribonucleoprotein D3 polypeptide 18kDa
Bt.28423.1.S1_at	LOC541051	similar to KIAA0984 protein
Bt.28392.1.S1_at	LOC531539	Similar to KIAA1609 protein
Bt.28358.1.A1_at	MLZE	melanoma-derived leucine zipper, extra-nuclear factor
Bt.28335.1.A1_at	ITLN2 /// LOC786046 /// LOC788773	intelectin 2 /// similar to endothelial lectin HL-2
Bt.28329.1.S1_at	MGC155124	hypothetical LOC510914
Bt.28307.1.S1_at	LOC525823	hypothetical LOC525823
Bt.28276.1.S1_at	MGC127939	similar to beta-casein-like protein
Bt.28268.1.A1_at	LOC509874	Similar to general transcription factor IIIC, polypeptide 1, alpha 220kDa
Bt.28241.1.A1_at	ITPK1	inositol 1,3,4-triphosphate 5/6 kinase
Bt.28230.1.S1_at	LOC519127	similar to Cfh protein
Bt.28228.1.S1_at	LYSB	intestinal lysozyme
Bt.28196.1.S1_at	LOC518699	similar to sphingomyelin phosphodiesterase, acid-like 3B
Bt.28168.1.A1_at	MGC166050	similar to insulin gene enhancer binding protein Isl-1
Bt.28162.2.A1_at	PLN	phospholamban
Bt.28148.2.A1_at	LOC517805	similar to fork head-related protein like A
Bt.2813.2.S1_at	PRKCA	Protein kinase C, alpha
Bt.28125.1.S1_at	LOC613954	similar to RAB37, member RAS oncogene family
Bt.28098.1.S1_at	AMICA1	adhesion molecule, interacts with CXADR antigen 1
Bt.28056.1.S1_at	LOC781559	similar to enterocytin
Bt.28031.1.S1_s_at	LOC789287 /// SQSTM1	sequestosome 1 /// similar to Sequestosome 1
Bt.28027.1.S1_at	LOC513731 /// LOC618831 /// LOC785752 /// LOC789653 ///	T-cell receptor delta chain /// similar to bovine T cell receptor delta chain //

Probe Set ID	Gene Symbol	Gene Title
	TRD@	
Bt.28022.1.A1_at	BOLA-NC1	Non-classical MHC class I antigen
Bt.28015.1.S1_at	LOC407171	Fc gamma 2 receptor
Bt.28007.2.A1_at	LOC407198	T cell receptor delta chain
Bt.28004.4.A1_at	---	T cell receptor delta chain variable region precursor (BVd1.23)
Bt.28004.2.S1_x_at	LOC505306	Hypothetical LOC505306
Bt.27993.1.S1_at	5htr1a	5-hydroxytryptamine 1A receptor
Bt.27989.1.S1_at	5htr2b	5-hydroxytryptamine 2B receptor
Bt.27987.1.A1_at	nk1R	tachikinin receptor 1
Bt.279.1.S1_at	LOC281812	fibroblast growth factor-binding protein (FGF-BP)
Bt.27883.1.S1_at	MGC155188	similar to Efs1
Bt.27882.1.S1_at	RECQL4	RecQ protein-like 4
Bt.27877.1.S1_at	LOC532964	similar to Myosin IF
Bt.27868.1.S1_at	LOC781667	similar to Kin of IRRE-like protein 1 precursor (Kin of irregular chiasm-like pr
Bt.27844.1.S1_at	LOC515433	similar to glucagon receptor
Bt.27816.3.S1_a_at	STAC3	SH3 and cysteine rich domain 3
Bt.27816.2.S1_a_at	STAC3	SH3 and cysteine rich domain 3
Bt.27815.1.S1_at	LOC509227	similar to src related tyrosine kinase
Bt.27784.2.S1_a_at	PPP1R10	protein phosphatase 1, regulatory (inhibitor) subunit 10
Bt.27731.1.A1_at	ABCG2 /// LOC505219	similar to ATP-binding cassette sub-family G member 2 (CD338 antigen) /// ATP-bi
Bt.27601.1.A1_at	LOC782354 /// SLC39A4	solute carrier family 39 (zinc transporter), member 4 /// similar to SLC39A4 pro
Bt.27547.1.A1_at	LOC509490	similar to eIF4E-binding protein 3
Bt.27535.1.A1_at	LOC783806	hypothetical protein LOC783806
Bt.27514.1.A1_at	LOC615299	hypothetical LOC615299
Bt.27486.1.A1_at	LOC786312	similar to Uncharacterized protein C20orf26
Bt.27481.1.A1_at	SPG3A	spastic paraplegia 3A (autosomal dominant)
Bt.27445.2.S1_at	LOC520376	similar to ELAV-like protein 3
Bt.27445.1.A1_at	LOC520376	similar to ELAV-like protein 3
Bt.27444.2.S1_at	LOC506508	similar to phospholipase B1
Bt.27421.2.S1_at	MGC152523	similar to rho/rac guanine nucleotide exchange factor (GEF) 2
Bt.27409.1.A1_at	LOC504406 /// LOC532419	similar to hydrocephalus inducing /// hypothetical LOC532419
Bt.27383.1.A1_at	MGC142877	similar to aarF domain containing kinase 1
Bt.27343.1.A1_at	LOC534114	similar to Rab3A-interacting molecule
Bt.27328.1.S1_at	UHRF1	ubiquitin-like, containing PHD and RING finger domains, 1
Bt.27319.2.S1_at	MGC151855	hypothetical LOC508022
Bt.27310.2.A1_at	LOC533526	similar to G1/S-specific cyclin-E1
Bt.27304.2.S1_a_at	MGC139492	similar to Poly(rC)-binding protein 3 (Alpha-CP3)
Bt.27292.1.S1_at	LOC617150	similar to ATP-binding cassette transporter C4
Bt.27270.1.A1_at	LOC526583	similar to NPAT
Bt.27245.1.A1_at	LOC527362	Similar to FLJ00128 protein
Bt.27219.1.A1_at	LOC540893	similar to heparan sulfate 3-O-sulfotransferase 6
Bt.27185.1.S1_at	POLR3F	Polymerase (RNA) III (DNA directed) polypeptide F, 39 kDa
Bt.27175.1.A1_at	---	Transcribed locus, strongly similar to NP_001014171.1 hypothetical protein LOC36
Bt.27093.1.S1_at	MGC157047	similar to zinc finger protein 189
Bt.27059.1.S1_at	LOC511050	similar to alpha-L-iduronidase
Bt.27048.1.A1_at	LOC518599	Similar to Lactase-like protein precursor (Klotho/lactase-phlorizin hydrolase-re
Bt.27001.2.S1_at	MGC139710	similar to CG18177-PB
Bt.26985.1.A1_at	LOC506540	similar to T cell leukemia/lymphoma 1
Bt.26973.1.S1_at	LOC504975	similar to tolloid-like 2 protein
Bt.26917.2.A1_at	LOC511497	Similar to arginyl aminopeptidase (aminopeptidase B)-like 1
Bt.26911.1.A1_at	LOC506674	similar to TAFII140 protein
Bt.26902.1.A1_at	GATAD2A	GATA zinc finger domain containing 2A
Bt.26896.1.S1_at	LOC533359	similar to MAX dimerization protein 3
Bt.26891.1.S1_at	LOC534348	similar to IgG Fc binding protein
Bt.26880.1.A1_at	LOC514524	similar to Leucine rich repeat containing 45
Bt.26855.1.S1_at	LOC506746	hypothetical LOC506746
Bt.26849.3.S1_at	LOC784605	similar to ADAM15 isoform 6a
Bt.26839.1.S1_at	LOC507057	similar to PHD finger protein 12 (PHD factor 1) (Pf1)
Bt.26824.1.A1_a_at	MRPL46	mitochondrial ribosomal protein L46
Bt.26822.1.A1_at	LOC510012	similar to SCL/TAL1 interrupting locus
Bt.26819.3.S1_at	FLJ36874	Hypothetical protein LOC537453
Bt.268.1.S1_at	F12 /// LOC785029	coagulation factor XII /// similar to Coagulation factor XII
Bt.26781.1.A1_at	MGC139340	similar to Ectoderm-neural cortex-1 protein (ENC-1) (p53-induced protein 10) (Nu
Bt.26769.1.S1_at	LOC531516	similar to GTPase, IMAP family member 8
Bt.26758.1.A1_at	LOC539500	similar to Zinc finger protein 710
Bt.26715.1.S1_at	ST14	suppression of tumorigenicity 14
Bt.26707.2.S1_at	LOC539236	similar to LY6G5B protein
Bt.26706.1.S1_at	LOC618116 /// LOC787378	similar to IQ motif containing with AAA domain

Probe Set ID	Gene Symbol	Gene Title
Bt.26688.2.S1_a_at	FRMD3	FERM domain containing 3
Bt.26678.1.S1_at	LOC789892	similar to BCR variant protein
Bt.26665.3.S1_at	LOC510748	similar to Pleckstrin homology domain containing, family A (phosphoinositide bin
Bt.26652.1.S1_at	LOC523793	similar to anchor protein
Bt.26649.1.A1_at	LOC783512 /// TST	thiosulfate sulfurtransferase (rhodanese) /// similar to Thiosulfate sulfurtrans
Bt.26604.1.S1_at	AGTRL1	angiotensin II receptor-like 1
Bt.26599.1.S1_a_at	ZNF414	zinc finger protein 414
Bt.26575.2.A1_at	BLR1	Burkitt lymphoma receptor 1
Bt.26562.2.S1_at	CCDC86	coiled-coil domain containing 86
Bt.26556.1.A1_at	LOC528050	Similar to glycine transporter GLYT2
Bt.26514.1.A1_at	OSBPL2	oxysterol binding protein-like 2
Bt.26472.1.A1_at	C-MOS	C-MOS protein
Bt.26470.1.S1_at	LOC524593	hypothetical LOC524593
Bt.26421.1.A1_at	LOC782416 /// LOC787497 /// NDUFAB1	NADH dehydrogenase (ubiquinone) 1, alpha/beta subcomplex, 1, 8kDa /// similar to
Bt.26399.1.A1_at	MGC166237	similar to EF-hand calcium binding protein 2
Bt.26387.1.A1_at	GRIK1	glutamate receptor, ionotropic, kainate 1
Bt.26350.1.A1_at	LOC529109	similar to cofactor required for Sp1 transcriptional activation, subunit 2, 150k
Bt.26349.1.A1_at	LOC513885	similar to Chromosome 12 open reading frame 26
Bt.26338.1.A1_at	---	Transcribed locus, weakly similar to XP_001115384.1 PREDICTED: hypothetical prot
Bt.26336.1.A1_at	NXPH1	neurexophilin 1
Bt.26293.3.S1_at	LOC616292	hypothetical LOC616292
Bt.26229.1.A1_at	LOC507627	hypothetical LOC507627
Bt.26222.1.A1_at	LOC504995 /// LOC786521	similar to growth differentiation factor 3
Bt.26221.1.A1_at	---	Homo sapiens Similar to hypothetical gene supported by AL050367; AK022946 (MGC34
Bt.26169.1.A1_at	LOC786540	hypothetical protein LOC786540
Bt.26151.1.A1_at	LOC539328	similar to Protein 7 transactivated by hepatitis B virus X antigen (HBxAg)
Bt.26096.1.A1_at	LOC510218	similar to heart alpha-kinase
Bt.26088.1.A1_at	STXBP2	syntaxin binding protein 2
Bt.25975.1.A1_at	---	Transcribed locus, moderately similar to NP_001074391.1 hypothetical protein LOC
Bt.25908.3.S1_at	CCHCR1	coiled-coil alpha-helical rod protein 1
Bt.259.2.S1_a_at	PAG7	pregnancy-associated glycoprotein 7
Bt.25810.1.S1_at	MGC142865	similar to numb homolog (Drosophila)-like
Bt.25738.1.A1_at	MGC134360	similar to Protein Disulfide Isomerase family member (pdi-2)
Bt.25709.1.S1_at	LOC521616	similar to calcium channel gamma subunit 6
Bt.25700.1.A1_at	CLCN2	chloride channel 2
Bt.25682.1.A1_at	DIO1 /// LOC782446	deiodinase, iodothyronine, type I /// similar to type I iodothyronine deiodinase
Bt.25678.1.A1_at	---	Transcribed locus, strongly similar to XP_001000072.1 PREDICTED: similar to Exos
Bt.25670.1.A1_at	NFE2L2	Nuclear factor (erythroid-derived 2)-like 2
Bt.25641.2.S1_at	MGC143399	nuclear prelamin A recognition factor-like
Bt.25633.1.A1_at	LOC617133	similar to Regulator of G-protein signalling 22
Bt.25616.1.S1_at	LOC782069	hypothetical protein LOC782069
Bt.25570.1.S1_at	LOC516784	similar to bactericidal/permeability-increasing protein-like 2
Bt.2557.1.S1_at	IFRD2	interferon-related developmental regulator 2
Bt.25562.1.S1_at	---	Transcribed locus, moderately similar to NP_660337.3 WD repeat domain 90 [Homo s
Bt.25548.1.A1_at	LOC511770	hypothetical LOC511770
Bt.25544.1.A1_at	MGC139051	similar to tectorin beta
Bt.25541.1.A1_at	CCDC135	coiled-coil domain containing 135
Bt.25469.1.A1_at	MGC139293	similar to MDC3
Bt.25424.1.A1_at	LOC538817	hypothetical LOC538817
Bt.25414.1.A1_at	---	Transcribed locus, strongly similar to NP_006303.2 nuclear receptor co-repressor
Bt.25412.1.A1_at	NUSAP1	nucleolar and spindle associated protein 1
Bt.25405.1.A1_at	PLAC1	placenta-specific 1
Bt.25380.1.A1_at	LOC519193	similar to putative G protein-coupled receptor
Bt.25362.1.A1_at	---	Transcribed locus, strongly similar to XP_947066.1 PREDICTED: similar to Small V
Bt.25359.1.A1_at	LOC789937	Similar to WD and tetratricopeptide repeats protein 1
Bt.2529.1.S1_at	MT-2	metallothionein-2
Bt.2527.1.S1_at	LOC539203	Similar to dishevelled 3
Bt.25269.1.S1_at	LOC507139	similar to Gca protein
Bt.25247.1.A1_at	LOC786372	similar to 200 kDa antigen p200
Bt.25164.1.A1_at	LOC781222	hypothetical protein LOC781222
Bt.25133.1.A1_at	LOC787034	hypothetical protein LOC787034
Bt.25125.1.A1_at	LOC508574	similar to Kinesin family member 9
Bt.25102.1.S1_a_at	MGC139164	hypothetical LOC509649
Bt.25095.1.A1_at	LOC509596 /// LOC787462	similar to cation-transporting P5-ATPase
Bt.25073.1.A1_at	LOC616071	Hypothetical LOC616071
Bt.25055.1.A1_at	IPMK	inositol polyphosphate multikinase
Bt.25034.1.A1_at	MGC142439	similar to olfactory receptor, family 7, subfamily A, member 17

Probe Set ID	Gene Symbol	Gene Title
Bt.25023.1.A1_at	CLEC6A	C-type lectin domain family 6, member A
Bt.24992.1.S1_at	LOC618086	Similar to transmembrane protein 7
Bt.24990.1.S1_at	USP21	ubiquitin specific peptidase 21
Bt.24966.1.S1_at	CHAF1B	chromatin assembly factor 1, subunit B (p60)
Bt.24925.2.A1_at	RHAG	Rh-associated glycoprotein
Bt.24923.2.S1_a_at	LOC535060	hypothetical LOC535060
Bt.24850.1.S1_at	MGC157325	similar to copine-like protein
Bt.24836.1.A1_at	LOC514561	similar to retinoblastoma-associated factor 600 (RBAF600)
Bt.24743.1.S1_at	LOC521454	similar to solute carrier family 12, member 8
Bt.24694.2.S1_at	LOC511689	similar to KIAA1237 protein
Bt.24688.1.S1_at	MGC152294	similar to M83
Bt.24664.1.S1_at	LOC536439	similar to NAALADase II protein
Bt.24661.1.S1_at	LOC533455	similar to Sck
Bt.24645.1.A1_at	LOC613372	hypothetical LOC613372
Bt.24635.2.A1_at	IGFALS	insulin-like growth factor binding protein, acid labile subunit
Bt.24629.3.S1_at	LOC509859	similar to KIAA0342 protein
Bt.24594.2.S1_at	MGC139844	similar to malic enzyme 3, NADP(+)-dependent, mitochondrial
Bt.24594.1.A1_at	MGC139844	similar to malic enzyme 3, NADP(+)-dependent, mitochondrial
Bt.24542.2.S1_a_at	LOC512034	similar to neurotrypsin
Bt.24532.1.A1_at	MGC148783	similar to Interleukin 17 receptor B
Bt.24526.1.S1_at	LOC507318 /// LOC781116	hypothetical LOC507318 /// hypothetical protein LOC781116
Bt.24519.1.S1_at	LOC783266	similar to Hlcs
Bt.24517.1.S1_at	GPRC5B	G protein-coupled receptor, family C, group 5, member B
Bt.24516.2.A1_a_at	VSIG2	V-set and immunoglobulin domain containing 2
Bt.24499.1.A1_at	LOC618639	similar to potassium voltage-gated channel, subfamily H, member 8
Bt.24494.2.S1_at	LOC512321	hypothetical LOC512321
Bt.24490.2.S1_at	RPP38	ribonuclease P/MRP 38kDa subunit
Bt.24488.1.A1_at	LOC782819	similar to zinc finger protein 35
Bt.24485.1.S1_at	ZNF746	zinc finger protein 746
Bt.24455.2.A1_at	LOC510922	hypothetical LOC510922
Bt.24437.1.S1_at	MGC165851	similar to serine/threonine protein kinase
Bt.24430.1.S1_at	LOC529593	hypothetical LOC529593
Bt.24416.1.S1_at	MGC152089	similar to Rho GDP-dissociation inhibitor 3 (Rho GDI 3) (Rho-GDI gamma)
Bt.24411.1.A1_at	LOC618360	hypothetical LOC618360
Bt.24393.2.S1_at	MGC157235	similar to Def-6 protein
Bt.24218.1.S1_at	LOC515301	similar to Cdc6-related protein
Bt.24217.1.S1_at	NFE2	nuclear factor (erythroid-derived 2), 45kDa
Bt.242.1.S1_at	OPRM1	opioid receptor, mu 1
Bt.24157.1.A1_at	MGC152175	similar to DKFZP564O0823 protein
Bt.241.1.S1_at	NR2E3	nuclear receptor subfamily 2, group E, member 3
Bt.24023.1.A1_at	LOC654400	GATA-6
Bt.23998.1.A1_a_at	LOC524491	similar to cut-like 2
Bt.23953.1.A1_at	MGC126989	similar to Putative deoxyribose-phosphate aldolase (Phosphodeoxyriboaldolase) (D
Bt.23678.1.A1_at	LOC536537	Hypothetical LOC536537
Bt.23652.1.A1_at	APOB	apolipoprotein B
Bt.23513.1.S1_at	TAT	tyrosine aminotransferase
Bt.23375.1.S1_at	---	Transcribed locus, moderately similar to NP_115955.1 esophagus cancer-related ge
Bt.23367.2.S1_at	LOC505399	similar to hook1 protein
Bt.23367.1.S1_at	LOC505399	similar to hook1 protein
Bt.23294.1.A1_at	PDLIM3	PDZ and LIM domain 3
Bt.23250.4.A1_at	AHSG	Alpha-2-HS-glycoprotein
Bt.232.1.S1_at	SVS8	seminal vesicle secretion 8
Bt.23176.2.S1_a_at	IGF2	insulin-like growth factor 2
Bt.23094.6.A1_at	AKR1C3	aldo-keto reductase family 1, member C3 (3-alpha hydroxysteroid dehydrogenase, t
Bt.23094.3.S1_x_at	LOC782061	similar to AKR1C1 protein
Bt.23094.2.A1_x_at	LOC785762	similar to prostaglandin F synthase-like1 protein
Bt.23081.1.S1_at	---	Transcribed locus, weakly similar to XP_998493.1 PREDICTED: hypothetical protein
Bt.23042.1.S1_at	MT-1A	metallothionein-1A
Bt.22948.1.S1_s_at	KIR2DS1 /// KIR3DL1 /// KIR3DL2	killer cell immunoglobulin-like receptor, three domains, long cytoplasmic tail,
Bt.22948.1.S1_at	KIR3DL1	killer cell immunoglobulin-like receptor, three domains, long cytoplasmic tail,
Bt.22867.2.A1_at	BOLA-DQA1	histocompatibility complex, class II, DQ alpha, type 1
Bt.22846.1.S1_at	TSPAN33	tetraspanin 33
Bt.22843.3.S1_at	LOC515398	similar to Proprotein convertase subtilisin/kexin type 7
Bt.22801.1.S1_at	LOC507464	similar to keratin 15
Bt.22756.1.A1_at	MGC152033	Hypothetical LOC515055
Bt.22742.1.A1_at	LOC507595	Similar to My030 protein
Bt.22741.1.S1_at	LOC507243	similar to chloride channel form A
Bt.22727.1.S1_at	CLDN18	claudin 18
Bt.22696.1.A1_at	TMEM35	transmembrane protein 35
Bt.22642.1.A1_at	LOC530095	similar to diacylglycerol kinase iota

Probe Set ID	Gene Symbol	Gene Title
Bt.22639.2.S1_at	LOC618779	similar to NOL1/NOP2/Sun domain family 4 protein
Bt.22639.1.A1_at	LOC618779	similar to NOL1/NOP2/Sun domain family 4 protein
Bt.22586.1.A1_at	MGC129108	Similar to myo-inositol monophosphatase A3
Bt.22561.1.A1_at	RPLP0	ribosomal protein, large, P0
Bt.22525.1.A1_at	LOC540254	similar to DGCR8 protain
Bt.22422.1.S1_at	MGC127459	similar to small nuclear RNA activating complex, polypeptide 2, 45kDa
Bt.224.1.S1_at	LOC317699	seminal plasma 30K protein
Bt.22388.1.S1_at	FLJ10458	Notchless gene homolog
Bt.22371.2.S1_at	MOG	Myelin oligodendrocyte glycoprotein
Bt.22369.1.S1_at	MGC142472	similar to bromodomain containing protein 3
Bt.22334.1.S1_at	LOC616898	hypothetical protein LOC616898
Bt.22316.1.S1_at	IQCC	IQ motif containing C
Bt.22268.1.S1_at	LOC781073	similar to KIAA1831 protein
Bt.22237.1.A1_at	LOC538699	hypothetical LOC538699
Bt.22229.2.S1_at	MGC126900	similar to Proto-oncogene tyrosine-protein kinase LCK (P56-LCK) (LSK) (T cell-sp
Bt.22206.1.S1_at	---	Transcribed locus, moderately similar to XP_944914.1 PREDICTED: similar to CG176
Bt.22174.1.S1_at	LOC523661	similar to neural plakophilin-related arm-repeat protein (NPRAP)
Bt.22115.1.S1_at	LOC510792	similar to putative N-ATPase
Bt.22094.1.A1_at	MGC142386	similar to chromosome 9 open reading frame 26 (NF-HEV)
Bt.22088.3.S1_at	PFDN4	prefoldin subunit 4
Bt.21997.2.A1_at	PPM1K	protein phosphatase 1K (PP2C domain containing)
Bt.21988.1.S1_at	LOC523257 /// LOC786973	hypothetical LOC523257 /// hypothetical protein LOC786973
Bt.21975.1.S1_at	PRF1	perforin 1 (pore forming protein)
Bt.21766.2.S1_at	MLF1	myeloid leukemia factor 1
Bt.21749.2.S1_at	LOC533805	similar to KIAA0467 protein
Bt.21749.1.S1_at	LOC533805	similar to KIAA0467 protein
Bt.21690.2.S1_at	TUT1	terminal uridylyl transferase 1, U6 snRNA-specific
Bt.21685.2.S1_at	LOC516875	Similar to phosphoinositide-binding proteins
Bt.21667.2.S1_a_at	LOC506936	similar to RPUSD2 protein
Bt.21648.1.S1_at	CIDEB	cell death-inducing DFFA-like effector b
Bt.21621.1.S1_at	TMED1	transmembrane emp24 protein transport domain containing 1
Bt.21604.2.S1_at	LOC534284	similar to senataxin
Bt.21483.2.A1_at	APC	adenomatosis polyposis coli
Bt.21459.1.S1_at	NCAPH2	non-SMC condensin II complex, subunit H2
Bt.21422.2.S1_at	LOC514230	hypothetical LOC514230
Bt.21401.1.S1_at	MGC137196	Similar to CG31803-PA
Bt.21365.1.S1_at	LOC513829	similar to Eukaryotic translation initiation factor 2-alpha kinase 4 (GCN2-like
Bt.21348.1.A1_at	LOC513601	similar to Chromosome 6 open reading frame 151
Bt.21341.1.S1_at	TNRC4	trinucleotide repeat containing 4
Bt.21333.1.A1_at	MGC126900	similar to Proto-oncogene tyrosine-protein kinase LCK (P56-LCK) (LSK) (T cell-sp
Bt.21310.1.S1_at	LOC508569	similar to Family with sequence similarity 98, member C
Bt.21284.2.S1_at	LOC506264	similar to Cysteine rich transmembrane BMP regulator 1 (chordin like)
Bt.21126.1.S1_at	SNCB	synuclein, beta
Bt.21088.1.S1_at	MGC152608	similar to macrophage-derived chemokine
Bt.21079.2.S1_at	LOC533008	similar to Solute carrier family 35, member F2
Bt.21056.1.S1_at	MGC142482	similar to Derlin-3 (Der1-like protein 3) (DERtrin 3)
Bt.21019.2.S1_at	LOC538483	hypothetical LOC538483
Bt.21013.1.S1_at	PLK3	polo-like kinase 3 (Drosophila)
Bt.20969.1.S1_at	PEMT	phosphatidylethanolamine N-methyltransferase
Bt.209.2.S1_at	LYZ	lysozyme (renal amyloidosis)
Bt.20872.3.S1_a_at	LOC783989	similar to phosphatidylinositol glycan anchor biosynthesis, class O
Bt.20866.1.A1_at	LIPC	Lipase, hepatic
Bt.20759.1.A1_at	---	Transcribed locus, strongly similar to NP_055554.1 BCL2-associated transcription
Bt.20736.1.S1_at	LOC522566	similar to Zinc finger protein PLAGL2 (Pleiomorphic adenoma-like protein 2)
Bt.20735.2.A1_at	LOC514182	Similar to CG10341-PA
Bt.2069.2.S1_at	MGC179370	Similar to Docking protein 2, 56kDa
Bt.20593.1.A1_at	MGC140018	similar to Peptidyl-prolyl cis-trans isomerase C (PPIase) (Rotamase) (Cyclophili
Bt.20557.1.S1_at	---	Transcribed locus
Bt.20546.1.S1_a_at	LOC528487	similar to protein tyrosine phosphatase HD-PTP
Bt.20525.1.S1_at	MGC139756	similar to F-box only protein 2
Bt.20523.1.S1_at	PRSS16	Protease, serine, 16
Bt.20511.1.S1_at	LOC783943 /// MGC152121	similar to Ral guanine nucleotide dissociation stimulator A
Bt.20495.1.S1_at	LOC504985	similar to tuberin
Bt.20478.1.S1_at	LOC512021	similar to Rho guanine exchange factor 15
Bt.20431.3.S1_at	MGC140538	similar to Max interacting protein 1
Bt.20419.2.S1_a_at	---	Transcribed locus, strongly similar to XP_588451.3 PREDICTED: similar to NFBD1 [
Bt.20399.1.S1_at	HSD17B13	hydroxysteroid (17-beta) dehydrogenase 13
Bt.20382.1.S1_at	MGC152539	similar to ankyrin repeat domain 29
Bt.20362.2.S1_at	LOC516567	similar to KIAA0365 protein
Bt.20330.1.S1_at	MGC139156	hypothetical LOC538575
Bt.20278.1.S1_at	LOC522721	similar to KIAA0385

Probe Set ID	Gene Symbol	Gene Title
Bt.20277.1.S1_at	LOC787696	similar to topoisomersae II
Bt.20243.3.A1_at	LOC783394 /// SLC25A26	solute carrier family 25, member 26 /// similar to solute carrier family 25, mem
Bt.20152.1.S1_at	LOC535381	similar to 85 kDa calcium-independent phospholipase A2
Bt.2013.1.S1_at	LOC539996	similar to semaphorin V
Bt.20093.1.S1_at	---	Transcribed locus
Bt.20057.1.S1_at	LOC505658 /// LOC509956	similar to cathepsin G
Bt.19958.1.A1_at	---	Transcribed locus, moderately similar to NP_035214.1 phosphatidylinositol 3-kina
Bt.1984.1.S1_at	MGC10471	hypothetical protein MGC10471
Bt.19824.2.S1_at	FLJ14213	hypothetical protein FLJ14213
Bt.19796.1.S1_at	B3GALT2	UDP-Gal:betaGlcNAc beta 1,3-galactosyltransferase, polypeptide 2
Bt.19782.2.S1_a_at	IRAK1BP1	interleukin-1 receptor-associated kinase 1 binding protein 1
Bt.1978.1.S1_at	LOC614950 /// LOC617281 /// LOC784182	similar to T-cell receptor beta chain C region /// similar to T-cell receptor be
Bt.1978.1.S1_a_at	LOC509513 /// LOC614950 /// LOC617281 /// LOC784182 /// LOC784307	hypothetical LOC509513 /// similar to T-cell receptor beta chain C region /// si
Bt.19756.1.S1_at	APOB	apolipoprotein B
Bt.19574.1.A1_at	LOC536103	similar to putative 4 repeat voltage-gated ion channel
Bt.19568.1.A1_at	LOC515085	Similar to SH2 domain-containing phosphatase anchor protein 2a
Bt.19544.1.A1_at	MGC179444	similar to putative protein product of HYST1046
Bt.19509.1.A1_at	LOC505588	Similar to cordon-bleu homolog (mouse)
Bt.19501.1.A1_at	MGC140472	similar to Cytochrome P450 2C23 (CYPIIC23) (Arachidonic acid epoxygenase)
Bt.19419.1.A1_at	---	Transcribed locus, moderately similar to XP_942891.1 PREDICTED: similar to SET d
Bt.19386.1.A1_at	---	Transcribed locus
Bt.19333.2.A1_at	SLC35C2	solute carrier family 35, member C2
Bt.19304.1.A1_at	MGC142440	Similar to DAZ interacting protein 1
Bt.19281.2.S1_at	LOC515490	similar to Cdc42 GTPase-activating protein
Bt.19251.1.S1_at	LMO1	LIM domain only 1 (rhombotin 1)
Bt.19244.1.A1_at	SERPINB9	Serpin peptidase inhibitor, clade B (ovalbumin), member 9
Bt.19186.1.A1_at	---	Transcribed locus, strongly similar to NP_999035.1 antileukoproteinase [Sus scro
Bt.19109.1.A1_at	LOC788854	hypothetical protein LOC788854
Bt.19064.2.S1_at	MGC159696	similar to Biotinidase
Bt.19043.2.A1_at	MGC151539	Similar to beta(1,6)-N-acetylglucosaminyltransferase V
Bt.19006.2.A1_at	LOC504557	Similar to beta-ureidopropionase
Bt.18973.1.S1_a_at	MGC139025	hypothetical LOC506184
Bt.18959.1.A1_at	LOC515155	similar to LAG-3 protein
Bt.18853.1.A1_at	LOC790875	Hypothetical protein LOC790875
Bt.18832.1.S1_at	MGC142353	Similar to centrin 3
Bt.18821.1.A1_at	LOC513810	similar to RIKEN cDNA C230043N17 gene
Bt.18815.2.A1_at	LOC509768	GTPase-like protein
Bt.18776.1.S1_at	KIAA0101	KIAA0101 protein
Bt.18756.1.S1_at	CDC42SE2	CDC42 small effector 2
Bt.18748.1.A1_at	LOC505696	similar to Protein tyrosine phosphatase, receptor type, B
Bt.18653.1.A1_at	MGC133901	Similar to CG11760-PB
Bt.18585.1.S1_at	LOC504856	Similar to myeloid/lymphoid or mixed-lineage leukemia (trithorax homolog, Drosop
Bt.18571.1.S1_at	MGC155295	similar to disks large-associated protein 4
Bt.18565.1.S1_at	LOC534714	Similar to zinc finger and BTB domain containing 40
Bt.18504.1.S1_at	MMP3	matrix metallopeptidase 3 (stromelysin 1, progelatinase)
Bt.18501.1.A1_at	LOC537171	similar to Diacylglycerol kinase beta (Diglyceride kinase beta) (DGK-beta) (DAG
Bt.18476.2.S1_at	IRF5	interferon regulatory factor 5
Bt.18466.1.A1_at	LOC513431	Hypothetical LOC513431
Bt.18435.2.S1_a_at	LOC508197	similar to KIAA0759 protein
Bt.18435.1.S1_at	LOC508197	similar to KIAA0759 protein
Bt.18347.1.A1_at	---	Transcribed locus, strongly similar to XP_922484.2 PREDICTED: similar to thrombo
Bt.18329.1.A1_at	LOC533491	Similar to human ras GTPase-activating protein, Gap1m
Bt.18323.1.A1_at	LOC509506	similar to Cytochrome P450, family 4, subfamily F, polypeptide 2
Bt.1828.1.A1_at	SLC27A3	solute carrier family 27 (fatty acid transporter), member 3
Bt.18260.1.A1_at	LOC515359	similar to carbonic anhydrase V
Bt.18241.1.A1_at	PPARA	Peroxisome proliferator-activated receptor alpha
Bt.1818.1.S1_at	LOC514360	similar to desmoplakin isoform II
Bt.1815.2.A1_at	MGC157300	Hypothetical LOC534625
Bt.18081.1.A1_at	KIF20A	kinesin family member 20A
Bt.18037.1.S1_at	LOC540860	hypothetical LOC540860
Bt.18016.1.A1_at	LOC782347	Similar to TUBA
Bt.17964.1.S1_at	LOC615386	similar to light ear protein
Bt.17957.1.A1_at	ICOS	inducible T-cell co-stimulator
Bt.17938.2.S1_at	MGC127503	Similar to Argininosuccinate lyase (Arginosuccinase) (ASAL)
Bt.17932.1.S1_at	LOC514613	similar to cyclin L ania-6a
Bt.17922.1.A1_at	MGC140268	Similar to ADP-sugar pyrophosphatase (Nucleoside diphosphate-linked moiety X mot

Probe Set ID	Gene Symbol	Gene Title
Bt.17901.1.S1_at	LOC526887	similar to RALBP1 associated Eps domain containing protein 2a
Bt.17879.1.A1_at	LOC515342	similar to lipase-like, ab-hydrolase domain containing 1
Bt.17857.1.A1_at	MGC151651	hypothetical LOC613490
Bt.1782.2.S1_at	MGC127999	similar to HSPC171 protein
Bt.17816.1.A1_at	LOC615443	Similar to BB128963 protein
Bt.17773.1.S1_at	GNGT2	Guanine nucleotide binding protein (G protein), gamma transducing activity polyp
Bt.17756.1.A1_at	LOC616498	similar to piggyBac transposable element derived 5
Bt.17654.1.A1_at	LOC781492	similar to NIPA-like domain containing 2
Bt.1763.1.S1_at	HAND1	heart and neural crest derivatives expressed 1
Bt.17570.2.A1_at	LOC539968	similar to RP11-438B23.1
Bt.17543.1.A1_at	LOC509065	hypothetical LOC509065
Bt.17433.1.S1_at	CHCHD5	Coiled-coil-helix-coiled-coil-helix domain containing 5
Bt.17372.1.A1_at	LOC505134	Similar to RNA adenosine deaminase
Bt.17314.1.S1_at	CLGN	calmegin
Bt.17242.1.A1_at	CYP2B	cytochrome P450 subfamily 2B
Bt.17232.1.A1_at	AVPR1A	arginine vasopressin receptor 1A
Bt.17200.1.A1_at	C5orf32	C5orf32 protein
Bt.17159.1.A1_at	---	Transcribed locus, strongly similar to NP_783573.3 brain-specific angiogenesis i
Bt.17105.1.A1_at	MGC160076	similar to Zinc finger, ZZ-type containing 3
Bt.17046.1.A1_at	LOC785410	similar to RLTPR protein
Bt.1697.2.S1_at	MGC142933	similar to Amyloid beta A4 precursor protein-binding family B member 3 (Fe65-lik
Bt.16957.1.A1_at	MRPL30	Mitochondrial ribosomal protein L30
Bt.16949.1.A1_at	FAM86A	Hypothetical protein LOC531984
Bt.16878.1.A1_at	LOC535214	similar to C2H2 type Kruppel-like zinc finger protein
Bt.16798.1.A1_at	GNAS1	Guanine nucleotide binding protein (G protein), alpha stimulating activity polyp
Bt.16676.1.A1_at	LOC784449	similar to KIAA1324 protein
Bt.16674.1.A1_at	LOC534614	hypothetical LOC534614
Bt.16646.1.S1_at	LOC785057	similar to F-box protein 44
Bt.166.1.S1_at	PENK	proenkephalin
Bt.16595.1.A1_at	LOC517284	Similar to Protein piccolo (Aczonin)
Bt.16483.2.A1_at	MGC142920	Similar to Zinc finger protein 567
Bt.16447.1.A1_at	LOC515330	Similar to myosin-IXa
Bt.16427.1.S1_at	CCBP2	chemokine binding protein 2
Bt.16375.1.A1_at	LOC504591 /// LOC784995	similar to kinase suppressor of Ras-2
Bt.16353.1.A1_at	LOC529881	similar to CG6818-PA
Bt.16344.1.A1_at	LOC504288	similar to A-kinase anchor protein 13
Bt.16338.2.A1_at	MBL-A	mannose binding lectin, liver (A)
Bt.16275.1.A1_at	LOC529494	similar to KIAA1636 protein
Bt.16141.1.S1_at	CCNE2	cyclin E2
Bt.16128.1.S1_at	HDAC8	histone deacetylase 8
Bt.16101.1.S1_at	GNLY /// LOC780979	granulysin /// hypothetical protein LOC780979
Bt.16051.3.S1_at	LOC513279	similar to KIAA0595 protein
Bt.1605.3.S1_at	MGC138923	Similar to selenoprotein N, 1 isoform 1 precursor
Bt.16029.1.S2_at	FUT1	fucosyltransferase 1
Bt.16027.1.A1_at	LEPR	leptin receptor
Bt.15990.1.S1_at	SLC8A1	solute carrier family 8 (sodium/calcium exchanger), member 1
Bt.15984.1.S1_at	LOC782451 /// PAG12	pregnancy-associated glycoprotein 12 /// similar to pregnancy-associated glycopr
Bt.15958.2.A1_a_at	ABCB1 /// LOC781361 /// LOC785554	ATP-binding cassette, sub-family B (MDR/TAP), member 1 /// similar to Multidrug
Bt.15910.1.S1_at	LOC523429	Similar to interleukin 1 family, member 6 (epsilon)
Bt.15875.1.S1_at	TRADD	TNFRSF1A-associated via death domain
Bt.15767.1.A2_at	UGT1A1	UDP glucuronosyltransferase 1 family, polypeptide A1
Bt.15751.1.S1_at	LOC514185	similar to AMP deaminase
Bt.15675.1.S1_at	ADAMTS4	ADAM metallopeptidase with thrombospondin type 1 motif, 4
Bt.15667.2.S1_at	SREBF1	sterol regulatory element binding transcription factor 1
Bt.15569.1.A1_at	LOC782689	similar to ST6 (alpha-N-acetyl-neuraminyl-2,3-beta-galactosyl-1,3)-N-acetylgalac
Bt.154.1.S1_at	CCL8 /// LOC788169	chemokine (C-C motif) ligand 8 /// similar to chemoattractant protein 2
Bt.1536.2.S1_at	LOC506727	similar to nuclear factor of kappa light polypeptide gene enhancer in B-cells in
Bt.1449.1.S1_at	LOC516332	similar to UDP-glucose:glycoprotein glucosyltransferase 1
Bt.14395.1.A1_at	C3orf57	hypothetical protein LOC780785
Bt.14326.2.A1_at	SMS	Spermine synthase
Bt.14304.2.S1_at	LOC539922	hypothetical LOC539922
Bt.14298.1.A1_at	ZDHHC1	Zinc finger, DHHC-type containing 1
Bt.14093.1.S1_at	---	Transcribed locus, strongly similar to NP_035251.2 polo-like kinase [Mus musculu
Bt.14083.1.A1_at	MASP1	Mannan-binding lectin serine peptidase 1 (C4/C2 activating component of Ra-react
Bt.14026.1.A1_at	BRCA1	Breast cancer 1, early onset
Bt.139.1.A1_at	ADAM2	ADAM metallopeptidase domain 2 (fertilin beta)
Bt.13880.2.S1_at	LOC504445	similar to Dickkopf-1 (hdkk-1)
Bt.13860.2.A1_at	KDR	kinase insert domain receptor (a type III receptor tyrosine kinase)

Probe Set ID	Gene Symbol	Gene Title
Bt.13751.2.S1_at	GSTK1	glutathione S-transferase kappa 1
Bt.137.1.S1_at	ANGPT2	angiopoietin 2
Bt.13695.1.S1_at	MGRN1	mahogunin, ring finger 1
Bt.13670.1.S2_at	ALPL	alkaline phosphatase, liver/bone/kidney
Bt.13670.1.S1_at	ALPL	alkaline phosphatase, liver/bone/kidney
Bt.13466.1.S1_at	LOC533634	similar to oxysterol-binding protein-like protein 6
Bt.13448.2.S1_at	GNPAT	Glyceronephosphate O-acyltransferase
Bt.13310.1.S1_at	LOC782446	similar to type I iodothyronine deiodinase
Bt.13291.2.S1_at	LOC535254	similar to pogo transposable element with ZNF domain
Bt.13287.1.S1_at	AGXT2L1	alanine-glyoxylate aminotransferase 2-like 1
Bt.13278.2.S1_a_at	LOC504235	hypothetical LOC504235
Bt.13235.2.S1_at	MGC148992	Similar to RGC-32
Bt.13201.1.S1_at	DSC2	desmocollin 2
Bt.13159.1.A1_at	PTPRZ1	protein tyrosine phosphatase, receptor-type, Z polypeptide 1
Bt.13145.1.S1_at	ALDH5	aldehyde dehydrogenase 5, mitochondrial X
Bt.13142.1.A1_at	PRKCD	protein kinase C, delta
Bt.13136.1.S1_at	GDF5	growth differentiation factor 5
Bt.13122.1.S1_at	COL6A2	collagen, type VI, alpha 2
Bt.13122.1.A1_at	COL6A2	collagen, type VI, alpha 2
Bt.13121.1.S1_at	SHH	sonic hedgehog homolog (Drosophila)
Bt.13117.1.S1_at	AMELY	amelogenin, Y-linked
Bt.13073.1.S1_at	SERPINB2	serpin peptidase inhibitor, clade B (ovalbumin), member 2
Bt.13069.1.S1_at	CACNA1D	calcium channel, voltage-dependent, L type, alpha 1D
Bt.13055.1.A1_at	CACNA1L	alpha1I T-type calcium channel subunit
Bt.13044.1.A1_at	CLN2	ceroid-lipofuscinosis, neuronal 2, late infantile (Jansky-Bielschowsky disease)
Bt.13040.1.A1_at	HCRT	hypocretin (orexin) neuropeptide precursor
Bt.13033.1.A1_at	FOXL2	forkhead box L2
Bt.13003.15.A1_at	TRA@	T cell receptor, alpha
Bt.13003.11.S1_at	TRA@	T cell receptor, alpha
Bt.12990.1.S1_at	FGF8	fibroblast growth factor 8 (androgen-induced)
Bt.12932.1.S1_s_at	FGFR3	fibroblast growth factor receptor 3
Bt.12926.1.S1_at	LOC786429	similar to Lutropin subunit beta precursor (Luteinizing hormone subunit beta) (L
Bt.12907.2.S1_a_at	---	Transcribed locus, strongly similar to XP_221962.3 PREDICTED: similar to tweety
Bt.12891.1.S1_at	RRAD	Ras-related associated with diabetes
Bt.12849.1.S1_at	SLCO2B1	solute carrier organic anion transporter family, member 2B1
Bt.12836.1.S1_at	PROC	protein C (inactivator of coagulation factors Va and VIIIa)
Bt.12823.1.S1_at	VWF	von Willebrand factor
Bt.12818.3.A1_at	TSPY	testis-specific protein, Y-encoded
Bt.12810.1.S1_at	TLR9	toll-like receptor 9
Bt.12801.1.S1_at	ALOX15B	arachidonate 15-lipoxygenase, type B
Bt.12770.1.A1_at	SNCA	synuclein, alpha (non A4 component of amyloid precursor)
Bt.12764.1.S1_at	RDHL	NADP-dependent retinol dehydrogenase/reductase
Bt.12761.1.S1_at	ITGA2	integrin, alpha 2 (CD49B, alpha 2 subunit of VLA-2 receptor)
Bt.12689.1.A1_at	MGC155293	similar to vasoactive intestinal peptide receptor
Bt.12625.1.S1_at	LOC615883	similar to SLIT3
Bt.12561.3.S1_at	RHOF	ras homolog gene family, member F (in filopodia)
Bt.12510.1.S1_at	LOC509824	similar to Os08g0528700
Bt.12478.3.S1_a_at	C20ORF18	ubiquitin conjugating enzyme 7 interacting protein 3
Bt.12425.2.S1_at	LOC533229	similar to ETNK2 protein
Bt.12405.1.S1_at	LOC538276	similar to JAK3_HUMAN; JANUS KINASE 3; JAK-3; LEUKOCYTE JANUS KINASE; L-JAK
Bt.12379.1.S1_at	MGC139265	similar to Prostate tumor over expressed gene 1
Bt.12300.1.S1_at	MYH1	myosin, heavy chain 1, skeletal muscle, adult
Bt.12180.2.S1_at	EXOSC8	exosome component 8
Bt.12175.1.A1_at	CADPS	Ca2+-dependent secretion activator
Bt.12139.2.S1_at	ADPRHL2	ADP-ribosylhydrolase like 2
Bt.12065.1.S1_at	LOC618071	Hypothetical LOC618071
Bt.1206.1.S1_at	LOC510681	similar to B-box and SPRY domain containing
Bt.1187.1.S1_at	LOC514688	similar to protein phosphatase 1, regulatory subunit 15A
Bt.11853.1.S1_at	LOC508042	similar to UnpES
Bt.11847.1.A1_at	XIST	X (inactive)-specific transcript
Bt.11816.2.S1_at	MGC142695	similar to C04F5.8
Bt.11683.1.A1_at	---	Transcribed locus, moderately similar to XP_416866.1 PREDICTED: similar to prote
Bt.11444.1.S1_at	LOC614457	hypothetical LOC614457
Bt.11438.1.S1_at	LOC511094	similar to Troponin I, cardiac muscle (Cardiac troponin I)
Bt.11190.1.S1_at	PHKG2	phosphorylase kinase, gamma 2 (testis)
Bt.11180.1.A1_a_at	LRRN5	leucine rich repeat neuronal 5 precursor
Bt.1116.1.A1_at	MGC140191	similar to GABA-B receptor
Bt.11133.3.S1_at	MGC140764	similar to USE1-like protein (Hematopoietic stem/progenitor cells protein MDS032
Bt.11057.1.S1_at	LOC781091	hypothetical protein LOC781091
Bt.11044.1.S1_at	ARPP-21	cyclic AMP-regulated phosphoprotein, 21 kDa
Bt.11039.1.S1_at	LOC505497	similar to Qtrt1 protein
Bt.11004.1.S1_at	MYOZ3	myozenin 3

Probe Set ID	Gene Symbol	Gene Title
Bt.10954.1.S1_at	CD2	CD2 molecule
Bt.1088.1.S1_at	MGC127192	Hypothetical LOC510988
Bt.10878.1.S1_at	HPS1	Hermansky-Pudlak syndrome 1
Bt.10851.1.S1_at	MGC143149	similar to likely ortholog of kinesin light chain 2
Bt.10704.1.S1_at	LPPR2	lipid phosphate phosphatase-related protein type 2
Bt.10524.2.S1_at	ZNF821	zinc finger protein 821
Bt.1037.1.S1_at	REEP2	receptor accessory protein 2
Bt.10312.2.S1_at	TMEM148B	transmembrane protein 184B
Bt.10259.1.A1_at	LOC539449	similar to serum-inducible kinase
Bt.10194.1.A1_x_at	LOC404051	similar to thrombin inhibitor
Bt.10085.1.A1_at	MGC142726	similar to UDP-Gal:betaGal beta 1,3-galactosyltransferase polypeptide 7
Bt.10002.1.S1_at	LOC784163	similar to AP-3 complex beta3B subunit
Bt.9974.1.S1_at	CCL3L1	chemokine (C-C motif) ligand 3-like 1
Bt.9633.2.S1_at	LOC518540	similar to MEOX2
Bt.9560.1.S1_at	CCL20	chemokine (C-C motif) ligand 20
Bt.9455.1.A1_at	MGC152031	similar to CD5 antigen-like
Bt.9289.1.S1_at	LOC506812	similar to carnitine O-palmitoyltransferase
Bt.9288.2.A1_at	LOC510738	similar to FLJ00258 protein
Bt.9211.1.S1_at	APBB1IP	amyloid beta (A4) precursor protein-binding, family B, member 1 interacting prot
Bt.8678.1.A1_at	---	LERK-5 gene, partial sequence
Bt.8548.1.S1_at	ADIPOQ	adiponectin
Bt.836.1.S1_at	FAHD1 /// LOC787486	fumarylacetoacetate hydrolase domain containing 1 /// similar to Fumarylacetoace
Bt.8106.1.S1_at	NID1	nidogen 1
Bt.7425.1.S1_at	SDF1	stromal cell-derived factor 1
Bt.7319.1.S1_at	LOC509657	similar to protein tyrosine phosphatase, receptor type, K
Bt.7165.1.S1_at	CXCL6	chemokine (C-X-C motif) ligand 6 (granulocyte chemotactic protein 2)
Bt.7066.1.S1_at	ALOX5AP	arachidonate 5-lipoxygenase-activating protein
Bt.6972.1.S1_at	KBTBD10	kelch repeat and BTB (POZ) domain containing 10
Bt.690.1.S1_at	LOC512018	similar to brother of CDO
Bt.6796.1.A1_at	MGC157214	hypothetical LOC524166
Bt.6542.1.S1_at	SLC22A5	solute carrier family 22 (organic cation transporter), member 5
Bt.6504.1.S1_at	LOC526200	similar to AIM1
Bt.611.1.S2_at	CXCL1	chemokine (C-X-C motif) ligand 1
Bt.610.1.A1_at	CXCL2	chemokine (C-X-C motif) ligand 2
Bt.5851.2.S1_at	SEP11	Septin 11
Bt.5522.1.S1_at	THBS2	thrombospondin 2
Bt.5395.1.S1_a_at	CSPG2	chondroitin sulfate proteoglycan 2 (versican)
Bt.5392.1.S1_at	CD36	CD36 molecule (thrombospondin receptor)
Bt.5193.2.S1_a_at	LOC517002	similar to uteroferrin
Bt.5193.1.S1_at	LOC517002	similar to uteroferrin
Bt.5180.1.S1_at	UCP2	uncoupling protein 2 (mitochondrial, proton carrier)
Bt.4846.1.S1_at	LOC506009	similar to novel transcript
Bt.4817.1.A1_at	MGC128478	similar to claudin 11
Bt.4732.1.S1_at	ALDH1A1	aldehyde dehydrogenase 1 family, member A1
Bt.4679.1.S1_at	FCGR2A	Fc fragment of IgG, low affinity IIa, receptor (CD32)
Bt.4482.2.S1_a_at	MSR1	macrophage scavenger receptor 1
Bt.4439.1.S1_at	PLA2G1B	phospholipase A2, group IB (pancreas)
Bt.4417.1.S1_at	CDH2	cadherin 2
Bt.4394.1.S1_at	GUCY1B3	guanylate cyclase 1, soluble, beta 3
Bt.4310.1.A1_at	MGC152252	similar to regulator of G-protein signalling 1
Bt.3870.1.S1_at	TTLL3	Tubulin tyrosine ligase-like family, member 3
Bt.357.1.S1_at	S100A12	S100 calcium binding protein A12 (calgranulin C)
Bt.3540.1.S1_at	MGC139918	similar to Secreted frizzled-related protein 4 precursor (sFRP-4) (Frizzled prot
Bt.3402.3.A1_at	MGC165864	similar to Katanin p80 (WD repeat containing) subunit B 1
Bt.3374.1.A1_a_at	LOC517876	similar to AT rich interactive domain 2 (ARID, RFX-like)
Bt.29965.1.S1_at	---	Transcribed locus, strongly similar to XP_001257270.1 PREDICTED: similar to T ce
Bt.29946.1.S1_s_at	ANPEP	alanyl (membrane) aminopeptidase
Bt.29913.1.S1_at	G6PD	glucose-6-phosphate dehydrogenase
Bt.29772.1.A1_at	SLC8A1	solute carrier family 8 (sodium/calcium exchanger), member 1
Bt.29717.1.S1_a_at	GHR	growth hormone receptor
Bt.29697.1.S1_at	ART3	ADP-ribosyltransferase 3
Bt.29393.1.A1_at	ABHD5	abhydrolase domain containing 5
Bt.29264.1.A1_at	LOC522691	hypothetical LOC522691
Bt.2903.1.S1_at	CXADR	coxsackie virus and adenovirus receptor
Bt.28853.1.A1_at	LOC508297	similar to ankyrin repeat domain 43
Bt.28837.1.S1_at	LOC789978	Hypothetical protein LOC789978
Bt.28709.1.A1_at	LOC537873	hypothetical LOC537873
Bt.287.1.S1_at	RNASE6	ribonuclease, RNase A family, k6
Bt.28461.2.S1_a_at	INSR	insulin receptor
Bt.28258.1.S1_at	MGC138926	similar to intestinal peptide-associated transporter HPT-1
Bt.28243.2.S1_at	VNN1	vanin 1
Bt.27634.1.A1_a_at	LOC534112	similar to connector enhancer of KSR2A

Probe Set ID	Gene Symbol	Gene Title
Bt.27430.2.S1_at	LOC506029	similar to amyotrophic lateral sclerosis 2
Bt.27425.1.A1_a_at	EGFR	epidermal growth factor receptor (erythroblastic leukemia viral (v-erb-b) oncoge
Bt.27036.1.S1_at	CYP4F2	cytochrome P450, family 4, subfamily F, polypeptide 2
Bt.26983.1.S1_at	CASP1	caspase 1
Bt.26980.1.S1_at	LOC785895 /// LOC786146	hypothetical protein LOC785895 /// hypothetical protein LOC786146
Bt.26772.1.S1_at	MGC137966	similar to Protein FAM26B
Bt.26578.1.S1_at	MGC140507	similar to energy metabolism-related sodium-dependent high-affinity dicarboxylat
Bt.26426.1.A1_at	MGC159967	hypothetical LOC617625
Bt.26051.1.A1_at	LOC521326	similar to OTTHUMP00000065631
Bt.25316.1.A1_at	LOC523889	similar to type V P-type ATPase
Bt.24911.1.A1_at	LOC533620	similar to Ankyrin repeat domain-containing protein 26
Bt.24899.1.A1_at	LOC539563	similar to MAP/microtubule affinity-regulating kinase
Bt.24821.1.S1_at	MGC137561	similar to acyl-Coenzyme A binding domain containing 4
Bt.24770.1.S1_at	CORO7	coronin 7
Bt.24724.1.S1_at	LOC509296	similar to gasdermin-like
Bt.24550.1.S1_a_at	COMTD1	catechol-O-methyltransferase domain containing 1
Bt.24515.1.S1_at	LOC507082	Akt substrate AS250
Bt.24495.1.A1_at	LOC514322	similar to AarF domain containing kinase 4
Bt.24447.2.S1_at	F2RL2	coagulation factor II (thrombin) receptor-like 2
Bt.24447.1.S1_at	F2RL2	coagulation factor II (thrombin) receptor-like 2
Bt.24012.1.A1_at	LOC511531	similar to guanylate binding protein 1
Bt.23640.1.A1_at	TLR3	toll-like receptor 3
Bt.23640.1.A1_a_at	TLR3	Toll-like receptor 3
Bt.23499.1.S1_at	LOC786335	similar to muscle glycogen synthase
Bt.23354.1.S1_at	MGC126963	similar to epoxide hydrolase 1
Bt.23171.2.S1_at	PCBD1	pterin-4 alpha-carbinolamine dehydratase/dimerization cofactor of hepatocyte nuc
Bt.23126.1.S1_at	NOS2A	nitric oxide synthase 2A (inducible, hepatocytes)
Bt.23094.4.S1_at	LOC782922	similar to prostaglandin F synthetase II
Bt.23094.1.A1_at	AKR1C1	aldo-keto reductase family 1, member C1 (dihydrodiol dehydrogenase 1; 20-alpha (
Bt.23093.1.S1_at	CXCL3	chemokine (C-X-C motif) ligand 3
Bt.23002.1.S1_at	COX6A1	cytochrome c oxidase subunit VIa polypeptide 1
Bt.22699.1.S1_at	NFIA	nuclear factor I/A
Bt.22577.2.S1_at	MGC139420	similar to mitochondrial carrier protein MGC4399
Bt.22468.2.A1_at	MGC128008	hypothetical LOC510399
Bt.22384.1.A1_at	MGC139294	similar to immunoglobulin superfamily, member 4B
Bt.22359.2.A1_at	RIOK3	RIO kinase 3 (yeast)
Bt.22322.1.S1_at	LOC506412 /// LOC616035 /// LOC618238 /// SAA3	serum amyloid A 3 /// serum amyloid A-like /// hypothetical LOC616035 /// simila
Bt.22160.1.S1_at	MGC152609	similar to chromosome 1 open reading frame 26
Bt.22144.2.S1_at	MGC155130	similar to START domain-containing 5 protein
Bt.22144.1.A1_at	MGC155130	similar to START domain-containing 5 protein
Bt.22085.1.S1_at	---	Transcribed locus
Bt.22056.2.S1_a_at	MGC127615	similar to abhydrolase domain containing 1 (predicted)
Bt.22012.1.S1_at	---	Transcribed locus
Bt.21950.1.S1_at	LOC616732	similar to IL-10-inducible chemokine
Bt.21909.1.S1_at	LOC514831 /// LOC782775 /// LOC784320 /// MGC160062	hypothetical LOC514831 /// hypothetical LOC617160 /// hypothetical protein LOC78
Bt.218.1.S1_at	AKAP4	A kinase (PRKA) anchor protein 4
Bt.21331.2.S1_at	CCR5	chemokine (C-C motif) receptor 5
Bt.21192.2.A1_at	LOC613658	hypothetical LOC613658
Bt.21156.1.S1_at	LOC505802	similar to telomerase-associated protein TP-1
Bt.20890.1.S1_at	AMY2B	amylase, alpha 2B (pancreatic)
Bt.20861.2.S1_at	---	Transcribed locus, moderately similar to NP_032704.1 nuclear receptor coactivato
Bt.20683.1.S1_at	---	Transcribed locus, moderately similar to NP_001071470.1 eukaryotic translation i
Bt.20384.1.S1_at	MGC159638	similar to branched chain acyl-CoA oxidase
Bt.20372.1.S1_at	MGC139085	similar to paraoxonase 3
Bt.19818.1.A1_at	DDX9	Nuclear DNA helicase II
Bt.1928.1.S1_at	LOC526642	similar to WD repeat domain 59
Bt.19247.1.S1_at	SULT1C2	sulfotransferase family, cytosolic, 1C, member 2
Bt.18965.1.A1_at	LOC537901	Similar to Na+-driven Cl-HCO3 exchanger
Bt.18908.1.S1_at	MGC139688	Similar to heterogeneous nuclear ribonucleoprotein L-like
Bt.18889.1.S1_at	LAT2	linker for activation of T cells family, member 2
Bt.18801.1.A1_at	CREB1	CAMP responsive element binding protein 1
Bt.18689.2.A1_at	LOC538401	similar to Arylsulfatase B precursor (ASB) (N-acetylgalactosamine-4-sulfatase) (
Bt.18631.1.A1_at	SPRY4	Sprouty homolog 4 (Drosophila)
Bt.18492.1.A1_at	---	Transcribed locus, strongly similar to XP_001001712.1 PREDICTED: similar to zinc
Bt.18484.1.A1_at	NT5DC1	5'-nucleotidase domain containing 1
Bt.18349.1.A1_at	---	Transcribed locus, strongly similar to XP_582187.3 PREDICTED: hypothetical prote
Bt.18233.1.A1_s_at	BCL2	B-cell CLL/lymphoma 2

Probe Set ID	Gene Symbol	Gene Title
Bt.18075.1.A1_at	LOC616404	Similar to actin-related protein 3-beta
Bt.17766.1.S1_at	MGC160071	similar to Chromosome 3 open reading frame 23
Bt.17607.2.A1_at	PLD1	phospholipase D1, phosphatidylcholine-specific
Bt.17499.1.A1_at	LOC524684	similar to subtilisin-like proprotein convertase (EC 3.4.21.-) PACE4
Bt.17496.2.A1_at	LOC511508	Similar to KIAA0438
Bt.17386.1.A1_at	MGC152005	Similar to PABP1-dependent poly A-specific ribonuclease subunit PAN3
Bt.17349.1.A1_at	LOC537224	similar to KIAA0188
Bt.1658.1.S1_at	MKP-1	MAP kinase phosphatase-1
Bt.16568.2.A1_at	LOC538226	Hypothetical LOC538226
Bt.16514.1.S1_at	MGC127339	similar to cytochrome P450, family 4, subfamily v, polypeptide 2
Bt.16402.1.A1_at	STAT1	Signal transducer and activator of transcription 1
Bt.16382.1.A1_at	MGC155061	similar to calcitonin receptor-like receptor
Bt.16021.1.S1_at	CHRNA1	cholinergic receptor, nicotinic, alpha 1 (muscle)
Bt.15996.1.S2_at	ACAS2L	acetyl-Coenzyme A synthetase 2 (AMP forming)-like
Bt.15978.1.S1_at	MOCS1	molybdenum cofactor synthesis 1
Bt.15908.1.S1_at	LOC781892 /// METTL7A	methyltransferase like 7A /// hypothetical protein LOC781892
Bt.15842.1.S1_at	THRSP	thyroid hormone responsive (SPOT14 homolog, rat)
Bt.14570.2.S1_at	MGC137464	similar to 4-aminobutyrate aminotransferase, mitochondrial precursor ((S)-3-amin
Bt.14366.1.S1_at	LOC532209	Similar to AML1-EVI-1 fusion protein
Bt.1409.1.S1_at	MGC127860	similar to Protein CGI-38
Bt.13796.1.S1_at	LOC783399	similar to Equ c1
Bt.13708.2.S1_a_at	LOC781217	similar to ATM/ATR-Substrate Chk2-Interacting Zn2+-finger protein
Bt.13650.1.S1_at	LOC514078	similar to KIAA1119 protein
Bt.13556.1.S1_at	LOC514792 /// LOC788826	similar to H factor 1 (complement)
Bt.1345.1.S1_at	F2RL2	coagulation factor II (thrombin) receptor-like 2
Bt.13381.1.S1_at	MGC139113	similar to Cell death activator CIDE-3 (Cell death-inducing DFFA-like effector p
Bt.13345.1.A1_at	LOC784739	hypothetical protein LOC784739
Bt.13251.1.S1_at	MFNG	MFNG O-fucosylpeptide 3-beta-N-acetylglucosaminyltransferase
Bt.132.1.S1_at	DEFB1	defensin, beta 1
Bt.13125.1.S1_s_at	BNBD-4 /// LOC783935 /// LOC786536	neutrophil beta-defensin 4 /// hypothetical protein LOC783935 /// similar to neu
Bt.13125.1.S1_at	LOC783935	hypothetical protein LOC783935
Bt.13096.1.A1_at	FIGF	c-fos induced growth factor (vascular endothelial growth factor D)
Bt.1300.1.S1_at	LOC509642	similar to oxidized-LDL responsive gene 2
Bt.12991.1.S1_at	FGF10	fibroblast growth factor 10
Bt.12991.1.A1_at	FGF10	fibroblast growth factor 10
Bt.12745.2.A1_at	ANTXR2	anthrax toxin receptor 2
Bt.12565.1.S1_at	MGC127362	similar to solute carrier family 31, member 2
Bt.12403.1.S1_at	MGC137880	similar to p76RBE protein
Bt.12319.1.S1_at	MGC139145	similar to Protein C11orf13 homolog
Bt.12301.1.S1_at	PTGER2	prostaglandin E receptor 2 (subtype EP2), 53kDa
Bt.12206.1.S1_x_at	BNBD-9-LIKE /// DEFB7 /// DEFB8	neutrophil beta-defensin-9 like peptide /// defensin beta 7 /// defensin beta 8
Bt.12081.1.S1_at	LOC782347	similar to TUBA
Bt.12010.2.S1_at	LOC512171	similar to ADAMTS1
Bt.11446.1.A1_at	LDB2	LIM domain binding 2
Bt.1116.2.S1_at	MGC140191	similar to GABA-B receptor
Bt.1115.1.S1_at	LOC533323	similar to cyclic nucleotide phophodiesterase
Bt.10996.1.S1_at	GDPD2	glycerophosphodiester phosphodiesterase domain containing 2
Bt.10941.1.S1_at	LOC540550	similar to CHCR
Bt.10831.1.S1_at	LOC534996	similar to Tyrosine-protein kinase Lyn
Bt.10232.1.A1_at	MGC149024	Similar to PAR-6 beta
BtAffx.1.20.S1_at	RSG20	regulator of G-protein signalling 20
Bt.9997.1.S1_at	LOC511958	similar to KIAA0056 protein
Bt.9982.1.S1_at	MGC128443	similar to proline-rich protein 3
Bt.9974.2.S1_at	CCL3L1	chemokine (C-C motif) ligand 3-like 1
Bt.9972.1.S1_at	ITGB6	integrin, beta 6
Bt.976.1.A1_at	ILF3	Interleukin enhancer binding factor 3
Bt.9704.1.S1_at	COX19	COX19 cytochrome c oxidase assembly homolog (S. cerevisiae)
Bt.9682.1.S1_at	LYZ1	lysozyme 1
Bt.9678.1.S1_at	---	Transcribed locus, strongly similar to XP_001254389.1 PREDICTED: hypothetical pr
Bt.9649.1.A1_at	LOC507169	similar to TRRAP protein
Bt.9599.1.A1_at	MGC128671	Similar to Inositol hexakisphosphate kinase 2 (InsP6 kinase 2) (Inositol hexakis
Bt.9460.1.S1_at	ELF1	E74-like factor 1 (ets domain transcription factor)
Bt.9416.1.S1_at	MGC143300	similar to CasL interacting molecule MICAL
Bt.9350.1.A1_at	LOC613472	similar to ganglioside-induced differentiation-associated protein 1
Bt.935.1.A1_at	LOC539354	similar to solute carrier family 35, member A4
Bt.9296.1.A1_at	LOC512486	similar to Interferon-induced guanylate-binding protein 1 (GTP-binding protein 1
Bt.9292.1.A1_at	LOC508406	similar to Chromosome 1 open reading frame 166
Bt.9268.1.S1_at	LOC537028	hypothetical LOC537028

Probe Set ID	Gene Symbol	Gene Title
Bt.9267.1.A1_at	APOBEC3F	apolipoprotein B mRNA editing enzyme, catalytic polypeptide-like 3F
Bt.9263.1.S1_at	---	Transcribed locus, moderately similar to XP_001106673.1 PREDICTED: similar to zi
Bt.9241.1.A1_at	TBC1D20	TBC1 domain family, member 20
Bt.9233.1.A1_at	ADRM1	adhesion regulating molecule 1
Bt.9229.1.A1_at	LOC512949 /// LOC789693	hypothetical LOC512949 /// hypothetical protein LOC789693
Bt.9200.1.A1_at	MGC134424	Similar to CG5543-PA
Bt.9179.2.S1_at	LOC509283	similar to chromosome 17 open reading frame 27
Bt.9172.1.A1_at	LOC526702	similar to putative nuclear protein
Bt.9162.1.A1_at	CHORDC1	cysteine and histidine-rich domain (CHORD)-containing 1
Bt.9131.1.S1_at	LOC618514	similar to LAIR hlog
Bt.9128.1.A1_at	LOC509859	similar to KIAA0342 protein
Bt.9099.1.A1_at	MGC138130	Similar to small nuclear RNA activating complex, polypeptide 5, 19kDa
Bt.9071.1.S1_at	MGC139710	similar to CG18177-PB
Bt.9045.1.S1_at	RAVER1	ribonucleoprotein, PTB-binding 1
Bt.9044.1.S1_at	LOC538493	similar to chromosome 14 open reading frame 173
Bt.9034.1.S1_at	LOC538952	similar to Proline rich 15
Bt.9027.1.S1_at	NFKBIA	nuclear factor of kappa light polypeptide gene enhancer in B-cells inhibitor, al
Bt.901.2.S1_a_at	LOC509354	similar to type 6 nucleoside diphosphate kinase NM23-H6
Bt.8979.1.A1_at	LOC538880	similar to cytoplasmic polyadenylation element binding protein CPEB2b
Bt.8902.2.S1_at	ICA1	islet cell autoantigen 1, 69kDa
Bt.8887.1.S1_at	LOC515078	similar to transmembrane protein 62
Bt.8850.1.S1_at	SARS2	seryl-tRNA synthetase 2
Bt.88.1.S1_at	CHRNA7	cholinergic receptor, nicotinic, alpha 7
Bt.8745.1.S1_at	MGC159813	hypothetical LOC535344
Bt.8699.1.S1_at	LOC540045	similar to zinc finger protein 385
Bt.8586.1.S1_at	LOC512149 /// LOC512150	similar to Myeloid-associated differentiation marker
Bt.8563.1.S1_at	LOC506370	similar to cytochrome b5 outer mitochondrial membrane precursor
Bt.8518.1.S1_at	LOC539768	similar to phosphodiesterase 8B4
Bt.8476.1.A1_at	DLX5	distal-less homeobox 5
Bt.8473.2.S1_at	PEX11B	peroxisomal biogenesis factor 11B
Bt.8435.1.S1_at	ACTA1	actin, alpha 1, skeletal muscle
Bt.8348.1.S1_at	LOC517133	hypothetical LOC517133
Bt.8316.1.S1_at	LOC782502	hypothetical protein LOC782502
Bt.8166.1.S1_at	CXXC5	CXXC finger 5
Bt.8128.1.S1_at	ETAA16	ETAA16 protein
Bt.8117.1.S1_at	MGC160050	similar to ULK2 protein
Bt.8090.2.S1_at	LOC513045	similar to Myb-binding protein 1A
Bt.7990.1.S1_at	LOC517259	similar to molecule interacting with Rab13
Bt.7894.1.S1_at	LOC531974	similar to mKIAA1151 protein
Bt.776.1.S1_at	LOC528990	similar to KIAA0690
Bt.7651.1.S1_at	ASB11	ankyrin repeat and SOCS box-containing 11
Bt.7639.1.S1_at	MGC142929	similar to CG11986-PA
Bt.763.1.S1_at	LOC514844	similar to expressed in synovial lining protein
Bt.7620.1.S1_at	ERCC6L	excision repair cross-complementing rodent repair deficiency, complementation gr
Bt.7619.1.S1_at	TTYH1	tweety homolog 1 (Drosophila)
Bt.7600.1.S1_at	LOC506900	histone H2A.I (H2A/I)
Bt.759.1.S1_at	SLC4A2	solute carrier family 4, anion exchanger, member 2 (erythrocyte membrane protein
Bt.7561.1.S1_at	LOC781024 /// LOC781057 /// LOC781072 /// LOC781114 /// LOC781191 /// LOC781232	hypothetical protein LOC781024 /// hypothetical protein LOC781057 /// hypothetic
Bt.7542.1.S1_at	BCL2A1	BCL2-related protein A1
Bt.7535.1.A1_at	DLST	dihydrolipoamide S-succinyltransferase (E2 component of 2-oxo-glutarate complex)
Bt.7484.1.S1_at	LOC504530	similar to FLJ00018 protein
Bt.7451.1.S1_at	MGC160130	hypothetical LOC617610
Bt.7447.1.A1_at	B3GALT2	UDP-Gal:betaGlcNAc beta 1,3-galactosyltransferase, polypeptide 2
Bt.737.1.S1_a_at	LIG3	ligase III, DNA, ATP-dependent
Bt.7272.1.S1_at	RNPEP	arginyl aminopeptidase (aminopeptidase B)
Bt.7263.1.S1_at	LOC510413	similar to PCAF associated factor 65 beta
Bt.7251.1.S1_at	B3GALT2	UDP-Gal:betaGlcNAc beta 1,3-galactosyltransferase, polypeptide 2
Bt.72.1.S1_at	MMP1	matrix metallopeptidase 1 (interstitial collagenase)
Bt.6980.1.S1_at	LOC790164	similar to 19A protein
Bt.6976.2.S1_at	SELPG	selectin P ligand
Bt.6963.1.A1_at	MGC152610	similar to Ecotropic viral integration site 2B
Bt.6842.1.S1_at	LOC520428	similar to Cdc14B2 phosphatase
Bt.6783.1.A1_at	LOC508660	hypothetical LOC508660
Bt.6705.1.S1_at	LOC527162	similar to TBC1 domain family, member 8
Bt.6680.3.S1_at	FKBP2 /// LOC783065	FK506 binding protein 2, 13kDa /// hypothetical protein LOC783065
Bt.6657.1.S1_at	LOC534891	similar to transmembrane protein 63B

Probe Set ID	Gene Symbol	Gene Title
Bt.6657.1.S1_a_at	LOC534891	similar to transmembrane protein 63B
Bt.6575.1.A1_at	---	Transcribed locus, strongly similar to XP_423069.1 PREDICTED: similar to phospha
Bt.6521.1.A1_at	MGC149024	similar to PAR-6 beta
Bt.6520.1.A1_at	LOC539144	similar to FRAT2
Bt.6261.1.S1_at	LOC614323	similar to carbonic anhydrase
Bt.6140.1.S1_at	LOC535992	similar to Rab11 interacting protein Rip11a
Bt.6105.1.S1_at	LOC619120	hypothetical LOC619120
Bt.6086.1.S1_at	ANK3	ankyrin 3, node of Ranvier (ankyrin G)
Bt.6020.1.S1_at	DNAJC11	DnaJ (Hsp40) homolog, subfamily C, member 11
Bt.6014.2.S1_at	RNF168	ring finger protein 168
Bt.6001.1.S1_s_at	LOC530342	similar to Chromosome 16 open reading frame 24
Bt.5858.1.S1_at	MGC139676	similar to Serine/threonine-protein kinase PAK 1 (p21-activated kinase 1) (PAK-1
Bt.5760.1.S1_at	MGC140597	similar to FtsJ homolog 3
Bt.5634.1.S1_at	SCAMP2	secretory carrier membrane protein 2
Bt.5603.2.S1_at	LOC534759	similar to G patch domain containing 8
Bt.5590.2.S1_at	PTPN2	Protein tyrosine phosphatase, non-receptor type 2
Bt.5589.1.S1_at	MGC142822	similar to SPATA20 protein
Bt.557.1.S1_at	SLC1A1	solute carrier family 1 (neuronal/epithelial high affinity glutamate transporter
Bt.5563.1.S1_at	PCSK2	proprotein convertase subtilisin/kexin type 2
Bt.5496.2.S1_at	LOC511673	similar to methylmalonic aciduria type A
Bt.5445.3.A1_at	MGC137802	similar to tubulin, beta 6
Bt.5432.2.S1_at	TNIP1	TNFAIP3 interacting protein 1
Bt.5420.3.A1_at	PCP4L1	Purkinje cell protein 4 like 1
Bt.5413.2.S1_at	MGC137522	similar to glucocerebrosidase precursor
Bt.5413.1.S1_at	MGC137522	similar to glucocerebrosidase precursor
Bt.5403.1.S1_at	XDH	xanthine dehydrogenase
Bt.5401.1.S1_at	TGM2	transglutaminase 2 (C polypeptide, protein-glutamine-gamma-glutamyltransferase)
Bt.5381.2.S1_x_at	CSN2	casein beta
Bt.5287.1.S1_at	BCKDHA	branched chain keto acid dehydrogenase E1, alpha polypeptide
Bt.5259.1.S1_at	BIRC4BP	XIAP associated factor-1
Bt.5220.1.S1_at	SHBG	sex hormone-binding globulin
Bt.5121.1.S1_at	CASR	calcium-sensing receptor
Bt.5074.1.S1_at	LOC618226	Similar to SFPQ protein
Bt.5007.1.A1_at	LOC508098 /// LOC790292	hypothetical LOC508098 /// hypothetical protein LOC790292
Bt.50.1.S1_at	CD8A	CD8a molecule
Bt.4984.1.A1_a_at	MUTYH	mutY homolog (E. coli)
Bt.4950.1.S1_at	NDST2	N-deacetylase/N-sulfotransferase (heparan glucosaminyl) 2
Bt.4946.1.S1_at	RAC2	ras-related C3 botulinum toxin substrate 2 (rho family, small GTP binding protei
Bt.4932.1.S1_at	TBC1D1	TBC1 (tre-2/USP6, BUB2, cdc16) domain family, member 1
Bt.4911.1.S1_at	CPSF1	cleavage and polyadenylation specific factor 1
Bt.4909.1.S1_at	LOC511267	similar to START domain containing 3
Bt.4894.1.S1_at	CPSF3L	cleavage and polyadenylation specific factor 3-like
Bt.4863.1.S1_at	MGC128242	similar to neuronal protein
Bt.4856.1.S2_at	IL1B	interleukin 1, beta
Bt.4735.1.S1_at	ACACA /// LOC787813	acetyl-coenzyme A carboxylase alpha /// similar to acetyl-CoA-carboxylase
Bt.4709.1.S1_at	LOC782522 /// LOC782961 /// LOC788268 /// STAR	steroidogenic acute regulator /// similar to Steroidogenic acute regulatory prot
Bt.4648.1.S1_at	FANCC	Fanconi anemia, complementation group C
Bt.460.1.S1_s_at	LOC783512 /// TST	thiosulfate sulfurtransferase (rhodanese) /// similar to Thiosulfate sulfurtrans
Bt.445.1.S1_at	PDE6H	phosphodiesterase 6H, cGMP-specific, cone, gamma
Bt.4390.1.S1_at	TEK	TEK tyrosine kinase, endothelial (venous malformations, multiple cutaneous and m
Bt.4378.2.S1_a_at	ECE1	endothelin converting enzyme 1
Bt.4323.2.S1_at	AMZ2	archaemetzincins-2
Bt.4289.1.S1_at	LOC785621 /// TRA@	T cell receptor, alpha /// hypothetical protein LOC785621
Bt.425.1.S2_a_at	RBP3	retinol binding protein 3, interstitial
Bt.4232.2.S1_at	LOC508023	similar to KIAA1395 protein
Bt.4220.1.S1_at	LOC286844	pyruvate dehydrogenase phosphatase regulatory subunit precursor
Bt.4216.1.S1_at	PGF	placental growth factor, vascular endothelial growth factor-related protein
Bt.4111.1.A1_at	LOC510124	similar to OTTHUMP00000016605
Bt.4057.1.S1_at	MYH10	myosin, heavy chain 10, non-muscle
Bt.4010.1.S1_at	---	Transcribed locus, moderately similar to XP_851133.1 PREDICTED: similar to rever
Bt.3992.1.S1_at	PISD	phosphatidylserine decarboxylase
Bt.3981.2.S1_at	LOC788761	similar to C20orf94 protein
Bt.3923.1.S1_at	MGC155009	similar to Protein C21orf63 precursor (SUE21)
Bt.39.1.S1_at	MMP13	matrix metallopeptidase 13 (collagenase 3)
Bt.3885.5.S1_x_at	CLCA3	chloride channel, calcium activated, family member 3
Bt.3877.2.S1_a_at	CD37	CD37 molecule
Bt.3766.1.A1_at	MGC166276	hypothetical LOC520250

Probe Set ID	Gene Symbol	Gene Title
Bt.3753.3.A1_at	LOC534434	Similar to KIAA0614 protein
Bt.3704.1.S1_at	TCN2	transcobalamin II
Bt.3685.2.S1_at	LOC512915	Similar to zinc finger and BTB domain containing 17
Bt.3547.1.A1_at	MGC152116	similar to Stac protein (SRC homology 3 and cysteine-rich domain protein)
Bt.352.5.S1_a_at	PTGFR	prostaglandin F receptor (FP)
Bt.3516.1.S1_at	LOC527449	similar to mannosidase, alpha, class 2A, member 2
Bt.3414.2.A1_at	HRB	HIV-1 Rev binding protein
Bt.3361.1.S1_at	CDC42BPG	CDC42 binding protein kinase gamma
Bt.3339.2.S1_a_at	SEMA4A	sema domain, immunoglobulin domain (Ig), transmembrane domain (TM) and short cyt
Bt.333.1.S1_at	TNP1	transition protein 1 (during histone to protamine replacement)
Bt.3317.1.A1_at	LOC523202	similar to cubilin
Bt.3309.1.A1_at	LOC535933	hypothetical LOC535933
Bt.3308.1.S1_at	MGC137396	similar to CG9339-PF
Bt.3300.1.S1_at	LOC511523	similar to SLC2A4 regulator
Bt.3245.1.S1_at	RHCG	Rh family, C glycoprotein
Bt.3221.2.S1_at	MBD1	Methyl-CpG binding domain protein 1
Bt.3221.1.A1_at	MBD1	Methyl-CpG binding domain protein 1
Bt.3201.1.S1_at	MGC139107	similar to Glutamate-rich WD-repeat protein 1
Bt.3199.3.S1_at	RUSC1	RUN and SH3 domain containing 1
Bt.3196.1.S1_at	STRA6	stimulated by retinoic acid gene 6 homolog
Bt.3170.3.S1_at	LOC517531	similar to Mitochondrial intermediate peptidase
Bt.3060.3.S1_at	LOC781477	hypothetical protein LOC781477
Bt.3015.2.S1_at	MGC157216	similar to HMGIC fusion partner-like 2
Bt.29964.1.S1_at	MGC140199	similar to Zinc finger protein 200
Bt.29962.3.S1_at	MAP3K12	mitogen-activated protein kinase kinase kinase 12
Bt.29957.2.S1_a_at	LOC786176 /// ZFP2	zinc finger protein 2 homolog /// similar to Kruppel-type zinc-finger protein
Bt.29907.2.S1_a_at	KLHDC8B	kelch domain containing 8B
Bt.2989.2.S1_at	LOC539494	similar to Solute carrier family 25 (mitochondrial carrier, Aralar), member 12
Bt.29845.1.A1_at	---	B11 cell-line anti-idiotype Ig heavy chain V region (IgH)
Bt.29829.1.A1_at	NALP5	NACHT, leucine rich repeat and PYD containing 5
Bt.29804.1.S1_at	---	Clone 4 immunoglobulin heavy chain variable region (VH)
Bt.29752.1.S1_at	LOC613361	Hypothetical LOC613361
Bt.2973.3.A1_at	PDHB	Pyruvate dehydrogenase (lipoamide) beta
Bt.29621.1.S1_at	LOC533088	similar to glutathione peroxidase 2
Bt.29605.1.A1_at	LOC515218	Similar to SAPS3 protein
Bt.29569.2.S1_at	ZC3H8	zinc finger CCCH-type containing 8
Bt.29569.1.A1_at	ZC3H8	zinc finger CCCH-type containing 8
Bt.29563.1.A1_at	---	Transcribed locus, strongly similar to XP_622559.3 PREDICTED: similar to Adenoma
Bt.29530.1.S1_at	LOC781470 /// LOC781867	hypothetical protein LOC781470 /// similar to Pol; truncated polymerase
Bt.29480.1.S1_at	LOC517559	hypothetical LOC517559
Bt.29231.1.A1_at	MGC152225	Hypothetical LOC533952
Bt.29226.1.A1_at	LOC100125413	hypothetical protein LOC100125413
Bt.29152.1.S1_at	TSPAN12	tetraspanin 12
Bt.29086.1.S1_at	SVOPL	SVOP-like
Bt.29074.1.A1_at	MGC142645	Similar to SET and MYND domain containing 3
Bt.29035.1.A1_at	LOC539674	similar to B12 protein
Bt.28907.1.S1_at	NDUFS1	NADH dehydrogenase (ubiquinone) Fe-S protein 1, 75kDa (NADH-coenzyme Q reductase
Bt.28904.1.A1_at	MGC139461	Similar to LBP-1c=transcription factor alpha-globin CP2 homolog (alternatively s
Bt.28896.1.S1_at	LOC781067	similar to jumonji domain containing 1C
Bt.28874.1.S1_at	LOC540004	similar to nucleoporin 98kD
Bt.28797.1.A1_at	CENP-N /// LOC783804	centromere protein N /// similar to Centromere protein N
Bt.28738.1.S1_at	ALPI	Alkaline phosphatase, intestinal
Bt.28718.1.A1_at	LOC538754	Similar to Protein phosphatase 1, regulatory (inhibitor) subunit 15B
Bt.28666.1.S1_at	LOC512168	similar to Transmembrane and coiled-coil domains 4
Bt.28626.1.S1_at	LOC521363	similar to Chromosome 2 open reading frame 3
Bt.28592.1.S1_at	LOC518260	similar to Paf1/RNA polymerase II complex component
Bt.28559.1.S1_a_at	DNASE1L1	deoxyribonuclease I-like 1
Bt.28532.1.S1_at	MMRN1	Multimerin 1
Bt.28487.1.A1_at	ART4	ADP-ribosyltransferase 4 (Dombrock blood group)
Bt.28403.1.A1_at	LOC783837	hypothetical protein LOC783837
Bt.28352.1.S1_at	CENPI	centromere protein I
Bt.28346.2.S1_at	BRRN1	barren homolog 1 (Drosophila)
Bt.28320.1.A1_at	LOC613826	hypothetical LOC613826
Bt.28250.1.A1_at	LOC508176	hypothetical LOC508176
Bt.28245.1.S1_at	MGC148361	similar to organic solute transporter beta
Bt.28240.1.S1_at	EPS8L3	EPS8-like 3
Bt.28234.1.S1_at	LOC781514	similar to FLJ00044 protein
Bt.28182.1.A1_at	RGS5	regulator of G-protein signaling 5

Probe Set ID	Gene Symbol	Gene Title
Bt.28165.1.A1_at	MGC154978	Similar to androgen-regulated serine protease TMPRSS2
Bt.28162.3.S1_at	PLN	phospholamban
Bt.28129.1.S1_at	Idlr	low density lipoprotein receptor
Bt.28020.1.A1_at	LOC407189	KERIA
Bt.28004.2.A1_a_at	LOC505306	Hypothetical LOC505306
Bt.27995.1.S1_at	adra2c	alpha-2C adrenergic receptor
Bt.27990.1.S1_at	5HTR2A	5-hydroxytryptamine receptor 2A
Bt.27940.1.A1_at	RHBG	Rh family, B glycoprotein
Bt.27874.2.S1_at	PTDSR	Phosphatidylserine receptor
Bt.27859.1.S1_at	LOC538956	hypothetical LOC538956
Bt.27816.1.S1_at	STAC3	SH3 and cysteine rich domain 3
Bt.27773.1.A1_at	LOC540258	similar to RNA binding motif protein 25
Bt.27622.1.A1_at	LOC538331	similar to myosin tail domain-containing protein
Bt.27584.1.S1_at	LOC538513	hypothetical LOC538513
Bt.27564.1.A1_at	LGP2	RNA helicase LGP2
Bt.27560.1.A1_at	LOC534432	hypothetical LOC534432
Bt.27537.1.A1_at	MAP1D	methionine aminopeptidase 1D
Bt.27458.1.A1_at	NR1H3	nuclear receptor subfamily 1, group H, member 3
Bt.27449.1.A1_at	LOC531405	similar to Sortilin-related VPS10 domain containing receptor 3
Bt.27423.1.S1_at	LOC539203	similar to dishevelled 3
Bt.27409.2.S1_at	LOC504406	similar to hydrocephalus inducing
Bt.27374.1.S1_at	LOC511212 /// LOC790064	hypothetical LOC511212 /// hypothetical protein LOC790064
Bt.27356.1.S1_at	MGC152577	similar to Chromatin assembly factor 1, subunit A (p150)
Bt.27242.2.S1_at	MGC151790	similar to nucleolar RNA-associated protein alpha
Bt.27223.2.S1_a_at	LOC508130	similar to Malonyl CoA:ACP acyltransferase (mitochondrial)
Bt.27212.1.A1_at	LOC783524	similar to cardiac muscle ryanodine receptor
Bt.27064.1.A1_at	LOC514726	similar to methionine-tRNA synthetase 2 precursor
Bt.27012.1.A1_at	LOC510408	similar to KIAA1092 protein
Bt.26993.1.S1_at	LOC514446	similar to see GenBank Accession Number U01184 for cDNA
Bt.26982.1.S1_at	LOC523815	similar to myeloid translocation gene-related protein 2 isoform MTG16a
Bt.26979.1.A1_at	MGC137696	similar to KIAA0517 protein
Bt.26935.3.S1_at	LOC790401 /// TAF13	TAF13 RNA polymerase II, TATA box binding protein (TBP)-associated factor, 18kDa
Bt.26850.1.S1_at	LOC508443	similar to ATP-binding cassette sub-family G member 4
Bt.26786.1.S1_at	MGC139038	similar to RNF185 protein
Bt.26780.1.S1_at	LOC511191	similar to Golgi complex autoantigen golgin-97
Bt.26753.1.A1_at	LOC533403	Similar to protein inhibitor of activated STAT X isoform beta
Bt.26740.1.S1_at	LOC510032	similar to Transcription factor EB
Bt.26727.1.S1_at	DHDDS	dehydrodolichyl diphosphate synthase
Bt.26691.1.S1_a_at	TNFSF13	tumor necrosis factor (ligand) superfamily, member 13
Bt.26651.1.S1_at	LOC534619	similar to beta-1,3-N-acetylglucosaminyltransferase bGn-T4
Bt.26643.2.S1_at	LOC511168	similar to NFBD1
Bt.26640.1.S1_at	LOC784717	similar to ZNF239 protein
Bt.26623.1.S1_at	TTLL3	tubulin tyrosine ligase-like family, member 3
Bt.26617.1.A1_at	LEP	leptin
Bt.26568.2.S1_a_at	LOC531049	similar to Putative eukaryotic translation initiation factor 3 subunit (eIF-3)
Bt.26510.1.S1_at	PLP1	proteolipid protein
Bt.26405.1.A1_at	MGC166351	Similar to KIAA0026
Bt.26315.1.A1_at	MGC137255	Hypothetical protein MGC137255
Bt.26312.1.A1_at	LOC528108	similar to Scavenger receptor class F member 2 precursor (Scavenger receptor exp
Bt.26293.1.A1_at	LOC616292	Hypothetical LOC616292
Bt.26272.1.S1_at	LOC507407	similar to Musculin (activated B-cell factor-1)
Bt.26271.1.A1_at	MGC143024	similar to fructosamine 3 kinase
Bt.26258.1.A1_at	MGC139179	similar to mitochondrial translation optimization 1 homolog
Bt.26234.1.A1_at	---	Transcribed locus, strongly similar to NP_065971.1 chromodomain helicase DNA bin
Bt.26184.1.S1_at	LOC540500	similar to UDP-N-acetyl-alpha-D-galactosamine:polypeptide N-acetylgalactosaminyl
Bt.26172.1.S1_at	MGC139845	similar to Rap2 interacting protein
Bt.26111.1.A1_at	KIAA1549	hypothetical protein LOC512679
Bt.26093.1.A1_at	ZFP341	zinc finger protein 341
Bt.26039.1.A1_at	LOC540964	similar to transcription elongation regulator 1
Bt.26037.1.A1_at	LOC534539	similar to bromodomain and WD repeat domain containing 3 variant BRWD3-A
Bt.25950.1.A1_at	ATP6V0B	ATPase, H+ transporting, lysosomal 21kDa, V0 subunit b
Bt.25948.1.A1_at	LOC512873	Similar to Deltex protein 1 (Deltex-1) (Deltex1) (hDTX1)
Bt.25888.1.A1_at	LOC785211	hypothetical protein LOC785211
Bt.25858.1.A1_at	NDUFA7	NADH dehydrogenase (ubiquinone) 1 alpha subcomplex, 7, 14.5kDa
Bt.25834.1.A1_at	MELK	maternal embryonic leucine zipper kinase
Bt.25793.1.S1_at	LOC527701	similar to KIAA2019 protein
Bt.25783.1.A1_at	SP2	Sp2 transcription factor
Bt.25770.1.A1_at	APC	adenomatosis polyposis coli
Bt.25746.1.A1_at	MGC140754	hypothetical LOC508613
Bt.25724.1.A1_at	LOC613929	hypothetical LOC613929
Bt.25697.1.A1_a_at	CCR9	chemokine (C-C motif) receptor 9

Probe Set ID	Gene Symbol	Gene Title
Bt.25685.1.A1_at	ASPHD1	aspartate beta-hydroxylase domain containing 1
Bt.25673.1.A1_at	LOC615476	similar to actinfilin
Bt.25622.1.A1_at	VNN1	vanin 1
Bt.25617.1.A1_at	LOC526780	similar to ADAMTS-like 2
Bt.25609.1.A1_at	GPR61	G protein-coupled receptor 61
Bt.25596.1.A1_at	LOC615059	similar to huntingtin
Bt.25567.1.A1_at	MGC139640	similar to Amyloid beta A4 precursor protein-binding family B member 2 (Fe65-lik
Bt.25560.1.A1_at	MGC140383	similar to Skeletal muscle and kidney enriched inositol phosphatase
Bt.25509.1.A1_at	---	Transcribed locus, moderately similar to NP_982279.1 hypothetical protein LOC403
Bt.25501.1.A1_at	LOC505613	similar to BoWC1.1
Bt.25463.1.S1_at	OAT3	organic anion transporter 3
Bt.25416.1.A1_at	LOC538233	Similar to hSSH-1L
Bt.25388.1.A1_at	LOC527499	similar to P2X2B receptor
Bt.2537.1.S1_at	CHRNA3	cholinergic receptor, nicotinic, alpha 3
Bt.25344.1.S1_at	---	Transcribed locus, weakly similar to NP_062566.1 zinc finger protein 386 (Kruppe
Bt.25342.1.A1_at	MGC159591	similar to coiled-coil domain containing 132
Bt.25326.1.A1_at	RPH3AL	Rabphilin 3A-like (without C2 domains)
Bt.25305.1.A1_at	LOC790079	hypothetical protein LOC790079
Bt.25289.1.A1_at	MGC128518	Similar to CG14966-PA
Bt.25262.1.A1_at	LOC508660	hypothetical LOC508660
Bt.25214.1.A1_at	SPIN2	spindlin family, member 2
Bt.2510.1.A1_at	MGC166270	similar to SRp40-1
Bt.2509.1.S1_at	MEF2B	myocyte enhancer factor 2B
Bt.25084.1.S1_at	---	Transcribed locus, weakly similar to NP_001012749.1 hypothetical protein LOC2838
Bt.25083.1.A1_at	MGC128237	Similar to ubiquinol-cytochrome c reductase binding protein
Bt.25049.1.S1_at	LOC505068	similar to Translocation associated membrane protein 1-like 1
Bt.24912.1.A1_at	---	Transcribed locus, moderately similar to XP_937072.1 PREDICTED: hypothetical pro
Bt.2490.1.A1_at	AGP	alpha-1 acid glycoprotein
Bt.249.1.S1_at	NMT2	N-myristoyltransferase 2
Bt.24881.1.S1_at	LOC539690	similar to C1qR(p)
Bt.24832.1.A1_a_at	MGC142764	similar to 2-phosphodiesterase
Bt.24825.1.S1_at	CDH3	Cadherin 3, type 1, P-cadherin (placental)
Bt.24821.2.S1_a_at	MGC137561	similar to acyl-Coenzyme A binding domain containing 4
Bt.24813.2.S1_at	LOC787267 /// RTP4	receptor (chemosensory) transporter protein 4 /// similar to Receptor transporte
Bt.24811.1.A1_at	LOC515718	vav 2 protein
Bt.24808.1.A1_at	HUWE1	HECT, UBA and WWE domain containing 1
Bt.24807.1.S1_at	LOC540683	similar to vacuolar protein sorting 13D
Bt.24780.1.S1_at	LOC783538	similar to modulator recognition factor 2 (MRF2)
Bt.24697.1.A1_at	LOC541246	similar to Kinesin-like protein KIF3A (Microtubule plus end-directed kinesin mot
Bt.24690.1.S1_at	LOC505073	similar to RP11-334J6.1
Bt.24642.1.A1_at	LOC526505 /// LOC785905	similar to Ankyrin repeat domain-containing protein 26
Bt.24629.1.S1_at	LOC509859	similar to KIAA0342 protein
Bt.24569.1.A1_at	LOC517240	similar to KIAA1345 protein
Bt.24565.3.A1_a_at	LOC507256	similar to RAI16 protein
Bt.24559.1.A1_at	CD1D	CD1D antigen, d polypeptide
Bt.24554.1.S1_at	LOC507268	hypothetical LOC507268
Bt.24525.1.S1_at	LOC531863	similar to FLJ00174 protein
Bt.24501.1.A1_at	LOC539689	similar to Cartilage paired-class homeoprotein 1
Bt.24478.1.S1_at	LOC540132	Similar to TNE5
Bt.24412.1.S1_at	MGC139150	Hypothetical LOC540648
Bt.24394.1.S1_at	---	Transcribed locus, moderately similar to XP_001158686.1 PREDICTED: SA hypertensi
Bt.24370.1.A1_at	CXorf45	hypothetical protein LOC515282
Bt.24233.1.S1_at	NSF	N-ethylmaleimide-sensitive factor
Bt.24219.1.A1_at	LOC540563	similar to ash1 (absent, small, or homeotic)-like
Bt.24069.1.A1_at	LOC617565	Similar to Ocil/Clrb-like protein
Bt.24008.1.A1_at	MGC165775	similar to solute carrier 19A3
Bt.23968.1.S1_at	LOC782635	similar to KIAA1040 protein
Bt.23857.2.S1_at	MGC157214	hypothetical LOC524166
Bt.23857.1.A1_at	MGC157214	hypothetical LOC524166
Bt.23801.1.A1_at	LOC519409	Similar to origin recognition complex subunit 5 homolog
Bt.23650.1.S1_at	PRKRIP1	PRKR interacting protein 1
Bt.23600.2.A1_at	TMEM93	Transmembrane protein 93
Bt.23588.1.S1_at	LOC539235	similar to casein kinase 2, beta subunit
Bt.23585.1.S1_at	GDNF	glial cell derived neurotrophic factor
Bt.23571.2.A1_at	LOC534896	similar to centrosome-associated protein 350
Bt.23267.1.S1_at	LYVE-1	lymphatic vessel endothelial hyaluronan receptor 1
Bt.23152.1.S1_at	RETN	resistin
Bt.23106.1.S1_at	HN1 /// MGC127173	hematological and neurological expressed 1 /// similar to hematological and neur
Bt.23078.1.S1_at	LOC783510	similar to diacylglycerol kinase zeta

Probe Set ID	Gene Symbol	Gene Title
Bt.23030.2.A1_at	LOC518806	Similar to KIAA0840 protein
Bt.22998.1.S1_at	SLC5A6	solute carrier family 5 (sodium-dependent vitamin transporter), member 6
Bt.22982.1.A1_at	RTN1	reticulon 1
Bt.22872.1.A1_at	NGFR	nerve growth factor receptor
Bt.22871.1.A1_at	ANK1	ankyrin 1, erythrocytic
Bt.22856.1.S1_at	LOC787355 /// NEF3	neurofilament, medium polypeptide /// neurofilament triplet M protein
Bt.22809.2.S1_at	DFFB	DNA fragmentation factor, 40kDa, beta polypeptide (caspase-activated DNase)
Bt.22766.2.S1_at	MGC152480	similar to KIAA0156
Bt.22735.1.S1_at	MGC151530	similar to synaptotagmin-like 2
Bt.2268.1.S1_at	LASS4	LAG1 homolog, ceramide synthase 4
Bt.22574.1.S1_at	AMD1	Adenosylmethionine decarboxylase 1
Bt.22499.2.S1_at	MGC133722	hypothetical LOC505437
Bt.22499.1.S1_at	MGC133722	hypothetical LOC505437
Bt.22466.2.S1_at	MGC140624	Similar to Septin-8
Bt.22431.1.S1_at	LOC787244	similar to LOC285193 protein
Bt.22415.2.A1_at	LOC512863	similar to Sialic acid binding Ig-like lectin 5
Bt.22320.3.S1_at	TARDBP	TAR DNA binding protein
Bt.22320.2.S1_at	TARDBP	TAR DNA binding protein
Bt.223.1.S1_at	AMBN	ameloblastin (enamel matrix protein)
Bt.22290.1.S1_at	ESAM	endothelial cell adhesion molecule
Bt.22275.1.A1_at	LOC506604	similar to HEM45
Bt.2222.2.S1_at	LOC537096	similar to WD repeat and FYVE domain containing 3
Bt.2217.1.S1_at	APBB1	amyloid beta (A4) precursor protein-binding, family B, member 1 (Fe65)
Bt.22150.2.S1_at	LZTFL1	leucine zipper transcription factor-like 1
Bt.22106.2.S1_at	MGC139676	similar to Serine/threonine-protein kinase PAK 1 (p21-activated kinase 1) (PAK-1
Bt.22086.2.A1_at	ALDH7A1	aldehyde dehydrogenase 7 family, member A1
Bt.22072.1.A1_at	MBNL2	Muscleblind-like 2
Bt.2203.1.S1_at	ABHD12	abhydrolase domain containing 12
Bt.22006.1.S1_at	LOC527362	similar to FLJ00128 protein
Bt.22001.1.A1_at	MGC143168	hypothetical LOC512635
Bt.21993.1.A1_at	---	Transcribed locus, moderately similar to XP_342030.2 PREDICTED: similar to Expre
Bt.21989.1.A1_at	THRAP4	thyroid hormone receptor associated protein 4
Bt.21964.1.S1_at	ACS	1-aminocyclopropane-1-carboxylate synthase
Bt.21937.1.A1_at	LOC539495	hypothetical LOC539495
Bt.21907.1.S1_at	MGC165906	hypothetical LOC512477
Bt.21861.2.A1_at	MGC139330	similar to Carbohydrate sulfotransferase 9 (N-acetylgalactosamine-4-O-sulfotrans
Bt.21842.1.A1_at	LOC535064	similar to U2 small nuclear RNA auxiliary factor 1-like 2
Bt.21833.2.S1_at	MGC152436	hypothetical LOC516995
Bt.21789.1.S1_at	LOC617344	Similar to SH3 binding protein 3BP2
Bt.21775.2.S1_at	LOC513377	similar to Rho guanine nucleotide exchange factor 1
Bt.21759.1.S1_at	MGC165687	similar to gamma-butyrobetaine 2-oxoglutarate dioxygenase
Bt.21669.1.A1_at	ZNF274	Zinc finger protein 274
Bt.21630.1.S1_at	DNAJB5	DnaJ (Hsp40) homolog, subfamily B, member 5
Bt.21504.1.A1_at	LOC540351	similar to Zyg-11 homolog B (C. elegans)-like
Bt.21475.3.S1_a_at	LOC786013	similar to Ded protein
Bt.21448.2.S1_at	LOC528038	similar to mFLJ00098 protein
Bt.21430.1.S1_at	MGC166357	similar to Synovial apoptosis inhibitor 1, synoviolin
Bt.21413.2.S1_at	MGC151768	similar to Solute carrier family 44, member 2
Bt.214.1.S1_at	DDEF1	development and differentiation enhancing factor 1
Bt.21336.2.S1_a_at	MAD2L2	MAD2 mitotic arrest deficient-like 2 (yeast)
Bt.21249.1.S1_at	LOC509555	similar to CDNA sequence BC046404
Bt.21247.1.S1_at	---	Transcribed locus, moderately similar to NP_064327.1 poly (A) polymerase beta (t
Bt.21228.1.A1_a_at	PAXIP1	PAX interacting (with transcription-activation domain) protein 1
Bt.21225.1.S1_at	LOC514364	similar to eyes absent 3
Bt.21223.1.S1_at	ATP1A1	ATPase, Na+/K+ transporting, alpha 1 polypeptide
Bt.21165.1.A1_at	MGC152214	similar to gamma tubulin ring complex protein (76p gene)
Bt.21099.2.S1_at	MGC143052	similar to Breast cancer metastasis-suppressor 1-like
Bt.2105.1.S1_at	LOC535935	similar to large tumor suppressor 1
Bt.21039.1.A1_at	LOC507449	similar to Dexamethasone-induced Ras-related protein 1
Bt.21037.2.S1_at	MGC157143	similar to Transcription factor 7 (T-cell specific, HMG-box)
Bt.21034.1.A1_at	LOC511350	hypothetical LOC511350
Bt.21009.1.S1_at	LOC532887	similar to phosphoinositol 3-phosphate-binding protein-2
Bt.2096.2.S1_at	LOC505206	similar to pincher
Bt.2092.1.S1_at	LOC506953	similar to Integrin alpha-7 precursor
Bt.20835.1.A1_at	LOC525143	Similar to PI-3-kinase-related kinase SMG-1
Bt.20742.1.A1_at	LOC508405	similar to ankyrin repeat domain protein 17
Bt.20712.1.A1_at	LOC790501	Hypothetical protein LOC790501
Bt.20709.1.A1_at	LOC789017	similar to ras responsive element binding protein 1
Bt.20687.2.A1_at	LOC510651	hypothetical LOC510651
Bt.20652.1.A1_at	LOC790246 /// MAP1D	methionine aminopeptidase 1D /// similar to Methionine aminopeptidase 1D
Bt.20600.2.A1_a_at	MINA	MYC induced nuclear antigen

Probe Set ID	Gene Symbol	Gene Title
Bt.20584.1.S1_at	MGC127609	similar to NAD(P) dependent steroid dehydrogenase-like
Bt.20549.2.S1_at	MGC142862	similar to Regulator of G-protein signaling 19 (RGS19) (G-alpha interacting prot
Bt.20533.1.S1_at	ZA20D3	zinc finger, A20 domain containing 3
Bt.20532.1.S1_at	PSMB9	proteasome (prosome, macropain) subunit, beta type, 9 (large multifunctional pep
Bt.20505.1.S1_at	LOC532427	similar to tigger transposable element derived 2
Bt.20423.1.S1_at	LOC540021	similar to polyhomeotic 1-like
Bt.20394.1.A1_at	MGC148818	similar to Kruppel-like factor 13
Bt.20368.2.S1_at	MGC134421	hypothetical LOC540543
Bt.20352.1.S1_at	SEP2	Septin 2
Bt.20343.2.S1_a_at	LOC506146	similar to mammalian unc13-4
Bt.20322.2.S1_at	WDR18	WD repeat domain 18
Bt.20320.1.S1_at	DKFZP761P1121	similar to Ser/Thr-rich protein T10 in DGCR region
Bt.20311.2.S1_at	LOC787681	similar to peptidyl-prolyl cis-trans isomerase E
Bt.20310.1.S1_at	LOC505572	similar to dedicator of cytokinesis 5
Bt.20244.1.S1_at	MGC166124	similar to CAAX prenyl protein protease RCE1
Bt.20198.1.S1_at	LOC526529	similar to spindle pole body protein spc98 homolog GCP3
Bt.20189.1.S1_at	MGC148378	similar to KIAA0082
Bt.20146.1.S1_at	ATP2B4	ATPase, Ca++ transporting, plasma membrane 4
Bt.2007.2.S1_at	LOC525750	similar to tetratricopeptide repeat domain 32
Bt.20045.1.A1_at	LOC534212	similar to arylacetamide deacetylase-like 1
Bt.20043.3.A1_at	DUSP14	Dual specificity phosphatase 14
Bt.20043.2.S1_at	DUSP14	dual specificity phosphatase 14
Bt.20019.1.S1_at	LOC530692	unc-13 B-like protein
Bt.20008.2.S1_at	NUDT17	nudix (nucleoside diphosphate linked moiety X)-type motif 17
Bt.19994.1.S1_at	LOC789597	similar to PDZ domain-containing guanine nucleotide exchange factor PDZ-GEF2
Bt.19954.1.A1_at	ERCC3	excision repair cross-complementing rodent repair deficiency, complementation gr
Bt.199.1.S1_at	PNOC	prepronociceptin
Bt.19889.1.A1_at	IGSF1	immunoglobulin superfamily, member 1
Bt.19810.1.A1_at	MGC166311	hypothetical LOC540970
Bt.19781.1.A1_at	MGC137859	similar to Ubiquitin ligase protein DZIP3 (DAZ-interacting protein 3) (RNA-bindi
Bt.1978.10.S1_a_at	TRB@	T cell receptor, beta cluster
Bt.19754.1.A1_at	---	Transcribed locus, moderately similar to XP_001255373.1 PREDICTED: hypothetical
Bt.19702.1.S1_at	LYPD1	LY6/PLAUR domain containing 1
Bt.19681.1.A1_at	LOC538547	Hypothetical LOC538547
Bt.19629.2.S1_at	HSPH1	heat shock 105kDa/110kDa protein 1
Bt.19614.1.A1_at	LIPC	lipase, hepatic
Bt.19612.1.S1_at	LOC541096	Similar to pad-1-like
Bt.19611.1.S1_at	LOC512135	Hypothetical LOC512135
Bt.1960.2.S1_a_at	LOC616609	similar to Y38F2AL.2
Bt.19564.1.A1_at	LOC540109	similar to transducer of regulated CREB protein 3
Bt.19563.1.A1_at	TCP11L1	t-complex 11 (mouse)-like 1
Bt.19552.1.A1_at	LOC614987	similar to LOC220416 protein
Bt.1953.3.S1_at	LOC515593	similar to microtubule-associated protein 1A
Bt.19500.2.A1_at	MGC137400	Similar to splicing factor 3B, 14 kDa subunit
Bt.19482.1.A1_at	LOC504698	similar to transferrin receptor
Bt.19405.1.A1_at	LOC782774	similar to G-protein coupled receptor GPR86
Bt.19370.1.A1_at	---	Transcribed locus, strongly similar to XP_871659.1 PREDICTED: hypothetical prote
Bt.19338.2.A1_at	LOC790072	hypothetical protein LOC790072
Bt.19309.1.S1_at	LOC616742	similar to Ephrin-A5 precursor (EPH-related receptor tyrosine kinase ligand 7) (
Bt.19241.1.A1_at	LOC508899	similar to Nuclear receptor coactivator 6
Bt.19220.1.A1_at	LOC510341	similar to AHNAK nucleoprotein
Bt.19199.1.A1_at	DCLK1	Doublecortin-like kinase 1
Bt.19093.1.S1_at	LOC535075	Similar to aldehyde dehydrogenase 1A2
Bt.1908.1.S1_at	LOC536558	similar to heat shock 70kDa protein 4
Bt.19079.1.A1_s_at	LOC785805	Hypothetical protein LOC785805
Bt.19059.1.A1_at	LOC504792	Similar to TBP-associated factor 1
Bt.19053.1.A1_at	LOC534067	similar to ubiquitin specific protease 34
Bt.18968.1.A1_at	MGC137317	similar to Protein C6orf165
Bt.18851.1.S1_at	NRBF1	nuclear receptor binding factor 1
Bt.18835.2.S1_at	CARS	cysteinyl-tRNA synthetase
Bt.18802.1.A1_at	LMO7	LIM domain 7
Bt.18751.1.S1_at	LOC533289	similar to type II phosphatidylinositol-4-phosphate 5-kinase 53K
Bt.18744.2.A1_at	WBP4	WW domain binding protein 4 (formin binding protein 21)
Bt.18718.1.S1_at	LOC514189	hypothetical LOC514189
Bt.18640.1.A1_at	VTI1A	Vesicle transport through interaction with t-SNAREs homolog 1A
Bt.18564.1.A1_at	LOC509744	alcohol dehydrogenase LOC509744
Bt.18546.1.A1_at	LOC508931	similar to Zinc finger protein 624
Bt.18512.1.A1_at	---	Transcribed locus, strongly similar to XP_342147.2 PREDICTED: similar to minichr
Bt.18469.1.S1_at	LOC784517	hypothetical protein LOC784517
Bt.18460.1.A1_at	MGC142807	Similar to alpha/beta hydrolase domain containing protein 3
Bt.18414.1.S1_at	GK	glycerol kinase
Bt.18392.1.A1_at	AMBP	alpha-1-microglobulin/bikunin precursor
Bt.18320.1.A1_at	---	Transcribed locus, strongly similar to NP_033801.4 ankyrin repeat and FYVE domai

Probe Set ID	Gene Symbol	Gene Title
Bt.18290.1.A1_at	LOC506182	similar to Tnf receptor-associated factor 3
Bt.18253.1.A1_at	LOC518313	similar to glutamate receptor interacting protein 1
Bt.18221.2.A1_s_at	LOC524692	Similar to KIAA0299
Bt.18196.1.S1_at	MGC128572	similar to mitochondrial Rho 1
Bt.1815.3.S1_at	MGC157300	Hypothetical LOC534625
Bt.18139.1.A1_at	LOC617808	hypothetical LOC617808
Bt.18126.1.A1_at	PRICKLE1	prickle homolog 1
Bt.18119.1.A1_at	FAF1	Fas (TNFRSF6) associated factor 1
Bt.18105.1.A1_at	LOC786620	hypothetical protein LOC786620
Bt.18101.1.A1_at	MGC148570	similar to olfactomedin related ER localized protein
Bt.18043.1.S1_at	LOC526616	similar to mKIAA1856 protein
Bt.1801.3.S1_at	TSPAN31	Tetraspanin 31
Bt.18002.2.S1_at	ZNF470	zinc finger protein 470
Bt.1797.1.S1_at	LOC506830	hypothetical LOC506830
Bt.17969.1.A1_at	MGC140375	similar to PP203
Bt.17964.2.A1_s_at	---	Transcribed locus, weakly similar to NP_690054.1 light ear protein isoform b [Ho
Bt.17948.2.A1_at	LOC513153	hypothetical LOC513153
Bt.17933.1.A1_at	LOC515358	Hypothetical LOC515358
Bt.17871.1.S1_a_at	LOC510737	similar to RNA binding protein DEF-3
Bt.17852.1.A1_at	LOC506353	Similar to KIAA0166
Bt.1780.1.S1_at	CTBP1	C-terminal binding protein 1
Bt.1774.1.S1_at	LOC513493	similar to myosin IXB
Bt.17734.1.A1_at	MGC157341	hypothetical LOC613974
Bt.17670.1.A1_at	LOC517995	similar to GPRIN family member 3
Bt.17669.1.S1_a_at	LOC522670	similar to I-REL
Bt.17656.1.A1_at	IL17	interleukin 17 (cytotoxic T-lymphocyte-associated serine esterase 8)
Bt.17637.3.A1_at	MGC139640	Similar to Amyloid beta A4 precursor protein-binding family B member 2 (Fe65-lik
Bt.17581.2.S1_at	LOC506952	similar to Methyltransferase-like protein 7B
Bt.17510.1.A1_at	PAM	Peptidylglycine alpha-amidating monooxygenase
Bt.17492.1.S1_at	MGC166379	similar to transcriptional regulatory protein p54
Bt.17473.2.S1_at	RPE	ribulose-5-phosphate-3-epimerase
Bt.17460.1.A1_at	LOC540117	similar to SLIT and NTRK-like family, member 2
Bt.17440.1.A1_at	MGC139708	similar to G+C-rich promoter-binding protein
Bt.17402.1.S1_at	MGC157323	Similar to Tripeptidyl peptidase II
Bt.17357.1.A1_at	LOC513610	Similar to CRSP3
Bt.17310.2.A1_at	LOC514509	similar to Agmatine ureohydrolase (agmatinase)
Bt.17229.1.A1_at	LOC539807	similar to KIAA1404 protein
Bt.17213.1.A1_at	SLC10A1	solute carrier family 10 (sodium/bile acid cotransporter family), member 1
Bt.17172.1.S1_at	GJA5	gap junction protein, alpha 5
Bt.17158.1.S1_at	LOC512933	similar to KIAA0753
Bt.17144.1.A1_s_at	LOC536676	similar to putative acetyltransferase
Bt.17124.1.A1_s_at	NUDT14	nudix (nucleoside diphosphate linked moiety X)-type motif 14
Bt.17096.2.A1_at	SYCP3	synaptonemal complex protein 3
Bt.17045.1.A1_at	LOC506159	similar to G protein-coupled receptor 52
Bt.17026.1.S1_at	LOC504245	similar to Rho GTPase activating protein 17
Bt.17.1.S1_at	PRP6	prolactin-related protein 6 /// prolactin-related protein VI
Bt.16985.1.S1_at	ELMO1	engulfment and cell motility 1
Bt.16958.1.A1_at	LOC788422	Hypothetical protein LOC788422
Bt.16889.1.A1_at	LTB4R	leukotriene B4 receptor
Bt.1682.1.S1_at	LOC534620	similar to serine/threonine kinase
Bt.16794.1.A1_at	LOC527607	Similar to elongation factor Tu GTP binding domain containing 1
Bt.16784.1.S1_at	LOC527394	similar to pygopus 1
Bt.16776.1.S1_at	LOC540422	similar to tigger transposable element derived 5
Bt.16725.1.S1_at	MGC152289	similar to ubiquitin-conjugating enzyme RIG-B
Bt.16652.1.A1_at	LOC510507	similar to cholesterol 7alpha-hydroxylase
Bt.16602.1.A1_at	PRPF38A	PRP38 pre-mRNA processing factor 38 (yeast) domain containing A
Bt.16594.1.A1_at	LOC505073	similar to RP11-334J6.1
Bt.16585.1.A1_at	MGC142680	Similar to PHD finger protein 6
Bt.16534.1.A1_at	DCTN2	Dynactin 2 (p50)
Bt.16521.2.A1_at	LOC615147	hypothetical LOC615147
Bt.16521.1.S1_at	LOC615147	hypothetical LOC615147
Bt.16464.1.A1_at	LOC784987	hypothetical protein LOC784987
Bt.16412.1.S1_a_at	FAA	fumarylacetoacetate hydrolase
Bt.16407.1.A1_at	NSF	N-ethylmaleimide-sensitive factor
Bt.16372.1.A1_at	LOC535887	similar to pantothenate kinase 1alpha
Bt.16338.1.S1_at	MBL-A	mannose binding lectin, liver (A)
Bt.16326.3.S1_at	LOC616626	hypothetical LOC616626
Bt.16271.2.A1_at	LOC514797	similar to macrophage C-type lectin Mincle
Bt.16212.2.S1_at	LOC617368	Hypothetical LOC617368
Bt.16210.1.S1_at	PRPSAP1	Phosphoribosyl pyrophosphate synthetase-associated protein 1
Bt.16188.2.S1_at	CYYR1	cysteine/tyrosine-rich 1
Bt.1616.1.A1_at	ECSOD	extracellular superoxide dismutase
Bt.16149.2.A1_at	MGC143009	hypothetical protein LOC783805

Probe Set ID	Gene Symbol	Gene Title
Bt.161.1.S2_at	DSG1	desmoglein 1
Bt.16077.1.S1_at	MGC140177	similar to receptor activity-modifying protein
Bt.1605.2.S1_at	MGC138923	similar to selenoprotein N, 1 isoform 1 precursor
Bt.1593.1.S1_at	SEZ6L2	seizure related 6 homolog (mouse)-like 2
Bt.15912.1.S1_at	LOC767910	placenta-specific 8
Bt.15890.1.S1_at	APOA4	apolipoprotein A-IV
Bt.15873.1.A1_at	MGC157081	similar to Nuclear pore complex protein Nup93 (Nucleoporin Nup93) (93 kDa nucleo
Bt.15866.3.S1_a_at	LOC784219	similar to nucleoporin 214kDa
Bt.15828.2.S1_at	LOC521857	similar to G-protein-coupled receptor induced protein GIG2
Bt.15769.1.S1_at	MGC139596	hypothetical LOC534262
Bt.15733.1.A1_at	LOC510012	similar to SCL/TAL1 interrupting locus
Bt.15732.1.S1_at	MGC157216	similar to HMGIC fusion partner-like 2
Bt.15531.1.S1_at	MGC142841	similar to tuberin-like protein 1
Bt.15466.1.A1_at	UNC50	unc-50 homolog
Bt.14921.1.A1_at	MGC137188	similar to Collagen alpha 1(X) chain precursor
Bt.1472.1.S1_at	IKBKE	inhibitor of kappa light polypeptide gene enhancer in B-cells, kinase epsilon
Bt.14676.1.S1_at	LOC540789	similar to poly (ADP-ribose) polymerase family, member 14
Bt.1463.1.S1_at	LOC504245	similar to Rho GTPase activating protein 17
Bt.146.1.S1_at	BNBD-4	neutrophil beta-defensin 4
Bt.1458.1.S1_at	MGC138036	similar to phosphoglucomutase 5
Bt.1436.1.S1_at	LOC788843	similar to pregnancy-associated glycoprotein 11
Bt.14165.1.S1_at	MGC133533	hypothetical LOC512692
Bt.14136.1.A1_at	ENDOD1	endonuclease domain containing 1
Bt.14000.1.S1_at	LOC789594	Hypothetical protein LOC789594
Bt.13927.2.S1_at	MGC134318	similar to Protein C22orf8
Bt.13894.1.S1_at	LOC527699	Similar to kalirin, RhoGEF kinase
Bt.13886.1.S1_at	LOC534067	Similar to ubiquitin specific protease 34
Bt.13868.1.S1_at	OCLN	occludin
Bt.13834.1.S1_at	LOC504698	similar to transferrin receptor
Bt.13810.1.S1_at	MGC152593	hypothetical LOC617594
Bt.13809.1.S1_at	LOC511191	similar to Golgi complex autoantigen golgin-97
Bt.13791.1.A1_at	LOC508196	similar to KIAA0476 protein
Bt.13645.2.S1_at	MGC159622	Hypothetical LOC513649
Bt.13556.1.S1_a_at	HF1 /// LOC788826	H factor 1 (complement) /// similar to H factor 1 (complement)
Bt.13553.2.S1_at	SPCS3	signal peptidase complex subunit 3
Bt.13549.2.S1_at	SRRP130	splicing factor, arginine/serine-rich 130
Bt.13549.1.A1_at	SRRP130	splicing factor, arginine/serine-rich 130
Bt.13484.1.A1_at	PPP1R3C	protein phosphatase 1, regulatory (inhibitor) subunit 3C
Bt.13478.1.A1_at	MGC155164	similar to LSM10, U7 small nuclear RNA associated
Bt.13470.3.S1_a_at	LOC787630	hypothetical protein LOC787630
Bt.13428.2.S1_at	FBP2	fructose-1,6-bisphosphatase 2
Bt.13427.1.S1_at	LOC781315	similar to C5orf25 protein
Bt.13410.1.S1_at	MGC160087	similar to ribosomal protein S6 kinase, 90kDa, polypeptide 3
Bt.1341.1.S1_at	LOC527172	hypothetical LOC527172
Bt.13390.1.A1_at	DECR1	2,4-dienoyl CoA reductase 1, mitochondrial
Bt.13375.1.S1_at	MGC128216	similar to S-adenosylmethionine synthetase alpha and beta forms (Methionine aden
Bt.13370.3.S1_at	LOC527459	similar to rapamycin insensitive companion of mTOR; rictor
Bt.13294.1.A1_at	LOC510378	similar to Transmembrane protein 161B
Bt.13147.1.A1_at	B4GALT5	UDP-Gal:betaGlcNAc beta 1,4- galactosyltransferase, polypeptide 5
Bt.13142.1.A1_x_at	PRKCD	protein kinase C, delta
Bt.13139.1.S1_at	TRPC3	transient receptor potential cation channel, subfamily C, member 3
Bt.13115.2.S1_at	P2RX7	purinergic receptor P2X, ligand-gated ion channel, 7
Bt.13115.1.S1_at	P2RX7	purinergic receptor P2X, ligand-gated ion channel, 7
Bt.13111.1.S1_at	FGFR4	fibroblast growth factor receptor 4
Bt.13094.1.A1_at	TXNRD3	thioredoxin reductase 3
Bt.13087.1.S1_at	CD6	CD6 molecule
Bt.13084.1.S1_at	MET	met proto-oncogene (hepatocyte growth factor receptor)
Bt.12952.2.A1_at	DNASE1	deoxyribonuclease I
Bt.12943.1.S1_at	LGTN	ligatin
Bt.12936.1.S1_at	CATHL5	cathelicidin 5
Bt.12894.1.S1_at	MGC159470	similar to transcript expressed during hematopoiesis 2
Bt.12871.1.S1_at	LOC788113	hypothetical protein LOC788113
Bt.12867.3.S1_at	LOC786496	similar to zinc finger protein 318
Bt.1284.1.S1_at	FLAD1	FAD1 flavin adenine dinucleotide synthetase homolog (S. cerevisiae)
Bt.12803.1.S1_at	PPARA	peroxisome proliferator-activated receptor alpha
Bt.12773.1.S1_at	SLC2A8	solute carrier family 2, (facilitated glucose transporter) member 8
Bt.1275.1.S1_at	LOC517354	similar to fractalkine
Bt.12744.1.S1_at	LOC510329	hypothetical LOC510329
Bt.12710.2.S1_at	MAP4K1	mitogen-activated protein kinase kinase kinase kinase 1
Bt.12569.1.A1_at	LOC539069 /// LOC789470	similar to copper amine oxidase
Bt.12431.1.S1_at	LOC504649	similar to Sorting nexin-19

Probe Set ID	Gene Symbol	Gene Title
Bt.1242.1.S1_at	ATP5G1	ATP synthase, H+ transporting, mitochondrial F0 complex, subunit C1 (subunit 9)
Bt.12293.1.S1_at	LOC786485	similar to limbin
Bt.12217.1.S1_at	NTRK2	Neurotrophic tyrosine kinase, receptor, type 2
Bt.12063.1.S1_at	LOC514537	similar to protocadherin 7
Bt.12010.1.S1_at	LOC512171	similar to ADAMTS1
Bt.1194.1.S1_at	LOC518086	similar to CANT1 protein
Bt.11885.1.S1_a_at	MGC139596	hypothetical LOC534262
Bt.11869.1.S1_at	LOC785548	hypothetical protein LOC785548
Bt.1184.1.S1_at	APEX2	APEX nuclease (apurinic/apyrimidinic endonuclease) 2
Bt.1180.2.A1_at	LOC529373	similar to monocytic leukaemia zinc finger protein
Bt.1180.1.A1_at	LOC529373	similar to monocytic leukaemia zinc finger protein
Bt.11797.3.A1_at	MGC148776	Hypothetical LOC535746
Bt.11763.2.S1_at	---	Transcribed locus, strongly similar to XP_213362.3 PREDICTED: similar to Camta2
Bt.11761.1.A1_at	LOC528972	similar to retinoic acid induced 1
Bt.1176.1.A1_at	MGC151719	similar to cell division cycle protein 23
Bt.11751.1.A1_at	---	Transcribed locus, strongly similar to XP_230006.3 PREDICTED: similar to Hypothe
Bt.11656.1.S1_at	CGN	cingulin
Bt.11651.1.A1_at	SCAND1	SCAN domain containing 1
Bt.11580.1.S1_at	LOC539650	similar to IGF-II mRNA-binding protein 3
Bt.11532.1.A1_at	CRYGB	crystallin, gamma B
Bt.11525.3.S1_at	LOC614417 /// LOC787851	similar to RNA-binding protein with multiple splicing (RBP-MS) /// similar to RB
Bt.11417.1.A1_at	LOC616483 /// LOC787261	similar to translation initiation factor eIF4A I
Bt.11368.1.A1_at	LOC541061	similar to 43 kD receptor-associated protein of the synapse
Bt.11362.1.A1_at	---	Transcribed locus, moderately similar to XP_343493.2 PREDICTED: similar to Arpp2
Bt.11277.2.S1_at	LOC789590	similar to ZXD family zinc finger C
Bt.11277.1.A1_at	LOC524085	similar to Solute carrier family 41, member 3
Bt.11195.1.S1_at	PLUNC	palate, lung and nasal epithelium carcinoma associated
Bt.11182.2.S1_at	GCFC	GC-rich sequence DNA-binding factor homolog
Bt.11126.2.A1_at	MGC137397	Similar to Phosphatidylcholine-sterol acyltransferase precursor (Lecithin-choles
Bt.11124.1.S1_at	VPS25	vacuolar protein sorting 25 homolog (S. cerevisiae)
Bt.11100.1.S1_at	LOC509260	Similar to nuclear DEAF-1 related transcriptional regulator
Bt.11017.1.S1_at	LOC540504	similar to Nesprin-2 (Nuclear envelope spectrin repeat protein 2) (Syne-2) (Syna
Bt.11010.1.S1_at	ATP6V0D2	ATPase, H+ transporting, lysosomal 38kDa, V0 subunit d2
Bt.10953.2.S1_at	MGC128409	Similar to TSC22 domain family protein 1 (Transforming growth factor beta 1 indu
Bt.10878.2.S1_a_at	HPS1	Hermansky-Pudlak syndrome 1
Bt.10604.1.A1_at	FYN	FYN oncogene related to SRC, FGR, YES
Bt.1054.1.S1_at	LOC522521	similar to KIAA0521 protein
Bt.10524.3.S1_at	ZNF821	zinc finger protein 821
Bt.10374.3.A1_at	VPS33B	Vacuolar protein sorting 33 homolog B (yeast)
Bt.10261.1.S1_at	LOC525095	similar to Phosphatidylinositol glycan anchor biosynthesis, class N
Bt.10180.1.A1_at	LOC524813	similar to forkhead box F1
Bt.10140.1.S1_at	LOC510456	hypothetical LOC510456
Bt.10124.1.S1_at	LOC513129	hypothetical LOC513129
Bt.10087.1.A1_at	LOC509257	similar to KIAA0672 gene product
Bt.10077.1.S3_at	LOC789216	similar to interferon regulatory factor 1
Bt.10046.2.S1_a_at	KLHDC2	kelch domain containing 2
Bt.10033.1.S1_at	LOC541118	similar to GW182 autoantigen
Bt.100.1.S1_at	ADRB2	adrenergic, beta-2-, receptor, surface

Complete list of genes that were down-regulated (>3-fold) at week 6 with dynamic compressive loading compared to CM+ free-swelling control.

Probe Set ID	Gene Symbol	Gene Title
Bt.9807.2.S1_at	GPNMB	glycoprotein (transmembrane) nmb
Bt.9675.1.S1_at	LOC787253	similar to Extracellular proteinase inhibitor
Bt.9351.2.S1_at	MGC139990	similar to EVIN1
Bt.9082.1.S1_at	LGALS4	lectin, galactoside-binding, soluble, 4 (galectin 4)
Bt.8421.2.S1_at	---	Transcribed locus, strongly similar to NP_001002374.1 hypothetical protein LOC43
Bt.8328.1.S1_at	LOC521189	similar to NRAMP2
Bt.7210.1.S1_at	PRND	prion protein 2 (dublet)
Bt.6392.1.S1_at	LOC527597	similar to transient receptor potential cation channel subfamily M member 6
Bt.5373.1.S1_at	SLC11A1	solute carrier family 11 (proton-coupled divalent metal ion transporters), membe
Bt.502.1.A1_at	RGN	regucalcin (senescence marker protein-30)
Bt.4781.1.S1_at	ADAM10	ADAM metallopeptidase domain 10
Bt.4604.1.S1_a_at	BUCS1	butyryl Coenzyme A synthetase 1
Bt.422.1.S2_at	IGFBP3	insulin-like growth factor binding protein 3
Bt.390.1.S1_at	CALB3	calbindin 3, (vitamin D-dependent calcium binding protein)
Bt.361.1.S1_at	SLC1A3	solute carrier family 1 (glial high affinity glutamate transporter), member 3
Bt.352.1.S1_at	PTGFR	prostaglandin F receptor (FP)
Bt.3189.1.A1_at	LOC540831	similar to FLJ20273 protein
Bt.29882.1.S1_at	MITF	microphthalmia-associated transcription factor
Bt.29718.1.S1_a_at	GHR	growth hormone receptor
Bt.28685.1.S1_at	LOC540831	similar to FLJ20273 protein
Bt.2846.1.A1_at	MGC154996	similar to ras homolog gene family, member U
Bt.28393.1.S1_at	DAF	decay-accelerating factor 1
Bt.28073.1.S1_at	LOC523223	similar to macrophage actin-associated-tyrosine-phosphorylated protein
Bt.27893.3.S1_a_at	---	Transcribed locus, strongly similar to NP_055053.1 kinase suppressor of ras [Hom
Bt.26343.1.S1_at	MTP	microsomal triglyceride transfer protein
Bt.26041.1.A1_at	LOC538782	hypothetical LOC538782
Bt.25926.1.A1_at	LOC533323	similar to cyclic nucleotide phophodiesterase
Bt.24864.2.A1_at	LOC508763	similar to Tissue factor pathway inhibitor precursor (TFPI) (Lipoprotein-associa
Bt.24830.1.A1_at	ITIH5	Inter-alpha (globulin) inhibitor H5
Bt.2481.1.A1_at	MGC128787	similar to CG3625-PB
Bt.24687.1.A1_at	LOC533427	hypothetical LOC533427
Bt.24238.1.A1_at	MPEG1	macrophage expressed gene 1
Bt.23523.1.S1_at	TUSC5	tumor suppressor candidate 5
Bt.23089.1.S1_at	LOC783547	similar to mannose receptor C1
Bt.22987.2.S1_at	PRG4	proteoglycan 4
Bt.22672.1.A1_at	PGDH	hydroxyprostaglandin dehydrogenase 15-(NAD)
Bt.22429.1.S1_at	LOC535378	similar to PAR3 beta
Bt.21962.1.S1_at	MGC165819	similar to ependymin related protein 1
Bt.21615.1.A1_at	MGC140693	similar to transmembrane protein 22
Bt.20381.2.S1_at	F2R	coagulation factor II (thrombin) receptor
Bt.19959.2.A1_at	LOC505317	similar to ankyrin-like protein
Bt.19945.1.A1_at	LOC616344	hypothetical LOC616344
Bt.1983.1.S1_at	LOC508459	similar to EMR1
Bt.19479.1.A1_at	LOC504217 /// LOC788273	hypothetical LOC504217 /// hypothetical protein LOC788273
Bt.18072.1.A1_at	MGC148318	hypothetical protein LOC782788
Bt.17607.1.A1_at	PLD1	phospholipase D1, phosphatidylcholine-specific
Bt.17309.2.A1_at	LOC518403	hypothetical LOC518403
Bt.16048.1.S1_at	LOC509501	proteoglycan 1 precursor-like
Bt.15925.1.S1_at	EPHX2 /// LOC785508	epoxide hydrolase 2, cytoplasmic /// hypothetical protein LOC785508
Bt.15895.2.S1_at	LOC614402	hypothetical LOC614402
Bt.15895.1.A1_at	LOC614402	hypothetical LOC614402
Bt.15731.1.A1_at	VSIG4	V-set and immunoglobulin domain containing 4
Bt.14566.2.S1_at	MGC157129	Similar to KIAA0936 protein
Bt.14143.1.S1_at	CPE	carboxypeptidase E
Bt.14056.1.A1_at	ARHGAP18	Rho GTPase activating protein 18
Bt.13996.3.A1_at	PLD1	phospholipase D1, phosphatidylcholine-specific
Bt.13542.1.S1_at	MGC137125	similar to Complement factor B precursor (C3/C5 convertase)
Bt.13330.2.A1_at	MGC166250	similar to pyruvate dehydrogenase kinase
Bt.12964.1.A1_at	GPM6B	Glycoprotein M6B
Bt.12768.1.S1_at	PCK1	phosphoenolpyruvate carboxykinase 1 (soluble)
Bt.12598.1.S1_at	LOC505573	similar to Cartilage intermediate layer protein, nucleotide pyrophosphohydrolase
Bt.12443.1.S1_at	CD82 /// LOC783413	CD82 molecule /// similar to CD82 molecule
Bt.11576.1.S1_at	SSAT2	polyamine N-acetyltransferase
Bt.11019.1.S1_at	LOC613597	similar to KIAA1195 protein
Bt.10980.1.S1_at	LOC522913	similar to ATP-binding cassette, sub-family C, member 9 isoform SUR2B
Bt.10076.1.S1_at	RCSD1	RCSD domain containing 1

Probe Set ID	Gene Symbol	Gene Title
Bt.8141.1.S1_at	UGT8	UDP glycosyltransferase 8 (UDP-galactose ceramide galactosyltransferase)
Bt.5013.1.A1_at	LOC789183	similar to Mib
Bt.430.2.S1_a_at	CSH1 /// PRCII	chorionic somatomammotropin hormone 1 (placental lactogen) /// prolactin-related
Bt.3101.1.A1_at	LOC539379	similar to STARS
Bt.29752.1.A1_at	LOC613361	Hypothetical LOC613361
Bt.28735.1.A1_at	LOC781271	similar to Gag-Pro-Pol-Env protein
Bt.26959.2.S1_at	MVK	mevalonate kinase (mevalonic aciduria)
Bt.23852.1.A1_at	RPS4X /// RPS4Y1	ribosomal protein S4, X-linked /// ribosomal protein S4, Y-linked 1
Bt.22555.2.S1_at	LOC514045	Hypothetical LOC514045
Bt.21798.1.S1_at	LOC528288	Similar to FLJ00102 protein
Bt.20832.1.S1_at	HNF-3a	hepatocyte nuclear factor 3 alpha
Bt.1978.14.A1_at	LOC613389	T-cell receptor beta chain V region
Bt.1920.1.S1_at	LOC514624	similar to Stard10 protein
Bt.16477.1.A1_at	LOC520327	Similar to Kynureninase (L-kynurenine hydrolase)
Bt.9838.1.S1_at	FABP6	fatty acid binding protein 6, ileal
Bt.9759.1.S1_at	NGDN	neuroguidin, EIF4E binding protein
Bt.9699.1.S1_at	CYP26	cytochrome P450 retinoic acid hydroxylase
Bt.9596.1.S1_at	MGC127202	similar to Chain A, High Resolution Solution Structure Of Human Intestinal Trefo
Bt.9233.2.S1_at	LOC506751	similar to Laminin alpha-5 chain
Bt.9225.1.A1_at	MGC152634	similar to Hexokinase 3 (white cell)
Bt.9075.1.S1_at	LOC510923	Similar to estrogen responsive finger protein
Bt.9071.2.S1_a_at	MGC139710	similar to CG18177-PB
Bt.9053.2.S1_a_at	LRP16	LRP16 protein
Bt.9.2.S1_a_at	PRKG1	protein kinase, cGMP-dependent, type I
Bt.8957.1.S1_at	CXCR4	chemokine (C-X-C motif) receptor 4
Bt.8925.2.S1_at	TMEM15	transmembrane protein 15
Bt.879.1.S1_at	---	Transcribed locus, moderately similar to NP_001008802.1 type II keratin Kb1 [Rat
Bt.8788.2.S1_a_at	LOC514115	similar to Wdr33 protein
Bt.8719.1.S1_a_at	LOC511744	similar to L-seryl-tRNA(Ser/Sec) kinase (Phosphoseryl-tRNA(Ser/Sec) kinase)
Bt.8549.2.S1_at	MGC137169	hypothetical LOC511765
Bt.8504.1.A1_at	LOC507482	similar to fragile X mental retardation 1
Bt.8436.1.S1_at	IFI6	interferon, alpha-inducible protein 6
Bt.83.1.S1_a_at	DNAJC5	DnaJ (Hsp40) homolog, subfamily C, member 5
Bt.8286.1.S1_at	PDK2	pyruvate dehydrogenase kinase, isozyme 2
Bt.8250.1.S1_at	---	Transcribed locus, strongly similar to NP_776612.1 secreted phosphoprotein 1 [Bo
Bt.8247.1.A1_at	LOC518364	similar to OHCU decarboxylase
Bt.8238.1.A1_at	TRIB3	tribbles homolog 3 (Drosophila)
Bt.8080.1.S1_at	LOC531018	similar to putative membrane steroid receptor
Bt.8024.2.S1_at	LOC541155	similar to myotubularin-related protein 1
Bt.7555.2.S1_at	SMAP1L	stromal membrane-associated protein 1-like
Bt.7449.1.A1_at	RFWD2	ring finger and WD repeat domain 2
Bt.7339.1.S1_at	LOC513110	amino acid transporter
Bt.7337.1.A1_at	LOC781512	similar to ARAP2
Bt.7237.2.S1_a_at	HADHA	hydroxyacyl-Coenzyme A dehydrogenase/3-ketoacyl-Coenzyme A thiolase/enoyl-Coenzy
Bt.7161.2.A1_at	MGC139542	Similar to spermatid perinuclear RNA-binding protein
Bt.7056.2.A1_at	HBG	Hemoglobin, gamma
Bt.7003.1.S1_at	LPXN	leupaxin
Bt.687.1.S1_at	MGC165904	similar to caspase recruitment domain family, member 11
Bt.6851.1.S1_at	B4GALT5	UDP-Gal:betaGlcNAc beta 1,4- galactosyltransferase, polypeptide 5
Bt.6805.2.S1_at	SMNDC1	survival motor neuron domain containing 1
Bt.6775.1.S1_at	ANXA3	annexin A3
Bt.6646.2.S1_a_at	LOC516199	similar to nuclear LIM interactor-interacting factor
Bt.6586.2.S1_at	LOC789485	similar to Notch3
Bt.6556.1.S1_at	LOC504773	regakine-1 protein
Bt.6523.2.S1_at	LOC613977	similar to TPA-induced transmembrane protein
Bt.6434.1.S1_at	LOC506267	hypothetical LOC506267
Bt.6410.2.A1_s_at	LOC505518	Similar to placenta expressed transcript protein
Bt.6408.1.S1_at	LOC506809	similar to transcription factor GATA-2
Bt.6068.3.S1_a_at	MGC142307	similar to topoisomerase (DNA) III alpha
Bt.605.1.S1_at	GDF8	growth differentiation factor 8
Bt.6048.2.S1_at	LOC532237	similar to pleckstrin and Sec7 domain containing 4
Bt.6028.2.S1_at	LOC514160	similar to ubiquitin ligase
Bt.6012.1.S1_at	TNNC1	troponin C type 1 (slow)
Bt.5789.1.S1_at	SPNS1	spinster homolog 1 (Drosophila)
Bt.5503.2.S1_at	NME4	non-metastatic cells 4, protein expressed in
Bt.5193.2.S1_at	LOC517002	similar to uteroferrin
Bt.5152.1.S1_at	FECH	ferrochelatase
Bt.5151.1.S1_at	EFNA2	ephrin-A2
Bt.5141.1.S2_at	B4GALT1	UDP-Gal:betaGlcNAc beta 1,4- galactosyltransferase, polypeptide 1
Bt.5003.1.S1_at	EMCN	endomucin
Bt.4977.1.S1_at	IGF2R	insulin-like growth factor 2 receptor

Probe Set ID	Gene Symbol	Gene Title
Bt.4856.1.S1_at	IL1B	interleukin 1, beta
Bt.4811.3.A1_at	MGC166020	Similar to Rac3
Bt.4811.1.S1_at	MGC166020	similar to Rac3
Bt.4774.1.S2_at	GNAT1	guanine nucleotide binding protein (G protein), alpha transducing activity polyp
Bt.4772.2.S1_a_at	MGC154983	Similar to ataxin-1 ubiquitin-like interacting protein
Bt.468.1.S1_at	CFTR	cystic fibrosis transmembrane conductance regulator
Bt.4675.1.S1_a_at	MX1	myxovirus (influenza virus) resistance 1, interferon-inducible protein p78 (mous
Bt.4653.1.S2_at	PECAM1	platelet/endothelial cell adhesion molecule
Bt.462.1.S1_at	PRKAR2B	protein kinase, cAMP-dependent, regulatory, type II, beta
Bt.4547.1.S1_at	NTT73	homolog of rat orphan transporter v7-3
Bt.4529.1.S1_at	FNTB	farnesyltransferase, CAAX box, beta
Bt.4477.2.S1_at	C2orf24	chromosome 2 open reading frame 24
Bt.4462.1.S1_at	MGC140564	similar to Type-1 angiotensin II receptor-associated protein (AT1 receptor-assoc
Bt.4430.1.S1_at	ATP6V0A1 /// LOC785923	ATPase, H+ transporting, lysosomal V0 subunit a1 /// similar to vacuolar H+-ATPa
Bt.4389.1.S1_at	LOC404103	spleen trypsin inhibitor
Bt.4360.1.S1_at	CYB561	cytochrome b-561
Bt.4336.1.S1_at	DF	D component of complement (adipsin)
Bt.4153.1.S1_at	DUSP12	dual specificity phosphatase 12
Bt.4147.1.S1_at	PDE6A	phosphodiesterase 6A, cGMP-specific, rod, alpha
Bt.4109.1.S1_at	LOC510024	similar to A-kinase anchor protein 13
Bt.3885.2.S1_at	LOC784768	similar to calcium-activated chloride channel
Bt.3763.1.S1_at	MGC138063	hypothetical LOC533158
Bt.376.1.S2_at	NPR3	natriuretic peptide receptor C
Bt.3753.2.S1_at	LOC534434	Similar to KIAA0614 protein
Bt.373.2.S1_a_at	AMELX /// AMELY	amelogenin (amelogenesis imperfecta 1, X-linked) /// amelogenin, Y-linked
Bt.3717.1.A1_at	ZFAND5	Zinc finger, AN1-type domain 5
Bt.3460.1.A1_at	SH3BGRL	SH3 domain binding glutamic acid-rich protein like
Bt.3451.1.A1_at	LOC787340	hypothetical protein LOC787340
Bt.3402.1.S1_at	MGC165864	similar to Katanin p80 (WD repeat containing) subunit B 1
Bt.3362.1.S1_at	LOC522886	similar to periplakin
Bt.3273.2.S1_at	MGC139254	hypothetical LOC510183
Bt.3258.2.S1_at	ZNF435	zinc finger protein 435
Bt.3253.3.S1_at	LOC617871	hypothetical LOC617871
Bt.3238.1.S1_at	FLJ36874	hypothetical protein LOC537453
Bt.3236.2.S1_at	LOC782247	similar to RhoGEF protein
Bt.3052.1.S1_at	LOC509972	Similar to Ocil/Clrb-like protein
Bt.29963.1.S1_at	FGD1	FYVE, RhoGEF and PH domain containing 1
Bt.29878.1.A1_at	GR-A	alpha-glucocorticoid receptor
Bt.29824.1.S1_s_at	BOLA	MHC class I heavy chain
Bt.29806.1.S1_at	LOC407113 /// LOC407991	growth hormone receptor
Bt.29793.1.A1_at	IGHG1	Immunoglobulin heavy constant gamma 1
Bt.29786.1.S1_x_at	---	Glutathione-S-transferase (GST) specific immunoglobulin light chain variable reg
Bt.29778.1.A1_at	bTrappin-5	trappin 5
Bt.29760.1.A1_s_at	LOC507050	Similar to T-cell receptor beta chain variable segment
Bt.29757.1.A1_x_at	LOC783911	Hypothetical protein LOC783911
Bt.29741.1.A1_at	---	Immunoglobulin heavy chain mRNA, variable region, partial cds, 5' end
Bt.29735.1.S1_at	---	Immunoglobulin variable region
Bt.29718.2.A1_at	GHR	growth hormone receptor
Bt.29717.2.A1_a_at	GHR	growth hormone receptor
Bt.29695.1.A1_s_at	TRGV3-2	T cell receptor gamma variable 3-2
Bt.29686.1.S1_at	FGFR2	fibroblast growth factor receptor 2
Bt.29666.1.A1_at	MGC138924	similar to G protein-coupled receptor 128
Bt.29328.1.S1_at	ASPH	aspartate beta-hydroxylase
Bt.29290.1.S1_at	LOC525143	similar to PI-3-kinase-related kinase SMG-1
Bt.29277.1.S1_at	LRRC51	leucine rich repeat containing 51
Bt.29152.2.A1_at	TSPAN12	tetraspanin 12
Bt.29143.1.S1_at	MGC139389	similar to B-cell CLL/lymphoma 11A
Bt.29025.1.A1_at	LOC523809	similar to KIAA1959 protein
Bt.28871.1.A1_at	MGC152152	Similar to GINS complex subunit 1 (Psf1 homolog)
Bt.28792.1.S1_at	---	CDNA clone IMAGE:8310187
Bt.28780.2.A1_at	LOC505234	similar to FYVE, RhoGEF and PH domain-containing protein 4 (Actin filament-bindi
Bt.28744.1.S1_at	MGC157238	similar to mFLJ00316 protein
Bt.28667.2.S1_at	MGC159992	similar to Armadillo repeat-containing protein 6
Bt.28625.1.S1_at	LOC538219	similar to ARHGAP26 protein
Bt.28605.1.S1_at	MGC148293	similar to phospholipase inhibitor
Bt.28604.2.S1_a_at	MGC137499	hypothetical LOC511775
Bt.28494.7.A1_x_at	LOC524810	IgM
Bt.28459.1.S1_at	BMP4	bone morphogenetic protein 4
Bt.28446.1.S1_at	BVd1.25 /// LOC613744 ///	T cell receptor delta chain variable region /// hypothetical LOC613744 /// hypot

Probe Set ID	Gene Symbol	Gene Title
	LOC786775	
Bt.28444.1.S1_at	LOC617281	similar to T-cell receptor beta chain variable segment
Bt.28438.2.S1_at	RGS13	regulator of G-protein signaling 13
Bt.28338.1.S1_at	MGC166160	hypothetical LOC514617
Bt.28313.1.S1_at	LOC512905	similar to CDNA sequence BC085284
Bt.28252.2.S1_a_at	LOC525379	similar to syntaxin 10
Bt.28225.2.S1_at	SAMSN1	SAM domain, SH3 domain and nuclear localization signals 1
Bt.28191.2.S1_at	LOC511230	similar to DENN/MADD domain containing 1C
Bt.28172.2.A1_at	VSIG1	V-set and immunoglobulin domain containing 1
Bt.28022.1.A1_s_at	BOLA-NC1	Non-classical MHC class I antigen
Bt.27983.1.S1_at	BMPRIB	bone morphogenetic protein receptor IB
Bt.27979.1.A1_at	cd4	CD4 antigen
Bt.27978.1.S1_at	ITGAM	integrin, alpha M (complement component 3 receptor 3 subunit)
Bt.27976.1.A1_at	TIMP1	TIMP metallopeptidase inhibitor 1
Bt.27974.1.A1_at	LOC407094	similar to heregulin-beta1
Bt.27866.1.A1_at	LOC508591	similar to myo-inositol oxygenase
Bt.27852.2.S1_at	PGPEP1	pyroglutamyl-peptidase I
Bt.27838.2.S1_a_at	LOC513374 /// MGC152326	similar to PHLDB3 protein /// similar to Pleckstrin homology-like domain family
Bt.27826.1.S1_at	RASGEF1B	RasGEF domain family, member 1B
Bt.27790.1.A1_at	MGC148413	Similar to dynactin 1 p150
Bt.27757.1.S1_at	LOC513513	similar to chitinase
Bt.27720.1.A1_at	Oasl	2'-5' oligoadenylate synthetase-like protein
Bt.27621.1.A1_at	MGC155048	similar to autoantigen
Bt.27616.1.A1_at	LOC541035	similar to zinc-finger protein of the cerebellum 3
Bt.27605.1.A1_at	MGC160064	similar to Potassium inwardly-rectifying channel, subfamily J, member 15
Bt.27538.1.A1_at	LOC509789	hypothetical LOC509789
Bt.27517.2.A1_at	LOC515764	similar to Pancreatic triacylglycerol lipase precursor (Pancreatic lipase) (PL)
Bt.27460.1.A1_at	LOC538665	similar to MAGEL2 protein
Bt.27442.1.S1_at	LOC535260	similar to AASA9217
Bt.27419.1.S1_at	SOX2	SRY (sex determining region Y)-box 2
Bt.27400.1.S1_at	PCDHA13	protocadherin alpha 13
Bt.2737.1.S1_at	MGC127744	similar to Carbonic anhydrase III (Carbonate dehydratase III) (CA-III)
Bt.27339.2.S1_at	LOC536741	similar to Mme protein
Bt.27338.1.S1_at	MGC139028	hypothetical LOC508965
Bt.27320.2.S1_at	LOC532412	similar to Shugoshin-like 2 (S. pombe)
Bt.27313.1.A1_at	CSPG5	chondroitin sulfate proteoglycan 5 (neuroglycan C)
Bt.27311.1.A1_at	GPR173	G protein-coupled receptor 173
Bt.27208.2.S1_at	AGPAT3	1-acylglycerol-3-phosphate O-acyltransferase 3
Bt.27163.1.A1_at	LOC784144	hypothetical protein LOC784144
Bt.26990.2.S1_at	LOC517833 /// LOC788103	similar to TWEAK
Bt.26968.1.S1_at	LOC518168	similar to VESPR
Bt.26929.1.S1_at	TUBGCP5	tubulin, gamma complex associated protein 5
Bt.26874.1.S1_at	DKFZP761E198	hypothetical protein LOC509087
Bt.26851.1.S1_at	DRAM	damage-regulated autophagy modulator
Bt.26690.1.S1_at	MGC148790	similar to CDC-like kinase 1
Bt.26613.1.A1_at	LOC615530	hypothetical LOC615530
Bt.2659.1.A1_at	LOC618375	similar to Fanconi anemia, complementation group A
Bt.26570.1.S1_at	LOC513885	similar to Chromosome 12 open reading frame 26
Bt.26545.1.A1_at	LOC536269	similar to methylenetetrahydrofolate dehydrogenase (NADP+ dependent) 2-like
Bt.26428.1.A1_at	MGC137752	similar to Y55F3AM.9
Bt.26309.1.A1_at	LOC781881	hypothetical protein LOC781881
Bt.26254.1.A1_at	LOC505383	similar to chapsyn-110
Bt.26235.1.A1_at	ELMO1	Engulfment and cell motility 1
Bt.26192.1.A1_at	LOC534164	similar to SLIT2
Bt.26155.1.A1_at	NPL	N-acetylneuraminate pyruvate lyase (dihydrodipicolinate synthase)
Bt.26077.1.A1_at	NRXN3	neurexin 3
Bt.26046.1.A1_at	LOC507731	similar to cdc25 protein
Bt.2598.1.S1_at	ALOX15	arachidonate 15-lipoxygenase
Bt.25880.1.A1_at	LOC537141	similar to mKIAA1921 protein
Bt.25874.3.S1_a_at	MST1	macrophage stimulating 1 (hepatocyte growth factor-like)
Bt.25874.2.S1_at	MST1	macrophage stimulating 1 (hepatocyte growth factor-like)
Bt.25846.1.A1_at	LOC525946	similar to Ephrin type-A receptor 1 precursor (Tyrosine-protein kinase receptor
Bt.25789.1.A1_at	LOC785219	Similar to Mono (ADP-ribosyl)transferase
Bt.25767.1.S1_at	LOC527517	similar to putative G protein-coupled receptor
Bt.25743.1.A1_at	UOX	urate oxidase
Bt.25690.1.S1_at	MGC45404	mitogen-activated protein kinase kinase kinase 7 interacting protein 3
Bt.25668.1.S1_at	MGC128628	similar to F37C4.6
Bt.25662.1.A1_at	MTG1	mitochondrial GTPase 1 homolog (S. cerevisiae)
Bt.256.1.S1_at	PAG4	pregnancy-associated glycoprotein 4
Bt.25587.1.A1_at	MGC157389	similar to SERPINI2 protein
Bt.25576.1.A1_at	LOC615880	similar to KIAA1910 protein

Probe Set ID	Gene Symbol	Gene Title
Bt.25550.1.A1_at	LOC534284	similar to senataxin
Bt.25422.1.A1_at	AP1G2	Adaptor-related protein complex 1, gamma 2 subunit
Bt.25404.2.S1_at	LOC531254	similar to alpha 1 type XXIV collagen
Bt.25393.1.A1_at	GABRA1	gamma-aminobutyric acid (GABA) A receptor, alpha 1
Bt.25374.1.A1_at	LOC789280	hypothetical protein LOC789280
Bt.25320.1.S1_at	SCRN3	secernin 3
Bt.25031.1.S1_at	LOC528870	similar to neuron navigator 3
Bt.25030.1.A1_a_at	MGC152009	similar to transmembrane 9 superfamily member 2
Bt.25008.1.A1_at	LOC534053	Similar to laminin B2
Bt.24997.1.S1_at	---	Transcribed locus, strongly similar to XP_996409.1 PREDICTED: similar to CG4502-
Bt.24884.1.A1_a_at	LOC511847	similar to GMCSFR receptor
Bt.24849.1.A1_at	FLAD1	FAD1 flavin adenine dinucleotide synthetase homolog (S. cerevisiae)
Bt.248.1.S1_at	CD38	CD38 molecule
Bt.24783.2.S1_at	LOC504869	similar to FRAP-related protein
Bt.24694.1.A1_at	LOC511689	Similar to KIAA1237 protein
Bt.24598.1.A1_at	MGC137508	similar to CG10053-PA
Bt.24583.1.A1_at	MGC157094	similar to NG7
Bt.24512.1.A1_at	LOC538746	similar to Membrane-associated transporter protein (Solute carrier family 45 mem
Bt.24467.1.S1_at	MGC128573	similar to radical S-adenosyl methionine domain containing 2
Bt.24318.1.A1_at	SLC22A9	solute carrier family 22 (organic anion/cation transporter), member 9
Bt.24288.2.S1_at	LOC513059	similar to ATP(GTP)-binding protein
Bt.24225.1.S1_at	---	Clone NG010006B11A03 mRNA, complete sequence
Bt.24133.1.A1_at	---	Transcribed locus, strongly similar to NP_777000.1 phosphoinositide-3-kinase, re
Bt.24098.1.A1_at	LOC535490	similar to melanoma differentiation associated protein-5
Bt.23912.1.A1_a_at	CYP2E1	cytochrome P450 subfamily IIE polypeptide 1
Bt.23775.1.A1_at	LOC520530	similar to HIC protein isoform p32
Bt.23729.1.A1_at	PLAC8	placenta-specific 8
Bt.23559.1.S1_at	TPK1	thiamin pyrophosphokinase 1
Bt.23523.2.S1_at	TUSC5	tumor suppressor candidate 5
Bt.23503.2.S1_a_at	DOM3Z	DOM-3 homolog Z
Bt.234.1.S1_at	IL18	interleukin 18 (interferon-gamma-inducing factor)
Bt.23355.1.S1_at	LOC615191	similar to protein tyrosine phosphatase-like protein PTPLA
Bt.2333.1.S1_at	LOC618893	similar to JNK MAP kinase scaffold protein JIP2
Bt.23055.3.S1_at	DLG5	discs, large homolog 5 (Drosophila)
Bt.22978.1.S1_at	IFITM1	interferon induced transmembrane protein 1 (9-27)
Bt.22832.1.S1_at	LOC513951	hypothetical LOC513951
Bt.22773.2.S1_at	SLC25A19	solute carrier family 25 (mitochondrial thiamine pyrophosphate carrier), member
Bt.22770.1.S1_at	LOC511229	similar to CARD8 protein
Bt.22768.1.A1_at	LOC781282	similar to polydom
Bt.22739.2.S1_at	SOCS4	suppressor of cytokine signaling 4
Bt.22726.3.S1_a_at	MGC157244	similar to Carbonic anhydrase-related protein (CARP) (CA-VIII)
Bt.22715.1.A1_at	ROPN1L	ropporin 1-like
Bt.227.3.A1_x_at	GSTA1	glutathione S-transferase A1
Bt.22692.1.A1_at	IL6R	interleukin 6 receptor
Bt.22647.3.A1_at	LOC532952	similar to membrane-associated guanylate kinase-related 3 (MAGI-3)
Bt.22629.1.A1_at	LOC515053	hypothetical LOC515053
Bt.22430.1.A1_at	CYBB	cytochrome b-245, beta polypeptide
Bt.22410.2.S1_at	ARF3	ADP-ribosylation factor 3
Bt.22285.2.S1_at	LSS	lanosterol synthase (2,3-oxidosqualene-lanosterol cyclase)
Bt.22279.1.S1_at	LOC614739	hypothetical LOC614739
Bt.22264.1.S1_at	MGC140699	similar to p53-induced protein
Bt.22234.1.S1_at	LOC505901	similar to protein kinase C-theta
Bt.22119.1.S1_at	E2F1	E2F transcription factor 1
Bt.22058.1.A1_at	MGC151596	Similar to hect domain and RLD 5
Bt.22056.1.S1_a_at	MGC127615	similar to abhydrolase domain containing 1 (predicted)
Bt.21943.1.S1_at	LOC524460	similar to UDP-Gal:glucosylceramide beta-1,4-galactosyltransferase
Bt.21924.2.S1_at	LOC535975	similar to dermatan/chondroitin sulfate 2-sulfotransferase
Bt.21914.1.S1_at	LOC785293	similar to actin-binding protein
Bt.21845.1.S1_at	LOC614141	hypothetical LOC614141
Bt.2179.1.S1_at	MGC166009	similar to KIAA0360
Bt.21766.1.A1_at	MLF1	Myeloid leukemia factor 1
Bt.2172.1.S1_at	LOC510736	similar to HEPH
Bt.21706.2.A1_a_at	MGC152081	similar to carboxypeptidase A5
Bt.21673.1.S1_at	CSNK1E	casein kinase 1, epsilon
Bt.21672.1.S1_at	---	Transcribed locus, moderately similar to XP_993763.1 PREDICTED: hypothetical pro
Bt.21662.2.S1_at	ATP6V0E2	ATPase, H+ transporting V0 subunit e2
Bt.21658.1.S1_at	MGC139070	similar to inositol 1,4,5-trisphosphate 3-kinase C
Bt.21467.1.S1_at	MGC129017	similar to Conserved oligomeric Golgi complex component 4
Bt.21420.1.A1_at	LOC505228	Similar to thyroid hormone receptor associated protein 3
Bt.21366.1.A1_at	MGC166108	similar to GUF1 GTPase homolog (S. cerevisiae)
Bt.21354.1.A1_at	LOC514036	Similar to GDNF family receptor alpha 2 preproprotein
Bt.21300.1.S1_at	LOC513253	hypothetical LOC513253
Bt.21177.1.A1_s_at	LOC511229	similar to CARD8 protein

Probe Set ID	Gene Symbol	Gene Title
Bt.21113.1.S1_a_at	CPT1B	carnitine palmitoyltransferase 1B
Bt.20921.1.A1_at	BSG	basigin
Bt.209.2.S1_a_at	LYZ /// LYZ2 /// LYZ3	lysozyme C-2 /// lysozyme 3 /// lysozyme (renal amyloidosis)
Bt.20860.3.A1_at	MGC165794	similar to calcyphosine-like
Bt.20850.2.A1_at	LOC520186	similar to centrosomal protein 110kDa
Bt.20836.1.S1_at	LOC783547	similar to mannose receptor C1
Bt.20833.3.A1_at	MGC140213	hypothetical LOC534327
Bt.20833.1.S1_at	MGC140213	hypothetical LOC534327
Bt.20817.2.S1_at	POLA1	polymerase (DNA directed), alpha
Bt.20799.3.A1_at	DOCK1	dedicator of cytokinesis 1
Bt.20733.1.S1_at	LOC532836	similar to Adenosylhomocysteinase 3
Bt.20613.3.S1_at	BCAR3	breast cancer anti-estrogen resistance 3
Bt.20521.2.S1_at	LOC510910	similar to leukocyte differentiation antigen CD84
Bt.20520.1.S1_at	LOC506858	similar to Solute carrier family 25 (mitochondrial carrier; dicarboxylate transp
Bt.20416.1.S1_at	LOC524959	similar to transporter 1 ATP-binding cassette sub-family B
Bt.20381.1.A1_at	F2R	coagulation factor II (thrombin) receptor
Bt.20318.2.S1_at	NQO2	NAD(P)H dehydrogenase, quinone 2
Bt.20219.3.S1_at	LOC504724	similar to phosphatidyl inositol glycan class T
Bt.20131.1.S1_at	MGC151555	similar to fatty acid desaturase domain family, member 6
Bt.20015.1.S1_at	CART	cocaine and amphetamine responsive transcript
Bt.20005.1.S1_at	LOC513482	putative oxidoreductase
Bt.20003.1.A1_at	TAT	tyrosine aminotransferase
Bt.19972.1.S1_at	PEPT1	proton-dependent gastrointestinal peptide transporter 1
Bt.19899.1.A1_at	HGD	homogentisate 1,2-dioxygenase (homogentisate oxidase)
Bt.19825.1.S1_at	LOC510467	similar to UDP glucuronosyltransferase 2 family, polypeptide B4
Bt.19790.1.A1_at	TRIM22	tripartite motif-containing 22
Bt.19647.2.S1_at	LOC529062	similar to Ankyrin repeat domain-containing protein 28
Bt.19620.1.A1_at	LOC508348 /// LOC781857	similar to Interferon-induced protein 44 (Antigen p44) (Non-A non-B hepatitis-as
Bt.1948.1.S1_at	MAEA	macrophage erythroblast attacher
Bt.1945.1.A1_at	LOC537451	similar to glycogen synthase
Bt.19408.1.A1_at	MGC148776	Hypothetical LOC535746
Bt.19305.1.A1_at	MGC139794	Similar to Transmembrane protein 17
Bt.19111.1.A1_at	MGC152108	similar to zinc finger protein 211
Bt.19083.1.S1_at	ANKRD22	ankyrin repeat domain 22
Bt.19028.1.A1_at	trp6	Transient receptor potential channel 6
Bt.19001.1.S1_at	MT-2	metallothionein-2
Bt.18918.1.S1_at	SEC22C	SEC22 vesicle trafficking protein homolog C (S. cerevisiae)
Bt.18895.1.A1_at	---	Transcribed locus, strongly similar to NP_001028686.1 G protein-coupled receptor
Bt.18860.1.A1_at	LOC531875	similar to protocadherin 10
Bt.18837.2.A1_at	LOC512304	similar to ENPP5
Bt.18827.1.A1_at	LOC529195	similar to PYRIN
Bt.18750.1.A1_at	LOC540473	similar to Achaete-scute complex homolog 1 (Drosophila)
Bt.18739.1.A1_at	MGC134379	Similar to serine active site containing 1
Bt.18710.2.A1_at	---	Transcribed locus, strongly similar to NP_056629.1 dickkopf homolog 3 [Mus muscu
Bt.18639.2.S1_at	FBXO32	F-box protein 32
Bt.18557.1.S1_at	C7	complement component 7
Bt.18526.1.A1_at	LOC617176	Hypothetical LOC617176
Bt.18476.1.A1_at	IRF5	interferon regulatory factor 5
Bt.18473.1.S1_at	MGC142910	similar to CSaids binding protein
Bt.18444.1.A1_at	LOC538492	Hypothetical LOC538492
Bt.18440.3.A1_at	LOC510382	hypothetical LOC510382
Bt.18426.1.A1_s_at	---	Transcribed locus, moderately similar to NP_001005369.1 mitochondrial translatio
Bt.18316.2.S1_at	LOC513587	similar to Adult retina protein
Bt.18292.1.A1_at	LOC616277	similar to MOK protein kinase
Bt.18116.3.A1_s_at	LOC513185	hypothetical LOC513185
Bt.18114.1.A1_at	---	Transcribed locus, strongly similar to NP_803474.1 uridine monophosphate synthet
Bt.18080.3.A1_at	LOC509794	similar to TESC protein
Bt.17994.2.A1_at	CENPO	Centromere protein O
Bt.17898.1.A1_at	LOC613821	similar to aster-associated protein
Bt.17878.1.A1_at	---	Transcribed locus, strongly similar to NP_001070405.1 hypothetical protein LOC61
Bt.17868.1.A1_at	LOC506859	similar to KIAA1588 protein
Bt.17854.1.A1_at	POU2AF1	POU class 2 associating factor 1
Bt.17805.1.S1_at	NUDT12	nudix (nucleoside diphosphate linked moiety X)-type motif 12
Bt.17758.1.S1_at	LOC541088 /// LOC784529	similar to BCL-6 corepressor
Bt.17754.1.A1_at	LOC515491	Similar to KIAA1412 protein
Bt.17731.2.S1_at	MGC148584	Similar to KIAA0843 protein
Bt.17701.1.A1_at	ZFP2	zinc finger protein 2 homolog
Bt.17685.1.A1_at	MGC133676	hypothetical LOC504348
Bt.17682.1.A1_s_at	LOC514596	similar to Chromosome 3 open reading frame 29
Bt.17594.1.S1_at	WDR5	WD repeat domain 5

Probe Set ID	Gene Symbol	Gene Title
Bt.17585.1.S2_at	ST3GAL-V	alpha2,3-sialyltransferase
Bt.17479.1.A1_at	MGC133968	similar to calcium-binding tyrosine-phosphorylation regulated protein
Bt.17468.1.A1_at	---	Transcribed locus, moderately similar to NP_694591.1 tudor domain containing 9 [
Bt.17311.2.S1_at	RP2	retinitis pigmentosa 2 (X-linked recessive)
Bt.17295.1.A1_at	LOC524465	Similar to CG9003-PA
Bt.17265.2.S1_at	NR1H3	nuclear receptor subfamily 1, group H, member 3
Bt.17227.1.A1_at	LOC532564	Similar to leishmanolysin-like (metallopeptidase M8 family)
Bt.17116.1.A1_at	LOC507749	similar to Complement component C6 precursor
Bt.16997.1.A1_at	LOC790043	Hypothetical protein LOC790043
Bt.16924.1.A1_at	SEPP1	selenoprotein P, plasma, 1
Bt.16838.1.S1_at	LOC512905	similar to CDNA sequence BC085284
Bt.16782.2.S1_at	MGC143433	similar to adenylosuccinate synthetase
Bt.16689.2.A1_at	LOC538447	Similar to serine/threonine kinase
Bt.16668.1.A1_at	TRIM45	tripartite motif-containing 45
Bt.16666.1.A1_at	LOC519739	hypothetical LOC519739
Bt.16495.2.A1_at	LOC511602	similar to alpha-5 type IV collagen
Bt.16481.2.A1_at	---	Transcribed locus, weakly similar to XP_001496051.1 PREDICTED: similar to zinc f
Bt.16450.2.A1_at	LOC540735	Similar to Protein KIAA0853
Bt.16350.1.S1_at	MGC142842	Similar to guanylate-binding protein 5
Bt.16331.1.S1_at	PDHB	Pyruvate dehydrogenase (lipoamide) beta
Bt.16291.1.A1_at	TEX12	testis expressed 12
Bt.16175.1.A1_at	LOC536187	similar to cytoplasmic activation/proliferation-associated protein 2
Bt.16119.1.S1_at	MGC157040	hypothetical LOC513646
Bt.1607.2.S1_at	LOC526310	similar to KIAA0722 protein
Bt.16046.1.A1_at	LOC532798	similar to Chromosome 1 open reading frame 96
Bt.16016.1.S1_at	P2RX5	purinergic receptor P2X, ligand-gated ion channel, 5
Bt.160.3.S1_a_at	DSC1	desmocollin 1
Bt.15987.1.S1_at	LOC784833 /// PAG19	pregnancy-associated glycoprotein 19 /// similar to pregnancy-associated glycopr
Bt.15887.1.S1_at	LOC509076	hypothetical LOC509076
Bt.15836.2.S1_at	ANKRD1	ankyrin repeat domain 1 (cardiac muscle)
Bt.15797.1.S1_at	LOC507834	Hypothetical LOC507834
Bt.15788.3.S1_at	LOC507402	Similar to Bone marrow stromal cell antigen 2
Bt.15736.1.S1_at	LOC512972	similar to Histocompatibility (minor) HA-1
Bt.15653.1.S1_at	DSC2	desmocollin 2
Bt.1525.1.S1_at	Aqp1	aquaporin 1
Bt.152.1.S1_at	LOC282685	rhesus-like protein
Bt.14734.2.A1_at	MGC137099	hepatitis A virus cellular receptor 1 N-terminal domain containing protein
Bt.14568.1.A1_at	LOC508264	similar to afamin
Bt.145.1.S1_at	RGS9	regulator of G-protein signaling 9
Bt.14266.1.A1_a_at	LOC514509	similar to Agmatine ureohydrolase (agmatinase)
Bt.14238.1.A1_at	CRYAA	crystallin, alpha A
Bt.14153.1.S1_at	LOC407121	nebulin
Bt.13974.1.A1_at	LOC617055	similar to BANK
Bt.13968.2.S1_at	---	Transcribed locus, strongly similar to XP_989204.1 PREDICTED: similar to phospho
Bt.13940.1.S1_at	LOC535138	similar to CDC91 cell division cycle 91-like 1 (S. cerevisiae)
Bt.13850.3.S1_a_at	LYPLA1	lysophospholipase I
Bt.13807.1.S1_at	SART1	squamous cell carcinoma antigen recognized by T cells
Bt.13798.2.S1_at	LOC615685	hypothetical LOC615685
Bt.13651.1.S1_at	LOC504822	similar to aminopeptidase P
Bt.13629.1.A1_at	MGC139474	similar to Inward rectifier potassium channel 16 (Potassium channel, inwardly re
Bt.13624.2.S1_at	FBXO15	F-box protein 15
Bt.13617.2.S1_a_at	MGC139118	similar to RIKEN cDNA 2810451A06
Bt.1344.1.S1_at	MGC140553	similar to Iron-responsive element binding protein 1 (IRE-BP 1) (Iron regulatory
Bt.13434.3.A1_at	MKRN1	Makorin, ring finger protein, 1
Bt.13428.1.S1_at	FBP2	fructose-1,6-bisphosphatase 2
Bt.134.1.S1_at	EPB42	erythrocyte membrane protein band 4.2
Bt.1332.1.S1_a_at	LOC511440	hypothetical LOC511440
Bt.13147.1.S1_at	B4GALT5	UDP-Gal:betaGlcNAc beta 1,4- galactosyltransferase, polypeptide 5
Bt.13114.1.S1_at	TTPA	tocopherol (alpha) transfer protein
Bt.13106.1.A1_at	F9	coagulation factor IX
Bt.13079.1.S1_at	MYOG	myogenin (myogenic factor 4)
Bt.13069.3.A1_at	CACNA1D	calcium channel, voltage-dependent, L type, alpha 1D
Bt.13065.1.S1_at	KCNJ8	potassium inwardly-rectifying channel, subfamily J, member 8
Bt.13051.1.S1_at	POLR1B	polymerase (RNA) I polypeptide B
Bt.13031.1.A1_at	MTR	5-methyltetrahydrofolate-homocysteine methyltransferase
Bt.12938.1.S1_at	NRXN3	neurexin 3
Bt.12904.2.S1_at	LOC506290	Hypothetical LOC506290
Bt.12902.1.S1_at	MGC165678	similar to ZNF304 protein
Bt.12783.1.A1_at	PDC	phosducin
Bt.12641.2.S1_at	PLVAP	plasmalemma vesicle associated protein
Bt.126.1.S2_at	KCNJ2	potassium inwardly-rectifying channel, subfamily J, member 2
Bt.12589.1.S1_at	LOC532965	similar to alpha3A chain laminin

Probe Set ID	Gene Symbol	Gene Title
Bt.12574.2.S1_at	LOC508320	similar to serine/threonine kinase 19
Bt.12452.1.A1_at	LOC536143	similar to GCN1 general control of amino-acid synthesis 1-like 1
Bt.12345.2.S1_at	LOC506730	similar to microfilament and actin filament cross-linker protein
Bt.12261.2.S1_at	C20orf13	taspase 1
Bt.12196.1.S1_at	cd45	membrane tyrosine phosphatase
Bt.12186.1.S1_at	INSL3	insulin-like 3 (Leydig cell)
Bt.11907.1.A1_at	MCPH1	microcephalin 1
Bt.11759.1.A1_at	PAX6	paired box 6
Bt.11590.1.A1_at	COL11A1	collagen, type XI, alpha 1
Bt.11459.2.A1_at	MGC152256	Similar to CG16790-PA
Bt.11455.1.A1_at	LOC505600 /// LOC782675 /// UTP14C	UTP14, U3 small nucleolar ribonucleoprotein, homolog C (yeast) /// similar to UT
Bt.1140.1.S1_at	MGC166188	similar to Non-metastatic cells 3, protein expressed in
Bt.11315.2.S1_at	LOC538958 /// LOC790188	similar to NCAG1
Bt.11262.1.S1_at	PEG3	paternally expressed 3
Bt.11218.1.S1_at	LRRC25	leucine rich repeat containing 25
Bt.11174.1.S1_at	KIR2DL1	killer cell immunoglobulin-like receptor, two domains, long cytoplasmic tail, 1
Bt.11167.1.S1_at	LOC505935	hypothetical LOC505935
Bt.11152.1.S1_at	LOC785246	similar to SAMD1 protein
Bt.11130.1.S1_at	DNMT1	DNA (cytosine-5-)-methyltransferase 1
Bt.11103.2.S1_at	LOC505541	similar to Ras-interacting protein 1
Bt.11080.1.S1_at	IL2RG	interleukin 2 receptor, gamma
Bt.1106.1.S1_at	MGC128574	similar to hsp70-interacting protein
Bt.10981.1.A1_at	MGC128728	similar to RNA polymerase I associated factor 53
Bt.10811.1.S1_at	MAPRE3	microtubule-associated protein, RP/EB family, member 3
Bt.10543.1.S1_at	LOC784675	Similar to KIAA1462 protein
Bt.1047.1.S1_at	LOC508291	similar to Huntingtin-interacting protein 1-related protein (Hip1-related) (Hip
Bt.10144.1.A1_s_at	MGC142564	similar to T-lymphoma invasion and metastasis inducing protein 1 (TIAM1 protein)
Bt.10102.2.S1_a_at	CCDC84 /// LOC785267	coiled-coil domain containing 84 /// similar to DLNB14
Bt.10089.1.S1_at	MGC152258	hypothetical LOC535263
Bt.9849.1.A1_at	LOC508470	hypothetical LOC508470
Bt.9745.1.A1_at	LOC507464	similar to keratin 15
Bt.9576.3.S1_at	COMMD4	COMM domain containing 4
Bt.9564.1.S1_at	LYPLA3	lysophospholipase 3 (lysosomal phospholipase A2)
Bt.8946.2.S1_a_at	SLCO1A2	solute carrier organic anion transporter family, member 1A2
Bt.8798.1.S1_at	LOC507093 /// LOC534200	similar to retinaldehyde dehydrogenase 3 /// similar to aldehyde dehydrogenase 6
Bt.8797.1.S1_at	MGC139675	similar to Rap1 GTPase-activating protein 1 (Rap1GAP)
Bt.8451.2.S1_at	MMAB	methylmalonic aciduria (cobalamin deficiency) cblB type
Bt.8427.1.S1_at	LOC537594	similar to phosphatase and actin regulator 1
Bt.8166.2.S1_at	CXXC5	CXXC finger 5
Bt.8144.1.S1_at	XCL1	chemokine (C motif) ligand 1
Bt.800.1.S1_at	MAPK13	mitogen-activated protein kinase 13
Bt.7919.1.A1_at	FXYD7	FXYD domain containing ion transport regulator 7
Bt.7873.1.S2_at	LU	Lutheran blood group (Auberger b antigen included)
Bt.7873.1.S1_at	LU	Lutheran blood group (Auberger b antigen included)
Bt.748.2.A1_at	POLR2J2	DNA directed RNA polymerase II polypeptide J-related gene
Bt.744.1.S1_at	ARID5A	AT rich interactive domain 5A (MRF1-like)
Bt.7346.1.S1_at	LOC507464	similar to keratin 15
Bt.7220.1.S1_at	BLA-DQB	MHC class II antigen
Bt.7056.5.A1_x_at	HBG /// LOC788610	hemoglobin, gamma /// hemoglobin, gamma 2
Bt.701.1.S1_at	LOC788007	similar to Fibronectin leucine rich transmembrane protein 1
Bt.6897.1.S1_at	LOC504848	similar to adaptor molecule-1
Bt.6702.1.S1_at	LOC538659	hypothetical LOC538659
Bt.6685.1.S1_at	MGC142685	similar to Bifunctional methylenetetrahydrofolate dehydrogenase/cyclohydrolase,
Bt.6653.1.S1_at	ALKBH4	AlkB, alkylation repair homolog 4
Bt.6141.1.S1_at	DES	desmin
Bt.5951.1.S1_at	LOC512922	similar to SplA/ryanodine receptor domain and SOCS box containing 4
Bt.5934.1.S1_at	---	Transcribed locus, strongly similar to NP_002488.1 NIMA (never in mitosis gene a
Bt.5919.2.S1_at	GDAP1L1	ganglioside-induced differentiation-associated protein 1-like 1
Bt.5848.2.S1_at	ATP2A1	ATPase, Ca++ transporting, cardiac muscle, fast twitch 1
Bt.55.1.S1_at	PDE6B	phosphodiesterase 6B, cGMP-specific, rod, beta (congenital stationary night blin
Bt.5488.1.S1_at	LOC514313	similar to phosphofurin acidic cluster sorting protein 1
Bt.5427.1.A1_at	SCG2	secretogranin II (chromogranin C)
Bt.538.1.S1_at	IL3	interleukin 3
Bt.537.1.S1_at	CRYGD	crystallin, gamma D
Bt.5348.1.S1_at	H19 /// LOC511905	hypothetical LOC511905 /// H19, imprinted maternally expressed untranslated mRNA
Bt.508.1.A1_at	SPP2	secreted phosphoprotein 2, 24kDa
Bt.5050.1.A1_at	CDH16	cadherin 16, KSP-cadherin

Probe Set ID	Gene Symbol	Gene Title
Bt.5014.1.S1_at	FGFR1	fibroblast growth factor receptor 1
Bt.501.1.S1_at	CHRM3	cholinergic receptor, muscarinic 3
Bt.5003.2.S1_a_at	EMCN	endomucin
Bt.49.1.S1_at	TNFSF5	tumor necrosis factor (ligand) superfamily, member 5
Bt.4867.2.S1_at	MYH8	myosin, heavy chain 8, skeletal muscle, perinatal
Bt.4804.3.A1_at	CDKN1C	cyclin-dependent kinase inhibitor 1C
Bt.4799.1.S1_at	SLC4A1	solute carrier family 4, anion exchanger, member 1 (erythrocyte membrane protein
Bt.4751.2.S1_at	BOLA-DQA2	major histocompatibility complex, class II, DQ alpha 2
Bt.4665.1.S1_at	GLYCAM1	glycosylation-dependent cell adhesion molecule 1
Bt.4662.1.S1_at	NOS3	nitric oxide synthase 3 (endothelial cell)
Bt.4536.1.S1_at	---	Transcribed locus, strongly similar to XP_606704.2 PREDICTED: similar to FLJ0010
Bt.4447.3.A1_at	CYP19	Cytochrome P450, family XIX (conversion of androgen to estrogen), aromatase
Bt.4303.1.S1_at	ADA	adenosine deaminase
Bt.4208.1.S1_at	IL8RB	interleukin 8 receptor, beta
Bt.4060.2.A1_at	LOC782642 /// MAL	mal, T-cell differentiation protein /// similar to Mal, T-cell differentiation p
Bt.37.2.A1_at	LHCGR	luteinizing hormone/choriogonadotropin receptor
Bt.3554.1.S1_at	LOC529049	similar to mannose receptor, C type 2
Bt.350.1.S1_at	BLA-DQB	MHC class II antigen
Bt.3307.1.A1_at	NDP	Norrie disease (pseudoglioma)
Bt.3282.1.S1_at	MGC126924	similar to dipeptidase 1 (renal)
Bt.3046.2.S1_at	FCNB	ficolin B
Bt.29884.1.S1_at	st6GalNAc-VI	beta-galactosamide alpha-2,6-sialyltransferase
Bt.29873.1.S1_at	MEST	mesoderm specific transcript homolog (mouse)
Bt.29856.1.S1_at	GNG7	guanine nucleotide binding protein (G protein), gamma 7
Bt.29853.1.S1_at	LOC407121	nebulin
Bt.29851.1.S1_at	BLA-DQB	MHC class II antigen
Bt.29838.1.A1_at	GlyT-1Ab	glycine transporter
Bt.29828.1.A1_at	---	Immunoglobulin light chain variable region
Bt.29813.1.S1_at	---	Hybridoma BL2C7 immunoglobulin heavy chain variable region
Bt.29813.1.A1_at	---	Hybridoma BL2C7 immunoglobulin heavy chain variable region
Bt.29811.1.A1_at	---	Hybridoma BL5H4 immunoglobulin heavy chain variable region
Bt.29788.1.S1_at	SIAT1	Sialyltransferase 1 (beta-galactoside alpha-2,6-sialytransferase)
Bt.29786.1.A1_at	---	Glutathione-S-transferase (GST) specific immunoglobulin light chain variable reg
Bt.29765.1.S1_at	LOC505349	similar to TCRVB17
Bt.29758.1.S1_x_at	LOC506453 /// LOC514734 /// LOC613323 /// LOC613361 /// LOC617183 /// LOC783357	similar to T-cell receptor beta chain V region C5 precursor /// hypothetical LOC
Bt.29677.1.S1_at	OPTC	opticin
Bt.29389.1.S1_at	---	Transcribed locus, weakly similar to XP_942890.1 PREDICTED: similar to SET domai
Bt.2933.1.S1_at	LOC788205	hypothetical protein LOC788205
Bt.2927.1.A1_at	C20orf55	chromosome 20 open reading frame 55
Bt.29144.1.S1_at	CLRN3	Clarin 3
Bt.29099.1.S1_at	MGC152111	Hypothetical LOC507206
Bt.29011.1.A1_at	BCKDHA	branched chain keto acid dehydrogenase E1, alpha polypeptide
Bt.29000.1.S1_at	LOC539158	similar to HATH1
Bt.28983.1.A1_a_at	LOC515285	similar to Centrosomal protein 76kDa
Bt.28774.1.A1_at	EIF1	eukaryotic translation initiation factor 1
Bt.28742.1.S1_at	MGC155102	similar to Probable transcription factor CST (Castor-related protein)
Bt.28717.1.S1_at	USF1	upstream transcription factor 1
Bt.28534.2.S1_at	MGC142714	similar to pleckstrin 2
Bt.28518.1.S1_s_at	LOC404103 /// PTI	spleen trypsin inhibitor /// pancreatic trypsin inhibitor
Bt.28453.1.S1_at	VpreB	immunoglobulin light chain variable region
Bt.28453.1.A1_at	VpreB	immunoglobulin light chain variable region
Bt.28294.1.S1_at	LOC615733	similar to human immunity associated protein 1
Bt.28173.2.S1_at	LOC512700	similar to Flt3
Bt.28024.1.A1_at	LOC407111	Fas ligand
Bt.28020.1.S1_at	LOC407189	KERIA
Bt.28008.1.S1_s_at	KCNN2	potassium intermediate/small conductance calcium-activated channel, subfamily N,
Bt.28004.2.S1_a_at	LOC505306 /// LOC785621 /// TRD@	T-cell receptor delta chain /// hypothetical LOC505306 /// hypothetical protein
Bt.28003.1.S1_at	---	TCR mRNA for T cell receptor gamma chain, partial cds, clone: BTGV17
Bt.28003.1.A1_at	---	TCR mRNA for T cell receptor gamma chain, partial cds, clone: BTGV17
Bt.28001.1.S1_at	---	T cell receptor gamma TRGV5-1
Bt.28000.1.S1_at	TRGC4	T cell receptor gamma C4
Bt.27992.1.S1_at	5htr1d	5-hydroxytryptamine 1D receptor
Bt.27992.1.A1_at	5htr1d	5-hydroxytryptamine 1D receptor
Bt.27984.1.A1_x_at	---	Immunoglobulin heavy chain variable region (IGHV gene)
Bt.27981.1.S1_at	cd21	complement receptor type 2

Probe Set ID	Gene Symbol	Gene Title
Bt.27927.1.S1_at	LOC532674	similar to OTTHUMP00000016557
Bt.27855.1.S1_at	LOC788252	similar to Iatrophilin-1
Bt.27805.2.S1_a_at	CENPM	centromere protein M
Bt.27803.1.A1_at	LOC522810	similar to testis expressed sequence 14
Bt.277.1.S1_at	EXPI	extracellular proteinase inhibitor
Bt.27531.1.A1_at	LOC787969	similar to cancer susceptibility candidate 5
Bt.27334.1.A1_at	SLC35C1	solute carrier family 35, member C1
Bt.27333.1.S1_at	KRT17	keratin 17
Bt.27308.1.S1_at	MGC137932	similar to empty spiracles homolog 2
Bt.27296.1.S1_at	LOC404171	sodium chloride cotransporter
Bt.27134.1.A1_at	LOC522307	similar to DNA polymerase lambda
Bt.26886.1.S1_at	TOP3B	topoisomerase (DNA) III beta
Bt.26766.1.S1_at	---	Transcribed locus, moderately similar to NP_478067.2 chromosome 21 open reading
Bt.26644.2.S1_at	LOC613386	similar to fibroblast growth factor homologous factor 3
Bt.26637.2.S1_at	MGC138046	similar to chromatin modifying protein 4C
Bt.26590.1.A1_at	TRIM10	tripartite motif-containing 10
Bt.26583.1.S1_a_at	MGC157157	similar to euchromatic histone methyltransferase 1
Bt.26544.1.S1_at	LOC784636	hypothetical protein LOC784636
Bt.26506.1.S1_at	ORF1	ORF1 protein
Bt.26462.1.S1_at	MGC143242	similar to preproendothelin-3
Bt.26351.1.A1_at	LOC516661	similar to putative leucine-rich glioma inactivated 3
Bt.26255.1.S1_at	LOC528492	similar to c-myeloproliferative leukemia virus type P
Bt.26160.1.A1_at	MAEL	maelstrom homolog (Drosophila)
Bt.26080.3.S1_at	LOC532872	hypothetical LOC532872
Bt.26057.1.A1_at	ARL3	ADP-ribosylation factor-like 3
Bt.25983.1.A1_at	LOC510260	hypothetical LOC510260
Bt.25977.2.A1_at	LOC540703	similar to FOXJ2 forkhead factor
Bt.25875.1.A1_at	LOC506152	similar to Guanine nucleotide binding protein-like 3 (nucleolar)
Bt.25775.1.A1_at	PDE1B	phosphodiesterase 1B, calmodulin-dependent
Bt.25723.1.A1_at	LOC616656	hypothetical LOC616656
Bt.25706.1.A1_at	TARBP2	TAR (HIV-1) RNA binding protein 2
Bt.25543.1.A1_at	LOC518023	hypothetical LOC518023
Bt.25528.1.S1_at	PTP	pancreatic thread protein
Bt.25506.1.A1_at	EFCAB1	EF-hand calcium binding domain 1
Bt.25458.1.A1_at	---	Transcribed locus, moderately similar to NP_001025472.1 TIR domain containing ad
Bt.25428.1.A1_at	LOC781497	similar to HLH-PAS transcription factor NXF
Bt.25383.1.A1_at	LOC617967	similar to interleukin 21 receptor
Bt.25382.1.A1_at	LOC506037	similar to netrin receptor Unc5h1
Bt.25018.1.A1_at	MGC159655	similar to fibroblast growth factor 13
Bt.24854.1.A1_at	LOC618224	similar to peptidylarginine deiminase type I
Bt.24779.2.S1_at	CREM	cAMP responsive element modulator
Bt.24771.2.S1_at	CPNE6	copine VI (neuronal)
Bt.24663.1.A1_at	LOC540142	Similar to Forkhead-like 18 (Drosophila)
Bt.2462.1.S1_at	SH2D2A	SH2 domain protein 2A
Bt.24584.1.S1_at	MGC139629	similar to UDP-N-acetyl-alpha-D-galactosamine:polypeptide N-acetylgalactosaminyl
Bt.24568.1.A1_at	MGC139944	similar to Kallikrein 10 precursor (Protease serine-like 1) (Normal epithelial c
Bt.24564.1.A1_a_at	LOC519331	similar to voltage-dependent calcium channel gamma-4 subunit
Bt.24542.2.S1_at	LOC512034	similar to neurotrypsin
Bt.24466.1.S1_at	MGC148717	similar to Transmembrane protein 130
Bt.24460.1.S1_at	MGC143376	similar to zinc finger, CCHC domain containing 12
Bt.24392.1.S1_at	LOC537808	similar to neurexin II
Bt.24341.1.S1_at	TSPAN2	tetraspanin 2
Bt.24298.1.A1_at	LOC617934	Hypothetical LOC617934
Bt.24218.2.S1_a_at	LOC515301	similar to Cdc6-related protein
Bt.24081.1.A1_at	TDO2	tryptophan 2,3-dioxygenase
Bt.23731.1.A1_at	TAT	Tyrosine aminotransferase
Bt.23703.1.A1_at	LOC508455	similar to Putative steroid dehydrogenase KIK-I
Bt.23658.2.S1_at	MGC139875	similar to anti-silencing function 1B
Bt.23521.2.S1_a_at	DUSP26	dual specificity phosphatase 26
Bt.23521.1.S1_at	DUSP26	dual specificity phosphatase 26
Bt.23465.1.S1_at	LOC785186 /// MGC139984	similar to keratin 25A /// hypothetical protein LOC785186
Bt.23349.1.A1_a_at	LOC509593	similar to Rho-GTPase-activating protein 8
Bt.23309.1.S1_at	MYPN	myopalladin
Bt.23195.2.S1_at	NR5A1	Nuclear receptor subfamily 5, group A, member 1
Bt.2314.1.S1_at	SELL	selectin L
Bt.23.2.S1_at	SLC6A2	solute carrier family 6 (neurotransmitter transporter, noradrenalin), member 2
Bt.23.2.S1_a_at	SLC6A2	solute carrier family 6 (neurotransmitter transporter, noradrenalin), member 2
Bt.22938.1.S1_at	CYLC2	cylicin, basic protein of sperm head cytoskeleton 2
Bt.22879.1.S1_at	HSD17B1 /// LOC785989	hydroxysteroid (17-beta) dehydrogenase 1 /// similar to Hydroxysteroid (17-beta)
Bt.22877.1.S1_at	CBP40	catecholamine binding protein CBP40
Bt.22873.1.A1_at	NTRK1	neurotrophic tyrosine kinase, receptor, type 1

Probe Set ID	Gene Symbol	Gene Title
Bt.22863.1.A1_at	C20ORF18	ubiquitin conjugating enzyme 7 interacting protein 3
Bt.22853.1.S1_at	MGC155311	similar to C22orf13 protein
Bt.22846.2.S1_a_at	TSPAN33	tetraspanin 33
Bt.22165.1.S1_at	MGC137948	similar to KIAA1914 protein
Bt.22163.1.S1_at	DNAJB5	DnaJ (Hsp40) homolog, subfamily B, member 5
Bt.22083.2.S1_at	---	Transcribed locus, moderately similar to NP_003990.1 oncostatin M receptor [Homo
Bt.21773.2.S1_at	MGC142842	similar to guanylate-binding protein 5
Bt.21614.2.S1_at	LOC782984 /// MGC148653	hypothetical LOC508790 /// hypothetical protein LOC782984
Bt.21579.2.S1_at	LOC519461	similar to renal organic cation transporter
Bt.21388.3.S1_at	LOC617684	similar to Bromo adjacent homology domain containing 1
Bt.21252.2.S1_at	---	Transcribed locus, moderately similar to NP_032218.1 guanylate cyclase 2e [Mus m
Bt.20968.1.S1_at	VSNL1	visinin-like 1
Bt.20848.1.A1_at	LOC510592	similar to F52H3.5
Bt.20596.2.S1_at	EVA1	epithelial V-like antigen 1
Bt.20543.1.S1_at	LOC513662	hypothetical LOC513662
Bt.20540.3.A1_at	LOC509801	similar to immunoglobulin-associated beta
Bt.20403.1.S1_at	LOC789882	hypothetical protein LOC789882
Bt.20359.1.S1_at	MGC148465	similar to IKAROS family zinc finger 3 (Aiolos)
Bt.20328.3.S1_at	MGC166079	Similar to PHD finger protein 2
Bt.20228.1.S1_at	RTN2	reticulon 2
Bt.20136.1.S1_at	LOC529808	similar to KIAA0404
Bt.19930.1.A1_at	LOC505056	similar to GPR35
Bt.19877.1.A1_at	PSMC5	proteasome (prosome, macropain) 26S subunit, ATPase, 5
Bt.1978.9.S1_at	TRB@	T cell receptor, beta cluster
Bt.1976.2.S1_at	MGC139033	similar to suppression of tumorigenicity 5
Bt.19750.1.A1_at	MGC140234	Similar to tRNA selenocysteine associated protein
Bt.197.1.S1_at	SELE	selectin E
Bt.19517.1.S1_at	ERBB3	v-erb-b2 erythroblastic leukemia viral oncogene homolog 3 (avian)
Bt.19295.2.S1_at	LOC538827	similar to Apolipoprotein-L domain-containing protein 1 (Vascular early response
Bt.18983.1.A1_at	MGC159441	Hypothetical LOC511455
Bt.18962.1.A1_at	AOAH	acyloxyacyl hydrolase
Bt.18325.2.A1_a_at	MGC151537	microtubule-associated protein 7
Bt.18009.1.A1_at	C8orf13	chromosome 8 open reading frame 13
Bt.17723.1.A1_s_at	MGC133619	hypothetical protein MGC133619
Bt.176.1.S1_at	GAL	galanin
Bt.17599.1.A1_at	CDH8	cadherin 8, type 2
Bt.17314.2.A1_at	CLGN	calmegin
Bt.16873.1.S1_at	HSD17B2	hydroxysteroid (17-beta) dehydrogenase 2
Bt.16735.1.A1_at	LOC527732	Similar to plakophilin 4
Bt.16332.1.A1_at	LOC534842	similar to Roundabout homolog 2 precursor
Bt.16238.2.S1_at	LOC614598	similar to mitogen-activated protein kinase kinase kinase 6
Bt.16200.1.A1_at	LOC506520	similar to WNK lysine deficient protein kinase 2
Bt.16103.1.S1_at	APOB	apolipoprotein B
Bt.16062.1.A1_at	LOC781013	hypothetical protein LOC781013
Bt.16037.1.S1_at	LOC783982 /// MGC140602	similar to globoside alpha-1,3-N-acetylgalactosaminyltransferase 1 /// hypotheti
Bt.15988.1.S1_at	PAG20	pregnancy-associated glycoprotein 20
Bt.15986.1.S1_at	PAG18	pregnancy-associated glycoprotein 18
Bt.15981.1.S1_at	GPR44	G protein-coupled receptor 44
Bt.15900.2.S1_at	LOC532836	similar to Adenosylhomocysteinase 3
Bt.15822.1.S1_at	MGC159776	similar to Proto-oncogene tyrosine-protein kinase FGR (P55-FGR) (C-FGR)
Bt.15713.2.S1_at	LOC518658	similar to Pleckstrin
Bt.15301.1.A1_at	DUSP3	dual specificity phosphatase 3 (vaccinia virus phosphatase VH1-related)
Bt.1493.1.S1_at	LOC536316	similar to polymerase (RNA) I polypeptide A, 194kDa
Bt.14726.1.A1_at	LOC510506	similar to carbamoyl phosphate synthetase 1
Bt.14202.2.S1_at	LGI4	leucine-rich repeat LGI family, member 4
Bt.14139.1.A1_at	C9	complement component 9
Bt.1366.1.S1_at	CLEC3B	C-type lectin domain family 3, member B
Bt.13469.1.S1_at	MGC159817	similar to Serine dehydratase-like
Bt.1333.1.S1_at	LOC505697	similar to Ryanodine receptor 1 (Skeletal muscle-type ryanodine receptor) (RyR1)
Bt.13211.1.A1_at	LOC509824	similar to Os08g0528700
Bt.13105.1.S1_at	ADRA2A	adrenergic, alpha-2A-, receptor
Bt.13102.1.S1_at	CACNG2	calcium channel, voltage-dependent, gamma subunit 2
Bt.13095.1.A1_at	HAS3	hyaluronan synthase 3
Bt.13055.1.S1_at	CACNA1L	alpha1I T-type calcium channel subunit
Bt.13003.8.A1_at	TRA@	T cell receptor, alpha
Bt.13003.4.S1_at	TRA@	T cell receptor, alpha
Bt.12930.1.S1_a_at	TAC1	tachykinin, precursor 1
Bt.12928.1.S1_at	IL13	interleukin 13
Bt.12847.1.S1_at	STATH	statherin
Bt.12804.1.S1_at	KIT	v-kit Hardy-Zuckerman 4 feline sarcoma viral oncogene homolog
Bt.12781.2.S1_a_at	MYB	v-myb myeloblastosis viral oncogene homolog (avian)

Probe Set ID	Gene Symbol	Gene Title
Bt.12537.1.S1_at	ASB15	ankyrin repeat and SOCS box-containing 15
Bt.1232.1.S1_at	LOC511230	similar to DENN/MADD domain containing 1C
Bt.12300.2.S1_at	LOC788772	similar to myosin heavy chain 2a
Bt.12240.1.A1_at	---	Transcribed locus, strongly similar to XP_001255051.1 PREDICTED: similar to OTTH
Bt.122.1.S1_at	ATP1B2	ATPase, Na+/K+ transporting, beta 2 polypeptide
Bt.12083.1.S1_s_at	LOC507139	similar to Gca protein
Bt.11675.1.A1_at	LOC784738 /// RPS12	ribosomal protein S12 /// hypothetical protein LOC784738
Bt.11666.3.S1_a_at	MGC157202	similar to sterol response element binding protein cleavage-activating protein
Bt.11659.1.S1_at	MRP63	mitochondrial ribosomal protein 63
Bt.11639.1.A1_at	MGC140008	Similar to Myosin light chain 1, slow-twitch muscle A isoform (MLC1sa) (Alkali)
Bt.11541.2.S1_at	LOC516041	hypothetical LOC516041
Bt.11266.2.S1_s_at	MGC166040	hypothetical LOC506374
Bt.11215.1.S1_a_at	TNNT3	troponin T type 3 (skeletal, fast)
Bt.11214.1.S1_at	RP1	retinitis pigmentosa 1 (autosomal dominant)
Bt.11204.1.S1_at	PROKR2	prokineticin receptor 2
Bt.10921.1.S1_at	TBX19	T-box 19
Bt.10696.1.S1_at	CDCA3	cell division cycle associated 3
Bt.10310.1.S1_at	MYBPC1	myosin binding protein C, slow type
BtAffx.1.5.S1_at	TRHR	thyrotropin-releasing hormone receptor
BtAffx.1.13.S1_at	TAC3	tachykinin 3 (neuromedin K, neurokinin beta)
Bt.9944.1.S1_at	DPYSL5	dihydropyrimidinase-like 5
Bt.9909.1.S1_at	CCDC22	coiled-coil domain containing 22
Bt.9850.1.A1_at	PRP2	proline-rich protein PRP2
Bt.9736.1.S1_at	LOC512548	hypothetical LOC512548
Bt.9735.2.A1_at	APOM	apolipoprotein M
Bt.9697.1.A1_at	MGC137543	similar to Alcohol dehydrogenase 6
Bt.9692.1.S1_at	BSP30C	common salivary protein BSP30 form C
Bt.965.1.S1_at	MATN1	matrilin 1, cartilage matrix protein
Bt.9648.1.S1_at	LOC505595	similar to Ost-II
Bt.9622.2.S1_at	LOC538901	hypothetical LOC538901
Bt.9599.3.S1_at	MGC128671	Similar to Inositol hexakisphosphate kinase 2 (InsP6 kinase 2) (Inositol hexakis
Bt.9590.1.S1_at	LOC530483	similar to C21orf108
Bt.9556.1.S1_at	MEST	mesoderm specific transcript homolog (mouse)
Bt.9535.1.S1_at	TRGC6	T-cell receptor gamma chain TRGC6
Bt.950.1.S1_at	ANKZF1	ankyrin repeat and zinc finger domain containing 1
Bt.9431.2.S1_at	LOC512048 /// LOC788506	similar to KIAA1138 protein /// similar to REX1, RNA exonuclease 1 homolog (S. c
Bt.9420.1.S1_at	LOC786966	similar to plectin 6
Bt.9390.1.S1_at	MGC160028	similar to tumor endothelial marker 7
Bt.9353.1.S1_at	EMILIN2	elastin microfibril interfacer 2
Bt.9308.1.S1_at	PTPRCAP	protein tyrosine phosphatase, receptor type, C-associated protein
Bt.9221.1.A1_at	LOC788760	similar to tangerin C
Bt.9163.2.S1_at	P2RY10	purinergic receptor P2Y, G-protein coupled, 10
Bt.9111.1.S1_at	LOC514967	similar to K+ channel tetramerization protein
Bt.9097.1.S1_at	GRAMD1A	hypothetical protein LOC507027
Bt.9035.1.S1_at	LOC506974	hypothetical LOC506974
Bt.9032.1.S1_a_at	TCRG	T-cell receptor gamma chain
Bt.9012.1.S1_at	LOC508247	similar to KIAA1639 protein
Bt.8984.1.S1_at	MGC152112	similar to MIB006
Bt.8967.1.S1_at	GDF8	growth differentiation factor 8
Bt.8946.1.S1_at	SLCO1A2	solute carrier organic anion transporter family, member 1A2
Bt.8941.1.S1_at	CHIA	chitinase, acidic
Bt.8861.1.S1_at	AIPL1	aryl hydrocarbon receptor interacting protein-like 1
Bt.8547.1.S1_at	SLAM	signaling lymphocytic activation molecule
Bt.8299.1.S1_at	MGC165989	similar to MGC2641 protein
Bt.8282.1.S1_at	DPP4	dipeptidyl-peptidase 4 (CD26, adenosine deaminase complexing protein 2)
Bt.8257.2.A1_at	LOC508697	similar to protein BAP28 (FLJ10359)
Bt.8247.2.S1_at	LOC518364	similar to OHCU decarboxylase
Bt.82.1.A1_at	CYP3A4	cytochrome P450, subfamily IIIA (niphedipine oxidase), polypeptide 4
Bt.8180.2.S1_at	LOC782388	similar to copine III-like related protein
Bt.8146.1.S1_at	EVC	Ellis van Creveld syndrome
Bt.8103.1.S1_a_at	LOC505556	similar to Valyl-tRNA synthetase
Bt.8090.1.A1_at	LOC513045	similar to Myb-binding protein 1A
Bt.8079.2.S1_at	LOC509045	similar to KIAA0138
Bt.8064.1.S1_at	LIMD2	LIM domain containing 2
Bt.8053.3.S1_at	LOC506045	hypothetical LOC506045
Bt.8048.1.S1_at	LOC506434 /// LOC790768	similar to troponin I
Bt.7988.1.A1_at	LOC614413	similar to Etr-3
Bt.7907.2.S1_a_at	CDK10 /// LOC785111	cyclin-dependent kinase 10 /// hypothetical protein LOC785111
Bt.7780.1.S1_at	LTF	Lactotransferrin

Probe Set ID	Gene Symbol	Gene Title
Bt.7763.1.S1_at	LOC514326	similar to TLE3 protein
Bt.771.2.S1_at	NFATC4	nuclear factor of activated T-cells, cytoplasmic, calcineurin-dependent 4
Bt.771.1.S1_at	NFATC4	nuclear factor of activated T-cells, cytoplasmic, calcineurin-dependent 4
Bt.7696.1.S1_at	RABGGTA	Rab geranylgeranyltransferase, alpha subunit
Bt.7597.1.S1_at	LOC537511	similar to polyhomeotic 2
Bt.7587.3.S1_a_at	PCBP4	poly(rC) binding protein 4
Bt.7435.1.S1_at	UNC119	unc-119 homolog (C. elegans)
Bt.7416.2.S1_at	LOC521413	similar to G protein-coupled receptor kinase 6, splice variant B; GRK6B
Bt.7404.1.S1_s_at	CENTB1	centaurin, beta 1
Bt.7356.2.S1_at	LOC535403	similar to MYST histone acetyltransferase (monocytic leukemia) 4
Bt.7304.1.S1_at	MGC129010	similar to eNOS interacting protein
Bt.7208.1.S1_at	ZP2	zona pellucida glycoprotein 2 (sperm receptor)
Bt.7207.1.S1_at	ZP4	zona pellucida glycoprotein 4
Bt.7197.2.A1_at	PRL	prolactin
Bt.7179.3.S1_a_at	MMP23B	matrix metallopeptidase 23B
Bt.7173.1.S1_at	LOC513500	similar to Chromosome 17 open reading frame 68
Bt.7172.1.S1_at	MOG	myelin oligodendrocyte glycoprotein
Bt.7150.3.A1_at	LOC533514	similar to KIAA1289 protein
Bt.7141.1.S1_at	LOC503858	aromatase cytochrome P450 pseudogene
Bt.7039.2.S1_at	MGC134398	similar to mitogen-activated protein kinase kinase 2
Bt.7016.1.S1_at	MGC126906	similar to MON1 homolog B
Bt.7013.1.S1_at	LOC505800	similar to interleukin 32
Bt.6886.1.S1_at	MGC137960	similar to ATP-binding cassette, sub-family F (GCN20), member 3
Bt.6823.1.S1_at	FGD3	FYVE, RhoGEF and PH domain containing 3
Bt.6650.1.S1_at	LOC525303	similar to human gamma-glutamyl hydrolase
Bt.6608.1.S1_at	LOC518168	Similar to VESPR
Bt.6583.1.S1_at	LOC511762	similar to ATP-binding cassette sub-family A member 7 (Macrophage ABC transporte
Bt.657.1.S1_at	LOC506074 /// LOC782744	similar to Chromosome 17 open reading frame 63
Bt.6509.1.S1_at	LOC511043	similar to laminin 5 gamma 2 subunit
Bt.6410.1.A1_at	LOC505518	similar to placenta expressed transcript protein
Bt.6409.1.S1_at	LOC532789	Similar to PAWR
Bt.6405.1.S1_at	MBP	myelin basic protein
Bt.6403.1.A1_at	LOC534923	Similar to protein serine/threonine kinase
Bt.6177.2.S1_at	SNX21	sorting nexin family member 21
Bt.6167.1.S1_at	LOC617087	similar to Transmembrane anchor protein 1
Bt.616.2.S1_a_at	MGC160024	similar to Ring finger protein 166
Bt.6151.1.S1_at	CSF1R	colony stimulating factor 1 receptor
Bt.6095.2.A1_at	GPR137	G protein-coupled receptor 137
Bt.6068.2.S1_at	MGC142307	similar to topoisomerase (DNA) III alpha
Bt.6067.2.S1_at	LOC515820	similar to SH2 domain containing 3C
Bt.6002.1.S1_at	LOC505787	similar to ABC-C transporter
Bt.5919.1.S1_at	GDAP1L1	ganglioside-induced differentiation-associated protein 1-like 1
Bt.583.1.S1_a_at	CSN3	casein kappa
Bt.580.1.S1_at	NEFL	neurofilament, light polypeptide
Bt.5768.2.S1_at	IRF7	interferon regulatory factor 7
Bt.570.1.S1_at	UMOD	uromodulin
Bt.5666.1.S1_at	MGC159743	similar to unnamed secretory protein
Bt.562.1.S1_at	PFKFB1	6-phosphofructo-2-kinase/fructose-2,6-biphosphatase 1
Bt.5562.1.S1_at	PCSK1	proprotein convertase subtilisin/kexin type 1
Bt.555.1.S1_at	CA4	carbonic anhydrase IV
Bt.554.1.S1_at	DMP1	dentin matrix acidic phosphoprotein
Bt.5531.3.S1_at	BACE1	beta-site APP-cleaving enzyme 1
Bt.5497.1.S1_a_at	NRXN1	neurexin 1
Bt.5456.1.S2_at	AQP4	aquaporin 4
Bt.5456.1.S1_at	AQP4	aquaporin 4
Bt.5381.2.A1_at	CSN2	casein beta
Bt.5362.2.S1_at	SERPINA3-7	endopin 2
Bt.5353.1.S1_a_at	SSBP4	single stranded DNA binding protein 4
Bt.5336.1.A1_a_at	TF	transferrin
Bt.5333.3.S1_a_at	CRELD1	cysteine-rich with EGF-like domains 1
Bt.5306.1.S1_at	TCAP	titin-cap
Bt.5277.3.S1_at	CCRK	cell cycle related kinase
Bt.5219.1.S1_at	TCF21	transcription factor 21
Bt.5192.3.S1_at	LOC617546	similar to chromosome 6 open reading frame 47
Bt.5192.1.S1_at	LOC617546	similar to chromosome 6 open reading frame 47
Bt.5175.1.S1_at	RNH1	ribonuclease/angiogenin inhibitor 1
Bt.5130.1.A1_a_at	ALB	albumin
Bt.5126.2.S1_a_at	COMMD5	COMM domain containing 5
Bt.5116.2.S1_a_at	LOC506831	hypothetical LOC506831
Bt.5084.1.S1_at	CKB	creatine kinase, brain
Bt.5.1.S1_at	IL5 /// LOC785154	interleukin 5 /// similar to interleukin-5

Probe Set ID	Gene Symbol	Gene Title
Bt.4993.1.S1_at	MGC142408	similar to protein kinase N1
Bt.4886.1.A1_at	LRRC17	leucine rich repeat containing 17
Bt.4833.3.S1_a_at	VRK3	vaccinia related kinase 3
Bt.4817.2.S1_at	MGC128478	similar to claudin 11
Bt.4795.1.S1_at	SLC6A4	solute carrier family 6 (neurotransmitter transporter, serotonin), member 4
Bt.4735.1.S2_at	ACACA	acetyl-coenzyme A carboxylase alpha
Bt.4734.1.S1_at	GNA14	guanine nucleotide binding protein (G protein), alpha 14
Bt.472.1.S1_at	GNAT2	guanine nucleotide binding protein (G protein), alpha transducing activity polyp
Bt.47.1.S1_at	CA6	carbonic anhydrase VI
Bt.467.1.S1_at	MAPT	microtubule-associated protein tau
Bt.4621.1.S1_a_at	SMTN	smoothelin
Bt.4619.2.S1_at	LOC514958	hypothetical LOC514958
Bt.4589.1.S1_at	MGC140424	similar to death effector domain-containing DNA binding protein 2
Bt.4588.1.S1_at	PLEKHQ1	pleckstrin homology domain containing, family Q member 1
Bt.4575.1.S1_at	LOC100125320	hypothetical protein LOC100125320
Bt.457.1.S1_at	SPADH1	spermadhesin 1
Bt.4559.1.S1_at	MGC151650	similar to SCG10-related protein HiAT3
Bt.4557.1.S1_at	IFNAR1	interferon, alpha; receptor
Bt.4553.1.S1_at	LOC526472	similar to CLIM2
Bt.4552.4.A1_at	PLCB4	phospholipase C, beta 4
Bt.4481.1.S1_at	DBH	dopamine beta-hydroxylase
Bt.4474.2.S1_a_at	LOC507590	similar to Protein C20orf35 (HSMNP1)
Bt.4461.1.S1_at	CKMT1	creatine kinase, mitochondrial 1 (ubiquitous)
Bt.44.1.S1_at	C4BPB	complement component 4 binding protein, beta
Bt.4397.2.S1_a_at	POMT1	protein-O-mannosyltransferase 1
Bt.438.1.S1_at	MYO1A	myosin IA
Bt.4378.1.S1_at	ECE1	endothelin converting enzyme 1
Bt.4357.1.S1_at	TSPAN7	tetraspanin 7
Bt.4307.1.S1_at	MGC140398	similar to GTPase
Bt.4293.1.S1_at	ICAM3	intercellular adhesion molecule 3
Bt.4238.1.S1_at	LOC616557	hypothetical LOC616557
Bt.4233.1.S1_at	SMYD5	SMYD family member 5
Bt.4219.1.A1_at	LOC528818	Similar to Fuzzy homolog (Drosophila)
Bt.4196.1.S1_at	LOC539462 /// LOC790208	similar to Myelin P0 protein precursor (Myelin protein zero) (Myelin peripheral
Bt.4126.2.S1_at	MGC159729	similar to Cytochrome P450, family 4, subfamily A, polypeptide 11
Bt.412.1.S1_at	QPCT	glutaminyl-peptide cyclotransferase (glutaminyl cyclase)
Bt.410.1.S1_at	GCG /// LOC789291	glucagon /// similar to Glucagon precursor
Bt.4091.2.S1_at	LOC782204 /// MGC134173	similar to Epsin 1 /// hypothetical protein LOC782204
Bt.408.1.S1_at	GABRG2	gamma-aminobutyric acid (GABA) A receptor, gamma 2
Bt.4015.1.S1_at	MGC139434	similar to F46F6.4
Bt.4011.1.S1_at	LOC520173	similar to transmembrane protein induced by tumor necrosis factor alpha
Bt.3985.1.S1_at	CYP17 /// LOC782561 /// LOC784256 /// LOC784299 /// LOC785462	cytochrome P450, subfamily XVII /// similar to Cytochrome P450 17A1 (CYPXVII) (P
Bt.394.4.S1_a_at	CYM	chymosin
Bt.394.3.A1_a_at	CYM	chymosin
Bt.3875.1.S1_at	RLBP1	retinaldehyde binding protein 1
Bt.3841.2.S1_at	CD83	CD83 molecule
Bt.3787.1.A1_at	LOC785692	Hypothetical protein LOC785692
Bt.3683.1.S1_at	CSN1S1	casein alpha s1
Bt.368.1.S1_at	CENTA1	centaurin, alpha 1
Bt.353.1.S1_at	RPH3A	rabphilin 3A homolog (mouse)
Bt.348.2.S1_a_at	PTGER3	prostaglandin E receptor 3 (subtype EP3)
Bt.3415.1.A1_at	LOC504513	hypothetical LOC504513
Bt.34.1.S1_at	TSHR	thyroid stimulating hormone receptor
Bt.3372.3.S1_a_at	LOC511614	similar to putative lysophosphatidic acid acyltransferase
Bt.3313.1.A1_at	ARHGAP24	Rho GTPase activating protein 24
Bt.3306.1.S1_at	LOC512397	similar to ProSAPiP1 protein
Bt.329.1.S1_at	DNTT	deoxynucleotidyltransferase, terminal
Bt.3253.2.S1_at	LOC617871	hypothetical LOC617871
Bt.3242.1.S1_at	CLDN2	claudin 2
Bt.324.1.S1_at	LOC280905	seminalplasmin
Bt.3201.2.S1_at	MGC139107	similar to Glutamate-rich WD-repeat protein 1
Bt.3196.2.S1_a_at	STRA6	stimulated by retinoic acid gene 6 homolog
Bt.3189.2.S1_at	LOC540831	similar to FLJ20273 protein
Bt.3185.1.A1_at	MGC151883	similar to ectonucleoside triphosphate diphosphohydrolase 8
Bt.3093.1.S1_at	IMPACT	Impact homolog (mouse)
Bt.3066.1.A1_at	LOC539411	Hypothetical LOC539411
Bt.305.1.S1_at	PKP1	plakophilin 1 (ectodermal dysplasia/skin fragility syndrome)

Probe Set ID	Gene Symbol	Gene Title
Bt.29962.1.S1_at	MAP3K12	Mitogen-activated protein kinase kinase kinase 12
Bt.29931.2.S1_at	LOC514928	similar to Kinesin family member 1C
Bt.29912.1.S1_at	MGC159765	hypothetical LOC513430
Bt.29872.1.S1_at	CCNT1	cyclin T1
Bt.29871.1.S1_at	BOLA-DYA	major histocompatibility complex, class II, DY alpha
Bt.29870.1.S1_at	BOLA-DYB	major histocompatibility complex, class II, DY beta
Bt.29865.1.A1_at	CYP1A2	cytochrome P450, family 1, subfamily a, polypeptide 2
Bt.29848.1.S1_at	LOC407174	NTT4-like neurotransmitter transporter
Bt.29848.1.A1_at	LOC407174	NTT4-like neurotransmitter transporter
Bt.29842.1.A1_at	---	B4 cell-line anti-respiratory syncytial virus Ig lambda chain V region (IgL)
Bt.29841.1.A1_at	---	B4 cell-line anti-respiratory syncytial virus Ig lambda chain V region (IgL)
Bt.29820.1.S1_s_at	BOLA	MHC class I heavy chain
Bt.29780.1.A1_at	GJB1	gap junction protein, beta 1, 32kDa
Bt.29779.1.S1_s_at	bTrappin-4 /// bTrappin-5	trappin 5 /// trappin 4
Bt.29779.1.A1_at	bTrappin-4	trappin 4
Bt.29774.1.S1_at	LOC407162	chloride-bicarbonate exchanger
Bt.29773.1.A1_at	LOC407112	sodium proton exchanger
Bt.29771.1.A1_at	bsc1	apical Na(2Cl)K cotransporter
Bt.29758.1.A1_x_at	LOC783615	Similar to TRB@ protein
Bt.29755.1.A1_at	---	Cyp19 mRNA; untranslated exon 1 region, variant 1, placental transcript
Bt.29750.1.A1_x_at	LOC617169	Hypothetical LOC617169
Bt.29749.1.S1_x_at	LOC615995 /// LOC617169 /// LOC783128 /// LOC783206 /// LOC783317 /// LOC783647	hypothetical LOC615995 /// hypothetical LOC617169 /// hypothetical protein LOC78
Bt.29748.1.A1_at	LOC783317	Hypothetical protein LOC783317
Bt.29743.1.A1_at	---	Immunoglobulin heavy chain mRNA, variable region, partial cds, 5' end
Bt.29742.1.A1_at	---	Immunoglobulin heavy chain mRNA, variable region, partial cds, 5' end
Bt.29738.1.A1_at	---	B4 cell-line anti-respiratory syncytial virus Ig lambda chain V region (IgL)
Bt.29736.1.A1_at	---	Immunoglobulin variable region
Bt.29726.1.A1_at	---	B4 cell-line anti-respiratory syncytial virus Ig lambda chain V region (IgL)
Bt.29722.1.S1_at	at2	angiotensin receptor 2
Bt.29718.2.S1_at	GHR	growth hormone receptor
Bt.29702.1.A1_at	---	Immunoglobulin rearranged heavy chain variable region
Bt.29693.1.A1_at	TRGV7-1	T cell receptor gamma variable 7-1
Bt.29689.1.S1_s_at	LOC407199 /// TRD@	T-cell receptor delta chain /// T cell receptor delta chain
Bt.29681.1.A1_at	PRP6	prolactin-related protein VI
Bt.2964.2.S1_at	ZNF330	zinc finger protein 330
Bt.29634.1.A1_at	---	Transcribed locus
Bt.29614.1.A1_at	LOC511043	similar to laminin 5 gamma 2 subunit
Bt.29579.1.A1_at	LOC515340	N-acetylgalactosaminyltransferase A blood group-like
Bt.29528.1.A1_at	GPRC5A	G protein-coupled receptor, family C, group 5, member A
Bt.29509.1.A1_at	RNASE6	ribonuclease, RNase A family, k6
Bt.29479.1.S1_at	MGC179481	similar to carotene-9,10-monooxygenase
Bt.29365.1.A1_at	LOC513032	similar to Nedd4 binding protein 3
Bt.29351.1.A1_at	LOC510394	similar to serine protease PRSS22
Bt.293.1.S1_at	PAG21	pregnancy-associated glycoprotein 21
Bt.29281.1.S1_at	MGC127475	similar to Adaptor-related protein complex 1, mu 2 subunit (Mu-adaptin 2) (Adapt
Bt.29262.1.S1_at	LOC512001	similar to GDDR
Bt.29253.1.S1_at	PDIA5	protein disulfide isomerase family A, member 5
Bt.29219.1.A1_at	LOC514701	hypothetical LOC514701
Bt.29208.1.S1_at	LOC535967	similar to KIAA0715 protein
Bt.29198.1.S1_a_at	MEP1B	meprin A, beta
Bt.29157.1.A1_at	MGC140405	similar to Growth arrest-specific 2 like 1
Bt.29132.1.A1_at	LOC521868	similar to protein tyrosine phosphatase
Bt.2913.1.A1_at	CRYM	crystallin, mu
Bt.29113.1.A1_at	LOC505468	hypothetical LOC505468
Bt.29079.1.A1_at	UQCRC1	UQCRC1 protein
Bt.29068.1.A1_at	PLA2G7	phospholipase A2, group VII (platelet-activating factor acetylhydrolase, plasma)
Bt.29060.1.A1_at	HPS1	Hermansky-Pudlak syndrome 1
Bt.2902.2.S1_at	LOC613943	similar to ZDHHC22 protein
Bt.28974.1.A1_at	TMEM141	transmembrane protein 141
Bt.28967.1.S1_at	LOC408018	C-C motif chemokine receptor 3
Bt.28954.1.S1_at	MGC159504	Similar to DEP domain containing 6
Bt.28921.1.S1_at	LOC785197	similar to multi-specific organic anion tranporter-E
Bt.28811.1.A1_at	REG4	Regenerating islet-derived family, member 4
Bt.28798.1.A1_at	ANKRD22	Ankyrin repeat domain 22
Bt.28781.1.A1_at	MGC155072	similar to NADPH oxidase activator 1
Bt.28776.1.A1_at	---	Transcribed locus, strongly similar to XP_215812.3 PREDICTED: similar to 53BP1 p
Bt.28734.1.S1_at	LOC617096	similar to cadherin-like 26

Probe Set ID	Gene Symbol	Gene Title
Bt.28727.1.A1_at	NFKBIL1	nuclear factor of kappa light polypeptide gene enhancer in B-cells inhibitor-lik
Bt.28716.2.S1_at	MGC128448	similar to F26A3.7
Bt.28679.1.A1_at	LOC521542	similar to KIAA0645 protein
Bt.28663.1.A1_at	HNF-1a	hepatocyte nuclear factor 1 alpha
Bt.28647.1.S1_at	PAG15	pregnancy-associated glycoprotein 15
Bt.28537.1.S1_at	MGC138951	similar to harmonin-interacting ankyrin-repeat containing protein
Bt.28494.7.A1_at	LOC524810	IgM
Bt.28494.5.S1_at	LOC524810	IgM
Bt.28494.5.A1_at	LOC524810	IgM
Bt.28494.2.A1_x_at	LOC524810	IgM
Bt.28446.1.S1_x_at	BVd1.25	T cell receptor delta chain variable region
Bt.28444.1.A1_x_at	---	T-cell receptor beta chain variable segment, clone C20
Bt.28439.2.S1_at	MGC139478	similar to lymphocyte antigen 9
Bt.28370.1.A1_at	CPB1	carboxypeptidase B1 (tissue)
Bt.28365.1.A1_at	LOC521163	similar to H+/K+-exchanging ATPase (EC 3.6.3.10) alpha chain
Bt.28364.1.S1_a_at	LOC613996	similar to FLJ10769 protein
Bt.28353.1.A1_at	LOC525692	similar to mucin 5
Bt.28347.1.S1_at	LOC540000	hypothetical LOC540000
Bt.28323.1.S1_at	LOC517820	similar to tumor-associated hydroquinone (NADH) oxidase tNOX
Bt.28317.1.S1_at	LOC511923	similar to p54/58N
Bt.28316.1.S1_at	SH2D3A	SH2 domain containing 3A
Bt.28246.1.S1_at	GPA33	glycoprotein A33 (transmembrane)
Bt.28236.2.A1_at	LOC521163	Similar to H+/K+-exchanging ATPase (EC 3.6.3.10) alpha chain
Bt.2823.3.S1_a_at	C1orf35	chromosome 1 open reading frame 35
Bt.28227.1.S1_at	LOC787926	similar to transmembrane mucin 12
Bt.28220.1.S1_at	LOC615263	hypothetical protein LOC615263
Bt.28216.1.S1_at	LOC783851	similar to RIKEN cDNA 1600002O04 gene
Bt.28208.1.S1_at	MGC127579	similar to Fructose-1,6-bisphosphatase isozyme 2 (D-fructose-1,6-bisphosphate 1-
Bt.28192.1.S1_at	MGC143192	similar to Interferon regulatory factor 6 (IRF-6)
Bt.28150.1.S1_at	TRIM52	tripartite motif-containing 52
Bt.28140.2.S1_at	KCTD15	potassium channel tetramerisation domain containing 15
Bt.28132.1.S1_at	MGC165793	tRNA (adenine-N(1)-)-methyltransferase catalytic subunit TRM61
Bt.2813.1.A1_at	PRKCA	Protein kinase C, alpha
Bt.28103.1.S1_at	LOC535376	similar to transforming growth factor beta type II receptor, TGF beta R-II
Bt.28083.1.S1_at	MGC128725	similar to SH2 domain protein 1A
Bt.28069.1.S1_at	TMIGD	transmembrane and immunoglobulin domain containing
Bt.28033.1.S1_at	LOC788991	hypothetical protein LOC788991
Bt.28024.1.S1_at	LOC407111 /// LOC784352 /// LOC785839	Fas ligand /// similar to Fas-ligand
Bt.28009.1.S1_at	KRT8 /// LOC515823	keratin 8 /// similar to Keratin 8
Bt.28007.1.A1_s_at	BVd1.20	T cell receptor delta chain variable region
Bt.28006.1.S1_at	LOC407197	T cell receptor gamma chain
Bt.28006.1.A1_at	LOC407197	T cell receptor gamma chain
Bt.28005.1.S1_at	LOC509374	Similar to TCR delta
Bt.28005.1.A1_at	LOC509374	Similar to TCR delta
Bt.28004.2.A1_x_at	LOC505306	Hypothetical LOC505306
Bt.27999.1.S1_at	LOC444875	IgM
Bt.27994.1.S1_at	ANPEP	alanyl (membrane) aminopeptidase
Bt.27984.1.S1_x_at	---	Immunoglobulin heavy chain variable region (IGHV gene)
Bt.27981.1.A1_at	cd21	complement receptor type 2
Bt.27977.1.A1_at	IMPDH1	IMP (inosine monophosphate) dehydrogenase 1
Bt.27881.1.A1_at	LOC533085	similar to RanBP17
Bt.27853.1.S1_at	OSGEP	O-sialoglycoprotein endopeptidase
Bt.27850.2.S1_at	LOC535353	similar to Pleckstrin homology domain containing, family G (with RhoGef domain)
Bt.27834.1.A1_at	MGC137817	similar to CG7139-PA
Bt.27821.1.S1_at	MGC152614	similar to NOL1/NOP2/Sun domain family, member 5
Bt.27819.1.S1_at	LOC787487	similar to von Willebrand factor C and EGF domains
Bt.27767.2.S1_at	LOC784831 /// SLC28A3	solute carrier family 28 (sodium-coupled nucleoside transporter), member 3 /// s
Bt.27767.1.A1_at	LOC784831 /// SLC28A3	solute carrier family 28 (sodium-coupled nucleoside transporter), member 3 /// s
Bt.2771.1.A1_at	MGC142450	similar to seizure related gene 6
Bt.27692.1.A1_at	LOC613858	similar to splicing factor YT521-B
Bt.27643.1.A1_at	ZNF410	zinc finger protein 410
Bt.2761.1.S1_a_at	LOC614755	hypothetical LOC614755
Bt.27581.1.A1_at	LOC540175	similar to KIAA0514
Bt.27570.1.A1_at	LOC513236	similar to tigger transposable element derived 3
Bt.27525.1.S1_at	MGC165851	similar to serine/threonine protein kinase
Bt.27495.1.A1_at	LOC506293	similar to DEAD/H (Asp-Glu-Ala-Asp/His) box polypeptide 11
Bt.27468.1.A1_at	MGC179401	similar to acyl-CoA:cholesterol acyltransferase 2
Bt.27453.1.A1_at	MGC139257	hypothetical LOC520468

Probe Set ID	Gene Symbol	Gene Title
Bt.27444.1.A1_at	LOC506508	similar to phospholipase B1
Bt.27428.2.A1_at	GPM6A	Glycoprotein M6A
Bt.27428.1.A1_at	GPM6A	Glycoprotein M6A
Bt.27397.1.A1_at	LOC617312	similar to Centrosomal protein 72kDa
Bt.27389.2.S1_a_at	MGC159994	similar to KIAA0014
Bt.27378.1.A1_at	---	---
Bt.27364.1.S1_at	LOC518283	Platelet-activating factor receptor
Bt.27307.1.S1_at	---	Transcribed locus
Bt.27304.2.S1_at	MGC139492	similar to Poly(rC)-binding protein 3 (Alpha-CP3)
Bt.27304.1.S1_at	MGC139492	similar to Poly(rC)-binding protein 3 (Alpha-CP3)
Bt.27261.2.S1_at	LOC784347	Similar to multidrug resistance-associated protein
Bt.27254.1.A1_at	WNT2B	wingless-type MMTV integration site family, member 2B
Bt.27250.1.S1_at	LOC506751	similar to Laminin alpha-5 chain
Bt.27241.1.S1_at	LOC527711	similar to Spectrin beta chain, erythrocyte (Beta-I spectrin)
Bt.27234.1.S1_at	SPINT1	serine peptidase inhibitor, Kunitz type 1
Bt.27229.1.S1_at	MGC140809	similar to Folate transporter 1 (Solute carrier family 19 member 1) (Placental f
Bt.27175.2.S1_at	RELL2	RELT-like 2
Bt.27053.1.A1_at	LOC509707	similar to G protein-coupled receptor 1
Bt.27052.1.S1_at	PSCD4	pleckstrin homology, Sec7 and coiled-coil domains 4
Bt.27043.2.S1_at	LOC506783	similar to high affinity immunoglobulin E receptor alpha subunit
Bt.27029.1.S1_at	LOC784875 /// TMEM45B	transmembrane protein 45B /// similar to Transmembrane protein 45B
Bt.27015.1.A1_at	LOC516048	similar to ARF GTPase-activating protein GIT2
Bt.27001.1.S1_at	MGC139710	similar to CG18177-PB
Bt.26994.1.A1_at	KCNB2	potassium voltage-gated channel, Shab-related subfamily, member 2
Bt.26982.2.S1_at	LOC523815	similar to myeloid translocation gene-related protein 2 isoform MTG16a
Bt.26970.1.S1_at	LOC507860	similar to Phosphatidylinositol 4-kinase type II
Bt.26952.2.A1_at	LOC614351	similar to CGI-122 protein
Bt.26934.1.A1_at	LOC506914	similar to testis specific protein A14
Bt.26927.2.S1_at	C10orf77	similar to hypothetical protein FLJ22529
Bt.26927.2.S1_a_at	C10orf77	similar to hypothetical protein FLJ22529
Bt.26895.2.S1_at	LOC521099	hypothetical LOC521099
Bt.26865.3.S1_a_at	LOC785670	similar to Myosin head domain containing 1
Bt.26864.2.S1_at	LOC516012	hypothetical LOC516012
Bt.26860.1.A1_at	LOC521190	Similar to axonemal heavy chain dynein type 3
Bt.26859.2.S1_at	MGC143089	similar to family 3, member A protein
Bt.26852.1.S1_at	MGC143166	similar to Fetal brain protein 239 (239FB)
Bt.26832.1.S1_at	LOC518086	similar to CANT1 protein
Bt.26827.2.S1_at	KLHL12	kelch-like 12
Bt.26775.1.S1_at	LOC511514	similar to HIR (histone cell cycle regulation defective, S. cerevisiae) homolog
Bt.26757.2.A1_a_at	LOC515677	similar to chromosome 20 open reading frame 17
Bt.26737.1.S1_at	USP52	ubiquitin specific peptidase 52
Bt.26725.1.S1_at	LOC537773	growth factor independent 1B-like protein
Bt.26698.1.S1_at	LOC511966	similar to DLNB23
Bt.26691.3.S1_at	TNFSF13	tumor necrosis factor (ligand) superfamily, member 13
Bt.26674.1.S1_at	LOC517405	similar to Jagged2
Bt.26654.1.S1_at	LOC617764	hypothetical LOC617764
Bt.26629.1.S1_a_at	MGC139849	similar to F-box protein FBW7
Bt.26592.2.A1_at	GALGT	UDP-N-acetyl-alpha-D-galactosamine:(N-acetylneuraminyl)-galactosylglucosylcerami
Bt.26591.1.S1_at	MGC152584	similar to TBC1 domain family, member 10C
Bt.26587.2.S1_at	MGC148838	similar to Histone deacetylase 11 (HD11)
Bt.26565.1.A1_at	LOC541226	similar to Zinc finger protein Helios (IKAROS family zinc finger protein 2)
Bt.26555.1.S1_at	GGTL3	gamma-glutamyltransferase-like 3
Bt.26546.1.S1_at	MUS81	MUS81 endonuclease homolog
Bt.26544.2.S1_at	LOC784636	hypothetical protein LOC784636
Bt.26537.1.S1_at	LRRC33	leucine rich repeat containing 33
Bt.26530.2.S1_at	LOC511425	similar to ACAD 10
Bt.26518.3.S1_a_at	MGC157040	hypothetical LOC513646
Bt.26409.1.A1_at	LOC787393	hypothetical protein LOC787393
Bt.26356.2.S1_at	MGC142602	similar to Glutamate decarboxylase 1 (Glutamate decarboxylase, 67 kDa isoform) (
Bt.26352.1.A1_at	LOC613428	Similar to Zinc finger FYVE domain-containing protein 9 (Mothers against decapen
Bt.26326.1.A1_at	LOC617904	similar to Mdm2, transformed 3T3 cell double minute 2, p53 binding protein (mous
Bt.26307.1.A1_at	LOC505477	similar to regulator of G protein signaling RGS12
Bt.26294.1.A1_at	LOC407169	12-lipoxygenase
Bt.26259.3.A1_at	LOC515561	similar to zinc finger protein 462
Bt.26204.1.A1_at	LOC532895	similar to C18orf17 protein
Bt.26197.1.A1_at	CARD9	caspase recruitment domain family, member 9
Bt.26180.2.A1_at	LOC504294	similar to KIAA1206 protein
Bt.26147.1.A1_at	LOC782935	similar to TAFA1
Bt.26128.1.A1_at	MGC157183	similar to class-I MHC-restricted T cell associated molecule
Bt.26125.1.A1_at	GFAP	glial fibrillary acidic protein
Bt.26101.1.A1_at	COLQ	collagen-like tail subunit (single strand of homotrimer) of asymmetric acetylcho
Bt.26075.1.S1_at	MGC143176	similar to Sorting nexin-11

Probe Set ID	Gene Symbol	Gene Title
Bt.26060.1.A1_at	BTK	Bruton agammaglobulinemia tyrosine kinase
Bt.26010.1.A1_at	LOC513625	similar to SPA-1-like 3
Bt.25958.2.S1_at	LOC514870	similar to WD repeat protein WDR3
Bt.25957.2.S1_at	VISA	virus-induced signaling adapter
Bt.25951.1.A1_at	MGC155119	similar to lethal giant larvae homolog 2
Bt.25947.1.A1_at	ITGB4BP	integrin beta 4 binding protein
Bt.25924.2.S1_at	MGC160119	similar to Family with sequence similarity 64, member A
Bt.25904.1.A1_at	LOC539074	similar to transient receptor potential V1
Bt.25882.1.A1_at	FHL3	four and a half LIM domains 3
Bt.25860.1.A1_at	MYBPC1	Myosin binding protein C, slow type
Bt.25856.1.A1_at	---	Transcribed locus, weakly similar to XP_001518985.1 PREDICTED: hypothetical prot
Bt.25807.1.A1_at	LOC540876	similar to proto-oncogene tyrosine-protein kinase
Bt.25804.1.A1_at	MGC139931	similar to PDZ domain containing ring finger 1
Bt.25773.2.S1_at	IQCA	IQ motif containing with AAA domain
Bt.25736.1.A1_at	MGC157237	hypothetical LOC511175
Bt.25732.1.A1_at	LOC618549	hypothetical LOC618549
Bt.25702.1.A1_at	TMEM145	transmembrane protein 145
Bt.25693.1.S1_at	LOC504530	similar to FLJ00018 protein
Bt.25668.2.S1_at	MGC128628	similar to F37C4.6
Bt.25648.1.A1_at	SPPL2B	signal peptide peptidase-like 2B
Bt.25628.1.A1_at	GMFG	glia maturation factor, gamma
Bt.25599.1.A1_at	LOC540087	similar to corticotropin releasing factor binding protein
Bt.25582.1.A1_at	CHRM4	Cholinergic receptor, muscarinic 4
Bt.25568.1.S1_at	MGC148650	similar to Gamma-aminobutyric acid (GABA) A receptor, delta
Bt.25530.1.A1_at	LOC615161	similar to FERM domain containing 5
Bt.25510.2.S1_at	LOC513740	hypothetical LOC513740
Bt.255.1.S1_at	SDR3	short-chain dehydrogenase/reductase
Bt.25486.1.A1_at	---	Transcribed locus, strongly similar to NP_001071589.1 hypothetical protein LOC76
Bt.25476.1.S1_at	LOC538433	hypothetical LOC538433
Bt.25473.1.A1_at	MGC151963	Similar to Metabotropic glutamate receptor 7 precursor (mGluR7)
Bt.25456.1.S1_a_at	LOC786296	hypothetical protein LOC786296
Bt.25447.1.A1_at	LOC538797	similar to receptor protein-tyrosine kinase
Bt.25423.1.S1_at	---	Transcribed locus, strongly similar to NP_999393.1 prostaglandin H2 D-isomerase
Bt.25420.1.A1_at	LOC408019	C-C motif chemokine receptor 4
Bt.25413.1.A1_at	GBL	G protein beta subunit-like
Bt.25411.1.A1_at	SLC17A6	solute carrier family 17 (sodium-dependent inorganic phosphate cotransporter), m
Bt.25407.1.S1_at	LOC507696	similar to G-protein coupled receptor-associated sorting protein 1 (GASP-1)
Bt.25355.1.A1_at	NALP5	NACHT, leucine rich repeat and PYD containing 5
Bt.2532.1.S1_at	UBL7	ubiquitin-like 7 (bone marrow stromal cell-derived)
Bt.25279.1.A1_at	LRSAM1	Leucine rich repeat and sterile alpha motif containing 1
Bt.25088.1.A1_at	GCSH	Glycine cleavage system protein H (aminomethyl carrier)
Bt.25062.1.A1_at	FGF12	fibroblast growth factor 12
Bt.24995.1.A1_at	THEX1	Three prime histone mRNA exonuclease 1
Bt.24993.1.A1_at	LOC537017	Similar to CMP-N-acetylneuraminic acid hydroxylase
Bt.24962.1.A1_at	COL18A1	collagen, type XVIII, alpha 1
Bt.24875.1.S1_at	LOC617922	myeloid-associated differentiation marker-like
Bt.24813.3.S1_at	RTP4	receptor (chemosensory) transporter protein 4
Bt.24786.1.S1_at	MGC142630	similar to syntaxin 1A (brain)
Bt.24771.1.A1_at	CPNE6	copine VI (neuronal)
Bt.24748.1.A1_at	AMOTL2	angiomotin like 2
Bt.24742.1.S1_at	LOC505683	similar to Tubulin polyglutamylase complex subunit 1 (PGs1)
Bt.24737.1.S1_at	MGC143184	similar to Armadillo repeat containing 7
Bt.24675.1.S1_at	LOC614838	similar to p101 protein
Bt.24673.1.A1_at	---	Transcribed locus, strongly similar to XP_595458.3 PREDICTED: similar to Lipl3 p
Bt.24665.1.S1_at	LOC508720	similar to (MHC) class II transactivator
Bt.24644.1.S1_at	CPXM	carboxypeptidase X
Bt.24627.2.A1_a_at	MGC128227	similar to GIY-YIG domain containing 2
Bt.24624.1.S1_at	MRPS9	mitochondrial ribosomal protein S9
Bt.24605.1.S1_at	LOC787326	similar to Gamma-glutamyltransferase-like activity 1
Bt.24573.2.S1_at	MGC143056	similar to polynucleotide kinase-3-phosphatase
Bt.24565.1.S1_at	LOC507256	similar to RAI16 protein
Bt.24521.2.S1_at	LOC539174	similar to myotubularin related protein 9
Bt.24513.1.S1_at	USP12	ubiquitin specific peptidase 12
Bt.24475.1.S1_at	LOC515758	hypothetical LOC515758
Bt.24445.1.A1_at	LOC513676	similar to sine oculis homeobox homolog 5
Bt.24442.3.S1_at	LOC511220	Similar to Rho guanine nucleotide exchange factor (GEF) 11
Bt.24441.3.S1_at	---	CDNA clone IMAGE:7956285
Bt.24438.1.S1_a_at	LOC511511	similar to granulocyte colony stimulating factor receptor 25-1
Bt.24426.1.A1_at	---	Transcribed locus, strongly similar to XP_218506.3 PREDICTED: similar to carbohy
Bt.24399.1.A1_at	LOC537964	Similar to odz, odd Oz/ten-m homolog 1(Drosophila)
Bt.24396.3.A1_at	NUDT11	nudix (nucleoside diphosphate linked moiety X)-type motif 11
Bt.24378.1.S1_at	MAPK8IP3	mitogen-activated protein kinase 8 interacting protein 3
Bt.2436.1.A1_at	GH	growth hormone

Probe Set ID	Gene Symbol	Gene Title
Bt.24359.3.S1_at	ALS2CL	ALS2 C-terminal like
Bt.24351.1.A1_at	MGC142689	similar to limb expression 1
Bt.24323.1.A1_at	LOC528040	similar to Chain A, Structure Of Mammalian C3 With An Intact Thioester At 3a Res
Bt.24293.1.A1_at	BHMT	betaine-homocysteine methyltransferase
Bt.2426.2.S1_at	MGC137376	hypothetical LOC515507
Bt.2421.1.A1_at	LOC782309	similar to Pleckstrin homology domain containing, family F (with FYVE domain) me
Bt.24201.1.A1_at	F9	coagulation factor IX
Bt.24176.1.A1_at	MGC143302	similar to Interleukin-1 receptor accessory protein precursor (IL-1 receptor acc
Bt.24101.1.A1_at	LOC533798	hypothetical LOC533798
Bt.24020.1.A1_at	LOC533203	Similar to matrix metalloproteinase 19 isoform rasi-6
Bt.24.1.S1_at	OPCML	opioid binding protein/cell adhesion molecule-like
Bt.23987.1.A1_at	EIF3S7	eukaryotic translation initiation factor 3, subunit 7 zeta, 66/67kDa
Bt.23963.1.A1_s_at	SULT2A1	sulfotransferase family, cytosolic, 2A, dehydroepiandrosterone (DHEA)-preferring
Bt.23872.1.A1_at	MGC128787	Similar to CG3625-PB
Bt.23855.1.A1_at	ALB	Albumin
Bt.23853.3.S1_a_at	FES	feline sarcoma oncogene
Bt.23827.1.A1_at	LOC616400 /// PAPOLB	poly(A) polymerase beta (testis specific) /// similar to Chain A, Crystal Struct
Bt.238.1.S1_at	HOXB7	homeobox B7
Bt.23750.1.A1_at	GJA1	Gap junction protein, alpha 1, 43kDa
Bt.2373.2.S1_at	PAQR6	progestin and adipoQ receptor family member VI
Bt.23608.1.S1_s_at	KRT8	keratin 8
Bt.23602.2.A1_at	LOC539205	similar to BRUNO-like 6 RNA-binding protein
Bt.23583.1.S1_at	IL21	interleukin 21
Bt.23565.1.S1_at	LOC533909	hypothetical LOC533909
Bt.23501.2.S1_at	LOC616142	hypothetical protein LOC616142
Bt.23501.1.S1_at	LOC616142	hypothetical protein LOC616142
Bt.23298.1.S1_at	CCDC84	coiled-coil domain containing 84
Bt.23246.1.S1_at	CDH5	cadherin 5, type 2, VE-cadherin (vascular epithelium)
Bt.23205.1.S1_s_at	LOC787239	similar to Synaptotagmin-1 (Synaptotagmin I) (SytI) (p65)
Bt.23174.1.S1_at	MGC127643	similar to CD74 antigen
Bt.23153.1.S1_at	DSSDR2	double substrate-specificity short chain dehydrogenase/reductase 2
Bt.23079.2.A1_at	ORP150	Oxygen regulated protein, 150 kDa
Bt.23079.1.S1_at	LOC508773	similar to Hyou1 protein
Bt.22992.2.S1_at	LOC527819	similar to keratin 4
Bt.22984.1.S1_a_at	GCNT3	glucosaminyl (N-acetyl) transferase 3, mucin type
Bt.22973.1.S1_at	MYF6	myogenic factor 6 (herculin)
Bt.22967.1.A1_at	SPAM1	sperm adhesion molecule 1
Bt.22876.1.A1_at	SOX9	SRY (sex determining region Y)-box 9 (campomelic dysplasia, autosomal sex-revers
Bt.22875.1.A1_at	CACNA1E	calcium channel, voltage-dependent, R type, alpha 1E subunit
Bt.22861.1.S1_at	GRP	gastrin-releasing peptide
Bt.22788.1.S1_at	RAF1	v-raf-1 murine leukemia viral oncogene homolog 1
Bt.227.3.A1_a_at	GSTA1 /// GSTA2	glutathione S-transferase A2 /// glutathione S-transferase A1
Bt.22692.2.S1_at	IL6R	interleukin 6 receptor
Bt.2266.3.S1_at	TRAF3IP3	TRAF3 interacting protein 3
Bt.22646.2.S1_at	LOC539884	similar to binding regulatory factor
Bt.2258.1.A1_at	LOC523809	Similar to KIAA1959 protein
Bt.22545.1.S1_a_at	MGC148755	similar to fibulin-1 C
Bt.22541.1.A1_at	ARF1 /// ARF3 /// LOC785421	ADP-ribosylation factor 1 /// ADP-ribosylation factor 3 /// similar to ADP-ribos
Bt.22475.1.S1_at	LOC539413	similar to aortic preferentially expressed gene 1
Bt.22400.1.A1_at	LOC615883	similar to SLIT3
Bt.22325.1.S1_at	MGC151722	hypothetical protein LOC783439
Bt.22277.1.S1_at	LOC538843	similar to LRMR5827
Bt.22264.2.A1_a_at	MGC140699	similar to p53-induced protein
Bt.22223.2.S1_at	JOSD1	Josephin domain containing 1
Bt.22221.1.S1_at	LOC540530	similar to fibronectin type III and SPRY domain containing 2
Bt.22180.1.S1_at	LOC507332	similar to DTTR431
Bt.22128.2.S1_at	LOC507361	hypothetical protein LOC507361
Bt.2212.1.S1_at	LOC616136	similar to OTTHUMP00000017061
Bt.22104.1.S1_at	IHH	indian hedgehog
Bt.22094.2.S1_at	MGC142386	similar to chromosome 9 open reading frame 26 (NF-HEV)
Bt.22048.1.S1_at	LOC615922	similar to KIAA1793 protein
Bt.21997.1.S1_at	PPM1K	protein phosphatase 1K (PP2C domain containing)
Bt.21980.1.S1_at	LOC783725	similar to B-cell differentiation antigen CD72 (Lyb-2)
Bt.21959.3.S1_at	LOC536822	Hypothetical LOC536822
Bt.21939.2.S1_at	LOC537594	similar to phosphatase and actin regulator 1
Bt.21926.2.S1_a_at	LOC508142	similar to translocase of outer mitochondrial membrane 34
Bt.21918.1.S1_at	CARS2	cysteinyl-tRNA synthetase 2, mitochondrial (putative)
Bt.21903.1.S1_at	MOBKL2C	MOB1, Mps One Binder kinase activator-like 2C
Bt.219.1.S1_at	AKAP3	A kinase (PRKA) anchor protein 3
Bt.21851.2.S1_at	---	Transcribed locus, moderately similar to NP_001096709.1 F-box protein 17 [Bos ta

Probe Set ID	Gene Symbol	Gene Title
Bt.21827.2.S1_at	THOP1	thimet oligopeptidase 1
Bt.21731.2.S1_a_at	DBN1	drebrin 1
Bt.21722.1.S1_at	MGC137405	GTPase, IMAP family member
Bt.21706.2.A1_at	MGC152081	similar to carboxypeptidase A5
Bt.21655.1.S1_at	FUT2	fucosyltransferase 2 (secretor status included)
Bt.21570.3.A1_at	LOC533096	Similar to CD39L4
Bt.2156.2.S1_a_at	LOC508598	hypothetical LOC508598
Bt.21534.3.S1_a_at	LOC533826	similar to TIP120-family protein TIP120B
Bt.21501.2.S1_a_at	DECR2	2,4-dienoyl CoA reductase 2, peroxisomal
Bt.21498.1.S1_at	CPSF4	cleavage and polyadenylation specific factor 4, 30kDa
Bt.21482.2.S1_at	LOC538384	similar to beta-interferon gene positive-regulatory domain I binding factor
Bt.21407.2.S1_at	TNMD	tenomodulin
Bt.21360.1.S1_at	LOC539901	hypothetical LOC539901
Bt.21308.1.A1_at	RAPGEF3	Rap guanine nucleotide exchange factor (GEF) 3
Bt.21221.1.S1_at	LOC615744	similar to Lst-1 gene product
Bt.21215.2.S1_at	LOC506721	similar to ALL1 responsive protein ARP1c
Bt.21215.1.A1_at	LOC506721	similar to ALL1 responsive protein ARP1c
Bt.2114.1.S1_at	---	CDNA clone IMAGE:8220921
Bt.21126.2.S1_at	SNCB	synuclein, beta
Bt.210.1.S1_at	PRH	preproprolactin-releasing peptide
Bt.20999.1.S1_at	COLEC11	collectin sub-family member 11
Bt.20921.1.S1_at	BSG	basigin
Bt.20901.1.A1_at	LOC507162	Similar to Apobec3G
Bt.20884.1.S1_at	MGC137881	Similar to RNA-binding protein 5 (RNA-binding motif protein 5) (Putative tumor s
Bt.20867.1.A1_at	RPUSD3	RNA pseudouridylate synthase domain containing 3
Bt.20850.1.S1_at	LOC520186	similar to centrosomal protein 110kDa
Bt.20828.1.A1_at	LOC617365	similar to Chromosome 14 open reading frame 143
Bt.20795.1.A1_at	PARD6A	par-6 partitioning defective 6 homolog alpha (C. elegans)
Bt.20771.2.S1_at	LOC505771	similar to Pex1pL664P
Bt.20723.1.A1_at	LOC514108	Similar to Eukaryotic translation initiation factor 4E transporter (eIF4E transp
Bt.20698.1.A1_at	ETAA16	ETAA16 protein
Bt.20653.1.A1_at	LOC539392	similar to programmed death ligand 2
Bt.20522.1.S1_at	---	Transcribed locus, moderately similar to XP_943264.1 PREDICTED: similar to Serin
Bt.20513.2.S1_a_at	MGC140219	similar to Serine/threonine-protein kinase MARK2 (MAP/microtubule affinity-regul
Bt.20513.1.S1_at	MGC140219	similar to Serine/threonine-protein kinase MARK2 (MAP/microtubule affinity-regul
Bt.20491.1.S1_at	---	Transcribed locus, strongly similar to XP_342578.2 PREDICTED: similar to RIKEN c
Bt.20478.2.S1_at	LOC512021	similar to Rho guanine exchange factor 15
Bt.20471.2.S1_a_at	SHARPIN	SHANK-associated RH domain interactor
Bt.20455.1.S1_at	MAPT	Microtubule-associated protein tau
Bt.20453.1.S1_at	LOC515122	similar to Abhydrolase domain containing 14A
Bt.20431.2.S1_at	MGC140538	similar to Max interacting protein 1
Bt.2039.2.S1_at	LOC514971	similar to cytochrome P450 2S1
Bt.2039.1.S1_at	LOC514971	similar to cytochrome P450 2S1
Bt.20388.1.S1_at	TM4SF4	transmembrane 4 L six family member 4
Bt.20362.1.S1_at	LOC516567	similar to KIAA0365 protein
Bt.20361.3.S1_at	FBXL2	F-box and leucine-rich repeat protein 2
Bt.20241.1.S1_at	LOC510602 /// LOC786774	similar to 3-hydroxyanthranilate 3,4-dioxygenase (3-HAO) (3-hydroxyanthranilic a
Bt.20232.1.S1_at	LOC511420	hypothetical LOC511420
Bt.20212.1.S1_at	MGC152565	similar to adenylate cyclase type IV
Bt.20180.1.S1_at	RAB25	RAB25, member RAS oncogene family
Bt.20178.2.S1_at	MGC152142	similar to nuclear factor of kappa light polypeptide gene enhancer in B-cells in
Bt.20120.3.S1_at	LOC511801	Similar to ubiquitin-conjugating enzyme E2D 4 (putative)
Bt.20092.2.S1_at	MGC140362	similar to Rab GTPase-binding effector protein 2 (Rabaptin-5beta)
Bt.20088.2.S1_a_at	TPPP	tubulin polymerization promoting protein
Bt.20085.2.S1_at	LOC510966	hypothetical LOC510966
Bt.20081.1.S1_at	MGC137224	similar to PET112-like
Bt.20058.1.S1_at	MGC138975	Similar to mitochondrial ribosomal protein L14
Bt.20018.2.S1_a_at	LOC100126544	hypothetical LOC100126544
Bt.20012.1.S1_at	LOC516256	similar to glucocorticoid-induced TNFR-related protein
Bt.19980.1.A1_at	ApoN	ovarian and testicular apolipoprotein N
Bt.19884.2.S1_at	PLA1A	phospholipase A1 member A
Bt.19795.1.S1_at	BREH1	retinyl ester hydrolase type 1
Bt.1978.9.A1_at	TRB@	T cell receptor, beta cluster
Bt.1978.8.A1_at	LOC507049	T-cell receptor beta chain V region
Bt.1978.10.A1_a_at	TRB@	T cell receptor, beta cluster
Bt.19753.1.S1_at	LOC783335	similar to IL-17RE
Bt.19717.1.S1_at	LOC785809	similar to Family with sequence similarity 109, member A
Bt.19629.3.A1_at	HSPH1	heat shock 105kDa/110kDa protein 1
Bt.19619.1.A1_at	HRMT1L2	HMT1 hnRNP methyltransferase-like 2
Bt.19578.1.S1_at	LOC618914	hypothetical LOC618914
Bt.195.2.S1_at	LOC540141	similar to F-box and leucine-rich repeat protein 11
Bt.19470.1.A1_at	MGC166329	hypothetical LOC525941

Probe Set ID	Gene Symbol	Gene Title
Bt.19334.3.S1_at	JUND	jun D proto-oncogene
Bt.19309.3.A1_at	LOC616742	similar to Ephrin-A5 precursor (EPH-related receptor tyrosine kinase ligand 7) (
Bt.19296.2.S1_a_at	SLC39A3	solute carrier family 39 (zinc transporter), member 3
Bt.19274.1.A1_at	C1QTNF7	C1q and tumor necrosis factor related protein 7
Bt.19232.1.A1_at	---	Transcribed locus, strongly similar to NP_001071497.1 hypothetical protein LOC54
Bt.19148.1.S1_a_at	KHDRBS1	KH domain containing, RNA binding, signal transduction associated 1
Bt.191.1.S1_at	IL1A	interleukin 1, alpha
Bt.19060.1.A1_at	LOC523081	similar to Solute carrier family 23 (nucleobase transporters), member 3
Bt.1905.1.S1_at	MYL2	myosin, light chain 2, regulatory, cardiac, slow
Bt.19008.1.A1_at	---	Transcribed locus, weakly similar to NP_001028798.1 fibrinogen A-alpha chain [Bo
Bt.18927.1.A1_at	KIAA1189	hypothetical protein LOC617274
Bt.18901.1.S1_at	LOC539749	similar to Homeobox protein SIX6 (Sine oculis homeobox homolog 6) (Optic homeobo
Bt.18868.1.S1_at	---	Transcribed locus, strongly similar to NP_001098481.1 tripartite motif-containin
Bt.18864.1.A1_at	---	Transcribed locus, weakly similar to NP_001073867.1 KIAA0368 protein [Homo sapie
Bt.18804.2.S1_at	LOC784914	similar to Zinc finger protein 26
Bt.18804.1.A1_at	LOC784914	similar to Zinc finger protein 26
Bt.18793.2.S1_at	SVOP	SV2 related protein
Bt.18752.1.S1_at	MGC143150	similar to SET and MYND domain containing protein 2 (HSKM-B)
Bt.18735.2.S1_at	ITGB3BP	integrin beta 3 binding protein
Bt.18682.1.A1_at	CST6	cystatin E/M
Bt.18571.2.S1_at	MGC155295	similar to disks large-associated protein 4
Bt.18522.1.A1_at	---	Transcribed locus, strongly similar to NP_056558.1 nuclear receptor subfamily 4,
Bt.18506.1.S1_at	DLG5	discs, large homolog 5 (Drosophila)
Bt.18487.3.S1_at	MGC140386	hypothetical LOC527134
Bt.18487.2.S1_at	LOC617939	similar to FLJ00248 protein
Bt.18422.1.S1_at	LOC515581	similar to MGC21874 protein
Bt.18418.1.A1_at	LOC532674	similar to OTTHUMP00000016557
Bt.18342.2.A1_at	---	Transcribed locus, strongly similar to XP_986810.1 PREDICTED: similar to HECT do
Bt.18290.2.S1_at	LOC506182	similar to Tnf receptor-associated factor 3
Bt.18285.1.A1_at	LOC531695	similar to homeodomain protein
Bt.18238.1.S1_at	MGC152584	similar to TBC1 domain family, member 10C
Bt.18231.1.S1_at	CYP2C87	cytochrome P450, family 2, subfamily C, polypeptide 87
Bt.18189.1.A1_at	LOC504803	similar to 12R-lipoxygenase
Bt.18180.1.A1_at	LOC781707	hypothetical protein LOC781707
Bt.18120.1.A1_at	DDX5	DEAD (Asp-Glu-Ala-Asp) box polypeptide 5
Bt.18085.2.A1_at	MGC157202	Similar to sterol response element binding protein cleavage-activating protein
Bt.17935.1.S1_at	LOC514212	similar to myosin, heavy chain 14
Bt.17792.1.S1_at	LOC506859	similar to KIAA1588 protein
Bt.17780.2.S1_at	LOC510185	similar to IL2RB
Bt.1776.2.S1_a_at	LOC509964	hypothetical LOC509964
Bt.17756.2.S1_at	LOC616498	similar to piggyBac transposable element derived 5
Bt.17742.1.A1_at	LOC507082	Akt substrate AS250
Bt.17737.1.A1_at	---	Transcribed locus, weakly similar to NP_001012749.1 hypothetical protein LOC2838
Bt.17711.1.A1_at	LOC533355	similar to ENaCB, amiloride sensitive sodium channel beta subunit
Bt.17673.1.A1_at	LOC788986	Similar to HZFW1
Bt.17642.1.A1_at	LOC784036	similar to Zinc finger protein 323
Bt.17537.1.A1_at	SAA4	serum amyloid A4, constitutive
Bt.17520.1.S1_at	LOC506571	hypothetical LOC506571
Bt.1748.2.S1_a_at	KLC4 /// LOC784355	kinesin light chain 4 /// similar to LOC767885 protein
Bt.174.1.S1_at	GABRA2	gamma-aminobutyric acid (GABA) A receptor, alpha 2
Bt.1739.3.S1_at	---	Transcribed locus, strongly similar to NP_989430.1 frizzled homolog 4 [Gallus ga
Bt.17332.1.S1_at	LOC613833	similar to mineralocorticoid receptor
Bt.17305.1.A1_at	MGC152385	similar to Fragile X mental retardation 1 neighbor
Bt.17291.1.A1_at	TEX12	Testis expressed 12
Bt.1726.2.S1_at	MGC179414	hypothetical LOC514858
Bt.1722.3.S1_a_at	LOC538270	similar to skeletrophin
Bt.17187.1.A1_at	ARRB1	Arrestin, beta 1
Bt.17170.1.A1_at	LOC504622	similar to killer cell lectin-like receptor family I member 1
Bt.17133.1.A1_at	MGC143419	Similar to KIAA1819 protein
Bt.17078.1.S1_at	LOC516019	similar to semaphorin SEMA6A1
Bt.17059.2.S1_at	LOC618228	similar to nucleolar protein with MIF4G domain 1
Bt.17054.2.A1_at	LOC528960	Hypothetical LOC528960
Bt.17048.1.S1_at	SPATS1	spermatogenesis associated, serine-rich 1
Bt.16964.1.A1_at	---	Transcribed locus, strongly similar to NP_776378.2 prolactin precursor [Bos taur
Bt.16930.1.A1_at	LOC531942	similar to B-cell lymphoma 3-encoded protein (Protein Bcl-3)
Bt.16903.1.A1_at	XAB2	XPA binding protein 2
Bt.1688.1.A1_at	LOC514669 /// LOC789691	hypothetical LOC514669 /// hypothetical protein LOC789691
Bt.16874.1.A1_at	LOC617120	Hypothetical LOC617120
Bt.16822.1.S1_at	MGC157129	similar to KIAA0936 protein
Bt.16810.1.S1_at	LOC509616	similar to Wbscr27 protein
Bt.16801.1.A1_at	MGC151542	Similar to COPG2 protein

Probe Set ID	Gene Symbol	Gene Title
Bt.16795.1.A1_at	SPAG6	sperm associated antigen 6
Bt.16789.1.A1_at	MGC137384	similar to Protein C12orf11 (Sarcoma antigen NY-SAR-95)
Bt.16785.1.A1_at	LOC505819	similar to mannan-binding lectin serine protease 2
Bt.16761.1.S1_a_at	100125581 /// LOC614260 /// LOC783192	similar to zinc finger protein 75 /// hypothetical protein LOC783192 /// hypothe
Bt.16748.1.A1_at	---	---
Bt.16747.1.A1_at	LOC524776	similar to chromodomain helicase DNA binding protein 6
Bt.16745.1.A1_at	CCL28	Chemokine (C-C motif) ligand 28
Bt.16727.2.S1_at	MGC139174	similar to CLN8 protein
Bt.16713.1.A1_at	LOC510356	similar to Non-receptor tyrosine-protein kinase TNK1 (CD38 negative kinase 1)
Bt.16712.1.A1_at	LOC782368	similar to aquaporin 5
Bt.16632.1.A1_at	LOC613276	hypothetical LOC613276
Bt.1661.1.S1_at	LOC100124517	hypothetical protein LOC100124517
Bt.16596.2.S1_at	MGC165823	similar to leucine-rich repeat domain-containing protein
Bt.16583.1.S1_at	MGC126930	similar to Voltage-dependent calcium channel gamma-like subunit (Neuronal voltag
Bt.16580.3.A1_at	MGC139899	similar to leader-binding protein 32
Bt.16532.1.A1_at	LOC506965	similar to DEAH (Asp-Glu-Ala-His) box polypeptide 34
Bt.16498.1.A1_at	LOC615968	similar to chromosome 9 open reading frame 11
Bt.16469.3.S1_at	TRABD	TraB domain containing
Bt.16390.2.A1_at	---	---
Bt.16362.1.S1_at	LOC512324	similar to CG32732-PA
Bt.16307.1.A1_s_at	MGC140803	similar to Pulmonary surfactant-associated protein B precursor (SP-B) (6 kDa pro
Bt.16279.1.A1_at	MGC148626	Similar to Regulated endocrine specific protein 18 precursor
Bt.16211.2.S1_at	LOC789894	similar to PAP-associated domain-containing protein 5 (Topoisomerase-related fun
Bt.16206.1.A1_at	LOC618234	similar to zinc finger protein 258
Bt.16173.1.A1_at	LOC782597	hypothetical protein LOC782597
Bt.16098.1.S1_at	LOC617882	hypothetical LOC617882
Bt.16057.1.S1_at	MGC159903	hypothetical LOC540019
Bt.16042.1.S1_at	LOC539467	hypothetical LOC539467
Bt.16004.1.A1_at	MYH8	myosin, heavy chain 8, skeletal muscle, perinatal
Bt.16003.1.S1_at	PYGM	phosphorylase, glycogen; muscle (McArdle syndrome, glycogen storage disease type
Bt.160.2.S1_x_at	DSC1	desmocollin 1
Bt.15989.1.S1_at	IRF2	interferon regulatory factor 2
Bt.15965.1.S1_at	LOC505878	similar to hSOX20 protein
Bt.15950.2.S1_at	GORASP1	Golgi reassembly stacking protein 1, 65kDa
Bt.15914.2.S1_at	KHK	ketohexokinase (fructokinase)
Bt.15907.1.A1_at	MMACHC	methylmalonic aciduria (cobalamin deficiency) cblC type, with homocystinuria
Bt.15827.1.S1_a_at	LOC534944	similar to Pxaaa1p
Bt.1567.2.S1_a_at	LOC508510	similar to secretory carrier membrane protein 5
Bt.15666.1.S1_at	PXMP2	peroxisomal membrane protein 2, 22kDa
Bt.1559.3.S1_a_at	THAP3	THAP domain containing, apoptosis associated protein 3
Bt.15405.1.A1_at	PRP9	prolactin-related protein IX
Bt.15401.1.S1_at	PAG1B	pregnancy-associated glycoprotein 1
Bt.1536.3.S1_at	LOC506727	similar to nuclear factor of kappa light polypeptide gene enhancer in B-cells in
Bt.14681.1.A1_at	ARG1	arginase, liver
Bt.14637.1.A1_at	CARKL	carbohydrate kinase-like
Bt.14590.1.A1_at	MGC142356	similar to Tyrosine-protein kinase BLK (B lymphocyte kinase) (p55-BLK)
Bt.14576.1.A1_at	LOC515324	similar to Prospero-related homeobox 1
Bt.141.2.S1_a_at	BSM	submaxillary mucin 2
Bt.13990.2.S1_at	LOC539598	similar to zinc finger, CCHC domain containing 8
Bt.13845.2.S1_at	LOC786764 /// MGC151851	similar to HSPC230 /// similar to ATP sulfurylase/APS kinase
Bt.13771.2.S1_at	MGC152529	Similar to CD134 homologue
Bt.13730.2.S1_at	LOC408003	Aut2a
Bt.13716.3.S1_at	NFKBIL2	nuclear factor of kappa light polypeptide gene enhancer in B-cells inhibitor-lik
Bt.13716.2.S1_at	NFKBIL2	nuclear factor of kappa light polypeptide gene enhancer in B-cells inhibitor-lik
Bt.1369.1.S1_at	LOC508989	hypothetical LOC508989
Bt.13668.1.A1_at	TLCD1	TLC domain containing 1
Bt.13583.1.A1_at	LOC510745	similar to ATP-binding cassette transporter G1
Bt.13581.1.S1_at	LOC783908	hypothetical protein LOC783908
Bt.13523.2.A1_at	LOC512538	Similar to RLSS299
Bt.13518.2.S1_at	CRYZL1	crystallin, zeta (quinone reductase)-like 1
Bt.13510.1.S1_at	---	Transcribed locus, strongly similar to NP_001013618.1 major histocompatibility c
Bt.13499.1.S1_at	MGC179503	similar to p87 phosphoinositide 3-kinase gamma adapter protein
Bt.13466.2.A1_at	LOC533634	Similar to oxysterol-binding protein-like protein 6
Bt.13265.1.A1_at	MGC166233	similar to plasmolipin
Bt.13250.1.S1_at	MGC139913	hypothetical LOC513150
Bt.13205.1.A1_at	MRPS35	mitochondrial ribosomal protein S35
Bt.13160.1.S1_at	CEL	carboxyl ester lipase
Bt.13159.1.S1_at	PTPRZ1	protein tyrosine phosphatase, receptor-type, Z polypeptide 1
Bt.13148.1.A1_at	LOC503620	VEGF-receptor
Bt.13146.1.S1_at	ESR1	estrogen receptor 1

Probe Set ID	Gene Symbol	Gene Title
Bt.13116.1.S1_at	ALDH3	dehydrogenase 3, dimeric NAPD-prefering
Bt.13115.1.A1_at	P2RX7	purinergic receptor P2X, ligand-gated ion channel, 7
Bt.13102.1.A1_at	CACNG2	calcium channel, voltage-dependent, gamma subunit 2
Bt.13090.1.S1_at	MMP15	matrix metallopeptidase 15 (membrane-inserted)
Bt.13087.1.A1_at	CD6	CD6 molecule
Bt.13081.1.A1_at	CYP1A1	cytochrome P450, subfamily I (aromatic compound-inducible), polypeptide 1
Bt.13078.1.S2_at	MYOD1	myogenic differentiation 1
Bt.13071.2.A1_at	CACNA1A	calcium channel, voltage-dependent, P/Q type, alpha 1A subunit
Bt.13067.1.S1_at	PAPPA	pregnancy-associated plasma protein A
Bt.13057.2.A1_at	CACNA1H	calcium channel, voltage-dependent, T type, alpha 1H subunit
Bt.13057.1.S1_at	LOC789778	similar to low-voltage-activated calcium channel alpha13.2 subunit
Bt.13048.1.S1_at	CHRM1	cholinergic receptor, muscarinic 1
Bt.13036.1.A1_at	PGR	progesterone receptor
Bt.13024.2.S1_at	P2RY2	purinergic receptor P2Y, G-protein coupled, 2
Bt.13024.2.A1_at	P2RY2	purinergic receptor P2Y, G-protein coupled, 2
Bt.13024.1.S1_at	P2RY2	purinergic receptor P2Y, G-protein coupled, 2
Bt.13003.8.S1_at	TRA@	T cell receptor, alpha
Bt.13003.7.S1_at	TRA@	T cell receptor, alpha
Bt.13003.2.A1_at	TRA@	T cell receptor, alpha
Bt.13003.16.A1_a_at	TRA@	T cell receptor, alpha
Bt.13003.14.S1_at	TRA@	T cell receptor, alpha
Bt.13003.11.A1_at	TRA@	T cell receptor, alpha
Bt.12894.2.S1_a_at	MGC159470	similar to transcript expressed during hematopoiesis 2
Bt.12823.2.S1_at	VWF	von Willebrand factor
Bt.12818.2.A1_a_at	TSPY	testis-specific protein, Y-encoded
Bt.12818.1.A1_at	TSPY	testis-specific protein, Y-encoded
Bt.12807.1.S1_at	LOC317708	5-hydroxytryptamine (serotonin) receptor 4
Bt.12807.1.A1_at	LOC317708	5-hydroxytryptamine (serotonin) receptor 4
Bt.12806.1.S1_at	HR44	Hr44 antigen
Bt.12801.1.A1_at	ALOX15B	arachidonate 15-lipoxygenase, type B
Bt.128.1.S1_at	LOC286848	acetoin reductase
Bt.12781.1.S1_at	MYB	v-myb myeloblastosis viral oncogene homolog (avian)
Bt.12759.1.S1_at	IGF1R	insulin-like growth factor 1 receptor
Bt.12750.2.S1_x_at	IGF1	Insulin-like growth factor 1 (somatomedin C)
Bt.12721.1.A1_at	PSCD2	pleckstrin homology, Sec7 and coiled-coil domains 2 (cytohesin-2)
Bt.12705.2.S1_at	ACTR8	ARP8 actin-related protein 8
Bt.12703.2.S1_at	LOC539882 /// LOC789768	similar to tubulin, alpha 1 /// similar to THAP domain containing 7
Bt.12643.1.A1_at	LOC517043	similar to VTS20631
Bt.12641.1.S1_at	PLVAP	plasmalemma vesicle associated protein
Bt.12577.1.A1_at	LOC517987	Similar to nebulette
Bt.12561.2.S1_at	LOC782984	hypothetical protein LOC782984
Bt.12553.1.S1_at	HP	haptoglobin
Bt.12536.1.S1_at	KCNK2	potassium channel, subfamily K, member 2
Bt.12519.1.S1_at	FMO3	flavin containing monooxygenase 3
Bt.12445.2.S1_at	FSCN1	fascin homolog 1, actin-bundling protein (Strongylocentrotus purpuratus)
Bt.12356.1.S1_at	MGC157300	hypothetical LOC534625
Bt.12330.2.S1_at	CCDC71	coiled-coil domain containing 71
Bt.12296.1.S1_at	ATRN	attractin
Bt.12294.1.S1_at	AMIGO2	amphoterin induced gene 2
Bt.12261.2.S1_a_at	C20orf13	taspase 1
Bt.12245.1.S1_at	LOC508513	similar to ubiquitin protein ligase E3C
Bt.12177.1.S1_at	CLDN4	claudin 4
Bt.12118.1.A1_at	MGC142928	similar to natural killer cell-specific antigen KLIP1
Bt.12105.1.A1_at	LOC539567	similar to Protein phosphatase 1J (PP2C domain containing)
Bt.11724.1.A1_at	alpha globin	hemoglobin alpha chain
Bt.11687.3.A1_at	LOC513912	similar to sarcoplasmic reticulum glycoprotein
Bt.11684.1.A1_at	MGC142747	similar to Neurogenic differentiation factor 6 (NeuroD6)
Bt.11666.3.S1_at	MGC157202	similar to sterol response element binding protein cleavage-activating protein
Bt.11660.1.A1_at	LOC789390	similar to naked cuticle-2
Bt.11553.1.A1_at	NEK3	NIMA (never in mitosis gene a)-related kinase 3
Bt.11478.1.A1_at	LOC523124	similar to KIAA2011 protein
Bt.11477.1.A1_at	LOC509540	Hypothetical LOC509540
Bt.11428.1.A1_at	LOC540879	similar to TAK1-like protein
Bt.11352.2.A1_at	MGC127555	similar to Probable rRNA processing protein EBP2 (EBNA1 binding protein 2) (Nucl
Bt.11327.1.S1_at	MGC137477	similar to CG14648-PA
Bt.11301.3.A1_at	MGC148584	Similar to KIAA0843 protein
Bt.11301.1.S1_at	MGC148584	similar to KIAA0843 protein
Bt.11220.2.S1_a_at	RALB	v-ral simian leukemia viral oncogene homolog B
Bt.11212.1.S1_at	LOC781759 /// VIP	vasoactive intestinal peptide /// similar to vasoactive intestinal polypeptide
Bt.11199.1.S1_at	MYOZ1	myozenin 1
Bt.11171.2.S1_at	FLCN	folliculin

Probe Set ID	Gene Symbol	Gene Title
Bt.11170.2.S1_a_at	TNPO2	transportin 2 (importin 3, karyopherin beta 2b)
Bt.11097.1.S1_at	LOC525506	similar to ZIP-kinase
Bt.11079.1.A1_at	MGC179327	hypothetical LOC616055
Bt.11078.2.S1_at	MGC148743	similar to aflatoxin B1-aldehyde reductase
Bt.1107.1.S1_at	MGC148626	similar to Regulated endocrine specific protein 18 precursor
Bt.11043.1.S1_a_at	LOC533338	similar to Bcl-2 related proline-rich protein
Bt.11032.2.S1_at	EPB49	erythrocyte membrane protein band 4.9 (dematin)
Bt.11027.1.A1_at	LOC516232	similar to Zinc finger protein 653
Bt.11015.1.S1_at	LOC539015	similar to LMBR1L protein
Bt.11005.1.S1_at	SH3BP5L	SH3-binding domain protein 5-like
Bt.10898.1.S1_at	TDE2L	tumor differentially expressed 2-like
Bt.10874.1.S1_at	MGC134253	similar to CG11334-PB
Bt.10844.2.S1_at	LOC529829	Similar to Phosphatidylserine synthase 2
Bt.10842.2.S1_a_at	LOC537017	similar to CMP-N-acetylneuraminic acid hydroxylase
Bt.10831.3.A1_at	LOC534996	Similar to Tyrosine-protein kinase Lyn
Bt.1068.1.A1_at	MGC143401	similar to myosin binding protein H
Bt.1059.3.S1_a_at	LOC540568	Atp2a2
Bt.1052.2.S1_at	CH25H	cholesterol 25-hydroxylase
Bt.1040.2.S1_at	MGC165889	similar to nucleolar protein 1, 120kDa
Bt.10391.1.S1_at	PSRC1	proline/serine-rich coiled-coil 1
Bt.10281.1.S1_at	TKDP5	trophoblast Kunitz domain protein 5
Bt.1009.1.A1_at	PLD2	Phospholipase D2

APPENDIX 2: COMPLETE LIST OF GENES DIFFERENTIALLY EXPRESSED IN MSCS COMPARED TO CHONDROCYTES

Complete list of genes that were at least 2 fold higher in CH vs MSCs (10% FDR); M28 must not be 2 fold lower than M0 or more than 3 fold higher (no FDR)

Probeset ID	Gene Symbol	Gene Title
Bt.22987.2.S1_at	PRG4	proteoglycan 4
Bt.22987.2.A1_at	PRG4	proteoglycan 4
Bt.25045.1.S1_at	LOC538287	similar to Teneurin-2 (Ten-2) (Tenascin-M2) (Ten-m2) (Protein Odd Oz/ten-m homol
Bt.13954.1.S1_at	LUZP5	leucine zipper protein 5
Bt.9697.1.A1_at	MGC137543	similar to Alcohol dehydrogenase 6
Bt.594.1.S1_at	LOC286871	uterine milk protein precursor
Bt.10144.1.A1_s_at	MGC142564	similar to T-lymphoma invasion and metastasis inducing protein 1 (TIAM1 protein)
Bt.8797.1.S1_at	MGC139675	similar to Rap1 GTPase-activating protein 1 (Rap1GAP)
Bt.18860.1.A1_at	LOC531875	similar to protocadherin 10
Bt.1969.1.S1_at	CACNA1H	calcium channel, voltage-dependent, T type, alpha 1H subunit
Bt.20262.1.S1_at	MCM4	minichromosome maintenance complex component 4
Bt.5959.1.S1_at	LOC526726	similar to Retinal short chain dehydrogenase reductase
Bt.25345.1.A1_at	LOC781304	hypothetical protein LOC781304
Bt.29264.1.A1_at	LOC522691	hypothetical LOC522691
Bt.25616.1.S1_at	LOC782069	hypothetical protein LOC782069
Bt.24549.1.A1_at	TKTL1	transketolase-like 1
Bt.20617.1.S1_at	BEX5	BEX family member 5
Bt.24181.1.S1_at	LBP	lipopolysaccharide binding protein
Bt.24199.1.A1_s_at	LOC286871	uterine milk protein precursor
Bt.19449.1.A1_at	LOC540081	similar to CAGR1
Bt.10212.1.S1_at	PHLDA1	Pleckstrin homology-like domain, family A, member 1
Bt.14143.1.S1_at	CPE	carboxypeptidase E
Bt.4231.1.S1_at	CHRNE	cholinergic receptor, nicotinic, epsilon
Bt.22389.1.S1_at	LOC617336	similar to WGAR9166
Bt.23857.1.A1_at	MGC157214	hypothetical LOC524166
Bt.16861.2.S1_at	LOC515128	hypothetical LOC515128
Bt.7447.1.A1_at	B3GALT2	UDP-Gal:betaGlcNAc beta 1,3-galactosyltransferase, polypeptide 2
Bt.4105.2.A1_at	MGC143272	similar to putative GPCR interacting protein GIP
Bt.21547.1.A1_at	MGC140246	similar to plakophilin 2a
Bt.11130.1.S1_at	DNMT1	DNA (cytosine-5-)-methyltransferase 1
Bt.2933.1.S1_at	LOC788205	hypothetical protein LOC788205
Bt.27202.1.A1_at	SOSTDC1	sclerostin domain containing 1
Bt.19482.1.A1_at	LOC504698	similar to transferrin receptor
Bt.13181.2.S2_at	LOC788252	similar to latrophilin-1
Bt.1115.1.S1_at	LOC533323	similar to cyclic nucleotide phophodiesterase
Bt.8091.1.S1_at	LOC527837	similar to hematopoietic progenitor protein
Bt.6056.1.S1_at	LOC615408	similar to septin 5
Bt.9300.1.A1_at	LOC519626	similar to opioid growth factor receptor-like 1
Bt.24902.1.S1_at	LOC540358	similar to 5T4 oncofoetal antigen
Bt.858.1.S1_at	LOC517007	similar to CTF18, chromosome transmission fidelity factor 18 homolog (S. cerevis
Bt.17935.1.S1_at	LOC514212	similar to myosin, heavy chain 14
Bt.29026.1.A1_at	LOC507682	similar to Bone morphogenetic protein 5 precursor (BMP-5)
Bt.7677.1.S1_at	TMEM59L	transmembrane protein 59-like
Bt.25052.1.S1_at	LOC539360	similar to calpain 6
Bt.12599.1.S1_at	LOC507133	similar to type VII collagen
Bt.16886.1.A1_a_at	MGC157096	similar to DNA polymerase epsilon small subunit

Probeset ID	Gene Symbol	Gene Title
Bt.16087.1.S1_at	MGC159943	similar to nidogen-2
Bt.12936.1.S1_at	CATHL5	cathelicidin 5
Bt.13870.1.A1_at	LOC508668	similar to probable dual-specificity Ser/Thr/Tyr kinase
Bt.11057.1.S1_at	LOC781091	hypothetical protein LOC781091
Bt.9789.1.S1_at	mash2	achaete-scute complex-like protein 2 /// achaete scute-like protein 2
Bt.7208.1.S1_at	ZP2	zona pellucida glycoprotein 2 (sperm receptor)
Bt.14207.1.S1_at	GCAT	glycine C-acetyltransferase (2-amino-3-ketobutyrate coenzyme A ligase)
Bt.19372.1.A1_at	LOC527979	similar to leucine rich repeat containing 6 (testis)
Bt.8743.1.S1_at	LOC506194	similar to ERIC1
Bt.1676.1.A1_at	MGC140394	similar to SIGIRR
Bt.16094.1.S1_at	LOC509106	similar to enhancer of zeste homolog 2
Bt.5445.2.A1_at	TUBB	tubulin, beta
Bt.17697.1.A1_at	MGC159632	hypothetical LOC538280
Bt.18280.1.S1_at	SPON2	spondin 2, extracellular matrix protein
Bt.22699.1.S1_at	NFIA	nuclear factor I/A
Bt.24523.1.S1_at	MGC148435	similar to Septin 1
Bt.1818.1.S1_at	LOC514360	similar to desmoplakin isoform II
Bt.21924.1.A1_at	LOC535975	similar to dermatan/chondroitin sulfate 2-sulfotransferase
Bt.20883.1.S1_at	ANG	angiogenin, ribonuclease, RNase A family, 5
Bt.7251.1.S1_at	B3GALT2	UDP-Gal:betaGlcNAc beta 1,3-galactosyltransferase, polypeptide 2
Bt.23857.2.S1_at	MGC157214	hypothetical LOC524166
Bt.13689.1.A1_at	LOC504531	similar to phosphoinositide 3-kinase
Bt.5578.1.S1_at	FLJ40629	hypothetical protein LOC507498
Bt.11030.1.S1_at	LOC514557	similar to OAF homolog (Drosophila)
Bt.27356.1.S1_at	MGC152577	similar to Chromatin assembly factor 1, subunit A (p150)
Bt.26125.1.A1_at	GFAP	glial fibrillary acidic protein
Bt.21355.1.S1_at	LOC789363	similar to Neuronal pentraxin II
Bt.6004.1.S1_at	LOC507012	similar to TACC1
Bt.9194.1.S1_at	LOC534230	similar to microtubule associated serine/threonine kinase 2
Bt.5027.1.A1_at	PEG3	paternally expressed 3
Bt.15927.1.S1_at	MGC159964	similar to WD repeat domain, phosphoinositide interacting 1
Bt.176.1.S1_at	GAL	galanin
Bt.6728.1.A1_at	Ndn	necdin
Bt.16861.1.A1_at	LOC515128	hypothetical LOC515128
Bt.2327.1.S1_at	PPP2R5B	protein phosphatase 2, regulatory subunit B', beta isoform
Bt.27361.1.A1_at	LOC789154	similar to decoy receptor 3
Bt.28710.2.A1_a_at	MGC139457	similar to ALK-1
Bt.4060.1.S1_at	LOC782642 /// MAL	mal, T-cell differentiation protein /// similar to Mal, T-cell differentiation p
Bt.27401.1.A1_at	RNF128	ring finger protein 128
Bt.15730.1.S1_at	LOC533161	similar to Kinesin family member 2C
Bt.8872.1.S2_at	ATP2B1	ATPase, Ca++ transporting, plasma membrane 1
Bt.16838.2.A1_at	LOC512905	Similar to CDNA sequence BC085284
Bt.28269.1.S1_at	MGC143367	similar to TC10-like Rho GTPase
Bt.11129.1.S1_at	MCM3	minichromosome maintenance complex component 3
Bt.4412.1.S1_at	LOC511619	similar to conductin
Bt.17928.1.A1_at	LOC532126	similar to transmembrane protein 16A
Bt.6796.1.A1_at	MGC157214	hypothetical LOC524166
Bt.17928.2.A1_at	LOC532126	similar to transmembrane protein 16A
Bt.9593.1.S1_at	LOC533151	similar to multidrug resistance-associated protein 3
Bt.14398.1.S1_at	MGC127772	similar to phosphatidylethanolamine-binding protein 4
Bt.26692.1.S1_a_at	BNIP3	BCL2/adenovirus E1B 19kDa interacting protein 3
Bt.12403.1.S1_at	MGC137880	similar to p76RBE protein
Bt.18484.1.A1_at	NT5DC1	5'-nucleotidase domain containing 1

Probeset ID	Gene Symbol	Gene Title
Bt.15675.1.S1_at	ADAMTS4	ADAM metallopeptidase with thrombospondin type 1 motif, 4
Bt.958.2.S1_at	TNFAIP6	tumor necrosis factor, alpha-induced protein 6
Bt.27778.1.A1_at	MGC142820	similar to BMP-binding endothelial regulator precursor protein
Bt.2786.1.S1_at	MGC139603	hypothetical LOC509055
Bt.8220.3.S1_at	LOC507012	similar to TACC1
Bt.10898.1.S1_at	TDE2L	tumor differentially expressed 2-like
Bt.3206.1.A1_at	SUSD2	sushi domain containing 2
Bt.20478.1.S1_at	LOC512021	similar to Rho guanine exchange factor 15
Bt.21037.1.S1_at	MGC157143	similar to Transcription factor 7 (T-cell specific, HMG-box)
Bt.24288.1.A1_at	LOC513059	similar to ATP(GTP)-binding protein
Bt.18478.2.A1_at	LOC784124	hypothetical protein LOC784124
Bt.21999.1.S1_at	LOC533248	similar to Hook-related protein 1
Bt.24859.2.S1_at	MGC140467	similar to oncostatin-M specific receptor beta subunit
Bt.25236.1.A1_at	LOC786844	similar to adlican
Bt.3046.1.S1_at	SNAI1	snail homolog 1 (Drosophila)
Bt.997.1.S1_at	CYB5R1	cytochrome b5 reductase 1
Bt.9206.1.S1_at	LOC527641	hypothetical LOC527641
Bt.26852.1.S1_at	MGC143166	similar to Fetal brain protein 239 (239FB)
Bt.12912.1.S1_at	COL4A1	collagen, type IV, alpha 1
Bt.10852.1.S1_at	MGC142936	similar to DNA damage binding protein 2 (Damage-specific DNA binding protein 2)
Bt.13336.1.A1_at	SMC4	Structural maintenance of chromosomes 4
Bt.5538.1.S1_at	UGDH	UDP-glucose dehydrogenase
Bt.25390.1.A1_at	MGC138090	similar to leukemogenic homolog protein
Bt.6544.1.S1_at	MGC151756	similar to small trans-membrane and glycosylated protein
Bt.4703.1.S1_at	MYOC	myocilin, trabecular meshwork inducible glucocorticoid response
Bt.1402.2.S1_at	GNAO1	guanine nucleotide binding protein (G protein), alpha activating activity polype
Bt.1151.1.S1_at	CRABP2	cellular retinoic acid binding protein 2
Bt.25870.1.S1_at	MGC134617	similar to Histone-lysine N-methyltransferase, H3 lysine-9 specific 1 (Histone H
Bt.21037.2.S1_at	MGC157143	similar to Transcription factor 7 (T-cell specific, HMG-box)
Bt.28296.1.A1_at	IL16	Interleukin 16
Bt.5618.1.A1_at	LOC516395	similar to KIAA0868 protein
Bt.26151.1.A1_at	LOC539328	similar to Protein 7 transactivated by hepatitis B virus X antigen (HBxAg)
Bt.7418.1.S1_at	MGC166183	similar to KIAA1581 protein
Bt.1730.2.A1_at	ID1	Inhibitor of DNA binding 1, dominant negative helix-loop-helix protein
Bt.19509.1.A1_at	LOC505588	Similar to cordon-bleu homolog (mouse)
Bt.9202.1.S1_at	FGL2	fibrinogen-like 2
Bt.11436.1.A1_at	---	Transcribed locus, strongly similar to XP_947682.1 PREDICTED: similar to SH3 and
Bt.23216.1.S1_at	ENPP2	ectonucleotide pyrophosphatase/phosphodiesterase 2 (autotaxin)
Bt.13376.1.S1_at	DHRS1	dehydrogenase/reductase (SDR family) member 1
Bt.19790.1.A1_at	TRIM22	tripartite motif-containing 22
Bt.27221.1.S1_at	LOC535872	similar to X-linked PEST-containing transporter
Bt.4318.1.S1_a_at	MGC151532	hypothetical LOC513195
Bt.15740.1.A1_at	LOC534629	similar to tumor protein D52-like 1
Bt.800.1.S1_at	MAPK13	mitogen-activated protein kinase 13
Bt.11420.1.A1_at	P4HA3	procollagen-proline, 2-oxoglutarate 4-dioxygenase (proline 4-hydroxylase), alpha
Bt.28287.1.S1_at	MGC148296	similar to UNC93A protein
Bt.12654.1.S1_at	MGC155116	similar to EGF-like, fibronectin type III and laminin G domains
Bt.28346.1.A1_at	BRRN1	barren homolog 1 (Drosophila)
Bt.4285.1.S1_at	CD14	CD14 molecule
Bt.24915.1.A1_at	CNTNAP3	contactin associated protein-like 3
Bt.24446.1.A1_at	LOC506636	similar to Sema domain, seven thrombospondin repeats (type 1 and type 1-like), t
Bt.26865.1.S1_at	MYOHD1	Myosin head domain containing 1
Bt.23504.1.A1_at	LOC533264	similar to sulfatase 2

Probeset ID	Gene Symbol	Gene Title
Bt.4886.1.A1_at	LRRC17	leucine rich repeat containing 17
Bt.9997.1.S1_at	LOC511958	similar to KIAA0056 protein
Bt.25730.1.S1_at	CDC45L	CDC45 cell division cycle 45-like (S. cerevisiae)
Bt.16141.1.S1_at	CCNE2	cyclin E2
Bt.12885.1.S1_at	LOC790609 /// MGC127073	hypothetical protein MGC127073 /// similar to aminoacylase-1
Bt.10007.1.A1_at	MGC148979	Similar to LB1
Bt.17810.1.S1_a_at	RBP1	retinol binding protein 1, cellular
Bt.4154.1.S1_at	LOC522613	similar to kinase Myt1
Bt.561.1.S1_at	MAP2K6	mitogen-activated protein kinase kinase 6
Bt.8775.1.S1_at	AP1B1	adaptor-related protein complex 1, beta 1 subunit
Bt.8872.1.S1_at	ATP2B1	ATPase, Ca++ transporting, plasma membrane 1
Bt.22854.2.S1_at	FASN	fatty acid synthase
Bt.21852.1.S1_at	MGC151581	similar to CDNA sequence BC011487
Bt.12315.1.S1_at	---	Transcribed locus, strongly similar to XP_587714.3 PREDICTED: similar to TGF-bet
Bt.10169.1.S1_at	LOC614166	hypothetical LOC614166
Bt.1112.1.S1_at	LOC618204	similar to Sodium channel beta-1 subunit precursor
Bt.793.1.S1_at	MGC128730	similar to ribosomal protein S6 kinase-like 1
Bt.7603.1.S1_at	PLK1	polo-like kinase 1 (Drosophila)
Bt.23094.1.A1_at	AKR1C1	aldo-keto reductase family 1, member C1 (dihydrodiol dehydrogenase 1; 20-alpha (
Bt.16556.1.A1_at	LOC527595	Similar to MCM10 homolog
Bt.25265.1.A1_at	MGC142770	similar to CG7568-PA
Bt.27940.1.A1_at	RHBG	Rh family, B glycoprotein
Bt.16309.1.S1_at	LOC510369	similar to hypoxanthine phosphoribosyltransferase 1
Bt.13912.2.A1_at	LOC540357	Similar to carbohydrate (N-acetylglucosamine 6-O) sulfotransferase 7
Bt.6021.1.S1_at	DKFZP586H2123	regeneration associated muscle protease
Bt.29563.1.A1_at	---	Transcribed locus, strongly similar to XP_622559.3 PREDICTED: similar to Adenoma
Bt.27849.2.S1_a_at	LOC506353	similar to KIAA0166
Bt.18009.1.A1_at	C8orf13	chromosome 8 open reading frame 13
Bt.3051.1.S1_at	PHLDA1	Pleckstrin homology-like domain, family A, member 1
Bt.303.1.S1_at	P2RY1	purinergic receptor P2Y, G-protein coupled, 1
Bt.21648.1.S1_a_at	CIDEB	cell death-inducing DFFA-like effector b
Bt.12722.1.A1_at	LOC616089	similar to PDZ domain containing 6
Bt.6509.1.S1_at	LOC511043	similar to laminin 5 gamma 2 subunit
Bt.20160.1.A1_at	PAH	phenylalanine hydroxylase
Bt.27248.1.A1_at	MMP16	matrix metallopeptidase 16 (membrane-inserted)
Bt.10169.2.S1_at	LOC614166	hypothetical LOC614166
Bt.22366.1.S1_at	TROAP	trophinin associated protein (tastin)
Bt.14369.1.A1_at	MGC160008	hypothetical LOC511195
Bt.15733.1.A1_at	LOC510012	similar to SCL/TAL1 interrupting locus
Bt.12498.1.A1_at	LOC530657	similar to alpha 3 type VI collagen isoform 5 precursor
Bt.13880.2.S1_at	LOC504445	similar to Dickkopf-1 (hdkk-1)
Bt.25082.1.A1_at	LOC514345	Similar to mucolipin-3
Bt.24859.1.A1_at	MGC140467	similar to oncostatin-M specific receptor beta subunit
Bt.24288.2.S1_at	LOC513059	similar to ATP(GTP)-binding protein
Bt.24200.1.S1_at	LOC787049	similar to FAM122B protein
Bt.22459.1.S1_at	LOC785319	similar to Neural cell adhesion molecule 1, 180 kDa isoform precursor (N-CAM 180
Bt.24447.2.S1_at	F2RL2	coagulation factor II (thrombin) receptor-like 2
Bt.26788.1.S1_at	LOC535329	hypothetical LOC535329
Bt.16495.1.A1_at	LOC511602	similar to alpha-5 type IV collagen
Bt.9412.3.S1_at	LOC781493	similar to collagen, type XIV, alpha 1
Bt.25834.1.A1_at	MELK	maternal embryonic leucine zipper kinase
Bt.27531.1.A1_at	LOC787969	similar to cancer susceptibility candidate 5

Probeset ID	Gene Symbol	Gene Title
Bt.11040.1.S1_at	LOC785319	similar to Neural cell adhesion molecule 1, 180 kDa isoform precursor (N-CAM 180
Bt.28603.1.A1_at	LOC512154	similar to PAS-kinase
Bt.20401.1.A1_at	TMC4	transmembrane channel-like 4
Bt.17579.1.A1_at	LRRN1	leucine rich repeat neuronal 1
Bt.24830.1.A1_at	ITIH5	Inter-alpha (globulin) inhibitor H5
Bt.5922.1.S1_at	HOMER2	homer homolog 2 (Drosophila)
Bt.27063.1.A1_at	PDE9A	phosphodiesterase 9A
Bt.15707.1.S1_at	ITGA5	integrin, alpha 5 (fibronectin receptor, alpha polypeptide)
Bt.10343.1.A1_at	PALMD	palmdelphin
Bt.13468.1.S1_at	LOC535603	similar to type III adenylyl cyclase
Bt.9605.1.S1_at	ms4A8B	membrane spanning 4-domain subfamily A member 8B
Bt.28346.2.S1_a_at	BRRN1	barren homolog 1 (Drosophila)
Bt.2172.1.S1_at	LOC510736	similar to HEPH
Bt.20272.1.S1_at	MGC143103	hypothetical LOC538515
Bt.5055.1.S1_at	MGC128881	similar to solute carrier family 22 (organic cation transporter), member 17
Bt.7357.1.A1_at	LOC528939	hypothetical LOC528939
Bt.22987.1.S1_at	PRG4	proteoglycan 4
Bt.22987.1.A1_at	LOC507869	similar to Tpr
Bt.6054.1.S1_at	MGC143138	similar to claudin-like protein 24
Bt.4105.1.S1_at	MGC143272	similar to putative GPCR interacting protein GIP
Bt.4804.1.S1_at	CDKN1C	Cyclin-dependent kinase inhibitor 1C
Bt.27460.1.A1_at	LOC538665	similar to MAGEL2 protein
Bt.22812.1.S1_at	---	Transcribed locus, strongly similar to XP_983710.1 PREDICTED: similar to Ras-rel
Bt.24555.1.S1_at	LOC528253	similar to jumonji, AT rich interactive domain 2 protein
Bt.3736.1.A1_at	---	CDNA clone IMAGE:8141299
Bt.26111.1.A1_at	KIAA1549	hypothetical protein LOC512679
Bt.13435.1.A1_at	LOC539445	similar to serine/threonine protein kinase MASK
Bt.19891.1.A1_at	LOC512164	similar to inter-alpha-trypsin inhibitor heavy chain2
Bt.22149.1.S1_at	LOC614841	hypothetical protein LOC614841
Bt.29677.1.S1_at	OPTC	opticin
Bt.9487.1.S1_at	LOC616969	Rho-guanine nucleotide exchange factor
Bt.6958.1.A1_at	BNIP3	BCL2/adenovirus E1B 19kDa interacting protein 3
Bt.11017.1.S1_at	LOC540504	similar to Nesprin-2 (Nuclear envelope spectrin repeat protein 2) (Syne-2) (Syna
Bt.115.1.S1_at	DDC	dopa decarboxylase (aromatic L-amino acid decarboxylase)
Bt.22165.1.S1_at	MGC137948	similar to KIAA1914 protein
Bt.3194.1.S1_at	LOC511594	similar to cell adhesion molecule JCAM
Bt.25305.1.A1_at	LOC790079	hypothetical protein LOC790079
Bt.958.1.A1_at	TNFAIP6	tumor necrosis factor, alpha-induced protein 6
Bt.1229.1.S1_at	APOA1	apolipoprotein A-I
Bt.1730.1.A1_at	ID1	inhibitor of DNA binding 1, dominant negative helix-loop-helix protein
Bt.12177.1.S1_at	CLDN4	claudin 4
Bt.5951.1.S1_at	LOC512922	similar to SplA/ryanodine receptor domain and SOCS box containing 4
Bt.12147.1.S1_at	---	Transcribed locus, strongly similar to NP_002630.1 serine (or cysteine) proteina
Bt.8825.1.S1_at	MGC142803	similar to Dynamin-2 (Dynamin UDNM)
Bt.28799.1.S1_at	LOC615798	similar to cAMP-dependent protein kinase inhibitor beta
Bt.23360.1.S1_at	LOC399559	nicotinate phosphoribosyltransferase-like
Bt.21648.1.S1_at	CIDEB	cell death-inducing DFFA-like effector b
Bt.4216.1.S1_at	PGF	placental growth factor, vascular endothelial growth factor-related protein

Complete list of genes that were at least 2 fold lower in CH vs MSCs (10% FDR); M28 must not be 2 fold lower than M0 or more than 3 fold higher (no FDR)

Probeset ID	Gene Symbol	Gene Title
Bt.27560.1.A1_at	LOC534432	hypothetical LOC534432
Bt.18420.2.A1_at	---	Transcribed locus
Bt.19423.2.S1_at	ABCA1	ATP-binding cassette, sub-family A (ABC1), member 1
Bt.2849.1.S1_at	---	Transcribed locus
Bt.20027.1.S1_at	---	Transcribed locus
Bt.23597.1.S1_at	MGC128797	similar to Nuclear protein 1 (Protein p8) (Candidate of metastasis 1)
Bt.28387.1.S1_at	LOC784334	hypothetical protein LOC784334
Bt.3191.1.A1_at	LOC533510	similar to DRE1 protein
Bt.3804.1.S1_at	LOC513618	similar to Procollagen C-endopeptidase enhancer 2 precursor (Procollagen COOH-te
Bt.9519.1.S1_at	SESN2	sestrin 2
Bt.20501.1.S1_at	---	Transcribed locus
Bt.26402.1.A1_at	---	Transcribed locus
Bt.11001.1.S1_at	---	Transcribed locus
Bt.27004.1.A1_at	---	Transcribed locus
Bt.27834.1.A1_at	MGC137817	similar to CG7139-PA
Bt.27807.1.A1_at	LOC782359	similar to PUMA/JFY1 protein
Bt.26303.1.A1_at	NEIL2	nei like 2 (E. coli)
Bt.9519.3.S1_at	SESN2	sestrin 2
Bt.13906.1.S1_at	---	Transcribed locus, strongly similar to NP_542763.1 sulfiredoxin 1 homolog [Homo
Bt.17355.1.S1_at	---	Transcribed locus
Bt.27864.1.S1_at	TPD52	tumor protein D52
Bt.12179.1.S1_at	LOC518469	similar to RP5-1022P6.2
Bt.21229.1.S1_at	MGC151593	similar to ST7L
Bt.20588.1.S1_at	---	Transcribed locus
Bt.16761.1.S1_at	LOC614260	similar to zinc finger protein 75
Bt.3447.2.S1_at	LOC509885	similar to isoleucyl-tRNA synthetase
Bt.24718.1.S1_at	MGC148411	similar to LETM1 domain containing 1
Bt.10098.1.S1_at	TSPAN13	tetraspanin 13
Bt.9828.1.S2_at	HINT3	histidine triad nucleotide binding protein 3
Bt.2416.1.S1_at	TEGT	testis enhanced gene transcript (BAX inhibitor 1)
Bt.11301.1.S1_at	MGC148584	similar to KIAA0843 protein
Bt.25218.1.S1_at	---	Transcribed locus
Bt.24386.1.A1_at	MGC159798	similar to UTP18, small subunit (SSU) processome component, homolog (yeast)
Bt.28725.1.A1_at	LOC613578 /// LOC790548	similar to UBX domain containing 4 /// hypothetical protein LOC790548
Bt.28163.1.S1_at	LOC514132	hypothetical LOC514132
Bt.1205.2.S1_at	ELP2	elongation protein 2 homolog (S. cerevisiae)
Bt.29464.1.A1_at	LOC614047	hypothetical protein LOC614047
Bt.1801.2.S1_a_at	TSPAN31	tetraspanin 31
Bt.6063.1.S1_at	LOC784459	similar to Heat shock 70kDa protein 9B (mortalin-2)
Bt.1185.2.S1_at	MGC148910	hypothetical LOC515777
Bt.21177.1.A1_s_at	LOC511229	similar to CARD8 protein
Bt.20613.1.A1_at	BCAR3	Breast cancer anti-estrogen resistance 3
Bt.17731.1.A1_at	MGC148584	Similar to KIAA0843 protein
Bt.2589.1.S1_at	UTP14C	UTP14, U3 small nucleolar ribonucleoprotein, homolog C (yeast)
Bt.20918.1.A1_at	LOC512082	similar to HGFL protein
Bt.25953.1.A1_at	PAX6	Paired box 6
Bt.26339.1.A1_at	EYA2	eyes absent homolog 2 (Drosophila)
Bt.17725.1.A1_at	---	Transcribed locus
Bt.26379.1.A1_at	---	Transcribed locus
Bt.26100.2.A1_at	GDPD1	glycerophosphodiester phosphodiesterase domain containing 1
Bt.17272.1.A1_at	---	Transcribed locus
Bt.4345.1.S1_at	TNFRSF6	apoptosis (APO-1) antigen 1 (FAS), member 6

Probeset ID	Gene Symbol	Gene Title
Bt.20105.2.S1_at	TAX1BP1	Tax1 (human T-cell leukemia virus type I) binding protein 1
Bt.19945.1.A1_at	LOC616344 100125581 /// LOC614260 ///	hypothetical LOC616344
Bt.16761.1.S1_a_at	LOC783192	similar to zinc finger protein 75 /// hypothetical protein LOC783192 /// hypothe
Bt.10101.1.S1_at	MGC139044	Similar to WD repeat- and FYVE domain-containing protein 2
Bt.24984.1.A1_at	---	Transcribed locus
Bt.3454.1.S1_at	---	Transcribed locus
Bt.1985.1.S1_at	MGC140251	similar to Protein SYS1 homolog
Bt.2587.2.S1_a_at	MGC140701	similar to Fumarate hydratase, mitochondrial precursor (Fumarase)
Bt.18835.1.S1_at	CARS	cysteinyl-tRNA synthetase
Bt.5302.1.S1_a_at	MRVI1 LOC532072 ///	murine retrovirus integration site 1 homolog
Bt.16262.1.S1_at	LOC784584	similar to kinase A anchor protein /// hypothetical protein LOC784584
Bt.21051.1.S1_at	MGC137630	similar to mitochondrial ribosomal protein L50
Bt.19945.2.A1_at	LOC616344	hypothetical LOC616344
Bt.2187.1.S1_at	HKE6	hydroxysteroid (17-beta) dehydrogenase 8
Bt.10101.2.S1_at	MGC139044	Similar to WD repeat- and FYVE domain-containing protein 2
Bt.25099.1.A1_at	PSPH	phosphoserine phosphatase
Bt.9072.1.S1_at	SCYE1	small inducible cytokine subfamily E, member 1 (endothelial monocyte-activating)
Bt.22494.1.S1_at	---	Transcribed locus
Bt.4462.1.S1_at	MGC140564	similar to Type-1 angiotensin II receptor-associated protein (AT1 receptor-assoc
Bt.13313.2.S1_at	LOC525346	similar to nuclear receptor coactivator-1
Bt.27655.1.S1_at	LOC534112	similar to connector enhancer of KSR2A
Bt.27130.1.S1_at	SCCPDH	saccharopine dehydrogenase (putative)
Bt.3458.2.S1_at	EIF2S2	eukaryotic translation initiation factor 2, subunit 2 beta, 38kDa
Bt.17499.1.A1_at	LOC524684	similar to subtilisin-like proprotein convertase (EC 3.4.21.-) PACE4
Bt.16018.1.S2_at	CASP4	caspase 4, apoptosis-related cysteine peptidase
Bt.5296.1.S1_at	SQRDL	sulfide quinone reductase-like (yeast)
Bt.20382.1.S1_at	MGC152539	similar to ankyrin repeat domain 29
Bt.9287.1.S1_at	LOC100124511	Hypothetical protein LOC100124511
Bt.16464.1.A1_at	LOC784987	hypothetical protein LOC784987
Bt.19366.1.A1_at	---	Transcribed locus
Bt.16018.1.S1_a_at	CASP4	caspase 4, apoptosis-related cysteine peptidase
Bt.4767.1.S3_at	CHS1	lysosomal trafficking regulator
Bt.13224.1.A1_at	MGC127339	similar to cytochrome P450, family 4, subfamily v, polypeptide 2
Bt.5478.1.S1_at	CACNB3	calcium channel, voltage-dependent, beta 3 subunit
Bt.23734.1.A1_at	LOC532789	similar to PAWR
Bt.8290.1.S1_at	LOC507982	similar to WDSUB1 protein
Bt.4655.1.S1_at	MSRA	methionine sulfoxide reductase A
Bt.21424.1.A1_at	MGC139607	similar to receptor Pit2
Bt.2674.1.A1_at	MEIS2	Meis homeobox 2
Bt.21050.1.S1_at	LOC506520	similar to WNK lysine deficient protein kinase 2
Bt.7938.1.S1_at	CTSS	cathepsin S
Bt.4767.1.S2_at	CHS1	lysosomal trafficking regulator
Bt.22282.1.S1_at	---	Transcribed locus
Bt.27966.1.S1_at	LOC532789 LOC507856 ///	similar to PAWR
Bt.26846.1.A1_at	MGC166388	similar to La ribonucleoprotein domain family, member 6
Bt.1938.2.S1_at	LOC784005	similar to Chromosome 10 open reading frame 72
Bt.27082.1.S1_at	---	Transcribed locus
Bt.16118.1.S1_at	LOC504309	similar to C-type lectin domain family 2, member h
Bt.234.1.S1_at	IL18	interleukin 18 (interferon-gamma-inducing factor)
Bt.12294.2.A1_at	AMIGO2	amphoterin induced gene 2
Bt.4474.1.S1_at	LOC507590	similar to Protein C20orf35 (HSMNP1)
Bt.10111.1.S1_at	---	Transcribed locus
Bt.786.1.S1_a_at	MGC151829	similar to Leiomodin 1 (smooth muscle)
Bt.196.1.S1_at	S100A13	8KDa amlexanox-binding protein

Probeset ID	Gene Symbol	Gene Title
Bt.22081.1.S1_at	LMO7	LIM domain 7
Bt.16194.1.A1_at	KLHL13	kelch-like 13
Bt.12294.1.S1_at	AMIGO2	amphoterin induced gene 2
Bt.28956.1.A1_at	MGC142528	hypothetical LOC538579
Bt.22409.1.S1_at	LOC540050	similar to KIAA0417
Bt.2114.1.S1_at	---	CDNA clone IMAGE:8220921
Bt.26051.1.A1_at	LOC521326	similar to OTTHUMP00000065631

APPENDIX 3: COMPLETE LIST OF MECHANICALLY SENSITIVE GENES MIS-REGULATED IN MSCS COMPARED TO CHONDROCYTES

Complete list of genes that were improved by dynamic compression (>2-fold) and were previously identified as under-expressed in day 0 and day 28 MSCs (>3-fold) compared to day 28 chondrocytes.

Gene Symbol	Gene Title	Fold Change (C28 v M0)	Fold Change (C28 v M28)	Fold Change (DL v CM+)
PPP1R3C	protein phosphatase 1, regulatory (inhibitor) subunit 3C	3	3	2
BLA-DQB	MHC class II antigen	4	3	2
ECSOD	extracellular superoxide dismutase	5	3	3
CATHL5	cathelicidin 5	4	3	13
NFIA	nuclear factor I/A	4	3	8
RHBG	Rh family, B glycoprotein	3	3	3
LOC511958	similar to KIAA0056 protein	3	3	10
LOC506412 /// LOC616035 /// LOC618238 /// SAA3	serum amyloid A 3 /// serum amyloid A-like /// hypothetical LOC616035 /// simila	4	3	28
LOC533151	similar to multidrug resistance-associated protein 3	4	3	3
LOC504531	similar to phosphoinositide 3-kinase	5	3	3
LOC790079	hypothetical protein LOC790079	8	3	4
LOC505588	Similar to cordon-bleu homolog (mouse)	5	4	4
LOC539146	similar to G protein-coupled receptor	12	4	2
SLC27A3	solute carrier family 27 (fatty acid transporter), member 3	6	4	26
LOC614166	hypothetical LOC614166	4	4	2
LOC615798	similar to cAMP-dependent protein kinase inhibitor beta	10	4	2
DAX-1	orphan nuclear receptor DAX-1	3	4	2
LOC504445	similar to Dickkopf-1 (hdkk-1)	21	4	2
MGC142803	similar to Dynamin-2 (Dynamin UDNM)	11	4	3
LOC540358	similar to 5T4 oncofoetal antigen	7	4	3
MMP16	matrix metallopeptidase 16 (membrane-inserted)	4	4	2
LOC509824	similar to Os08g0528700	10	4	19
MGC157143	similar to Transcription factor 7 (T-cell specific, HMG-box)	3	5	8
LOC785319	similar to Neural cell adhesion molecule 1, 180 kDa isoform precursor (N-CAM 180	5	5	5
SNAI1	snail homolog 1 (Drosophila)	5	5	81
LOC511043	similar to laminin 5 gamma 2 subunit	4	5	8
B3GALT2	UDP-Gal:betaGlcNAc beta 1,3-galactosyltransferase, polypeptide 2	7	5	20
LOC504698	similar to transferrin receptor	4	6	6
LOC539328	similar to Protein 7 transactivated by hepatitis B virus X antigen (HBxAg)	11	6	7
LOC506636	similar to Sema domain, seven thrombospondin repeats (type 1 and type 1-like), t	7	6	2
MGC152519	similar to Uridine phosphorylase 1	19	6	2
ADAMTS4	ADAM metallopeptidase with thrombospondin type 1 motif, 4	6	6	16
LOC510012	similar to SCL/TAL1 interrupting locus	4	6	16
TMEM59L	transmembrane protein 59-like	10	6	12
PEG3	paternally expressed 3	9	6	2
CA13	carbonic anhydrase XIII	7	6	2
LOC532126	similar to transmembrane protein 16A	10	7	6
BRCA1	Breast cancer 1, early onset	3	7	7

Gene Symbol	Gene Title	Fold Change (C28 v M0)	Fold Change (C28 v M28)	Fold Change (DL v CM+)
MGC148382	similar to kinesin family member 23	3	7	3
LOC404111	epidermal keratin VII	11	8	13
F2RL2	coagulation factor II (thrombin) receptor-like 2	9	8	7
LOC511043	Similar to laminin 5 gamma 2 subunit	6	8	4
LOC522691	hypothetical LOC522691	12	8	8
LOC513643	similar to Forkhead box protein M1 (Forkhead-related protein FKHL16) (Hepatocyte	4	8	19
CIDEB	cell death-inducing DFFA-like effector b	18	8	5
MGC157214	hypothetical LOC524166	9	9	3
LOC781892 /// METTL7A	methyltransferase like 7A /// hypothetical protein LOC781892	6	9	4
ms4A8B	membrane spanning 4-domain subfamily A member 8B	5	9	3
LOC511594	similar to cell adhesion molecule JCAM	26	9	72
B3GALT2	UDP-Gal:betaGlcNAc beta 1,3-galactosyltransferase, polypeptide 2	9	10	3
LOC515301	similar to Cdc6-related protein	3	10	8
LOC533359	similar to MAX dimerization protein 3	3	10	7
AKR1C1	aldo-keto reductase family 1, member C1 (dihydrodiol dehydrogenase 1; 20-alpha (	19	11	5
CDCA5	cell division cycle associated 5	4	11	3
LOC786844	similar to adlican	15	11	3
LOC511100	Similar to Opa interacting protein 5	3	11	59
MGC157214	hypothetical LOC524166	8	12	21
MGC140246	similar to plakophilin 2a	13	12	3
PGF	placental growth factor, vascular endothelial growth factor-related protein	36	13	16
mash2	achaete-scute complex-like protein 2 /// achaete scute-like protein 2	13	13	16
MGC137880	similar to p76RBE protein	13	13	15
LOC514360	similar to desmoplakin isoform II	14	14	11
MGC157214	hypothetical LOC524166	22	14	4
TROAP	trophinin associated protein (tastin)	8	14	2
MGC157179	similar to Cyclin F	5	16	9
NUSAP1	nucleolar and spindle associated protein 1	3	17	4
LOC532126	similar to transmembrane protein 16A	31	18	4
LBP	lipopolysaccharide binding protein	34	20	2
KIF20A	kinesin family member 20A	3	20	14
LOC617336	similar to WGAR9166	22	24	3
LOC533089	similar to centromere protein F (350/400kD)	3	25	9
MGC151855	hypothetical LOC508022	3	26	4
LOC539360	similar to calpain 6	490	32	3
THBS4	thrombospondin 4	163	33	2
LOC533323	similar to cyclic nucleotide phophodiesterase	39	41	4
LOC781091	hypothetical protein LOC781091	47	54	6
LOC782069	hypothetical protein LOC782069	59	57	36
LOC286871	uterine milk protein precursor	218	263	4

Complete list of genes that were improved by dynamic compression (>2-fold) and were previously identified as under-expressed in day 0 and day 28 MSCs (>3-fold) compared to day 28 chondrocytes.

Gene Symbol	Gene Title	Fold Change (C28 v M0)	Fold Change (C28 v M28)	Fold Change (DL v CM+)
LOC512082	similar to HGFL protein	-3	-3	-3
DSC2	desmocollin 2	-4	-4	-6
LOC616344	hypothetical LOC616344	-5	-4	-3
RASGEF1B	RasGEF domain family, member 1B	-22	-5	-7
LOC616344	hypothetical LOC616344	-5	-5	-4
IL18	interleukin 18 (interferon-gamma-inducing factor)	-13	-5	-4
LOC511229	similar to CARD8 protein	-8	-6	-13
FBXO32	F-box protein 32	-4	-6	-3
LOC511229	similar to CARD8 protein	-6	-6	-5
ABCA1	ATP-binding cassette, sub-family A (ABC1), member 1	-3	-7	-2
ISG15	ISG15 ubiquitin-like modifier	-4	-7	-2
MX1	myxovirus (influenza virus) resistance 1, interferon-inducible protein p78 (mous	-13	-8	-4
MEIS2	Meis homeobox 2	-20	-9	-2

APPENDIX 4: RELATED PUBLICATIONS

BOOK CHAPTERS

1. **Huang AH**, Hung CT, Mauck RL: Functional Cartilage Tissue Engineering with Adult Stem Cells: Current Status and Future Directions. In: Stem Cells and Regenerative Medicine. Ed by Herman Cheung. Oak Park, IL, Bentham Science Publishers, in press.

FULL-LENGTH MANUSCRIPTS

1. **Huang AH**, Farrell MJ, Kim M, Mauck RL. "Long-term Dynamic Compressive Loading Improves the Mechanical Properties of Mesenchymal Stem Cell-Laden Hydrogels," 2010, *European Cells and Materials*, 19:72-85.

2. **Huang AH**, Baker BM, Ateshian GA, Mauck RL. "Sliding Contact Loading Enhances Chondrogenesis and Mechanical Function of Mesenchymal Stem Cells in 3D Culture," 2010, in preparation.

3. **Huang AH**, Stein A, Mauck RL. "Evaluation of the Complex Molecular Topography of Mesenchymal Stem Cell Chondrogenesis for Cartilage Tissue Engineering," 2010, *Tissue Engineering: Part A*, in press (PMID: 20367254).

4. Nerurkar NL, Sen S, **Huang AH**, Elliott DM, Mauck RL. "Engineered Disc-Like Angle-Ply Structures for Intervertebral Disc Replacement," 2010, *Spine*, in press (PMID: 20354467).

5. **Huang AH**, Farrell MJ, Mauck RL. "Mechanics and Mechanobiology of Mesenchymal Stem Cell-Based Engineered Cartilage," 2010, *Journal of Biomechanics*, 43(1): 128-36.

6. Erickson IE, **Huang AH**, Sengupta S, Kestle S, Burdick JA, Mauck RL. "Macromer Density Influences Mesenchymal Stem Cell Chondrogenesis and Maturation in Photocrosslinked Hyaluronic Acid Hydrogels," 2009, *Osteoarthritis and Cartilage*, 17(12):1639-48.

7. **Huang AH**, Stein A, Tuan RS, Mauck RL. "Transient Exposure to TGF-B3 Improves the Mechanical Properties of Mesenchymal Stem Cell-Laden Constructs in a Density Dependent Manner," 2009, *Tissue Engineering: Part A,* 15(11): 3461-72.

8. **Huang AH**, Motlekar NA, Stein A, Diamond SL, Shore EM, Mauck RL. "High Throughput Screening for Modulators of Mesenchymal Stem Cell Chondrogenesis," 2008, *Annals of Biomedical Engineering*, 36(11):1909-21.

9. Erickson IE, **Huang AH**, Chung C, Li R, Burdick JA, Mauck RL. "Differential Maturation and Structure-Function Relationships in MSC and Chondrocyte Seeded Hydrogels," 2008, *Tissue Engineering*, 15(5):1041-52.

10. **Huang AH**, Yeger-McKeever M, Stein A, Mauck RL. "Tensile Properties of Engineered Cartilage Formed From Chondrocyte- and MSC-Laden Hydrogels," 2008, *Osteoarthritis and Cartilage*, 16(9):1074-1082.

APPENDIX 5: RELATED CONFERENCE ABSTRACTS

1. **Huang AH**, Farrell MJ, Baker BM, Kim M, Mauck RL. "Mechanical Stimulation Enhances Functional Mesenchymal Stem Cell Chondrogenesis," *World Congress on Biomechanics*, Singapore, August 1-6, 2010, submitted.

2. Baker BM, Shah RP, **Huang AH**, Mauck RL. "Dynamic Tensile Stimulation of MSC-Seeded Nanofibrous Constructs," *World Congress on Biomechanics*, Singapore, August 1-6, 2010, submitted.

3. Elliott DM, Nerurkar NL, **Huang AH**, Kluge JA, Smith LJ, Martin JT, Hebela N, Mauck RL. "Disc Tissue Engineering – Can We Make It Stick?" *World Congress on Biomechanics*, Singapore, August 1-6, 2010, submitted.

4. **Huang AH**, Baker BM, Ateshian GA, Mauck RL. "Sliding Contact Loading Improves the Tensile Properties of MSC-Based Engineered Cartilage," *Proceedings of ASME 2010 Summer Bioengineering Conference*, Naples, FL, June 16-19, 2010, paper 19292 (podium).

5. **Huang AH**, Mauck RL. "Extended Long-Term Culture of MSC-Laden Agarose Constructs Does Not Produce Functional Tissue Comparable to Primary Chondrocytes," *Proceedings of ASME 2010 Summer Bioengineering Conference*, Naples, FL, June 16-19, 2010, paper 19643 (podium).

6. **Huang AH**, Baker BM, Ateshian GA, Mauck RL. "Sliding Contact Enhances Mesenchymal Stem Cell Chondrogenesis in 3D Culture," *Transactions of the 56th Annual Orthopaedic Research Society Meeting*, New Orleans, LA, March 6-9, 2009, 35:315 (podium).

7. **Huang AH**, Farrell MJ, Mauck RL. "Dynamic Compression Initiated After Chondrogenesis Improves Mechanical Properties of Mesenchymal Stem Cell Seeded Hydrogel Constructs," *56th Annual Orthopaedic Research Society Meeting*, New Orleans, LA, March 6-9, 2009, 35:1336.

8. Nerurkar NL, Sen S, **Huang AH**, Elliott DM, Mauck RL. "Functional Maturation of Engineered Composites that Mimic the Hierarchical Organization of the Intervertebral Disc," *Transactions of the 56th Annual Orthopaedic Research Society Meeting*, New Orleans, LA, March 6-9, 2009 (podium).

9. **Huang AH**, Farrell MJ, Mauck RL. "Delayed Dynamic Compression Improves the Mechanical Properties of MSC-Laden Constructs," *Biomedical Engineering Society Meeting*, Pittsburgh, PA, October 7-10, 2009.

10. **Huang AH**, Mauck RL. "Repeated Dynamic Loading Modulates Cartilage Gene Expression but Does Not Improve Mechanical Properties of MSC-Laden Hydrogels,"

Proceedings of ASME 2009 Summer Bioengineering Conference, Lake Tahoe, CA, June 17-21, 2009, paper 204339 (podium).

11. **Huang AH**, Stein A, Mauck RL. "Genome-Wide Analysis to Identify Functional Determinants of Mesenchymal Stem Cell Chondrogenesis," *Transactions of the 55th Annual Orthopaedic Research Society Meeting,* Las Vegas, NV, February 22-25, 2009, 34:279 (podium).

12. Ionescu L, Gee AO, **Huang AH**, Sennett B, Liechty K, Mauck RL. "Regenerative Potential of Fetal Meniscus Fibrochondrocytes," *Transactions of the 55th Annual Orthopaedic Research Society Meeting,* Las Vegas, NV, February 22-25, 2009, 34:1208.

13. **Huang AH**, Stein A, Yeger-McKeever M, Tuan RS, Mauck RL. "Transient Exposure to TGF-B3 Improves Mechanical Properties of MSC-Laden Constructs," *Proceedings of ASME 2008 Summer Bioengineering Conference,* Marco Island, FL, June 25-29, paper 193130 (podium).

14. **Huang AH**, Motlekar NA, Stein A, Shore EM, Diamond SL, Mauck RL. "High-Throughput Screening of Chemical Libraries for Moduluators of Mesenchymal Stem Cell Chondrogenesis," *Proceedings of ASME 2008 Summer Bioengineering Conference,* Marco Island, FL, June 25-29, paper 193118 (podium).

15. **Huang AH**, Stein A, Diamond SL, Shore EM, Mauck RL. "High-Throughput Screening of MSC Chondrogenesis: Assay Development and Application," *Transactions of the 54th Annual Orthopaedic Research Society Meeting*, San Francisco, CA, March 2-5, 2008 33:520.

16. **Huang AH**, Yeger-McKeever M, Stein A, Mauck RL. "Identification of Molecular Antecedents Limiting Functional Maturation of MSC-Laden Hydrogels," *Transactions of the 54th Annual Orthopaedic Research Society Meeting*, San Francisco, CA, March 2-5, 2008, 33:549.

17. Erickson IE, Chung C, **Huang AH**, Li R, Burdick JA, Mauck RL. "Hydrogel Effects on Long-Term Maturation of Chondrocyte and MSC Laden Hydrogels," *Transactions of the 54th Annual Orthopaedic Research Society Meeting*, San Francisco, CA, March 2-5, 2008, 33:557.

18. Yeger-McKeever M, **Huang AH**, Stein AF, Mauck RL. "Engineered MSC-Laden Cartilage Constructs are Sensitive to Infllammatory Cytokine-Mediated Degradation," *Proceedings of ASME 2007 Summer Bioengineering Conference*, Keystone, CO, June 20-24, paper 176186 (podium).

19. **Huang AH**, Mauck RL. "Sliding Contact Modulates ECM Expression in Chondrocyte-Laden Agarose Gels," *Proceedings of ASME 2007 Summer Bioengineering Conference*, Keystone, CO, June 20-24, paper 176427 (podium).

20. **Huang AH**, Yeger-McKeever M, Yuan X, Mauck RL. "Direct Measurement of Tensile Properties of Chondrocyte- and MSC-laden Hydrogels," 2007, *Transactions of the 53rd Annual Orthopaedic Research Society Meeting*, 32:345 (podium).

21. **Huang AH**, Mauck RL. "Sliding Contact Enhances Cartilage ECM Gene Expression in Chondrocyte-Laden Hydrogels," 2006, *Gordon Research Conference on Musculoskeletal Biology and Bioengineering*.

BIBLIOGRAPHY

Adamson, L. F. and C. S. Anast (1966). "Amino acid, potassium, and sulfate transport and incorporation by embryonic chick cartilage: the mechanism of the stimulatory effects of serum." Biochim Biophys Acta **121**(1): 10-20.

Ahmed, A. M., D. L. Burke and A. Yu (1983). "In-vitro measurement of static pressure distribution in synovial joints--Part II: Retropatellar surface." J Biomech Eng **105**(3): 226-36.

Akizuki, S., V. C. Mow, F. Muller, J. C. Pita, D. S. Howell and D. H. Manicourt (1986). "Tensile properties of human knee joint cartilage: I. Influence of ionic conditions, weight bearing, and fibrillation on the tensile modulus." J Orthop Res **4**(4): 379-92.

Albro, M. B., N. O. Chahine, R. Li, K. Yeager, C. T. Hung and G. A. Ateshian (2008). "Dynamic loading of deformable porous media can induce active solute transport." J Biomech **41**(15): 3152-7.

Angele, P., R. Kujat, M. Nerlich, J. Yoo, V. Goldberg and B. Johnstone (1999). "Engineering of osteochondral tissue with bone marrow mesenchymal progenitor cells in a derivatized hyaluronan-gelatin composite sponge." Tissue Eng **5**(6): 545-54.

Angele, P., D. Schumann, M. Angele, B. Kinner, C. Englert, R. Hente, B. Fuchtmeier, M. Nerlich, C. Neumann and R. Kujat (2004). "Cyclic, mechanical compression enhances chondrogenesis of mesenchymal progenitor cells in tissue engineering scaffolds." Biorheology **41**(3-4): 335-46.

Angele, P., J. U. Yoo, C. Smith, J. Mansour, K. J. Jepsen, M. Nerlich and B. Johnstone (2003). "Cyclic hydrostatic pressure enhances the chondrogenic phenotype of human mesenchymal progenitor cells differentiated in vitro." J Orthop Res **21**(3): 451-7.

Antoci, V., Jr., C. S. Adams, N. J. Hickok, I. M. Shapiro and J. Parvizi (2007). "Antibiotics for local delivery systems cause skeletal cell toxicity in vitro." Clin Orthop Relat Res **462**: 200-6.

Appelman, T. P., J. Mizrahi, J. H. Elisseeff and D. Seliktar (2009). "The differential effect of scaffold composition and architecture on chondrocyte response to mechanical stimulation." Biomaterials **30**(4): 518-25.

Archer, C. W., G. P. Dowthwaite and P. Francis-West (2003). "Development of synovial joints." Birth Defects Res C Embryo Today **69**(2): 144-55.

Archer, C. W., G. P. Dowthwaite and P. H. Francis-West (2003). "Development of synovial joints." Birth Def Res (Part C) **69**: 144-55.

Armstrong, C. G., A. S. Bahrani and D. L. Gardner (1979). "In vitro measurement of articular cartilage deformations in the intact human hip joint under load." J Bone Joint Surg Am **61**(5): 744-55.

Ateshian, G. A. and C. T. Hung (2003). Functional properties of native articular cartilage. Functional Tissue Engineering. F. Guilak, D. L. Butler, S. A. Goldstein and D. J. Mooney. New York, Springer-Verlag**:** 46-68.

Ateshian, G. A. and H. Wang (1995). "A theoretical solution for the frictionless rolling contact of cylindrical biphasic articular cartilage layers." J Biomech **28**(11): 1341-55.

Ateshian, G. A., W. H. Warden, J. J. Kim, R. P. Grelsamer and V. C. Mow (1997). "Finite deformation biphasic material properties of bovine articular cartilage from confined compression experiments." J Biomech **30**(11-12): 1157-64.

Athanasiou, K. A., M. P. Rosenwasser, J. A. Buckwalter, T. I. Malinin and V. C. Mow (1991). "Interspecies comparisons of in situ intrinsic mechanical properties of distal femoral cartilage." J Orthop Res **9**(3): 330-40.

Athanasiou, K. A., C. F. Zhu, X. Wang and C. M. Agrawal (2000). "Effects of aging and dietary restriction on the structural integrity of rat articular cartilage." Ann Biomed Eng **28**(2): 143-9.

Audhya, T. K. and K. D. Gibson (1976). "Effects of medium composition and metabolic inhibitors on glycosaminoglycan synthesis in chick embryo cartilage and its stimulation by serum and triiodothyronine." Biochim Biophys Acta **437**(2): 364-76.

Awad, H. A., Y. D. Halvorsen, J. M. Gimble and F. Guilak (2003). "Effects of transforming growth factor beta1 and dexamethasone on the growth and chondrogenic differentiation of adipose-derived stromal cells." Tissue Eng **9**(6): 1301-12.

Awad, H. A., M. Q. Wickham, H. A. Leddy, J. M. Gimble and F. Guilak (2004). "Chondrogenic differentiation of adipose-derived adult stem cells in agarose, alginate, and gelatin scaffolds." Biomaterials **25**(16): 3211-22.

Baker, B. M. and R. L. Mauck (2007). "The effect of nanofiber alignment on the maturation of engineered meniscus constructs." Biomaterials **28**(11): 1967-77.

Ballock, R. T., A. Heydemann, L. M. Wakefield, K. C. Flanders, A. B. Roberts and M. B. Sporn (1993). "TGF-beta 1 prevents hypertrophy of epiphyseal chondrocytes: regulation of gene expression for cartilage matrix proteins and metalloproteases." Dev Biol **158**(2): 414-29.

Barry, F., R. E. Boynton, B. Liu and J. M. Murphy (2001). "Chondrogenic differentiation of mesenchymal stem cells from bone marrow: differentiation-dependent gene expression of matrix components." Exp Cell Res **268**(2): 189-200.

Barry, F. P., J. M. Murphy, K. English and B. P. Mahon (2005). "Immunogenicity of adult mesenchymal stem cells: lessons from the fetal allograft." Stem Cells Dev **14**(3): 252-65.

Below, S., S. P. Arnoczky, J. Dodds, C. Kooima and N. Walter (2002). "The split-line pattern of the distal femur: A consideration in the orientation of autologous cartilage grafts." Arthroscopy **18**(6): 613-7.

Benya, P. D. and J. D. Shaffer (1982). "Dedifferentiated chondrocytes reexpress the differentiated collagen phenotype when cultured in agarose gels." Cell **30**(1): 215-24.

Betre, H., L. A. Setton, D. E. Meyer and A. Chilkoti (2002). "Characterization of a genetically engineered elastin-like polypeptide for cartilaginous tissue repair." Biomacromolecules **3**(5): 910-6.

Bi, X., G. Li, S. B. Doty and N. P. Camacho (2005). "A novel method for determination of collagen orientation in cartilage by Fourier transform infrared imaging spectroscopy (FT-IRIS)." Osteoarthritis Cartilage **13**(12): 1050-8.

Bian, L., J. V. Fong, E. G. Lima, A. M. Stoker, G. A. Ateshian, J. L. Cook and C. T. Hung "Dynamic Mechanical Loading Enhances Functional Properties of Tissue-Engineered Cartilage Using Mature Canine Chondrocytes." Tissue Eng Part A.

Blunk, T., A. L. Sieminski, K. J. Gooch, D. L. Courter, A. P. Hollander, A. M. Nahir, R. Langer, G. Vunjak-Novakovic and L. E. Freed (2002). "Differential effects of growth factors on tissue-engineered cartilage." Tissue Eng **8**(1): 73-84.

Boeuf, S., E. Steck, K. Pelttari, T. Hennig, A. Buness, K. Benz, D. Witte, H. Sultmann, A. Poustka and W. Richter (2007). "Subtractive gene expression profiling of articular cartilage and mesenchymal stem cells: serpins as cartilage-relevant differentiation markers." Osteoarthritis Cartilage.

Boskey, A. and N. Pleshko Camacho (2007). "FT-IR imaging of native and tissue-engineered bone and cartilage." Biomaterials **28**(15): 2465-78.

Brittberg, M., E. Sjogren-Jansson, A. Lindahl and L. Peterson (1997). "Influence of fibrin sealant (Tisseel) on osteochondral defect repair in the rabbit knee." Biomaterials **18**(3): 235-42.

Brown, P. D. and P. D. Benya (1988). "Alterations in chondrocyte cytoskeletal architecture during phenotypic modulation by retinoic acid and dihydrocytochalasin B-induced reexpression." J Cell Biol **106**(1): 171-9.

Brown, T. D. and D. T. Shaw (1983). "In vitro contact stress distributions in the natural human hip." J Biomech **16**(6): 373-84.

Bryant, S. J. and K. S. Anseth (2001). "The effects of scaffold thickness on tissue engineered cartilage in photocrosslinked poly(ethylene oxide) hydrogels." Biomaterials **22**(6): 619-26.

Bryant, S. J. and K. S. Anseth (2003). "Controlling the spatial distribution of ECM components in degradable PEG hydrogels for tissue engineering cartilage." J Biomed Mater Res A **64**(1): 70-9.

Bryant, S. J., K. S. Anseth, D. A. Lee and D. L. Bader (2004). "Crosslinking density influences the morphology of chondrocytes photoencapsulated in PEG hydrogels during the application of compressive strain." J Orthop Res **22**(5): 1143-9.

Bryant, S. J., T. T. Chowdhury, D. A. Lee, D. L. Bader and K. S. Anseth (2004). "Crosslinking density influences chondrocyte metabolism in dynamically loaded photocrosslinked poly(ethylene glycol) hydrogels." Ann Biomed Eng **32**(3): 407-17.

Bryant, S. J., C. R. Nuttelman and K. S. Anseth (1999). "The effects of crosslinking density on cartilage formation in photocrosslinkable hydrogels." Biomed Sci Instrum **35**: 309-14.

Burdick, J. A., C. Chung, X. Jia, M. A. Randolph and R. Langer (2005). "Controlled degradation and mechanical behavior of photopolymerized hyaluronic acid networks." Biomacromolecules **6**(1): 386-91.

Burdick, J. A., A. J. Peterson and K. S. Anseth (2001). "Conversion and temperature profiles during the photoinitiated polymerization of thick orthopaedic biomaterials." Biomaterials **22**(13): 1779-86.

Burdick, J. A., L. M. Philpott and K. S. Anseth (2001). "Synthesis and characterization of tetrafunctional lactic acid oligomers: A potential in situ forming degradable orthopaedic biomaterial." Journal of Polymer Science Part a-Polymer Chemistry **39**(5): 683-692.

Bursac, P., C. V. McGrath, S. R. Eisenberg and D. Stamenovic (2000). "A microstructural model of elastostatic properties of articular cartilage in confined compression." J Biomech Eng **122**(4): 347-53.

Buschmann, M. D., Y. A. Gluzband, A. J. Grodzinsky and E. B. Hunziker (1995). "Mechanical compression modulates matrix biosynthesis in chondrocyte/agarose culture." J Cell Sci **108 (Pt 4)**: 1497-508.

Buschmann, M. D., Y. A. Gluzband, A. J. Grodzinsky, J. H. Kimura and E. B. Hunziker (1992). "Chondrocytes in agarose culture synthesize a mechanically functional extracellular matrix." J Orthop Res **10**(6): 745-58.

Butler, D. L., S. A. Goldstein and F. Guilak (2000). "Functional tissue engineering: the role of biomechanics." J Biomech Eng **122**(6): 570-5.

Buxton, A. N., J. Zhu, R. Marchant, J. L. West, J. U. Yoo and B. Johnstone (2007). "Design and characterization of poly(ethylene glycol) photopolymerizable semi-interpenetrating networks for chondrogenesis of human mesenchymal stem cells." Tissue Eng **13**(10): 2549-60.

Byers, B. A., R. L. Mauck, I. E. Chiang and R. S. Tuan (2008). "Transient exposure to transforming growth factor beta 3 under serum-free conditions enhances the biomechanical and biochemical maturation of tissue-engineered cartilage." Tissue Eng Part A **14**(11): 1821-34.

Caligaris, M. and G. A. Ateshian (2008). "Effects of sustained interstitial fluid pressurization under migrating contact area, and boundary lubrication by synovial fluid, on cartilage friction." Osteoarthritis Cartilage **16**(10): 1220-7.

Caplan, A. I. (1991). "Mesenchymal stem cells." J Orthop Res **9**(5): 641-50.

Caterson, E. J., L. J. Nesti, W. J. Li, K. G. Danielson, T. J. Albert, A. R. Vaccaro and R. S. Tuan (2001). "Three-dimensional cartilage formation by bone marrow-derived cells seeded in polylactide/alginate amalgam." J Biomed Mater Res **57**(3): 394-403.

Chahine, N. O., M. B. Albro, E. G. Lima, V. I. Wei, C. R. Dubois, C. T. Hung and G. A. Ateshian (2009). "Effect of dynamic loading on the transport of solutes into agarose hydrogels." Biophys J **97**(4): 968-75.

Chahine, N. O., C. C. Wang, C. T. Hung and G. A. Ateshian (2004). "Anisotropic strain-dependent material properties of bovine articular cartilage in the transitional range from tension to compression." J Biomech **37**(8): 1251-61.

Chang, C. F., M. W. Lee, P. Y. Kuo, Y. J. Wang, Y. H. Tu and S. C. Hung (2007). "Three-dimensional collagen fiber remodeling by mesenchymal stem cells requires the integrin-matrix interaction." J Biomed Mater Res A **80**(2): 466-74.

Chang, S. C., J. A. Rowley, G. Tobias, N. G. Genes, A. K. Roy, D. J. Mooney, C. A. Vacanti and L. J. Bonassar (2001). "Injection molding of chondrocyte/alginate constructs in the shape of facial implants." J Biomed Mater Res **55**(4): 503-11.

Charlebois, M., M. D. McKee and M. D. Buschmann (2004). "Nonlinear tensile properties of bovine articular cartilage and their variation with age and depth." J Biomech Eng **126**(2): 129-37.

Chen, J., R. L. Horan, D. Bramono, J. E. Moreau, Y. Wang, L. R. Geuss, A. L. Collette, V. Volloch and G. H. Altman (2006). "Monitoring mesenchymal stromal cell developmental stage to apply on-time mechanical stimulation for ligament tissue engineering." Tissue Eng **12**(11): 3085-95.

Chen, S. S., Y. H. Falcovitz, R. Schneiderman, A. Maroudas and R. L. Sah (2001). "Depth-dependent compressive properties of normal aged human femoral head articular cartilage: relationship to fixed charge density." Osteoarthritis Cartilage **9**(6): 561-9.

Chen, X., C. M. Macica, A. Nasiri and A. E. Broadus (2008). "Regulation of articular chondrocyte proliferation and differentiation by indian hedgehog and parathyroid hormone-related protein in mice." Arthritis Rheum **58**(12): 3788-97.

Cheng, N. C., B. T. Estes, H. A. Awad and F. Guilak (2008). "Chondrogenic Differentiation of Adipose-Derived Adult Stem Cells by a Porous Scaffold Derived from Native Articular Cartilage Extracellular Matrix." Tissue Eng Part A.

Choi, Y. S., S. E. Noh, S. M. Lim, C. W. Lee, C. S. Kim, M. W. Im, M. H. Lee and D. I. Kim (2008). "Multipotency and growth characteristic of periosteum-derived progenitor cells for chondrogenic, osteogenic, and adipogenic differentiation." Biotechnol Lett **30**(4): 593-601.

Chung, C., M. Beecham, R. L. Mauck and J. A. Burdick (2009). "The Influence of Degradation Characteristics of Hyaluronic Acid Hydrogels on in Vitro Neocartilage Formation by Mesenchymal Stem Cells." Biomaterials **30**(26): 4287-96.

Chung, C. and J. A. Burdick (2009). "Influence of three-dimensional hyaluronic Acid microenvironments on mesenchymal stem cell chondrogenesis." Tissue Eng Part A **15**(2): 243-54.

Chung, C., I. E. Erickson, R. L. Mauck and J. A. Burdick (2008). "Differential Behavior of Auricular and Articular Chondrocytes in Hyaluronic Acid Hydrogels." Tissue Eng Part A.

Chung, C., J. Mesa, M. A. Randolph, M. Yaremchuk and J. A. Burdick (2006). "Influence of gel properties on neocartilage formation by auricular chondrocytes photoencapsulated in hyaluronic acid networks." J Biomed Mater Res A **77**(3): 518-25.

Clarke, I. C. (1971). "Articular cartilage: a review and scanning electron microscope study. 1. The interterritorial fibrillar architecture." J Bone Joint Surg Br **53**(4): 732-50.

Cohen, B., W. M. Lai and V. C. Mow (1998). "A transversely isotropic biphasic model for unconfined compression of growth plate and chondroepiphysis." J Biomech Eng **120**(4): 491-6.

Connelly, J. T., A. J. Garcia and M. E. Levenston (2007). "Inhibition of in vitro chondrogenesis in RGD-modified three-dimensional alginate gels." Biomaterials **28**(6): 1071-83.

Connelly, J. T., A. J. Garcia and M. E. Levenston (2008). "Interactions between integrin ligand density and cytoskeletal integrity regulate BMSC chondrogenesis." J Cell Physiol **217**(1): 145-54.

Connelly, J. T., E. J. Vanderploeg and M. E. Levenston (2004). "The influence of cyclic tension amplitude on chondrocyte matrix synthesis: experimental and finite element analyses." Biorheology **41**(3-4): 377-87.

Connelly, J. T., E. J. Vanderploeg, J. K. Mouw, C. Wilson and M. E. Levenston (2010). "Tensile Loading Modulates BMSC Differentiation and the Development of Engineered Fibrocartilage Constructs." Tissue Eng Part A.

Davisson, T., S. Kunig, A. Chen, R. Sah and A. Ratcliffe (2002). "Static and dynamic compression modulate matrix metabolism in tissue engineered cartilage." J Orthop Res **20**(4): 842-8.

De Croos, J. N., S. S. Dhaliwal, M. D. Grynpas, R. M. Pilliar and R. A. Kandel (2006). "Cyclic compressive mechanical stimulation induces sequential catabolic and anabolic gene changes in chondrocytes resulting in increased extracellular matrix accumulation." Matrix Biol **25**(6): 323-31.

Derfoul, A., A. D. Miyoshi, D. E. Freeman and R. S. Tuan (2007). "Glucosamine promotes chondrogenic phenotype in both chondrocytes and mesenchymal stem cells and inhibits MMP-13 expression and matrix degradation." Osteoarthritis Cartilage **15**(6): 646-55.

Dickhut, A., E. Gottwald, E. Steck, C. Heisel and W. Richter (2008). "Chondrogenesis of mesenchymal stem cells in gel-like biomaterials in vitro and in vivo." Front Biosci **13**: 4517-28.

Dillman, C. J. (1975). "Kinematic analyses of running." Exerc Sport Sci Rev **3**: 193-218.

Eckstein, F., M. Tieschky, S. C. Faber, M. Haubner, H. Kolem, K. H. Englmeier and M. Reiser (1998). "Effect of physical exercise on cartilage volume and thickness in vivo: MR imaging study." Radiology **207**(1): 243-8.

Elder, S. H. (2002). "Conditioned medium of mechanically compressed chick limb bud cells promotes chondrocyte differentiation." J Orthop Sci **7**(5): 538-43.

Elder, S. H., S. A. Goldstein, J. H. Kimura, L. J. Soslowsky and D. M. Spengler (2001). "Chondrocyte differentiation is modulated by frequency and duration of cyclic compressive loading." Ann Biomed Eng **29**(6): 476-82.

Elder, S. H., J. H. Kimura, L. J. Soslowsky, M. Lavagnino and S. A. Goldstein (2000). "Effect of compressive loading on chondrocyte differentiation in agarose cultures of chick limb-bud cells." J Orthop Res **18**(1): 78-86.

Elisseeff, J., W. McIntosh, K. Fu, B. T. Blunk and R. Langer (2001). "Controlled-release of IGF-I and TGF-beta1 in a photopolymerizing hydrogel for cartilage tissue engineering." J Orthop Res **19**(6): 1098-104.

Elisseeff, J. H., A. Lee, H. K. Kleinman and Y. Yamada (2002). "Biological response of chondrocytes to hydrogels." Ann N Y Acad Sci **961**: 118-22.

Elliott, D. M., F. Guilak, T. P. Vail, J. Y. Wang and L. A. Setton (1999). "Tensile properties of articular cartilage are altered by meniscectomy in a canine model of osteoarthritis." J Orthop Res **17**(4): 503-8.

Erickson, G. R., J. M. Gimble, D. M. Franklin, H. E. Rice, H. Awad and F. Guilak (2002). "Chondrogenic potential of adipose tissue-derived stromal cells in vitro and in vivo." Biochem Biophys Res Commun **290**(2): 763-9.

Erickson, I. E., A. H. Huang, C. Chung, R. T. Li, J. A. Burdick and R. L. Mauck (2009). "Differential maturation and structure-function relationships in mesenchymal stem cell- and chondrocyte-seeded hydrogels." Tissue Eng Part A **15**(5): 1041-52.

Erickson, I. E., A. H. Huang, S. Sengupta, S. Kestle, J. A. Burdick and R. L. Mauck (2009). "Macromer Density Influences Mesenchymal Stem Cell Chondrogenesis and Maturation in Photocrosslinked Hyaluronic Acid Hydrogels." Osteoarthritis Cartilage **17**(12): 1639-1648.

Estes, B. T., A. W. Wu and F. Guilak (2006). "Potent induction of chondrocytic differentiation of human adipose-derived adult stem cells by bone morphogenetic protein 6." Arthritis Rheum **54**(4): 1222-32.

Eyre, D. R. (1980). "Collagen: molecular diversity in the body's protein scaffold." Science **207**(4437): 1315-22.

Eyre, D. R. (2004). "Collagens and cartilage matrix homeostasis." Clin Orthop Relat Res(427 Suppl): S118-22.

Farndale, R. W., D. J. Buttle and A. J. Barrett (1986). "Improved quantitation and discrimination of sulphated glycosaminoglycans by use of dimethylmethylene blue." Biochim Biophys Acta **883**(2): 173-7.

Felson, D. T., R. C. Lawrence, P. A. Dieppe, R. Hirsch, C. G. Helmick, J. M. Jordan, R. S. Kington, N. E. Lane, M. C. Nevitt, Y. Zhang, M. Sowers, T. McAlindon, T. D. Spector, A. R. Poole, S. Z. Yanovski, G. Ateshian, L. Sharma, J. A. Buckwalter, K. D. Brandt and J. F. Fries (2000). "Osteoarthritis: new insights. Part 1: the disease and its risk factors." Ann Intern Med **133**(8): 635-46.

Finger, A. R., C. Y. Sargent, K. O. Dulaney, S. H. Bernacki and E. G. Loboa (2007). "Differential effects on messenger ribonucleic acid expression by bone marrow-derived

human mesenchymal stem cells seeded in agarose constructs due to ramped and steady applications of cyclic hydrostatic pressure." Tissue Eng **13**(6): 1151-8.

Frank, E. H. and A. J. Grodzinsky (1987). "Cartilage electromechanics--I. Electrokinetic transduction and the effects of electrolyte pH and ionic strength." J Biomech **20**(6): 615-27.

Freed, L. E., R. Langer, I. Martin, N. R. Pellis and G. Vunjak-Novakovic (1997). "Tissue engineering of cartilage in space." Proc Natl Acad Sci U S A **94**(25): 13885-90.

Fukubayashi, T. and H. Kurosawa (1980). "The contact area and pressure distribution pattern of the knee. A study of normal and osteoarthrotic knee joints." Acta Orthop Scand **51**(6): 871-9.

Gemmiti, C. V. and R. E. Guldberg (2006). "Fluid flow increases type II collagen deposition and tensile mechanical properties in bioreactor-grown tissue-engineered cartilage." Tissue Eng **12**(3): 469-79.

Gepstein, A., G. Arbel, I. Blumenfeld, M. Peled and E. Livne (2003). "Association of metalloproteinases, tissue inhibitors of matrix metalloproteinases, and proteoglycans with development, aging, and osteoarthritis processes in mouse temporomandibular joint." Histochem Cell Biol **120**(1): 23-32.

Gepstein, A., S. Shapiro, G. Arbel, N. Lahat and E. Livne (2002). "Expression of matrix metalloproteinases in articular cartilage of temporomandibular and knee joints of mice during growth, maturation, and aging." Arthritis Rheum **46**(12): 3240-50.

Gilbert, S. J. (2000). Developmental Biology. New York, Sinauer Assoc.

Gleghorn, J. P., A. R. Jones, C. R. Flannery and L. J. Bonassar (2007). "Boundary mode frictional properties of engineered cartilaginous tissues." Eur Cell Mater **14**: 20-8; discussion 28-9.

Gomez, S., R. Toffanin, S. Bernstorff, M. Romanello, H. Amenitsch, M. Rappolt, R. Rizzo and F. Vittur (2000). "Collagen fibrils are differently organized in weight-bearing and not-weight-bearing regions of pig articular cartilage." J Exp Zool **287**(5): 346-52.

Gooch, K. J., T. Blunk, D. L. Courter, A. L. Sieminski, P. M. Bursac, G. Vunjak-Novakovic and L. E. Freed (2001). "IGF-I and mechanical environment interact to modulate engineered cartilage development." Biochem Biophys Res Commun **286**(5): 909-15.

Gooch, K. J., T. Blunk, D. L. Courter, A. L. Sieminski, G. Vunjak-Novakovic and L. E. Freed (2002). "Bone morphogenetic proteins-2, -12, and -13 modulate in vitro development of engineered cartilage." Tissue Eng **8**(4): 591-601.

Grad, S., S. Gogolewski, M. Alini and M. A. Wimmer (2006). "Effects of simple and complex motion patterns on gene expression of chondrocytes seeded in 3D scaffolds." Tissue Eng **12**(11): 3171-9.

Grad, S., C. R. Lee, K. Gorna, S. Gogolewski, M. A. Wimmer and M. Alini (2005). "Surface motion upregulates superficial zone protein and hyaluronan production in chondrocyte-seeded three-dimensional scaffolds." Tissue Eng **11**(1-2): 249-56.

Grad, S., C. R. Lee, M. A. Wimmer and M. Alini (2006). "Chondrocyte gene expression under applied surface motion." Biorheology **43**(3-4): 259-69.

Grodzinsky, A. J., M. E. Levenston, M. Jin and E. H. Frank (2000). "Cartilage tissue remodeling in response to mechanical forces." Annu Rev Biomed Eng **2**: 691-713.

Grodzinsky, A. J., V. Roth, E. Myers, W. D. Grossman and V. C. Mow (1981). "The significance of electromechanical and osmotic forces in the nonequilibrium swelling behavior of articular cartilage in tension." J Biomech Eng **103**(4): 221-31.

Guerin, H. L. and D. M. Elliott (2007). "Quantifying the contributions of structure to annulus fibrosus mechanical function using a nonlinear, anisotropic, hyperelastic model." J Orthop Res **25**(4): 508-16.

Guilak, F., R. L. Sah and L. A. Setton (1997). Physical regulation of cartilage metabolism. Basic Orthopaedic Biomechanics. V. C. Mow and W. C. Hayes. Philadelphia, Lippincott-Raven**:** 179-207.

Hashimoto, K., M. Noshiro, S. Ohno, T. Kawamoto, H. Satakeda, Y. Akagawa, K. Nakashima, A. Okimura, H. Ishida, T. Okamoto, H. Pan, M. Shen, W. Yan and Y. Kato (1997). "Characterization of a cartilage-derived 66-kDa protein (RGD-CAP/beta ig-h3) that binds to collagen." Biochim Biophys Acta **1355**(3): 303-14.

Hauselmann, H. J., R. J. Fernandes, S. S. Mok, T. M. Schmid, J. A. Block, M. B. Aydelotte, K. E. Kuettner and E. J. Thonar (1994). "Phenotypic stability of bovine articular chondrocytes after long-term culture in alginate beads." J Cell Sci **107 (Pt 1)**: 17-27.

Hayes, A. J., M. Benjamin and J. R. Ralphs (1999). "Role of actin stress fibres in the development of the intervertebral disc: cytoskeletal control of extracellular matrix assembly." Dev Dyn **215**(3): 179-89.

Hillenkamp, F., M. Karas, R. C. Beavis and B. T. Chait (1991). "Matrix-assisted laser desorption/ionization mass spectrometry of biopolymers." Anal Chem **63**(24): 1193A-1203A.

Hofmann, S., S. Knecht, R. Langer, D. L. Kaplan, G. Vunjak-Novakovic, H. P. Merkle and L. Meinel (2006). "Cartilage-like tissue engineering using silk scaffolds and mesenchymal stem cells." Tissue Eng **12**(10): 2729-38.

Hu, J. C. and K. A. Athanasiou (2006). "The effects of intermittent hydrostatic pressure on self-assembled articular cartilage constructs." Tissue Eng **12**(5): 1337-44.

Hu, K., L. Xu, L. Cao, C. M. Flahiff, J. Brussiau, K. Ho, L. A. Setton, I. Youn, F. Guilak, B. R. Olsen and Y. Li (2006). "Pathogenesis of osteoarthritis-like changes in the joints of mice deficient in type IX collagen." Arthritis Rheum **54**(9): 2891-900.

Huang, A. H., M. J. Farrell, M. Kim and R. L. Mauck (2010). "Long-term dynamic loading improves the mechanical properties of chondrogenic mesenchymal stem cell-laden hydrogel." Eur Cell Mater **19**: 72-85.

Huang, A. H., M. J. Farrell and R. L. Mauck (2010). "Mechanics and mechanobiology of mesenchymal stem cell-based engineered cartilage." J Biomech **43**(1): 128-136.

Huang, A. H., N. A. Motlekar, A. Stein, S. L. Diamond, E. M. Shore and R. L. Mauck (2008). "High-Throughput Screening for Modulators of Mesenchymal Stem Cell Chondrogenesis." Ann Biomed Eng **36**(11): 1909-21.

Huang, A. H., A. Stein, R. S. Tuan and R. L. Mauck (2009). "Transient exposure to TGF-beta3 improves the mechanical properties of MSC-laden cartilage constructs in a density dependent manner." Tissue Eng Part A **15**(11): 3461-3472.

Huang, A. H., M. Yeger-McKeever, A. Stein and R. L. Mauck (2008). "Tensile properties of engineered cartilage formed from chondrocyte- and MSC-laden hydrogels." Osteoarthritis Cartilage **16**(9): 1074-82.

Huang, C. Y., K. L. Hagar, L. E. Frost, Y. Sun and H. S. Cheung (2004). "Effects of cyclic compressive loading on chondrogenesis of rabbit bone-marrow derived mesenchymal stem cells." Stem Cells **22**(3): 313-23.

Huang, C. Y., V. C. Mow and G. A. Ateshian (2001). "The role of flow-independent viscoelasticity in the biphasic tensile and compressive responses of articular cartilage." J Biomech Eng **123**(5): 410-7.

Huang, C. Y., P. M. Reuben and H. S. Cheung (2005). "Temporal expression patterns and corresponding protein inductions of early responsive genes in rabbit bone marrow-derived mesenchymal stem cells under cyclic compressive loading." Stem Cells **23**(8): 1113-21.

Huang, C. Y., P. M. Reuben, G. D'Ippolito, P. C. Schiller and H. S. Cheung (2004). "Chondrogenesis of human bone marrow-derived mesenchymal stem cells in agarose culture." Anat Rec A Discov Mol Cell Evol Biol **278**(1): 428-36.

Huang, C. Y., A. Stankiewicz, G. A. Ateshian and V. C. Mow (2005). "Anisotropy, inhomogeneity, and tension-compression nonlinearity of human glenohumeral cartilage in finite deformation." J Biomech **38**(4): 799-809.

Huddleston, P. M., J. M. Steckelberg, A. D. Hanssen, M. S. Rouse, M. E. Bolander and R. Patel (2000). "Ciprofloxacin inhibition of experimental fracture healing." J Bone Joint Surg Am **82**(2): 161-73.

Hui, T. Y., K. M. Cheung, W. L. Cheung, D. Chan and B. P. Chan (2008). "In vitro chondrogenic differentiation of human mesenchymal stem cells in collagen microspheres: influence of cell seeding density and collagen concentration." Biomaterials **29**(22): 3201-12.

Hung, C. T., R. L. Mauck, C. C. Wang, E. G. Lima and G. A. Ateshian (2004). "A paradigm for functional tissue engineering of articular cartilage via applied physiologic deformational loading." Ann Biomed Eng **32**(1): 35-49.

Hunter, C. J., S. M. Imler, P. Malaviya, R. M. Nerem and M. E. Levenston (2002). "Mechanical compression alters gene expression and extracellular matrix synthesis by chondrocytes cultured in collagen I gels." Biomaterials **23**(4): 1249-59.

Hunziker, E. B. (1999). "Articular cartilage repair: are the intrinsic biological constraints undermining this process insuperable?" Osteoarthritis Cartilage **7**(1): 15-28.

Hyde, G., R. P. Boot-Handford and G. A. Wallis (2008). "Col2a1 lineage tracing reveals that the meniscus of the knee joint has a complex cellular origin." J Anat **213**(5): 531-8.

Im, G. I., N. H. Jung and S. K. Tae (2006). "Chondrogenic differentiation of mesenchymal stem cells isolated from patients in late adulthood: the optimal conditions of growth factors." Tissue Eng **12**(3): 527-36.

Indrawattana, N., G. Chen, M. Tadokoro, L. H. Shann, H. Ohgushi, T. Tateishi, J. Tanaka and A. Bunyaratvej (2004). "Growth factor combination for chondrogenic induction from human mesenchymal stem cell." Biochem Biophys Res Commun **320**(3): 914-9.

Iwamoto, M., Y. Tamamura, E. Koyama, T. Komori, N. Takeshita, J. A. Williams, T. Nakamura, M. Enomoto-Iwamoto and M. Pacifici (2007). "Transcription factor ERG and joint and articular cartilage formation during mouse limb and spine skeletogenesis." Dev Biol **305**(1): 40-51.

Jadin, K. D., B. L. Wong, W. C. Bae, K. W. Li, A. K. Williamson, B. L. Schumacher, J. H. Price and R. L. Sah (2005). "Depth-varying density and organization of chondrocytes in immature and mature bovine articular cartilage assessed by 3d imaging and analysis." J Histochem Cytochem **53**(9): 1109-19.

Janjanin, S., W. J. Li, M. T. Morgan, R. M. Shanti and R. S. Tuan (2008). "Mold-shaped, nanofiber scaffold-based cartilage engineering using human mesenchymal stem cells and bioreactor." J Surg Res **149**(1): 47-56.

Jimenez, M. J., M. Balbin, J. Alvarez, T. Komori, P. Bianco, K. Holmbeck, H. Birkedal-Hansen, J. M. Lopez and C. Lopez-Otin (2001). "A regulatory cascade involving retinoic acid, Cbfa1, and matrix metalloproteinases is coupled to the development of a process of perichondrial invasion and osteogenic differentiation during bone formation." J Cell Biol **155**(7): 1333-44.

Johnstone, B., T. M. Hering, A. I. Caplan, V. M. Goldberg and J. U. Yoo (1998). "In vitro chondrogenesis of bone marrow-derived mesenchymal progenitor cells." Exp Cell Res **238**(1): 265-72.

Jukes, J. M., S. K. Both, A. Leusink, L. M. Sterk, C. A. van Blitterswijk and J. de Boer (2008). "Endochondral bone tissue engineering using embryonic stem cells." Proc Natl Acad Sci U S A **105**(19): 6840-5.

Kafienah, W., S. Mistry, M. J. Perry, G. Politopoulou and A. P. Hollander (2007). "Pharmacological regulation of adult stem cells: chondrogenesis can be induced using a synthetic inhibitor of the retinoic acid receptor." Stem Cells **25**(10): 2460-8.

Kahn, J., Y. Shwartz, E. Blitz, S. Krief, A. Sharir, D. A. Breitel, R. Rattenbach, F. Relaix, P. Maire, R. B. Rountree, D. M. Kingsley and E. Zelzer (2009). "Muscle contraction is necessary to maintain joint progenitor cell fate." Dev Cell **16**(5): 734-43.

Kaplan, F. S., D. L. Glaser, R. J. Pignolo and E. M. Shore (2007). "A new era for fibrodysplasia ossificans progressiva: a druggable target for the second skeleton." Expert Opin Biol Ther **7**(5): 705-12.

Kavalkovich, K. W., R. E. Boynton, J. M. Murphy and F. Barry (2002). "Chondrogenic differentiation of human mesenchymal stem cells within an alginate layer culture system." In Vitro Cell Dev Biol Anim **38**(8): 457-66.

Kawamura, S., S. Wakitani, T. Kimura, A. Maeda, A. I. Caplan, K. Shino and T. Ochi (1998). "Articular cartilage repair. Rabbit experiments with a collagen gel-biomatrix and chondrocytes cultured in it." Acta Orthop Scand **69**(1): 56-62.

Kearney, E. M., P. J. Prendergast and V. A. Campbell (2008). "Mechanisms of strain-mediated mesenchymal stem cell apoptosis." J Biomech Eng **130**(6): 061004.

Kelly, T. A., K. W. Ng, C. C. Wang, G. A. Ateshian and C. T. Hung (2006). "Spatial and temporal development of chondrocyte-seeded agarose constructs in free-swelling and dynamically loaded cultures." J Biomech **39**(8): 1489-97.

Kempson, G. E. (1982). "Relationship between the tensile properties of articular cartilage from the human knee and age." Ann Rheum Dis **41**(5): 508-11.

Kempson, G. E. (1991). "Age-related changes in the tensile properties of human articular cartilage: a comparative study between the femoral head of the hip joint and the talus of the ankle joint." Biochim Biophys Acta **1075**(3): 223-30.

Kim, M., X. Bi, W. E. Horton, R. G. Spencer and N. P. Camacho (2005). "Fourier transform infrared imaging spectroscopic analysis of tissue engineered cartilage: histologic and biochemical correlations." J Biomed Opt **10**(3): 031105.

Kisiday, J., D. D. Frisbie, W. McIlwraith and A. Grodzinsky (2009). "Dynamic compression stimulates proteoglycan synthesis by mesenchymal stem cells in the absence of chondrogenic cytokines." Tissue Eng Part A.

Kisiday, J., M. Jin, B. Kurz, H. Hung, C. Semino, S. Zhang and A. J. Grodzinsky (2002). "Self-assembling peptide hydrogel fosters chondrocyte extracellular matrix production and cell division: implications for cartilage tissue repair." Proc Natl Acad Sci U S A **99**(15): 9996-10001.

Kisiday, J. D., M. Jin, M. A. DiMicco, B. Kurz and A. J. Grodzinsky (2004). "Effects of dynamic compressive loading on chondrocyte biosynthesis in self-assembling peptide scaffolds." J Biomech **37**(5): 595-604.

Kisiday, J. D., P. W. Kopesky, C. H. Evans, A. J. Grodzinsky, C. W. McIlwraith and D. D. Frisbie (2008). "Evaluation of adult equine bone marrow- and adipose-derived progenitor cell chondrogenesis in hydrogel cultures." J Orthop Res **26**(3): 322-31.

Kisiday, J. D., B. Kurz, M. A. DiMicco and A. J. Grodzinsky (2005). "Evaluation of medium supplemented with insulin-transferrin-selenium for culture of primary bovine calf chondrocytes in three-dimensional hydrogel scaffolds." Tissue Eng **11**(1-2): 141-51.

Koyama, E., Y. Shibukawa, M. Nagayama, H. Sugito, B. Young, T. Yuasa, T. Okabe, T. Ochiai, N. Kamiya, R. B. Rountree, D. M. Kingsley, M. Iwamoto, M. Enomoto-Iwamoto and M. Pacifici (2008). "A distinct cohort of progenitor cells participates in synovial joint and articular cartilage formation during mouse limb skeletogenesis." Dev Biol **316**(1): 62-73.

Kurtz, S., K. Ong, E. Lau, F. Mowat and M. Halpern (2007). "Projections of primary and revision hip and knee arthroplasty in the United States from 2005 to 2030." J Bone Joint Surg Am **89**(4): 780-5.

Laasanen, M. S., J. Toyras, R. K. Korhonen, J. Rieppo, S. Saarakkala, M. T. Nieminen, J. Hirvonen and J. S. Jurvelin (2003). "Biomechanical properties of knee articular cartilage." Biorheology **40**(1-3): 133-40.

Lee, H. J., C. Yu, T. Chansakul, N. S. Hwang, S. Varghese, S. M. Yu and J. H. Elisseeff (2008). "Enhanced chondrogenesis of mesenchymal stem cells in collagen mimetic peptide-mediated microenvironment." Tissue Eng Part A **14**(11): 1843-51.

Lee, R. C., E. H. Frank, A. J. Grodzinsky and D. K. Roylance (1981). "Oscillatory compressional behavior of articular cartilage and its associated electromechanical properties." J Biomech Eng **103**(4): 280-92.

Li, L., A. Shirazi-Adl and M. D. Buschmann (2003). "Investigation of mechanical behavior of articular cartilage by fibril reinforced poroelastic models." Biorheology **40**(1-3): 227-33.

Li, Q., C. G. Williams, D. D. Sun, J. Wang, K. Leong and J. H. Elisseeff (2004). "Photocrosslinkable polysaccharides based on chondroitin sulfate." J Biomed Mater Res A **68**(1): 28-33.

Li, W. J., Y. J. Jiang and R. S. Tuan (2006). "Chondrocyte phenotype in engineered fibrous matrix is regulated by fiber size." Tissue Eng **12**(7): 1775-85.

Li, W. J., R. Tuli, X. Huang, P. Laquerriere and R. S. Tuan (2005). "Multilineage differentiation of human mesenchymal stem cells in a three-dimensional nanofibrous scaffold." Biomaterials **26**(25): 5158-66.

Li, W. J., R. Tuli, C. Okafor, A. Derfoul, K. G. Danielson, D. J. Hall and R. S. Tuan (2005). "A three-dimensional nanofibrous scaffold for cartilage tissue engineering using human mesenchymal stem cells." Biomaterials **26**(6): 599-609.

Li, Z., L. Kupcsik, S. J. Yao, M. Alini and M. J. Stoddart (2009). "Mechanical Load Modulates Chondrogenesis of Human Mesenchymal Stem Cells through the TGF-beta Pathway." J Cell Mol Med.

Li, Z., S. J. Yao, M. Alini and M. J. Stoddart (2009). "Chondrogenesis of Human Bone Marrow Mesenchymal Stem Cells in Fibrin-Polyurethane Composites is Modulated by Frequency and Amplitude of Dynamic Compression and Shear Stress." Tissue Eng Part A.

Lima, E. G., L. Bian, R. L. Mauck, B. A. Byers, R. S. Tuan, G. A. Ateshian and C. T. Hung (2006). "The effect of applied compressive loading on tissue-engineered cartilage constructs cultured with TGF-beta3." Conf Proc IEEE Eng Med Biol Soc **1**: 779-82.

Lima, E. G., L. Bian, K. W. Ng, R. L. Mauck, B. A. Byers, R. S. Tuan, G. A. Ateshian and C. T. Hung (2007). "The beneficial effect of delayed compressive loading on tissue-engineered cartilage constructs cultured with TGF-beta3." Osteoarthritis Cartilage.

Lima, E. G., L. Bian, K. W. Ng, R. L. Mauck, B. A. Byers, R. S. Tuan, G. A. Ateshian and C. T. Hung (2007). "The beneficial effect of delayed compressive loading on tissue-

engineered cartilage constructs cultured with TGF-beta3." Osteoarthritis Cartilage **15**(9): 1025-33.

Lipshitz, H., R. Etheredge, 3rd and M. J. Glimcher (1976). "Changes in the hexosamine content and swelling ratio of articular cartilage as functions of depth from the surface." J Bone Joint Surg Am **58**(8): 1149-53.

Longobardi, L., L. O'Rear, S. Aakula, B. Johnstone, K. Shimer, A. Chytil, W. A. Horton, H. L. Moses and A. Spagnoli (2006). "Effect of IGF-I in the chondrogenesis of bone marrow mesenchymal stem cells in the presence or absence of TGF-beta signaling." J Bone Miner Res **21**(4): 626-36.

Lutolf, M. P. and J. A. Hubbell (2005). "Synthetic biomaterials as instructive extracellular microenvironments for morphogenesis in tissue engineering." Nat Biotechnol **23**(1): 47-55.

Lutolf, M. P., J. L. Lauer-Fields, H. G. Schmoekel, A. T. Metters, F. E. Weber, G. B. Fields and J. A. Hubbell (2003). "Synthetic matrix metalloproteinase-sensitive hydrogels for the conduction of tissue regeneration: engineering cell-invasion characteristics." Proc Natl Acad Sci U S A **100**(9): 5413-8.

Macirowski, T., S. Tepic and R. W. Mann (1994). "Cartilage stresses in the human hip joint." J Biomech Eng **116**(1): 10-8.

Majumdar, M. K., E. Wang and E. A. Morris (2001). "BMP-2 and BMP-9 promotes chondrogenic differentiation of human multipotential mesenchymal cells and overcomes the inhibitory effect of IL-1." J Cell Physiol **189**(3): 275-84.

Malemud, C. J. (2006). "Matrix metalloproteinases: role in skeletal development and growth plate disorders." Front Biosci **11**: 1702-15.

Malemud, C. J. and V. M. Goldberg (1999). "Future directions for research and treatment of osteoarthritis." Front Biosci **4**: D762-71.

Mankin, H. J., V. C. Mow, J. A. Buckwalter, J. P. Iannotti and A. Ratcliffe (1994). Form and Function of Articular Cartilage. Orthopaedic Basic Science. S. R. Simon. Rosemont, American Academy of Orthopaedic Surgeons.

Mauck, R. L., B. A. Byers, X. Yuan and R. S. Tuan (2007). "Regulation of cartilaginous ECM gene transcription by chondrocytes and MSCs in 3D culture in response to dynamic loading." Biomech Model Mechanobiol **6**(1-2): 113-25.

Mauck, R. L., B. A. Byers, X. Yuan and R. S. Tuan (2007). "Regulation of Cartilaginous ECM Gene Transcription by Chondrocytes and MSCs in 3D Culture in Response to Dynamic Loading." Biomech Model Mechanobiol **6**(1-2): 113-125.

Mauck, R. L., C. T. Hung and G. A. Ateshian (2003). "Modeling of neutral solute transport in a dynamically loaded porous permeable gel: implications for articular cartilage biosynthesis and tissue engineering." J Biomech Eng **125**(5): 602-14.

Mauck, R. L., S. B. Nicoll, S. L. Seyhan, G. A. Ateshian and C. T. Hung (2003). "Synergistic action of growth factors and dynamic loading for articular cartilage tissue engineering." Tissue Eng **9**(4): 597-611.

Mauck, R. L., S. L. Seyhan, G. A. Ateshian and C. T. Hung (2002). "Influence of seeding density and dynamic deformational loading on the developing structure/function relationships of chondrocyte-seeded agarose hydrogels." Ann Biomed Eng **30**(8): 1046-56.

Mauck, R. L., M. A. Soltz, C. C. Wang, D. D. Wong, P. H. Chao, W. B. Valhmu, C. T. Hung and G. A. Ateshian (2000). "Functional tissue engineering of articular cartilage through dynamic loading of chondrocyte-seeded agarose gels." J Biomech Eng **122**(3): 252-60.

Mauck, R. L., C. C. Wang, E. S. Oswald, G. A. Ateshian and C. T. Hung (2003). "The role of cell seeding density and nutrient supply for articular cartilage tissue engineering with deformational loading." Osteoarthritis Cartilage **11**(12): 879-90.

Mauck, R. L., X. Yuan and R. S. Tuan (2006). "Chondrogenic differentiation and functional maturation of bovine mesenchymal stem cells in long-term agarose culture." Osteoarthritis Cartilage **14**(2): 179-89.

McMahon, L. A., V. A. Campbell and P. J. Prendergast (2008). "Involvement of stretch-activated ion channels in strain-regulated glycosaminoglycan synthesis in mesenchymal stem cell-seeded 3D scaffolds." J Biomech **41**(9): 2055-9.

McMahon, L. A., P. J. Prendergast and V. A. Campbell (2008). "A comparison of the involvement of p38, ERK1/2 and PI3K in growth factor-induced chondrogenic differentiation of mesenchymal stem cells." Biochem Biophys Res Commun **368**(4): 990-5.

McMahon, L. A., A. J. Reid, V. A. Campbell and P. J. Prendergast (2008). "Regulatory effects of mechanical strain on the chondrogenic differentiation of MSCs in a collagen-GAG scaffold: experimental and computational analysis." Ann Biomed Eng **36**(2): 185-94.

Mehlhorn, A. T., H. Schmal, S. Kaiser, G. Lepski, G. Finkenzeller, G. B. Stark and N. P. Sudkamp (2006). "Mesenchymal stem cells maintain TGF-beta-mediated chondrogenic phenotype in alginate bead culture." Tissue Eng **12**(6): 1393-403.

Mikic, B., A. L. Isenstein and A. Chhabra (2004). "Mechanical modulation of cartilage structure and function during embryogenesis in the chick." Ann Biomed Eng **32**(1): 18-25.

Mikic, B., T. L. Johnson, A. B. Chhabra, B. J. Schalet, M. Wong and E. B. Hunziker (2000). "Differential effects of embryonic immobilization on the development of fibrocartilaginous skeletal elements." J Rehabil Res Dev **37**(2): 127-33.

Mitrovic, D. (1982). "Development of the articular cavity in paralyzed chick embryos and in chick embryo limb buds cultured on chorioallantoic membranes." Acta Anat (Basel) **113**(4): 313-24.

Miyanishi, K., M. C. Trindade, D. P. Lindsey, G. S. Beaupre, D. R. Carter, S. B. Goodman, D. J. Schurman and R. L. Smith (2006). "Effects of hydrostatic pressure and transforming growth factor-beta 3 on adult human mesenchymal stem cell chondrogenesis in vitro." Tissue Eng **12**(6): 1419-28.

Moioli, E. K., L. Hong, J. Guardado, P. A. Clark and J. J. Mao (2006). "Sustained release of TGFbeta3 from PLGA microspheres and its effect on early osteogenic differentiation of human mesenchymal stem cells." Tissue Eng **12**(3): 537-46.

Moioli, E. K., L. Hong and J. J. Mao (2007). "Inhibition of osteogenic differentiation of human mesenchymal stem cells." Wound Repair Regen **15**(3): 413-21.

Moutos, F. T., L. E. Freed and F. Guilak (2007). "A biomimetic three-dimensional woven composite scaffold for functional tissue engineering of cartilage." Nat Mater **6**(2): 162-7.

Mouw, J. K., N. D. Case, R. E. Guldberg, A. H. Plaas and M. E. Levenston (2005). "Variations in matrix composition and GAG fine structure among scaffolds for cartilage tissue engineering." Osteoarthritis Cartilage **13**(9): 828-36.

Mouw, J. K., J. T. Connelly, C. G. Wilson, K. E. Michael and M. E. Levenston (2007). "Dynamic compression regulates the expression and synthesis of chondrocyte-specific matrix molecules in bone marrow stromal cells." Stem Cells **25**(3): 655-63.

Mow, V. C. and X. E. Guo (2002). "Mechano-electrochemical properties of articular cartilage: their inhomogeneities and anisotropies." Annu Rev Biomed Eng **4**: 175-209.

Mow, V. C., S. C. Kuei, W. M. Lai and C. G. Armstrong (1980). "Biphasic creep and stress relaxation of articular cartilage in compression? Theory and experiments." J Biomech Eng **102**(1): 73-84.

Mueller, M. B. and R. S. Tuan (2008). "Functional characterization of hypertrophy in chondrogenesis of human mesenchymal stem cells." Arthritis Rheum **58**(5): 1377-1388.

Muir, H. (1970). "The intracellular matrix in the environment of connective tissue cells." Clin Sci **38**(2): 8P.

Muir, H. (1980). The chemistry of the ground substance of joint cartilage. The Joints and Synovial Fluid. L. Sokoloff. New York, Academic Press. **II:** 27-94.

Murphy, J. M., K. Dixon, S. Beck, D. Fabian, A. Feldman and F. Barry (2002). "Reduced chondrogenic and adipogenic activity of mesenchymal stem cells from patients with advanced osteoarthritis." Arthritis Rheum **46**(3): 704-13.

Nagase, H. and M. Kashiwagi (2003). "Aggrecanases and cartilage matrix degradation." Arthritis Res Ther **5**(2): 94-103.

Nehrer, S., H. A. Breinan, A. Ramappa, S. Shortkroff, G. Young, T. Minas, C. B. Sledge, I. V. Yannas and M. Spector (1997). "Canine chondrocytes seeded in type I and type II collagen implants investigated in vitro." J Biomed Mater Res **38**(2): 95-104.

Nesti, L. J., W. J. Li, R. M. Shanti, Y. J. Jiang, W. Jackson, B. A. Freedman, T. R. Kuklo, J. R. Giuliani and R. S. Tuan (2008). "Intervertebral disc tissue engineering using a novel hyaluronic acid-nanofibrous scaffold (HANFS) amalgam." Tissue Eng Part A **14**(9): 1527-37.

Nettles, D. L., T. P. Vail, M. T. Morgan, M. W. Grinstaff and L. A. Setton (2004). "Photocrosslinkable hyaluronan as a scaffold for articular cartilage repair." Ann Biomed Eng **32**(3): 391-7.

Neuman, R. E. and M. A. Logan (1950). "The determination of hydroxyproline." J Biol Chem **184**(1): 299-306.

Ng, K. W., L. E. Kugler, S. B. Doty, G. A. Ateshian and C. T. Hung (2009). "Scaffold degradation elevates the collagen content and dynamic compressive modulus in engineered articular cartilage." Osteoarthritis Cartilage **17**(2): 220-7.

Ng, K. W., C. C. Wang, R. L. Mauck, T. A. Kelly, N. O. Chahine, K. D. Costa, G. A. Ateshian and C. T. Hung (2005). "A layered agarose approach to fabricate depth-dependent inhomogeneity in chondrocyte-seeded constructs." J Orthop Res **23**(1): 134-41.

Nixon, A. J., L. A. Fortier, J. Williams and H. Mohammed (1999). "Enhanced repair of extensive articular defects by insulin-like growth factor-I-laden fibrin composites." J Orthop Res **17**(4): 475-87.

Normand, V., D. L. Lootens, E. Amici, K. P. Plucknett and P. Aymard (2000). "New insight into agarose gel mechanical properties." Biomacromolecules **1**(4): 730-8.

Noth, U., A. M. Osyczka, R. Tuli, N. J. Hickok, K. G. Danielson and R. S. Tuan (2002). "Multilineage mesenchymal differentiation potential of human trabecular bone-derived cells." J Orthop Res **20**(5): 1060-9.

O'Keefe, R. J., L. S. Loveys, D. G. Hicks, P. R. Reynolds, I. D. Crabb, J. E. Puzas and R. N. Rosier (1997). "Differential regulation of type-II and type-X collagen synthesis by parathyroid hormone-related protein in chick growth-plate chondrocytes." J Orthop Res **15**(2): 162-74.

Oberlender, S. A. and R. S. Tuan (1994). "Expression and functional involvement of N-cadherin in embryonic limb chondrogenesis." Development **120**(1): 177-87.

Ohno, S., T. Doi, K. Fujimoto, C. Ijuin, N. Tanaka, K. Tanimoto, K. Honda, M. Nakahara, Y. Kato and K. Tanne (2002). "RGD-CAP (betaig-h3) exerts a negative regulatory function on mineralization in the human periodontal ligament." J Dent Res **81**(12): 822-5.

Ohno, S., T. Doi, S. Tsutsumi, Y. Okada, K. Yoneno, Y. Kato and K. Tanne (2002). "RGD-CAP ((beta)ig-h3) is expressed in precartilage condensation and in prehypertrophic chondrocytes during cartilage development." Biochim Biophys Acta **1572**(1): 114-22.

Pacifici, M., E. Koyama and M. Iwamoto (2005). "Mechanisms of synovial joint and articular cartilage formation: recent advances, but many lingering mysteries." Birth Defects Res C Embryo Today **75**(3): 237-48.

Pacifici, M., E. Koyama, M. Iwamoto and C. Gentili (2000). "Development of articular cartilage: what do we know about it and how may it occur?" Connect Tissue Res **41**(3): 175-84.

Paige, K. T., L. G. Cima, M. J. Yaremchuk, J. P. Vacanti and C. A. Vacanti (1995). "Injectable cartilage." Plast Reconstr Surg **96**(6): 1390-8; discussion 1399-400.

Pajerowski, J. D., K. N. Dahl, F. L. Zhong, P. J. Sammak and D. E. Discher (2007). "Physical plasticity of the nucleus in stem cell differentiation." Proc Natl Acad Sci U S A **104**(40): 15619-24.

Palmer, G. D., A. Steinert, A. Pascher, E. Gouze, J. N. Gouze, O. Betz, B. Johnstone, C. H. Evans and S. C. Ghivizzani (2005). "Gene-induced chondrogenesis of primary mesenchymal stem cells in vitro." Mol Ther **12**(2): 219-28.

Park, H., J. S. Temenoff, Y. Tabata, A. I. Caplan and A. G. Mikos (2007). "Injectable biodegradable hydrogel composites for rabbit marrow mesenchymal stem cell and growth factor delivery for cartilage tissue engineering." Biomaterials **28**(21): 3217-27.

Park, H., J. S. Temenoff, Y. Tabata, A. I. Caplan, R. M. Raphael, J. A. Jansen and A. G. Mikos (2009). "Effect of dual growth factor delivery on chondrogenic differentiation of rabbit marrow mesenchymal stem cells encapsulated in injectable hydrogel composites." J Biomed Mater Res A **88**(4): 889-97.

Park, S. and G. A. Ateshian (2006). "Dynamic response of immature bovine articular cartilage in tension and compression, and nonlinear viscoelastic modeling of the tensile response." J Biomech Eng **128**(4): 623-30.

Park, S., C. T. Hung and G. A. Ateshian (2004). "Mechanical response of bovine articular cartilage under dynamic unconfined compression loading at physiological stress levels." Osteoarthritis Cartilage **12**(1): 65-73.

Park, S., S. B. Nicoll, R. L. Mauck and G. A. Ateshian (2008). "Cartilage mechanical response under dynamic compression at physiological stress levels following collagenase digestion." Ann Biomed Eng **36**(3): 425-34.

Park, Y., M. P. Lutolf, J. A. Hubbell, E. B. Hunziker and M. Wong (2004). "Bovine primary chondrocyte culture in synthetic matrix metalloproteinase-sensitive poly(ethylene glycol)-based hydrogels as a scaffold for cartilage repair." Tissue Eng **10**(3-4): 515-22.

Paul, J. P. and D. A. McGrouther (1975). "Forces transmitted at the hip and knee joint of normal and disabled persons during a range of activities." Acta Orthop Belg **41 Suppl 1**(1): 78-88.

Pei, M., J. Seidel, G. Vunjak-Novakovic and L. E. Freed (2002). "Growth factors for sequential cellular de- and re-differentiation in tissue engineering." Biochem Biophys Res Commun **294**(1): 149-54.

Pelaez, D., C. Y. Huang and H. S. Cheung (2008). "Cyclic Compression Maintains Viability and Induces Chondrogenesis of Human Mesenchymal Stem Cells in Fibrin Gel Scaffolds." Stem Cells Dev.

Pelttari, K., A. Winter, E. Steck, K. Goetzke, T. Hennig, B. G. Ochs, T. Aigner and W. Richter (2006). "Premature induction of hypertrophy during in vitro chondrogenesis of human mesenchymal stem cells correlates with calcification and vascular invasion after ectopic transplantation in SCID mice." Arthritis Rheum **54**(10): 3254-66.

Penick, K. J., L. A. Solchaga and J. F. Welter (2005). "High-throughput aggregate culture system to assess the chondrogenic potential of mesenchymal stem cells." Biotechniques **39**(5): 687-91.

Persson, M. (1983). "The role of movements in the development of sutural and diarthrodial joints tested by long-term paralysis of chick embryos." J Anat **137 (Pt 3)**: 591-9.

Pitsillides, A. A. (2003). "Identifying and characterizing the joint cavity-forming cell." Cell Biochem Funct **21**(3): 235-40.

Pittenger, M. F., A. M. Mackay, S. C. Beck, R. K. Jaiswal, R. Douglas, J. D. Mosca, M. A. Moorman, D. W. Simonetti, S. Craig and D. R. Marshak (1999). "Multilineage potential of adult human mesenchymal stem cells." Science **284**(5411): 143-7.

Ponticiello, M. S., R. M. Schinagl, S. Kadiyala and F. P. Barry (2000). "Gelatin-based resorbable sponge as a carrier matrix for human mesenchymal stem cells in cartilage regeneration therapy." J Biomed Mater Res **52**(2): 246-55.

Prockop, D. J. (1997). "Marrow stromal cells as stem cells for nonhematopoietic tissues." Science **276**(5309): 71-4.

Puelacher, W. C., S. W. Kim, J. P. Vacanti, B. Schloo, D. Mooney and C. A. Vacanti (1994). "Tissue-engineered growth of cartilage: the effect of varying the concentration of chondrocytes seeded onto synthetic polymer matrices." Int J Oral Maxillofac Surg **23**(1): 49-53.

Quinn, T. M., P. Schmid, E. B. Hunziker and A. J. Grodzinsky (2002). "Proteoglycan deposition around chondrocytes in agarose culture: construction of a physical and biological interface for mechanotransduction in cartilage." Biorheology **39**(1-2): 27-37.

Reginato, A. M. and B. R. Olsen (2002). "The role of structural genes in the pathogenesis of osteoarthritic disorders." Arthritis Res **4**(6): 337-45.

Reginster, J. Y., R. Deroisy, L. C. Rovati, R. L. Lee, E. Lejeune, O. Bruyere, G. Giacovelli, Y. Henrotin, J. E. Dacre and C. Gossett (2001). "Long-term effects of glucosamine sulphate on osteoarthritis progression: a randomised, placebo-controlled clinical trial." Lancet **357**(9252): 251-6.

Riesle, J., A. P. Hollander, R. Langer, L. E. Freed and G. Vunjak-Novakovic (1998). "Collagen in tissue-engineered cartilage: types, structure, and crosslinks." J Cell Biochem **71**(3): 313-27.

Roth, V. and V. C. Mow (1980). "The intrinsic tensile behavior of the matrix of bovine articular cartilage and its variation with age." J Bone Joint Surg Am **62**(7): 1102-17.

Rotter, N., L. J. Bonassar, G. Tobias, M. Lebl, A. K. Roy and C. A. Vacanti (2002). "Age dependence of biochemical and biomechanical properties of tissue-engineered human septal cartilage." Biomaterials **23**(15): 3087-94.

Rowley, J. A., G. Madlambayan and D. J. Mooney (1999). "Alginate hydrogels as synthetic extracellular matrix materials." Biomaterials **20**(1): 45-53.

Sakaguchi, Y., I. Sekiya, K. Yagishita and T. Muneta (2005). "Comparison of human stem cells derived from various mesenchymal tissues: superiority of synovium as a cell source." Arthritis Rheum **52**(8): 2521-9.

Salinas, C. N., B. B. Cole, A. M. Kasko and K. S. Anseth (2007). "Chondrogenic differentiation potential of human mesenchymal stem cells photoencapsulated within poly(ethylene glycol)-arginine-glycine-aspartic acid-serine thiol-methacrylate mixed-mode networks." Tissue Eng **13**(5): 1025-34.

Schaefer, D., I. Martin, G. Jundt, J. Seidel, M. Heberer, A. Grodzinsky, I. Bergin, G. Vunjak-Novakovic and L. E. Freed (2002). "Tissue-engineered composites for the repair of large osteochondral defects." Arthritis Rheum **46**(9): 2524-34.

Schmidt, M. B., V. C. Mow, L. E. Chun and D. R. Eyre (1990). "Effects of proteoglycan extraction on the tensile behavior of articular cartilage." J Orthop Res **8**(3): 353-63.

Schmitt, B., J. Ringe, T. Haupl, M. Notter, R. Manz, G. R. Burmester, M. Sittinger and C. Kaps (2003). "BMP2 initiates chondrogenic lineage development of adult human mesenchymal stem cells in high-density culture." Differentiation **71**(9-10): 567-77.

Schumacher, B. L., C. E. Hughes, K. E. Kuettner, B. Caterson and M. B. Aydelotte (1999). "Immunodetection and partial cDNA sequence of the proteoglycan, superficial zone protein, synthesized by cells lining synovial joints." J Orthop Res **17**(1): 110-20.

Seda Tigli, R., S. Ghosh, M. M. Laha, N. K. Shevde, L. Daheron, J. Gimble, M. Gumusderelioglu and D. L. Kaplan (2009). "Comparative chondrogenesis of human cell sources in 3D scaffolds." J Tissue Eng Regen Med.

Seidel, J. O., M. Pei, M. L. Gray, R. Langer, L. E. Freed and G. Vunjak-Novakovic (2004). "Long-term culture of tissue engineered cartilage in a perfused chamber with mechanical stimulation." Biorheology **41**(3-4): 445-58.

Sekiya, I., J. T. Vuoristo, B. L. Larson and D. J. Prockop (2002). "In vitro cartilage formation by human adult stem cells from bone marrow stroma defines the sequence of cellular and molecular events during chondrogenesis." Proc Natl Acad Sci U S A **99**(7): 4397-402.

Shieh, A. C. and K. A. Athanasiou (2003). "Principles of cell mechanics for cartilage tissue engineering." Ann Biomed Eng **31**(1): 1-11.

Shore, E. M., M. Xu, G. J. Feldman, D. A. Fenstermacher, T. J. Cho, I. H. Choi, J. M. Connor, P. Delai, D. L. Glaser, M. LeMerrer, R. Morhart, J. G. Rogers, R. Smith, J. T. Triffitt, J. A. Urtizberea, M. Zasloff, M. A. Brown and F. S. Kaplan (2006). "A recurrent mutation in the BMP type I receptor ACVR1 causes inherited and sporadic fibrodysplasia ossificans progressiva." Nat Genet **38**(5): 525-7.

Smith, R. L., S. F. Rusk, B. E. Ellison, P. Wessells, K. Tsuchiya, D. R. Carter, W. E. Caler, L. J. Sandell and D. J. Schurman (1996). "In vitro stimulation of articular chondrocyte mRNA and extracellular matrix synthesis by hydrostatic pressure." J Orthop Res **14**(1): 53-60.

Solchaga, L. A., K. Penick, J. D. Porter, V. M. Goldberg, A. I. Caplan and J. F. Welter (2005). "FGF-2 enhances the mitotic and chondrogenic potentials of human adult bone marrow-derived mesenchymal stem cells." J Cell Physiol **203**(2): 398-409.

Soltz, M. A. and G. A. Ateshian (1998). "Experimental verification and theoretical prediction of cartilage interstitial fluid pressurization at an impermeable contact interface in confined compression." J Biomech **31**(10): 927-34.

Soltz, M. A. and G. A. Ateshian (2000). "A Conewise Linear Elasticity mixture model for the analysis of tension-compression nonlinearity in articular cartilage." J Biomech Eng **122**(6): 576-86.

Soltz, M. A. and G. A. Ateshian (2000). "Interstitial fluid pressurization during confined compression cyclical loading of articular cartilage." Ann Biomed Eng **28**(2): 150-9.

Song, L. and R. S. Tuan (2004). "Transdifferentiation potential of human mesenchymal stem cells derived from bone marrow." Faseb J **18**(9): 980-2.

Song, L., N. E. Webb, Y. Song and R. S. Tuan (2006). "Identification and functional analysis of candidate genes regulating mesenchymal stem cell self-renewal and multipotency." Stem Cells **24**(7): 1707-18.

Soulhat, J., M. D. Buschmann and A. Shirazi-Adl (1999). "A fibril-network-reinforced biphasic model of cartilage in unconfined compression." J Biomech Eng **121**(3): 340-7.

Stanton, H., F. M. Rogerson, C. J. East, S. B. Golub, K. E. Lawlor, C. T. Meeker, C. B. Little, K. Last, P. J. Farmer, I. K. Campbell, A. M. Fourie and A. J. Fosang (2005). "ADAMTS5 is the major aggrecanase in mouse cartilage in vivo and in vitro." Nature **434**(7033): 648-52.

Stegemann, H. and K. Stalder (1967). "Determination of hydroxyproline." Clin Chim Acta **18**(2): 267-73.

Stewart, A. A., C. R. Byron, H. Pondenis and M. C. Stewart (2007). "Effect of fibroblast growth factor-2 on equine mesenchymal stem cell monolayer expansion and chondrogenesis." Am J Vet Res **68**(9): 941-5.

Stoddart, M. J., L. Ettinger and H. J. Hauselmann (2006). "Enhanced matrix synthesis in de novo, scaffold free cartilage-like tissue subjected to compression and shear." Biotechnol Bioeng **95**(6): 1043-51.

Stoller, P., K. M. Reiser, P. M. Celliers and A. M. Rubenchik (2002). "Polarization-modulated second harmonic generation in collagen." Biophys J **82**(6): 3330-42.

Tacchetti, C., S. Tavella, B. Dozin, R. Quarto, G. Robino and R. Cancedda (1992). "Cell condensation in chondrogenic differentiation." Exp Cell Res **200**(1): 26-33.

Terraciano, V., N. Hwang, L. Moroni, H. B. Park, Z. Zhang, J. Mizrahi, D. Seliktar and J. Elisseeff (2007). "Differential Response of Adult and Embryonic Mesenchymal Progenitor Cells to Mechanical Compression in Hydrogels." Stem Cells.

Thorpe, S. D., C. T. Buckley, T. Vinardell, F. J. O'Brien, V. A. Campbell and D. J. Kelly (2008). "Dynamic compression can inhibit chondrogenesis of mesenchymal stem cells." Biochem Biophys Res Commun **377**(2): 458-62.

Toh, W. S., H. Liu, B. C. Heng, A. J. Rufaihah, C. P. Ye and T. Cao (2005). "Combined effects of TGFbeta1 and BMP2 in serum-free chondrogenic differentiation of mesenchymal stem cells induced hyaline-like cartilage formation." Growth Factors **23**(4): 313-21.

Toyras, J., J. Rieppo, M. T. Nieminen, H. J. Helminen and J. S. Jurvelin (1999). "Characterization of enzymatically induced degradation of articular cartilage using high frequency ultrasound." Phys Med Biol **44**(11): 2723-33.

Tuli, R., M. R. Seghatoleslami, S. Tuli, M. S. Howard, K. G. Danielson and R. S. Tuan (2002). "p38 MAP kinase regulation of AP-2 binding in TGF-beta1-stimulated chondrogenesis of human trabecular bone-derived cells." Ann N Y Acad Sci **961**: 172-7.

Tuli, R., S. Tuli, S. Nandi, X. Huang, P. A. Manner, W. J. Hozack, K. G. Danielson, D. J. Hall and R. S. Tuan (2003). "Transforming growth factor-beta-mediated chondrogenesis of human mesenchymal progenitor cells involves N-cadherin and mitogen-activated protein kinase and Wnt signaling cross-talk." J Biol Chem **278**(42): 41227-36.

Vanderploeg, E. J., C. G. Wilson and M. E. Levenston (2008). "Articular chondrocytes derived from distinct tissue zones differentially respond to in vitro oscillatory tensile loading." Osteoarthritis Cartilage **16**(10): 1228-36.

Verbruggen, G. (2006). "Chondroprotective drugs in degenerative joint diseases." Rheumatology (Oxford) **45**(2): 129-38.

Vortkamp, A., K. Lee, B. Lanske, G. V. Segre, H. M. Kronenberg and C. J. Tabin (1996). "Regulation of rate of cartilage differentiation by Indian hedgehog and PTH-related protein." Science **273**(5275): 613-22.

Vunjak-Novakovic, G., I. Martin, B. Obradovic, S. Treppo, A. J. Grodzinsky, R. Langer and L. E. Freed (1999). "Bioreactor cultivation conditions modulate the composition and mechanical properties of tissue-engineered cartilage." J Orthop Res **17**(1): 130-8.

Vunjak-Novakovic, G., B. Obradovic, I. Martin, P. M. Bursac, R. Langer and L. E. Freed (1998). "Dynamic cell seeding of polymer scaffolds for cartilage tissue engineering." Biotechnol Prog **14**(2): 193-202.

Wagner, D. R., D. P. Lindsey, K. W. Li, P. Tummala, S. E. Chandran, R. L. Smith, M. T. Longaker, D. R. Carter and G. S. Beaupre (2008). "Hydrostatic pressure enhances chondrogenic differentiation of human bone marrow stromal cells in osteochondrogenic medium." Ann Biomed Eng **36**(5): 813-20.

Waldman, S. D., C. G. Spiteri, M. D. Grynpas, R. M. Pilliar and R. A. Kandel (2003). "Long-term intermittent shear deformation improves the quality of cartilaginous tissue formed in vitro." J Orthop Res **21**(4): 590-6.

Walters, W. P. and M. Namchuk (2003). "Designing screens: how to make your hits a hit." Nat Rev Drug Discov **2**(4): 259-66.

Wang, C. C., X. E. Guo, D. Sun, V. C. Mow, G. A. Ateshian and C. T. Hung (2002). "The functional environment of chondrocytes within cartilage subjected to compressive loading: a theoretical and experimental approach." Biorheology **39**(1-2): 11-25.

Wang, X., E. Wenk, X. Zhang, L. Meinel, G. Vunjak-Novakovic and D. L. Kaplan (2009). "Growth factor gradients via microsphere delivery in biopolymer scaffolds for osteochondral tissue engineering." J Control Release **134**(2): 81-90.

Wayne, J. S., C. W. Brodrick and N. Mukherjee (1998). "Measurement of articular cartilage thickness in the articulated knee." Ann Biomed Eng **26**(1): 96-102.

Weightman, B. (1976). "Tensile fatigue of human articular cartilage." J Biomech **9**(4): 193-200.

Welter, J. F., L. A. Solchaga and K. J. Penick (2007). "Simplification of aggregate culture of human mesenchymal stem cells as a chondrogenic screening assay." Biotechniques **42**(6): 732, 734-7.

Williams, G. M., T. J. Klein and R. L. Sah (2005). "Cell density alters matrix accumulation in two distinct fractions and the mechanical integrity of alginate-chondrocyte constructs." Acta Biomater **1**(6): 625-33.

Williamson, A. K., A. C. Chen, K. Masuda, E. J. Thonar and R. L. Sah (2003). "Tensile mechanical properties of bovine articular cartilage: variations with growth and relationships to collagen network components." J Orthop Res **21**(5): 872-80.

Williamson, A. K., A. C. Chen and R. L. Sah (2001). "Compressive properties and function-composition relationships of developing bovine articular cartilage." J Orthop Res **19**(6): 1113-21.

Williamson, A. K., K. Masuda, E. J. Thonar and R. L. Sah (2003). "Growth of immature articular cartilage in vitro: correlated variation in tensile biomechanical and collagen network properties." Tissue Eng **9**(4): 625-34.

Williamson, A. K., K. Masuda, E. J. Thonar and R. L. Sah (2003). "Growth of immature articular cartilage in vitro: correlated variation of tensile biomechanical and collagen network properties." Tiss Eng **9**(4): 625-34.

Woo, S. L., W. H. Akeson and G. F. Jemmott (1976). "Measurements of nonhomogeneous, directional mechanical properties of articular cartilage in tension." J Biomech **9**(12): 785-91.

Woods, A. and F. Beier (2006). "RhoA/ROCK signaling regulates chondrogenesis in a context-dependent manner." J Biol Chem **281**(19): 13134-40.

Woods, A., G. Wang and F. Beier (2005). "RhoA/ROCK signaling regulates Sox9 expression and actin organization during chondrogenesis." J Biol Chem **280**(12): 11626-34.

Woods, A., G. Wang, H. Dupuis, Z. Shao and F. Beier (2007). "Rac1 signaling stimulates N-cadherin expression, mesenchymal condensation, and chondrogenesis." J Biol Chem **282**(32): 23500-8.

Wu, X., S. Ding, Q. Ding, N. S. Gray and P. G. Schultz (2002). "A small molecule with osteogenesis-inducing activity in multipotent mesenchymal progenitor cells." J Am Chem Soc **124**(49): 14520-1.

Xu, J., W. Wang, M. Ludeman, K. Cheng, T. Hayami, J. C. Lotz and S. Kapila (2008). "Chondrogenic differentiation of human mesenchymal stem cells in three-dimensional alginate gels." Tissue Eng Part A **14**(5): 667-80.

Yamane, S., E. Cheng, Z. You and A. H. Reddi (2007). "Gene expression profiling of mouse articular and growth plate cartilage." Tissue Eng **13**(9): 2163-73.

Yates, K. E., F. Allemann and J. Glowacki (2005). "Phenotypic analysis of bovine chondrocytes cultured in 3D collagen sponges: effect of serum substitutes." Cell Tissue Bank **6**(1): 45-54.

Yu, P. B., C. C. Hong, C. Sachidanandan, J. L. Babitt, D. Y. Deng, S. A. Hoyng, H. Y. Lin, K. D. Bloch and R. T. Peterson (2008). "Dorsomorphin inhibits BMP signals required for embryogenesis and iron metabolism." Nat Chem Biol **4**(1): 33-41.

Zhang, J., L. Liu, Z. Gao, L. Li, X. Feng, W. Wu, Q. Ma, X. Cheng, F. Chen and T. Mao (2009). "Novel approach to engineer implantable nasal alar cartilage employing marrow precursor cell sheet and biodegradable scaffold." J Oral Maxillofac Surg **67**(2): 257-64.

Zhang, J. H., T. D. Chung and K. R. Oldenburg (1999). "A Simple Statistical Parameter for Use in Evaluation and Validation of High Throughput Screening Assays." J Biomol Screen **4**(2): 67-73.

Zhang, Z., J. Messana, N. S. Hwang and J. H. Elisseeff (2006). "Reorganization of actin filaments enhances chondrogenic differentiation of cells derived from murine embryonic stem cells." Biochem Biophys Res Commun **348**(2): 421-7.

Zhao, Y. and S. Ding (2007). "A high-throughput siRNA library screen identifies osteogenic suppressors in human mesenchymal stem cells." Proc Natl Acad Sci U S A **104**(23): 9673-8.

Zhou, X. Z., V. Y. Leung, Q. R. Dong, K. M. Cheung, D. Chan and W. W. Lu (2008). "Mesenchymal stem cell-based repair of articular cartilage with polyglycolic acid-hydroxyapatite biphasic scaffold." Int J Artif Organs **31**(6): 480-9.

Zhou, Z., S. S. Apte, R. Soininen, R. Cao, G. Y. Baaklini, R. W. Rauser, J. Wang, Y. Cao and K. Tryggvason (2000). "Impaired endochondral ossification and angiogenesis in mice deficient in membrane-type matrix metalloproteinase I." Proc Natl Acad Sci U S A **97**(8): 4052-7.